Rostyslav S. Stoika *Editor*

Biomedical Nanomaterials

From design and synthesis to imaging,
application, and environmental impact

Springer

Biomedical Nanomaterials

Rostyslav S. Stoika

Editor

Biomedical Nanomaterials

From design and synthesis to imaging,
application, and environmental impact

 Springer

Editor
Rostyslav S. Stoika
Head of Department of Regulation of Cell
Proliferation and Apoptosis
Institute of Cell Biology, National Academy
of Sciences of Ukraine
Lviv, Ukraine

Preface

My interest in specific nanomaterials and nanobiotechnologies for biology and medicine started in 2005, when a couple of my colleagues who are organic and physical chemists sent me a proposal to investigate the biological activities of their products in order to evaluate the potential biomedical applications of the synthesized products. The role of my department at the Institute of Cell Biology, NAS of Ukraine, was to study the possibility of using new products, organic polymers and C60-fullerene nanoparticles, as platforms for drug and gene delivery. The need for such platforms exists because of the inaction of many medicines and their adverse effects in the treated organism. In addition, the physicochemical properties of many drugs, for example, with their poor water solubility, do not allow for a convenient application of these drugs. As a result of the realization of joint research projects with my colleagues working in Eastern and Central European countries, several nanoplatforms were developed for drug and gene delivery. Thus, there was a need for the analysis and summarization of our experience in the molecular design, chemical synthesis, and biomedical application of novel nanomaterials in order to pass that experience to other scientists who work in this rapidly developing field of materials science.

Most co-authors of this book participated in the TechConnect World Innovation Conference in Washington, DC (USA), in 2017. Their oral and poster presentations were visited by Merry Stuber, Senior Editor with Springer Nature Publishers. She asked Dr. Sandor Vari, Director of International Research and Innovation in Medicine Program (Cedars-Sinai Medical Center, Los Angeles, CA, USA) and RECOOP Association (https://www.cedars-sinai.org/research/administration/recoop.html), who managed our participation at the TechConnect World Innovation Conference, if he would prepare a book devoted to our results in the development of novel nanomaterials and nanobiotechnologies for biomedical use. This initiative was interrupted by COVID-19-related problems, but finally, we can present our book to readers.

The logistics of composing the presented materials is based on offering to readers a unique manual for their strategy for developing their own nanomaterials for biomedical applications, starting from their molecular design and synthesis, and

moving to necessary steps of their physical-chemical and toxicological characteristics (biodegradability, biocompatibility, controlled delivery and clearance in the organism, as well as potential bio-risks for the environment). Both the organic (novel surface-active comb-like PEG-containing polymers) and mineral (novel water-soluble C60-fullerene-based nanoplatforms and magnetic iron oxide-based nano- and micro-particles for theranostics) materials used in biomedical applications are described by the leading specialists in the corresponding fields. The nano-toxicology-related aspects of these and other biomedical materials are described both in general, including genotoxicity and environmental toxicity, and specifically, hepato-, cardio-, nephro-, and immune-toxicities. Environmental aspects of the application of various nanomaterials have been characterized for freshwater and marine organisms, as well as for the multipollutant strategy of assessment of the environmental quality and health risks caused by air nano-pollutants. Bioimaging of nanomaterials is a central element for monitoring their biological action, and this aspect is described in the book as characterization of novel polymeric nanocarriers for gene delivery, which is a crucial step in gene therapy that is considered to be the future of medicine.

The co-authors of all chapters of this book are thankful to the people who initiated its writing, as well as to numerous members of the research teams who assisted in the experiments aimed at the development of novel nanomaterials and nanobio-technologies for biomedical applications.

Lviv, Ukraine   Rostyslav S. Stoika

Contents

Part IV   Environmental Impacts of Nanomaterials

Part I
Introduction

Principal Trends in Nanobiotechnology

Rostyslav S. Stoika

Abbreviations

CT	X-ray computed tomography
DNA	deoxyribonucleic acid
miRNA	micro ribonucleic acid
MRI	magnetic resonance imaging
NIR	near-infrared
PEG	polyethylene glycol
PEI	polyethylenimine

1 Multifunctional "Smart" Medicines

Trend 1 in nanobiotechnology is focused on the creation of nanomaterials for biomedical application that possess multifunctionality due to which they are also called "smart" or "intellectual" materials (Torchilin, 2014). The "smartness" of "drug delivery systems" means that the drugs are released only at the sites of their action and not before they reach the target tissues or organs. Historically, three generations of medicines might be considered (Deshaies, 2020; Wang & Yang, 2020): (1) drugs that passively penetrate the tissues and organs in order to reach target cells; (2) drugs immobilized on the developed carriers for better targeting of specific biomolecules or structures in the cells; (3) multifunctional "smart" medicines whose additional activities and characteristics are provided by the high-tech delivery systems (nanoshuttles, multistage self-assembling systems, other).

The nonaddressed action of the anticancer drugs causes severe adverse effects (hepato-, cardio-, nephro-, neuro-, and immunotoxicities) in the treated body, and it is one of the most serious problems in antitumor chemotherapy. Different approaches have been proposed to avoid negative side effects or at least diminish their consequences. They are based on immobilization of clinically approved antitumor drugs, for example, the lyposomal form of doxorubicin (Myocet), the PEGylated

R. S. Stoika (✉)
Institute of Cell Biology of National Academy of Sciences of Ukraine, Lviv, Ukraine

lyposomal form of doxorubicin (Doxil), albumin-bound paclitaxel (Abraxane), and others (for review see: Shetab Boushehri et al., 2020). We have used similar noncovalent immobilization of anticancer drugs on the experimental nanoplatforms, such as C60 fullerene (Prylutska et al., 2017) or synthetic amphiphilic polymers (Senkiv et al., 2014). The results of our studies demonstrated that a use of special drug-delivery nanoplatforms significantly increased the effectiveness of antitumor action of various drugs (Senkiv et al., 2014; Heffeter et al., 2014), and also reduced their overall toxicity in the preclinical experiments in laboratory animals bearing model tumors (Kobylinska et al., 2018). Besides, drug delivery on the functionalized nano-carriers enhanced drug engulfment by the target cells (Senkiv et al., 2014; Heffeter et al., 2014) and provided water solubility to insoluble drug substances (Kobylinska et al., 2019).

In this brief introduction chapter, it is not possible to report about all multifunctional nanomaterials that were created for biomedical use, since the number of experimental and review papers devoted to these materials is really huge (e.g., see: Pelaz et al., 2017). Thus, I would like to attract the readers' attention to four main issues:

1. Decoration of the multifunctional nanocomposites with the *Camelidae* small antibodies (nanobodies) for providing them with more addressed action toward the target cells (Steeland et al., 2016; Xiang et al., 2020), and use of "cell penetrating peptides" for improved penetration of the nanocomposites into the target cells (Torchilin, 2008; Hu et al., 2014)
2. Search for a substitute for the polyethylene glycol (PEG) that is widely used as a functional element of most drug and gene carriers (Ljubimova et al., 2017) for the prevention of their resorption by cells of the reticuloendothelial system, which, however, demonstrated adverse effects in some individuals (Andersen et al., 2013)
3. Creation of stimuli-responsive nanomaterials that are capable of changing their physicochemical properties (shape, solubility, wettability, color, conductivity, light transmitting abilities, or surface characteristics) in response to the effect of the environmental factors (temperature, pH, ionic strength, redox status, specific enzymes, electric and magnetic fields, mechanical force, light) (for review, see: Torchilin, 2014; Wei et al., 2017; Municoy et al., 2020)
4. Development of self-assembled nanomaterials for biomedical use

A dynamic self-assembly means that the pre-existing components are organized in specific patterns via local interactions. Self-assembly (self-organization) term originates from physics (Vladimirov & Ostrikov, 2004), but it is also applicable for characteristics of the behavior of the nanosystems of third generation proposed for addressed drug and gene delivery. In biology, a dynamic self-assembly means that a mixture of components of various activities are specifically organized at proper locations in tissues or organs due to local interactions of those components with formation of supramolecular structures that possess new activities. The alliances of cell signaling scaffold proteins can form similar higher-order macromolecular

complexes that facilitate their integration, regulation, crosstalk, and feedback of the target proteins. The formation of viral capsids might be another example of self-assembled structures with 3D surface topography. The team of André H. Gröschel in Germany nicely demonstrated control of size, shape, inner morphology, and chemistry of the multicompartment micelles (Malho et al., 2016; Tjaberings et al., 2020). In perspective, new challenges in the combinatorial nano-bio interfaces and multiparametric nano-combinatorics (composition, morphology, mechanics, surface chemistry) will be addressed to biomolecules, organelles, cells, tissues, and organs with the recruitment of the computational modeling and artificial intelligence (Brownlee, 2018).

2   Medicines Capable of Circumventing Multiple Drug Resistance

Trend 2 in nanobiotechnology is focused on the development of drugs that are capable of circumventing the multidrug resistance barriers in patients with malignant neoplasms and tuberculosis. There are two main ways to solve this problem of drug resistance: (1) "hide" the anticancer or anti-tuberculosis drugs in order to make them "invisible" for the transporting system of cell membrane that responsible for pumping out the drugs from target cells—this aim might be achieved through the encapsulation of drugs in the polymeric micelles or nanoparticles used as a container (Senkiv et al., 2014; Heffeter et al., 2014; Jin et al., 2014; Ljubimova et al., 2017) and (2) make the delivery of drugs to the target cells too complicated a task for blocking such delivery by systems of drug resistance in the cells—this might be achieved via the creation of the dual (multiple) targeting drug systems in which the cytomodulator or cytotoxicant is combined with the nucleic acid, thus, functioning as both the chemotherapeutic agent and the gene therapy remedy. For example, a hybrid system was created for cancer treatment (Zhang et al., 2016). It contains both the chemotherapeutic drug (dichloroacetate) that induces apoptosis in tumor, and intact gene coding for p53 protein functioning as growth inhibitor and apoptosis inducer. This anti-oncogene is mutated in a majority of tumors and, thus, it codes there for the inactive form of p53. miRNAs that block the expression of specific proteins (e.g., products of oncogenes) are also used as a nucleic acid component of hybrid drug-delivery systems (Xin et al., 2017).

3   Nanomaterials for Conjugation of Poorly Water-Soluble Drug Compounds

Trend 3 in nanobiotechnology is focused on the creation of nanomaterials that can efficiently conjugate poorly water-soluble medicines among which are various natural (e.g., taxol) or synthetic (heterocyclics) compounds, particularly the anticancer

drugs. These and many other biologically active substances can be solubilized only in the organic solvents that are highly toxic for the organism. Thus, their application in chemotherapies is blocked. It is known that >40% of the existing compounds cannot be easily solubilized in water (Merisko-Liversidge & Liversidge, 2008; Kakran et al., 2012). All known compounds have been categorized into four classes, starting from high solubility and high permeability (class 1) to low solubility and low permeability (class 4) (Saffie-Siebert et al., 2005). The application of particular biocompatible lipid systems is a simple, although not always easy, way to solve a solubility problem (Merisko-Liversidge & Liversidge, 2008; Da Silva et al., 2020). Another more complicated way is to use specific amphiphilic polymers that can encapsulate a water-insoluble substance inside the micelles exposing on their surface chemical groups which prefer water molecules (Djordjevic et al., 2005; Tao & Uhrich, 2006; see also Chap. 2 of this book). For such micellar structures, choosing the desired size, architecture, and chemical functionalization is of principal significance.

4   Nanomaterials for Gene Delivery

Trend 4 in nanobiotechnology is focused on the development of efficient nanocarriers for the delivery of DNA and miRNA in the organism. The market for these materials is rapidly growing due to the requirements of biotechnology aimed at producing new substances and of gene therapy that is, no doubt, a future of modern medicine. On that way, there is a problem of crossing by the negatively charged nucleic acid molecule of plasma membrane whose surface charge is also negative and which is composed of the hydrophobic lipid bi-layer that is another barrier for the hydrophilic compounds. Various approaches are used to secure crossing of cellular plasma membrane barrier by the nucleic acid. The biological approach is based on using viral vectors which are potentially dangerous for the organism. The physical approaches are not convenient because of the need for using complicated and expensive equipment and they frequently damage the targeted cells, which reduces the efficiency of delivery of nucleic acids to the target cells. Polyethylenimine (PEI) is widely used in chemical approaches for gene delivery (Lungwitz et al., 2005; Deng et al., 2009), although it is not the best reagent because of its bio-toxicity (see also Chap. 8 in this book). Thus, the development of novel materials for chemical transfection is currently a prospective trend, and new biocompatible cationic polymers are probably the most promising carriers of genetic materials (Agarwal et al., 2012; Bae et al., 2017; Santo et al., 2017; Rai et al., 2019). A possibility of additional functionalization of such polymers exists and this might provide them with functional components responsible for many useful activities (Ljubimova et al., 2017). The application of the nonviral vectors demonstrated their efficiency in gene therapeutic treatment of cancer and cardiovascular pathologies (Hardee et al., 2017; Hidai & Kitano, 2018).

5   Biocompatible Labels for Bioimaging of Pharmaceutics

Trend 5 in nanobiotechnology is focused on the creation of efficient and biocompatible labels for biomedical application, namely in the use of novel pharmaceutics. Labeling of drug- and gene-delivery carriers is important for monitoring their biodistribution, biological action, and clearance in the body. Such labels possess the physico-chemical properties that permit their monitoring in cell or the body, namely super-paramagnetism (Li et al., 2013), radioactivity (Lewis & Kannan, 2014), noble metal core/shell (Tiwari et al., 2011; Wen Zhou et al., 2015; Bartosewicz et al., 2017), rare earth and hybrid rare earth–polymeric nanoparticles (Chang et al., 2014; Shapoval et al., 2021), other metals (Yi Yan et al., 2016; Yaqoob et al., 2020), semiconductivity (Ichimura et al., 2014), luminescence/fluorescence (Reisch & Klymchenko, 2016; Zhang et al., 2017), graphene-based materials (Lin et al., 2016; Gu et al., 2019), quantum dots (Shen, 2011; Wagner et al., 2019), carbon-based nanoparticles (Liu et al., 2020), nanodiamonds (Kaur & Badea, 2013), silica-based nanoparticles (Narayan et al., 2018), optically active nanomaterials (Yang et al., 2019), polymer nanoparticles (Braeken et al., 2017), organic dyes (Lian et al., 2019), molecular fluorophores (Wang et al., 2020), green fluorescent protein (Schmidt et al., 2017), luciferase and luciferin system (Sun et al., 2011; Kaskova et al., 2016), and other properties. These properties might be either innate characteristics (e.g., luminescence/fluorescence) of the biomedical nanomaterials or provided via conjugation of the nanomaterials (e.g., polymer or mineral) with additional functional elements (labels). Thus, a number and variety of the bio-trackers are extremely big due to the involvement of chemists and physicists in the creation of these materials.

6   Nanomaterials for Bioimaging in Diagnostics

Trend 6 in nanobiotechnology is focused on the creation of nanomaterials for bioimaging to be used in diagnostics. These materials are needed for the visualization of time-dependent biodistribution of specific nanomedicines and their accumulation in the targeted organs or tissues of the body. Parallelly, specific bioimaging techniques should be developed. There are two main types of scanners for bioimaging in medicine and experimental biology: X-ray computed tomography (CT) and magnetic resonance imaging (MRI) (Wallyn et al., 2019). Many trackers noted above in the Trend 5 description are used as contrast agents for diagnostic bioimaging. The sensitivity of their detection is permanently increasing and this occurs in parallel with the improvement in the characteristics of the labeling materials.

Specific trackers have been proposed for tissue engineering and 3D printing (Li & Lee, 2020), monitoring the circumvention of blood-brain barrier and blood-brain tumor barrier during neuro-oncological surgery (Belykh et al., 2020; Hampel et al., 2009), study of dynamics of tumor development and regression evaluated by MRI

and CT (Shapoval et al., 2021), and biosensing and bioimaging with graphene for cancer diagnosis (Lin et al., 2016). The list of examples of the nanoparticle-based bio-trackers is very long (for review, see Rong et al., 2017; Ni et al., 2020).

It might be worth to address in more detail the use of the near-infrared (NIR, 700–2500 nm) light. It penetrates the tissues such as skin and is less harmful comparing with X-ray used in CT. There are two biological windows of the NIR wavelength applicable for bio-imaging: NIR-I (650–950 nm) and NIR-II (1000–1700 nm) (Smith et al., 2009; Welsher et al., 2009; Jie Cao et al., 2020). The drawbacks of the application of NIR-I are tissue autofluorescence, which produces background noise, limited tissue penetration (millimeters depth), and a need for using nonbiocompatible fluorescent probes for bioimaging. However, the application of the NIR-II permits deep-tissue exploration (centimeters range) using more biocompatible probes, for example, single-walled carbon nanotubes (Smith et al., 2009; Welsher et al., 2009). To improve the biocompatibility, the carbon nanotubes might be coated with sodium cholate lipid or with phospholipid-PEG, which did not interfere with their fluorescence (Welsher et al., 2009). High selectivity is the key issue of the bioimaging that is achieved by functionalization of the targeting contrast probes or delivery nanoplatforms. However, there is no big progress in the development of novel NIR-II probes for the biomedical application.

Nanotheranostics combines disease diagnosis and therapy based on the use of nanomaterials and nanobiotechnology approaches (Wang et al., 2012; Chen et al., 2017). In this field, novel nanomaterials are used for monitoring addressed delivery of drugs and their accumulation in the target tissues, sustained and triggered release of drugs, as well as response to drugs in the organism and a reduction in the adverse effects. The main functional elements of nanomaterials used in nanotheranostics are drugs, antibodies, cell penetration peptides, oligonucleotides, fluorophores, and plasmid DNA in gene delivery. The "*Theranostics*" journal has achieved an impact factor of 8.579 (2019–2020) in less than 10 years from the time its monitoring started. The main goals of nanotheranostics are (1) "targeted therapy," which is based on the advancements in the field of nanotechnology and is among the principal scopes of theranostics and (2) "biomarkers," whose study is based on new technologies in material science, such as biochips and other invented nano-analytical probes used in nanotheranostics. These issues are combined in "photodynamic therapy," which might be considered a specific branch of theranostics (Kufe et al., 2003).

In summary, six principal trends in nanobiotechnology with regard to the current demands in the pharmaceutical market are defined in this chapter. In other chapters of our book, these trends are considered in more detail by scientists who work in different fields of design, synthesis, and biomedical application of novel nanomaterials.

References

Agarwal, S., Zhang, Y., Maji, S., & Greiner, A. (2012). PDMAEMA based gene delivery materials. *Materials Today, 15*, 388–393. https://doi.org/10.1016/S1369-7021(12)70165-7

Andersen, A. J., Windschiegl, B., Ilbasmis-Tamer, S., Degim, I. T., Hunter, A. C., Andresen, T. L., & Moghimi, S. M. (2013). Complement activation by PEG-functionalized multi-walled carbon nanotubes is independent of PEG molecular mass and surface density. *Nanomedicine, 9*(4), 469–473. https://doi.org/10.1016/j.nano.2013.01.011

Bae, Y., Rhim, H., Lee, S., Ko, K., Han, J., & Choi, J. (2017). Apoptin gene delivery by the functionalized polyamidoamine dendrimer derivatives induces cell death of U87-MG glioblastoma cells. *Journal of Pharmaceutical Sciences, 106*, 1618–1633. https://doi.org/10.1016/j.xphs.2017.01.034

Bartosewicz, B., Michalska-Domańska, M., Liszewska, M., Zasada, D., & Jankiewicz, B. J. (2017). Synthesis and characterization of noble metal-titania core-shell nanostructures with tunable shell thickness. *Beilstein Journal of Nanotechnology*, *8*, 2083–2093. https://doi.org/10.3762/bjnano.8.208

Belykh, E., Shaffer, K. V., Lin, C., Byvaltsev, V. A., Preul, M. C., & Chen, L. (2020). Blood-brain barrier, blood-brain tumor barrier, and fluorescence-guided neurosurgical oncology: Delivering optical labels to brain tumors. *Frontiers in Oncology, 10*, 739. https://doi.org/10.3389/fonc.2020.00739

Braeken, Y., Cheruku, S., Ethirajan, A., & Maes, W. (2017). Conjugated Polymer nanoparticles for bioimaging. *Materials (Basel), 10*(12), 1420. https://doi.org/10.3390/ma10121420

Brownlee, C. (2018). Combinatorial nano–bio interfaces were created. *ACS Nano, 12*(6), 5069–5072. https://doi.org/10.1021/acsnano.8b04412

Cao, J., Zhu, B., Zheng, K., He, S., Meng, L., Song, J., & Yang, H. (2020). Recent progress in NIR-II contrast agent for biological imaging. *Frontiers in Bioengineering and Biotechnology, 7*, 487. https://doi.org/10.3389/fbioe.2019.00487

Chang, H., Xie, J., Zhao, B., Liu, B., Xu, S., Ren, N., Xie, X., Huang, L., & Huang, W. (2014). Rare earth ion-doped upconversion nanocrystals: Synthesis and surface modification. *Nanomaterials (Basel, Switzerland), 5*(1), 1–25. https://doi.org/10.3390/nano5010001

Chen, H., Zhang, W., Zhu, G., Xie, J., & Chen, X. (2017). Rethinking cancer nanotheranostics. *Nature Reviews. Materials, 2*, 17024. https://doi.org/10.1038/natrevmats.2017.24

Da Silva, F., Marques, M., Kato, K. C., & Carneiro, G. (2020). Nanonization techniques to overcome poor water-solubility with drugs. *Expert Opinion on Drug Discovery, 15*(7), 853–864. https://doi.org/10.1080/17460441.2020.1750591

Deng, R., Yue, Y., Jin, F., Chen, Y., Kung, H. F., Lin, M. C., & Wu, C. (2009). Revisit the complexation of PEI and DNA - how to make low cytotoxic and highly efficient PEI gene transfection non-viral vectors with a controllable chain length and structure? *Journal of Controlled Release: Official Journal of the Controlled Release Society, 140*(1), 40–46. https://doi.org/10.1016/j.jconrel.2009.07.009

Deshaies, R. J. (2020). Multispecific drugs herald a new era of biopharmaceutical innovation. *Nature, 580*(7803), 329–338. https://doi:10.1038/s41586-020-2168-1

Djordjevic, J., Barch, M., & Uhrich, K. E. (2005). Polymeric micelles based on amphiphilic scorpion-like macromolecules: Novel carriers for water-insoluble drugs. *Pharmaceutical Research, 22*(1), 24–32. https://doi.org/10.1007/s11095-004-9005-3

Gu, H., Tang, H., Xiong, P., & Zhou, Z. (2019). Biomarkers-based biosensing and bioimaging with graphene for cancer diagnosis. *Nanomaterials (Basel, Switzerland), 9*(1), 130. https://doi.org/10.3390/nano9010130

Hampel, H., Broich, K., Hoessler, Y., & Pantel, J. (2009). Biological markers for early detection and pharmacological treatment of Alzheimer's disease. *Dialogues in Clinical Neuroscience, 11*(2), 141–157. https://doi.org/10.31887/DCNS.2009.11.2/hhampel

Hardee, C. L., Arévalo-Solizm, L. M., Hornsteinm, B. D., & Zechiedrich, L. (2017). Advances in non-viral DNA vectors for gene therapy. *Genes (Basel), 8*(2), pii: E65. https://doi.org/10.3390/genes8020065

Heffeter, P., Riabtseva, A., Senkiv, Y., Kowol, C. R., Körner, W., Jungwith, U., … Berger, W. (2014). Nanoformulation improves activity of the (pre)clinical anticancer ruthenium complex KP1019. *Journal of Biomedical Nanotechnology, 10*(5), 877–884. https://doi.org/10.1166/jbn.2014.1763

Hidai, C., & Kitano, H. (2018). Nonviral gene therapy for cancer: A review. *Diseases (Basel, Switzerland), 6*(3), 57. https://doi:10.3390/diseases6030057

Hu, Y., Xu, B., Ji, Q., Shou, D., Sun, X., Xu, J., … Liang, W. (2014). A mannosylated cell-penetrating peptide-graft-polyethylenimine as a gene delivery vector. *Biomaterials, 35*(13), 4236–4246. https://doi.org/10.1016/j.biomaterials.2014.01.065

Ichimura, T., Jin, T., Fujita, H., Higuchi, H., & Watanabe, T. M. (2014). Nano-scale measurement of biomolecules by optical microscopy and semiconductor nanoparticles. *Frontiers in Physiology, 5*, 273. https://doi.org/10.3389/fphys.2014.00273

Jin, S. E., Jin, H. E., & Hong, S. S. (2014). Targeted delivery system of nanobiomaterials in anti-cancer therapy: From cells to clinics. *BioMed Research International, 2014*, 814208. https://doi.org/10.1155/2014/814208

Kakran, M., Lin, L., & Muller, R. H. (2012). Overcoming the challenge of poor drug solubility. *Pharmaceutical Engineering, 32*(4), 1–7.

Kaskova, Z. M., Tsarkova, A. S., & Yampolsky, I. V. (2016). 1001 lights: Luciferins, luciferases, their mechanisms of action and applications in chemical analysis, biology and medicine. *Chemical Society Reviews, 45*, 6048–6077. https://doi:10.1039/c6cs00296j

Kaur, R., & Badea, I. (2013). Nanodiamonds as novel nanomaterials for biomedical applications: Drug delivery and imaging systems. *International Journal of Nanomedicine, 8*, 203–220. https://doi.org/10.2147/IJN.S37348

Kobylinska, L., Patereha, I., Finiuk, N., Mitina, N., Riabtseva, A., Kotsyumbas, I., … Vari, S. G. (2018). Comb-like PEG-containing polymeric composition as low toxic drug nanocarrier. *Cancer Nanotechnology, 9*(1), 11. https://doi.org/10.1186/s12645-018-0045-5

Kobylinska, L., Ivasechko, I., Skorokhyd, N., Panchuk, R., Riabtseva, A., Mitina, N., … Vari, S. G. (2019). Enhanced proapoptotic effects of water dispersed complexes of 4-thiazolidinone-based chemotherapeutics with a peg-containing polymeric nanocarrier. *Nanoscale Research Letters, 14*(1), 140. https://doi.org/10.1186/s11671-019-2945-7

Kufe, D. W., Pollock, R. E., Weichselbaum, R. R., et al. (Eds.). (2003). *Holland-Frei cancer medicine* (6th ed.). BC Decker.

Lewis, M. R., & Kannan, R. (2014). Development and applications of radioactive nanoparticles for imaging of biological systems. *Wiley Interdisciplinary Reviews - Nanomedicine and Nanobiotechnology, 6*(6), 628–640. https://doi:10.1002/wnan.1292

Li, Y. E., & Lee, I. C. (2020). The current trends of biosensors in tissue engineering. *Biosensors, 10*(8), 88. https://doi.org/10.3390/bios10080088

Li, X., Zhao, D., & Zhang, F. (2013). Multifunctional upconversion-magnetic hybrid nanostructured materials: Synthesis and bioapplications. *Theranostics, 3*(5), 292–305. https://doi.org/10.7150/thno.5289

Lian, X., Wei, M. Y., & Ma, Q. (2019). Nanomedicines for near-infrared fluorescent lifetime-based bioimaging. *Frontiers in Bioengineering and Biotechnology, 7*, 386. https://doi.org/10.3389/fbioe.2019.00386

Lin, J., Chen, X., & Huang, P. (2016). Graphene-based nanomaterials for bioimaging. *Advanced Drug Delivery Reviews*, *105*(Pt B), 242–254. https://doi.org/10.1016/j.addr.2016.05.013

Liu, J., Li, R., & Yang, B. (2020). Carbon dots: A new type of carbon-based nanomaterial with wide applications. *ACS Central Science, 6*(12), 2179–2195. https://doi.org/10.1021/acscentsci.0c01306

Ljubimova, J. Y., Sun, T., Mashouf, L., Ljubimov, A. V., Israel, L. L., Ljubimov, V. A., … Holler, E. (2017). Covalent nano delivery systems for selective imaging and treatment of brain tumors. *Advanced Drug Delivery Reviews, 113*, 177–200. https://doi.org/10.1016/j.addr.2017.06.002

Lungwitz, U., Breunig, M., Blunk, T., & Göpferich, A. (2005). Polyethylenimine-based nonviral gene delivery systems. *European Journal of Pharmaceutics and Biopharmaceutics, 60*, 247e66. https://doi.org/10.1016/j.ejpb.2004.11.011

Malho, J.-M., Morits, M., Löbling, T. I., Nonappa, Majoinen, J., Schacher, F. H., … Gröschel, A. H. (2016). Rod-like nanoparticles with striped and helical topography. *ACS Macro Letters, 5*(10), 1185–1190. https://doi.org/10.1021/acsmacrolett.6b00645

Merisko-Liversidge, E. M., & Liversidge, G. G. (2008). Drug nanoparticles: Formulating poorly water-soluble compounds. *Toxicologic Pathology, 36*(1), 43–48. https://doi.org/10.1177/0192623307310946

Municoy, S., Álvarez Echazú, M. I., Antezana, P. E., Galdopórpora, J. M., Olivetti, C., Mebert, A. M., … Desimone, M. F. (2020). Stimuli-responsive materials for tissue engineering and drug delivery. *International Journal of Molecular Sciences, 21*(13), 4724. https://doi.org/10.3390/ijms21134724

Narayan, R., Nayak, U. Y., Raichur, A. M., & Garg, S. (2018). Mesoporous silica nanoparticles: A comprehensive review on synthesis and recent advances. *Pharmaceutics, 10*(3), 118. https://doi.org/10.3390/pharmaceutics10030118

Ni, J. S., Li, Y., Yue, W., Liu, B., & Li, K. (2020). Nanoparticle-based cell trackers for biomedical applications. *Theranostics, 10*(4), 1923–1947. https://doi.org/10.7150/thno.39915

Pelaz, B., Alexiou, C., Alvarez-Puebla, R. A., Alves, F., Andrews, A. M., Ashraf, S., … Parak, W. J. (2017). Diverse applications of nanomedicine. *ACS Nano, 11*(3), 2313–2381. https://doi.org/10.1021/acsnano.6b06040

Prylutska, S., Panchuk, R., Gołuński, G., Skivka, L., Prylutskyy, Y., Hurmach, V., … Scharff, P. (2017). C60 fullerene enhances cisplatin anticancer activity and overcomes tumor cell drug resistance. *Nano Research, 10*, 652–671. https://doi.org/10.1007/s12274-016-1324-2

Rai, R., Alwani, S., & Badea, I. (2019). Polymeric nanoparticles in gene therapy: New avenues of design and optimization for delivery applications. *Polymers, 11*, 745. https://doi.org/10.3390/polym11040745

Reisch, A., & Klymchenko, A. S. (2016). Fluorescent polymer nanoparticles based on dyes: Seeking brighter tools for bioimaging. *Small (Weinheim an der Bergstrasse, Germany), 12*(15), 1968–1992. https://doi.org/10.1002/smll.201503396

Rong, G., Corrie, S. R., & Clark, H. A. (2017). *In Vivo* biosensing: Progress and perspectives. *ACS Sensors, 2*(3), 327–338. https://doi.org/10.1021/acssensors.6b00834

Saffie-Siebert, R., Ogden, J., & Parry-Billings, M. (2005). Nanotechnology approaches to solving the problems of poorly water-soluble drugs. *Drug Discovery World, Summer*, 71–76.

Santo, D., Cordeiro, R. A., Sousa, A., Serra, A., Coelho, J. F. J., & Faneca, H. (2017). Combination of poly[(2-dimethylamino)ethyl methacrylate] and poly(β-amino ester) results in a strong and synergistic transfection activity. *Biomacromolecules, 18*, 3331–3342. https://doi.org/10.1021/acs.biomac.7b00983

Schmidt, S., Tavernaro, I., Cavelius, C., Weber, E., Kümper, A., Schmitz, C., … Kraegeloh, A. (2017). Silica nanoparticles for intracellular protein delivery: A novel synthesis approach using green fluorescent protein. *Nanoscale Research Letters, 12*(1), 545. https://doi.org/10.1186/s11671-017-2280-9

Senkiv, Y., Riabtseva, A., Heffeter, P., Boiko, N., Kowol, C. R., Jungwith, U., … Stoika, R. (2014). Enhanced anticancer activity and circumvention of resistance mechanisms by novel polymeric/phospholipidic nanocarriers of doxorubicin. *Journal of Biomedical Nanotechnology, 10*(7), 1369–1381. https://doi.org/10.1166/jbn.2014.1864

Shapoval, O., Oleksa, V., Šlouf, M., Lobaz, V., Trhlíková, O., Filipová, M., … Horák, D. (2021). Colloidally stable P(DMA-AGME)-Ale-coated Gd(Tb)F$_3$:Tb^{3+}(Gd^{3+}),Yb^{3+},Nd^{3+} nanoparticles as a multimodal contrast agent for down- and upconversion luminescence, magnetic

resonance imaging, and computed tomography. *Nanomaterials (Basel), 11*(1), 230. https://doi.org/10.3390/nano11010230

Shen, L. (2011). Biocompatible polymer/quantum dots hybrid materials: Current status and future developments. *Journal of Functional Biomaterials, 2*(4), 355–372. https://doi.org/10.3390/jfb2040355

Shetab Boushehri, M. A., Dietrich, D., & Lamprecht, A. (2020). Nanotechnology as a platform for the development of injectable parenteral formulations: A comprehensive review of the know-hows and state of the art. *Pharmaceutics, 12*(6), 510. https://doi.org/10.3390/pharmaceutics12060510

Smith, A. M., Mancini, M. C., & Shuming, N. (2009). Second window for *in vivo* imaging. *Nature Nanotechnology, 4*(11), 710–711. https://doi.org/10.1038/nnano.2009.326

Steeland, S., Vandenbroucke, R. E., & Libert, C. (2016). Nanobodies as therapeutics: big opportunities for small antibodies. *Drug Discovery Today, 21*(7), 1076–1113. https://doi.org/10.1016/j.drudis.2016.04.003

Sun, X., Zhao, Y., Lin, V. S., Slowing, I. I., & Trewyn, B. G. (2011). Luciferase and luciferin co-immobilized mesoporous silica nanoparticle materials for intracellular biocatalysis. *Journal of the American Chemical Society, 133*(46), 18554–18557. https://doi.org/10.1021/ja2080168

Tao, L., & Uhrich, K. E. (2006). Novel amphiphilic macromolecules and their in vitro characterization as stabilized micellar drug delivery systems. *Journal of Colloid and Interface Science, 298*(1), 102–110. https://doi.org/10.1016/j.jcis.2005.12.018

Tiwari, P. M., Vig, K., Dennis, V. A., & Singh, S. R. (2011). Functionalized gold nanoparticles and their biomedical applications. *Nanomaterials (Basel, Switzerland), 1*(1), 31–63. https://doi.org/10.3390/nano1010031

Tjaberings, S., Heidelmann, M., Tjaberings, A., Steinhaus, A., Franzka, S., Walkenfort, B., & Gröschel, A. H. (2020). Terpolymer multicompartment nanofibers as templates for hybrid pt double helices. *ACS Applied Materials & Interfaces, 12*(35), 39586–39594. https://doi.org/10.1021/acsami.0c10385

Torchilin, V. P. (2008). Cell penetrating peptide-modified pharmaceutical nanocarriers for intracellular drug and gene delivery. *Peptide Science, 90*(5), 604–610. https://doi:10.1002/bip.20989

Torchilin, V. P. (2014). Multifunctional, stimuli-sensitive nanoparticulate systems for drug delivery. *Nature Reviews Drug Discovery, 13*, 813–827. https://doi.org/10.1038/nrd4333

Vladimirov, S. V., & Ostrikov, K. (2004). Dynamic self-organization phenomena in complex ionized gas systems: New paradigms and technological aspects. *Physics Reports, 393*, 175–380. https://doi.org/10.1016/j.physrep.2003.12.003

Wagner, A. M., Knipe, J. M., Orive, G., & Peppas, N. A. (2019). Quantum dots in biomedical applications. *Acta Biomaterialia, 94*, 44–63. https://doi.org/10.1016/j.actbio.2019.05.022

Wallyn, J., Anton, N., Akram, S., & Vandamme, T. F. (2019). Biomedical imaging: Principles, technologies, clinical aspects, contrast agents, limitations and future trends in nanomedicines. *Pharmaceutical Research, 36*(6), 78. https://doi.org/10.1007/s11095-019-2608-5

Wang, Y., & Yang, S. (2020). Multispecific drugs: The fourth wave of biopharmaceutical innovation. *Signal Transduction and Targeted Therapy, 5*(1), 86. https://doi.org/10.1038/s41392-020-0201-3

Wang, L. S., Chuang, M. C., & Ho, J. A. (2012). Nanotheranostics--a review of recent publications. *International Journal of Nanomedicine, 7*, 4679–4695. https://doi.org/10.2147/IJN.S33065

Wang, S., Li, B., & Zhang, F. (2020). Molecular fluorophores for deep-tissue bioimaging. *ACS Central Science, 6*(8), 1302–1316. https://doi.org/10.1021/acscentsci.0c00544

Wei, M., Gao, Y., Xue, L., & Serpe, M. J. (2017). Stimuli-responsive polymers and their applications. *Polymer Chemistry, 8*, 127–143. https://doi.org/10.1039/C6PY01585A

Welsher, K., Liu, Z., Sherlock, S. P., Robinson, J. T., Chen, Z., Daranciang, D., & Dai, H. (2009). A route to brightly fluorescent carbon nanotubes for near-infrared imaging in mice. *Nature Nanotechnology, 4*(11), 773–780. https://doi:10.1038/nnano.2009.294

Xiang, Y., Nambulli, S., Xiao, Z., Liu, H., Sang, Z., Duprex, W. P., … Shi, Y. (2020). Versatile and multivalent nanobodies efficiently neutralize SARS-CoV-2. *Science, 370*(6523), 1479–1484. https://doi.org/10.1126/science.abe4747

Xin, Y., Huang, M., Guo, W. W., Huang, Q., Zhang, L. Z., & Jiang, G. (2017). Nano-based delivery of RNAi in cancer therapy. *Molecular Cancer, 16*(1), 134. https://doi.org/10.1186/s12943-017-0683-y

Yan, Y., Zhang, J., Ren, L., & Tang, C. (2016). Metal-containing and related polymers for biomedical applications. *Chemical Society Reviews, 45*(19), 5232–5263. https://doi.org/10.1039/c6cs00026f

Yang, Y., Wang, L., Wan, B., Gu, Y., & Li, X. (2019). Optically active nanomaterials for bioimaging and targeted therapy. *Frontiers in Bioengineering and Biotechnology, 7*, 320. https://doi.org/10.3389/fbioe.2019.00320

Yaqoob, A. A., Ahmad, H., Parveen, T., Ahmad, A., Oves, M., Ismail, I., Qari, H. A., Umar, K., & Mohamad Ibrahim, M. N. (2020). Recent advances in metal decorated nanomaterials and their various biological applications: A review. *Frontiers in Chemistry, 8*, 341. https://doi.org/10.3389/fchem.2020.00341

Zhang, F., Li, M., Su, Y., Zhou, J., & Wang, W. (2016). A dual-targeting drug co-delivery system for tumor chemo- and gene combined therapy. *Materials Science & Engineering C, Materials for Biological Applications, 64*, 208–218. https://doi.org/10.1016/j.msec.2016.03.083

Zhang, K., Yang, K., Ai, S., & Xu, J. (2017). Synthesis of novel cross-linked s-triazine-containing poly(aryl ether)s nanoparticles for biological fluorescent labeling. *Designed Monomers and Polymers, 20*(1), 389–396. https://doi.org/10.1080/15685551.2017.1281786

Zhou, W., Gao, X., Liu, D., & Chen, X. (2015). Gold nanoparticles for in vitro diagnostics. *Chemical Reviews, 115*(19), 10575–10636. https://doi.org/10.1021/acs.chemrev.5b00100

Part II
Design and Synthesis of Nanomaterials

Molecular Design, Synthesis, and Properties of Surface-Active Comb-Like PEG-Containing Polymers and Derived Supramolecular Structures for Drug Delivery

Nataliya Mitina, Anna Riabtseva, Olena Paiuk, Nataliya Finiuk, Miroslav Slouf, Ewa Pavlova, Lesya Kobylinska, Roman Lesyk, Orest Hevus, Vasyl Garamus, Rostyslav S. Stoika, and Alexander Zaichenko

Abbreviations

A_∞	Adsorption at water/air interface
AA	Acrylic acid
BA	Butyl acrylate
CGE	Cumene glycidyl ether, 2-{[(4-isopropyl benzyl)oxi]methyl}oxirane
CMC	Critical micelle concentration
DLS	Dynamic light scattering
DMAEMA	Dimethylaminoethyl methacrylate
DMM	Dimethyl maleate

N. Mitina · A. Riabtseva · O. Paiuk · O. Hevus · A. Zaichenko (✉)
Lviv Polytechnic National University, Lviv, Ukraine
e-mail: Oleksandr.S.Zaichenko@lpnu.ua

N. Finiuk
Institute of Cell Biology of National Academy of Sciences of Ukraine, Lviv, Ukraine

M. Slouf · E. Pavlova
Institute of Macromolecular Chemistry, Czech Academy of Sciences, Prague, Czech Republic

L. Kobylinska · R. Lesyk
Danylo Halytsky Lviv National Medical University, Lviv, Ukraine

V. Garamus
Helmholtz-Zentrum Geesthacht (HZG): Centre for Materials and Coastal Research, Geesthacht, Germany

R. S. Stoika
Institute of Cell Biology of National Academy of Sciences of Ukraine, Lviv, Ukraine

Danylo Halytsky Lviv National Medical University, Lviv, Ukraine

FCTA	Functional chain transfer agents
FT-IR	Fourier-transform infrared spectroscopy
GMA	Glycidyl methacrylate
GPC	Gel permeation chromatography
MP	Monoperoxine, 1-isopropyl-3(4)-[1-(tert-butyl peroxy)-1-methyle-thyl] benzene
mPEG	Poly(ethylene glycol) monomethyl ether
MWD	Molecular weight distribution
NMR	Nuclear magnetic resonance
NVP	N-vinylpyrrolidone
PEG	Polyethylene glycol
PEGMA	Polyethylene glycol methacrylate
PNC	Polymeric nanoscale carriers
RAMAN	Raman spectroscopy
S_0	Limiting area occupied by surfactant molecule
SAXS	Small-angle X-ray scattering
SEC	Size-exclusion chromatography
SEM	Scanning electron microscope
TEM	Transmission electron microscopy
VEP	5-(*tert*-butylperoxy)-5-methylhex-1-en-3-yne

1 Introduction

The problem of overcoming or decreasing the negative side effects of toxic anticancer drugs and expansion of their therapeutic application is of high importance (Chamundeeswari et al., 2019; ud Din et al., 2017). One of the most efficient ways to solve that problem is using multifunctional drug carriers capable of binding and delivering highly toxic drug directly to the target organ (Navya et al., 2019). The nanoscale supramolecular structures, micelles, vesicles, intermolecular complexes, and nanoparticles, with size in the 1–100 nm range, were suggested as promising carriers for drug delivery and overcoming biological barriers in the organism (Blanco et al., 2015; Patra et al., 2018). The waterborne drug delivery systems based on nanostructured polymeric and polymer/inorganic carriers were synthesized for water-insoluble substances. They were shown to prolong the circulation time of drugs in the organism, decrease their general toxicity, and improve the biocompatibility. Moreover, the availability of functional groups in the carrier structure provides a possibility of attachment of specific vectors, such as antibodies or lectins for recognizing the pathological cells and for addressed delivery of the drug to the target tissue or organ (Torchilin, 2010). The main characteristics of the polymer-based drug delivery systems are prolonged circulation in the blood, ability to accumulate

at the sites of the pathological processes, and an efficient drug transfer into the cells and/or their organelles. These systems must be stable without changing their colloidal-chemical properties, and, at the same time, they must possess an ability to be removed from the organism after a definite time (Lombardo et al., 2019; ud Din et al., 2017).

The functional polymeric surfactants are the most promising carriers for drug binding and delivery. They are designed and synthesized taking into consideration their biocompatibility, binding affinity, and controlled delivery. Some PEG-containing polymers of various architecture and functionality were successfully tested as waterborne systems of the carriers for delivery of anticancer drugs, for example, Doxil, which is a PEG-modified liposome (Lombardo et al., 2019; Patra et al., 2018; Suk et al., 2016). The enhanced ability of cell engulfment and high efficiency of the doxorubicin complexes with PEG-containing polymeric dendrimer, comparing the action of free Dox, was demonstrated (Zhu et al., 2010).

There is a large assortment of water-soluble surface-active polymers of block and branched structure. Star-like and dendritic polymers (Dong et al., 2014; Ren et al., 2016) that combine the hydrophilic and hydrophobic links and chains in their molecules (Cabral et al., 2011; Simone et al., 2008) were developed and studied as promising vehicles for the addressed delivery of drugs and nucleic acids. Three approaches were used for the synthesis of the comb-like and branched polymeric surfactants: (1) "grafting to" using covalent binding of the telechelic -OH, -NH$_2$, and other polymers, including mono-substituted polyethylene glycols and biopolymers, via their reactions with side anhydride, isocyanate, epoxide groups of the backbone (Tsarevsky et al., 2007; Tsuji et al., 2019); (2) polymerization and copolymerization of functional macromers, including PEG-containing ones (Najafi et al., 2013; Neugebauer et al., 2003); (3) "grafting from" via polymerization initiated by side peroxide-, azo-, hydroxyl-containing groups of the multisite macroinitiator backbone (Hu et al., 2006; Meng et al., 2009). The controlled biocompatibility, prolonged circulation in blood, ability to form stable water systems for targeted drug delivery, and overcoming protecting barriers in the organism are necessary requirements for the polymeric carriers of drugs and nucleic acids. Among them, PEG-containing polymers are considered to be the most promising macromolecules for controlled delivery and release of the drug due to the ability of PEG to interact with cell membranes and to protect drugs from the immune attack of the organism.

The first and second of the above-noted approaches of synthesis are of special importance at the creation of prospective comb-like polymeric drug carriers containing side PEG chains. The "grafting to" technique is one of the most efficient methods for the synthesis of the comb-like polymeric surfactants (Balci et al., 2010) due to the possibility of strict control of both the fine structure of the backbone that contains the reactive side fragments, and the structures and lengths of the grafted functional chains (Balci et al., 2010). However, the attachment of side polymeric chains via reactions with the active sites of the backbone is restricted due to the so-called "neighbor effect" and other steric hindrances specific to the macromolecules

(Zhang & Mischnick, 2017). The synthesis of the comb-like PEGylated copolymers via the reactions of mono-substituted PEGs with the maleic anhydride groups (Hou & Kuo, 2001) of the copolymer backbone is limited by the impossibility to attach more than 50% of the PEG chains per molecule, and also due to easy hydrolysis of anhydride groups, as well as insufficient durability of ester bonds formed as a result of esterification (Rzayev, 2011).

Earlier, we developed and described the comb-like polymeric surfactants combining the side peroxide groups and PEG-containing branches attached to the backbone via a controlled reaction of the mono-substituted mPEG with side epoxide groups of the backbone (Riabtseva et al., 2012, 2016). These copolymers contain a purposeful amount and disposition of the PEG branches and possess the durability toward the hydrolysis in the acidic and alkaline media. The polymerization and copolymerization of the PEG-containing macromers are also of great interest for the controlled synthesis of the comb-like polymeric surface-active carriers (Paiuk et al., 2018). The main disadvantages of this method are the limited assortment of the PEG-containing macromers and a complicated adjustment of the fine structure of the backbone due to the influence of the polymeric nature of the macromers on their reactivity and the peculiarities of chain propagation and termination.

A tailored synthesis of comb-like and branched surface-active polymers containing side polyethylene glycol or polyelectrolyte chains and the hydrophobic backbone consists of a complex approach combining radical and nonradical reactions and subsequent polymer analogous transformations, as shown in the scheme (Fig. 1). From this scheme, it is evident that at the first stage, the copolymer backbone containing side peroxide and epoxide groups was synthesized via radical copolymerization of the unsaturated peroxide monomer 5-(*tert*-butylperoxy)-5-methylhex-1-en-3-yne(VEP), glycidyl methacrylate (GMA), and other functional monomers.

The results of the kinetic study and molecular weight characteristics of copolymers showed that the copolymerization of VEP-containing monomer systems is in accordance with the known regularities of low-inhibition polymerization (Zaichenko et al., 1998). The resulting copolymers, combining two reactive sites, were used as the precursors for the molecular assemblage of the branched molecules via the addition reactions of side epoxide groups and/or radical polymerization initiated by side peroxide groups.

Another approach to the synthesis of comb-like surface-active polymers and copolymers containing side PEG chains of various lengths was developed via the polymerization of the PEG-methacrylate-based macromers in the presence of functional chain transfer agents offering the ability to control the backbone chain length and molecular weight distribution, as shown in the scheme (Fig. 2). Moreover, the terminal reactive fragments of functional chain transfer agents are included into the macromolecule structure.
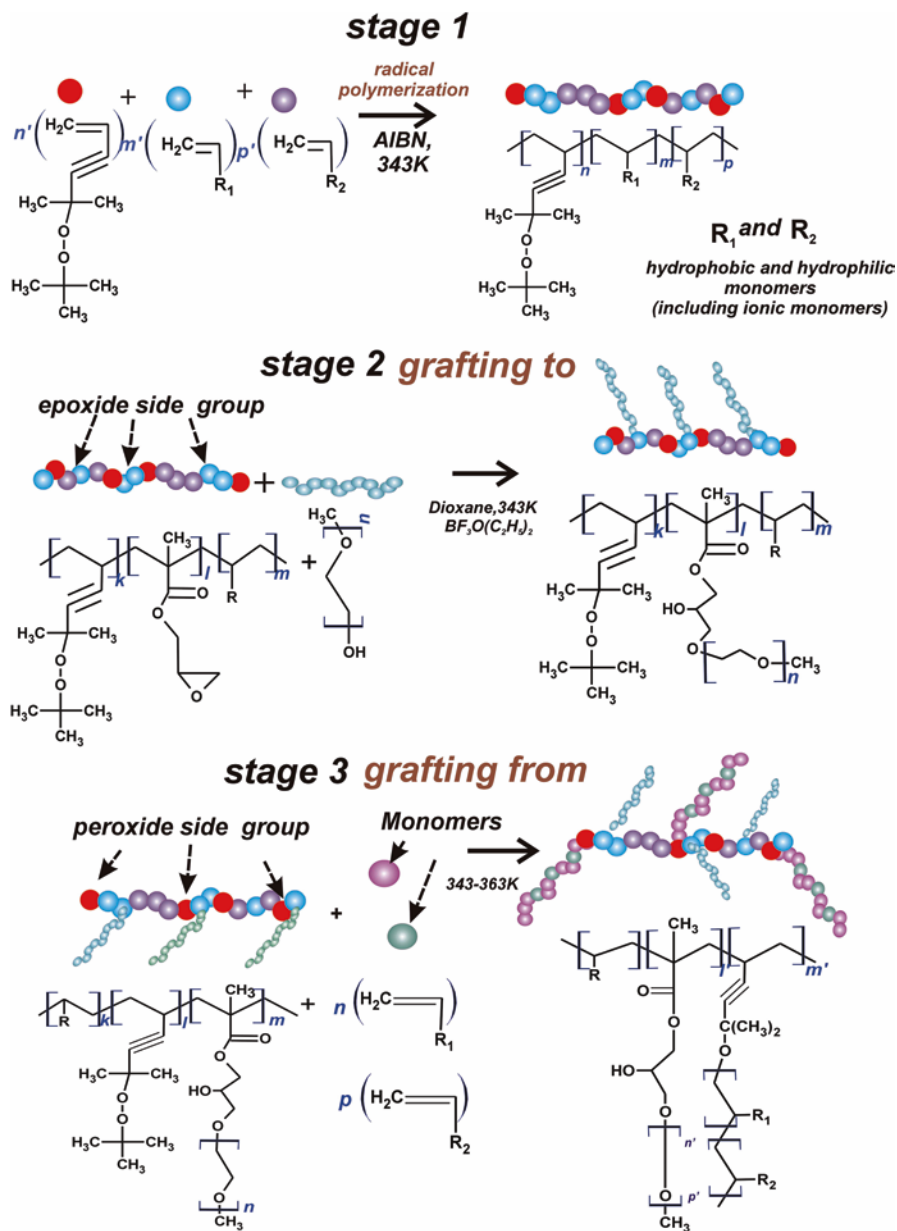
Fig. 1 Scheme of the molecular assembling of the comb-like and branched surface-active polymers
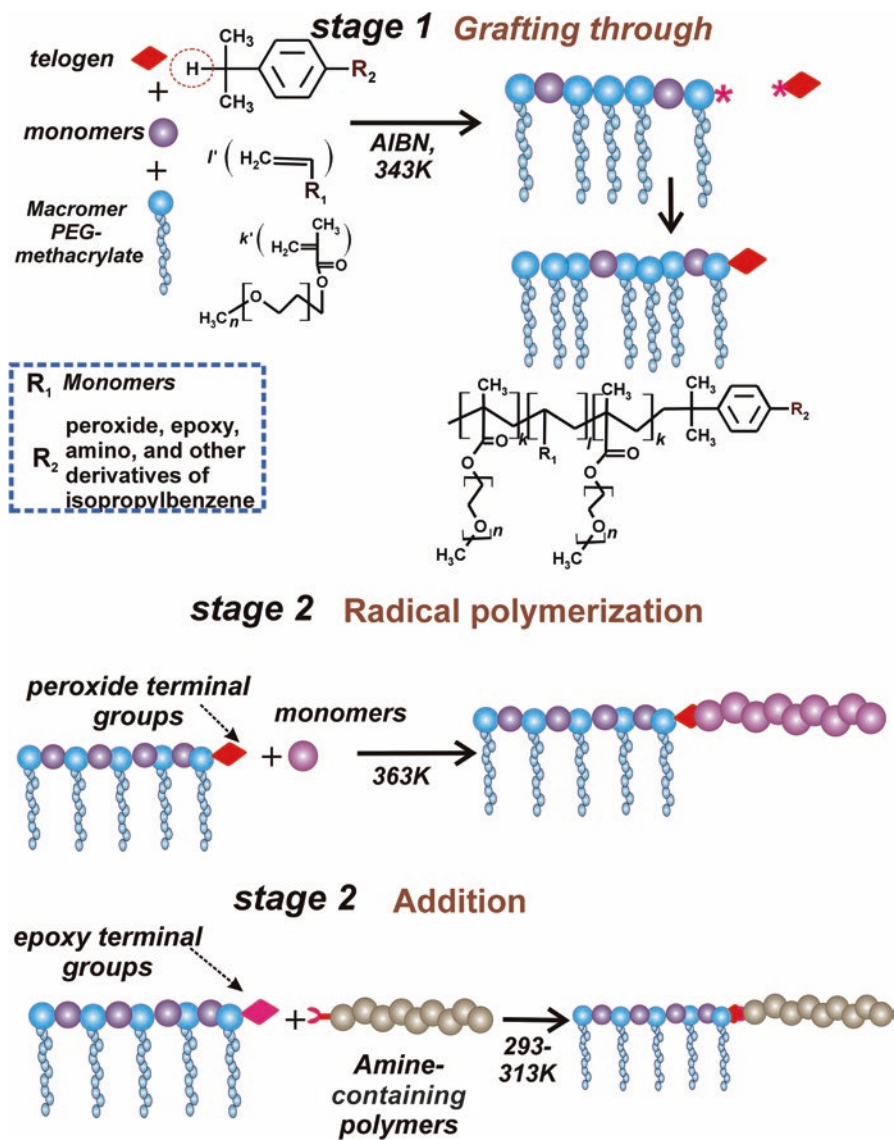
Fig. 2 Scheme of synthesis of the PEG-containing comb-like poly-amphiphiles

2 Synthesis, Structural, and Colloidal-Chemical Characteristics of Surface-Active Polymers with Side PEG and Polyelectrolyte Chains

Water-soluble comb-like copolymers with a desired content and length of side mPEG chains were synthesized via reaction of side epoxide groups of the polymer backbone with the monosubstituted polyethylene glycols, as shown in the scheme (Fig. 1).

The results of the kinetic study (Fig. 3) of interaction of epoxide containing GMA links with mPEG showed that the rate of the reaction and the maximal conversion degree of epoxide groups depended predominantly on mPEG concentration in the system. However, at the definite molar ratio of the reacting epoxide groups and mPEG, the rate of the reaction and content of the attached mPEG branches achieve maximally possible values and do not depend on mPEG concentration (Fig. 3b). The presence of two sections on the kinetic curves (Fig. 3a) might be explained by fast reaction with the accessible epoxide groups of the backbone at the first stage and visible deceleration of the reaction at the second stage. That happens due to a decrease in the amount of the accessible epoxide-containing GMA links, as well as a "neighbor effect" caused by the earlier attached PEG chains.

An increase in the length of the mPEG chain leads to a decrease in the epoxide group conversion (Fig. 4) due to a decrease in concentration of the mPEG in the reaction zone and an increase in the influence of the "neighbor effect" of attached side PEG chains.

A comparison of the molecular weight distribution of PEG-containing comb-like copolymers and initial epoxide-containing backbone copolymers demonstrates (Fig. 5) a visible narrowing of the molecular weight distribution (MWD) of the resulting copolymers. This is caused by the purification and washing out of the initial linear polymer that did not interact with the mPEG and did not form water-soluble comb-like PEGylated copolymers.
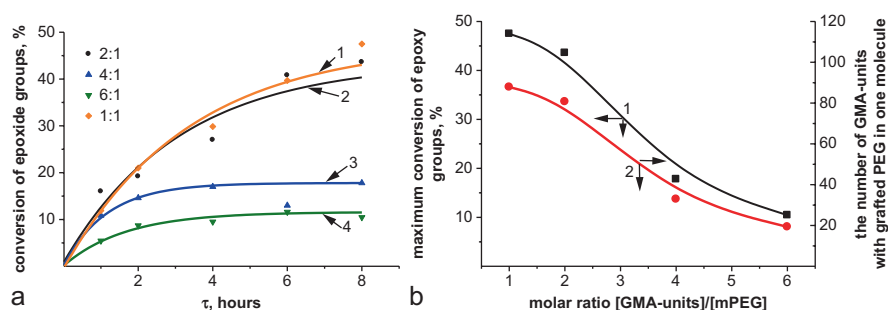

Fig. 3 Kinetic curves of the reaction of mPEG with side epoxide groups of the backbone at a mol ratio GMA-links: mPEG: *1* – 1:1, *2* – 2:1, *3* – 4:1, *4* – 6:1 (**a**) and dependences of maximal conversion of the epoxide groups (1) and the amount of attached PEG chains per comb-like copolymer (2) on a molar ratio GMA-links: mPEG
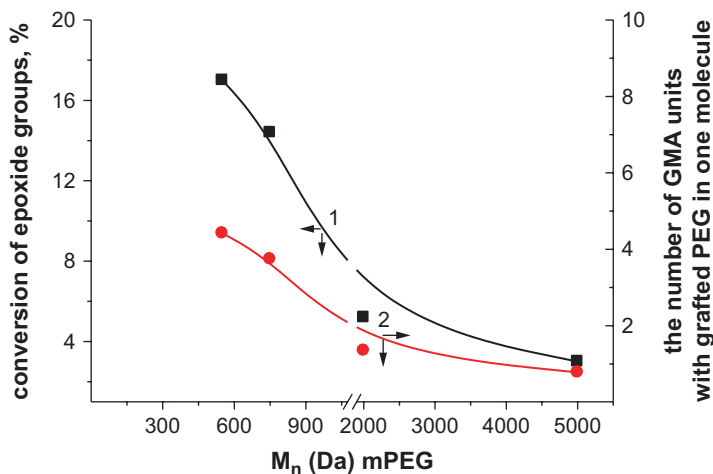
Fig. 4 The dependences of epoxide group conversion (%) (1) and the amount of attached PEG chains per molecule of poly(VEP-co-GMA) (25:75% moles) (2) on the molecular weight of PEG
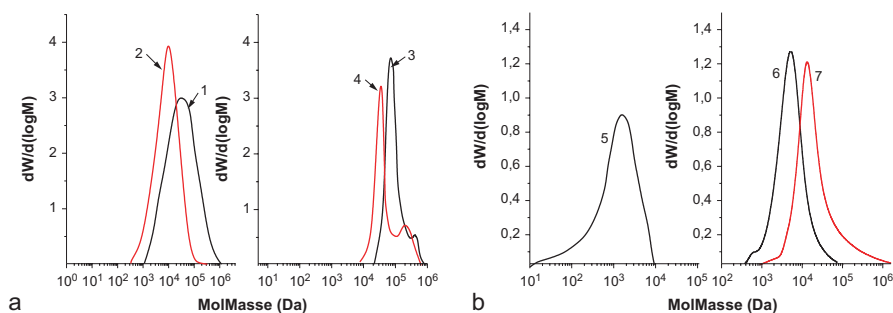
Fig. 5 Molecular weight distribution of poly(VEP-co-GMA): 2.0:98.0% mol (1) and 21:79% mol (2) and poly(NVP-co-VEP-co-GMA) 80:10:10% mol (5) and derived PEG-containing copolymers (3, 4 and 6, 7), mPEG molecular weight = 750 (4, 3, 6) and 900 (7)

The functional composition and structure of the poly(VEP-co-GMA) and derived comb-like poly(VEP-co-GMA)-graft-PEG were determined using elemental and functional analyses techniques, as well as by the NMR and IR-spectroscopy methods (Fig. 6).

The availability of the ditertiary peroxide side groups in the molecules of PEG-containing comb-like copolymers suggests their use as the multisite macroinitiators for the initiation of grafting various functional polymeric chains, including the polyelectrolytes, as shown in the scheme (Fig. 1).

The kinetic study revealed that the kinetic parameters of elementary stages of polymerization initiated by macroinitiator differ significantly from the kinetics of
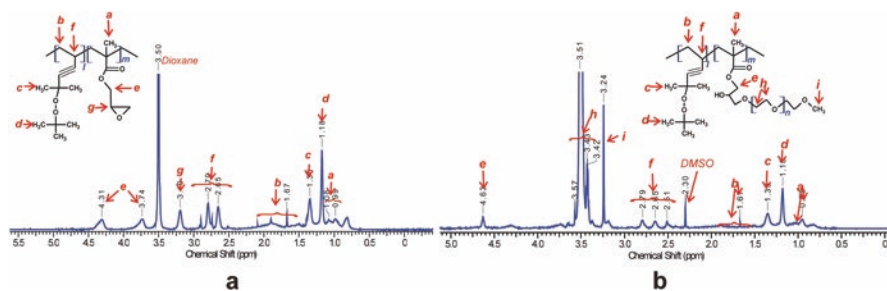
Fig. 6 ¹H NMR spectra of poly(VEP-co-GMA) (**a**) and poly(VEP-co-GMA)-graft- PEG (**b**)
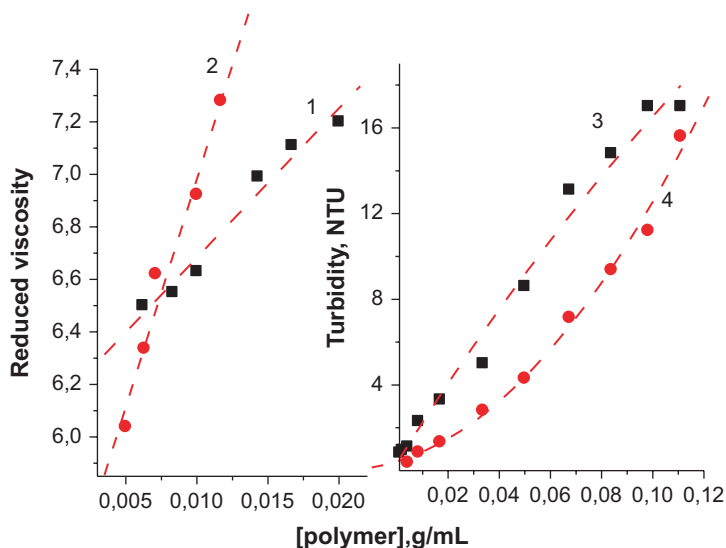
Fig. 7 The dependences of the reduced viscosity (1,2) and turbidity (3,4) of the solutions of poly(VEP-co-GMA) (1,3) and poly(VEP-co-GMA)-*graft*-PEG (2,4) on their concentration

polymerization initiated by the initial linear poly(VEP-co-GMA). That, as well as the dependences of reduced viscosity and turbidity of the solutions of PEG-containing peroxide macroinitiator on the concentration (Fig. 7a, b), can be explained by localization of elementary stages of polymerization initiated by macroinitiator in spatially restricted colloidal zones. Moreover, the change in the viscosity of the solution of the comb-like copolymer with an increase of its concentration is greater than the observed for the linear polyperoxide. The deviation from the linearity on the curve of the dependence of turbidity of comb-like copolymer solution on the concentration confirms an assumption of the existence of the microcolloidal zones in the solution.
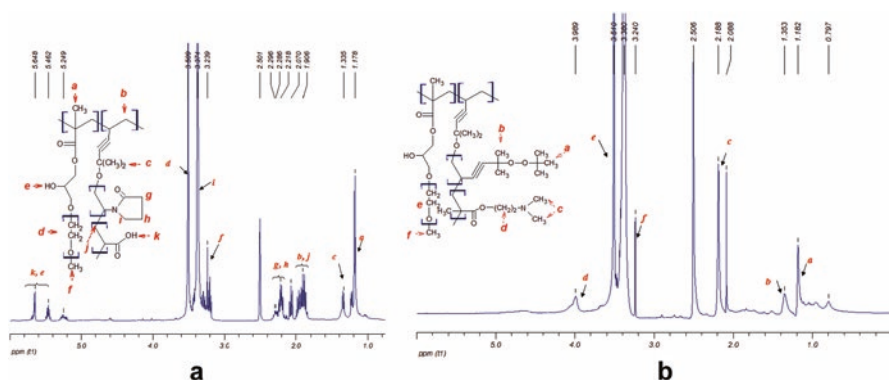
Fig. 8 ¹H NMR spectra of poly(VEP-co-GMA)-graft-PEG-graft-poly(NVP-co-AA) (**a**) and poly(VEP-co-GMA)-graft-PEG-graft-poly(DMAEMA) (**b**)

Table 1 Characteristics of PEG-containing comb-like copolymers

Composition, %						
Backbone composition, %		Grafted polymer chain				
VEP (*l*)	GMA(*m*)	mPEG(*n*) (M$_n$ 750 Da)	NVP	AA	DMAEMA	Molar weight, kDa
1.4	69.1	29.5	–	–	–	120.0
0.6	26.9	11.5	–	–	61.0	185.0
0.3	15.9	6.8	66.2	10.8	–	205.0

The functional composition of the resulting copolymers was determined by means of the NMR and IR-spectroscopy methods (Fig. 8), as well as by the elemental and functional analyses.

The characteristics of the branched polymers combining nonionic PEG and polyelectrolyte side chains synthesized via graft-polymerization of the acrylic acid (AA) and N-vinyl pyrrolidone (N-VP) initiated by side peroxide groups of VEP links are presented in the Table 1.

After the attachment of side PEG chains, a comb-like copolymer poly(VEP-co-GMA)-graft-PEG becomes water soluble. A combination of the hydrophobic backbone and hydrophilic side PEG chains in the molecules of the comb-like copolymers provides their surface activity and micelle forming ability (Fig. 9).

The isotherms of surface tension of comb-like polymers with side chains of different nature (Fig. 9) demonstrate the differences in their surface activities and sizes of the micelles formed by surfactants of different nature depending on the pH value. One can see (Fig. 9) that the surface activity of the nonionic PEG-containing comb-like copolymer does not depend on the pH value. In contrast, the surface activity of the branched copolymer combining PEG and anionic poly(NVP-co-AA) side chains
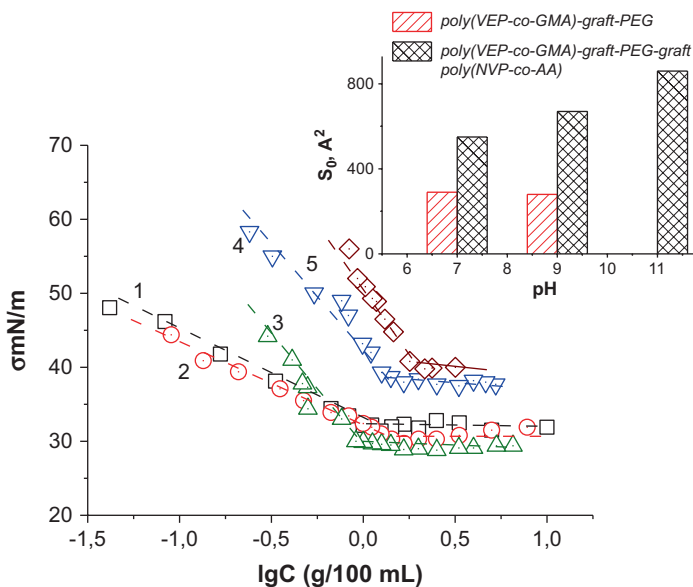
Fig. 9 Isotherms of surface tension of the solutions of 1,2 – poly(VEP-co-GMA)-graft-PEG(750); 3,4 – poly(VEP-co-GMA)-graft-PEG(750)-graft-poly(NVP-co-AA); pH = 7 (1,3); pH = 9 (2,4) (insertion: square areas per polymer micelles at the phase water-air boundary). (Reproduced with permission (Riabtseva et al., 2016))

Table 2 The characteristics of the micelles formed by the comb-like and branched polymers

Copolymer	DLS measured an average hydrodynamic diameter, nm	TEM measured diameter, nm	SEM measured diameter, nm	ξ-potential, mV
Poly(VEP-co-GMA)-graft-PEG(750)	59.0 ± 25.0	39.0 ± 6.5	35.0 ± 15.2	−0.25
Poly(VEP-co-GMA)-graft-PEG(750)-graft-poly(NVP-co-AA)	340.0 ± 35.0	300.0 ± 55.0	350.0 ± 105.0	−0.60

depends significantly on the pH value of the water solution. An increase in the pH value causes an enhancement of their solubility and unfolding carboxyl-containing side chains, resulting in a decrease in surface activity, compared to the initial PEG-containing surfactant. An increase in the micelle size and number of molecules per surface area for the branched copolymer at the phase boundary with an increase in the pH value of the solution confirms the suggested explanation (Fig. 9).

The size and charge of the micelles formed by the branched copolymer containing side PEG and poly(NVP-co-AA) chains are visibly larger than those for the initial PEG-containing comb-like copolymer (Table 2, Figs. 10 and 11). This
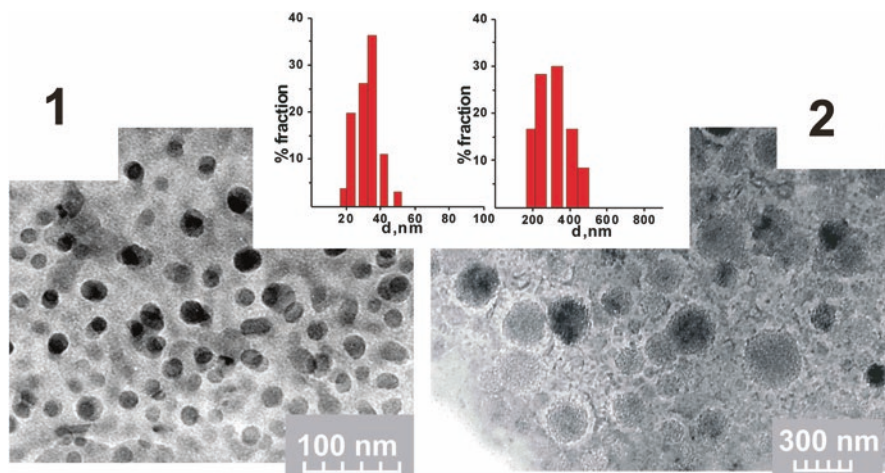
Fig. 10 TEM micrographs of the micelles formed by the poly(VEP-co-GMA)-*graft*-PEG(750) (1) and poly(VEP-co-GMA)-*graft*-PEG(750)-*graft*-poly(NVP-co-AA) (2), water solution, pH = 7 (×30,000). (Insets are bar graphs of the particle size distribution) (*Samples prepared by the method of spraying tested water solution (0.1%) on commercial C-coated Cu grid, by means of the ultrasonic dispersant*)
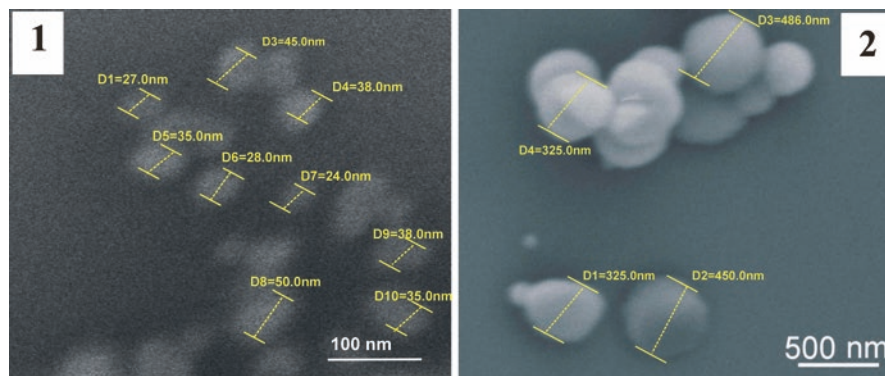
Fig. 11 SEM micrographs of the micelles formed by poly(VEP-co-GMA)-*graft*-PEG(750) (1) and poly(VEP-co-GMA)-*graft*-PEG(750)-*graft*-poly(NVP-co-AA) (2), water solution, pH = 7. *(Samples were prepared* via *known technique (*Reimer, 1998*) and covered with Gold).* (Reproduced with permission (Riabtseva et al., 2016))

suggests the existence of different mechanisms of micelle formation and the differences in their morphology.

The micelles formed by the copolymers containing side PEG and polyelectrolyte chains are larger than the micelles formed by the initial PEG-containing comb-like copolymer. It is evident (Fig. 12, Table 3) that branched copolymers combining side PEG and polyelectrolyte chains form predominantly monodisperse micelles, compared to the comb-like PEG-containing copolymer.
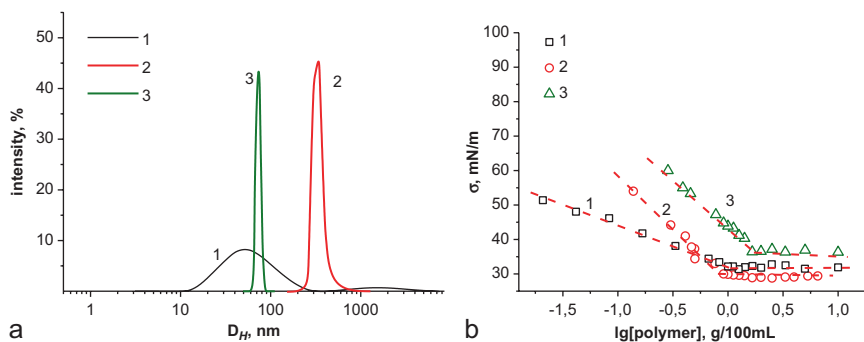
Fig. 12 The hydrodynamic diameters of the micelles (**a**) and isotherms of surface tension (**b**) of poly*(VEP-co-GMA)-graft-PEG(750)* (1.2:50.2:48.6% mol) (1) and derived poly(VEP-co-GMA)-graft-PEG)-graft-poly(NVP-co-AA) (2), poly(VEP-co-GMA)-graft-PEG)-graft-poly(DMAEMA) (3) (H$_2$O, pH 7)

Table 3 Comparative characteristics of the micelles formed by the comb-like surface-active copolymers

Copolymer	M$_n$, kDa	Average hydrodynamic diameter (nm)	ξ-potential (mV)	A$_\infty$x10^6, mol/m^{2a}	S$_0$^{a} Å^2
Poly*(VEP-co-GMA)-graft-PEG(750)*	120	59.0 ± 25.0	−0.25	0.56	292
Poly(VEP-co-GMA)-graft-PEG)-graft-poly(NVP-co-AA)	200	340.0 ± 35.0	−0.60	0.30	550
Poly(VEP-co-GMA)-*graft*-PEG)-*graft*-poly(DMAEMA)	185	90.0 ± 15.0	+4,5	0,45	370

[a]*Calculated from the isotherms of surface tension (water-air boundary)*

The functional micelles formed by the PEG-containing comb-like copolymer and derived branched copolymers combining side PEG and polyelectrolyte chains are promising nano- and microscale containers for the transportation of bioactive substances, as well as the nanoreactors for template synthesis of the polymer/inorganic nanoparticles.

3 Synthesis, Structural, and Colloidal-Chemical Characteristics of Surface-Active Comb-like Polymers Based on PEG-Methacrylates

The comb-like polymers based on the polyethylene glycol methacrylate macromers (PEGMA) are of both fundamental and applied interests due to the simplicity of synthesis of the polyamphiphiles with a controlled lengths of the backbone and side chains, and tunable structural and colloidal-chemical characteristics.
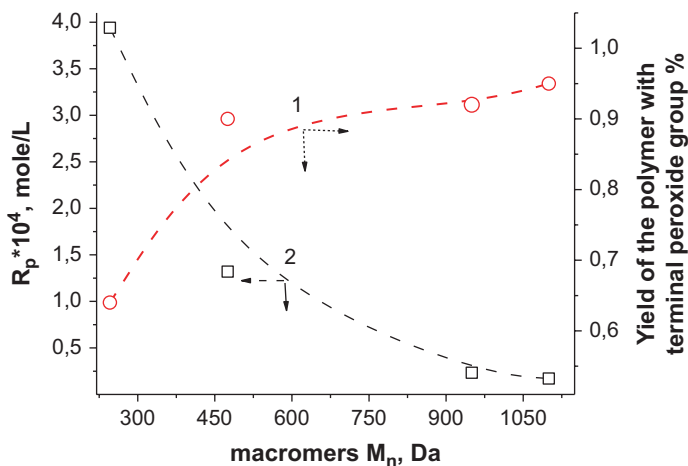
Fig. 13 The dependences of the rate of PEGMA polymerization (**a**) and content of terminal MP fragments per telechelic polymers (**b**) on the macromer PEG length

The polymerization of such macromers in the presence of functional chain transfer agents (FCTA) was studied in our lab for the first time.

It is evident (Fig. 13) that an increase in the PEG length of the macromer molecule causes an increase in the molecular weight of the polymer. At the same time, the diffusion control of the reactions in the colloidal zones formed by the macromer molecules does not restrict a diffusion of a low-molecular-weight chain transfer agent and the termination of growing radicals with the FCTA that results in higher values of an average terminal functionality (Fig. 13).

The dependences of the kinetic parameters of PEGMA polymerization, molecular weight, and structural characteristics of the resulting polymers on the nature and content of functional chain transfer agents (FCTA) (1-isopropyl-3(4)-[1-(tert-butyl peroxy)-1-methylethyl] benzene (MP) and 2-{[(4-isopropyl benzyl)oxi]methyl} oxirane (cumene glycidyl ether, CGE)) in the reaction system demonstrate that the polymerization obeys the laws of low-inhibition polymerization characterized by a decrease in the polymerization rate and molecular weight of the polymers. However, the oligomer nature of the macromers and formation of the spatially limited colloidal zones in the solution causes significant influence on kinetic parameters of the elementary stages of generation and termination of growing radicals. An increase in length of the side PEG chains in the macromer molecules leads to an enhancement of chain transfer constant to the FCTA. If kt (L/(mol·s) is equal 16.0 for PEGMA246, the values of the constants are 39.5 for PEGMA475 and 63.0 for PEGMA1100. This provides the availability of functional terminal group of chain transfer agent in almost every molecules of poly(PEGMA1100) and at the same time leads to formation of the telechelic polymers of a larger molecular weight. The copolymerization of the PEGMA with other functional hydrophobic and hydrophilic

Table 4 Characteristics of PEGMA475 (M_1) and DMM (M_2) copolymerization

Monomer system				
M_1	M_2	$r_{1(PEGMA475)}$	$r_{2(DMM)}$	$r_1 \cdot r_2$
PEGMA475	BA	1.94	0.17	0.33
	DMM	2.20	0.04	0.088
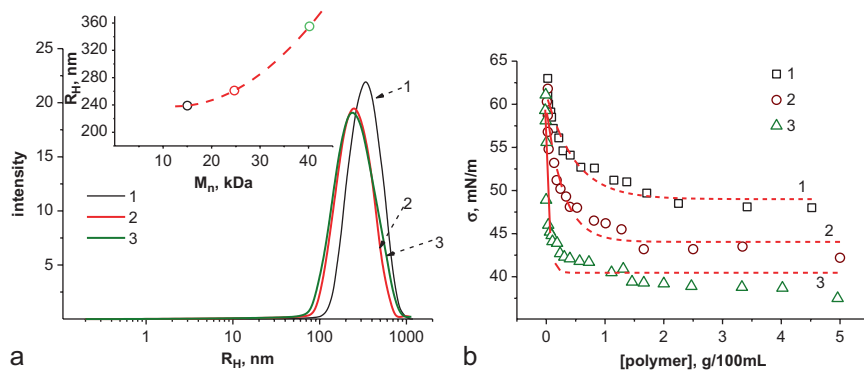
Fig. 14 The dependences of the hydrodynamic radii of the micelles (**a**) and isotherms of surface tension of polymer water solutions (**b**) on the molecular weight of poly(PEGMA)-MP backbone ($M_n \sim 40$ kDa (1), 24.7 kDa (2), 15 kDa (3))

monomers provides controlling the functionality, fine chain structure, molecular-weight, and colloidal-chemical characteristics of comb-like PEG containing surface-active copolymers.

In a result of a higher activity of the PEGMA as comonomer at the copolymerization with traditional low molecular weight monomers the resulting copolymers are enriched with the PEGMA links. The copolymer of PEGMA and dimethyl maleate (DMM) is characterized by an alternate disposition of the links along the backbone chain (Table 4).

The structure and functionality of the comb-like PEG-containing polymers synthesized via polymerization and copolymerization of PEGMA in the presence of FCTA were studied using functional and elemental analyses, as well as by means of the IR- and NMR spectroscopy methods. They confirmed the availability of side PEG chains and DMM links, as well as the terminal functional fragments of FCTA (MP or CGE).

The lengths of the backbone and side chains as well as the content of the hydrophobic terminal fragment in molecules of the poly(PEGMA)-MP surfactants are the main factors that define their surface activity (Fig. 14). It is obvious (Fig. 14) that the surface activity of the poly(PEGMA)-MP aqueous solutions and the amount of polymer molecules at the phase boundary increase with a decrease in the backbone
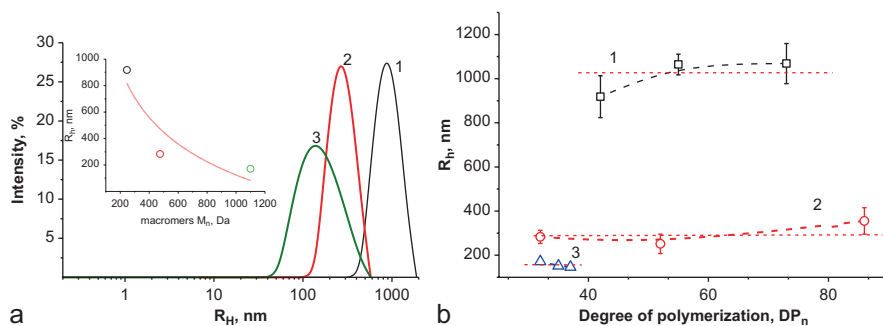
Fig. 15 Hydrodynamic radii of the micelles formed by the poly(PEGMA)-MP with different side PEG chains: 1a – poly(PEGMA246) (M_n = 10.5 kDa), 2a—poly(PEGMA475) (M_n = 15 kDa), 3a – poly(PEGMA1100) (M_n = 35.5 kDa) (a) and the dependence of sizes of micelles formed by the poly(PEGMA246) (1b), poly(PEGMA475) (2b), poly(PEGMA1100) (3b) – on the length of the backbone chain ([polymer] = 10 mg/mL, water, 298K)
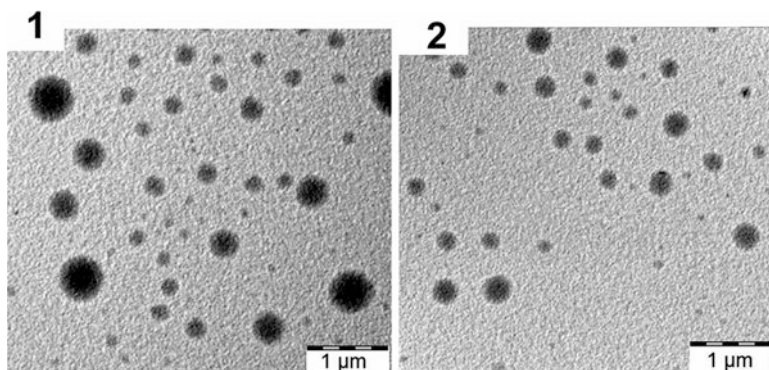
Fig. 16 TEM micrographs of the micelles formed by the poly(PEGMA)-MP: 1 poly(PEGMA475) (M_n = 15 kDa), 2 – poly(PEGMA1100) (M_n = 35.5 kDa). (*Sample preparation: 2 μL 0.1% of the solution on the commercial C-coated Cu grid and fast drying after 2 min*)

chain length and increase in the relative content of the terminal hydrophobic MP fragment. However, the results of DLS measurements revealed that the sizes of the polymeric micelles in the solution depend on the polymer surface activity and the length of the side PEG chains (Fig. 14), which define an ability of the comb-like polymer molecules to form aggregates and the amount of the molecules in these aggregates.

One can see (Figs. 15 and 16) that the values of the hydrodynamic sizes of the micelles formed by poly(PEGMA) molecules are defined mainly by the length of the side PEG chains. A decrease in the sizes of the micelles in the solution with an increase in the length of side PEG chains is caused, evidently, by the lower surface activity of the macromolecules and steric hindrances empeding their aggregation. .
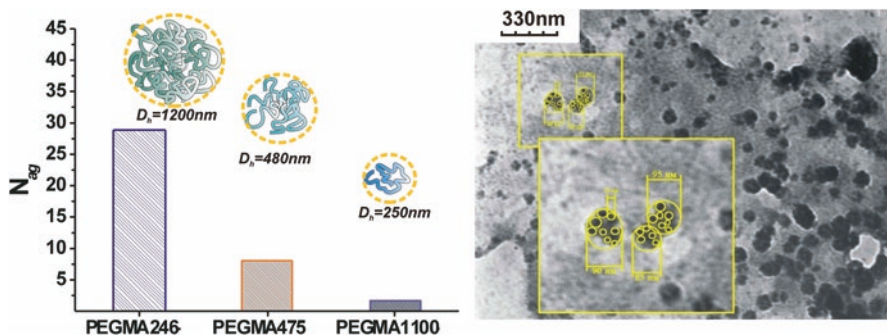
Fig. 17 The dependences of the aggregation numbers N_{ag} on the micelles formed by the poly(PEGMA)-MP in the solution on the length of PEG chains (left) and TEM micrographs of the aggregates of the poly(PEGMA475)-MP (M_n = 15 kDa) (*sample preparation: 2 μL 0.1% of the solution on commercial C-coated Cu grid and slow drying after 10 min*) (right)

The calculated amount of molecules in poly(PEGMA)-MP micelles formed in solutions (Fig. 17) confirms their different ability to form the aggregates. It is evident that such ability increases with a decrease in the side PEG length and increase in comb-like copolymer surface activity. The poly(PEGMA246)-MP forms micelles containing the largest amount of the molecules, and they are characterized by largest size of the aggregates, unlike the aggregation degree and size of the micelles formed by the poly(PEGMA1100) containing the longest side PEG chains. A decrease in the surface activity of the polymer in the studied range with an increase in both backbone and side PEG chains results in a decrease in the size of the aggregates formed in the solution due to their lower aggregation ability.

Moreover, the lengths of the backbone and PEG chains in molecules of comb-like polymeric surfactants define also their ability to form the micelle-like aggregates, aggregation number and packing density of the PEG chains in the micelles formed in the solutions. A disposition of PEG chains along the backbone depends on the method of synthesis of the comb-like PEG-containing copolymers, and it is an important factor causing the difference in their water solubility and colloidal-chemical characteristics. In spite of the large length of the hydrophobic backbone, the poly(VEP-co-GMA)-graft-PEG forms a highly transparent water solution after fast dissolution, while the poly(PEGMA)-MP dissolves in water for a long time and forms turbid solutions.

In our opinion, that is caused by the different disposition of side PEG chains and their different ability to form hydrogen bonds with water molecules. At the same time, due to high surface activity, the poly(VEP-co-GMA)-graft-PEG forms aggregates of a relatively large number of molecules. An alternate disposition of side PEG chains and DMM links along the backbone chain prevents the interaction of side PEG chains and promotes fast dissolution and formation of transparent water solution.
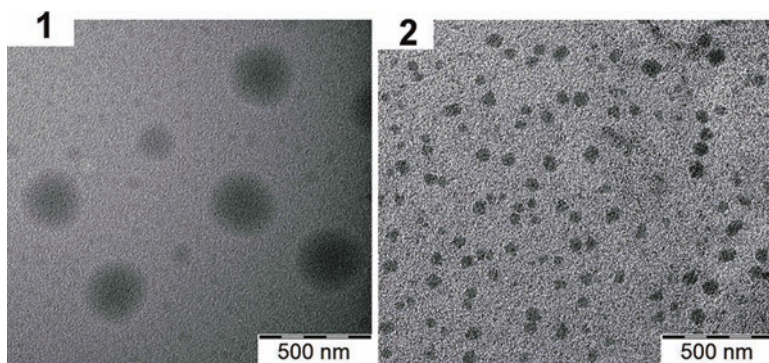
Fig. 18 TEM micrographs of the micelles formed by the poly(PEGMA)-MP (1) and poly(PEGMA-co-DMM)-MP (2) (10 mg/mL) (*sample preparation: 2 μL 0.1% of the solution on commercial C-coated Cu grid and fast drying after 2 min*)
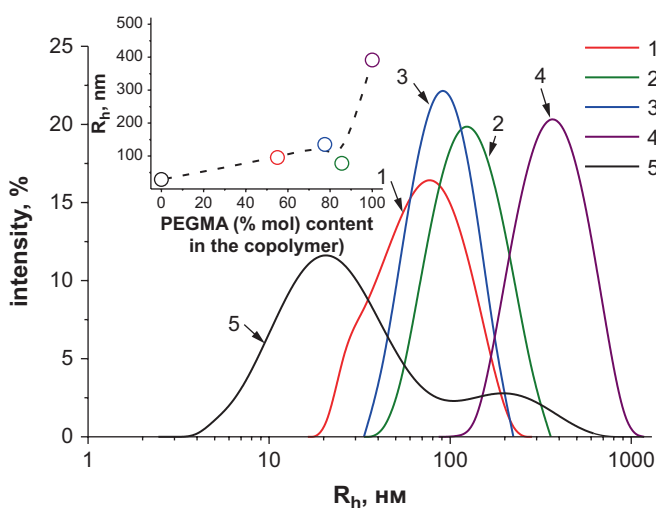
Fig. 19 The dependences of the hydrodynamic radii of the micelles formed by poly(PEGMA-co-DMM)-MP (1,2,3), poly(PEGMA)-MP (4), poly(VEP-co-GMA)-graft-PEG (5), [polymer] = 2.5 mg/mL (content of PEGMA475 links in the polymer −100% mol (4); 85.6% mol (1); 77.5% mol (2); 55.05% mol (3), 0% mol)

A significantly lower surface activity of the comb-like copolymer poly(PEGMA-co-DMM)-MP compared with the poly(PEGMA)-MP and poly(VEP-co-GMA)-graft-PEG causes a decrease in their ability to form aggregates and the aggregation number in the micelles. As a result, the poly(PEGMA-co-DMM)-MP molecules form aggregates of a smaller size and narrow size distribution (Fig. 18).

It is evident (Fig. 19) that the content, and thereby, the disposition of side PEG chains along the backbone of the comb-like copolymers, as well as the backbone nature and flexibility, define their ability to form aggregates, and affect their size and aggregation number.

The results of the SAXS study (Figs. 20 and 21) confirm the formation of orga-nized structures by molecules of the poly(PEGMA)-MP with the following values of fractal clusters: $\alpha_{(poly(PEGMA)-MP)}$ $1,06 - \alpha_{(poly(PEGMA-co-DMM)-MP)}$ $1,24$, respectively (Schmidt, 1995).
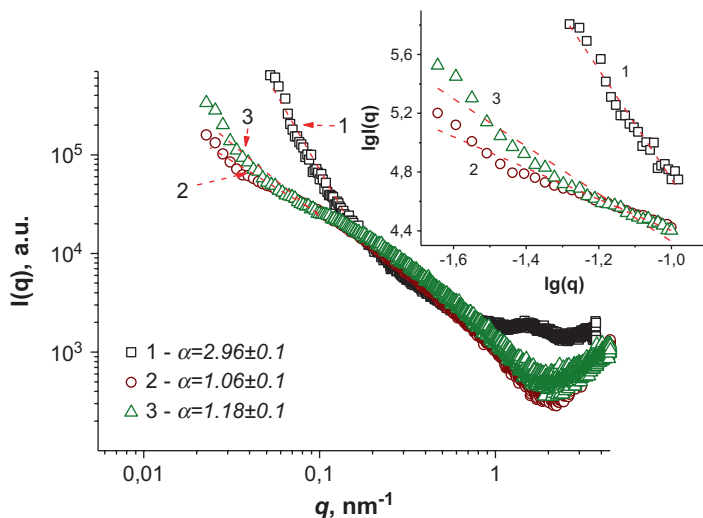
Fig. 20 SAXS diffractograms of the poly(VEP-co-GMA)-graft-PEG ($M_n \sim$ 90 kDa) (1), poly(PEGMA)-MP ($M_n \sim$ 15 kDa) (2) and poly(PEGMA-co-BA)-MP ($M_n \sim$ 16.5 kDa) (3) (poly-mer 0.01 g/mL) (The solid line is linear approximation in a respect of the scaling concept)
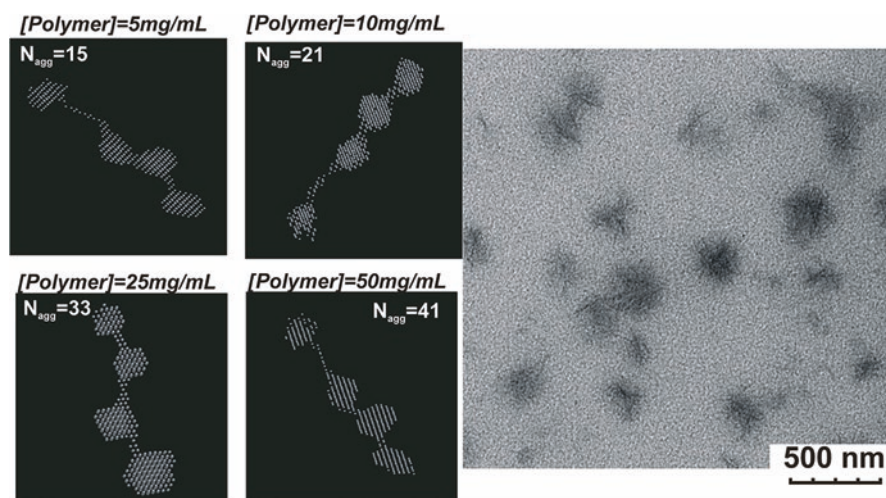
Fig. 21 3D models of the micelles formed by the poly(PEGMA475-co-BA)-MP at various con-centrations in water ([polymer] = 5 mg/mL (1); 10 mg/mL (2); 25 mg/mL (3) and 50 mg/mL (4)) (left); TEM micrographs of the micelles formed by the poly(PEGMA)-MP after slow drying on the grid (*sample preparation: 2 μL 0.1% of the solution on commercial C-coated Cu grid and slow drying after 10 min*) (right)

Table 5 SAXS parameters of the micelles formed by comb-like PEG containing polymers

Polymer	Polymer concentration in water mg/mL	Parameter α ($I(q) \sim q^{-\alpha}$)	$I(0)$	R_g^2 nm	N_{agg}[a]
Poly(PEGMA475)-MP ($M_n \sim 15$ kDa)	10	1.06 ± 0.1	0.0024	43.0 ± 0.7	36
	50	1.09 ± 0.1	0.0026	46.7 ± 0.8	42
Poly(PEGMA475-co-BA)-MP ($M_n \sim 16.5$ kDa)	5	1.12 ± 0.1	0.0026	37.5 ± 0.4	15
	10	1.18 ± 0.1	0.0026	38.5 ± 0.6	21
	25	1.24 ± 0.1	0.0027	39.8 ± 0.8	33
	50	1.27 ± 0.1	0.0030	46.5 ± 0.8	41
Poly(VEP-co-GMA)-graft-PEG750 ($M_n \sim 90$ kDa)	10	2.65 ± 0.1	0.0069	109.1 ± 0.7	26

[a]N_{agg} – aggregation number of macromolecules in the micelles

Table 6 Colloidal-chemical characteristics of poly(VEP-co-GMA)-graft-PEG475 and complex with Dox (pH = 7)

Polymer	CMC·10^4, mol/L	Σ_{CMC}, mN/m	$A_\infty \cdot 10^6$, mol/m^{2a}	S_0, Å^2
Poly(VEP-co-GMA)-graft-PEG750	1.42	32.0	0.56	292
Poly(VEP-co-GMA)-graft-PEG750 with Dox	0.69	28.2	0.66	260

[a]*Water-air boundary*

The models of the micelles formed by the comb-like copolymers containing side PEG chains have been created using the ATSAS 2.8.4(DAMMIN) computer program (Franke et al., 2017; Svergun, 1999) and presented by means of the RasMol 2.7.5 graphical program (Sayle & Milner-White, 1995) (Fig. 21a). Some of the calculated parameters of the micelles are summarized in Table 6. The interval of low scattering vectors is interpreted using power law $I(q) \sim q^{-\alpha}$ (Schmidt, 1995). Evidences of the existence of fractal structures in the micelles in submicron and nanoscale regions were also obtained using the TEM technique (Schmidt, 1991).

One can suggest from the characteristics of the diffractograms (Fig. 20, Table 5) that the micelle structures formed by poly(PEGMA475-co-BA)-MP and poly(PEGMA)-MP are close to the linear clusters with high packing density. An availability of the definite amount of PEGMA blocks in the poly(PEGMA475-co-BA)-MP promotes an interaction of side PEG chains and formation of clusters with enhanced density. However, this density is less than the packing density of the micelles formed by the poly(PEGMA)-MP with closely disposed PEG chains. The partition of the blocks from PEGMA links in poly(PEGMA475-co-BA)-MP decreases the density of packing in the micelles formed by the comb-like copolymer. At the same time, it is evident (Fig. 18) that an enhancement of the aggregation degree in micelles of the comb-like copolymers causes a formation of the thermodynamically favorable spherical aggregates.

The aggregates formed by macromolecules of the comb-like poly(VEP-co-GMA)-graft-PEG contain the side PEG chains distributed along backbone that

Fig. 22 Assumed morphology of the micelles formed by the comb-like copolymers with a different disposition of side PEG chains along the backbone
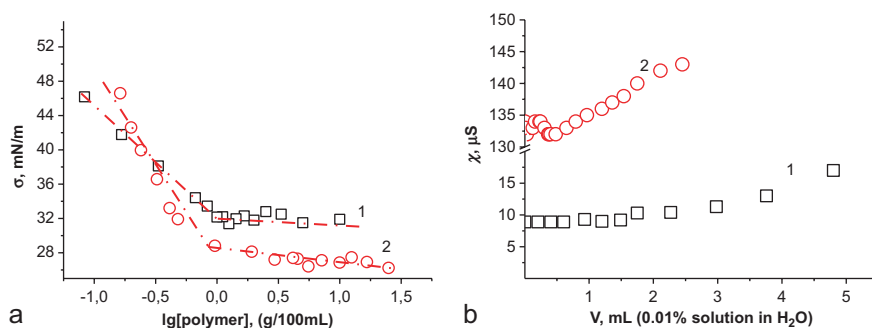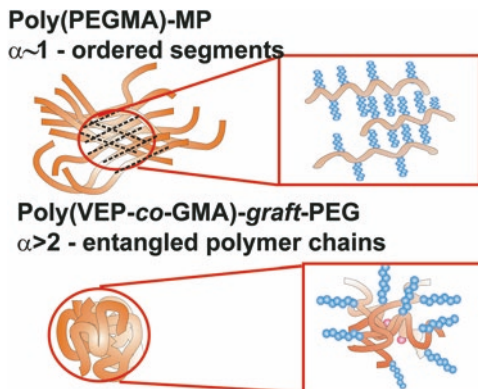
Fig. 23 Surface tension isotherms of water solutions of the poly(VEP-co-GMA)-graft-PEG750 (1) and complex of Dox with poly(VEP-co-GMA)-graft-PEG750 (2) (**a**) and the dependence of electroconductivity of water (1) and poly(VEP-*co*-GMA)-*graft*-PEG475 water solution (2) on amount of added Dox (**b**). (Reproduced with permission (Mitina et al., 2020))

prevents their interaction. Significantly bigger values of fractal cluster ($\alpha = 2.65 \pm 0.1$) on SAXS diffractograms (Fig. 20) and larger gyration radii (Table 5) suggest the formation of spherical micelles with soft core. This confirms a significant influence of the fine structure of the surface-active comb-like polymers on the morphology of the self-organized supramolecular structures formed in the solution.

The structures of the polymeric micelles formed by poly(PEGMA475)-MP and poly(VEP-co-GMA)-graft-PEG 750 were suggested to be based on the aforementioned results and these structures are presented in the scheme (Fig. 22).

We have established that fine structures, including the disposition of side PEG chains along the backbone of comb-like copolymers, define their ability to form the micelles of different packing density, size, morphology, and stability. This is important for using micelle-forming polymers as components of drug delivery systems for biomedical applications. The drug-binding ability and stability in the physiological liquids are significant factors for their use as drug carriers.

The possibilities of controlled formation of complexes of the comb-like PEG-containing polymers with water-soluble and water-insoluble anticancer drugs of different nature, as well as the proposed mechanisms of drug binding and formation of stable drug delivery systems, are considered below.

4 Structural and Colloidal-Chemical Characteristics of Complexes of Anticancer Drugs with Comb-Like PEG-Containing Copolymers

4.1 Complexes with Water-Soluble Drugs (e.g., Doxorubicin)

The surface activity of the complex formed by doxorubicin (Dox) with the poly(VEP-co-GMA)-graft-PEG475 is distinctly larger in comparison with the surface activity of the initial polymeric carrier (Fig. 23a). Moreover, such complexes form micelle-like structures at lower concentrations in the solution. This is important for using such micelle-like carriers for drug delivery systems, since the stability of the micelles at delivery in vitro and in vivo depends on the CMC value (Kulthe et al., 2012; Lu et al., 2018).

This might be explained by the hydrophobization of the polymer in the complex due to Dox binding via a formation of the hydrogen bonds with ether oxygen atoms of the PEG side chains. The area per micelle-like complex with the Dox at the phase boundary air/water solution is smaller than the area per polymeric micelles without Dox (Table 6). This confirms the evident compaction of the micelles caused by the binding of Dox molecules (Mitina et al., 2020; Riabtseva et al., 2016).

The complex is formed via the electrostatic noncovalent interaction between the positively charged Dox molecules and negatively charged PEG chains of the comb-like copolymer. The complex of poly(VEP-co-GMA)-graft-PEG750 with Dox has total positive charge of +1.6 mV, which suggests binding of Dox in the micelle-like structures formed by the polymeric surfactant containing PEG. An increase in the electroconductivity of a polymer solution after the addition of Dox (Fig. 23b) due to an increase in the amount of the hydronium ions confirms the possibility of the assumed mechanism.

The determined values of the SAXS α parameter of the micelles formed by the poly(VEP-co-GMA)-graft-PEG750 and complex of poly(VEP-co-GMA)-graft-PEG750 with Dox correspond to structures of mass fractal. Moreover, an increase in packing density of the micelle core with the increase in bound Dox content was observed. The increase in α parameter determined by SAXS is an evidence of the core compaction (Fig. 24).

The UV-Vis spectra of water solutions of the complex of carrier with Dox (Fig. 25a) confirm the presence of bound Dox in the micelles. The UV absorption band of Dox shifts as a result of its binding, which confirms the formation of the complex of poly(VEP-co-GMA)-graft-PEG750 with Dox (Fig. 25a). One can see
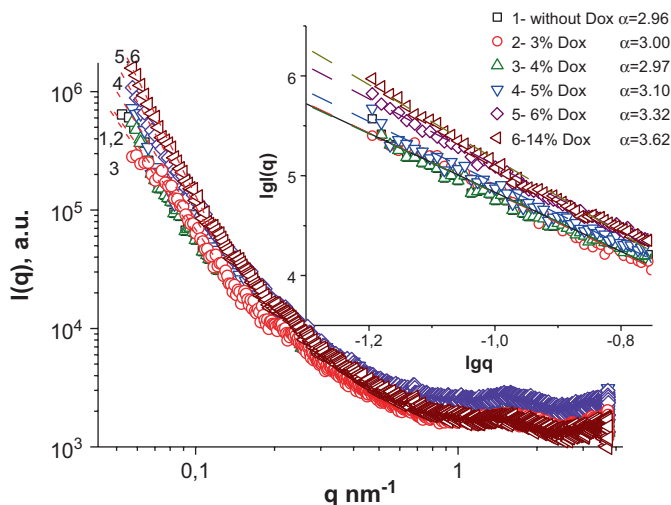
Fig. 24 SAXS diffractograms of the poly(VEP-co-GMA)-graft-PEG750 (1) and complex of poly(VEP-co-GMA)-graft-PEG750 with Dox (2–14) (polymer – 0.01 g/mL, [Dox] = 0.0003 g/mL (2); 0.0004 g/mL (3); 0.0005 g/mL (4); 0.0006 g/mL (5); 0.0014 g/mL (6)) (linear sections of the diffractograms are inserted) (The solid line is a linear approximation in respect of the scaling concept). (Reproduced with permission (Mitina et al., 2020))
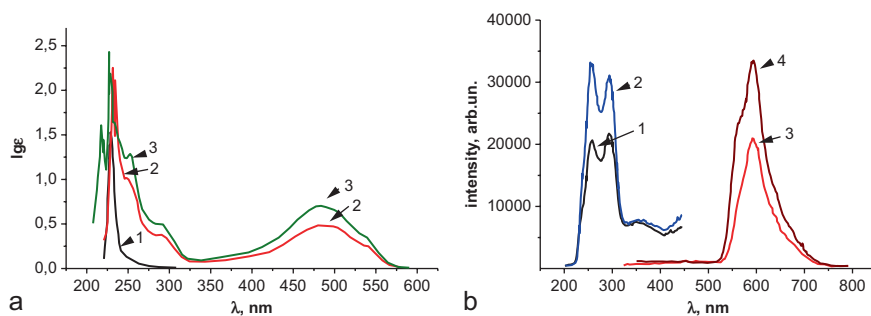
Fig. 25 UV-Vis spectra of the poly(VEP-co-GMA)-graft-PEG750 (1), complex of poly(VEP-co-GMA)-graft-PEG750 with Dox (2) and free Dox (3) (**a**) in water solutions; luminescent spectra of water solution of free Dox (1 – excitation, 2 – emission) and Dox complex with the polymer carrier (3 – excitation, 4 – emission) (**b**). (Reproduced with permission (Mitina et al., 2020))

from the excitation and emission luminescent spectra of water solutions of Dox in polymer micelles (Fig. 25b) that the main peaks attributed to Dox luminescence coincide. At the same time, a significant enhancement of the luminescent intensity of Dox in the micelles might be explained by its localization in the micelle core where it is protected from quenching by water.
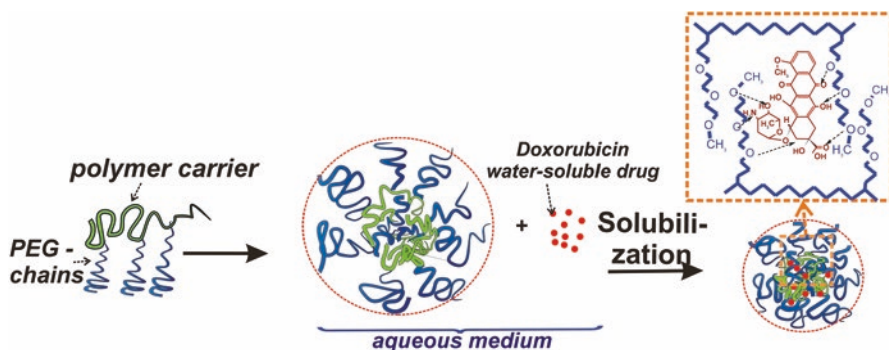
Fig. 26 Scheme of the formation of the complex of poly(VEP-co-GMA)-graft-PEG750 with Dox

Table 7 Characteristics of the micelle-like structures of the complexes of poly(VEP-co-GMA)-graft-PEG750 with Dox and the complexes of poly(VEP-co-GMA)-graft-PEG750-graft-poly(NVP-co-AA) with Dox (pH = 7)

Complex	Average hydrodynamic diameter DLS, nm	TEM-measured average diameter, nm	SEM-measured average diameter, nm	ξ-potential (mV)
Poly(VEP-co-GMA)-graft-PEG750 with Dox	40.6 ± 18.0	30.0 ± 11.0	–	+1.6… + 3.1
Poly(VEP-co-GMA)-graft-PEG750-graft-poly(NVP-co-AA) with Dox	250.0 ± 32.0	–	275.0 ± 25.0	+3.2…. + 6.0

Taking into account the results of the colloidal-chemical and spectral analyses, the scheme of the formation of the complex of poly(VEP-co-GMA)-graft-PEG750 with Dox was proposed in Fig. 26.

The results presented in Table 7 and Fig. 27 demonstrate a distinct decrease in the size and charge of the micelles containing Dox, compared to such micelles without Dox. Moreover, the complexes of Dox with the branched copolymer containing side PEG and poly(NVP-co-AA) chains possess a smaller size, comparing to complex of poly(VEP-co-GMA)-graft-PEG750 with Dox due to an additional compacting of the micelles as a result of the electrostatic interaction of Dox molecules with side anionic polymer chains.

The SAXS study of the micelle-like structures formed by the comb-like polymers and their complexes with Dox in the solution showed a difference in the morphology of the micelles formed by different carriers (Fig. 28). SAXS-produced results coincide well with the SEM images of the micelles.

The values of the α parameter determined by the analysis of linear sections of q dependences on the diffractograms are 4.6 ± 0.1 and 2.9 ± 0.1 for the poly(VEP-co-GMA)-graft-PEG-graft-poly(NVP-co-AA) and the poly(VEP-co-GMA)-graft-PEG,

Fig. 27 DLS measured hydrodynamic size of the micelles of poly(VEP-co-GMA)-graft-PEG750 (1); poly(VEP-co-GMA)-graft-PEG750 with Dox (2); poly(VEP-co-GMA)-graft-PEG750-graft-poly(NVP-co-AA) with Dox (93:7% mol) (3), poly(VEP-co-GMA)-graft-PEG750-graft-poly(NVP-co-AA) with Dox (93:7% mol) (4)
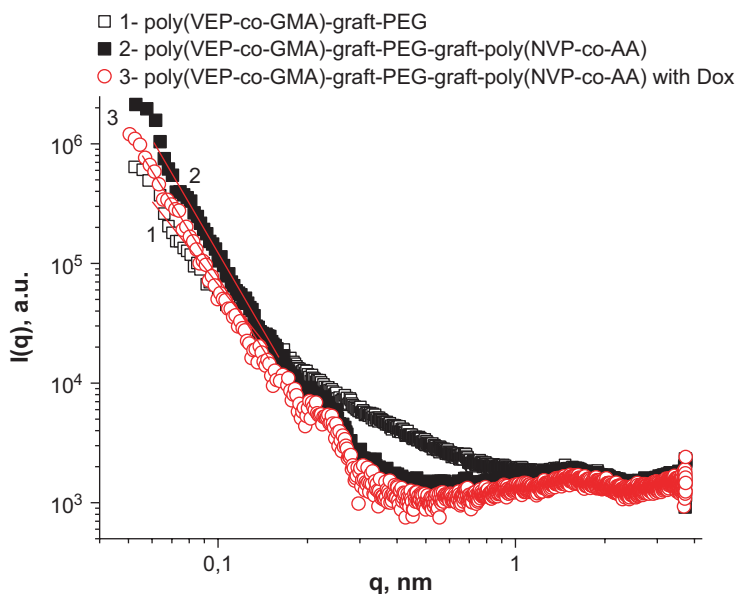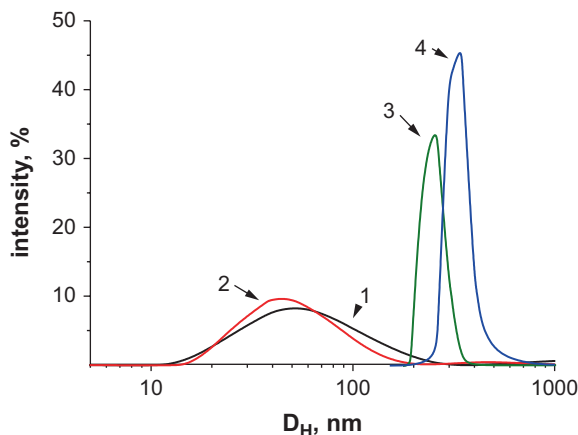
Fig. 28 SAXS diffractograms of poly(VEP-co-GMA)-graft-PEG (1), poly(VEP-co-GMA)-graft-PEG-graft-poly(NVP-co-AA) (2) and complex of poly(VEP-co-GMA)-graft-PEG-graft-poly(NVP-co-AA) with Dox (3) (polymer – 0.01 g/L, Dox – 0.0003 g/L), 293 K. (The solid line is a linear approximation in respect of the scaling concept). (Reproduced with permission (Riabtseva et al., 2016))

respectively. These α values confirm the formation of the micelles by the poly(VEP-co-GMA)-graft-PEG with a friable core and shell, and micelles formed by the poly(VEP-co-GMA)-graft-PEG-graft-poly(NVP-co-AA) with more densely packed core and developed nonfractal shell (Schmidt, 1991, 1995). The formation of the complex of poly(VEP-co-GMA)-graft-PEG-graft-poly(NVP-co-AA) with Dox
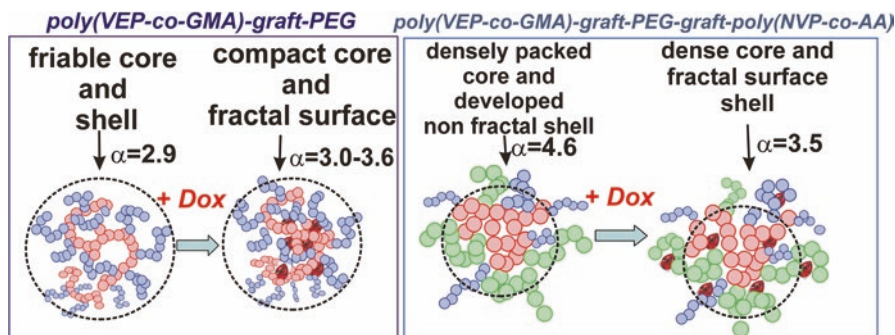
Fig. 29 Hypothetical scheme of the micelle morphology formed by the poly(VEP-co-GMA)-graft-PEG (**a**) and the poly(VEP-co-GMA)-graft-PEG-graft-poly(NVP-co-AA) (**b**)
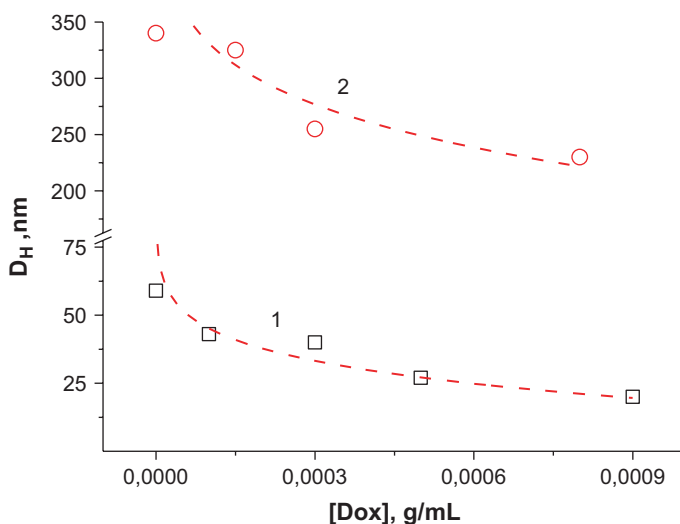
Fig. 30 Dependence of the micelle size on Dox content in complexes with the poly(VEP-co-GMA)-graft-PEG (1) and the poly(VEP-co-GMA)-graft-PEG-graft-poly(NVP-co-AA)(2) ([polymer] = $1.0 \cdot 10^{-2}$ g/mL, pH = 6.7; 1% NaCl)

leads to a change in α to 3.6 ± 0.1, which corresponds to compact aggregates possessing fractal surface shells. Dox molecules can be localized in the compact core and at the fractal surface (Fig. 29).

One can see (Figs. 30 and 31) that an increase in Dox content in the micelle-like complexes with the comb-like polymeric carriers provides a strong decrease in the micelle size due to their compaction caused by complex formation. This dependence is visible for the formation of complexes with the comb-like copolymer combing side PEG and the polyelectrolyte chains.

Fig. 31 Hydrodynamic diameters of the micelles formed by the complex of poly(VEP-co-GMA)-graft-PEG with Dox (1–4) and complex of poly(VEP-co-GMA)-graft-PEG-graft-poly(NVP-co-AA) with Dox (93:7% mol) (6–9): [Dox] = 0 g/mL (1, 6); $1.0 \cdot 10^{-4}$ g/mL (2, 7); $3.0 \cdot 10^{-4}$ g/mL (3, 8); $5.0 \cdot 10^{-4}$ g/mL (4), $9.0 \cdot 10^{-4}$ g/mL (5, 9). (Reproduced with permission (Riabtseva et al., 2016))

Different values of ξ-potential of Dox complexes formed by studied comb-like copolymers with the PEG chains only and combining PEG and the anionic chains prove various mechanisms of complex formation in water solutions (Table 7). The formation of the complex of comb-like copolymers combining side PEG and the anionic poly(NVP-co-AA) chains with Dox molecules causes their strong compaction in the solution, as well as recharging of the micelle-like structures from the negative to positive ξ-potential. These data can be explained by the binding of the positively charged Dox molecules not only with side PEG chains but also by the electrostatic interaction with carboxyls of the exterior side anionic polymer chains. As one can see (Fig. 32), the absorption band of $n \rightarrow \pi^*$ electron transfer for the complex of poly(VEP-co-GMA)-graft-PEG-graft-poly(NVP-co-AA) with Dox shifts as a result of Dox interaction with the COOH group due to a change in the solvation shell in comparison to the poly(VEP-co-GMA)-graft-PEG-graft-poly(NVP-co-AA).

A comparison of the hydrodynamic diameters with the intensity and number of the micelles containing bound Dox demonstrates (Figs. 32 and 33) that they do not form secondary aggregated structures even after three months of storage due to high durability of their hydrophilic shell.
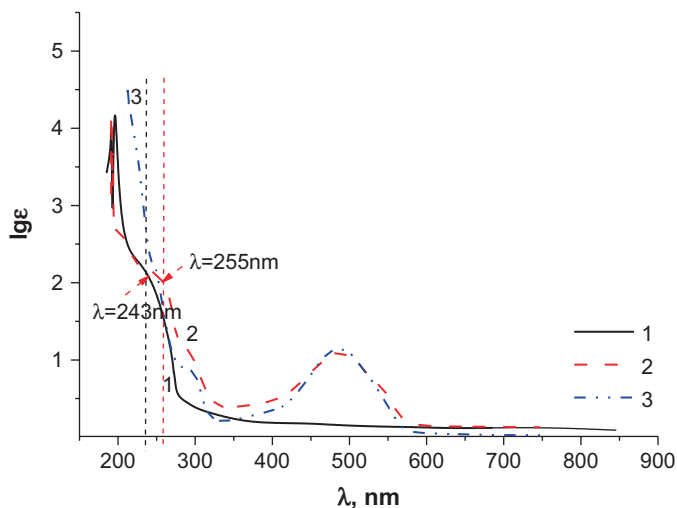
Fig. 32 Electronic spectra of water solutions of the poly(VEP-co-GMA)-graft-PEG-graft-poly(NVP-co-AA) (1), complex of poly(VEP-co-GMA)-graft-PEG-graft-poly(NVP-co-AA) with Dox (2), Dox (3). (Reproduced with permission (Riabtseva et al., 2016))

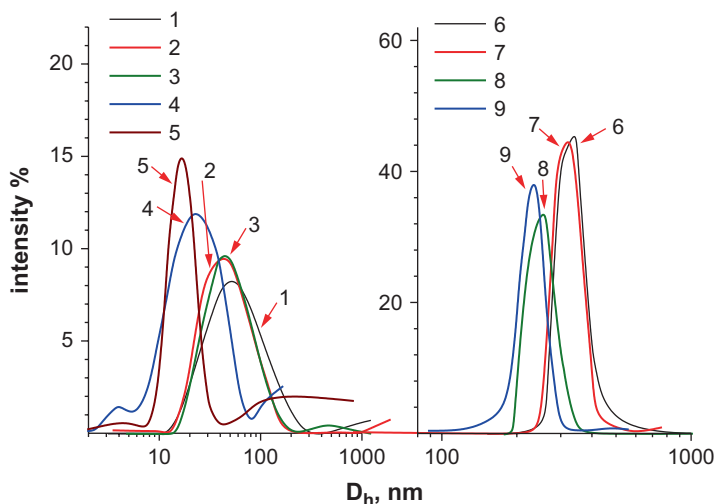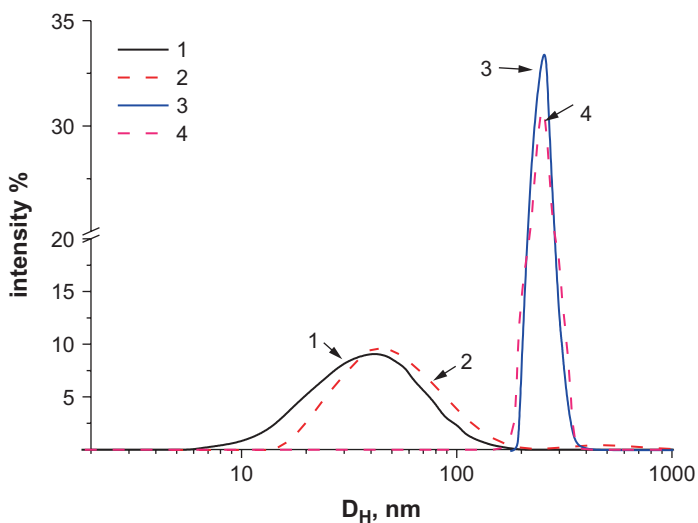**Fig. 33** Hydrodynamic diameters of the micelle-like complexes of the poly(VEP-co-GMA)-graft-PEG with Dox (1,2) and poly(VEP-co-GMA)-graft-PEG-graft-poly(NVP-co-AA) with Dox (3,4) (after a week (1,3) and after 3 months (2,4))

4.2 The Delivery Systems of Water-Insoluble Anticancer Ruthenium-Based Drug (Indazolium Trans-[Tetrachloridobis(1H-Indazole)Ruthenate (III))

The Ru^{+3}-based complex (KP1019) is a promising anticancer substance, especially for glioblastoma treatment (Heffeter et al., 2014). However, its water insolubility strongly impedes the development of stable water-based delivery systems and their use in anticancer chemotherapy. It is evident (Fig. 34a, b) that formation of the complex of comb-like copolymer poly(VEP-co-GMA)-graft-PEG with KP1019 does not influence significantly the polymer surface activity, as well as the size distribution of the formed micelle-like structures.

The CMC values of the comb-like polymer carrier poly(VEP-co-GMA)-graft-PEG and the complex of poly(VEP-co-GMA)-graft-PEG with KP1019 coincide well. That might be explained by the unchanged size and morphology of the micelle-like structures formed by the comb-like polymeric carrier after the formation of the KP1019 complex and its localization in the micelle core.

The results of the DLS study show that the main part of the micelles is of 16–20 nm size. These data coincide well with the results of measurements performed during TEM and SEM studies (Fig. 35).

The UV-Vis spectrum shows a significant enhancement in the intensity of the adsorption band at 226 nm and a shift of the band at 284 nm that corresponds to the Ru^{+3} complex and confirms its binding to the comb-like PEG containing copolymer (Fig. 36a). In spite of transparency of the polymeric carrier in the studied UV-region, one can see (Fig. 36b) that the linearity of the dependence of adsorption intensity on the concentration of KP1019 in solution of the complex of poly(VEP-co-GMA)-graft-PEG with KP1019 at the same polymer concentration is absent. That might be explained by the interaction of the Ru^{+3}-containing substance with the comb-like
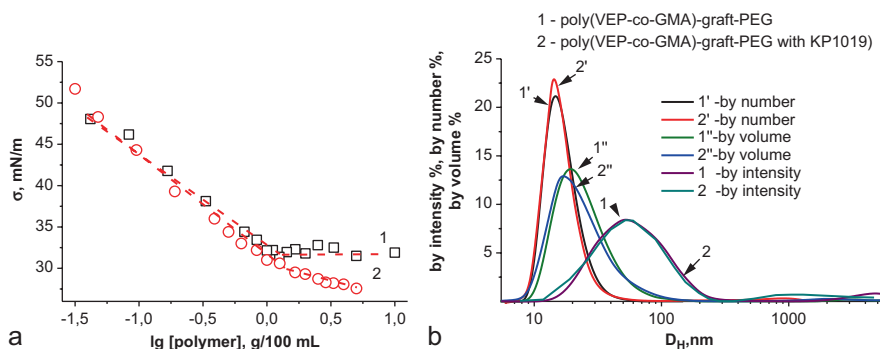
Fig. 34 Isotherms of the surface tension of water solutions (**a**) and size distribution of size of the formed micelles (**b**): *1* – poly(VEP-co-GMA)-graft-PEG; *2* – and complex of poly(VEP-co-GMA)-graft-PEG with KP1019
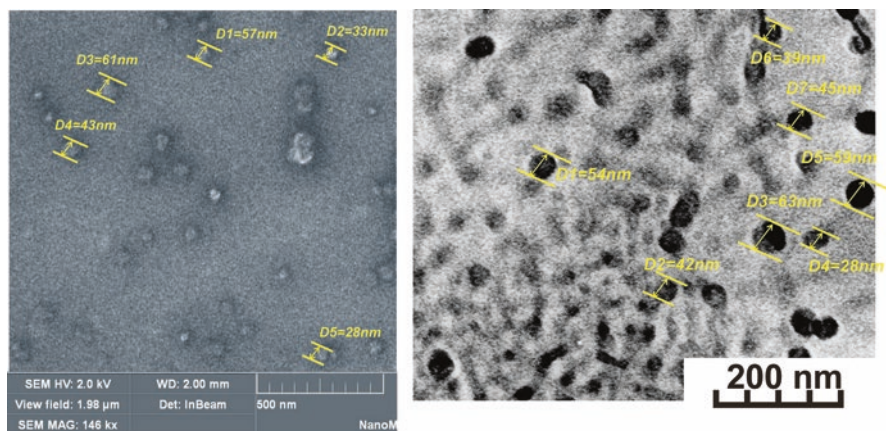
Fig. 35 SEM (left) and TEM (right) micrographs of the micelles formed by the complex of poly(VEP-co-GMA)-graft-PEG with KP1019. (*Samples were prepared in the same way as described in* Figs. 10 and 11)
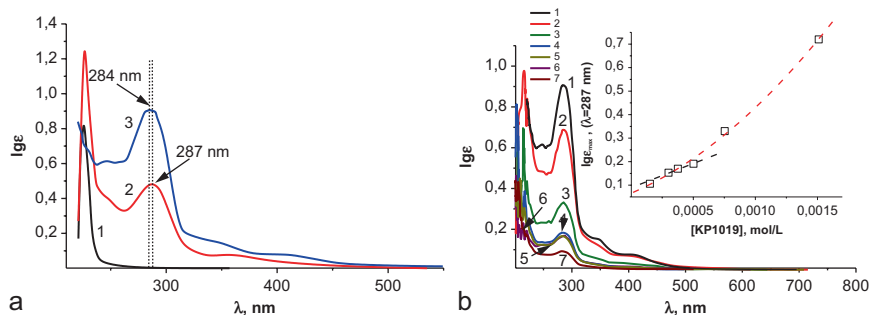
Fig. 36 UV-Vis spectra of water solutions of the poly(VEP-co-GMA)-graft-PEG (1) and complex of poly(VEP-co-GMA)-graft-PEG with KP1019 (2) as well as KP-1019 in DMSO (3) (**a**); as well as of solutions of the complex of poly(VEP-co-GMA)-graft-PEG with KP1019 at different content of bound KP-1019 per 100% of polymer in DMSO; 1–100% of polymer, 2–10:100; 3–5:100; 4–3,33:100; 5–2,5:100; 6–2:100; 7–1:100 (dependence of the adsorption band on KP-1019 concentration in water solution of the micelle-like carrier complex is inserted (**b**))

polymer and the formation of complex with side PEG chains that provide an elevated content in the molecules of KP-1019 in the micelle core.

The binding of KP-1019 with the polymeric carrier was also confirmed by a shift in the adsorption bands of the complexes of poly(VEP-co-GMA)-graft-PEG with KP1019 in a region of high frequency in the Raman spectrum (Fig. 37), as well as by an enhancement of the charge value of the KP-1019 complex (-0.2 mV) in comparison with the initial copolymer charge (-0.4 mV).
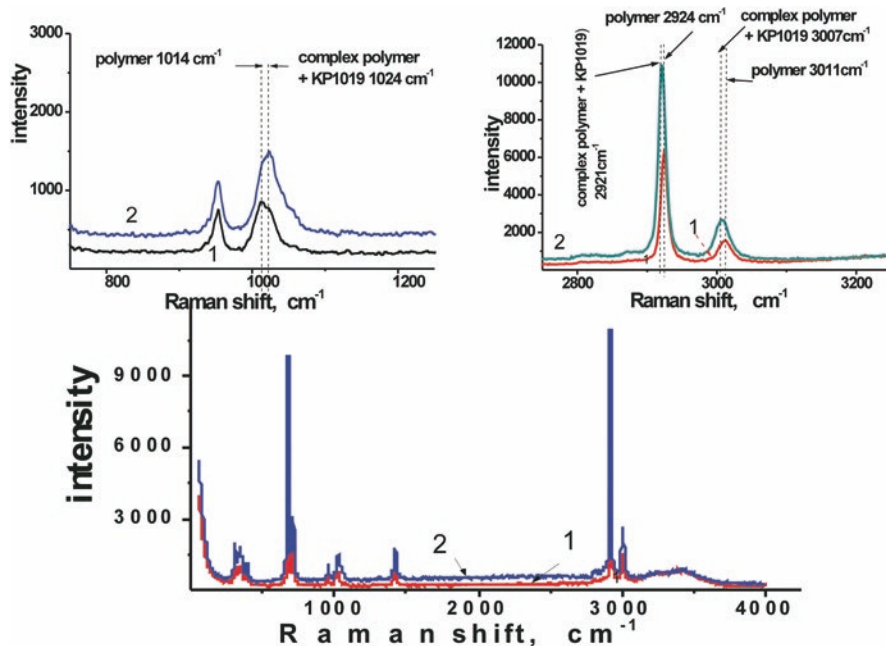
Fig. 37 Raman spectra of water solutions of the poly(VEP-co-GMA)-graft-PEG (1) and the complex of poly(VEP-co-GMA)-graft-PEG with KP1019 (2)

KP-1019 in complex with the polymeric carrier in the micelle-like structures is reliably protected from oxidation and saves its stability at storage at 278 K for 3 months, compared with the unstable free trans-[RuIIICl₄(Hind)₂] (Heffeter et al., 2014). The absence of a colored complex of serum albumin with KP-1019 in water systems containing a mixture of the micelles of the complex of polymer with KP1019 and the albumin proves that KP-1019 is localized in the micelle core, which prevents its interaction with the albumin (Heffeter et al., 2014).

4.3 Delivery Systems for Water-Insoluble 4-Thiazolidinone-Based Compounds with Anticancer Activity

It was shown that different 4-thiazolidinone derivatives possess anticancer potential (Finiuk et al., 2017; Kobylinska, Boiko, et al., 2016; Kobylinska, Havrylyuk, et al., 2016; Panchuk et al., 2012; Senkiv et al., 2016). The superfine complexes of water-insoluble 4-thiazolidinone derivatives (Les-3661 and Les-3120) of 90 nm and
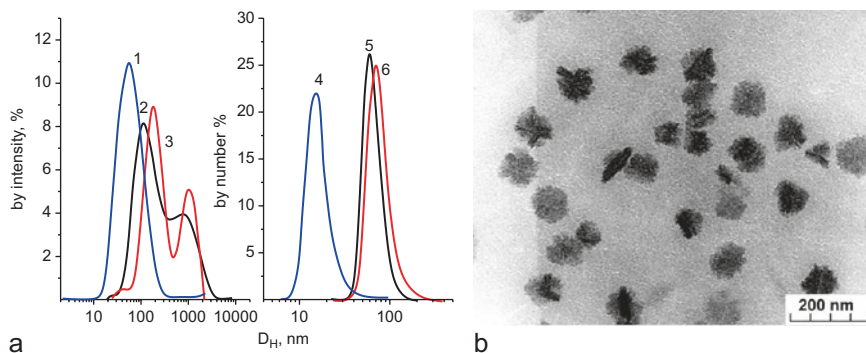
Fig. 38 DLS measured sizes of the micelles formed by poly(VEP-co-GMA)-graft-PEG (1,4), and complexes of Les-3661 (2,5) and Les-3120 (3,6) obtained and stabilized with the poly(VEP-co-GMA)-graft-PEG (intensity (1–3) and number (4–6)) (**a**); TEM micrographs of the nanoparticles of Les-3120 complex with the poly(VEP-co-GMA)-graft-PEG (*sample preparation: 2 μL 0.1% of the solution on commercial C-coated Cu grid and fast drying after 2 min*) (**b**)

140 nm size, respectively were formed and stabilized by the comb-like surfactant poly(VEP-co-GMA)-graft-PEG. Their size is distinctly bigger than the size of such complexes formed with Dox and KP-1019 (16–20 nm size, Fig. 35). In spite of the high stability of the water systems of Les-3661 and Les-3120, they contain a negligible content of 670 nm aggregates of Les-3661-containing complexes and 1260 nm aggregates of Les-3120-containing complexes (Fig. 38).

A possible explanation of that phenomenon is the formation of stable nanoparticles of water-insoluble 4-thiazolidinone derivatives as a result of their nucleation while transferring from the DMSO solution to water solution of the poly(VEP-co-GMA)-graft-PEG. The polymer behaves as a soft template that defines the size, functionality of the surface and stabilizes nanoparticles in the system. It is evident (Fig. 39a) that the adsorption of the surfactant molecules on the particle surface is reversible, and a part of the molecules desorbs into the water solution.

A study of the aggregation and sedimentation stabilities of 4-thiazolidinone-based nanoparticles modified by the comb-like PEG-containing surfactant combined with the study of the UV-spectra confirms the formation of stable bonds of the polymer molecules with the particle surface in the range of studied concentrations. One can see a shift in the adsorption bands of 4-thiazolidinone-based complexes in the bathochromic region of the UV-spectra (Fig. 39b), compared with the spectra of the solutions of free 4-thiazolidinone derivatives in the DMSO. We suggest a formation of the bonds between the surface of 4-thiazolidinone-based nanoparticle and chemically adsorbed molecules of the comb-like polymeric carrier. A decrease in the adsorption intensity of complexes of 4-thiazolidinones with the copolymer carrier in comparison with free 4-thiazolidinones in the DMSO at the same concentrations confirms this suggestion.
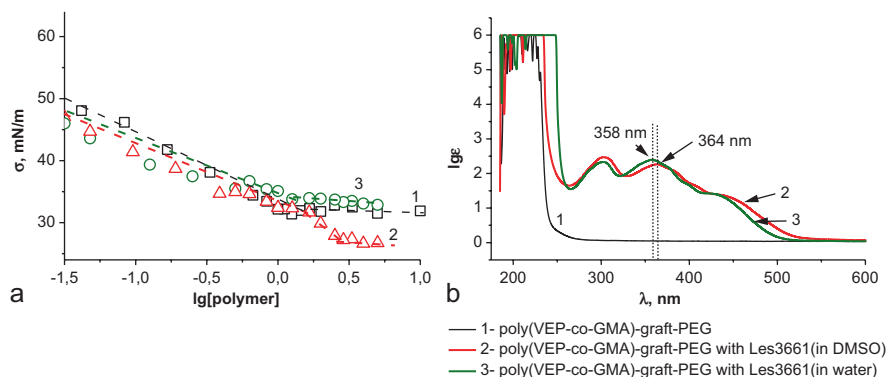
Fig. 39 Surface tension isotherms of water solutions of: *1* – poly(VEP-co-GMA)-graft-PEG (1), *2,3* – preparations of Les-3120 and Les-3661 nanoparticles stabilized by the poly(VEP-co-GMA)-graft-PEG (**a**) and electronic spectra of *1* – poly(VEP-co-GMA)-graft-PEG, *2* – preparation of Les-3661 nanoparticles stabilized by the poly(VEP-co-GMA)-graft-PEG in water, *3* – solution of Les-3661 in the DMSO (**b**)
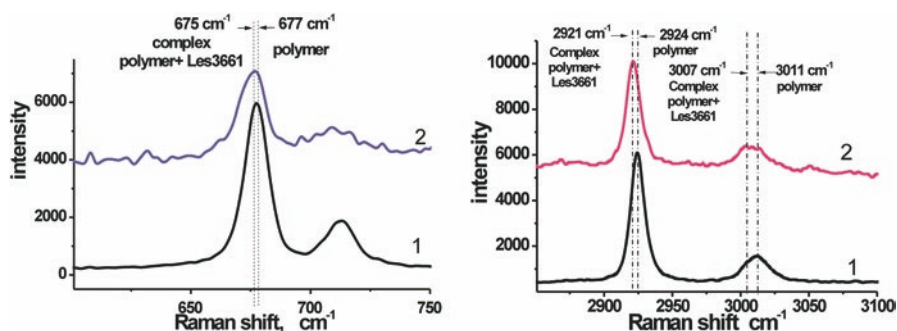
Fig. 40 Raman spectra of solutions of the poly(VEP-co-GMA)-graft-PEG (1) and dispersion of complexes of Les-3661 with the poly(VEP-co-GMA)-graft-PEG (2) in water

A formation of the chemical bonds between the polymer functional groups and the surface of the nanoparticles was proved by the detected shifts in the Raman spectra adsorption bands of the functional groups that correspond to the polymeric shell on the surface of Les-3661-containing nanoparticles (Fig. 40) stabilized by the comb-like surfactant in water.

SAXS diffractograms demonstrate (Fig. 41) a change in the α parameter. The slope of the linear function of the dependence of scattering intensity on scattering coordinate in binary logarithmic coordinates in the micelles containing water-insoluble substances is observed. This is explained by an increase in the micelle packing density. At the same time there was no significant change in the micelle

Fig. 41 SAXS
diffractograms of the
poly(VEP-co-GMA)-graft-
PEG (1) and its complexes
with Les-4523 (2), KP1019
(3) and Dox (4) (polymer –
0.01 g/L, substance –
0.0003 g/L), 20 °C. (The
solid line is a linear
approximation in respect
of the scaling concept)
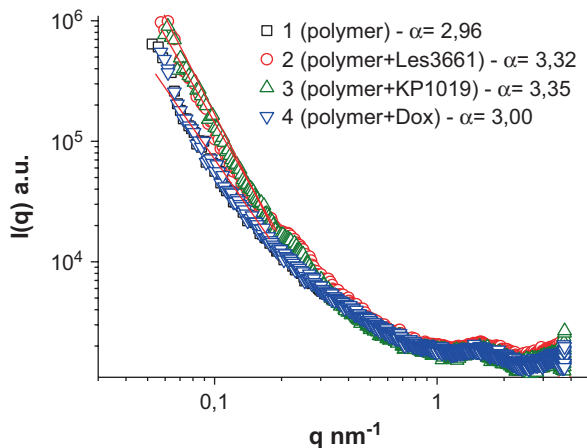
Fig. 42 DLS micelle size
of the poly(VEP-co-
GMA)-graft-PEG-graft-
poly(NVP-co-AA) (1) and
its complex with the
4-thiazolidinone derivative
Les-3120 nanoparticles (2)
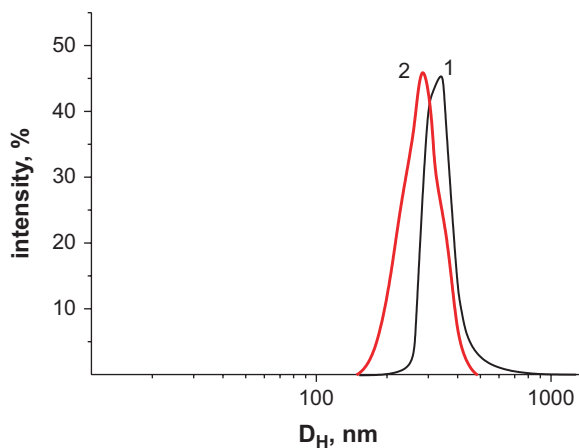
morphology in complexes formed by the same polymeric carrier with water-soluble Dox.

An increase in the micelles density and a decrease in their size witness the nucleation of 4-thiazolidinone Les-3120 nanoparticles in the presence of the poly(VEP-co-GMA)-graft-PEG-graft-poly(NVP-co-AA) surfactant as soft template and surface modifier (Fig. 42). The presence of polar carboxyl groups in the grafted side polyelectrolyte chains of the poly(VEP-co-GMA)-graft-PEG-graft-poly(NVP-co-AA) molecules causes a formation of strong chemical bonds between the polymer molecules and the surface of the 4-thiazolidinone nanoparticles.

The colloidal-chemical characteristics of complexes of the PEG-containing comb-like carriers with studied bioactive compounds (Table 8) demonstrate significant differences in the size of the micelles and derived particles, as well as differences in their ξ-potentials. To conclude, the aforementioned results confirm that the

Table 8 Colloidal-chemical characteristics of the micelles formed by the comb-like copolymers and their complexes with water-insoluble anticancer compounds

Surfactant	Average hydrodynamic diameter, nm	TEM-measured diameter, nm	SEM-measured diameter, nm	ξ-potential, mV	$A_\infty \cdot 10^6$, mol/m^{2a}	S_0, Å^2
Poly(VEP-co-GMA)-graft-PEG	59.0 ± 25.0	39.0 ± 6.5	35.0 ± 15.2	−0.25	0.50	292
Poly(VEP-co-GMA)-graft-PEG with KP1019	52.0 ± 17.0	30.0 ± 8.0	40.0 ± 8.0	+3.04	0.45	298
Poly(VEP-co-GMA)-graft-PEG with Les 3120	150.0 ± 26.0	120.0 ± 25.0	–	−0.7	–	–
Poly(VEP-co-GMA)-graft-PEG with Les3661	90.0 ± 20.0	100.0 ± 22.0	–	−0.9	–	–
Poly(VEP-co-GMA)-graft-PEG-graft-poly(NVP-co-AA)	340.0 ± 35.0	300.0 ± 55.0	350.0 ± 105.0	−0.60	–	–
Poly(VEP-co-GMA)-graft-PEG-graft-poly(NVP-co-AA) with Les 3120	320.0 ± 40.0	–	–	−1.20	–	–

[a]*Water-air boundary*
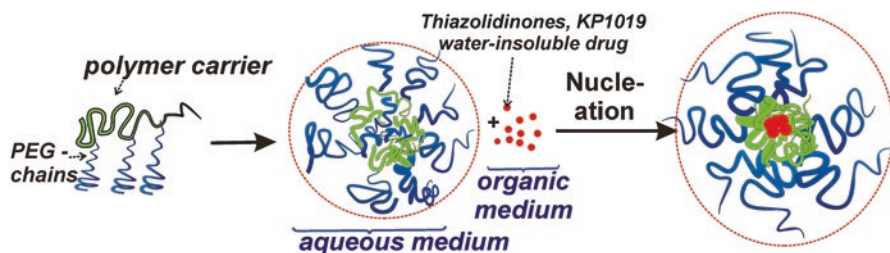
Fig. 43 Hypothetic scheme of the formation of the complexes of water insoluble drugs with the poly(VEP-co-GMA)-graft-PEG

created complexes can be formed and stabilized via different mechanisms. Their morphology, charge, and size depend on the nature and functionality of the polymer and the drug compound. The hypothetic scheme of the formation and morphology of water-insoluble drug complexes with the polymeric carrier is shown in Fig. 43.

5   Biocompatibility of Polymeric Systems for Drug Delivery

The high potential of the water-soluble PEGylated comb-like polymeric nanoscale systems (poly(VEP-co-GMA)-graft-PEG (PNC)) for delivery of both traditional and experimental drugs into tumor cells in vitro and in vivo was demonstrated (Kobylinska et al., 2015; Kobylinska, Boiko, et al., 2016; Kobylinska, Havrylyuk, et al., 2016). Here, the results of their testing for evaluation of their toxicity and biocompatibility are presented. The general toxicity of polymeric carriers of comb-like structure with side polyethylene glycol (PEG) chains was studied (Kobylinska et al., 2018).

In the MTT assay, the PNC demonstrated weak toxicity toward human leukemia (HL-60, Jurkat), hepatocellular (HepG2), colon (HCT116), and breast (MCF-7) cancer cell lines. At the highest dose of 50 μM, the PNC inhibited HL-60 cell viability by 35.7% and the viability of Jurkat cells by 27.2%. At 5μM, the PNC reduced the viability of HepG2 cells by 19%, and at 50 μM dose, it inhibited the viability of MCF-7 cells by 16% and that of HCT116 cells by 17% (Fig. 44).

The Trypan blue exclusion assay used for measuring the cytotoxic action of the PNC demonstrated results similar to the results of the MTT assay. There were 66.9%, 71.1%, 81.4%, and 83.0% of viable HL-60, Jurkat, MCF-7, and HCT116 cells, respectively, after their treatment (72 h) with the PNC in 50 μM dose (Fig. 45).

Thus, even in high doses equivalent to the amount of polymer used in a complex with the anticancer drug, the PNC itself did not significantly affect tumor cell viability in vitro.

The in vivo administration of the PNC in the highest doses (1 ml per one injection in mice and 10 ml in rats) induced a short suppression of the physical activity
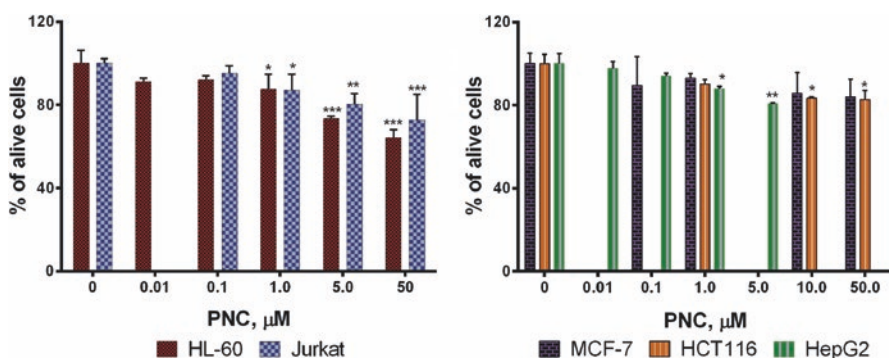
Fig. 44 Values of inhibition of the viability determined by means of the MTT assay under 72 h treatment of different tumor cell lines with the PNC: human leukemia (HL-60, Jurkat), hepatocellular (HepG2), colon (HCT116) and breast (MCF-7) carcinoma cells. *$P \leq 0.05$; **$P \leq 0.01$ (difference compared with the nontreated cells). (Reproduced with permission (Kobylinska et al., 2018))
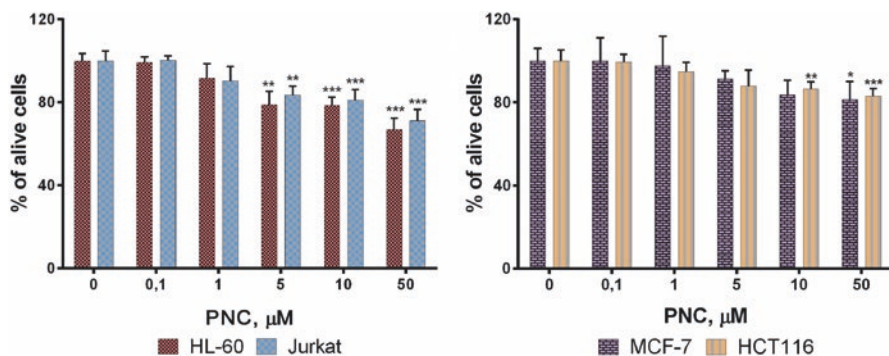
Fig. 45 Number of alive cells determined by the trypan blue exclusion testing of different tumor cell lines treated for 72 h with the PNC: human leukemia (HL-60, Jurkat), colon (HCT116), and breast (MCF-7) tumor. *$P \leq 0.05$; **$P \leq 0.01$ (difference compared with the nontreated control cells). (Reproduced with permission (Kobylinska et al., 2018))
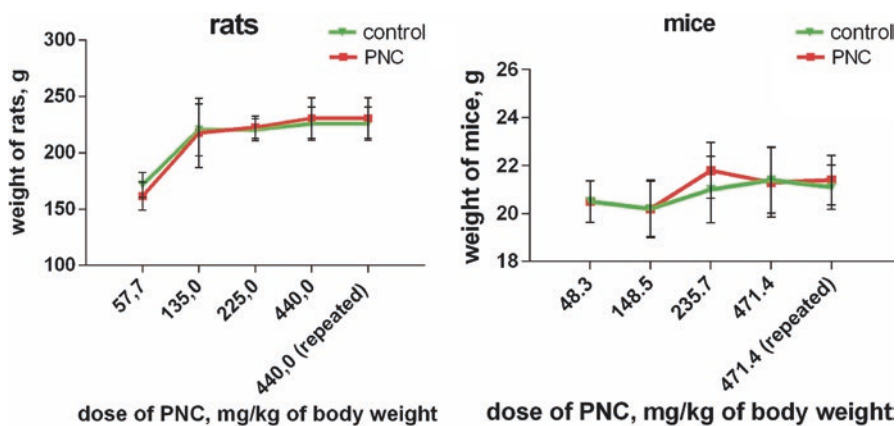
Fig. 46 The dynamics of body weight of rats and mice treated with the PNC used in different doses. (Reproduced with permission (Kobylinska et al., 2018))

of animals that happened due to a big volume of the injected PNC. However, the day after injection, there were no visible changes in the behavior or physiological status of the treated animals. The same results were obtained after the reinjecting of the PNC in rats (10.0 ml dose that corresponded to 9.9 mg of the PNC) and mice (1.0 ml dose that corresponded to 9.9 mg of the PNC)) (Kobylinska et al., 2018).

The body weight of animals treated with the PNC at the indicated doses did not differ substantially from the body weight measured before the administration of the PNC or at the end of the experiment (Fig. 46). In the administered doses, the PNC did not demonstrate any pronounced toxic effect on experimental animals, and there were no animals that died during the study.

The biochemical parameters of the PNC toxicity were also examined in vivo. There were no significant changes in the activity of the indicator enzymes and concentration of metabolites and ions in blood serum of rats treated with free PNC for 20 days. In more detail, these characteristics are described in another chapter of this monograph.

The chemical components of the PNC were examined in the urine and stool of rats treated with the PNC (Kobylinska et al., 2018). The obtained results allow one to suggest that the PNC is metabolized, probably, in liver tissue, while its clearance is carried out by kidney. The clearance of the PNC was estimated in daily urine and feces. It was found that rat feces contained 8–10% of the PNC in the native form, while urine contained 20% in the native form, 15–20% as fragments of backbone and 13–25% as PEG. Only traces of these products were detected in the liver tissue. Since the urine of the treated animals contained all components of the PNC, namely, fragments of the backbone, PEG, and PNC, clearance of the degraded PNC via kidney filtration looks the most likely.

Taken together, the results of this investigation of clearance of the PNC and the results of the study of general toxicity of free PNC (Kobylinska et al., 2015; Kobylinska, Boiko, et al., 2016; Kobylinska, Havrylyuk, et al., 2016) confirm the biocompatibility of the PNC. They are in agreement with our former data that demonstrated high potential of the use of the developed PNC as a drug delivery system (Heffeter et al., 2014; Senkiv et al., 2014).

In summary, the tailored synthesis of novel comb-like PEG-containing polymeric surfactants, derived micelles as well as stable complexes with the anticancer substances of controlled functionality and colloidal-chemical properties was considered and discussed. Low general toxicity, the biocompatibility, and the detected capability to enhance cytotoxic action of anticancer agents toward tumor cells in vitro and antitumor effect of those agents in vivo altogether suggest a possibility of application of these polymeric surfactants as safe drug delivery platforms for treatment of cancer patients.

References

Balci, M., Alli, A., Hazer, B., Güven, O., Cavicchi, K., & Cakmak, M. (2010). Synthesis and characterization of novel comb-type amphiphilic graft copolymers containing polypropylene and polyethylene glycol. *Polymer Bulletin, 64*(7), 691–705. https://doi.org/10.1007/s00289-009-0211-3

Blanco, E., Shen, H., & Ferrari, M. (2015). Principles of nanoparticle design for overcoming biological barriers to drug delivery. *Nature Biotechnology, 33*(9), 941. https://doi.org/10.1038/nbt.3330

Cabral, H., Matsumoto, Y., Mizuno, K., Chen, Q., Murakami, M., Kimura, M., et al. (2011). Accumulation of sub-100 nm polymeric micelles in poorly permeable tumours depends on size. *Nature Nanotechnology, 6*(12), 815. https://doi.org/10.1038/nnano.2011.166

Chamundeeswari, M., Jeslin, J., & Verma, M. L. (2019). Nanocarriers for drug delivery applications. *Environmental Chemistry Letters, 17*(2), 849–865. https://doi.org/10.1007/s10311-018-00841-1

Dong, R., Zhou, Y., & Zhu, X. (2014). Su pramolecular dendritic polymers: From synthesis to applications. *Accounts of Chemical Research, 47*(7), 2006–2016. https://doi.org/10.1021/ar500057e

Finiuk, N., Boiko, N., Klyuchivska, O., Kobylinska, L., Kril, I., Zimenkovsky, B., Lesyk, R., & Stoika, R. (2017). 4-Thiazolidinone derivative Les-3833 effectively inhibits viability of human melanoma cells through activating apop-totic mechanisms. *Croatian Medical Journal, 58*(2), 129–139. https://doi.org/10.3325/cmj.2017.58.129

Franke, D., Petoukhov, M. V., Konarev, P. V., Panjkovich, A., Tuukkanen, A., Mertens, H. D. T., et al. (2017). ATSAS 2.8: A comprehensive data analysis suite for small-angle scattering from macromolecular solutions. *Journal of Applied Crystallography, 50*(4), 1212–1225. https://doi.org/10.1107/S1600576717007786

Heffeter, P., Riabtseva, A., Senkiv, Y., Kowol, C. R., Körner, W., Jungwith, U., et al. (2014). Nanoformulation improves activity of the (pre) clinical anticancer ruthenium complex KP1019. *Journal of Biomedical Nanotechnology, 10*(5), 877–884. https://doi.org/10.1166/jbn.2014.1763

Hou, S. S., & Kuo, P. L. (2001). Synthesis and characterization of amphiphilic graft copolymers based on poly (sty-rene-co-maleic anhydride) with oligo (oxyethylene) side chains and their GPC behavior. *Polymer, 42*(6), 2387–2394. https://doi.org/10.1016/S0032-3861(00)00476-6

Hu, S., Wang, Y., McGinty, K., & Brittain, W. J. (2006). Surface modification of a silicate substrate by a "grafting from" methodology utilizing a perester initiator. *European Polymer Journal, 42*(9), 2053–2058. https://doi.org/10.1016/j.eurpolymj.2006.03.033

Kobylinska, L., Patereha, I., Finiuk, N., Mitina, N., Riabtseva, A., Kotsyumbas, I., Stoika, R., Zaichenko, A., & Vari, S. G. (2018). Comb-like PEG-containing polymeric composition as low toxic drug nanocarrier. *Cancer Nanotechnology, 9*(1), 11. https://doi.org/10.1186/s12645-018-0045-5

Kulthe, S. S., Choudhari, Y. M., Inamdar, N. N., & Mourya, V. (2012). Polymeric micelles: Authoritative aspects for drug delivery. *Designed Monomers and Polymers, 15*(5), 465–521. https://doi.org/10.1080/1385772X.2012.688328

Kobylinska, L. I., Boiko, N. M., Panchuk, R. R., Grytsyna, I. I., Klyuchivska, O. Y., Biletska, L. P., Lesyk, R. B., Zimenkovsky, B. S., & Stoika, R. S. (2016). Putative anticancer potential of novel 4-thiazolidinone derivatives: Cyto-toxicity toward rat C6 glioma in vitro and correlation of general toxicity with the balance of free radical oxidation in rats. *Croatian Medical Journal, 57*(2), 151–163. https://doi.org/10.3325/cmj.2016.57.151

Kobylinska, L. I., Havrylyuk, D. Y., Mitina, N. E., Zaichenko, A. S., Lesyk, R. B., Zimenkovsky, B. S., & Stoika, R. S. (2016). Biochemical indicators of nephrotoxicity in blood serum of rats treated with novel 4-thiazolidinone derivatives or their complexes with polyethylene glycol-containing nanoscale polymeric carrier. *The Ukrainian Biochemical Journal, 88*(1), 51–60. https://doi.org/10.15407/ubj88.01.051

Kobylinska, L. I., Havrylyuk, D. Y., Ryabtseva, A. O., Mitina, N. E., Zaichenko, O. S., Lesyk, R. B., et al. (2015). Biochemical indicators of hepatotoxicity in blood serum of rats under the effect of novel 4-thiazolidinone derivatives and doxorubicin and their complexes with polyethyleneglycol-containing nanoscale polymeric carrier. *The Ukrainian Biochemical Journal, 87*(2), 122–132. https://doi.org/10.15407/ubj87.02.122

Lombardo, D., Kiselev, M. A., & Caccamo, M. T. (2019). Smart nanoparticles for drug delivery application: Development of versatile nanocarrier platforms in biotechnology and nanomedicine. *Journal of Nanomaterials, 2019.* https://doi.org/10.1155/2019/3702518

Lu, Y., Zhang, E., Yang, J., & Cao, Z. (2018). Strategies to improve micelle stability for drug delivery. *Nano Research, 11*(10), 4985–4998. https://doi.org/10.1007/s12274-018-2152-3

Meng, T., Gao, X., Zhang, J., Yuan, J., Zhang, Y., & He, J. (2009). Graft copolymers prepared by atom transfer radical polymerization (ATRP) from cellulose. *Polymer, 50*(2), 447–454. https://doi.org/10.1016/j.polymer.2008.11.011

Mitina, N. E., Riabtseva, A. O., Garamus, V. M., Lesyk, R. B., Volianiuk, K. A., Izhyk, O. M., & Zaichenko, A. S. (2020). Morphology of the micelles formed by comb-like peg containing copolymer loaded with antitumor substances with different water solubility. *Ukrainian Journal of Physics, 65*(8), 670–678. https://doi.org/10.15407/ujpe65.8.670

Najafi, V., Kabiri, K., & Ziaee, F. (2013). Preparation and characterization of alcogels based on (poly ethylene glycol methyl ether methacrylate-acrylic acid) copolymers. *Polymer-Plastics Technology and Engineering, 52*(7), 667–673. https://doi.org/10.1080/03602559.2012.762664

Navya, P. N., Kaphle, A., Srinivas, S. P., Bhargava, S. K., Rotello, V. M., & Daima, H. K. (2019). Current trends and challenges in cancer management and therapy using designer nanomaterials. *Nano Convergence, 6*(1), 23. https://doi.org/10.1186/s40580-019-0193-2

Neugebauer, D., Zhang, Y., Pakula, T., Sheiko, S. S., & Matyjaszewski, K. (2003). Densely-grafted and double-grafted PEO brushes via ATRP. A route to soft elastomers. *Macromolecules, 36*(18), 6746–6755. https://doi.org/10.1021/ma0345347

Paiuk, O. L., Mitina, N. Y., Riabtseva, A. O., Haramus, V. M., Dolynska, L. V., Nadashkevych, Z. Y., & Zaichenko, A. S. (2018). Structure and colloidal-chemical characteristics of polymeric surface active substances based on polyethylene glycol-containing macromeres. *Voprosy Khimii i Khimicheskoi Tekhnologii, 6*, 63–71. (in Ukrainian).

Panchuk, R. R., Chumak, V. V., Fil, M. R., Havrylyuk, D. Y., Zimenkovsky, B. S., Lesyk, R. B., & Stoika, R. S. (2012). Study of molecular mechanisms of proapoptotic action of novel heterocyclic 4-thiazolidone derivatives. *Biopolymers and Cell, 28*(2), 121–128. https://doi.org/10.7124/bc.00003d

Patra, J. K., Das, G., Fraceto, L. F., Campos, E. V. R., del Pilar Rodriguez-Torres, M., Acosta-Torres, L. S., et al. (2018). Nano based drug delivery systems: Recent developments and future prospects. *Journal of Nanobiotechnology, 16*(1), 71. https://doi.org/10.1186/s12951-018-0392-8

Reimer, L. (1998). *Scanning electron microscopy: Physics of image formation and microanalysis*. Springer. https://doi.org/10.1007/978-3-540-38967-5

Ren, J. M., McKenzie, T. G., Fu, Q., Wong, E. H., Xu, J., An, Z., et al. (2016). Star polymers. *Chemical Reviews, 116*(12), 6743–6836. https://doi.org/10.1021/acs.chemrev.6b00008

Riabtseva, A., Mitina, N., Boiko, N., Garasevich, S., Yanchuk, I., Stoika, R., et al. (2012). Structural and colloidal-chemical characteristics of nanosized drug delivery systems based on pegylated comb-like carriers. *Chemistry & Chemical Technology, 6*(3), 291–295.

Riabtseva, A., Mitina, N., Grytsyna, I., Boiko, N., Garamus, V. M., Stryhanyuk, H., et al. (2016). Func-tional micelles formed by branched polymeric surfactants: Synthesis, characteristics, and application as nanoreactors and carriers. *European Polymer Journal, 75*, 406–422. https://doi.org/10.1016/j.eurpolymj.2016.01.006

Rzayev, Z. M. (2011). Graft copolymers of maleic anhydride and its isostructural analogues: High performance engineering materials. arXiv preprint arXiv:1105.1260.

Sayle, R. A., & Milner-White, E. J. (1995). RASMOL: Biomolecular graphics for all. *Trends in Biochemical Sciences, 20*(9), 374–376. https://doi.org/10.1016/S0968-0004(00)89080-5

Schmidt, P. W. (1991). Small-angle scattering studies of disordered, porous and fractal systems. *Journal of Applied Crystallography, 24*(5), 414–435. https://doi.org/10.1107/S0021889891003400

Schmidt, P. W. (1995). Some fundamental concepts and techniques useful in small-angle scattering studies of disor-dered solids. In H. Brumberger (Ed.), *Modern aspects of small-angle scattering. Nato ASI series (Series C: Mathemati-cal and physical sciences)* (Vol. vol 451, pp. 1–56). Springer. https://doi.org/10.1007/978-94-015-8457-9_1

Senkiv, J., Finiuk, N., Kaminskyy, D., Havrylyuk, D., Wojtyra, M., Kril, I., et al. (2016). 5-Ene-4-thiazolidinones induce apoptosis in mammalian leukemia cells. *European Journal of Medicinal Chemistry, 117*, 33–46. https://doi.org/10.1016/j.ejmech.2016.03.089

Senkiv, Y., Riabtseva, A., Heffeter, P., Boiko, N., Kowol, C. R., Jungwith, U., et al. (2014). Enhanced anticancer activity and circumvention of resistance mechanisms by novel polymeric/phospholipidic nanocarriers of doxorubicin. *Journal of Biomedical Nanotechnology, 10*(7), 1369–1381. https://doi.org/10.1166/jbn.2014.1864

Simone, E. A., Dziubla, T. D., & Muzykantov, V. R. (2008). Polymeric carriers: Role of geometry in drug delivery. *Expert Opinion on Drug Delivery, 5*(12), 1283–1300. https://doi.org/10.1517/17425240802567846

Suk, J. S., Xu, Q., Kim, N., Hanes, J., & Ensign, L. M. (2016). PEGylation as a strategy for improving nanoparticle-based drug and gene delivery. *Advanced Drug Delivery Reviews, 99*, 28–51. https://doi.org/10.1016/j.addr.2015.09.012

Svergun, D. I. (1999). Restoring low resolution structure of biological macromolecules from solution scattering using simulated annealing. *Biophysical Journal, 76*(6), 2879–2886. https://doi.org/10.1016/S0006-3495(99)77443-6

Torchilin, V. P. (2010). Passive and active drug targeting: Drug delivery to tumors as an example. In M. Schäfer-Korting (Ed.), *Drug delivery. Handbook of experimental pharmacology* (Vol. vol 197). Springer. https://doi.org/10.1007/978-3-642-00477-3_1

Tsarevsky, N. V., Bencherif, S. A., & Matyjaszewski, K. (2007). Graft copolymers by a combination of ATRP and two different consecutive click reactions. *Macromolecules, 40*(13), 4439–4445. https://doi.org/10.1021/ma070705m

Tsuji, S., Aso, Y., Ohara, H., & Tanaka, T. (2019). Polymeric water-soluble activated esters: Synthesis of polymer backbones with pendant N-hydoxy-sulfosuccinimide esters for post-polymerization modification in water. *Polymer Journal, 51*(10), 1015–1022. https://doi.org/10.1038/s41428-019-0221-4

ud Din, F., Aman, W., Ullah, I., Qureshi, O. S., Mustapha, O., Shafique, S., & Zeb, A. (2017). Effective use of nanocarriers as drug delivery systems for the treatment of selected tumors. *International Journal of Nanomedicine, 12*, 7291. https://doi.org/10.2147/IJN.S146315

Zaichenko, A. S., Voronov, S. A., Shevchuk, O. M., Vasilyev, V. P., & Kuzayev, A. I. (1998). Kinetic features and molecular-weight characteristics of terpolymerization products of the systems based on vinyl acetate and 2-tert-butyl-peroxy-2-methyl-5-hexene-3-yne. *Journal of Applied Polymer Science, 67*(6), 1061–1066. https://doi.org/10.1002/(SICI)1097-4628(19980207)67:6<1061::AID-APP13>3.0.CO;2-3

Zhang, Q., & Mischnick, P. (2017). Influence of stereochemistry on relative reactivities of glucosyl and mannosyl residues in Konjac glucomannan (KGM). *Macromolecular Chemistry and Physics, 218*(17), 1700119. https://doi.org/10.1002/macp.201700119

Zhu, S., Hong, M., Tang, G., Qian, L., Lin, J., Jiang, Y., & Pei, Y. (2010). Partly PEGylated polyamidoamine dendrimer for tumor-selective targeting of doxorubicin: The effects of PEGylation degree and drug conjugation style. *Biomaterials, 31*(6), 1360–1371. https://doi.org/10.1016/j.biomaterials.2009.10.044

A Novel Water-Soluble C₆₀ Fullerene-Based Nano-Platform Enhances Efficiency of Anticancer Chemotherapy

Yuriy Prylutskyy, Olga Matyshevska, Svitlana Prylutska, Anna Grebinyk, Maxim Evstigneev, Sergii Grebinyk, Larysa Skivka, Vsevolod Cherepanov, Anton Senenko, Rostyslav S. Stoika, Uwe Ritter, Peter Scharff, Thomas Dandekar, and Marcus Frohme

1 Introduction

C_{60} fullerene (C_{60}) is the third allotropic form of carbon materials that has a stable spherical-like hollow structure with a diameter of 0.72 nm, which is close to that of the polypeptides' α-helix and steroid molecules. Thus, the steric compatibility of C_{60} with biological structures such as the recognizing sites of the receptor molecules or active centers of the enzyme was suggested (Prylutska, Panchuk, et al., 2017; Prylutska, Politenkova, et al., 2017; Skivka et al., 2018). Sixty carbon atoms connected by sp^3 single and sp^2 double bonds are located on the surface of the C_{60} molecule. The ability of C_{60} to scavenge various free radicals is an important physicochemical property of C_{60} that is also responsible for its biomedical effects (Goodarzi et al., 2017; Kepley, 2012; Moussa, 2018; Sandoval et al., 2019; Zhang

Y. Prylutskyy (✉) · L. Skivka
Taras Shevchenko National University of Kyiv, Kyiv, Ukraine

O. Matyshevska
Palladin Institute of Biochemistry, NAS of Ukraine, Kyiv, Ukraine

S. Prylutska
Taras Shevchenko National University of Kyiv, Kyiv, Ukraine

National University of Life and Environmental Sciences of Ukraine, Kyiv, Ukraine

A. Grebinyk · S. Grebinyk · M. Frohme
Technical University of Applied Sciences Wildau, Wildau, Germany
e-mail: sgrebinyk@th-wildau.de; mfrohme@th-wildau.de

M. Evstigneev
Laboratory of Organic Synthesis and NMR Spectroscopy, Belgorod State University, Belgorod, Russian Federation

V. Cherepanov · A. Senenko
Institute of Physics, NAS of Ukraine, Kyiv, Ukraine

et al., 2019), in particular, for protecting the biological systems against cell and tissue damages (Eswaran, 2018; Gharbi et al., 2005). Wang et al., 1999, reported that C_{60} and some of its derivatives efficiently prevented peroxidation and membrane breakdown triggered by free radical species and were more effective in inhibiting lipid peroxidation compared to vitamin E, a natural antioxidant. They weakened certain inflammatory processes (e.g., arthritis and acute inflammation in rats) and possibly facilitate the recovery of damaged tissue (Dragojevic-Simic et al., 2011; Kuznietsova et al., 2020; Yudoh et al., 2009). The water-soluble derivatives of C_{60} with potent antioxidant properties demonstrated robust neuroprotection against excitotoxic, apoptotic, and metabolic insults in cortical cell cultures (Dugan et al., 2001).

C_{60} is a hydrophobic molecule that is embedded into biological membranes and, thus, penetrates the cell (Franskevych et al., 2017; Grebinyk et al., 2018a; Grebinyk et al., 2018b). Its water-soluble derivatives were found to accumulate in mitochondria (Foley et al., 2002). However, the pristine C_{60} diffuses through the bilayered membrane 6–9 times faster, as compared with its hydrophilic derivatives which interact with polar groups on the membrane surface instead of entering the cell (Qiao et al., 2007; Santos et al., 2014).

Although pristine C_{60} has very low solubility in water, it can form aggregates in aqueous solutions producing stable colloid solutions, which contain both individual C_{60} and its nanoclusters (Prilutski et al., 1998; Ritter et al., 2015). The mechanism of C_{60} molecule dispersal in aqueous solutions might be explained by the formation of a covalent bond between the hydroxyls and carbons in the C_{60} cage, as a result of ultrasound treatment that culminates in a consequent easy C_{60} dissolution (Prylutskyy, Petrenko, et al., 2014).

C_{60} is active only in a soluble form when its carbon double bounds are freely accessible (Gharbi et al., 2005). Recently, we demonstrated that water-soluble pristine C_{60} prevented restraint stress-induced oxidative disorders in rats' brain and heart tissues (Gonchar et al., 2018). It also caused CCl_4/acetaminophen-induced acute liver injury (Halenova et al., 2016; Kuznietsova, Lynchak, Dziubenko, Herheliuk, et al., 2019; Kuznietsova, Lynchak, Dziubenko, Osetskyi, et al., 2019), corrected skeletal muscle functioning at ischemic injury (Nozdrenko et al., 2017), diminished muscle fatigue in rats, comparable to known exogenous antioxidants

R. S. Stoika
Institute of Cell Biology, National Academy of Sciences of Ukraine, Lviv, Ukraine
e-mail: stoika@cellbiol.lviv.ua

U. Ritter · P. Scharff
Technical University of Ilmenau, Institute of Chemistry and Biotechnology,
Ilmenau, Germany
e-mail: uwe.ritter@tu-ilmenau.de; peter.scharff@tu-ilmenau.de

T. Dandekar
University of Würzburg, Würzburg, Germany
e-mail: dandekar@biozentrum.uni-wuerzburg.de

N-acetylcysteine or β-alanine (Vereshchaka et al., 2018), markedly decreased the level of oxidative stress and enhanced antioxidant enzyme activities in diet-induced obesity rats (Halenova et al., 2018), realized the anti-inflammatory and hepatoprotective effects in a model of acute colonic inflammation (Byelinska et al., 2018), reduced manifestations of acute cholangitis in rats (Kuznietsova, Lynchak, Dziubenko, Herheliuk, et al., 2019, Kuznietsova, Lynchak, Dziubenko, Osetskyi, et al., 2019), and protected the heart and liver of tumor-bearing mice against Doxorubicin (Dox)-induced oxidative stress (Prylutska et al., 2014).

It should be noted that water-soluble pristine C$_{60}$ at low concentrations is not toxic for normal cells (Prylutska et al., 2009; Tolkachov et al., 2016): at concentrations up to 14.4, as well as 24 μg/mL, C$_{60}$ did not manifest any toxic effects in rat erythrocytes and thymocytes, as well as in human mesenchymal stem cells, respectively. Recently, a low toxicity (IC$_{50}$ 383.4 μg/mL) of water-soluble pristine C$_{60}$ was revealed in human embryonic kidney (HEK293) cells (Prylutska, Grebinyk, et al., 2019). Its selective strong toxic effect against tumor cells (rat and human glioma cells) and transformed human phagocytes was demonstrated (Skivka et al., 2018).

A combination of C$_{60}$ antioxidant potential (Dragojevic-Simic et al., 2011; Dugan et al., 2001; Eswaran, 2018; Gharbi et al., 2005; Kuznietsova et al., 2020; Wang et al., 1999; Yudoh et al., 2009) and its ability for drug delivery (Kumar & Raza, 2017) make that nanostructure very attractive for anticancer therapy. A coupling of cargo molecules of C$_{60}$ for passive targeting of cancer cells was achieved through the noncovalent interactions (Prylutska, Panchuk, et al., 2017; Skivka et al., 2018). π-π stacking interactions between unsaturated (poly)cyclic molecules determine supramolecular nanosized self-assemblies, commonly used for fast, easy, and cost-effective coupling of the cargo molecules with carbon nanoparticles (Pérez & Martín, 2015), improving stability and drug-loading capacity (Yang et al., 2018). The choice of cargo molecules for C$_{60}$-based drug delivery into cancer cells had its main focus on the aromatic structure to enable π-π stacking interactions. Taking into account the high toxicity of common chemotherapeutics and relatively low bioavailability of alternative chemotherapeutics, gold standards chemotherapeutics—Dox and Cisplatin (Cis) and a known herbal alkaloid Berberine (Ber)—were selected in the current study.

Dox contains a quinone-based rigid planar aromatic ring bound by a glycosidic bond to an aminosugar daunosamine (Cortés-Funes & Coronado, 2007; Tacar et al., 2013). Dox, first extracted from *Streptomyces peucetius* in the 1970s, continues to be routinely used nowadays for the treatment of many cancers including breast, lung, gastric, ovarian, thyroid, non-Hodgkin's and Hodgkin's lymphoma, multiple myeloma, sarcoma, thyroid, and pediatric cancers (Kumar & Raza, 2017; Yang et al., 2018). The main mechanism of Dox toxicity against cancer cells is its intercalation in the molecule of nuclear DNA, followed by the inhibition of topoisomerase activity, DNA transcription, replication, and repair (Kizek et al., 2012; Tacar et al., 2013). While Dox's adverse side effects on the cardiomyocytes are considered to be determined by another mechanism, mainly via formation of iron-related reactive oxygen species (Kizek et al., 2012; Thorn et al., 2011) through metal chelation

and flavoprotein reductases-associated redox cycling (Finn et al., 2011; Kizek et al., 2012). The extended generation of the reactive oxygen species (ROS) causes serious adverse cardiotoxicity owing to a high content of mitochondria in the cardiomyocytes (Jung & Reszka, 2001; Tacar et al., 2013; Thorn et al., 2011) that limits the drug's clinical application.

Cis is an alkylating agent that becomes activated only in the cytoplasm due to its relatively low chloride ion concentration (Galluzzi et al., 2014), where chloride atoms are displaced by water molecules. The hydrolyzed product binds nonreversely to the DNA purine residues, which leads to inter- and intra-strand crosslinks, blocking both mitochondrial and nuclear DNA replication (Dasari & Tchounwou, 2014; Fennell et al., 2016). On the other hand, hydrolyzed Cis readily reacts with the sulfhydryl groups of cytosolic peptides and proteins, including reduced glutathione (Jung & Reszka, 2001), which depletes the cytosol of reducing equivalents and promotes oxidative stress (Florea & Büsselberg, 2011; Galluzzi et al., 2014). DNA damage and ROS generation trigger apoptotic cell death upon simultaneous activation of several signaling pathways (Galluzzi et al., 2014). Despite positive treatment effects of Cis, it is a poison; therefore, patients receiving this agent experience severe side effects that limit the administered clinical dose (Dasari & Tchounwou, 2014; Florea & Büsselberg, 2011).

Historically, natural products have always provided drugs against a wide variety of diseases, with cancer being no exception (Shewach & Kuchta, 2009). Herbal secondary metabolites exhibit multiple biological and pharmacological properties, representing a natural library of the bioactive compounds with potentially high safety, availability, and accessibility, and low cost. Ber is the isoquinoline quaternary alkaloid, also known as a common drug in Ayurvedic, Chinese, Middle-Eastern, and American folk medicines due to its board spectra of biological activities (Neag et al., 2018; Pereira et al., 2007). Ber applications as a low-cost therapeutic with anti-inflammatory, antimutagenic (Cernáková et al., 2002), antidiabetic (El-Wahab et al., 2013), antimicrobial, and antiviral medicne, seem promising (Cai et al., 2014). In recent years, Ber has been reported to inhibit proliferation of many cancer cell lines (Grebinyk, Yashchuk, Bashmakova, et al., 2019; Park et al., 2015; Seo et al., 2015; Zhang et al., 2013). However, the hormetic effect (Bao et al., 2015), poor water solubility, low stability, and bioavailability (Mirhadi et al., 2018) limit clinical applications of Ber.

An efficient clinical practice in cancer therapy is challenged with a number of setbacks, including poor specificity, high general toxicity, and induction of drug resistance in cancer cells (Chen et al., 2016; Shi et al., 2017). Thus, new approaches to improve efficiency and attenuate side effects are urgently needed. Reducing the side effects of these drugs might be achieved by creating an effective targeted delivery nanosystem based on a biocompatible and bioavailable C_{60} (Borowik et al., 2018; Ritter et al., 2015). One can suggest that C_{60} noncovalent complexation with a traditional drug is a promising nanoformulation for targeted drug delivery, substantially increasing its medico-biological effectiveness with a novel dosage form in a subsequent preclinical screening.
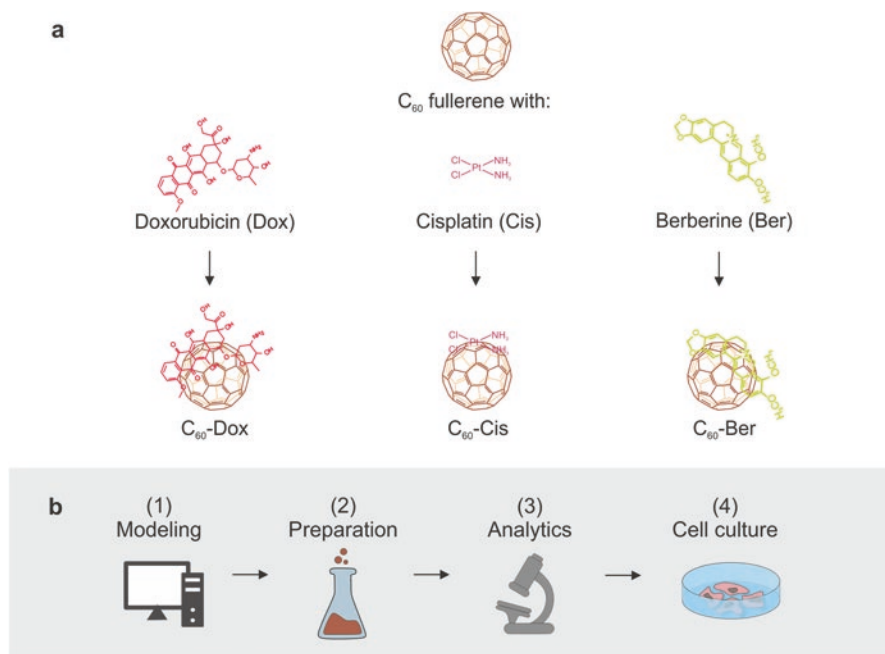
Fig. 1 Development of C$_{60}$-based cancer chemotherapy for optimization of efficiency of the chemotherapeutic drugs: (**a**) structure of drugs and their nanocomplexes with C$_{60}$; (**b**) workflow of the study: computer modeling of the C$_{60}$-drug nanocomplex (1); the fast and cost-effective preparation of nanocomplexes in different molar ratios in aqueous solution (2); the analytical assessment of nanocomplex stability in order to prove its biological applicability (3); noncovalent complexation of chemotherapy drug with C$_{60}$ improves its efficiency toward cancer cells in vitro (4)

The purposes of our work were to test the formation of the C$_{60}$-drug nanocomplexes in aqueous solutions using computer simulation and physicochemical characterization and to evaluate their toxic potential toward cancer cells compared to the action of free chemotherapeutic drugs in in vitro systems (Fig. 1).

2 Self-Organization of Pristine C$_{60}$ in Aqueous Solutions

In the late 1990s, much attention had been paid to the properties of C$_{60}$ in organic solvents, which had facilitated analogous studies in aqueous solutions (Deguchi et al., 2001; Mchedlov-Petrossyan, 2013; Ritter et al., 2015). To date, C$_{60}$ is considered as a colloidal particle due to the fact that its diameter is equal ~1 nm. This conclusion originates from the traditional point of view that the 1 nm corresponds to the lower border of the colloidal range of dispersity, and the range of true solutions is under this limit. Thus, aqueous solutions of C$_{60}$ must feature properties of

colloidal systems, which contain associates of solvated C_{60} of different sizes (Peudus et al., 2020; Prylutskyy et al., 2013). A further study of the pristine C_{60} aqueous solution (C_{60}FAS) was aimed at characterization of the clusters' structure and morphology.

Various complicated techniques are used for characterization of biomedical nanomaterials include the basic microscopic: scanning electron microscopy (SEM) or transmission electron microscopy (TEM), atomic-force microscopy (AFM) or scanning tunneling microscopy (STM)) and spectroscopic (UV-Vis, FTIR (Fourier transform infrared) and Raman spectroscopy, mass and energy-dispersive X-ray (EDX) spectrometry, dynamic light scattering (DLS) and small angle neutron scattering (SANS) techniques. Considering that biomaterials must be water soluble, monitoring their morphology in aqueous solutions is important for checking colloid stability (zeta-potential value (DLS)), shape (SEM) and size distribution profile (AFM and DLS) of particles, which can affect their specific bioactivity and toxicity.

A variety of physical methods has been applied in order to understand the specificity of C_{60} cluster formation. Characterization of C_{60} particles in aqueous solutions has been accomplished by means of UV-Vis spectroscopy (Bulavin et al., 2000; Ritter et al., 2015; Scharff et al., 2004), STM (Ritter et al., 2015), AFM (Prylutskyy, Evstigneev, et al., 2014; Prylutskyy, Petrenko, et al., 2014; Ritter et al., 2015), DLS (Brant et al., 2005; Meng et al., 2013; Ritter et al., 2015; Prylutska, Grebinyk, et al., 2019; Prylutska, Grynyuk, et al., 2019; Prylutska, Lynchak, et al., 2019), FTIR, and Raman (Prylutskyy, Evstigneev, et al., 2014; Prylutskyy, Petrenko, et al., 2014; Scharff et al., 2004) spectroscopy, as well as SANS technique (Borowik et al., 2018, Prylutska, Panchuk, et al., 2017, Prylutska, Politenkova, et al., 2017, Prylutskyy et al., 2016, Prylutskyy, Evstigneev, et al., 2014 , Prylutskyy, Petrenko, et al., 2014).

The purity of the prepared C_{60}FAS sample (i.e., the presence/absence of any residual impurities, for example carbon black, toluene phase) is an important factor that influences its toxicity. It was determined by the high-performance liquid chromatography (HPLC; Jasco PU-2086) and gas chromatography/mass spectrometry (GC/MS) techniques. Insoluble impurities in the prepared C_{60}FAS (0.15 mg/mL) samples were determined by ultra-centrifugation. It turned out that they were less than 1 μg/mL. Toluene from the synthesis could not be detected in the water by GC/MS analysis. ^{1}H NMR spectrum (400 MHz) of C_{60}FAS recorded in heavy water did not reveal any residual proton signals (Ritter et al., 2015).

The most direct and readily accessible UV-Vis (double-beam spectrophotometer SQ-4802; UNICO, USA) spectroscopy evidenced the existence of three most intense broad UV absorption bands with maxima at 208, 265, and 347 nm and generally resembles that in organic solvents (Ritter et al., 2015). The assignment of these bands to particular electron transitions, and the computation of the corresponding electronic parameters have been done (Prylutskyy et al., 2001). The common feature of the UV-Vis spectra of C_{60}FAS is light scattering, most evidently seen on dilution and affecting the value of absorption.

The composition of C_{60}FAS was typically monitored using AFM ("Solver Pro M" system; NT-MDT, Russia) technique (Prylutskyy, Evstigneev, et al., 2014, Prylutskyy, Petrenko, et al., 2014, Ritter et al., 2015). The AFM data demonstrate

randomly arranged individual C_{60} molecules with diameter ~0.7 nm and their bulk sphere-like aggregates with a height of 2–50 nm. Interestingly, some individual C_{60} aggregates with a height of ~100 nm were also reported in the probe microscopy images, indicating a polydisperse nature of $C_{60}FAS$, including either monomers or aggregates having diameters ranging from several to hundreds of nanometers.

The above results have also been confirmed by DLS (Zetasizer Nano-ZS90; Malvern, UK) data (Ritter et al., 2015). The wide distribution of hydrodynamic dimensions of C_{60} particles by intensity with Z-average ~70–120 nm most directly evidences the polydispersity. Moreover, experimental data indicate that the structural and morphological features of polydisperse C_{60} aggregates present in aqueous solutions remain essentially similar for different methods of $C_{60}FAS$ preparation as well (Prylutskyy, Evstigneev, et al., 2014, Prylutskyy, Petrenko, et al., 2014).

Thus, the prepared $C_{60}FAS$ contains mainly single C_{60} molecules and their nano-aggregates with a size of 2–100 nm, which can be a key stage in the mechanism of the in vivo and in vitro $C_{60}FAS$ biological synergy.

The magnitude of zeta-potential of C_{60} FAS which is related to the stability of colloid dispersions, spans a relatively wide range from −9 up to −38 mV (Deguchi et al., 2001; Prylutska, Grebinyk, et al., 2019; Prylutska, Grynyuk, et al., 2019; Prylutska, Lynchak, et al., 2019; Ritter et al., 2015; Wierzbicki et al., 2013) and evidences the presence of negative charge on the surface of C_{60} molecules in solution. A high negative charge of colloid clusters (or, more strictly, the electrostatic repulsion between the negatively charged clusters) plays a significant role in stabilization of $C_{60}FAS$ (i.e., it disfavors the aggregation and makes the solution electrically stable): the zeta-potential value (Zetasizer Nano-ZS90; Malvern, UK) was −25.3 mV at room temperature (Prylutska, Grebinyk, et al., 2019, Prylutska, Grynyuk, et al., 2019, Prylutska, Lynchak, et al., 2019), indicating a high solute stabilization.

The presence of negative charge on the C_{60} surface is a generally accepted fact and is considered the key, but not the sole, factor of C_{60} solubility in aqueous solutions. The formation of the ordered, H-bonded, and sphere-like hydrated shells around fullerene's surface is another important issue extensively discussed over the past decade (Bulavin et al., 2000; Choi et al., 2015; Prylutskyy, Evstigneev, et al., 2014; Prylutskyy, Petrenko, et al., 2014; Scharff et al., 2004). However, FTIR (Perkin-Elmer BX-II spectrophotometer) spectroscopy data suggested that there is one more factor that should also be considered (Prylutskyy, Evstigneev, et al., 2014, Prylutskyy, Petrenko, et al., 2014). The FTIR spectrum of $C_{60}FAS$ displays the typical pattern of peaks which could be expectedly assigned to C-C vibrational modes of C_{60} molecule. However, additional peaks were reported independent of the method of $C_{60}FAS$ preparation and corresponded to C-O stretching. It strongly suggests that C_{60} cage is hydroxylated and hydroxyls forming alcohol functional groups exist in the structure of C_{60} in water. Hence the primary mechanism of C_{60} solubilization in water could be the attachment of the OH-groups to C_{60} carbons (Prylutskyy, Evstigneev, et al., 2014, Prylutskyy, Petrenko, et al., 2014) which explains why the single C_{60} molecules and their clusters exist at equilibrium in solutions for quite a long time. It also explains the irreversible character of the adsorption/desorption

isotherms (Labille et al., 2006) and the minimal extraction of C_{60} from water colloid solutions by toluene (Deguchi et al., 2001). The covalent attachment of the OH-groups does not exclude the possibility of electron transfer from water molecules to C_{60}, enabling to explain the negative charge of C_{60} particles.

3   Self-Organization of C_{60}-Drug Mixture

The possibility of modification of biological and/or physicochemical properties of C_{60} or drug was mainly considered in terms of covalent conjugation of the drug molecules with C_{60} (Liu et al., 2010; Montellano et al., 2011). On the other hand, the presence in the structure of a C_{60} molecule of the aromatic surface composed of conjugated carbon rings suggests the possibility of its effective interactions via π-stacking with aromatic moieties of proteins, nucleic acid bases, aromatic vitamins, antibiotics, and other compounds that may be present in bio-system. Hence, the noncovalent complexation of C_{60} with bio-receptors and aromatic drugs may contribute to some extent to the observed biological effects at the cellular and organism levels. During the past few years, two sets of reports appeared evidencing a strong biological interaction in vitro and *in vivo* between C_{60} and the aromatic antitumor drugs (Panchuk et al., 2015; Prylutska et al., 2015; Prylutska, Panchuk, et al., 2017; Prylutska, Politenkova, et al., 2017; Skamrova et al., 2014). A peculiarity of that interaction was the following: (i) the most pronounced effect was observed during simultaneous administration of the drug and C_{60}; (ii) the physicochemical interaction of the drug with C_{60} is noncovalent; (iii) the preliminary indices of correlation of the in vitro biological effect with equilibrium constant of complexation of C_{60} with the aromatic drug molecules were noted (Skamrova et al., 2014). Thus, the knowledge of how C_{60} molecules interact with drugs is important for better understanding the mechanism of the medico-biological action of C_{60}.

Below, the main results of structural and thermodynamic analysis of the C_{60} interaction with Dox, Cis, and Ber as systems that have been most extensively investigated to date compared with others are presented.

3.1   *C_{60} Complexation with Dox*

In order to detect the complexation between C_{60} and antibiotic Dox, a range of physicochemical methods was applied (Evstigneev et al., 2013; Mosunov et al., 2017; Panchuk et al., 2015; Prylutskyy et al., 2016; Prylutskyy, Evstigneev, et al., 2014; Prylutskyy, Evstigneev, et al., 2015; Prylutskyy, Petrenko, et al., 2014). Under conditions of neutral aqueous solutions, the Dox molecule bears a positive charge, whereas the C_{60} is negatively charged. The AFM ("Solver Pro M" system; NT-MDT, Russia) study of the C_{60}-Dox mixture in a low concentration range in a nonsalted aqueous solution evidenced the formation of new island-type structures, which were assigned to the complexes between the C_{60} and Dox molecules (Prylutskyy,

Evstigneev, et al., 2014). Similar data were reported in the physiological solution, although in that case, the interpretation of the results was strongly obscured by the presence of salt crystals (Prylutskyy, Evstigneev, et al., 2015). The C$_{60}$-Dox interaction was also displayed by the UV-Vis (double-beam spectrophotometer SQ-4802; UNICO, USA) spectroscopy by hypochromic changes of the absorption maximum with a slight bathochromic shift with increasing C$_{60}$ concentration (Evstigneev et al., 2013; Panchuk et al., 2015; Prylutskyy, Evstigneev, et al., 2014). The DLS (Zetasizer Nano-ZS90; Malvern, UK) study of C$_{60}$-Dox mixture gave a pronounced positive shift of zeta-potential peak, evidencing shielding of the C$_{60}$ molecule negative charge and charging of these clusters by complexation of positively charged Dox with C$_{60}$ nanoclusters (Prylutskyy, Evstigneev, et al., 2015). A remarkable change in the translational diffusional motion of Dox molecules on the addition of C$_{60}$, monitored by diffusion-ordered NMR (Bruker Avance III NMR spectrometer, Bruker Biospin, Germany) spectroscopy (DOSY), supported the existence of complexation (Prylutskyy, Evstigneev, et al., 2014). Finally, the SANS (small-angle diffractometer YuMO at the IBR-2 pulsed reactor (JINR, Dubna, Russian Federation)) study yielded the distribution function of pair distances, pointing out the existence of at least two statistically different entities in aqueous solutions, which are the C$_{60}$ aggregates and nanocomplexes between the C$_{60}$ and Dox molecules (Prylutskyy et al., 2016). The qualitative experimental data were complemented by the calculation of the most probable structure of the C$_{60}$-Dox nanocomplex, from which the maximal filling of the C$_{60}$ surface by three Dox molecules was noted (Fig. 2a) (Evstigneev et al., 2013; Panchuk et al., 2015).

The physical model of C$_{60}$-Dox interaction is based on two main statements (Prylutskyy, Evstigneev, et al., 2014). The hydration shell around the C$_{60}$ cannot be detached by Dox complexation, resulting in a big distance (~0.5 Å) between the surfaces of Dox and C$_{60}$ molecules in the nanocomplex. As a consequence, magnetic ^{1}H NMR shielding should be minimal (as evidenced in the NMR (Bruker Avance III NMR spectrometer, Bruker Biospin, Germany) experiment), and the enthalpic contribution from the van der Waals and electrostatic forces should be damped (as
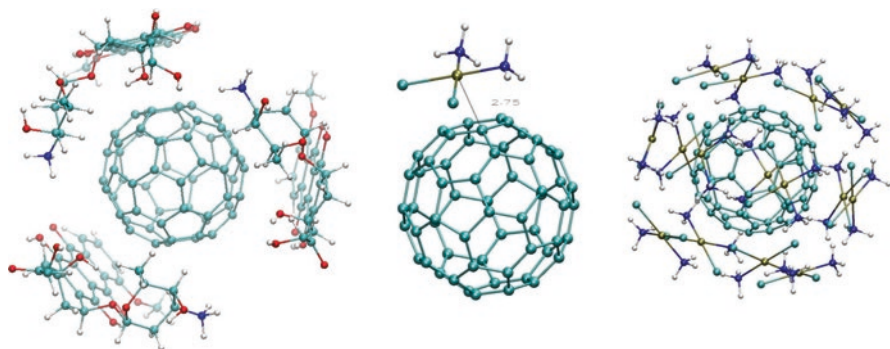

Fig. 2 The calculated structures of 1:3 C$_{60}$-Dox nanocomplex (**a**), 1:1 (**b**) and 1:15 (**c**) C$_{60}$-Cis nanocomplexes. (Reproduced with permission (Panchuk et al., 2015; Prylutska, Lynchak, et al., 2019))

evidenced in isothermal titration calorimetric (ITC; AutoITC isothermal titration calorimeter (MicroCal Inc. GE Healthcare, USA)) experiment). Hence, the C_{60}-Dox complexation appears to be the entropically driven, that is, mainly governed by hydrophobic forces due to the removal of water molecules from the second- and higher-level hydration shells around C_{60}. Binding of Dox molecules at moderate and high C_{60} concentrations mainly occurs by means of their adsorption into large C_{60} fullerene clusters, resulting in the effect called "ligand-induced C_{60} aggregation." In brief, positively charged Dox molecules being absorbed by the negatively charged C_{60} nanoclusters induce an additional cluster growth due to attenuated electrostatic repulsion between C_{60} molecules, displayed by additional light scattering (as evidenced in UV-Vis (double-beam spectrophotometer SQ-4802; UNICO, USA) experiment).

The proposed physical model of C_{60}-Dox interaction enabled us to build the thermodynamical model of their interaction and compute the corresponding equilibrium hetero-complexation constant, $K_L \approx 60,000$ M^{-1} (Evstigneev et al., 2013; Mosunov et al., 2017; Mosunov et al., 2019). This value was further used to correlate the relative in vitro biological effect of the action of C_{60}-Dox mixture on human buccal epithelium cells (Borowik et al., 2018) and to compare the C_{60} hetero-complexation affinity to various drugs (Evstigneev et al., 2013; Mosunov et al., 2017; Mosunov et al., 2019).

3.2 C_{60} Complexation with Cis

Investigation of possible complexation between the C_{60} and Cis molecules was carried out using a protocol generally similar to that reviewed above for C_{60}-Dox interaction (Prylutskyy, Cherepanov, et al., 2015, Prylutskyy, Evstigneev, et al., 2015). It should be noted that a direct complexation between these molecules should likely be relatively weak, as compared with the C_{60}-Dox system, because the π-stacking in the former case would be absent. Quite expectedly, the UV-Vis (double-beam spectrophotometer SQ-4802; UNICO, USA) spectra gave minor signs of interaction, and the ITC (AutoITC isothermal titration calorimeter (MicroCal Inc. GE Healthcare, USA)) data demonstrated nearly zero heat effect. In contrast, the SANS-derived pair distribution function (small-angle diffractometer YuMO at the IBR-2 pulsed reactor (JINR, Dubna, Russian Federation)) had evidenced the existence of two apparent statistically different entities in the aqueous solution, one of which was assigned to the C_{60}-Cis nanocomplex. This finding was partly supported by the results of SEM (JSM-35 SEM, Japan) and DLS (Zetasizer Nano-ZS90; Malvern, UK) studies. The latter investigation demonstrated an apparent shift in the distribution of the hydrodynamic radii of light-scattering nanoparticles to higher numbers on addition of Cis to the C_{60} solution. The energy-minimized structures with a minimal as well as theoretically maximal filling of the C_{60} surface with Cis molecules are shown in Fig. 2b, c (Prylutska, Grebinyk, et al., 2019, Prylutska, Grynyuk, et al., 2019, Prylutska, Lynchak, et al., 2019, Prylutska, Panchuk, et al., 2017, Prylutska, Politenkova, et al., 2017, Prylutskyy, Cherepanov, et al., 2015, Prylutskyy, Evstigneev, et al., 2015). The complexation of Cis with C_{60} is entropic by origin and

is totally driven by the hydrophobic interactions. The binding of Cis occurs mainly into large C_{60} nanoclusters via nonspecific adsorption, although the existence of weak 1:1 or 1:15 C_{60}-Cis nanocomplexes cannot be ruled out. Taking into account the fact that the adsorption into C_{60} clusters is relatively nonspecific to the type of drug, one could expect the value of equilibrium hetero-complexation constant for the C_{60}-Cis nanocomplex close to that reported for the adsorption phase for the aromatic molecules, that is, $K_L \approx 500$ M^{-1} (Mosunov et al., 2019).

3.3 C_{60} Complexation with Ber

The AFM ("Solver Pro M" system; NT-MDT, Russian Federation) characterization of the C_{60}-Ber nanocomplex films was challenged with the proximity of sizes of single C_{60} and Ber molecules. Our preliminary studies revealed that different nature of the intermolecular interaction of free C_{60} and Ber determines different types of adsorption of these substances. It was found (Grebinyk, Prylutska, Buchelnikov, et al., 2019, Grebinyk, Prylutska, Chepurna, et al., 2019, Grebinyk, Prylutska, Grebinyk, et al., 2019, Grebinyk, Yashchuk, Bashmakova, et al., 2019) that the continuous submonolayer was presented in the layer of the nanocomplex system is typical for the Ber films (its thickness is (0.35–0.5) nm); the single objects were identified as C_{60} molecules or their nanoclusters (0.7–2) nm. Besides, we observed conglomerates with a height of (1–2.5) nm, absent in the layers of free C_{60} and Ber. Therefore, one can assume that these conglomerates are the mixture of C_{60} and Ber. The origin of conglomerates can be explained by the fact that the interaction of negatively charged C_{60} nanoclusters with Ber$^+$ cations in aqueous solutions is accompanied by their coagulation (Fig. 3a, b).
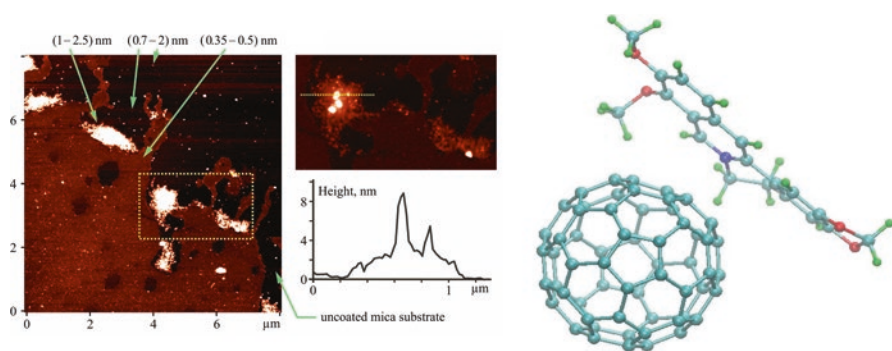
Fig. 3 AFM image of the C_{60}-Ber layer (**a**). Numbers with arrows show the height of nano-objects. Highlighted in image (**a**) 3.5 × 2μm^2 fragment with reduced contrast and its Z-profile along the marked line are shown in (**b**). Energy-minimized structure of 1:1 C_{60}-Ber nanocomplex (**c**). (Reproduced with permission (Grebinyk, Prylutska, Buchelnikov, et al., 2019, Grebinyk, Prylutska, Chepurna, et al., 2019, Grebinyk, Prylutska, Grebinyk, et al., 2019, Grebinyk, Yashchuk, Bashmakova, et al., 2019))

The UV-Vis (double-beam spectrophotometer SQ-4802; UNICO, USA) spectroscopy revealed that an increase in C_{60} concentration was followed by the nonmonotonic change in the Ber spectrum with a slight bathochromic shift of its absorption maximum that was induced by the ligand adsorption into large C_{60} nanoclusters. An increase in Ber concentrations in C_{60}-Ber nanocomplexes was followed by a gradual increase in the particle size and the zeta-potential value (Zetasizer Nano-ZS90; Malvern, UK) from -21.26 to -19.51 mV, which was linked to the Ber-induced C_{60} aggregation and the complexation of Ber cations with negatively charged C_{60}. The computer simulation revealed that π-stacking was the dominating force on Ber and C_{60} binding in aqueous solution and allowed to propose the energy-minimized structure of 1:1 C_{60}-Ber nanocomplex with a 1.05 nm minimum distance from C_{60} to Ber nitrogen atom and 1.42 nm maximum distance from C_{60} to the Ber hydrogen atom (Fig. 3c) (Grebinyk, Prylutska, Buchelnikov, et al., 2019, Grebinyk, Prylutska, Chepurna, et al., 2019, Grebinyk, Prylutska, Grebinyk, et al., 2019, Grebinyk, Yashchuk, Bashmakova, et al., 2019).

Although the investigated drugs are different in regard of chemical structure and properties, their thermodynamic patterns of binding with C_{60} were generally similar. Apart from certain specificities of binding, the complexation was found to be generally nonspecific, entropic by origin, and occurring mainly into large C_{60} nanoclusters, governed by hydrophobic interactions. This physicochemical mechanism may be further transferred onto the biological system, viz. on simultaneous administration, the hydrophobic C_{60} nanoclusters incorporating Dox, Cis, or Ber molecules protect them from the reactive environment when moving in biological fluid. Hence, both single C_{60} and its nanoclusters may act as a delivery system and elevate the active concentration of the drug inducing the biological effect.

In summary, a noncovalent complexation of the chemotherapy drugs with the C_{60} in aqueous solutions opens a new strategy in cancer therapy, namely the use of such nanoformulation for tumor treatment.

4   Anticancer Activity *In Vitro* of Chemotherapeutic Drugs Complexed with C_{60}

Nanocarriers have been extensively investigated as promising remedies for medical diagnostics, drug delivery, and cancer treatment. Owing to their high surface area to volume ratio, they possess the ability to alter basic properties and bioactivity of drugs, improving their stability, pharmacokinetics, bio-distribution, site-specific delivery, and controlled release, also providing decreased toxicity. Moreover, the physicochemical properties of nanocarriers can be finely tuned by altering their composition (organic, inorganic, or hybrid) and surface properties (charge, functional groups, PEGylation or other coating, attachment of targeting functional moieties) (Conde et al., 2013, see also part 2 of this chapter).

Due to the multidrug resistance of different cancer cells caused by the over-expression of drug export pumps, such as P-glycoprotein (P-gp), on cell membrane, an effective treatment of many cancers stays limited. The use of targeting the moiety of specific nanoparticles entering cells through endocytosis can bypass the P-gp efflux pump, leading to greater intracellular accumulation of drugs (Li et al., 2017). Thus, using nanoparticles provides an opportunity for designing properties that are not possible with other types of therapeutic drugs, and have a bright future as a new generation of anticancer therapeutics. Although there are certain critical questions and many challenges for the clinical development of nanoparticles, as more clinical data are available, further understanding in nanotechnology will certainly lead to a more rational design of optimized nanoparticles with improved selectivity, efficacy, and safety.

Below, the main results of toxic action in vitro of the created water-soluble C_{60}-Dox, C_{60}-Cis, and C_{60}-Ber nanocomplexes toward various cancer cell lines are presented.

4.1 Cytotoxic Action of C_{60}-Dox Nanocomplex

Viability of human leukemic cells of different lines (CCRF-CEM, Jurkat, THP1, and Molt-16) was estimated by using MTT-test at 24, 48, and 72 h incubation in the presence of C_{60}-Dox nanocomplexes, as well as of free Dox separately at equivalent concentrations (Grebinyk, Prylutska, Buchelnikov, et al., 2019, Grebinyk, Prylutska, Chepurna, et al., 2019, Grebinyk, Prylutska, Grebinyk, et al., 2019, Grebinyk, Yashchuk, Bashmakova, et al., 2019). It was found that C_{60} alone had no effect on the viability of the leukemic cells at concentrations equivalent to those in the nano-complexes (not shown).

Figure 4 shows the time- and concentration-dependent decrease in the viability of the leukemic cells under Dox treatment. The drug in the nM dose range exhibited toxicity toward leukemic cells. The sensitivity of leukemic cells to the Dox followed the order Molt-16 ˃ THP1 ˃ Jurkat ˃ CCRF-CEM (less sensitive).

Under the action of 100 nM Dox, the viability of CCRF-CEM cells was decreased to 84 ± 7, 50 ± 4, and $34 \pm 7\%$, compared to the control (nontreated cells) at 24, 48, and 72 h, respectively. A comparable pattern of 100 nM Dox toxic effect was also found in Jurkat cells. The viability of THP1 cells under treatment with 100 nM Dox cells was 50 ± 4, 47 ± 5, and $13 \pm 4\%$ at 24, 48, and 72 h, respectively. The estimated half-maximal inhibitory Dox concentrations (IC_{50}) for CCRF-CEM, THP1, and Jurkat cells at 72 h incubation were 80 ± 9, 43 ± 5, and 38 ± 6 nM, respectively. These results correspond to literature data (Antunovic et al., 2015; Scott et al., 1986).

Molt-16 cells were the most sensitive to the drug, since its toxic effect was detected within 1 to 25 nM range at all periods of cell incubation. The viability of Molt-16 cells treated with 5 nM Dox decreased to 75 ± 4, 28 ± 4, and $18 \pm 4\%$ of that in control at 24, 48, and 72 h, respectively, and the value of IC_{50} at 72 h was equal to 2.0 nM. Similar high sensitivity of Molt-16 cells with 10-times more
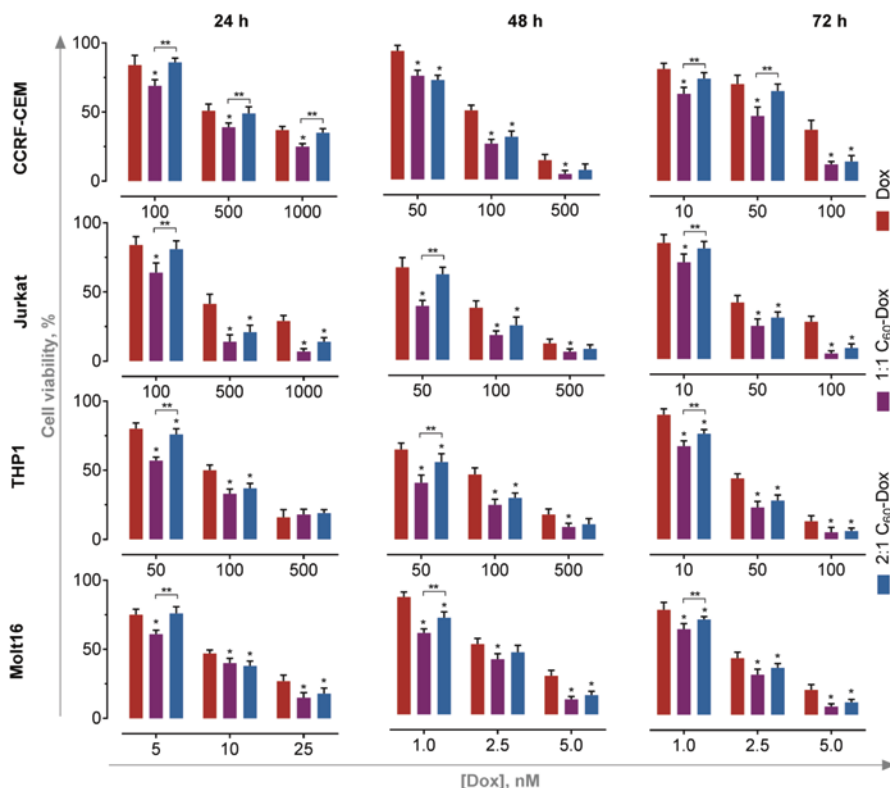
Fig. 4 Viability of CCRF-CEM, Jurkat, THP1, and Molt16 leukemic cells treated with equal doses of free Dox or C_{60}-Dox nanocomplexes for 24, 48, and 72 h. MTT-test. (Reproduced with permission (Grebinyk, Prylutska, Buchelnikov, et al., 2019)

intensive apoptosis induction in comparison with Jurkat T-cells under treatment of herbal alkaloid was reported by Cai et al., 2001.

Cells treated with free Dox were used as a control to assess cell viability under the action of C_{60}-Dox nanocomplexes at the equivalent doses of the drug. The value of IC_{50} for the free Dox and C_{60}-Dox nanocomplexes was calculated for each time point and cell line, and listed in Table 1.

It was shown that both C_{60}-Dox nanocomplexes possessed higher toxic potential than the free Dox against human leukemic cell lines (Fig. 4). So, the 100 nM 1:1 C_{60}-Dox nanocomplex exhibited 1.3, 2.1, and 6.8-fold enhanced toxicity toward Jurkat T-cells, in comparison with free drug at 24, 48, and 72 h, respectively. Under the treatment with the 100 nM 2:1 C_{60}-Dox nanocomplex, a decrease in the viability of Jurkat T-cells was estimated at the level of 1.5 and 3.4-fold, as compared with the effect of free drug at 48 and 72 h, respectively. A similar pattern of enhancement of drug toxicity after its complexation with C_{60} was found in other leukemic cell lines

Table 1 Half-maximal inhibitory concentration (IC_{50}, nM) of free and C_{60}-bound Dox in human leukemic cell lines

Cell line	Dox	24 h	48 h	72 h
CCRF-CEM	Dox	579 ± 51	98 ± 7	80 ± 9
	1:1 C_{60}-Dox	299 ± 54	71 ± 4*	23 ± 8*
	2:1 C_{60}-Dox	543 ± 48	72 ± 5*	32 ± 7*
Jurkat	Dox	419 ± 50	75 ± 9	38 ± 6
	1:1 C_{60}-Dox	148 ± 19*	35 ± 7*	19 ± 3*
	2:1 C_{60}-Dox	236 ± 33*,**	60 ± 5*	26 ± 3*,**
THP1	Dox	113 ± 16	93 ± 13	43 ± 5
	1:1 C_{60}-Dox	57 ± 11*	33 ± 7*	20 ± 3*
	2:1 C_{60}-Dox	77 ± 9*,**	56 ± 8*,**	21 ± 3*
Molt-16	Dox	23 ± 2	2.7 ± 0.2	2.0 ± 0.1
	1:1 C_{60}-Dox	16 ± 2*	1.5 ± 0.2*	1.3 ± 0.2*
	2:1 C_{60}-Dox	19 ± 2*,**	1.9 ± 0.1*,**	1.6 ± 0.1*,**

*$p \leq 0.05$ in comparison with the free Dox; **$p \leq 0.05$ in comparison with the 1:1 C_{60}-Dox nano-complex, $n = 5$

(Fig. 4). Under the treatment of 100 nM 1:1 C_{60}-Dox nanocomplex, the viability of CCRF-CEM cells decreased further by 1.2, 1.9, and 3.1 times, and the viability of THP1 cells by 1.5, 1.9, and 2.6-times at 24, 48, and 72 h, respectively. Under the treatment of 100 nM 2:1 C_{60}-Dox nanocomplex, the viability of CCRF-CEM cells decreased by 1.3 and 2.6 times at 48 and 72 h, and the viability of THP1 cells by 1.4, 1.6 and 2.2 at 24, 48 and 72 h, respectively. The enhancement of Dox toxicity due to its complexation with C_{60} was confirmed in experiments with Molt-16 cells. The 1:1 C_{60}-Dox nanocomplex decreased the viability by 1.2, 2.5, and 3.0 times at 24, 48, and 72 h, respectively, whereas the 2:1 C_{60}-Dox nanocomplex by 2.0 times at both 48 and 72 h, in comparison with the action of 5 nM Dox in free form.

In summary, our experiments showed enhanced toxicity of Dox up to 3.5-fold for four cell lines. The 1:1 C_{60}-Dox nanocomplex demonstrated higher toxicity in comparison with the 2:1 C_{60}-Dox nanocomplex. The less pronounced effect (IC_{50} decrease by ≥ 2.5 times, compared with that for free Dox) of the 2:1 C_{60}-Dox nanocomplex could be attributed to the higher concentration of C_{60} as a component. Due to its antioxidant activity (Castro et al., 2017; Gharbi et al., 2005), C_{60} can protect cells toward Dox-associated oxidative stress (Thorn et al., 2011).

In order to investigate a potential correlation between the enhanced toxic effect of C_{60}-Dox nanocomplexes and more effective intracellular drug accumulation, the cellular uptake of free Dox and C_{60}-Dox nanocomplex was studied. Since Dox possesses strong absorption and fluorescence in the visible spectral region (Changenet-Barret et al., 2013; Husseini et al., 2016), the tracking of C_{60}-Dox nanocomplexes is possible with noninvasive direct fluorescent-based techniques. CCRF-CEM cells were incubated in the presence of 1 μM Dox or C_{60}-Dox nanocomplexes in a drug-equivalent concentration, examined with fluorescent microscopy, and subjected to flow cytometry to quantify the intracellular level of the accumulated drug after 1, 3, and 6 h treatment (Fig. 5). The mean fluorescence intensity of each sample was
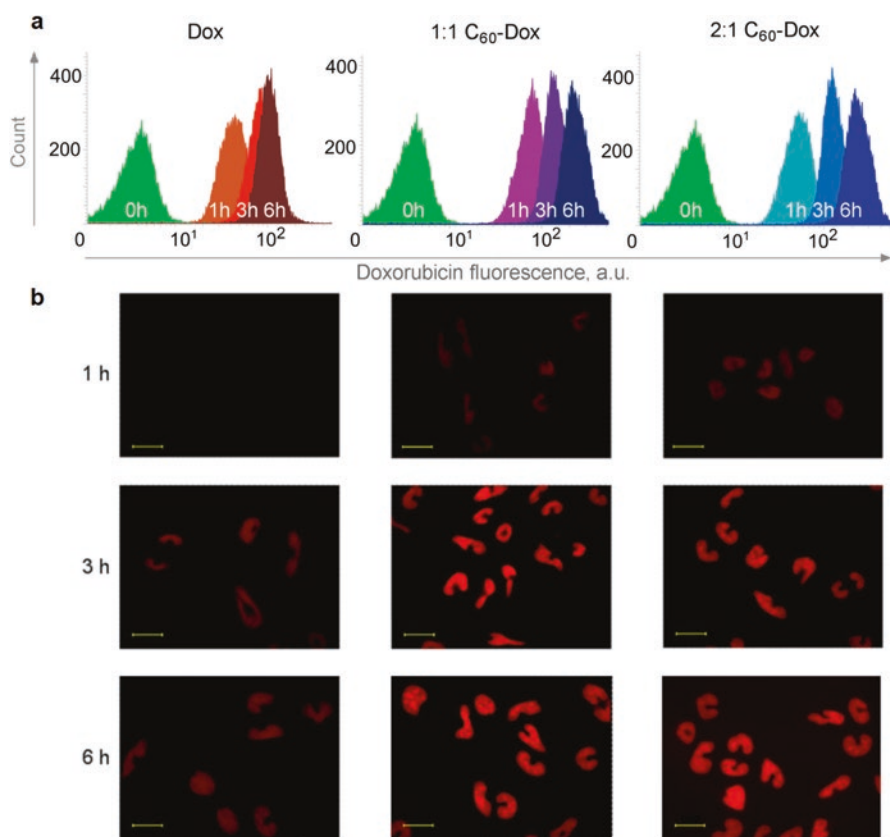
Fig. 5 Intracellular uptake of 1μM free or C_{60}-Dox nanocomplexes in a drug-equivalent concentration: flow cytometry (**a**) and fluorescence microscopy images (**b**) of CCRF-CEM cells incubated with Dox and C_{60}-Dox nanocomplex at the ratio 1:1 and 2:1 for 1, 3, and 6 h. Scale bar 20 μm. (Reproduced with permission (Grebinyk, Prylutska, Buchelnikov, et al., 2019))

calculated from the logarithmic FACS histograms by the value of the respective Dox red fluorescent signal ($\lambda_{ex} = 488$ nm, $\lambda_{em} = 585/29$ nm) and presented in Table 2. Auto-fluorescence of the untreated cells was used as a negative control (Fig. 5a).

Time-dependent accumulation of 1 μM Dox was measured by fluorescence intensity enhancement (Fig. 5, Table 2). The fluorescence microscopy images illustrate that C_{60}-Dox nanocomplexes are internalized faster than free drug, as evidenced by their much brighter intracellular fluorescence (Fig. 5b). The mean fluorescent intensities of the CCRF-CEM cells, treated with 1:1 C_{60}-Dox nanocomplex at 1 μM Dox-equivalent concentration, increased by 1.5, 1.7, and 2.2 times, compared to free Dox at 1, 3, and 6 h, respectively. The 2:1 C_{60}-Dox nanocomplex exhibited a delayed intracellular drug accumulation reaching the same level as the 1:1 C_{60}-Dox nanocomplex at 6 h (Fig. 5, Table 2).

Table 2 Mean fluorescence intensity (FI) of intracellular accumulated Dox estimated by FACS histograms

FI, a.u.	1 h	3 h	6 h
Dox	45 ± 7	85 ± 9	107 ± 11
1:1 C_{60}-Dox	68 ± 9*	145 ± 12*	236 ± 22*
2:1 C_{60}-Dox	57 ± 8*	131 ± 21*	234 ± 23*

*$p \leq 0.01$ in comparison with the free Dox

The obtained data demonstrate that Dox complexation with C_{60} promotes entry into the cells but does not affect its localization. The control staining of the studied cells with Hoechst 33342 (DNA binding dye) revealed its co-localization with Dox signal (data not shown). Evidently, Dox molecules from the C_{60}–Dox nanocomplexes, as well as the free drug, enter cell nucleus that reflects its antiproliferative impact through DNA damage (Kizek et al., 2012; Tacar et al., 2013). An increased intracellular drug's uptake upon complexation with C_{60} points toward the latter functioning as a drug transport promoter. C_{60} was shown to transmigrate the cellular plasma membrane due to a passive diffusion (Bedrov et al., 2008) and/or endocytosis/pinocytosis (Russ et al., 2016; Zhang et al., 2009), whereas small molecules such as Dox can penetrate the plasma membrane only via passive diffusion. C_{60} resembles the structure of clathrin (Schein, 2009; Schein & Sands-Kidner, 2008), the major coat component of vesicles formation during endocytosis. Therefore, C_{60} may function as a transporter of small aromatic molecules (Borowik et al., 2018). On the contrary, a covalent bond between the carrier and cargo introduces a structural alteration into the drug molecule. Consequently, the accumulation pattern and interaction with intracellular targets are altered, resulting in complete or partial loss of the drug's function. Liu et al., 2010, showed that C_{60} with two Dox molecules binds through an amide bond that takes place predominantly in the cytoplasm.

The content of 1:1 and 2:1 C_{60}-Dox nanocomplexes after incubation in the RPMI medium for 24 h was assessed to account 81.50 ± 5.03% and 83.83 ± 5.47%, correspondingly, of a respective 0 h in control (Fig. 6). For that, the C_{60}-Dox nanocomplexes were incubated in the RPMI culture medium up to 24 h under identical conditions adopted from cell-based experiments (450 nM, 2 mL, 37 °C). For sample purification from a released free drug, 500 μL of each sample was filtered with the centrifugal filter devices Amicon Ultra-0.5 3 K (Sigma-Aldrich Co., St- Louis, USA) according to the manufacturer's instructions: 14,000 g, 15 min for filtration; 1000 g, 2 min for the recovery (reverse spin upside down in a new centrifuge tube).

The content of the filter device was subjected to the optical analysis. Samples (50 μL) of C_{60}-Dox nanocomplexes were placed into 384-well plate Sarstedt and fluorescence intensities were measured with a multimode microplate spectrometer Tecan Infinite M200 Pro at the following parameters: λ_{ex} = 470 nm, λ_{em} = 595 nm, number of flashes per well—25, integration time—20 μs. The obtained data were normalized with the control (RPMI medium) and expressed as percentage of the respective control sample, analyzed at 0 h.
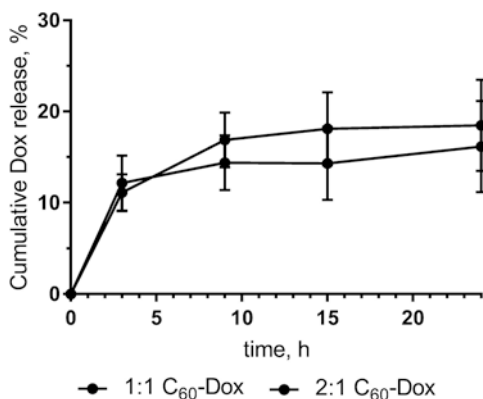
Computer simulation was applied for the disclosure of presumable molecular mechanisms of an increased receptivity of transformed cells to C_{60}-Dox nanocomplexes in comparison with Dox used alone. This methodological approach allows for conducting modeling of the behavior of small molecules in the binding sites of target cells (Guedes et al., 2014). As mentioned above, complexation of the chemotherapeutic agents with the nanocarriers could prevent their pumping out of tumor cells, and in such a way to eliminate one of the main reasons of chemotherapy failure. Strategies used currently for overcoming multidrug resistance were based on the application of the nanocarriers and are focused on the complexation of cytotoxic agents with P-gp inhibitors (Xue & Liang, 2012). However, such methodology has several drawbacks. First, it is necessary to avoid using P-gp substrates in such nanocomplexes. Second, P-gp is not the only agent interfering with drug sensitivity in tumor cells (Ughachukwu & Unekwe, 2012).

We addressed the CYP3A4 as cytochromes P450A belong to a big family of enzymes involved in xenobiotic metabolism. Among other CYP family members, CYP3A4 is involved in the oxidative metabolism of more than half of all drugs that are commonly used in humans. It is associated with 151 reactions in 11 different subsystems including plasma membrane, cytosol, endoplasmic reticulum, mitochondria, peroxisome, among others. Dox is a common CYP3A4 substrate (Feltrin & Oliveira Simões, 2019). CYP3A4 is overexpressed in drug-resistant tumor cells including cancer stem cells (Olszewski et al., 2011). The results of docking and molecular dynamics (MD) simulations indicate that C_{60} forms a stable complex with CYP3A4 (Fig. 7).

Therefore, CYP3A4 can be one of the intracellular receptive structures for C_{60} and its nanocomplexes. Moreover, one can suggest that the interaction of C_{60} with CYP3A4 results in the inactivation of the latter, and our experimental data confirm this assumption. As mentioned above, Molt-16 cells were more sensitive to the effect of C_{60}-Dox nanocomplexes than Jurkat T-cells. Nagai et al. revealed high expression of CYP3A4 in MOLT cells, and only a weak expression in Jurkat T-cells (Nagai et al., 2002). It is possible that the stabilization of this enzyme by C_{60} diminishes Dox degradation and that can be one of the reasons for the differential sensitivity of the tumor cells to the nano-formulation.
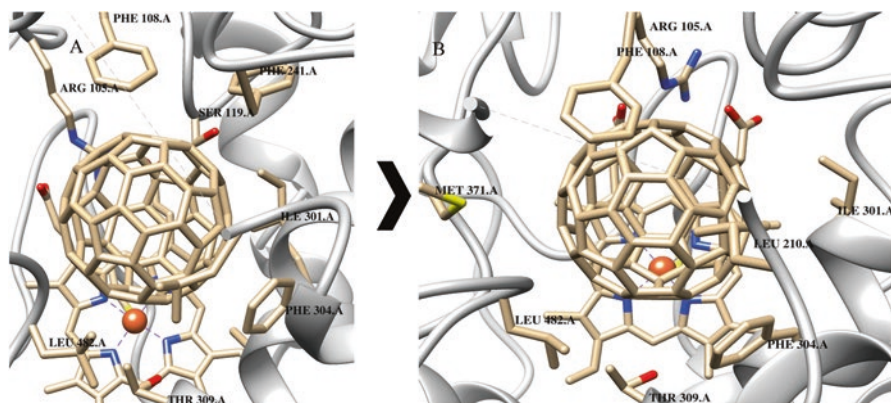
Fig. 7 Model of C$_{60}$-CYP3A4 binding: (**a**) docking and (**b**) MD simulation. (Reproduced with permission (Skivka et al., 2018))

The pattern-recognition receptors were another potential C$_{60}$ targets attracting our attention. As was noted above, C$_{60}$ can enter the cells not only by passive diffusion, but also by a receptor-mediated endocytosis. Cell endocytosis is regulated by the TLRs ligation (Lv et al., 2017). Our data on the molecular docking and MD simulation, as well as computational studies of other research groups (Skivka et al., 2018; Turabekova et al., 2014), have shown that the internal hydrophobic pockets of the Toll-like receptor 4 (TLR4) might be capable of binding C$_{60}$ and its nanocomplex (Fig. 8).

TLRs are mostly highlighted biological regulators in immunology and hematology. These pattern-recognition receptors are expressed by the immune cells and initiate a plethora of inflammatory and antimicrobial responses through the induction of the inflammatory signaling pathways (Takeda & Akira, 2015). Additionally, TLRs are expressed by the leukemic cells, and TLR ligands can inhibit leukemia development and lymphoma growth. The TLR signaling induces some forms of the leukemic cell differentiation, and this could be one of the mechanisms of a spontaneous disease remission associated with infection (Okamoto et al., 2009). In our experiments, THP1 cells were highly sensitive to a cytotoxic action of C$_{60}$-Dox nanocomplexes. It is possible that the high expression of TLR4 was one of the reasons of that effect, since the entry of the nano-formulation in tumor cells through endocytosis provides the escape of drug pumping out by the P-gp.

4.2 Cytotoxic Action of C$_{60}$-Cis Nanocomplex

A comparative analysis of the toxic activity of Cis in a range of 1–25 μM concentrations and C$_{60}$-Cis nanocomplex in Cis equivalent concentrations against LLC (Lewis lung carcinoma) cells after 24, 48, and 72 h of incubation was analyzed using the
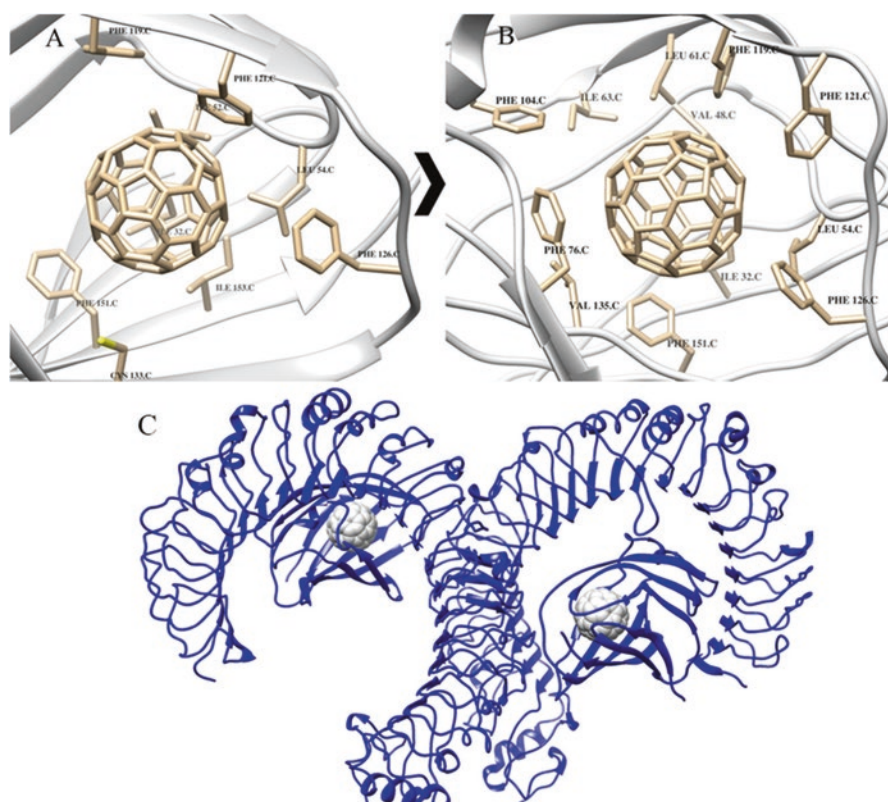
Fig. 8 C_{60}-TLR4/MD-2 bound structure: (**a**) docking and (**b**) MD simulation; C – C_{60}-TLR4/MD-2 bound structure. (Reproduced with permission (Skivka et al., 2018))

MTT-test (Prylutska, Grebinyk, et al., 2019, Prylutska, Grynyuk, et al., 2019, Prylutska, Lynchak, et al., 2019). It should be noted that no cytotoxic effect of C_{60} used alone in a range of 0.42–10.4 μM concentrations, equivalent to those in the C_{60}-Cis nanocomplex, on LLC cells' viability during the incubation period was detected (data not presented).

The results on the time- and concentration-dependent decrease in the viability of LLC cells induced by either Cis in a range of 1–25 μM concentrations or the C_{60}-Cis nanocomplex in Cis equivalent concentrations, as well as the corresponding IC_{50} values, are shown in Fig. 9. When LLC cells treated with free Cis were incubated for 24 h, a 26% decrease in cell viability was detected only at 25 μM concentration of the drug. The value of the calculated IC_{50} for Cis equal to 50 μM is in agreement with the literature value of 55 μM (Sarin et al., 2017) and 64 μM (Zhang et al., 2003) for A549 lung cancer cells. These data suggest a resistance of LLC cells to Cis treatment.

The complexation of Cis with C_{60} allowed to accelerate and potentiate the drug's effect at 24 h, as well as to reduce the IC_{50} value threefold (Fig. 9a). A similar effect
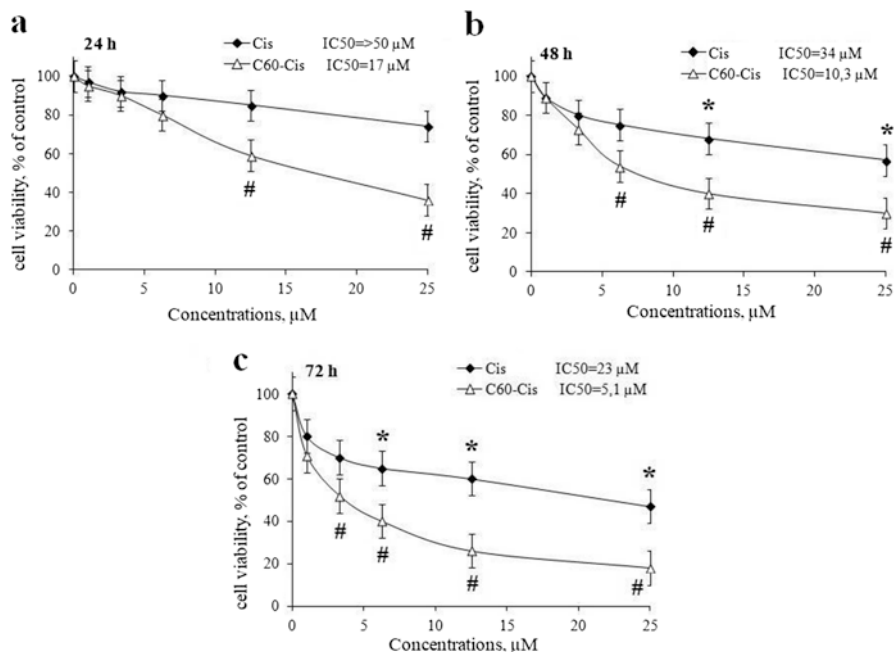
Fig. 9 Viability of LLC cells treated with either free Cis or C_{60}-Cis nanocomplex in Cis equivalent concentrations at 24, 48, and 72 h of incubation. (Data are presented as mean ± SEM of six independent experiments. *$p < 0.05$ in comparison with control; #$p < 0.05$ in comparison with Cis. Reproduced with permission (Prylutska, Grynyuk, et al., 2019))

of the C_{60}-Cis nanocomplex on enhanced cytotoxicity in comparison with the effect of free Cis was observed at 48 h and 72 h (Fig. 9 b,c). Thus, at 72 h incubation, the viability of LLC cells treated with the C_{60}-Cis nanocomplex was decreased by 82% and the value of IC_{50} was 4.5 times lower than that for free Cis (Fig. 9c).

These data demonstrate that the C_{60}-Cis nanocomplex possessed a higher cytotoxicity and induced earlier damage of LLC cells as compared with the free drug, in particular at low Cis equivalent concentrations. After the treatment of LLC cells with the studied nanocomplex, the cytotoxic effect was observed at Cis equivalent concentration at which the free drug has no effect on cell viability.

According to the flow cytometric analysis of LLC cells' cycle distribution (Fig. 10 a,b) after 24 h incubation, 44% of cells in control stayed in the G0/G1 phase. Accumulation of cancer cells of different origins in the G0/G1 phase of cell cycle ensures G1-S phase transition, mitosis, and intense proliferation (Horibe et al., 2015). LLC cells treated with 5.2μM C_{60} passed through the cell cycle without significant changes in the number of cells in different phases (Fig. 10b).

After the treatment of LLC cells with 12.5 μM Cis, the cytostatic effect of the drug was consisted in a simultaneous decrease in the number of cells in the G0/G1 phase and its increase in both S and G2/M phases (Fig. 10b). The accumulation in the G2/M phase was also detected after the treatment of A549 lung cancer cells with
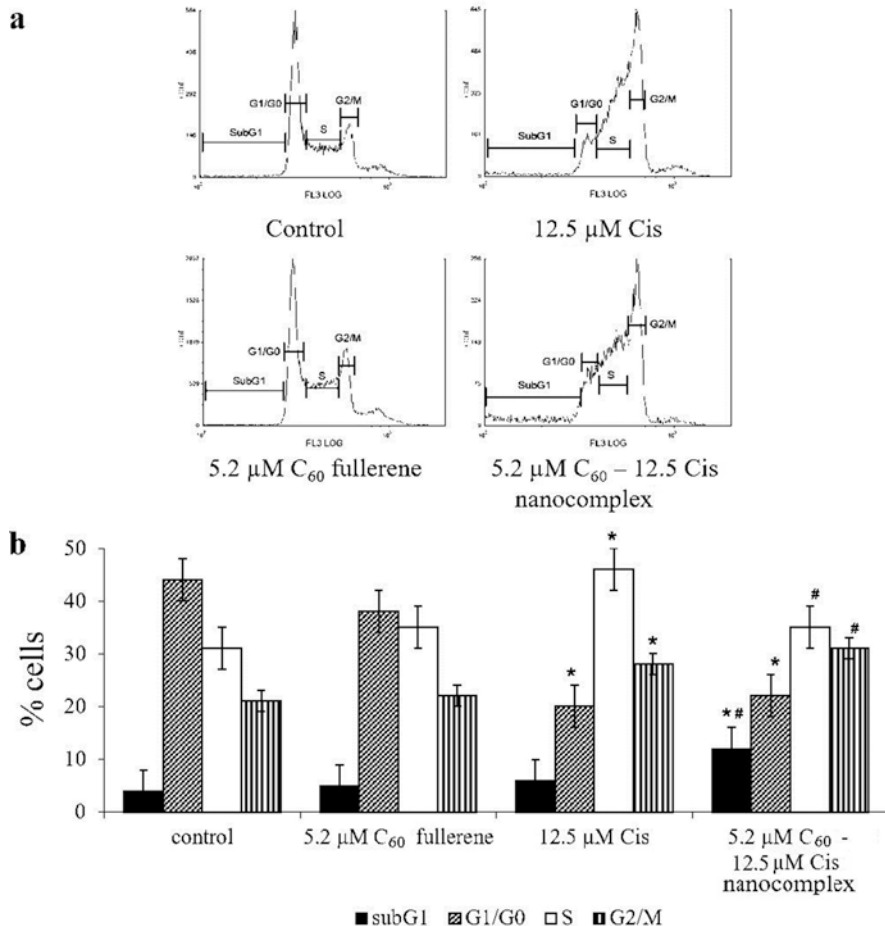
Fig. 10 Results pf analysis of cell cycle in LLC at 24 h after treatment with C_{60}, Cis or C_{60}-Cis nanocomplex. Representative histograms (**a**) and quantitative analysis of cells distribution on cycle phases (**b**); Data are presented as mean ± SEM of six independent experiments. *$p < 0.05$ in comparison with control; #$p < 0.05$ in comparison with Cis. (Reproduced with permission (Prylutska, Grynyuk, et al., 2019))

11 μM Cis (Sarin et al., 2017), and it was recognized to be the attribute of the effect of the anticancer drug. The cell cycle of LLC cells treated with the C_{60}-Cis nanocomplex was essentially disturbed. The number of cells in the S phase decreased, while further accumulation in the G2/M phase took place (Fig. 11). In addition, we detected cells arrest in the sub-G1 phase that is considered a marker of the apoptotic cell death induced by the anticancer drugs and Cis, particularly (Sarin et al., 2017; Velma et al., 2016). In order to determine whether the toxicity of the C_{60}-Cis nanocomplex toward LLC cells was associated with apoptosis, the induction of the caspase 3/7 activity and phosphatidylserine translocation into the outer lipid layer of
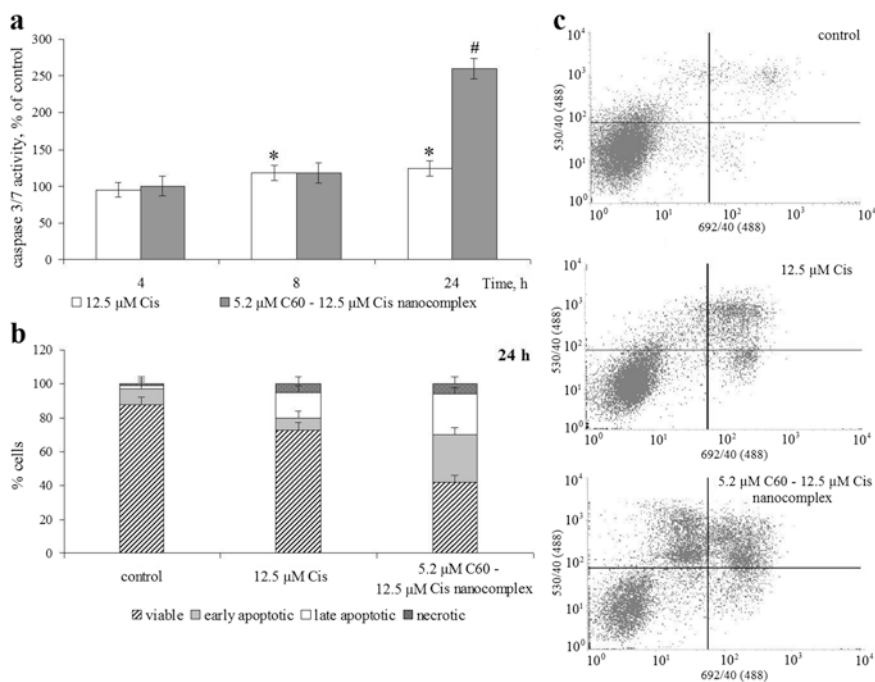
Fig. 11 Pattern of apoptosis induction by the C_{60}-Cis nanocomplex. Caspase 3/7 activity in LLC cells (**a**). Data are presented as mean ± SEM of four independent experiments. *$p < 0.05$ in comparison with control; #$p < 0.05$ in comparison with Cis; Quantitative analysis of cells number, differentiated with the double Annexin V-FITC/PI staining at 24 h of incubation (**b**); Fluorescence-activated cell sorting (FACS) histograms of cells stained with Annexin V-FITC/PI (in each panel the lower left quadrant shows the content of viable, upper left quadrant—early apoptotic, upper right quadrant—late apoptotic, lower right quadrant—necrotic cells populations) (**c**). (Reproduced with permission (Prylutska, Grynyuk, et al., 2019))

plasma membrane were studied. There was no effect of Cis at 12.5μM concentration on caspase 3/7 activity in LLC cells at 4 h treatment, and only a minor increase of such activity was found at 8 and 24 h in comparison with the control (Fig. 11a). Caspase 3 cleavage under treatment with 25 μM Cis was also demonstrated in experiments on lung cancer A549 cells (Rabik et al., 2008). Treatment of LLC cells for 24 h with the C_{60}-Cis nanocomplex enhanced caspase-3/7 activity by 2.1 times ($260 \pm 17\%$ vs. $124 \pm 11\%$ in Cis treated). This suggests that Cis complexation with C_{60} potentiates apoptosis development at longer incubation periods.

The results of analysis of cell populations at 24 h after treatment of LLC cells with 12.5μM Cis or C_{60}-Cis nanocomplex is presented in Fig. 11b, c. We have shown that C_{60} at 5.2 μM concentration equivalent to those in the C_{60}-Cis nanocomplex had no effect on caspase 3/7 activity and phosphatidylserine externalization on the surface of LLC cells (data not presented). The treatment of LLC cells with Cis was

followed by an increased percentage of the late apoptotic cells (15% vs. 2% in a control), while their treatment with the C_{60}-Cis nanocomplex was accompanied by an increased content of both early (28% vs. 7% in Cis treated) and late (24% vs. 15% in Cis treated) apoptotic cells, as well as by a significantly decreased content of the viable cells (58% vs. 27% in Cis treated) (Fig. 11 b, c). These data confirm that the toxic effect of the C_{60}-Cis nanocomplex against LLC cells is realized through apoptosis.

We suggest that C_{60}, as a component of the C_{60}-Cis nanocomplex, promotes Cis entry and intracellular accumulation (Franskevych et al., 2017; Grebinyk et al., 2018a; Grebinyk et al., 2018b), thus, contributing to the intensification of the drug's toxic effect toward lung cancer cells.

4.3   Cytotoxic Action of C_{60}-Ber Nanocomplex

Strong absorption and fluorescence of the Ber molecule in the visible spectral region (Gumenyuk et al., 2012) enables the tracking of its complexes with the noninvasive direct fluorescence-based techniques. CCRF-CEM cells were incubated in the presence of 10 μM Ber or C_{60}-Ber nanocomplexes for 0, 1, 3, and 6 h, and then examined with fluorescent microscopy and flow cytometry in order to visualize and quantify the intracellular uptake of Ber (Fig. 12). Autofluorescence of the untreated cells was used as a negative control. The mean fluorescence intensity of each sample, calculated from the logarithmic FACS histograms by the respective value of Ber green fluorescent signal (λ_{ex} = 488 nm, λ_{em} = 530/40 nm), is presented in Table 3.

Fluorescent microscopy demonstrated a time-dependent accumulation of 10μM Ber in CCRF-CEM cells (Fig. 12b). According to the literature data, after the uptake, Ber is localized in mitochondria (Zhang et al., 2019). It also binds with DNA, suggesting its high nuclear affinity (Wang et al., 2011; Zhang et al., 2013).

Once Ber is complexed with C_{60}, the detected intensity of fluorescence was significantly enhanced. The microscopic images demonstrated that the C_{60}-Ber nanocomplexes were internalized faster and more efficiently in comparison with the free Ber (Fig. 13b). The mean fluorescent intensity of the CCRF-CEM cells (Fig. 13a), treated with 1:2 C_{60}-Ber nanocomplex at 10μM Ber-equivalent concentration, increased by 31% at 6 h. In cells treated with C_{60}-Ber nanocomplexes at 1:1 and 2:1 molar ratio, the fluorescent signal reached the level of 130 and 140% of the control at 3 and 6 h, respectively (Table 3). These data showed that Ber complexation with C_{60} strongly promoted its uptake by the leukemic cells (Grebinyk, Prylutska, Buchelnikov, et al., 2019, Grebinyk, Prylutska, Chepurna, et al., 2019, Grebinyk, Prylutska, Grebinyk, et al., 2019, Grebinyk, Yashchuk, Bashmakova, et al., 2019).

In order to evaluate the effect of Ber on the proliferation of cancer cells, CCRF-CEM cells were treated with free Ber in increasing concentrations and C_{60}-Ber nanocomplexes in Ber-equivalent concentrations for 24, 48 and 72 h, and cell viability was estimated using the MTT-assay (Fig. 13). Free Ber exhibited dose- and time-dependent toxicity toward CCRF-CEM cells in a range of concentrations from
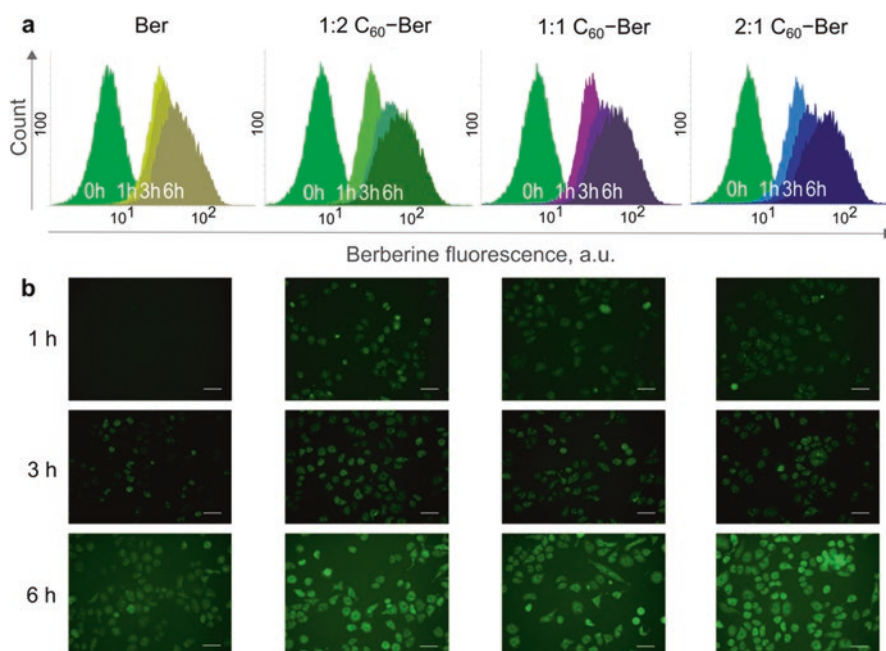
Fig. 12 Indicators of the intracellular accumulation of free 10 μM Ber and C$_{60}$-Ber nanocomplexes in a Ber-equivalent concentration: flow cytometry (**a**) and fluorescent microscopy (**b**) of CCRF-CEM cells incubated with Ber and C$_{60}$-Ber nanocomplexes at the molar ratios 1:2, 1:1, and 2:1. Scale bar equals 20 μm. (Reproduced with permission (Grebinyk, Prylutska, Buchelnikov, et al., 2019))

Table 3 Mean fluorescence intensity (FI) of the intracellular accumulated Ber measured with flow cytometry

FI, a.u.	1 h	3 h	6 h
Ber	39 ± 3	45 ± 3	57 ± 5
1:2 C$_{60}$-Ber	38 ± 2	49 ± 4	80 ± 7*
1:1 C$_{60}$-Ber	42 ± 4	59 ± 5*	79 ± 6*
2:1 C$_{60}$-Ber	38 ± 3	57 ± 6*	81 ± 6*

$^*p \leq 0.01$ in comparison with the free Ber

5 to 50 μM (data not shown). Taking into account the initial aim of the complexation of the anticancer agent with C$_{60}$ in order to potentiate its toxicity and, therefore, decrease efficient dose, we have chosen a concentration range from 1.3 to 20 μM for further investigation of the effects of such complexation. The noted concentrations of Ber exhibited no or mild cytotoxicity (Fig. 13a–c).

Ber in increasing concentrations inhibited cell growth in a time- and dose-dependent manner (Fig. 13a–c). Under the action of Ber in the concentration range of 1.3–20 μM, the number of viable cells was gradually decreased. Thus, 10 μM Ber
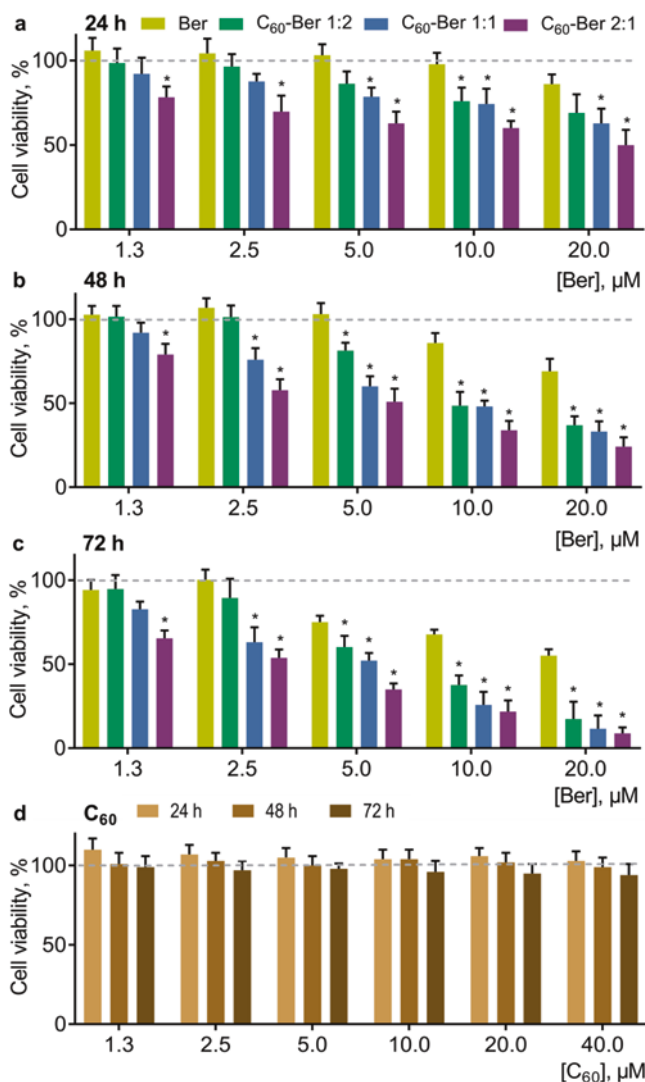
Fig. 13 Viability of CCRF-CEM cells, treated with free Ber or C_{60}-Ber nanocomplexes in the Ber-equivalent concentrations for 24 (**a**), 48 (**b**), and 72 h (**c**) (*$p \leq 0.01$ in comparison with the free Ber). Free C_{60} control: viability of CCRF-CEM cells, treated with a free C_{60} in nanocomplex-equivalent concentrations for 24, 48, and 72 h (**d**). (Reproduced with permission (Grebinyk, Prylutska, Buchelnikov, et al., 2019))

decreased the viability of CCRF-CEM cells to $71 \pm 9\%$ and $50 \pm 6\%$ of the control at 48 and 72 h, respectively

All C_{60}-Ber nanocomplexes exhibited stronger antiproliferative potential toward CCRF-CEM cells compared with such potential of free Ber (Grebinyk, Prylutska, Buchelnikov, et al., 2019, Grebinyk, Prylutska, Chepurna, et al., 2019, Grebinyk,

Table 4 Half-maximal inhibitory concentration (IC$_{50}$) of the free Ber and C$_{60}$-Ber nanocomplexes toward CCRF-CEM cells

IC$_{50}$, μM	24 h	48 h	72 h
Ber	58 ± 5	23 ± 2	19 ± 2
1:2 C$_{60}$-Ber	44 ± 4*	11.0 ± 1.2*	6.0 ± 0.4*
1:1 C$_{60}$-Ber	33 ± 3*	8.0 ± 0.7*	4.0 ± 0.3*
2:1 C$_{60}$-Ber	21 ± 2*	5.0 ± 0.6*	3.0 ± 0.2*

*$p \leq 0.01$ in comparison with the free Ber

Prylutska, Grebinyk, et al., 2019, Grebinyk, Yashchuk, Bashmakova, et al., 2019). However, the C$_{60}$ alone at concentrations equivalent to those used in the nanocomplexes did not have a significant effect on cell viability (Fig. 13d). With increase of C$_{60}$ concentration in the C$_{60}$-Ber nanocomplexes, higher toxic potential toward CCRF-CEM cells was observed, following the order 1:2 ‹ 1:1 ‹ 2:1 (most toxic). Thus, at 24, 48, and 72 h, 10μM 1:2 C$_{60}$-Ber nanocomplex decreased cell viability to 76 ± 8%, 49 ± 8%, 26 ± 7%, 1:1 C$_{60}$-Ber nanocomplex to 74 ± 9%, 48 ± 3%, 25 ± 7%, and 2:1 C$_{60}$-Ber nanocomplex—to 60 ± 4%, 34 ± 6%, 22 ± 7% of the control, respectively (Fig. 13a–c). The calculated IC$_{50}$ values for the free Ber and C$_{60}$-Ber nanocomplexes are listed in Table 4. These data evidence C$_{60}$-dependent enhancement of Ber cytotoxicity. Thus, at 24 h, the IC$_{50}$ value for the Ber complexed with C$_{60}$ at the molar ratio 1:2, 1:1, and 2:1 decreased by 1.3, 1.8, and 2.8 times, respectively. At 48 h, it decreased by 2.1, 2.9, and 4.6 times, respectively, and at 72 h, by 3.2, 4.8, and 6.3 times, respectively.

Complexation with C$_{60}$ enhanced Ber toxicity toward the leukemic cells more appreciably compared with C$_{60}$ complexation with a traditional anticancer therapeutic Dox that was followed by less than 3.5 times decrease in IC$_{50}$ at the same treatment duration. Such action could be linked to the higher safe concentration of Ber in the C$_{60}$-containing nanocomplex (μM of Ber against nM of Dox).

The obtained results encourage the strategy of the using of water-soluble pristine C$_{60}$ for safe delivery of the anticancer medicines.

5   Conclusion

The formation of stable noncovalent nanocomplexes of C$_{60}$ with chemotherapeutic drugs (in particular, Dox, Cis and Ber) in aqueous solution was confirmed by the microscopic and spectroscopic methods, as well as computer simulation. Studies on human leukemic cell lines revealed that C$_{60}$-Dox nanocomplexes possessed higher cytotoxicity than free drugs in equivalent concentrations. At 72 h incubation of cells, the IC$_{50}$ value for 1:1 and 2:1 C$_{60}$-Dox nanocomplexes decreased by ≤3.5 and ≤ 2.5 times, respectively, in comparison with IC$_{50}$ for the free Dox. Complexation with C$_{60}$ promoted Dox entry into the leukemic cells. A treatment of CCRF-CEM cells for 6 h with C$_{60}$-Dox nanocomplexes in 1μM Dox-equivalent concentration was followed by

2.2-fold increase of drug intracellular level, compared to treatment with free Dox. The toxic effect of the C_{60}-Cis nanocomplex toward LLC cells was higher with IC_{50} values of 3.3 and 4.5 times at 48 h and 72 h, respectively, compared to the effect of free drug. Cis at 12.5 μM concentration had no effect on LLC cell viability, while the C_{60}-Cis nanocomplex in Cis-equivalent concentration substantially decreased cell viability, impaired cell shape and adhesion, inhibited cell migration behavior, and induced the accumulation of cells in the pro-apoptotic sub-G1 phase of the cell cycle. Apoptosis development induced by the C_{60}-Cis nanocomplex was confirmed by a significant activation of the caspase 3/7 and externalization of phosphatidylserine on the outer surface of the plasma membrane of LLC cells. Fluorescence-based techniques evidenced that C_{60}-Ber nanocomplexes were faster and more intensely internalized by the leukemic CCRF-CEM cells. They also exhibited higher antiproliferative potential, as compared with free Ber. The IC_{50} value for Ber in the C_{60}-Ber nanocomplexes at 1:2, 1:1, and 2:1 molar ratio was decreased by 3.2, 4.8, and 6.3 times, respectively, compared with the IC_{50} value detected for free Ber.

Thus, we propose a novel water-soluble nano-formulation for usage in the anticancer chemotherapy, namely for the complexation of chemotherapeutic drugs with C_{60} that efficiently increases their toxicity toward the malignant cells.

References

Antunovic, M., Kriznik, B., Ulukaya, E., Yilmaz, V. T., Mihalic, K. C., Madunic, J., & Marijanovic, I. (2015). Cytotoxic activity of novel palladium-based compounds on leukemia cell lines. *Anti-Cancer Drugs, 26*(2), 180–186. https://doi.org/10.1097/cad.0000000000000174

Bao, J., Huang, B., Zou, L., Chen, S., Zhang, C., Zhang, Y., et al. (2015). Hormetic effect of Berberine attenuates the anticancer activity of chemotherapeutic agents. *PLoS One, 10*(9), e0139298. https://doi.org/10.1371/journal.pone.0139298

Bedrov, D., Smith, G. D., Davande, H., & Li, L. (2008). Passive transport of C_{60} fullerenes through a lipid membrane: A molecular dynamics simulation study. *The Journal of Physical Chemistry B, 112*(7), 2078–2084. https://doi.org/10.1021/jp075149c

Borowik, A., Prylutskyy, Y., Kawelski, Ł., Kyzyma, O., Bulavin, L., Ivankov, O., et al. (2018). Does C_{60} fullerene act as a transporter of small aromatic molecules? *Colloids and Surfaces B, Biointerfaces, 164*, 134–143. https://doi.org/10.1016/j.colsurfb.2018.01.026

Brant, J., Lecoanet, H., & Wiesner, M. R. (2005). Aggregation and deposition characteristics of fullerene nanoparticles in aqueous systems. *Journal of Nanoparticle Research, 7*, 545–553. https://doi.org/10.1007/s11051-005-4884-8

Bulavin, L., Adamenko, I., Prylutskyy, Y., Durov, S., Graja, A., Bogucki, A., & Scharff, P. (2000). Structure of fullerene C_{60} in aqueous solution. *Physical Chemistry Chemical Physics, 2*(8), 1627–1629. https://doi.org/10.1039/A907786C

Byelinska, I. V., Kuznietsova, H. M., Dziubenko, N. V., Lynchak, O. V., Rybalchenko, T. V., Prylutskyy, Y. I., et al. (2018). Effect of C_{60} fullerenes on the intensity of colon damage and hematological signs of ulcerative colitis in rats. *Materials Science & Engineering. C, Materials for Biological Applications, 93*, 505–517. https://doi.org/10.1016/j.msec.2018.08.033

Cai, Y., Xia, Q., Luo, R., Huang, P., Sun, Y., Shi, Y., & Jiang, W. (2014). Berberine inhibits the growth of human colorectal adenocarcinoma in vitro and in vivo. *Journal of Natural Medicines, 68*(1), 53–62. https://doi.org/10.1007/s11418-013-0766-z

Cai, Z., Lin, M., Wuchter, C., Ruppert, V., Dörken, B., Ludwig, W. D., & Karawajew, L. (2001). Apoptotic response to homoharringtonine in human wt p53 leukemic cells is independent of reactive oxygen species generation and implicates Bax translocation, mitochondrial cytochrome c release and caspase activation. *Leukemia, 15*(4), 567–574. https://doi.org/10.1038/sj.leu.2402067

Castro, E., Hernandez Garcia, A., Zavala, G., & Echegoyen, L. (2017). Fullerenes in biology and medicine. *Journal of Materials Chemistry B, 5*(32), 6523–6535. https://doi.org/10.1039/c7tb00855d

Cernáková, M., Kost'álová, D., Kettmann, V., Plodová, M., Tóth, J., & Drímal, J. (2002). Potential antimutagenic activity of berberine, a constituent of Mahonia aquifolium. *BMC Complementary and Alternative Medicine, 2*, 2. https://doi.org/10.1186/1472-6882-2-2

Changenet-Barret, P., Gustavsson, T., Markovitsi, D., Manet, I., & Monti, S. (2013). Unravelling molecular mechanisms in the fluorescence spectra of doxorubicin in aqueous solution by femtosecond fluorescence spectroscopy. *Physical Chemistry Chemical Physics, 15*(8), 2937–2944. https://doi.org/10.1039/c2cp44056c

Chen, G., Roy, I., Yang, C., & Prasad, P. N. (2016). Nanochemistry and nanomedicine for nanoparticle-based diagnostics and therapy. *Chemical Reviews, 116*(5), 2826–2885. https://doi.org/10.1021/acs.chemrev.5b00148

Choi, J., Snow, S. D., Kim, J.-H., & Jang, S. S. (2015). Interaction of C$_{60}$ with water: First-principles modeling and environmental implications. *Environmental Science and Technology, 49*(3), 1529–1536. https://doi.org/10.1021/es504614u

Conde, J., de la Fuente, J. M., & Baptista, P. V. (2013). Nanomaterials for reversion of multidrug resistance in cancer: A new hope for an old idea? *Frontiers in Pharmacology, 4*. https://doi.org/10.3389/fphar.2013.00134

Cortés-Funes, H., & Coronado, C. (2007). Role of anthracyclines in the era of targeted therapy. *Cardiovascular Toxicology, 7*(2), 56–60. https://doi.org/10.1007/s12012-007-0015-3

Dasari, S., & Tchounwou, P. B. (2014). Cisplatin in cancer therapy: Molecular mechanisms of action. *European Journal of Pharmacology, 740*, 364–378. https://doi.org/10.1016/j.ejphar.2014.07.025

Deguchi, S., Alargova, R. G., & Tsujii, K. (2001). Stable dispersions of fullerenes, C$_{60}$ and C$_{70}$, in water. Preparation and characterization. *Langmuir, 17*(19), 6013–6017. https://doi.org/10.1021/la010651o

Dragojevic-Simic, V., Jacevic, V., Dobric, S., Djordjevic, A., Bajcetic, M., & Injac, R. (2011). Anti-inflammatory activity of fullerenol C$_{60}$(OH)$_{24}$ nanoparticles in a model of acute inflammation in rats. *Digest Journal of Nanomaterials and Biostructures, 6*(2), 819–827.

Dugan, L. L., Lovett, E. G., Quick, K. L., Lotharius, J., Lin, T. T., & O'Malley, K. L. (2001). Fullerene-based antioxidants and neurodegenerative disorders. *Parkinsonism & Related Disorders, 7*(3), 243–246. https://doi.org/10.1016/s1353-8020(00)00064-x

El-Wahab, A. E.-S. A., Ghareeb, D. A., Sarhan, E. E., Abu-Serie, M. M., & Demellawy, M. A. E. (2013). In vitro biological assessment of berberis vulgaris and its active constituent, berberine: Antioxidants, anti-acetylcholinesterase, anti-diabetic and anticancer effects. *BMC Complementary and Alternative Medicine*. https://doi.org/10.1186/1472-6882-13-218

Eswaran, S. V. (2018). Water soluble nanocarbon materials: A panacea for all? *Current Science (Bangalore), 114*(9), 1846–1850.

Evstigneev, M. P., Buchelnikov, A. S., Voronin, D. P., Rubin, Y. V., Belous, L. F., Prylutskyy, Y. I., & Ritter, U. (2013). Complexation of C$_{60}$ fullerene with aromatic drugs. *A European Journal of Chemical Physics and Physical Chemistry, 14*(3), 568–578. https://doi.org/10.1002/cphc.201200938

Feltrin, C., & Oliveira Simões, C. M. (2019). Reviewing the mechanisms of natural product-drug interactions involving efflux transporters and metabolic enzymes. *Chemico-Biological Interactions, 314*, 108825. https://doi.org/10.1016/j.cbi.2019.108825

Fennell, D. A., Summers, Y., Cadranel, J., Benepal, T., Christoph, D. C., Lal, R., et al. (2016). Cisplatin in the modern era: The backbone of first-line chemotherapy for non-small cell lung cancer. *Cancer Treatment Reviews, 44*, 42–50. https://doi.org/10.1016/j.ctrv.2016.01.003

Finn, N. A., Findley, H. W., & Kemp, M. L. (2011). A switching mechanism in doxorubicin bio-activation can be exploited to control doxorubicin toxicity. *PLoS Computational Biology, 7*(9), e1002151. https://doi.org/10.1371/journal.pcbi.1002151

Florea, A. M., & Büsselberg, D. (2011). Cisplatin as an anti-tumor drug: Cellular mechanisms of activity, drug resistance and induced side effects. *Cancers, 3*(1), 1351–1371. https://doi.org/10.3390/cancers3011351

Foley, S., Crowley, C., Smaihi, M., Bonfils, C., Erlanger, B. F., Seta, P., & Larroque, C. (2002). Cellular localisation of a water-soluble fullerene derivative. *Biochemical and Biophysical Research Communications, 294*(1), 116–119. https://doi.org/10.1016/S0006-291X(02)00445-X

Franskevych, D., Palyvoda, K., Petukhov, D., Prylutska, S., Grynyuk, I., Schuetze, C., et al. (2017). Fullerene C_{60} penetration into leukemic cells and its Photoinduced cytotoxic effects. *Nanoscale Research Letters, 12*. https://doi.org/10.1186/s11671-016-1819-5

Galluzzi, L., Vitale, I., Michels, J., Brenner, C., Szabadkai, G., Harel-Bellan, A., et al. (2014). Systems biology of cisplatin resistance: Past, present and future. *Cell Death and Disease, 29*(5) https://doi.org/10.1038/cddis.2013.428

Gharbi, N., Pressac, M., Hadchouel, M., Szwarc, H., Wilson, S. R., & Moussa, F. (2005). [60]Fullerene is a powerful antioxidant *in vivo* with no acute or subacute toxicity. *Nano Letters, 5*(12), 2578–2585. https://doi.org/10.1021/nl051866b

Gonchar, O. O., Maznychenko, A. V., Bulgakova, N. V., Vereshchaka, I. V., Tomiak, T., Ritter, U., et al. (2018). C_{60} fullerene prevents restraint stress-induced oxidative disorders in rat tissues: Possible involvement of the Nrf2/ARE-antioxidant pathway. *Oxidative Medicine and Cellular Longevity, 17*. https://doi.org/10.1155/2018/2518676

Goodarzi, S., Da Ros, T., Conde, J., Sefat, F., & Mozafari, M. (2017). Fullerene: Biomedical engineers get to revisit an old friend. *Materials Today, 20*(8), 460–480. https://doi.org/10.1016/j.mattod.2017.03.017

Grebinyk, A., Grebinyk, S., Prylutska, S., Ritter, U., Matyshevska, O., Dandekar, T., & Frohme, M. (2018a). C_{60} fullerene accumulation in human leukemic cells and perspectives of LED-mediated photodynamic therapy. *Free Radical Biology & Medicine, 124*, 319–327. https://doi.org/10.1016/j.freeradbiomed.2018.06.022

Grebinyk, A., Grebinyk, S., Prylutska, S., Ritter, U., Matyshevska, O., Dandekar, T., & Frohme, M. (2018b). HPLC-ESI-MS method for C_{60} fullerene mitochondrial content quantification. *Data in Brief, 19*, 2047–2052. https://doi.org/10.1016/j.dib.2018.06.089

Grebinyk, A., Prylutska, S., Buchelnikov, A., Tverdokhleb, N., Grebinyk, S., Evstigneev, M., et al. (2019). C_{60} fullerene as an effective Nanoplatform of alkaloid Berberine delivery into leukemic cells. *Pharmaceutics, 11*(11) https://doi.org/10.3390/pharmaceutics11110586

Grebinyk, A., Prylutska, S., Chepurna, O., Grebinyk, S., Prylutskyy, Y., Ritter, U., et al. (2019). Synergy of chemo- and photodynamic therapies with C_{60} fullerene-doxorubicin Nanocomplex. *Nanomaterials (Basel, Switzerland), 9*(11) https://doi.org/10.3390/nano9111540

Grebinyk, A., Prylutska, S., Grebinyk, S., Prylutskyy, Y., Ritter, U., Matyshevska, O., et al. (2019). Complexation with C_{60} fullerene increases doxorubicin efficiency against leukemic cells *In Vitro*. *Nanoscale Research Letters, 14*. https://doi.org/10.1186/s11671-019-2894-1

Grebinyk, A., Yashchuk, V., Bashmakova, N., Gryn, D., Hagemann, T., Naumenko, A., et al. (2019). A new triple system DNA-Nanosilver-Berberine for cancer therapy. *Applied Nanoscience, 9*(5), 945–956. https://doi.org/10.1007/s13204-018-0688-x

Guedes, I. A., de Magalhães, C. S., & Dardenne, L. E. (2014). Receptor-ligand molecular docking. *Biophysical Reviews, 6*(1), 75–87. https://doi.org/10.1007/s12551-013-0130-2

Gumenyuk, V. G., Bashmakova, N. V., Kutovyy, S. Y., Yashchuk, V. M., & Zaika, L. A. (2012). Binding Parameters of Alkaloids Berberine and Sanguinarine with DNA. *arXiv:1201.2579 [physics, q-bio]*. Abgerufen von http://arxiv.org/abs/1201.2579.

Halenova, T., Raksha, N., Vovk, T., Savchuk, O., Ostapchenko, L., Prylutskyy, Y., et al. (2018). Effect of C_{60} fullerene nanoparticles on the diet-induced obesity in rats. *International Journal of Obesity, 42*(12), 1987–1998. https://doi.org/10.1038/s41366-018-0016-2

Halenova, T. I., Vareniuk, I. M., Roslova, N. M., Dzerzhynsky, M. E., Savchuk, O. M., Ostapchenko, L. I., et al. (2016). Hepatoprotective effect of orally applied water-soluble pristine C$_{60}$ fullerene against CCl4-induced acute liver injury in rats. *RSC Advances, 6*(102), 100046–100055. https://doi.org/10.1039/c6ra20291h

Horibe, S., Matsuda, A., Tanahashi, T., Inoue, J., Kawauchi, S., Mizuno, S., et al. (2015). Cisplatin resistance in human lung cancer cells is linked with dysregulation of cell cycle associated proteins. *Life Sciences, 124*, 31–40. https://doi.org/10.1016/j.lfs.2015.01.011

Husseini, G. A., Kanan, S., & Al-Sayah, M. (2016). Investigating the fluorescence quenching of doxorubicin in folic acid solutions and its relation to ligand-targeted Nanocarriers. *Journal of Nanoscience and Nanotechnology, 16*(2), 1410–1414. https://doi.org/10.1166/jnn.2016.10700

Jung, K., & Reszka, R. (2001). Mitochondria as subcellular targets for clinically useful anthracyclines. *Advanced Drug Delivery Reviews, 49*(1–2), 87–105. https://doi.org/10.1016/s0169-409x(01)00128-4

Kepley, C. (2012). Fullerenes in medicine; will it ever occur? *Journal of Nanomedicine & Nanotechnology, 3*(6) https://doi.org/10.4172/2157-7439.1000e111

Kizek, R., Adam, V., Hrabeta, J., Eckschlager, T., Smutny, S., Burda, J. V., et al. (2012). Anthracyclines and ellipticines as DNA-damaging anticancer drugs: Recent advances. *Pharmacology & Therapeutics, 133*(1), 26–39. https://doi.org/10.1016/j.pharmthera.2011.07.006

Kumar, M., & Raza, K. (2017). C$_{60}$-fullerenes as drug delivery carriers for anticancer agents: Promises and hurdles. *Pharmaceutical Nanotechnology, 5*(3), 169–179. https://doi.org/10.2174/2211738505666170301142232

Kuznietsova, H., Lynchak, O., Dziubenko, N., Herheliuk, T., Prylutskyy, Y., Rybalchenko, V., & Ritter, U. (2019). Water-soluble pristine C$_{60}$ fullerene attenuates acetaminophen-induced liver injury. *BioImpacts: BI, 9*(4), 227–237. https://doi.org/10.15171/bi.2019.28

Kuznietsova, H. M., Dziubenko, N. V., Lynchak, O. V., Herheliuk, T. S., Zavalny, D. K., Remeniak, O. V., et al. (2020). Effects of pristine C$_{60}$ fullerenes on liver and pancreas in α-Naphthylisothiocyanate-induced cholangitis. *Digestive Diseases and Sciences, 65*(1), 215–224. https://doi.org/10.1007/s10620-019-05730-3

Kuznietsova, H. M., Lynchak, O. V., Dziubenko, N. V., Osetskyi, V. L., Ogloblya, O. V., Prylutskyy, Y. I., et al. (2019). Water-soluble C$_{60}$ fullerenes reduce manifestations of acute cholangitis in rats. *Applied Nanoscience, 9*(5), 601–608. https://doi.org/10.1007/s13204-018-0700-5

Labille, J., Brant, J., Villieras, F., Pelletier, M., Thill, A., Masion, A., et al. (2006). Affinity of C$_{60}$ fullerenes with water. *Fullerenes, Nanotubes, and Carbon Nanostructures, 14*(2–3), 307–314. https://doi.org/10.1080/15363830600665250

Li, Z., Tan, S., Li, S., Shen, Q., & Wang, K. (2017). Cancer drug delivery in the nano era: An overview and perspectives (review). *Oncology Reports, 38*(2), 611–624. https://doi.org/10.3892/or.2017.5718

Liu, J.-H., Cao, L., Luo, P. G., Yang, S.-T., Lu, F., Wang, H., et al. (2010). Fullerene-conjugated doxorubicin in cells. *ACS Applied Materials & Interfaces, 2*(5), 1384–1389. https://doi.org/10.1021/am100037y

Lv, J., He, X., Wang, H., Wang, Z., Kelly, G. T., Wang, X., et al. (2017). TLR4-NOX2 axis regulates the phagocytosis and killing of Mycobacterium tuberculosis by macrophages. *BMC Pulmonary Medicine, 17*(1), 194. https://doi.org/10.1186/s12890-017-0517-0

Mchedlov-Petrossyan, N. O. (2013). Fullerenes in liquid media: An unsettling intrusion into the solution chemistry. *Chemical Reviews, 113*(7), 5149–5193. https://doi.org/10.1021/cr3005026

Meng, Z., Hashmi, S. M., & Elimelech, M. (2013). Aggregation rate and fractal dimension of fullerene nanoparticles via simultaneous multiangle static and dynamic light scattering measurement. *Journal of Colloid and Interface Science, 392*, 27–33. https://doi.org/10.1016/j.jcis.2012.09.088

Mirhadi, E., Rezaee, M., & Malaekeh-Nikouei, B. (2018). Nano strategies for berberine delivery, a natural alkaloid of Berberis. *Biomedicine & Pharmacotherapy, 104*, 465–473. https://doi.org/10.1016/j.biopha.2018.05.067

Montellano, A., Da Ros, T., Bianco, A., & Prato, M. (2011). Fullerene C_{60} as a multifunctional system for drug and gene delivery. *Nanoscale, 3*(10), 4035–4041. https://doi.org/10.1039/c1nr10783f

Mosunov, A., Evstigneev, V., Buchelnikov, A., Salo, V., Prylutskyy, Y., & Evstigneev, M. (2019). General up-scaled model of ligand binding with C_{60} fullerene clusters in aqueous solution. *Chemical Physics Letters, 721*, 22–26. https://doi.org/10.1016/j.cplett.2019.01.051

Mosunov, A. A., Pashkova, I. S., Sidorova, M., Pronozin, A., Lantushenko, A. O., Prylutskyy, Y. I., et al. (2017). Determination of the equilibrium constant of C_{60} fullerene binding with drug molecules. *Physical Chemistry Chemical Physics, 19*(9), 6777–6784. https://doi.org/10.1039/c6cp07140f

Moussa, F. (2018). [60]Fullerene and derivatives for biomedical applications. In R. Narayan (Hrsg.), *Nanobiomaterials,* 113–136. https://doi.org/10.1016/b978-0-08-100716-7.00005-2.

Nagai, F., Hiyoshi, Y., Sugimachi, K., & Tamura, H.-O. (2002). Cytochrome P450 (CYP) expression in human myeloblastic and lymphoid cell lines. *Biological & Pharmaceutical Bulletin, 25*(3), 383–385. https://doi.org/10.1248/bpb.25.383

Neag, M. A., Mocan, A., Echeverría, J., Pop, R. M., Bocsan, C. I., Crişan, G., & Buzoianu, A. D. (2018). Berberine: Botanical occurrence, traditional uses, extraction methods, and relevance in cardiovascular, metabolic, hepatic, and renal disorders. *Frontiers in Pharmacology, 9*, 557. https://doi.org/10.3389/fphar.2018.00557

Nozdrenko, D. M., Zavodovskyi, D. O., Matvienko, T. Y., Zay, S. Y., Bogutska, K. I., Prylutskyy, Y. I., et al. (2017). C_{60} fullerene as promising therapeutic agent for the prevention and correction of skeletal muscle functioning at ischemic injury. *Nanoscale Research Letters, 12*(1), 115. https://doi.org/10.1186/s11671-017-1876-4

Okamoto, M., Hirai, H., Taniguchi, K., Shimura, K., Inaba, T., Shimazaki, C., et al. (2009). Toll-like receptors (TLRs) are expressed by myeloid leukaemia cell lines, but fail to trigger differentiation in response to the respective TLR ligands. *British Journal of Haematology, 147*(4), 585–587. https://doi.org/10.1111/j.1365-2141.2009.07858.x

Olszewski, U., Liedauer, R., Ausch, C., Thalhammer, T., & Hamilton, G. (2011). Overexpression of CYP3A4 in a COLO 205 Colon cancer stem cell model in vitro. *Cancers, 3*(1), 1467–1479. https://doi.org/10.3390/cancers3011467

Panchuk, R. R., Prylutska, S. V., Chumakl, V. V., Skorokhyd, N. R., Lehka, L. V., Evstigneev, M. P., et al. (2015). Application of C_{60} fullerene-doxorubicin complex for tumor cell treatment *In Vitro* and *In Vivo*. *Journal of Biomedical Nanotechnology, 11*(7), 1139–1152. https://doi.org/10.1166/jbn.2015.2058

Park, S. H., Sung, J. H., Kim, E. J., & Chung, N. (2015). Berberine induces apoptosis via ROS generation in PANC-1 and MIA-PaCa2 pancreatic cell lines. *Brazilian Journal of Medical and Biological Research, 48*(2), 111–119. https://doi.org/10.1590/1414-431x20144293

Pereira, G. C., Branco, A. F., Matos, J. A. C., Pereira, S. L., Parke, D., Perkins, E. L., et al. (2007). Mitochondrially targeted effects of berberine [Natural Yellow 18, 5,6-dihydro-9,10-dimethoxybenzo(g)-1,3-benzodioxolo(5,6-a) quinolizinium] on K1735-M2 mouse melanoma cells: Comparison with direct effects on isolated mitochondrial fractions. *The Journal of Pharmacology and Experimental Therapeutics, 323*(2), 636–649. https://doi.org/10.1124/jpet.107.128017

Pérez, E. M., & Martín, N. (2015). π–π interactions in carbon nanostructures. *Chemical Society Reviews, 44*(18), 6425–6433. https://doi.org/10.1039/C5CS00578G

Peudus, D. A., Mosunov, A. A., Mykhina, Y. V., Prylutskyy, Y. I., & Evstigneev, M. P. (2020). Fractal C_{60} fullerene aggregation: Equilibrium thermodynamics approach. *Chemical Physics Letters, 742*, 137161. https://doi.org/10.1016/j.cplett.2020.137161

Prilutski, Y., Durov, S., Bulavin, L., Pogorelov, V., Astashkin, Y., Yashchuk, V., et al. (1998). Study of structure of colloidal particles of fullerenes in water solution. *Molecular Crystals and Liquid Crystals, 324*(1), 65–70. https://doi.org/10.1080/10587259808047135

Prylutska, S., Grynyuk, I., Matyshevska, O., Prylutskyy, Y., Evstigneev, M., Scharff, P., & Ritter, U. (2014). C_{60} fullerene as synergistic agent in tumor-inhibitory doxorubicin treatment. *Drugs in R&D, 14*(4), 333–340. https://doi.org/10.1007/s40268-014-0074-4

Prylutska, S., Grynyuk, I., Skaterna, T., Horak, I., Grebinyk, A., Drobot, L., et al. (2019). Toxicity of C$_{60}$ fullerene-cisplatin nanocomplex against Lewis lung carcinoma cells. *Archives of Toxicology, 93*(5), 1213–1226. https://doi.org/10.1007/s00204-019-02441-6

Prylutska, S., Panchuk, R., Gołuński, G., Skivka, L., Prylutskyy, Y., Hurmach, V., et al. (2017). C$_{60}$ fullerene enhances cisplatin anticancer activity and overcomes tumor cell drug resistance. *Nano Research, 10*(2), 652–671. https://doi.org/10.1007/s12274-016-1324-2

Prylutska, S., Politenkova, S., Afanasieva, K., Korolovych, V., Bogutska, K., Sivolob, A., et al. (2017). A nanocomplex of C$_{60}$ fullerene with cisplatin: Design, characterization and toxicity. *Beilstein Journal of Nanotechnology, 8*(1), 1494–1501. https://doi.org/10.3762/bjnano.8.149

Prylutska, S. V., Grebinyk, A. G., Lynchak, O. V., Byelinska, I. V., Cherepanov, V. V., Tauscher, E., et al. (2019). *In vitro* and *in vivo* toxicity of pristine C$_{60}$ fullerene aqueous colloid solution. *Fullerenes, Nanotubes, and Carbon Nanostructures, 27*(9), 715–728. https://doi.org/10.1080/1536383X.2019.1634055

Prylutska, S. V., Grynyuk, I. I., Grebinyk, S. M., Matyshevska, O. P., Prylutskyy, Y. I., Ritter, U., et al. (2009). Comparative study of biological action of fullerenes C$_{60}$ and carbon nanotubes in thymus cells. *Materialwissenschaft und Werkstofftechnik, 40*(4), 238–241. https://doi.org/10.1002/mawe.200900433

Prylutska, S. V., Lynchak, O. V., Kostjukov, V. V., Evstigneev, M. P., Remeniak, O. V., Rybalchenko, V. K., et al. (2019). Antitumor effects and hematotoxicity of C$_{60}$-Cis-Pt nanocomplex in mice with Lewis lung carcinoma. *Experimental Oncology, 41*(2), 106–111. https://doi.org/10.32471/exp-oncology.2312-8852.vol-41-no-2.13030

Prylutska, S. V., Skivka, L. M., Didenko, G. V., Prylutskyy, Y. I., Evstigneev, M. P., Potebnya, G. P., et al. (2015). Complex of C$_{60}$ fullerene with doxorubicin as a promising agent in antitumor therapy. *Nanoscale Research Letters, 10*(1), 499. https://doi.org/10.1186/s11671-015-1206-7

Prylutskyy, Y., Borowik, A., Gołuński, G., Woziwodzka, A., Piosik, J., Kyzyma, O., et al. (2016). Biophysical characterization of the complexation of C$_{60}$ fullerene with doxorubicin in a prokaryotic model. *Materialwissenschaft und Werkstofftechnik, 47*(2–3), 92–97. https://doi.org/10.1002/mawe.201600463

Prylutskyy, Y. I., Evstigneev, M., Cherepanov, V., Kyzyma, O., Bulavin, L. A., Davidenko, N., & Scharff, P. (2015). Structural organization of C$_{60}$ fullerene, doxorubicin, and their complex in physiological solution as promising antitumor agents. *Journal of Nanoparticle Research, 17*, 1–9. https://doi.org/10.1007/s11051-015-2867-y

Prylutskyy, Y. I., Evstigneev, M. P., Pashkova, I. S., Wyrzykowski, D., Woziwodzka, A., Gołuński, G., et al. (2014). Characterization of C$_{60}$ fullerene complexation with antibiotic doxorubicin. *Physical Chemistry Chemical Physics, 16*(42), 23164–23172. https://doi.org/10.1039/c4cp03367a

Prylutskyy, Y. I., Buchelnikov, A. S., Voronin, D. P., Kostjukov, V. V., Ritter, U., Parkinson, J. A., & Evstigneev, M. P. (2013). C$_{60}$ fullerene aggregation in aqueous solution. *Physical Chemistry Chemical Physics, 15*(23), 9351–9360. https://doi.org/10.1039/c3cp50187f

Prylutskyy, Y. I., Cherepanov, V. V., Evstigneev, M. P., Kyzyma, O. A., Petrenko, V. I., Styopkin, V. I., et al. (2015). Structural self-organization of C$_{60}$ and cisplatin in physiological solution. *Physical Chemistry Chemical Physics, 17*(39), 26084–26092. https://doi.org/10.1039/c5cp02688a

Prylutskyy, Y. I., Durov, S. S., Bulavin, L. A., Adamenko, I. I., Moroz, K. O., Geru, I. I., et al. (2001). Structure and thermophysical properties of fullerene C$_{60}$ aqueous solutions. *International Journal of Thermophysics, 22*(3), 943–956. https://doi.org/10.1023/a:1010791402990

Prylutskyy, Y. I., Petrenko, V. I., Ivankov, O. I., Kyzyma, O. A., Bulavin, L. A., Litsis, O. O., et al. (2014). On the origin of C$_{60}$ fullerene solubility in aqueous solution. *Langmuir, 30*(14), 3967–3970. https://doi.org/10.1021/la404976k

Qiao, R., Roberts, A. P., Mount, A. S., Klaine, S. J., & Ke, P. C. (2007). Translocation of C$_{60}$ and its derivatives across a lipid bilayer. *Nano Letters, 7*(3), 614–619. https://doi.org/10.1021/nl062515f

Rabik, C. A., Fishel, M. L., Holleran, J. L., Kasza, K., Kelley, M. R., Egorin, M. J., & Dolan, M. E. (2008). Enhancement of cisplatin [cis-Diammine Dichloroplatinum (II)] cytotoxicity by O6-Benzylguanine involves endoplasmic reticulum stress. *The Journal of Pharmacology and Experimental Therapeutics, 327*(2), 442–452. https://doi.org/10.1124/jpet.108.141291

Ritter, U., Prylutskyy, Y. I., Evstigneev, M. P., Davidenko, N. A., Cherepanov, V. V., Senenko, A. I., et al. (2015). Structural features of highly stable reproducible C_{60} fullerene aqueous colloid solution probed by various techniques. *Fullerenes, Nanotubes, and Carbon Nanostructures, 23*(6), 530–534. https://doi.org/10.1080/1536383x.2013.870900

Russ, K. A., Elvati, P., Parsonage, T. L., Dews, A., Jarvis, J. A., Ray, M., et al. (2016). C_{60} fullerene localization and membrane interactions in RAW 264.7 immortalized mouse macrophages. *Nanoscale, 8*(7), 4134–4144. https://doi.org/10.1039/c5nr07003a

Sandoval, J., Ventura-Sobrevilla, J., Boone-Villa, D., Ramos-González, R., Velázquez, M., Silva-Belmares, Y., et al. (2019). Chapter 14—Carbon nanomaterials as pharmaceutic forms for sustained and controlled delivery systems. In A. M. Grumezescu (Hrsg.), *Nanomaterials for drug delivery and therapy* (S. 403–434). https://doi.org/10.1016/b978-0-12-816505-8.00003-5.

Santos, S. M., Dinis, A. M., Peixoto, F., Ferreira, L., Jurado, A. S., & Videira, R. A. (2014). Interaction of fullerene nanoparticles with biomembranes: From the partition in lipid membranes to effects on mitochondrial bioenergetics. *Toxicological Sciences: An Official Journal of the Society of Toxicology, 138*(1), 117–129. https://doi.org/10.1093/toxsci/kft327

Sarin, N., Engel, F., Kalayda, G. V., Mannewitz, M., Cinatl, J., Rothweiler, F., et al. (2017). Cisplatin resistance in non-small cell lung cancer cells is associated with an abrogation of cisplatin-induced G2/M cell cycle arrest. *PLoS One, 12*(7), e0181081. https://doi.org/10.1371/journal.pone.0181081

Scharff, P., Risch, K., Carta-Abelmann, L., Dmytruk, I. M., Bilyi, M. M., Golub, O. A., et al. (2004). Structure of C_{60} fullerene in water: Spectroscopic data. *Carbon, 42*(5–6), 1203–1206. https://doi.org/10.1016/j.carbon.2003.12.053

Schein, S. (2009). Architecture of clathrin fullerene cages reflects a geometric constraint—The head-to-tail exclusion rule—And a preference for asymmetry. *Journal of Molecular Biology, 387*(2), 363–375. https://doi.org/10.1016/j.jmb.2009.01.044

Schein, S., & Sands-Kidner, M. (2008). A geometric principle may guide self-assembly of fullerene cages from Clathrin triskelia and from carbon atoms. *Biophysical Journal, 94*(3), 958–976. https://doi.org/10.1529/biophysj.107.110817

Scott, C. A., Westmacott, D., Broadhurst, M. J., Thomas, G. J., & Hall, M. J. (1986). 9-alkyl anthracyclines. Absence of cross-resistance to adriamycin in human and murine cell cultures. *British Journal of Cancer, 53*(5), 595–600. https://doi.org/10.1038/bjc.1986.101

Seo, Y.-S., Yim, M.-J., Kim, B.-H., Kang, K.-R., Lee, S.-Y., Oh, J.-S., et al. (2015). Berberine-induced anticancer activities in FaDu head and neck squamous cell carcinoma cells. *Oncology Reports, 34*(6), 3025–3034. https://doi.org/10.3892/or.2015.4312

Shewach, D. S., & Kuchta, R. D. (2009). Introduction to cancer chemotherapeutics. *Chemical Reviews, 109*(7), 2859–2861. https://doi.org/10.1021/cr900208x

Shi, J., Kantoff, P. W., Wooster, R., & Farokhzad, O. C. (2017). Cancer nanomedicine: Progress, challenges and opportunities. *Nature Reviews. Cancer, 17*, 20–37. https://doi.org/10.1038/nrc.2016.108

Skamrova, G. B., Laponogov, I., Buchelnikov, A. S., Shckorbatov, Y. G., Prylutska, S. V., Ritter, U., et al. (2014). Interceptor effect of C_{60} fullerene on the in vitro action of aromatic drug molecules. *European Biophysics Journal, 43*(6–7), 265–276. https://doi.org/10.1007/s00249-014-0960-2

Skivka, L. M., Prylutska, S. V., Rudyk, M. P., Khranovska, N. M., Opeida, I. V., Hurmach, V. V., et al. (2018). C_{60} fullerene and its nanocomplexes with anticancer drugs modulate circulating phagocyte functions and dramatically increase ROS generation in transformed monocytes. *Cancer Nanotechnology, 9*(1), 8. https://doi.org/10.1186/s12645-017-0034-0

Tacar, O., Sriamornsak, P., & Dass, C. R. (2013). Doxorubicin: An update on anticancer molecular action, toxicity and novel drug delivery systems. *The Journal of Pharmacy and Pharmacology, 65*(2), 157–170. https://doi.org/10.1111/j.2042-7158.2012.01567.x

Takeda, K., & Akira, S. (2015). Toll-like receptors. *Current Protocols in Immunology, 109*, 14121–141210. https://doi.org/10.1002/0471142735.im1412s109

Thorn, C. F., Oshiro, C., Marsh, S., Hernandez-Boussard, T., McLeod, H., Klein, T. E., & Altman, R. B. (2011). Doxorubicin pathways: Pharmacodynamics and adverse effects. *Pharmacogenetics and Genomics, 21*(7), 440–446. https://doi.org/10.1097/fpc.0b013e32833ffb56

Tolkachov, M., Sokolova, V., Loza, K., Korolovych, V., Prylutskyy, Y., Epple, M., et al. (2016). Study of biocompatibility effect of nanocarbon particles on various cell types *in vitro*. *Materialwissenschaft und Werkstofftechnik, 47*(2–3), 216–221. https://doi.org/10.1002/mawe.201600486

Turabekova, M., Rasulev, B., Theodore, M., Jackman, J., Leszczynska, D., & Leszczynski, J. (2014). Immunotoxicity of nanoparticles: A computational study suggests that CNTs and C$_{60}$ fullerenes might be recognized as pathogens by Toll-like receptors. *Nanoscale, 6*(7), 3488–3495. https://doi.org/10.1039/c3nr05772k

Ughachukwu, P., & Unekwe, P. (2012). Efflux pump-mediated resistance in chemotherapy. *Annals of Medical and Health Sciences Research, 2*(2), 191–198. https://doi.org/10.4103/2141-9248.105671

Velma, V., Dasari, S. R., & Tchounwou, P. B. (2016). Low doses of cisplatin induce gene alterations, cell cycle arrest, and apoptosis in human Promyelocytic leukemia cells. *Biomarker Insights, 11*, 113–121. https://doi.org/10.4137/bmi.S39445

Vereshchaka, I. V., Bulgakova, N. V., Maznychenko, A. V., Gonchar, O. O., Prylutskyy, Y. I., Ritter, U., et al. (2018). C$_{60}$ fullerenes diminish muscle fatigue in rats comparable to N-acetylcysteine or β-alanine. *Frontiers in Physiology, 9*. https://doi.org/10.3389/fphys.2018.00517

Wang, I. C., Tai, L. A., Lee, D. D., Kanakamma, P. P., Shen, C. K., Luh, T. Y., et al. (1999). C(60) and water-soluble fullerene derivatives as antioxidants against radical-initiated lipid peroxidation. *Journal of Medicinal Chemistry, 42*(22), 4614–4620. https://doi.org/10.1021/jm990144s

Wang, Y., Kheir, M. M., Chai, Y., Hu, J., Xing, D., Lei, F., & Du, L. (2011). Comprehensive study in the inhibitory effect of Berberine on gene transcription, including TATA box. *PLoS One, 6*(8) https://doi.org/10.1371/journal.pone.0023495

Wierzbicki, M., Sawosz, E., Grodzik, M., Prasek, M., Jaworski, S., & Chwalibog, A. (2013). Comparison of anti-angiogenic properties of pristine carbon nanoparticles. *Nanoscale Research Letters, 8*(1), 195. https://doi.org/10.1186/1556-276X-8-195

Xue, X., & Liang, X.-J. (2012). Overcoming drug efflux-based multidrug resistance in cancer with nanotechnology. *Chinese Journal of Cancer, 31*(2), 100–109. https://doi.org/10.5732/cjc.011.10326

Yang, D., Gao, S., Fang, Y., Lin, X., Jin, X., Wang, X., et al. (2018). The π-π stacking-guided supramolecular self-assembly of nanomedicine for effective delivery of antineoplastic therapies. *Nanomedicine (London, England), 13*(24), 3159–3177. https://doi.org/10.2217/nnm-2018-0288

Yudoh, K., Karasawa, R., Masuko, K., & Kato, T. (2009). Water-soluble fullerene (C60) inhibits the development of arthritis in the rat model of arthritis. *International Journal of Nanomedicine, 4*, 217–225.

Zhang, J., Cao, H., Zhang, B., Cao, H., Xu, X., Ruan, H., et al. (2013). Berberine potently attenuates intestinal polyps growth in ApcMin mice and familial adenomatous polyposis patients through inhibition of Wnt signalling. *Journal of Cellular and Molecular Medicine, 17*(11), 1484–1493. https://doi.org/10.1111/jcmm.12119

Zhang, L. W., Yang, J., Barron, A. R., & Monteiro-Riviere, N. A. (2009). Endocytic mechanisms and toxicity of a functionalized fullerene in human cells. *Toxicology Letters, 191*(2–3), 149–157. https://doi.org/10.1016/j.toxlet.2009.08.017

Zhang, P., Gao, W. Y., Turner, S., & Ducatman, B. S. (2003). Gleevec (STI-571) inhibits lung cancer cell growth (A549) and potentiates the cisplatin effect in vitro. *Molecular Cancer, 2*, 1. https://doi.org/10.1186/1476-4598-2-1

Zhang, X., Cong, H., Yu, B., & Chen, Q. (2019). Recent advances of water-soluble fullerene derivatives in biomedical applications. *Mini-Reviews in Organic Chemistry, 16*(1), 92–99. https://doi.org/10.2174/1570193x15666180712114405

Magnetic Iron Oxide Particles for Theranostics

Beata Zasońska and Daniel Horák

1 Introduction

With rapid development in nanotechnology, magnetic nanomaterials have received considerable attention in various industrial fields, such as wastewater treatment, pharmacology, electronics, and biotechnology (Cornell & Schwertmann, 2000). By definition, at least one dimension of nanomaterials is in nanoscale size (typically ≤100 nm) (Laurent et al., 2008). Magnetic nanoparticles exhibit unique properties, including a high surface-to-volume ratio and high magnetic moment, allowing potential manipulation by an external magnetic field. The particle biocompatibility, colloidal stability, and eco-friendliness have made them an ideal tool especially for biomedical applications (Gupta & Gupta, 2005; Neuberger et al., 2005). These involve mainly theranostics, incorporating both diagnostic and therapeutic uses, for example, controlled drug delivery systems, biosensors, cell separation and labeling, contrast agents for magnetic resonance imaging (MRI), and in cancer therapy, for example, hyperthermia (Fig. 1) (Zavaleta et al., 2018). In magnetic hyperthermia, magnetic nanoparticles induce local heat enhancement when submitted to an external magnetic field, killing cancer cells that cannot survive in the temperature ranging 42–49 °C. Also, other biomedical applications, like tissue repair and magnetofection, have been intensively investigated. A possibility to combine magnetic properties with antibacterial, conductive, fluorescence, and/or antitumor effects thus opens up a new range of possible exploitations (Musielak et al., 2019).

Magnetic nanoparticles are mostly made of iron oxides; iron is a crucial element in the organisms and is non-toxic at moderate concentrations. To interact with biological

B. Zasońska · D. Horák (✉)
Institute of Macromolecular Chemistry, Czech Academy of Sciences,
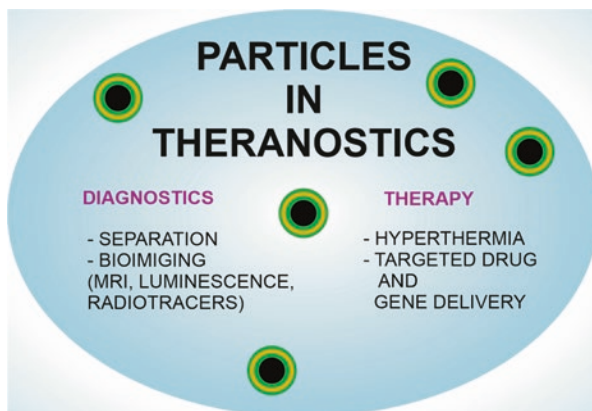Prague, Czech Republic
e-mail: horak@imc.cas.cz

Fig. 1 Schematic view of different applications of magnetic particles in theranostics

systems, the nanoparticle diameter has to be smaller or comparable to the size of proteins, viruses, or cells. The selection of synthetic methods that affect the particle size and its distribution, structural defects, surface chemistry, colloidal stability, and magnetic behavior is thus of crucial importance (Cornell & Schwertmann, 2000).

Another critical issue for the application is particle aggregation, which has to be prevented by coating particles with a proper polymer layer; uncoated iron oxides are usually not colloidally stable in biological media due to strong magnetic attraction between the particles, van der Waals forces, and high-energy surfaces (Cornell & Schwertmann, 2000). A common approach to increase biocompatibility and prevent particle aggregation in a physiological environment is coating with various inorganic and organic materials, involving, for example, dextran, chitosan, poly(ethylene glycol), silica, and albumin. Moreover, surface modification renders the particles with biofunctional groups necessary for the specific application.

Some of these issues have been recently summarized by us in a comprehensive review (Horák, 2020); this contribution then continues the above paper.

2   Synthesis of Magnetic Nano- and Microparticles

Synthesis of magnetic particles is usually a multistep procedure and many strategies have been developed to produce micro- and nanostructures based on iron oxides. All these methods have benefits as well as disadvantages, and various parameters have to be taken into consideration during the synthesis.
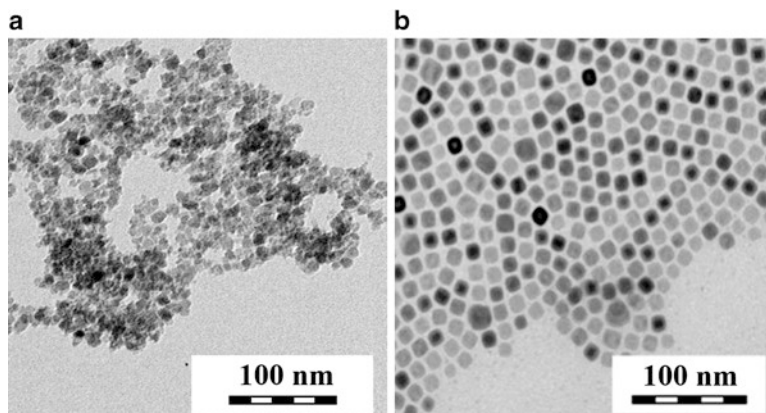
Fig. 2 TEM micrographs of (**a**) 9-nm γ-Fe$_2$O$_3$ and (**b**) 20-nm Fe$_3$O$_4$ particles

2.1 Iron Oxide Nanoparticles

Different methods have been utilized for the preparation of colloidally stable iron oxide nanoparticles of various sizes (1–100 nm), morphology (shape), and surface functionalization (Laurent et al., 2008; Varanda et al., 2019). Here, we provide a brief description of the existing strategies for the production of magnetite and maghemite particles. One of the oldest methods involves grinding of bulk magnetite; other synthetic approaches include coprecipitation, thermal decomposition, biomineralization, spray pyrolysis, sputter deposition, or sol-gel, bacterial, microemulsion, microwave plasma, and hydrothermal techniques (Horák, 2020). Nevertheless, the most widely used methods are coprecipitation of Fe salts and thermal decomposition of Fe organic precursors.

Coprecipitation method Maghemite (γ-Fe$_2$O$_3$) was prepared by coprecipitation of aqueous Fe(II) and Fe(III) chlorides with ammonium hydroxide, which was followed by oxidation of Fe$_3$O$_4$ with NaOCl or H$_2$O$_2$ (Fig. 2a) (Zasońska et al., 2016). A disadvantage of this method is that the iron oxide core is not protected from further oxidation and particles are not monodisperse in size and shape.

Thermal decomposition In contrast to the coprecipitation, thermal decomposition allows for the preparation of monodisperse Fe$_3$O$_4$ nanoparticles with controlled size (Fig. 2b). Typically, the particles are obtained from Fe(III) oleate in a high-boiling-point solvent (e.g., octadec-1-ene) and stabilized by oleic acid (Patsula et al., 2019a). The particles are hydrophobic and as such they have to be transferred from organic to aqueous solutions, where biological applications occur.
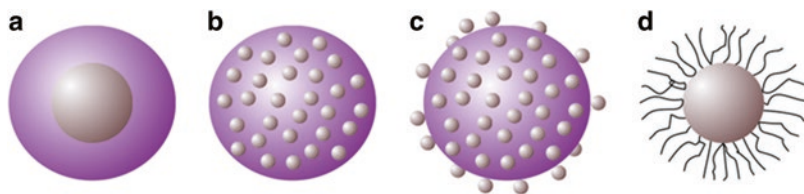
Fig. 3 Scheme of four main core-shell particle morphologies: (**a**) single core, (**b**) multicore, (**c**) strawberry, and (**d**) hairy. (Horák et al. (2007). Copyright Wiley-VCH. Reproduced with permission)

2.2 Core-Shell Nanoparticles and Modification with Biomolecules

Stability of the magnetic particles in biologically relevant media for a longer period is a key issue in many applications. It is a challenge to keep magnetic particles without aggregation or precipitation. In order to maintain chemical and colloidal stability of the iron oxide particles, their surface has to be coated with a proper protective layer. This protective shell not only prevents the particle core from oxidation and degradation but can also be useful for further modification with functional components such as drugs, biomolecules, and catalytically active species. It is still a challenge to produce stable and biocompatible magnetic particles with a narrow size distribution, high surface area, and high magnetization, which are environmentally friendly.

There are many ways to fabricate core-shell particles (Fig. 3). A relatively easy way of particle modification is adsorption of biomolecules. More challenging methods then provide steady immobilization, involving covalent binding of molecules to the iron oxide surface. The $\gamma\text{-}Fe_2O_3$ or Fe_3O_4 particles contain many hydroxyl groups at the surface that can be used for attachment of a polymer shell. Typically, the shells are made from organic [poly(ethylene glycol), poly(*N,N*-dimethylacrylamide), D-mannose, D-manitol] or inorganic materials (silica) (Pongrac et al., 2019; Patsula et al., 2019a; Zasońska et al., 2016).

2.3 Magnetic Microparticles

Polymer microparticles have found various applications in chromatography, drug delivery systems, tissue regeneration, and so on (Campos et al., 2013). Typically, the microparticles are made from silica (Girija & Balasubramanian, 2019), polystyrene (Šálek et al., 2011), poly(glycidyl methacrylate) (Fig. 4) (Koubková et al., 2014), and others. Many reports are available on the preparation of microparticles
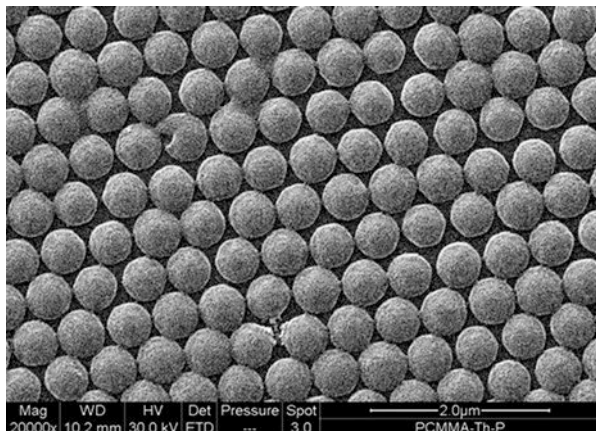
Fig. 4 SEM micrograph of poly(glycidyl methacrylate) microparticles

often also named microspheres (Horák et al., 2007; Agnihotri et al., 2004). The most common synthesis methods are emulsion polymerization, surfactant-free polymerization, and seeded-growth polymerization of styrene in an aqueous solution with potassium persulfate as a polymerization initiator. Depending on the purpose, the particles can be prepared with regulated size, shape, porosity, pore volume, pore size, and thickness of shell. Magnetic properties of the microparticles are derived from the presence of magnetic nanoparticles on the surface or within the microsphere bulk.

3   Properties and Characterization of Magnetic Particles

The characterization of physicochemical properties of iron oxide nanocomposites can be performed by several approaches. Below, we have chosen the most common techniques with a focus on the determination of shape, morphology, structure, size, size distribution, stability, magnetic properties of the particles, and others.

3.1   *Physicochemical Techniques*

Many spectroscopic techniques are used to characterize the magnetic particles. The important ones include FTIR spectroscopy, monitoring the presence of functional groups on the particle surface, and efficiency of the chemical modification. X-ray diffraction and highly surface-sensitive X-ray photoelectron spectroscopy provide information about the crystalline structure of the particles and surface composition,

respectively. The dynamic light scattering technique is of key importance for the analysis of particle dispersibility in aqueous media, informing about the hydrodynamic particle size and its distribution. The translational diffusion coefficient depends on the particle core size, surface modification, concentration, counter ions present in the medium, and pH. Another significant information is the ζ-potential (electrokinetic potential), which is not only a measure of the effective charge on the particle surface but also provides information about the particle colloidal stability (electrostatic repulsion, electrophoretic mobility, and colloidal stability). Fluorescence correlation spectroscopy (using the visible and UV light) is often employed for studying the concentration effects, chemical kinetics, and molecular diffusion. Atomic absorption spectroscopy and thermogravimetric analysis were used to determine the iron content in the particles. Elemental analysis provided the identification and quantification of carbon, hydrogen, nitrogen, and sulfur in nano- and microparticles. Scanning electron microscopy (SEM) and transmission electron microscopy (TEM) are used to determine the size and surface morphology of the magnetic particles. Dynamic desorption of nitrogen measures the specific surface area. Vibrating sample magnetometry allows for the measurement of the magnetic properties of a material as a function of magnetic field, temperature, and time. NMR spectra of a nonmagnetic particle coating allow for the characterization of the molecular structure and the organization (chain alignment) of the macromolecules. Finally, chromatography is a very important technique for the characterization of molecular weight and separation (purification).

3.2   Biological Properties

Novel materials, such as magnetic nanoparticles, can have a high impact on biological environment, affecting consequently the living organisms. A series of toxicology studies have, therefore, to be carried out before any biomedical application. These investigations include both *in vitro* and in vivo characterization of the nanomaterial behavior in cells, particle uptake, effects on living tissues, and evaluation of therapeutic and/or diagnostic efficiency. Cell viability tests should be incorporated at the beginning of these experiments.

4   Separation of Cells

Magnetic nano- and microparticles show great promise as novel medication, theranostic, and separation tools. Biologically active ligands can be specifically conjugated to the nanoparticles to separate cells from very complexed mixtures (Fig. 5).
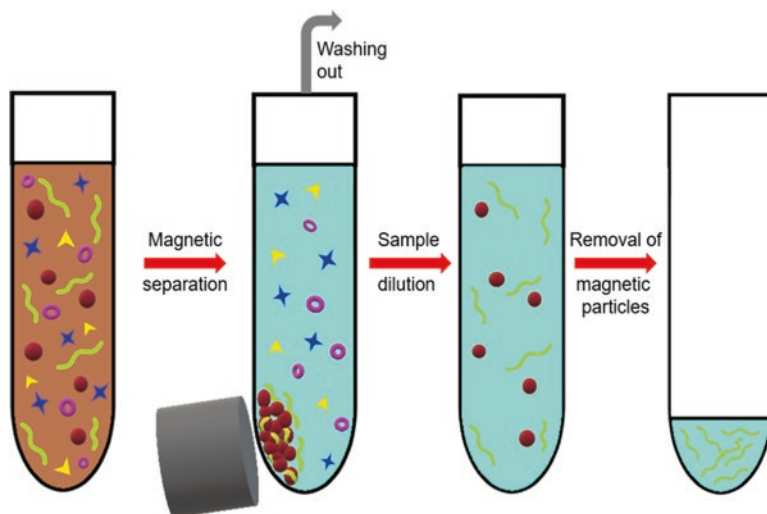
Fig. 5 Schematic illustration of the magnetic separation

It is very important that the magnetic separation does not affect cell viability and proliferation. Recently, molecular diagnostic methods based on DNA amplification are being used for the identification of beneficial microorganisms (probiotics) in foods or pathogenic bacteria in clinical samples, feces, and/or in archeology. In these isolation methods, in particular, the microspheres are preferable, as these operations are much easier than those with nanoparticles. As an example, solid phase DNA extraction from the real samples represented by *E. coli* lysate was performed on the monodisperse poly(methacrylic acid-*co*-ethylene dimethacrylate) microspheres without compromising the DNA integrity in the eluates (Šálek et al., 2019). DNA isolation on magnetic microspheres was also combined with polymerase chain reaction amplification (Konečná et al., 2019). Solid phase extraction thus represents an effective tool for the separation and purification of biomolecules from biological samples. In contrast to traditional extraction methods (phenol extraction, commercial kit), the magnetic particle-based approach allows for the simplification of the extraction procedures, the reduction of toxic solvents, and most importantly, the reduction of processing time from a few hours to less than half an hour. Ammonolyzed magnetic, monodisperse macroporous poly(glycidyl methacrylate) (PGMA–NH$_2$) microspheres were used for purification and identification of human blood serum, which has proteins with affinity to the antitumor active RL2 lactaptin. The data suggested that the RL2 protein could be engaged in interactions with blood serum, affecting protein activity (Manko et al., 2019).

5 Theranostic Applications

Theranostics is a relatively new term in medicine, which combines specific targeted therapy and diagnosis. For example, photothermal and/or photodynamic therapy involves imaging tools, such as optical, magnetic resonance, and ultrasound imaging. Nanotheranostics then applies to the use of magnetic nanoparticles, involving polymeric, metallic, and silica-based particulates, or micelles, dendrimers, and liposomes, in targeted delivery of diagnostic and therapeutic agents for synergic effects and reduced side-effects.

6 Anticancer Drug Delivery

Cancer remains one of the most fatal diseases worldwide, with surgery, chemo-, and radiotherapy being the most commonly used remedies. There is still need not only for improved and fast tumor detection and precise diagnosis, but also for selective treatment accompanied with low side-toxicity. These goals can be achieved using targeted anticancer drug delivery with magnetic nanoparticles.

As an example, transport of doxorubicin, which is the most often investigated anticancer agent, directly to cancer cells was achieved by magnetic nanoparticle-based delivery vehicles. To decrease the general toxicity, dose-dependent approaches were needed. The cytotoxicity of doxorubicin-conjugated poly[N-(2-hydroxypropyl) methacrylamide]-modified γ-Fe$_2$O$_3$ nanoparticles was analyzed toward human tumor cells (Fig. 6) (Plichta et al., 2018). Optionally, poly[N-(2-hydroxypropyl) methacrylamide-co-methyl 2-methacrylamidoacetate] [P(HP-MMAA)] was reacted with hydrazine to yield poly[N-(2-hydroxypropyl)methacrylamide-co-N-(2-hydrazinyl-2-oxoethyl)methacrylamide] [P(HP-MAH)] (Fig. 7) as a vehicle for anticancer drug transport into cells; its advantage was the presence of a hydrazone bond that was hydrolyzed in acidic milieu mimicking tumor environment and releasing the drug (Fig. 8) (Plichta et al., 2020). The P(HP-MAH)-Dox conjugate was then used as a coating of magnetic γ-Fe$_2$O$_3$ nanoparticles.
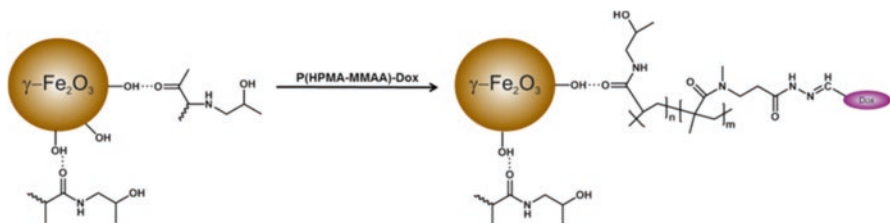

Fig. 6 Schematic illustration of the interaction between poly[N-(2-hydroxypropyl)methacrylamide] and a maghemite nanoparticle followed by the addition of doxorubicin-conjugated poly[N-(2-hydroxypropyl)methacrylamide-co-methyl 2-methacrylamidoacetate] (Plichta et al., 2018). (Reproduced with permission from Beilstein Institute for the Advancement of Chemical Sciences)
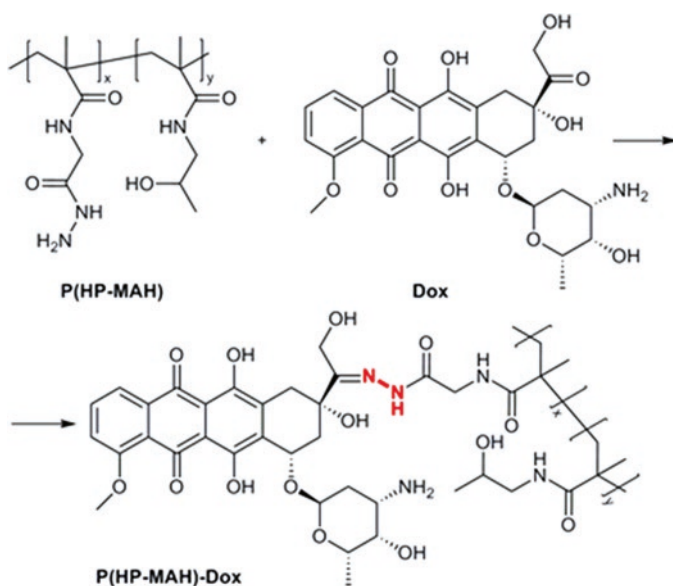
Fig. 7 Reaction of poly[*N*-(2-hydroxypropyl)methacrylamide-*co*-*N*-(2-hydrazinyl-2-oxoethyl) methacrylamide] [P(HP-MAH)] with doxorubicin (Dox) to yield doxorubicin-bound poly[*N*-(2-hydroxypropyl)methacrylamide-*co*-*N*-(2-hydrazinyl-2-oxoethyl)methacrylamide] [P(HP-MAH-Dox)]. (Plichta et al. (2020). Copyright Wiley-VCH. Reproduced with permission)

Fig. 8 Kinetics of doxorubicin (Dox) release from poly[*N*-(2-hydroxypropyl) methacrylamide-*co*-*N*-(2-hydrazinyl-2-oxoethyl) methacrylamide] [P(HP-MAH)-Dox] in various buffers at 37 °C. (Plichta et al. (2020). Copyright Wiley-VCH. Reproduced with permission)
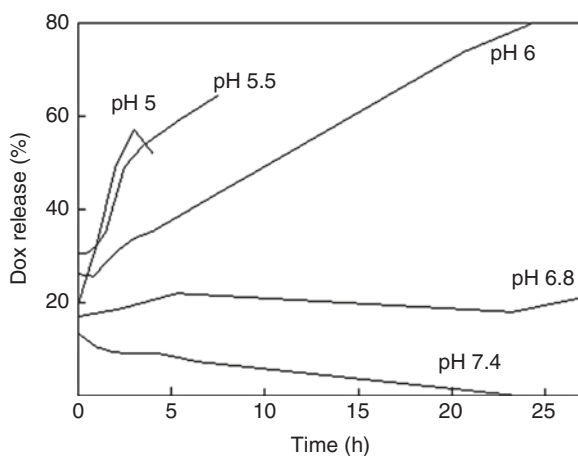
In vitro toxicity of various concentrations of doxorubicin, P(HP-MAH)-Dox, and γ-Fe$_2$O$_3$@P(HP-MAH)-Dox nanoparticles was determined on somatic healthy cells (human bone marrow stromal cells, hMSC), human glioblastoma line, and primary human glioblastoma cells isolated from patients both at a short and prolonged exposition time (up to 1 week) (Plichta et al., 2020). As expected,

Table 1 Combined antitumor effect of vitamin E analogue (Toc-6-Ac) and iron oxide nanoparticles administered per os in Wistar rats with Walker-256 mammary gland carcinosarcoma compared to tumor-bearing rats intraperitoneally treated with doxorubicin

Run	Active substance	Drug or particle dose (mg/kg)	Tumor volume reduction (vol.%)	No. and (%) of animals with complete tumor regression
1	Doxorubicin	1.5	$68.11 \pm 7.72^*$	1 (10)
2	Toc-6-Ac	25	$68.68 \pm 2.44^*$	1 (10)
3	$\gamma\text{-Fe}_2\text{O}_3$	10	$25.10 \pm 3.88^*$	1 (10)
4	$\gamma\text{-Fe}_2\text{O}_3@\text{SiO}_2$	10	12.03 ± 3.82	0 (0)
5	$\gamma\text{-Fe}_2\text{O}_3@\text{PDMA}$	10	$61.89 \pm 5.09^*$	0 (0)
6	$\gamma\text{-Fe}_2\text{O}_3$ + Toc-6-Ac	10 and 25	$36.25 \pm 2.92^{*,\#}$	4 (40)
7	$\gamma\text{-Fe}_2\text{O}_3@\text{SiO}_2$ + Toc-6-Ac	10 and 25	$57.88 \pm 10.47^{*,\S}$	2 (20)
8	$\gamma\text{-Fe}_2\text{O}_3@\text{PDMA}$ + Toc-6-Ac	10 and 25	$63.80 \pm 3.56^*$	0 (0)

Reprinted from Zasońska et al. (2019a). Copyright 2019, with permission from Elsevier
[*, #, §] Significantly different from control tumor-bearing animals without treatment and animals treated with nanoparticles No. 3 and 4, respectively. The data are means ± SE (number of animals $n = 10$)

$\gamma\text{-Fe}_2\text{O}_3@\text{P(HP-MAH)-Dox}$ nanoparticles significantly decreased the human glioblastoma line and primary human glioblastoma cell growth compared to free doxorubicin and P(HP-MAH)-Dox in low concentration (10 nM), although in hMSCs it remained without effect. $\gamma\text{-F}_2\text{O}_3@\text{PHP}$ nanoparticles alone did not affect the viability of the cells.

Analysis of current literature suggests that vitamin E may also be a suitable candidate for the adjuvant treatment of cancer. The tumor inhibitory effect of vitamin E, in particular, the acetate derivative of α-tocopherol (Toc-6-Ac) alone and together with the $\gamma\text{-Fe}_2\text{O}_3$ or $\gamma\text{-Fe}_2\text{O}_3@\text{SiO}_2$ nanoparticles, was investigated in Wistar rats with W-256 mammary gland carcinoma (Zasońska et al., 2019a). The antitumor effect of Toc-6-Ac and iron oxide nanoparticles was compared not only to that of doxorubicin, but also to poly(*N,N*-dimethylacrylamide)-coated maghemite abbreviated as $\gamma\text{-Fe}_2\text{O}_3@\text{PDMA}$ (Table 1).

Tumor inhibitory activity was expressed in terms of tumor volume decrease. Doxorubicin or Toc-6-Ac and $\gamma\text{-Fe}_2\text{O}_3$ reduced the tumor volume by ~70 and 25 vol.%, respectively. In contrast, $\gamma\text{-Fe}_2\text{O}_3@\text{SiO}_2$ nanoparticles reduced the tumor volume by only ~12 vol.%, which was due to the presence of the inert SiO_2 shell, which hindered the redox activity of maghemite nanoparticles alone. When Toc-6-Ac was administered in tumor-bearing animals, together with iron oxide nanoparticles, tumor volume reduction was moderate comparable to administration of neat $\gamma\text{-Fe}_2\text{O}_3$. Nevertheless, when Toc-6-Ac was jointly added with the $\gamma\text{-Fe}_2\text{O}_3@\text{SiO}_2$ nanoparticles, tumor inhibition was boosted, reducing the tumor volume by almost 60 vol.%. It was explained by the fact that $\gamma\text{-Fe}_2\text{O}_3$ redox activity in the $\gamma\text{-Fe}_2\text{O}_3@\text{SiO}_2$ nanoparticles was suppressed and the addition of Toc-6-Ac boosted the reduction of Fe^{3+} to Fe^{2+} ions even in the presence of the silica shell. The

Fig. 9 Schematic view of magnetic and temperature-sensitive solid lipid particles (Świętek et al., 2020). (Reproduced with permission from Frontiers Media SA)
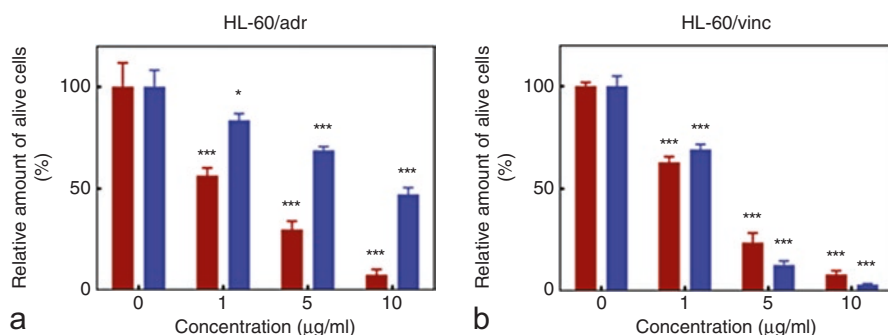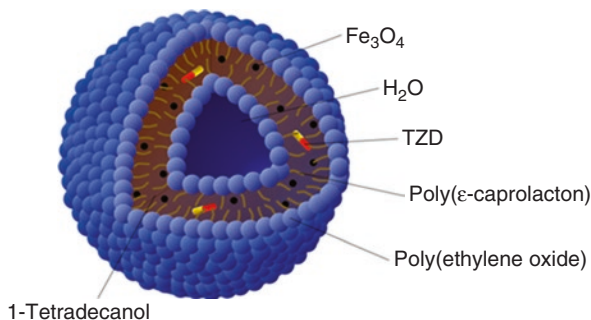

Fig. 10 Cytotoxicity of the magnetic solid lipid particles against (**a**) human myeloid leukemia HL-60/adr cells resistant to doxorubicin and (**b**) human myeloid leukemia HL-60/vinc cells resistant to vincristine determined by trypan blue exclusion test on 24 and 72 h (Świętek et al., 2020). (Reproduced with permission from Frontiers Media SA)

antitumor effect of γ-Fe$_2$O$_3$@SiO$_2$ nanoparticles was not so high as that of γ-Fe$_2$O$_3$@poly(N,N-dimethylacrylamide) (γ-Fe$_2$O$_3$@PDMA) nanoparticles (Table 1), which was interpreted by their quick engulfment by the cells.

Novel magnetic and temperature-sensitive solid lipid particles seem to be promising in anticancer therapy, especially in the context of therapy resistance. The particles (850 nm in size) were prepared in the presence of oleic acid-coated iron oxide nanoparticles with 1-tetradecanol and poly(ethylene oxide)-*block*-poly(ε-caprolactone) as lipid and stabilizing surfactant-like agents, respectively (Fig. 9) (Świętek et al., 2020).

The magnetic and nonmagnetic lipid particles exhibited dose-dependent cytotoxicity against human leukemia cell lines growing in suspension (Jurkat and HL 60/wt), as well as the doxorubicin did (Fig. 10 a,b). Moreover, higher cytotoxicity of the particles toward drug-resistant sublines was observed compared to doxorubicin. The human glioblastoma cell line U251 growing in a monolayer culture was also sensitive to magnetic lipid particles. Production of the reactive oxygen species was proposed as a potential mechanism of magnetic particle-induced cytotoxicity

(nonmagnetic lipid particles and neat iron oxides did not influence reactive oxygen species formation). Thus, the developed particles can be used for effective killing of human tumor cells.

7 Antioxidant Magnetic Nanoparticles

The effect of metal oxide nanoparticles on cells and tissues, as well as the particle biodistribution and clearance from the organism, is still not completely understood, mainly because of the existence of different nanoparticle-based toxic effects, when exposed in vitro and in vivo. The dominant toxic effect of nanoparticles is the production of reactive oxygen species (ROS). This induces imbalance in their amounts and scavenging molecules, which results in oxidative stress. Oxidative stress can be measured directly by monitoring the activity or gene expression of marker molecules of the antioxidant system (e.g., catalase) or production of glutathione, nicotinamide adenine dinucleotide phosphate, and so on. Oxidative stress can affect the cytoskeleton and therefore influence cell motility and proliferation, even cause mitochondrial damage, or result in oxidative damage of molecules like DNA, proteins, and so on (Fig. 11).

As the production of ROS is the leading cause of nanoparticle-induced toxicity, various antioxidants were investigated to reduce the negative effect of the particles on the cells. A recent study on L-929 and LN-229 cellular uptake proved that phenolic modification of the magnetic particles significantly reduced intracellular ROS levels and increased cellular uptake (Świętek et al., 2019). In that work, maghemite was coated with heparin and chitosan, which was modified with different phenolic compounds, including gallic acid (CS-G), hydroquinone (CS-H), and phloroglucinol (CS-P); antioxidant properties of the nanoparticles were analyzed using a DPPH assay (Fig. 12a–d).

To reveal the relation between the particle uptake and chemical structure of the phenolic antioxidants, phenol, phloroglucinol, chlorogenic, gallic, and tannic acid were introduced on modified maghemite nanoparticles (Fig. 13) (Patsula et al., 2019b). The phenol-modified nanoparticles were incubated with U87MG human glioma cells. Not surprisingly, intracellular levels of the ROS were reduced. The

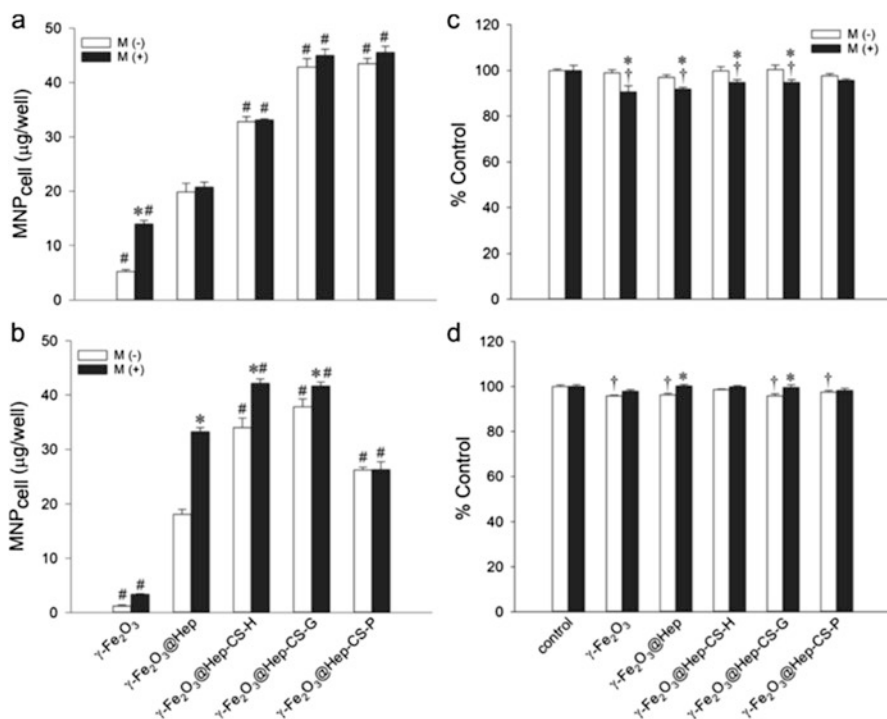**Fig. 11** DNA destruction by reactive oxygen species (ROS) in a cell
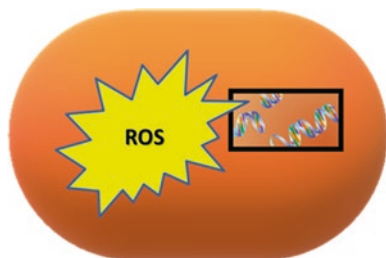
Fig. 12 Cellular uptake of the phenolic compound-modified particles by (**a**) L-929 and (**b**) LN-229 cells. A magnetic field was applied for 5 min, M (−), or 3 h, M (+), after administration of the particles (100μg/mL). Values are shown as the mean ± SE ($n = 3$). *, # $p < 0.05$ compared to the corresponding M (−) and γ-Fe$_2$O$_3$@Hep species, respectively. Cell viability of the phenolic compound-modified particles in (**c**) L-929 and (**d**) LN-229 cells. The control measurement was performed in the absence of the particles. Values are shown as the mean ± SE ($n = 3$). *, † $p < 0.05$ compared to the corresponding M (−) and control groups, respectively (Świętek et al., 2019). (Reproduced with permission from Beilstein Institute for the Advancement of Chemical Sciences)

Fig. 13 Functionalization of γ-Fe$_2$O$_3$ nanoparticle surface with silica, polyethyleneimine (PEI), poly(ethylene glycol) (PEG), poly(L-lysine) (PLL), and/or phenol-modified PLL. TMOS—tetramethyl orthosilicate, TMSPMA—3-(trimethoxysilyl)propyl methacrylate. (Reprinted from Patsula et al. (2019b). Copyright 2019, with permission from Elsevier)
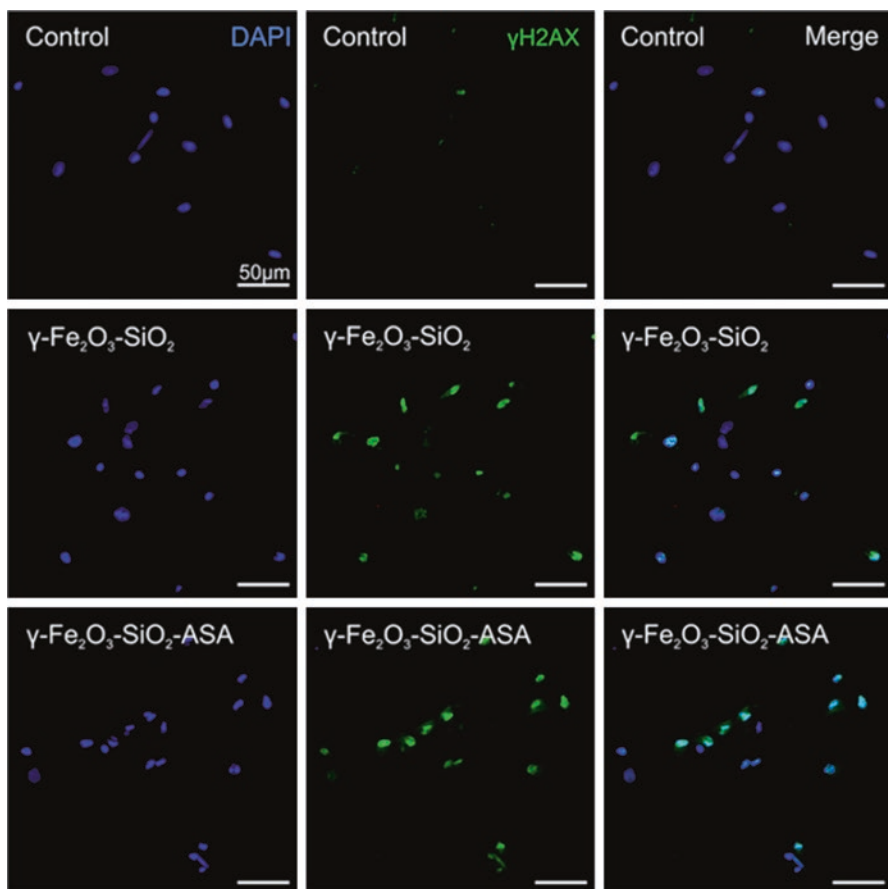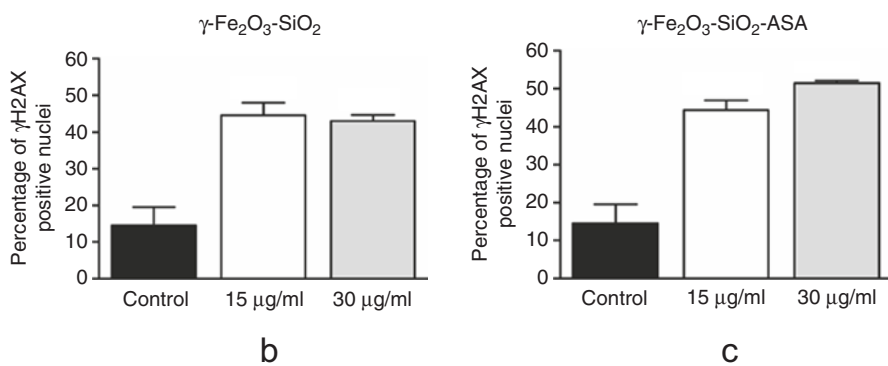
Fig. 14 (**a**) Percentage of phosphorylated H2A histone protein positive nuclei (γH2AX) and their immunocytochemistry. Cells were cultivated for 48 h without (control) or in the presence of

results suggested that the poly(L-lysine)-based coating was responsible for the anti-oxidant effects of the particles.

Among the carbohydrate derivatives, ascorbic acid is an effective ROS scavenger (Patsula et al., 2019b). However, γ-Fe_2O_3@SiO_2 nanoparticles, with or without modification by ascorbic acid, had only a minor effect on macrophage viability (Patsula et al., 2019b). The combination of iron and ascorbic acid was more toxic for the cells than nanoparticles alone. Also, an elevated expression of superoxide dismutase 2 and increased numbers of nuclei positivity for phosphorylated H2A histone family member X (γH2AX) in cells exposed to nanoparticles was observed (Fig. 14a–c) (Jiráková et al., 2020).

8   Autoimmune Diseases

There is a need for rapid and easy separation of biomolecules by using magnetic microspheres. In combination with bioaffinity ligands, for example, antibodies, proteins, or other biomolecules, the microspheres can also target bacteria or mammalian cells. Magnetic microspheres can efficiently isolate and concentrate protein antigens from biological complexes. This enrichment of specific protein biomarkers at very early stages of various diseases is essential. For example, the 46–48 kDa fragment of unconventional myosin IC isoform (p46/Myo1C), the potential biomarker of autoimmune diseases, was isolated and identified from the blood serum of multiple sclerosis and rheumatoid arthritis patients and attached to monodisperse magnetic microspheres (Zasońska et al., 2018a) (Fig. 15). The isolated protein
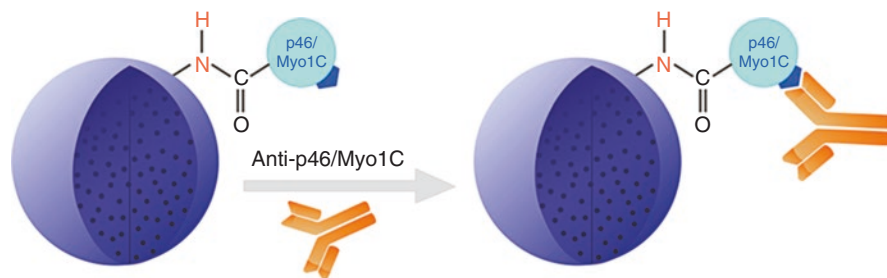

Fig. 15 Schematic view of immobilization of p46/Myo1C antigen on mgt.PGMA-NH$_2$ particle and capture of anti-p46/Myo1C auto-antibodies from blood serum; PGMA—poly(glycidyl methacrylate). (Reprinted by permission from Springer Nature, Zasońska et al. (2018a). Copyright 2018)

Fig. 14 (continued) nanoparticles in concentrations 15 and 30 μg Fe/mL. Nuclei were stained with phosphorylated H2A histone family member X (γH2AX; green) and 4′,6-diamidino-2-phenylindole (blue). Bar represents 50μm. Cells were labeled with different concentrations of (**b**) γ-Fe_2O_3–SiO_2 or (**c**) γ-Fe_2O_3@SiO_2-ASA for 48 h and analyzed for presence of γH2AX in nuclei; ASA—ascorbic acid. Results are expressed as mean ± SE. Statistically different from unlabeled control ** $p < 0.01$, *** $p < 0.001$. (Reprinted by permission from Springer Nature, Jiráková et al. (2020). Copyright 2020)

fractions (from human blood obtained by one-step affinity isolation using magnetic particles) were then separated by an SDS-PAGE electrophoresis, where the immunoglobulin subclasses were detected by Western blotting using anti-human IgG, IgA, and IgM antibodies. It was found that the affinity-purified protein fractions contained IgG and IgM subclasses of immunoglobulins, while IgA immunoglobulins were not detected.

9   Antibacterial Magnetic Nanoparticles

Several reports confirmed serious healthcare complications associated with growing antibiotic resistance worldwide. To overcome this problem, new antibiotics have to be developed or innovative approaches established that combine antimicrobial and targeting effect. For example, a combination of silver and magnetic nanoparticles not only allows for easy particle separation but also endows the particles with antibacterial properties. Inhibitory and toxic effects against *Staphylococcus aureus* and *Escherichia coli* were achieved after their incubation with $Fe_3O_4@SiO_2$-Ag nanoparticles (Shatan et al., 2019). Preparation of $Fe_3O_4@SiO_2$-Ag particles was quite complex. First, Fe_3O_4 nanoparticles were prepared by oleic acid-stabilized thermal decomposition of Fe(III) oleate. Second, the particles were coated with a silica shell; third, they were modified by (3-mercaptopropyl)trimethoxysilane to introduce sulfhydryl groups that finally enabled decoration with silver nanoclusters formed by the reduction of silver nitrate with $NaBH_4$ (Fig. 16).

The $Fe_3O_4@SiO_2$-Ag particles at low concentrations showed a direct bactericidal effect only on *S. aureus*, while the viability of *E. coli* remained unaffected (Fig. 17). Alternatively, introduction of Ag into magneto-conductive maghemite-polypyrrole composites also improved antibacterial activity. Minimal inhibitory concentration confirmed that not only the concentration but also the size of Ag particles is essential (Zasońska et al., 2018b).
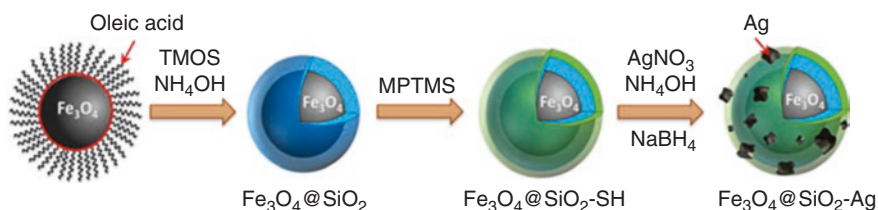

Fig. 16 Scheme of preparation of $Fe_3O_4@SiO_2$-Ag nanoparticles. TMOS—tetramethyl orthosilicate (TMOS), MPTMS—(3-mercaptopropyl)trimethoxy-silane. (Reprinted by permission from Springer Nature, Shatan et al. (2019). Copyright 2019)
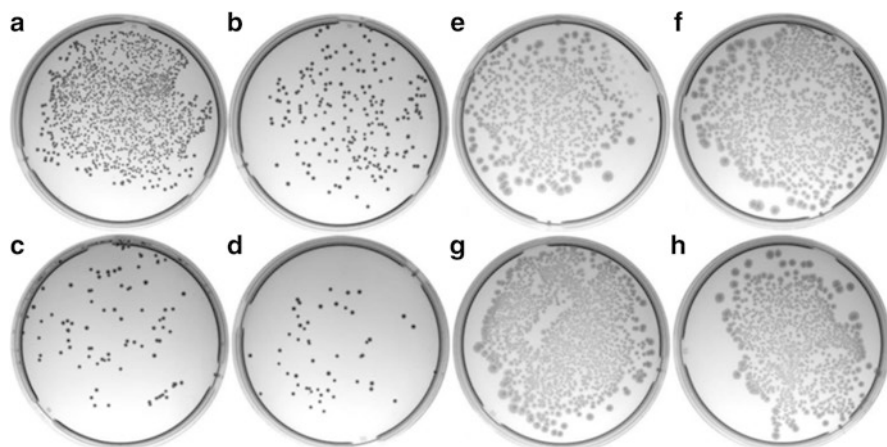
Fig. 17 Agar plates on Petri dishes with (**a–d**) *S. aureus* and (**e–h**) *E. coli* suspension after (**a, e**) 0, (**b, f**) 30, (**c, g**) 60, and (**d, h**) 90 min of incubation with $Fe_3O_4@SiO_2$-Ag nanoparticles (50 μg/mL). (Reprinted by permission from Springer Nature, Shatan et al. (2019). Copyright 2019)

10 Magnetic Nanoparticles for Treatment of Brain Disorders

Glutamate is the main excitatory neurotransmitter in the central nervous system and excessive extracellular glutamate concentration is associated with stroke, brain trauma, and epilepsy. Moreover, glutamate is a potential growth factor in tumor development. Glutamate-coated γ-Fe_2O_3 nanoparticles were suggested for glutamate delivery to the central nervous system (and other tissues) for modulation of extracellular glutamate homeostasis and synaptic neurotransmission. γ-Fe_2O_3 nanoparticles can be used for glutamate adsorption in stroke, brain trauma, epilepsy, and cancer treatment, which was followed by their consequent removal using a magnetic field (Patsula et al., 2019c). Glutamate coating on the surface of maghemite (γ-Fe_2O_3) nanoparticles was monitored using radiolabeled *L*-[^{14}C]-glutamate. In another study, different sizes of $Fe_3O_4@SiO_2$ nanoparticles were investigated as neuromodulators of rat synaptosomes. As mentioned above, the critical requirement for in vivo magnetic particle applications is the size, especially, hydrodynamic diameter. The size was controlled by changing various reaction parameters, such as the type of iron precursor, amount of oleic acid stabilizer, reaction time and temperature (Patsula et al., 2019c). For example, the decomposition of iron(III) oleate in octadec-1-ene (boiling point 320 °C) for 30 min in the presence of oleic acid produced 10 nm nanoparticles with dispersity $Đ = 1.05$. The 20-nm Fe_3O_4 particles (monodispersity was confirmed by very low $Đ = 1.03$) were obtained from iron(III) mandelate under similar reaction conditions, but with a slightly lower amount of oleic acid. Iron(III) mandelate decomposes faster; therefore, the nanoparticles nucleate and grow at a lower temperature than those from iron(III) oleate; as a

result, larger particles were prepared. With reaction temperature increasing to 343 °C and prolongation of the reaction time from 30 to 60 min, 31-nm Fe_3O_4 particles with a narrow size distribution ($Đ = 1.05$) were obtained. This result was attributed to both increased growth rate and prolonged reaction time at an elevated temperature. The particles increased the extracellular concentration and tonic release of L-[^{14}C]-glutamate, but decreased the transporter-mediated glutamate uptake, synaptic vesicle acidification, and membrane potential. The neuromodulatory properties of the $Fe_3O_4@SiO_2$ nanoparticles can be used in biotechnology and medicine, and the expected effects can be regulated via the nanoparticle size (Patsula et al., 2019c).

11   Magnetic Particles in Immunosensors

Functionalization of magnetic particles for nano- and microsensors has received considerable attention, especially in cancer diagnosis and treatment. For example, polymer microspheres decorated with magnetic nanoparticles were found useful in the development of a very sensitive sensor in the artificial enzyme-based immunoassay. It has been shown earlier that specific magnetic nanoparticles and their composites provide peroxidase-like activity, which enables oxidation of various substrates in the presence of hydrogen peroxide (Wei & Wang, 2008). In addition, it was established that electron-transfer mediators (e.g., thionine; Th) can intensify the electron transfer. The peroxidase-like activity was studied on poly(glycidyl methacrylate-*co*-ethylene dimethacrylate), magnetic poly(carboxymethyl methacrylate-*co*-ethylene dimethacrylate) [mag.P(CMMA-EDMA)], and thionine-conjugated P(CMMA-EDMA) [mag.P(CMMA-EDMA)-Th] particles (Zasońska et al., 2019b). The activity was determined by a photometric method with *N,N*-diethyl-1,4-phenylenediamine staining (Fig. 18).
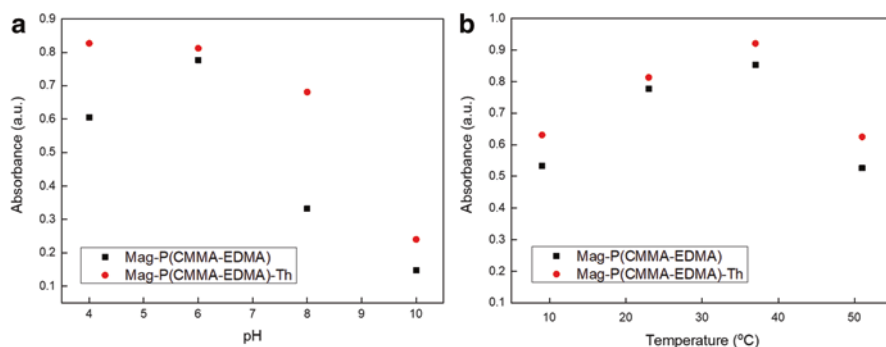

Fig. 18 (**a**) pH and (**b**) temperature dependence of the peroxidase-like activity of magnetic poly(carboxymethyl methacrylate-*co*-ethylene dimethacrylate) [mag.P(CMMA-EDMA)] and thionine-conjugated magnetic P(CMMA-EDMA) [mag.P(CMMA-EDMA)-Th] particles. The absorbance was recorded at 551 nm (Zasońska et al., 2019b). (Reproduced with permission from Nature Research)

Both mag.P(CMMA-EDMA) and mag.P(CMMA-EDMA)-Th microspheres exhibited similarly high peroxidase-like activity at 37 °C (opposite to nonmagnetic particles). pH dependence of enzymatic activity has shown that mag.P(CMMA-EDMA) microspheres had maximum peroxidase-like activity at pH ~6, while the mag.P(CMMA-EDMA)-Th particles were enzymatically active over a wider pH range (Fig. 18). The improved enzymatic activity was caused by the fact that the immobilized thionine supported the electron transfer between the iron oxide particles and the substrate.

12   Conclusions

There is a continuously growing research interest in new design, synthesis, modification, and use of magnetic iron oxide particles for cell separation, cell and tissue imaging, diagnosis, and finally treatment of various diseases. In this minireview, we have discussed several iron oxide functionalization strategies necessary to ensure proper interaction of the particles with biological systems. The magnetic feature of the nano- and microparticles allows for easy separation of the analyzed species from biofluids. The design of nanoparticles enabling efficient delivery of therapeutic compounds in targeted locations is now one of the major areas in cancer research. It has to be emphasized that translation of this research into real medical applications in everyday life in clinics is still some distance away; nevertheless, the particles discussed in this chapter are very promising for further biomedical investigations and implementation on a massive scale.

References

Agnihotri, S. A., Mallikarjuna, N. N., & Aminabhavi, T. M. (2004). Recent advances on chitosan-based micro- and nanoparticles in drug delivery. *Journal of Controlled Release, 100*(1), 5–28.

Campos, E., Branquinho, J., Carreira, A. S., Carvalho, A., Coimbra, P., Ferreira, P., & Gil, M. H. (2013). Designing polymeric microparticles for biomedical and industrial applications. *European Polymer Journal, 49*(8), 2005–2021.

Cornell, R. M., & Schwertmann, U. (2000). *The iron oxides: Structure, properties, reactions, occurrences and uses* (2nd ed.). Wiley.

Girija, A. R., & Balasubramanian, S. (2019). Theragnostic potentials of core/shell mesoporous silica nanostructures. *Nano, 3*(1), 1–40.

Gupta, A. K., & Gupta, M. (2005). Synthesis and surface engineering of iron oxide nanoparticles for biomedical applications. *Biomaterials, 26*, 3995–4021.

Horák, D. (2020). Magnetic nano- and microparticles in life sciences and medical imaging. In S. K. Sharma & Y. Javed (Eds.), *Magnetic nanoheterostructures*. Springer Nature. https://doi.org/10.1007/978-3-030-39923-8_5

Horák, D., Babič, M., Macková, H., & Beneš, M. J. (2007). Preparation and properties of magnetic nano- and microsized particles for biological and environmental separations. *Journal of Separation Science, 30*(11), 1751–1772.

Jiráková, K., Moskvin, M., Machová Urdzíková, L., Rossner, P., Elzeinová, F., Chudíčková, M., Jirák, D., Ziolkowska, N., Horák, D., Kubinová, Š., & Jendelová, P. (2020). The negative effect of magnetic nanoparticles with ascorbic acid on peritoneal macrophages. *Neurochemical Research, 45*, 159–170.

Konečná, J., Romanovská, D., Horák, D., & Trachtová, Š. (2019). Optimization of deoxyribonucleic acid extraction using various types of magnetic particles. *Chemical Papers, 73*, 1247–1255.

Koubková, J., Müller, P., Hlídková, H., Plichta, Z., Proks, V., Vojtěšek, B., & Horák, D. (2014). Magnetic poly(glycidyl methacrylate) microspheres for protein capture. *New Biotechnology, 31*(5), 482–491.

Laurent, S., Forge, D., Port, M., Roch, A., Robic, C., van der Elst, L., & Muller, R. N. (2008). Magnetic iron oxide nanoparticles: Synthesis, stabilization, vectorization, physicochemical characterizations, and biological applications. *Chemical Reviews, 108*, 2064–2110.

Manko, N., Starykovych, M., Bobak, Y., Stoika, R., Richter, V., Koval, O., Lavrik, I., Horák, D., Souchelnytskyi, S., & Kit, Y. (2019). The purification and identification of human blood serum proteins with affinity to the antitumor active RL2 lactaptin using magnetic microparticles. *Biomedical Chromatography, 33*(11), e4647.

Musielak, M., Piotrowski, I., & Suchorska, W. M. (2019). Superparamagnetic iron oxide nanoparticles (SPIONs) as a multifunctional tool in various cancer therapies. *Reports of Practical Oncology and Radiotherapy, 24*(4), 307–314.

Neuberger, T., Schöpf, B., Hofmann, H., Hofmann, M., & von Rechenberg, B. (2005). Superparamagnetic nanoparticles for biomedical applications: Possibilities and limitations of a new drug delivery system. *Journal of Magnetism and Magnetic Materials, 293*(1), 483–496.

Patsula, V., Horák, D., Kučka, J., Macková, H., Lobaz, V., Francová, P., Herynek, V., Heizer, T., Páral, P., & Šefc, L. (2019a). Synthesis and modification of uniform PEG-neridronate-modified magnetic nanoparticles determines prolonged blood circulation and biodistribution in a mouse preclinical model. *Scientific Reports, 9*, 10765.

Patsula, V., Moskvin, M., Siow, W. X., Konefal, R., Ma, Y.-H., & Horák, D. (2019b). Antioxidant polymer-modified maghemite nanoparticles. *Journal of Magnetism and Magnetic Materials, 473*, 517–526.

Patsula, V., Borisova, T., Kostiv, U., Galkin, M., Pastukhov, A., & Horák, D. (2019c). Effect of $Fe_3O_4@SiO_2$ nanoparticle diameter on glutamate transport in brain nerve terminals. *Nanoscience and Nanotechnology Letters, 11*, 1–9.

Plichta, Z., Kozak, Y., Panchuk, R., Sokolova, V., Epple, M., Kobylinska, L., Jendelová, P., & Horák, D. (2018). Cytotoxicity of doxorubicin-conjugated poly[*N*-(2-hydroxypropyl) methacrylamide]-modified γ-Fe_2O_3 nanoparticles towards human tumor cells. *Beilstein Journal of Nanotechnology, 9*, 2533–2545.

Plichta, Z., Horák, D., Mareková, D., Turnovcova, K., & Jendelová, P. (2020). Poly[*N*-(2-hydroxypropyl)methacrylamide]-modified magnetic γ-Fe_2O_3 nanoparticles conjugated with doxorubicin for glioblastoma treatment. *ChemMedChem, 15*, 96–104.

Pongrac, I. M., Dobrivojević Radmilović, M., Brkić Ahmed, L., Mlinarić, H., Regul, J., Škokić, S., Babič, M., Horák, D., Hoehn, M., & Gajović, S. (2019). D-mannose-coating of maghemite nanoparticles improved labeling of neural stem cells and allowed their visualization in the mouse brain by MRI. *Cell Transplantation, 28*, 553–567.

Šálek, P., Korecká, L., Horák, D., Petrovský, E., Kovářová, J., Metelka, R., Čadková, M., & Bílková, Z. (2011). Immunomagnetic sulfonated hypercrosslinked polystyrene microspheres for electrochemical detection of proteins. *Journal of Materials Chemistry, 21*(38), 14783–14792.

Šálek, P., Filipová, M., Horák, D., Proks, V., & Janoušková, O. (2019). Enhanced solid phase extraction of DNA using hydrophilic monodisperse poly(methacrylic acid-*co*-ethylene dimethacrylate) microparticles. *Molecular Biology Reports, 46*, 3063–3072.

Shatan, A. B., Venclíková, K., Zasońska, B. A., Patsula, V., Pop-Georgievski, O., Petrovský, E., & Horák, D. (2019). Antibacterial silver-conjugated magnetic nanoparticles: Design, synthesis and bactericidal effect. *Pharmaceutical Research, 36*, 147–159.

Świętek, M., Lu, Y.-C., Konefal, R., Ferreira, L. P., Cruz, M. M., Ma, Y.-H., & Horák, D. (2019). Scavenging of reactive oxygen species by phenolic compound-modified maghemite nanoparticles. *Beilstein Journal of Nanotechnology, 10*, 1073–1088.

Świętek, M., Skorokhyd, N., Černoch, P., Finiuk, N., Panchuk, R., Klyuchivska, O., Hrubý, M., Molčan, M., Berger, W., Trousil, J., Stoika, R., & Horák, D. (2020). Magnetic temperature-sensitive solid-lipid particles for targeting and killing tumor cell. *Frontiers in Chemistry, 8*, 205.

Varanda, L. C., Souza, C. G. S., Moraes, D. A., Neves, H. R., Souza Junior, J. B., Silva, M. F., Bini, R. A., Albers, R. F., Silva, T. L., & Beck Junior, W. (2019). Size and shape-controlled nanomaterials based on modified polyol and thermal decomposition approaches. A brief review. *Anais da Academia Brasileira de Ciências, 91*(4), e20181180.

Wei, H., & Wang, E. (2008). Fe_3O_4 magnetic nanoparticles as peroxidase mimetics and their applications in H_2O_2 and glucose detection. *Analytical Chemistry, 80*, 2250–2254.

Zasońska, B. A., Líšková, A., Kuricová, M., Tulinská, J., Pop-Georgievski, O., Ilavská, S., Horváthová, M., Jahnová, E., & Horák, D. (2016). Functionalized porous silica&maghemite core-shell nanoparticles for applications in medicine: Design, synthesis and immunotoxicity. *Croatian Medical Journal, 57*, 165–179.

Zasońska, B. A., Hlídková, H., Petrovský, E., Myronovskij, S., Nehrych, T., Negrych, N., Shorobura, M., Antonyuk, V., Stoika, R., Kit, Y., & Horák, D. (2018a). Monodisperse magnetic poly(glycidyl methacrylate) microspheres for isolation and determination of blood serum immunoglobulins with affinity to short form of unconventional Myo1C. *Microchimica Acta, 185*, 262.

Zasońska, B. A., Acharya, U., Pfleger, J., Humpolíček, P., Vajďák, J., Petrovský, E., Hromádková, J., Walterová, Z., & Bober, P. (2018b). Multifunctional polypyrrole@maghemite@silver composites: Synthesis, physico-chemical characterization and antibacterial properties. *Chemical Papers, 72*, 1789–1797.

Zasońska, B. A., Pustovyy, V. I., Babinskyi, A. V., Palyvoda, O. M., Chekhun, V. F., Todor, I. N., Petrovský, E., Kuzmenko, O. I., & Horák, D. (2019a). Combined antitumor effect of surface-modified superparamagnetic maghemite nanoparticles and a vitamin E derivative on experimental Walker-256 mammary gland carcinosarcoma. *Journal of Magnetism and Magnetic Materials, 471*, 381–387.

Zasońska, B. A., Šálek, P., Procházková, J., Müllerová, S., Svoboda, J., Petrovský, E., Proks, V., Horák, D., & Šafařík, I. (2019b). Peroxidase-like activity of magnetic poly(glycidyl mathacrylate-*co*-ethylene dimethacrylate) particles. *Scientific Reports, 9*, 1543.

Zavaleta, C., Ho, D., & Ji Chung, E. (2018). Theranostic nanoparticles for tracking and monitoring disease state. *SLAS Technology, 23*(3), 281–293.

Part III
Biological Applications of Nanomaterials

Controlled Delivery and Reduced Side Effects of Anticancer Drugs Complexed with Polymeric Nanocarrier

Lesya Kobylinska, Nataliya Mitina, Alexander Zaichenko, and Rostyslav S. Stoika

Abbreviations

ATM	Ataxia telangiectasia, mutated
DMSO	Dimethyl sulfoxide
DNA	Deoxyribonucleic acid
Dox	Doxorubicin
FDA	Food and Drug Administration
FRO	Free radical oxidation
HPMA	N-(2-hydroxypropyl)-methacrylamide copolymer
MPS	Mononuclear phagocytic system
mRNA	Messenger ribonucleic acid
NAD^+/NADH	Nicotinamide adenine dinucleotide/nicotinamide adenine dinucleotide reduced
PAA	Poly-aspartic acid
PCL	Polycaprolactone
PEG	Polyethylene glycol
PLA	Polylactic acid
PLGA	L-lactide-co-glycolic) acid

L. Kobylinska
Department of Biochemistry, Danylo Halytsky Lviv National Medical University, Lviv, Ukraine
e-mail: kobylinska_lesya@meduniv.lviv.ua

N. Mitina · A. Zaichenko
Department of Organic Chemistry, Lviv Polytechnic National University, Lviv, Ukraine
e-mail: zaichenk@polynet.lviv.ua

R. S. Stoika (✉)
Department of Regulation of Cell Proliferation and Apoptosis, Institute of Cell Biology, Lviv, Ukraine

PNC   Polymeric nanosized carrier
ROS   Reactive oxygen species
TEM   Transmission electron microscopy

1 Introduction

Nanomaterial-based drug design and development are priority tasks in modern pharmaceutical market (Dutta, 2007). Biocompatible and biodegradable multifunctional nanomaterials capable of targeted drug delivery and effectively crossing the biological barriers (e.g., blood–brain barrier) were created (Dutta, 2007; Bamrungsap et al., 2012). Many of them were also shown to be good tools for the diagnosis of different diseases (Bamrungsap et al., 2012).

The transition from macro- to nanosize particles is accompanied by a change in the interatomic distances and periods of the crystal lattice, which imparts new properties to the nanostructures. Because of their small size, most of the atoms in such particles are on the surface, thereby influencing the behavior of these atoms that leads to changes in their chemical, physical, biological, and pharmacological properties. The nanoparticles more easily penetrate the cells of tissues and organs of the human body, and are biologically more active through a large surface area per unit of mass, compared to the macro-sized particles (Bamrungsap et al., 2012). A particle size of <100 nm in diameter is considered to be optimum for in vivo application and biodistribution (Bamrungsap et al., 2012). An excessive reduction in particle size is undesirable, because nanoparticles sized <50 nm are more actively absorbed by the liver and spleen, which leads to increased toxicity, and extremely small nanoparticles (<5 nm) are intensively removed by diffusion in the kidney. Thus, the calculated optimal size of nanoparticles for biomedical application is within the range of 60–100 nm (Min et al., 2015).

In this chapter, polymeric nanomaterials of potential use as nanocarriers for controlled delivery of anticancer drugs with reduced side effects in the treated organism are considered.

2 Nanocarriers for Drug Delivery

Use of anticancer drugs can result in many side effects due to their action in the body. Non-addressed actions of drug delivery lead to undesirable effects in the body (Liu & Auguste, 2015). If the action of the drugs is properly addressed, then their concentration could be reduced accordingly, thereby minimizing the side effects. Thus, the ability of the nanocarriers to provide targeted delivery of drugs in the body would enhance the effectiveness of their action, simultaneously improving their biocompatibility and minimizing the adverse effects by reducing the overall toxicity to healthy organs and tissues. Finally, that would also reduce the cost of treatment.

The above-mentioned goals have led to the creation of "smart" drugs in which the active drug substance is combined with a specific nanocarrier (nanoparticles, polymeric micelles, liposomes, hydrogels, others) (Bamrungsap et al., 2012; Min et al., 2015). Special vector molecules, most frequently antibodies to specific antigens on the surface of the target cells, are included in the carrier that allows the drug-carrier complex interact with specific target cells. For monitoring the movement of a drug substance in vivo, biocompatible fluorescent or fluorescent labels are also included in the carrier's structure. The advantages of using drugs immobilized on such nanomaterials are prolonged duration of drug's circulation in the body and capacity to be presented at the required dose at a specific location (Bamrungsap et al., 2012; Liu & Auguste, 2015; Zhang et al., 2009).

The use of polymeric drug delivery systems in cancer chemotherapy started in 1976 after Langer and Folkman described the first controlled release system of macromolecules with polymers (Langer & Folkman, 1976). In 1979, Couvreur and colleagues in in vitro and in vivo studies described the results of using polymeric nanoparticles composed of poly-alkylcyanoacrylate for releasing doxorubicin (Couvreur et al., 1979). In the 1980s, early formulations of the polymeric nanoparticles were applied in cancer chemotherapy for the treatment of hepatocarcinoma, bronchopulmonary tumors, and myelomas (macrophage-infiltrated tumors). They were delivered directly to the mononuclear phagocytic system (MPS), exploiting the opsonization and clarification of the particles by the macrophages in the bloodstream (Brigger et al., 2012; Barraud et al., 2005).

The next step was done by targeting tumors by "stealth" polymeric nanoparticles with a long circulation period in the bloodstream and a reduced opsonization by the macrophages (Mitra et al., 2001; Onishi et al., 2003; Otsuka et al., 2003). In 1994, Langer and colleagues described the poly(lactic acid)/poly(lactic-co-glycolic acid) (PLA/PLGA) and PEG block copolymer nanoparticles as long-circulating stealth polymeric nanoparticles with important therapeutic applications (Langer, 1999). Then, due to progress in material science and engineering, the biodegradable polymeric nanoparticles have been developed as carriers for an advanced and personalized chemotherapy (Langer, 1999; Soppimath et al., 2001; Ravi Kumar & Kumar, 2001). Due to low number of conducted clinical trials, only one formulation based on polymeric nanoparticles has gotten the FDA approval for cancer therapy (Tang et al., 2010), and second one were "liposomes" (Barraud et al., 2005). Of all the papers devoted to cancer therapeutics with polymeric nanoparticles published recently, 90% show big interest in these formulations (Onishi et al., 2003). In the following, the most promising and advanced pre-clinical studies of polymeric nanoparticles used for cancer treatment are described.

The major challenges in developing safe nanoscale carriers are (a) low toxicity, (b) physical stability in blood vessels, (c) compatibility with body metabolites, (d) controlled effect on cell damage, and (e) the potential to improve targeted delivery of anticancer drugs to the tumor (Langer, 1999). The nanocarriers should be designed with high tumor selectivity and a capacity to slowly release the active cytotoxic compound, and these properties reduce the systemic toxicity of the drug and improve its distribution and circulation time in the body. The liposomes,

polymeric micelles, dendrimers, ceramic-based nanoparticles, and iron oxides, as well as some proteins, have been used for targeted delivery of anticancer drugs (Dutta, 2007).

As mentioned above, the drug delivery sheath should improve its biocompatibility. Such coating on the surface of the particles can be created on the basis of vinylpyrrolidone, vinyl alcohol, oxyethylated, and fluorinated co-polymers, as well as their complexes with various biopolymers, for example, blood serum albumin or bio-surfactants of bacterial origin (Brigger et al., 2012). Activation of certain chemical groups (hydroxyl, carboxyl, amino, aldehyde, or epoxy) on the surface of the nanoparticles is necessary for their further biofunctionalization. These reactive groups are introduced into the linear chain or branches of the polymer. The biocompatibility of nanomaterials in vivo strongly depends on the lack of their immunogenicity. Ideally, the nanocomposites should have minimal immunogenic activity.

A potential significance of the nanomaterials in medicine is also dependent on their biodegradability. Thus, the poly-aspartate, poly-glutamate, poly-malate, polylactate, polysaccharides, and other natural and synthetic polymers have been considered promising nanocarriers (Onishi et al., 2003).

Doxil is a liposome functionalized with the polyethylene glycol (PEG) and containing the encapsulated doxorubicin (Tang et al., 2010). In such form, the anticancer drug circulates 300 times longer and possesses improved pharmacokinetic characteristics compared to free doxorubicin (Zhang et al., 2009). The "masking" of highly toxic doxorubicin in the Doxil nanocomposite (approximately 100 nm) prevents its nonaddressed action in the body. However, the Doxil demonstrates immunogenic effect and the liposome cannot be further functionalized in order to increase its targeting properties.

The polymeric nanocarriers are the most promising platforms for the delivery of anticancer drugs (Zhang et al., 2009; Wilczewska et al., 2012; de Jong, 2008). In Fig. 1, other drug delivery platforms are shown. The effectiveness of the polymeric micelles in drug delivery is related to their ability to solubilize and immobilize the lipophilic drugs in the nucleus of micelles (Torchilin, 2001). Specific physicochemical properties of polymeric nanocarriers, such as molecular weight, size,
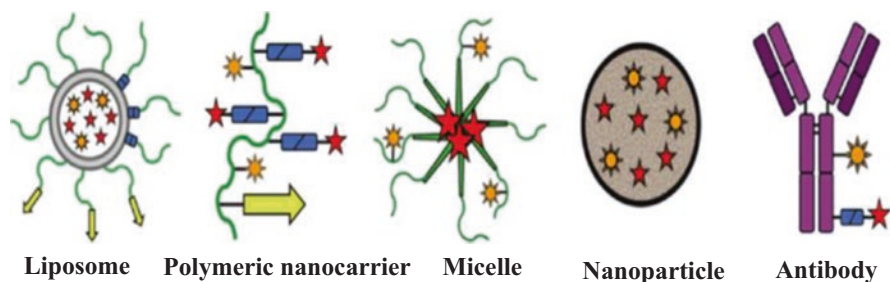

Liposome   Polymeric nanocarrier   Micelle   Nanoparticle   Antibody

Fig. 1 Main types of nanocarriers. Liposomal bilayers highlighted in gray; polymers and coatings—green; composite nanoparticles—brown; antibodies—purple; drug release linkers—blue; orientation ligands—yellow; contrast agents—orange; bound biologically active substances—red

solubility, density, specific gravity, pH, and dissociation, enhance their biocompatibility and biodegradability, and their capacity for functionalization should be taken into account while evaluating their drug delivery effectiveness (Li, 2003; Nath Roy et al., 2016; Riabtseva et al., 2012).

3   Modulation of Drug Action by the Nanocarriers

Exploring the molecular mechanisms involved in drug action is of great significance for developing better chemotherapeutics. The use of polymeric nanomaterials has established an innovative approach due to the possibility to conjugate different vector proteins, such as antibodies, and peptides to the nanoparticles. The polyethylene glycol (PEG), a water-soluble and biocompatible polymer, is the most common nonionic polymer that is conjugated to the polymer-based drug delivery platforms (Mishra et al., 2016).

New synthetic substances 4-thiazolidinone derivatives that possess high anticancer activity and lesser general toxicity in tumor-bearing animals were studied (Kobylinska et al., 2015, 2016). A novel drug delivery platform based on the PEGylated polymer was applied, which allows for the formation of stable water-based complexes of these water-insoluble compounds derivatives. The 4-thiazolidinone derivatives are heterocyclic compounds with a molecular mass of 400–600 Da. These and other related derivatives were synthesized at Lviv National Medical University (Ukraine), and most of them have been tested under the Developmental Therapeutic Program at the National Cancer Institute in Bethesda, Maryland (USA) (Boyd & Paull, 1995; Shoemaker, 2006). After evaluating their antineoplastic activity, the most promising substances were selected for further study of the mechanisms of their cytotoxic action and anticancer effects (Havrylyuk et al., 2012). Among the 4-thiazolidinone derivatives, the Les-3833 demonstrated the highest toxicity toward B16F10, WM793, and SK-Mel-28 melanoma cells, as well as human lung A549, breast MCF-7, colon HCT116, ovarian SKOV3 cancer cells, and leukemia cells (L1210, Jurkat, HL-60 lines) (Finiuk et al., 2017).

4   Increase in Water Solubility of Anticancer Agents Via Their Conjugation with Polymeric Nanocarriers

Many existing chemotherapeutic drugs, repurposed drug substances, as well as newly developed small-molecule anticancer compounds possess high lipophilicity and low water-solubility. These poorly water-soluble anticancer agents can be solubilized with surfactants and co-solvents used in high concentrations, which frequently leads to adverse effects (Bilia et al., 2019). Solubility is a physicochemical property of a substance which can be generally defined as the highest amount of a

substance that can be dissolved in a solvent, at a constant temperature and pressure. More specifically, solubility is considered to be the concentration that a solute reaches in a solution when equilibrium exists between the solid phase and the solution phase (saturated solution) at a defined temperature and pressure (Savjani et al., 2012).

Poor water solubility of drugs has been a serious problem in development and clinical application of efficient anticancer compounds. Many highly active and promising new substances are rejected because of their low solubility. The nanobiotechnologies proposed as an alternative to the solvent-based drug solubilization for encapsulation and delivery of the existing and new poorly water-soluble anticancer drugs might be based on lipid, polymer, and albumin (Narvekar et al., 2014). These nanocarriers may offer several additional advantages such as an enhanced tumor accumulation, reduced systemic toxicity, and improved therapeutic effectiveness.

The promotion of 4-thiazolidinones as anticancer drugs is limited due to their poor water solubility (Havrylyuk et al., 2012). This problem also exists for other anticancer medicines such as taxols (Jabir et al., 2012). When applied in the preparation of medicinal formulation, paclitaxel is dissolved in water by using a special oil (Ma, 2013; Tomao, 2009). Specific delivery platforms are more promising for creating "smart" drugs that possess effective action in the organism (Talukder et al., 2011; Wang et al., 2017; Iwamoto, 2013).

PEG is a hydrophilic and biocompatible polymer that is most often used in drug delivery platforms (Bunker, 2012; Mishra et al., 2016). Due to its relative biosafety and biocompatibility, it is widely used in the preparation of amphiphilic copolymers for drug delivery. PEG has previously been studied also as a drug, because it is relatively hydrophilic unlike many other synthetic polymers (Bunker, 2012; Mishra et al., 2016). PEG is soluble in both organic and inorganic solvents. The high surface hydrophilicity of PEG allows it to be conjugated to other polymers, increasing their solubility (i.e., PEGylation) (Mishra et al., 2016; Feng et al., 2015). PEG conjugation increases the solubility of the hydrophobic drug and prolongs its circulation time in the body. It is known that the surface of most cells has a negative electrical charge, and, therefore, the cationic nanoparticles are able to penetrate the cells, delivering a therapeutic substance. However, they can also more easily bind to cells in normal areas of tissues and organs. Thus, researchers have often introduced PEG to the coating of nanoparticles, because this electroneutral molecule reduces protein binding and particle uptake by the mononuclear phagocytic system. Due to this, the length of stay of the nanoparticles in the circulation increases, which facilitates their reaching the target cells in the body. The length of the PEG polymer chain and the density of PEG coatings influence both the binding of proteins to nanoparticles and their distribution in the body (Bunker, 2012).

PEG also minimizes nonspecific drug absorption, provides specific affinity for the target tumor, and increases drug accumulation in malignant tissue (Nath Roy et al., 2016; Narvekar et al., 2014). Changes in surface hydrophilicity prevent the adsorption of proteins and, therefore, permit cell adhesion and reproduction (Torchilin, 2001; Bunker, 2012; Feng et al., 2015). The presence of PEG in the polymeric nanocarriers is a valuable characteristic that allows for the

formation of micelles to make a molecule aggregate in a colloidal solution containing a hydrophobic compound, and to create a hydrophilic environment for drug delivery in the living organism. In addition, PEG protects the nanocomplex from the attack of the immune cells. Thus, encapsulation of anticancer drugs in the nanosheets composed of its copolymer derivatives can improve their uptake, distribution, metabolism, and excretion, which also provides better release and action toward tumor cells.

Since PEG is included in many modern drug carriers (both polymeric and nanoparticles), its role is actively studied. It was shown that PEG possessed low toxicity, and a dose of 10 mg/kg body weight is considered acceptable for animals (Bunker, 2012; Feng et al., 2015). However, free PEG causes acute intoxication in humans in excess of 500 mg/l of blood, and the minimum lethal dose for humans per os is 50 g of pure ethylene glycol (Feng et al., 2015). The ethylene glycol is rapidly absorbed in the gut, and it can be detected in blood within 1–2 h, while its half-life is about 3 h. The organic acids (glycolic, oxalic, formic) are the main toxic metabolites of PEG because they cause metabolic acidosis and nephrotoxic effects (Bunker, 2012; Feng et al., 2015). In addition, under the influence of the ethylene glycol, the NAD^+/NADH ratio decreases, and the activity of gluconeogenesis in liver is inhibited, which leads to an increase in lactate levels and metabolic acidosis (Feng et al., 2015). PEG also disrupts the electrolyte balance in the body and often accompanies hypocalcemia, which develops due to the chelating action of oxalic acid on calcium ions and produces poorly water-soluble calcium oxalate, which crystallizes in the kidney and lowers blood plasma Ca^{2+} cations (Feng et al., 2015).

Encapsulation of existing and new antitumor drugs in nanoparticles based on lipids and polymers has been used to increase the solubility of drugs that will increase the effectiveness of anticancer chemotherapy (Kobylinska, Patereha, et al., 2018; Kobylinska, Skorohyd, et al., 2018).

Earlier, we found that Les-3833 was the most toxic compound among the other studied 4-thiazolidinone derivatives used to treat rat glioma C6 cells and human glioblastoma U251 cells (Kobylinska et al., 2016). As already noted, application of these agents is problematic because of their water insolubility, and the DMSO, together with additional heating, was necessary to prepare the liquid form of those derivatives. In order to improve the delivery of these derivatives to target cells, a synthetic polymeric nanosized carrier (PNC) was used. It should be noted that the complexation of the 4-thiazolidinone derivatives with the applied PNC also enhanced the effectiveness of their antineoplastic action (Kobylinska et al., 2016; Finiuk et al., 2017). The enhanced pro-apoptotic action of these compounds was demonstrated in the Western-blot and FACS analyses (Finiuk et al., 2017).

We have developed the technique for obtaining highly stable water dispersions of the 4-thiazolidinone-based chemotherapeutics or other water-insoluble compounds. It is based on the nucleation of a solution of these compounds in the DMSO by the nanoscale micellar polymer structures that provides polymer coating at the surface of the nanoparticle and leads to their stabilization (Fig. 2). Besides, such coating prevents the aggregation and sedimentation of the nanoparticles. That technique
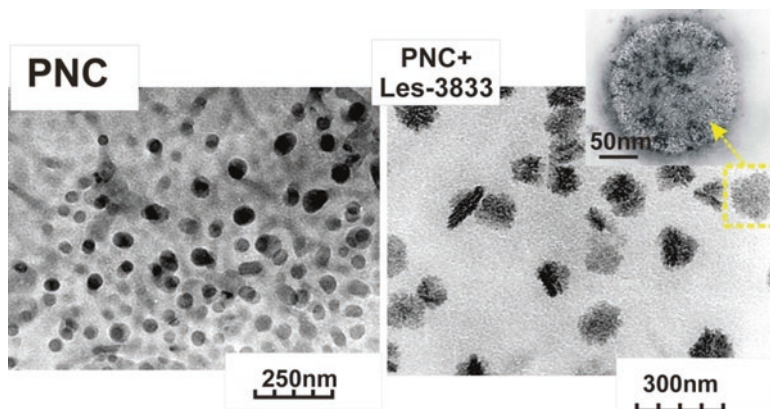
Fig. 2 Transmission electron microscopy (TEM) images of the PNC (*left*) and complex of PNC + Les3833 (right). (Reproduced with permission (Kobylinska et al., 2019))

was applied for the preparation of highly stable water dispersions of the 4-thiazolidinone-based chemotherapeutics and other water-insoluble compounds (Fig. 2).

5   Enhanced Uptake of Drug-Loaded Nanoconjugates by Target Cells

There are different biological barriers that prevent the penetration and biological action of various foreign agents, including drugs. It is known that some anticancer drugs can pass through the blood-brain barrier. For example, procarbazine, temozolomide (Temodar), and methotrexate overcome the blood-brain barrier, while the doxorubicin cannot cross it and about 35% of this drug is bound to plasma proteins. It is not so easy to predict which compound would cross the blood-brain barrier and which would not. To answer this question, a complex analysis of the molecular properties, surface activity of a molecule, and its size is necessary. For establishing the ability of different compounds to cross the blood-brain barrier by passive diffusion, a model water-air system was developed since air has a dielectric constant similar to the carbohydrate layer of the lipid plasma membrane. The air-to-water partition coefficient (K_{aw}) provides the characteristic that determines the ability of a drug compound to cross the blood-brain barrier (Narvekar et al., 2014). In addition, Gibbs adsorption isotherm analysis shows the physicochemical parameters of the drug molecule: minimum concentration for induction of surface activity (C_0), surface area of the molecule at the air-water interface, and critical micelles concentration. These parameters, together with drug ionization constants, allow for the separation of compounds that reach the central nervous system and those that do not achieve it with a predicted rate of better than 90% (Narvekar et al., 2014).

A delivery of the anticancer drug to brain might be assisted by the multifunctional nanocomposites "programmed" to pass through the blood-brain barrier to successfully transfer a drug substance to a lesion area, such as tumor. It has been shown that the polymeric carriers used for delivery of the antisense oligodeoxynucleotides by prenatal administration of appropriate oligonucleotide carrier complexes are capable of inhibiting the expression of the protein to which this oligonucleotide mRNA was generated in rats (de Jong, 2008; Li, 2003). These data indirectly indicate that the blood-brain barrier has been overcome; however, its direct evidence can be obtained only by attaching a special label to this carrier in order to follow its behavior after administration to experimental animals.

6 Increased Stability of Drugs in Complex with Polymeric Nanocarriers

Among the different carriers developed for a selective delivery of cytotoxic drugs, polymeric nanoparticles seem to be the more promising ones for cancer-targeted therapy. They can provide enhanced stability of drugs in the biological fluids, chemistry of tunable surface conjugation, more monodisperse size distributions, more controllable physicochemical properties, higher drug loading, and more controlled rate of drug release. In addition to these characteristics, they share with the other nanocarriers longer circulation in blood, reduced toxicity, improved pharmacokinetics, and efficient co-delivery of multiple cytotoxic compounds to tumors. The polymeric nanoparticles are efficient vehicles for the delivery of poorly soluble cytotoxic drugs that allow for controlled drug release.

The polymeric micelles are composed of amphiphilic block copolymers that form nanosized spheroidal micellar structures with a hydrophobic core that may contain poorly water-soluble anticancer drugs and a hydrophilic shell that allows for the inclusion of hydrophilic drugs and provides stability to the micelle. This property provides a long circulation time of the drug in blood, which makes this formulation an appropriate carrier for intravenous administration (Torchilin, 2007; Kwon, 2003; Tong & Cheng, 2007). To solve the solubility problem, numerous anticancer drugs have been included into the polymeric micelles. The reduced size of the micelles (20–80 nm) is sufficient to accommodate a high amount of anticancer drugs, as well as their uniformity. Small size does not only increase the circulation time of the drug in the bloodstream but also provides better permeability of the drug, improving its delivery from the blood vessels into the tumor and generating a uniform distribution of the cytotoxic drug throughout the anomalous tissue (Kwon & Kataoka, 2012; Cabral et al., 2011). The polymeric micelles will get more clinical significance when some drawbacks of their action, like insufficient stability in systemic circulation and premature drug leakage that may cause side effects and a decrease in effectiveness, are overcome (Pérez-Herrero & Fernández-Medarde, 2015).

Eight polymeric micelle-based formulations that include anticancer agents have been used in clinical trials (Talelli et al., 2012; Gong et al., 2012; Lu & Park, 2013). The polymeric micelle, Genexol-PM (paclitaxel encapsulated in the monomethoxy-poly(ethylene glycol)-block-poly(D,L-lactide)), has been involved in several clinical trials. It was under phase II, III, and IV clinical trials for the treatment of advanced, recurrent, or metastatic breast cancer. Besides, it was under phase II for the treatment of advanced urothelial cancer, advanced head and neck cancer, and advanced nonsmall-cell lung cancer, and it is under phase I/II clinical trial for the treatment of ovarian cancer and advanced or metastatic pancreatic cancer. It has been approved by the Korean drug administration for the treatment of breast and lung cancer (Lammers et al., 2012). The other described clinical trials with using this structure are the phase I trial with polymeric micelles composed of methoxy-poly(ethylene glycol)-block-poly(D,L-lactide) loaded with docetaxel (Nanoxel-PM) (Lee et al., 2011), the phase I trial of NC 4016, a PEG-poly(glutamic acid) polymeric micelle of oxaliplatin, the polymeric micelles composed of PEG and PAA that incorporate doxorubicin (NK911) (phase I/II trials) (Matsumura et al., 2004) or paclitaxel (NK105) (phase II/III trials) (Kato et al., 2011; Hamaguchi et al., 2007), the phase I/II trials of the PEGylated polymeric micelles NC-6004 (Nanoplain: PEG + poly-glutamic acid) (Plummer et al., 2011) and NK012 (PEG + poly-glycolic acid) (Hamaguchi et al., 2010), containing cisplatin or SN38, respectively, and the phase II/III trials of the P-glycoprotein-targeting pluronic micelle of doxorubicin (SP1049C) that was labeled as orphan drug by the FDA.

This group includes the effective carriers for the controlled and prolonged anticancer targeted drug delivery. These carriers are biodegradable colloidal systems with spherical nano-sized polymeric particles in which the cytotoxic drugs can be encapsulated or physically entrapped within a polymeric matrix (nanospheres) or entrapped into a cavity surrounded by a polymeric membrane (nanocapsules). They can also be used for conjugation of the anticancer drug to the surface or the core of the particles (Sahoo & Labhasetwar, 2003; Hillaireau & Couvreur, 2009).

In case of the insoluble drugs, it is possible to produce a hydrophobic interaction between the drug and the core of the particle, increasing in that way its solubility (Park et al., 2006). When a drug is conjugated to the particle, the properties of the linkers play a crucial role in the pharmacological properties of the complex. For example, they can make them stable in the bloodstream at pH = 7, and be decomposed at pH = 5.5, which can exist in tumors, or be stable in blood, but be cleaved by the lysosomal enzymes in tumors (Ulbrich, 2004). In addition to their protective properties, these carriers also provide multiple deliveries of the synergic drugs, reduced toxicity with a limited interaction with healthy cells, long circulation times (stealth nanoparticles), and enhanced uptake by cancer cells. They also showed higher stability, more homogeneous size distribution, better controllable physico-chemical properties, higher drug payload, and more controlled drug release via diffusion through the polymer matrix or by erosion and degradation of the particles, compared with other colloidal systems such as liposomes or polymeric micelles (Hu et al., 2010). The generation of nanoparticles includes biodegradable and biocompatible natural or synthetic polymers, which have already got FDA approval.

Synthetic polymers, like polyglutamic acid and polyglycolic acid (PGA), polyethylene glycol (PEG), polycaprolactone (PCL), polylactic acid (PLA), poly aspartate (PAA), poly(D, L-lactide-co-glycolic) acid (PLGA), and N-(2-hydroxypropyl)-methacrylamide copolymer (HPMA), are frequently used since they are easily manufactured and degraded after use, and they produce a sustained release of the active compounds (Wang et al., 2009).

The polymers of natural origin, like chitosan, alginate, dextran, heparin, albumin, gelatin, or collagen, are used less, in spite of being nontoxic, abundant in nature, inexpensive, easily biodegradable, and having high releasing properties. However, they are not naturally pure and homogeneous, thus requiring an additional purification step before their use (Brigger et al., 2012; Liu et al., 2008). The generation of the nanocarriers with natural polymers is gaining growing interest because it is performed by mild treatments, such as ionic gelation, coacervation, or complexation (Pérez-Herrero & Fernández-Medarde, 2015).

7   Enhanced Biological Activity of Drugs Immobilized on Polymeric Nanocarriers

To evaluate the efficiency of new anticancer drugs, it is important to measure their cytotoxic activity and potency of targeting various human cancer cells in an in vitro cell-based assay, and compare the action of new drugs to that of the traditional ones. The use of nanocomposites as drug delivery systems permits incorporation of molecules of anticancer drugs with different properties. The majority of anticancer drugs belong to xenobiotics, and most cells have a transport system on their plasma membrane whose function is to protect cells from the entry of various toxic substances with molecular weight less than 1000 Da, which is close to the size of most drugs. This system provides the multiple resistance of cell to drugs, and genes that encode the structure of these membrane proteins are often activated in tumor cells. Therefore, the transportation of drug substances under the cover of a polymer or other nanoscale particles will protect the tumor cells from the action of the chemotherapeutics. Thus, the use of nanoshell in drug delivery is a way to overcome drug resistance mechanisms and to reduce the total amount of medicines needed to achieve a therapeutic effect.

A number of synthetic polymers have been proposed for the enhancement of the biological action of anticancer drugs in vitro and in vivo (Ravi Kumar & Kumar, 2001; Wilczewska et al., 2012). The use of special carriers for drug delivery reduces their side effects in the body and increases the effectiveness of their therapeutic action (Wilczewska et al., 2012). Besides, the multifunctional nanoscale delivery systems provide a longer action and greater bioavailability of drugs in the body (Tang et al., 2010; de Jong, 2008).

We have applied the water-soluble form of 4-thiazolidinone derivatives complexed with the synthetic PNC to treat rat C6 glioma cells. It was found that such

complexation significantly enhanced the cytotoxic effect (Trypan blue exclusion test) of those derivatives compared to their unbound forms (Kobylinska et al., 2019). The highest cytotoxicity effect was observed at 0.1 and 0.5μM doses of Les-3833 complexes with the PNC at 24 h and at 0.1μM dose at 48 h (Fig. 3).

Taking into account these and other results of antitumor action in vitro of complexes of 4-thiazolidinone derivatives with the PNC, we moved to preclinical studies on animal tumor models. As one can see in Fig. 4, Dox and the water-soluble form of Les-3833 stabilized by the polymeric surfactant demonstrated the best treatment effects in mice bearing NK/Ly lymphoma. The antitumor effect of Les-3833 + PNC complex toward murine NK/Ly lymphoma was comparable with the effect of doxorubicin, which is considered to be a "golden standard" in cancer chemotherapy.

The treatment effect based on the evaluation of animal survival indicator correlated with a treatment-induced decrease in tumor mass that was monitored as a change of animal weight due to a decrease in the volume of the ascitic fluid that contains lymphoma cells. While in the untreated mice (control group), it was elevated by 1.5 times, and under the action of Dox and Les-3833, it was significantly decreased.

The results of anticancer action of 4-thiazolidinone derivative Les-3833 and its water-soluble complex with novel synthetic PNC toward NK/Ly lymphoma grafted to BALB/C mice (Fig. 4) are in agreement with the results of cytotoxicity experiments conducted in vitro using rat glioma cells of C6 line (Fig. 3). These anticancer effects of Les-3833 in complex with the PNC in vitro and in vivo are comparable with such effects of Dox (Kobylinska, Patereha, et al., 2018, Kobylinska, Skorohyd, et al., 2018).
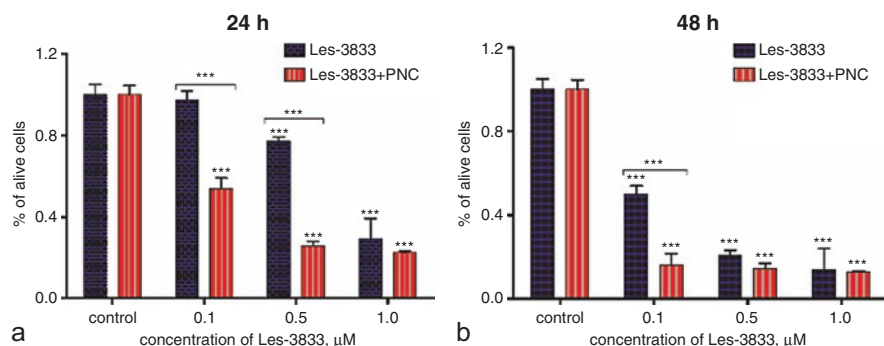

Fig. 3 Relative number of living C6 cells of rat glioma measured by Trypan blue exclusion test after treatment for 24 and 48 h with different doses (0.1, 0.5, and 1.0μM) of Les-3833 alone, compared with the action of its complex with the polymeric nanocarrier (PNC) *P < 0.05; **P < 0.01; ***P < 0.001 (difference in comparison to the control—100%). (Reproduced with permission (Kobylinska et al., 2019))
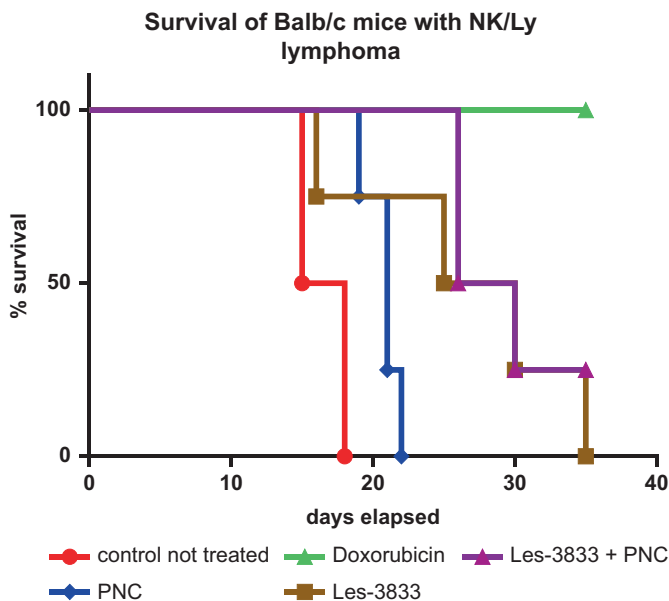
Fig. 4 Survival dynamics of mice bearing NK/Ly lymphoma treated with Doxorubicin (1 mg/kg of body weight), Les-3833 compound (2.5 mg/kg of body weight), and Les-3833 + PNC complex (1 mg of Les-3833/kg of body weight). (Reproduced with permission (Kobylinska, Patereha, et al., 2018; Kobylinska, Skorohyd, et al., 2018))

8   Biodistribution and Pharmacokinetics of Poorly Soluble Compounds

We studied the biodistribution of a synthetic 4-thiazolidinone derivative, the Les-3833, that might be a prospective anticancer agent. This compound, similar to many other anticancer drugs, is practically not soluble in water. Thus, measuring its concentration depending on time after administration, in blood plasma and selected tissues might define the character of the pharmacological response. The biodistribution parameters of Les-3833 in mice are important for the pre-clinical toxicology investigation, because the drug levels in plasma and tissues are often predictive for the evaluation of its toxicity and are important for effective therapeutic application. These parameters can be used for predicting the exposure of the investigated drug in the human body. The biodistribution can also reveal differences between various treatment groups, duration of treatment, and other factors, as well as permit estimating the variability between animals and identify cases with abnormal levels of the drug (Rollerova et al., 2015; Wilsker et al., 2019).

The results on the biodistribution and pharmacokinetics of Dox in rats demonstrated that after intravenous administration, the C_{max} (1.7μg/mL) in plasma was achieved immediately after injection, and in 1 h, the concentration was reduced to 0.3μg/mL (Rahman et al., 1986). In the experiments of treating mice with free Les-3833, its rapid clearance from blood plasma of animals was found. Its mean maximum concentration (5.55 ng/mL) was achieved in 2.08 min after administration, and after that, its concentration in blood plasma gradually decreased below the limit of quantitation.

When the clearance of water-soluble Dox was monitored in the liver and kidney of rats, a decrease from 26.4 ± 0.2μg/g (30 min) to 4.1 ± 0.6μg/g (24 h) in liver and from 37.2 ± 5.8μg/g (30 min) to 5.2 ± 0.2μg/g (24 h) in kidney was observed (Rahman et al., 1986). In our study, the water-insoluble Les-3833 compound was cleared from these organs of treated mice in a similar dynamics—from 1.02μg/g (15 min) to 0.42μg/g (24 h) in liver, and from 0.4μg/g (15 min) to 0.2μg/g (24 h) in kidney. The revealed differences in clearance doses of the Dox-treated rats and clearance doses of the Les-3833 in treated mice were probably caused by the differences in body masses of these animals—300–350 g in rats (Rahman et al., 1986) and 26.3 ± 2.1 g in mice (our study). Besides, the injected doses of these drugs were also different—6 mg/kg in rats and 2.5 mg/kg in mice (Rahman et al., 1986).

We found that Les-3833 was rapidly eliminated from the brain, and did not accumulate in the brain tissue of the treated mice (Fig. 5).

The liposomal encapsulation of Dox was shown to affect its pharmacokinetics in blood plasma (Rahman et al., 1986). Its terminal half-life was 69.3 h compared to
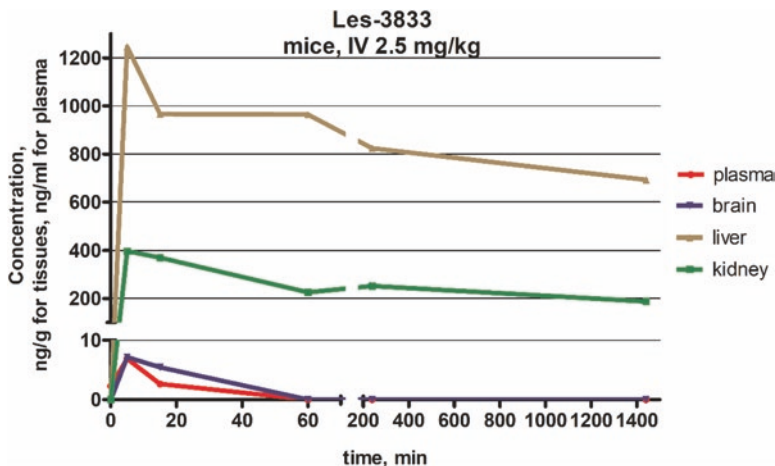

Fig. 5 Concentration/time dependence curves for Les-3833 following its dosing during 24 h in blood plasma, brain, liver, and kidney of male Balb/c mice. Since the concentrations of Les-3833 were very low for blood plasma (approximately 5 ng/mL) and brain (<10 ng/g), the X-axis and Y-axis each consist of two segments. (Reproduced with permission (Kobylinska et al., 2020))

17.3 h for free Dox, and the area under the blood plasma concentration curve for the liposomal Dox was 40-fold higher than that for the free drug.

The distribution and binding characteristics of the applied drug can also affect its renal clearance (Rollerova et al., 2015; Beechinor & Gonzalez, 2017). Usually, a drug that is extensively bound to proteins has a long half-life because its renal clearance is low and the urine flow rate is 1–2 mL/min (Beechinor & Gonzalez, 2017; Marenberg, 2004). The glomerular filtration and re-absorption are passive processes directly affected by the drug concentration in blood plasma. A drug that is not bound to plasma proteins and is excreted by filtration only shows a linear relationship between the rate of excretion and plasma drug concentration (Beechinor & Gonzalez, 2017; Marenberg, 2004).

The results of our study demonstrate that the distribution and elimination of Les-3833 take place in the liver and kidney. A very small half-life for this compound detected in blood plasma and brain suggests that it is not accumulated in these tissues.

9   Reduction of Side-Effects of Drugs Delivered by Polymeric Nanocarriers

In order to evaluate the effectiveness of action of anticancer drugs, it is not only important to determine their toxic effects at cellular and tissue levels but also necessary to study the biosafety of the action of the applied drugs in the treated organism (Wang et al., 2017). It is known that the effect of drugs with high biological activity may be accompanied by the adverse reactions of different severity. Thus, a critical requirement of the applied drugs is the optimal balance between their efficacy (therapeutic effect) and toxicity (Wang et al., 2017; Kobylinska, Patereha, et al., 2018, Kobylinska, Skorohyd, et al., 2018; Milane et al., 2011). The undesirable effects of medication should be considered during both the pre-clinical and clinical trials of new medicines.

Mechanisms related to the cytotoxic action of anticancer drugs include impaired energy metabolism and intracellular calcium homeostasis, activation of free radical processes in the cell, inhibition of matrix synthesis and cell division processes, and cell destruction (Wilsker et al., 2019). The molecular mechanisms of endogenous intoxication based on the membrane-destructive processes should also be considered (Tong & Cheng, 2007). Changes in the structure and function of cell membranes are due mainly to the effects of products of free radical oxidation (FRO), which are generated during the toxicosis switched on by the chemotherapeutics (Wilsker et al., 2019).

10   Hepatotoxicity

In healthy experimental animals, side effects such as cardiotoxicity (Kobylinska et al., 2014), hepatotoxicity (Kobylinska et al., 2015), and nephrotoxicity (Kobylinska et al., 2016) of the 4-thiazolidinone derivatives were much less expressed than the effects of the widely used anticancer agent, Dox. The action of anticancer drugs is most often accompanied by the pathophysiological and morphological manifestations in the liver, which is the central organ for metabolism in the body (Joshi et al., 2015; Ramadori & Cameron, 2010). It also provides a variety of hematopoietic, protective, and excretory processes, playing a key role in the intermediate metabolism as the main organ responsible for the detoxification processes (Ramadori & Cameron, 2010; Zimmerman, 1999). The metabolism of most pharmaceuticals takes place in the hepatocytes, which contain enzymes that catalyze chemical modifications and conjugation of substances of endogenous and exogenous origin.

According to the results of clinical studies, liver injury accounts for about 10% of all adverse reactions associated with the use of anticancer medicines (Ramadori & Cameron, 2010; Zimmerman, 1999). In the liver, the metabolism of most cytostatics occurs and, thus, it is the target for their toxic action (Joshi et al., 2015). During the processes of biotransformation, biochemical and physicochemical changes in drug molecules take place, which, in turn, may form polar water-soluble compounds which lose their pharmacological activity, become less toxic, and are more readily excreted (Navarro & Senior, 2006). The removal of xenobiotics from the internal environment of the body occurs in two stages: (1) the metabolic stage, which consists in the introduction of polar groups into the molecule with the participation of cytochrome P-450-hydroxylase system; (2) the conjugation stage of the attachment of certain water-soluble ligands to the molecules (Ramadori & Cameron, 2010). These are chemical reaction such as sulfation, acetylation, methylation, or attachment to natural compounds (glucuronidation, conjugation with glutathione, or single amino acids, such as glycine, taurine, glutamine). In addition, anticancer drugs can have a cumulative toxic effect on the functional state of the liver (Navarro & Senior, 2006).

The best-known manifestations of liver damage include bile duct lesions, destruction of hepatocytes and transport proteins, cytolytic activation of T-cells, apoptosis of hepatocytes, and disintegration of their mitochondria (Joshi et al., 2015; Ramadori & Cameron, 2010; Zimmerman, 1999; Navarro & Senior, 2006). It was shown that toxic effects of the anticancer drugs are due to both a decrease in the absorption of drugs by the hepatocytes and changes in the activity of certain enzymes, and is associated with the impaired interaction of these drugs with blood plasma proteins (Joshi et al., 2015; Ramadori & Cameron, 2010; Zimmerman, 1999; Navarro & Senior, 2006).

Marker enzymes and metabolites are used as an indicator of toxic damage caused by chemical compounds. Their level reflects the state of metabolic processes in the liver, heart, and kidney. The pathophysiological manifestations of drug hepatotoxicity are characterized by both hepatocellular and extracellular changes (Joshi et al., 2015; Ramadori & Cameron, 2010; Zimmerman, 1999; Navarro & Senior, 2006). Hepatocytes function at high concentrations of drugs that can be toxic even in the native state or become more toxic due to their metabolism (Zimmerman, 1999). The biological effect of drugs depends on the dose of their administration, the concentration of the active substance, route of administration, and duration of the

therapeutic effect of the drug. The hepatocyte lesions are more often caused by not the medicinal substances themselves, but by the toxic products formed during their metabolic detoxification reactions (Zimmerman, 1999; Navarro & Senior, 2006).

We have shown that after the injection of investigated compounds to laboratory rats, the activities of alanine aminotransferase, creatine kinase, alkaline phosphatase, and α-amylase increased compared to such activities in control animals (Kobylinska et al., 2014, 2015). Dox injection was accompanied by a fourfold increase in the activity of γ-glutamyltransferase, and the injection of Les-3833 compound led to a 2.5-fold elevation in the activity of this enzyme (Kobylinska et al., 2014, 2015). Complexation of these antineoplastic derivatives with a synthetic nanocarrier lowered the activity of the investigated enzymes substantially, as compared to the effect of these compounds applied in free form. The most evident decrease was measured for the activities of α-amylase, γ-glutamyltransferase, and lactate dehydrogenase. Thus, high general toxicity of anticancer drugs in the treated organism is abrogated by their immobilization on the polymeric carrier that is evident as the normalization of specific biochemical indicators of the hepatodestructive effects of the action of these drugs (Figs. 6, 7 and Table 1).
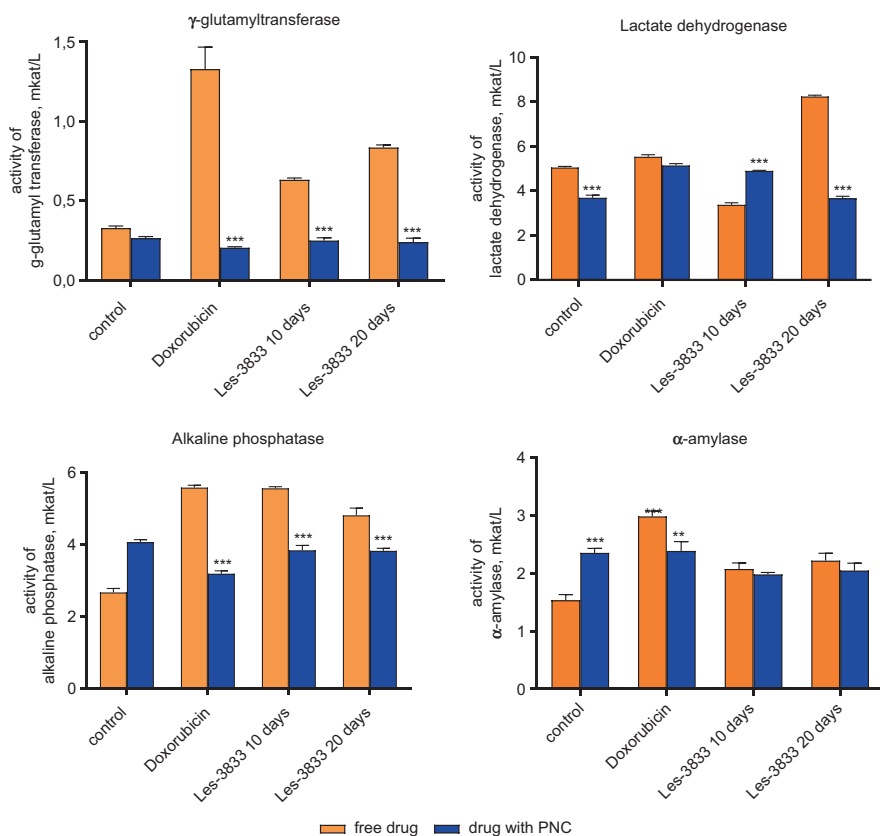

Fig. 6 Activity of γ-glutamyltransferase, lactate dehydrogenase alkaline phosphatase and α-amylase in blood serum of rats injected with free drug—doxorubicin, 4-thiazolidinone derivative Les-3833 (orange), and complexes of these substances with the polymeric nanocarrier (blue) (25.85). ***$P < 0.01$ (difference compare to the free drug)
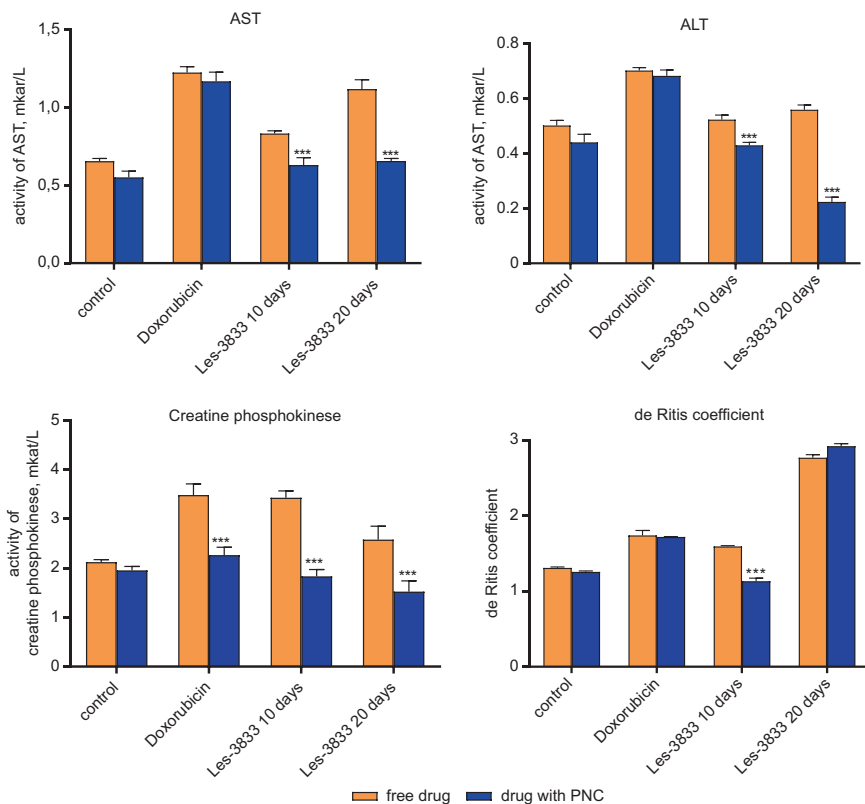
Fig. 7 Activity of alanine aminotransferase, aspartate aminotransferase, creatine kinase, and de Ritis coefficient in blood serum of rats injected with free drug—doxorubicin, 4-thiazolidinone derivative Les-3833 (orange), and complexes of these substances with the polymeric nanocarrier (blue). (86) ***$P < 0.01$ (difference compared to the free drug)

11 Cardiotoxicity

Numerous studies have shown the violation in the functions of the cardiovascular system under the influence of chemotherapeutic agents (Ramadori & Cameron, 2010). Dox is one of the most common and effective antitumor agents; however, its use is accompanied by a number of side effects—first, a powerful cardiotoxic effect, in particular, impairment of the cardiovascular functions and myocardial lesions in treated patients (Shi et al., 2011). Even in therapeutic doses, Dox causes destructive-dystrophic changes in the myocardium of animals, and in high doses of Dox, the mortality of animals reaches 67% (Mitry & Edwards, 2016).

Table 1 Concentrations of metabolites in blood serum of rats injected with free drug—doxorubicin, compound Les-3833, and their complexes with the polymeric nanocarrier (PNC)

Experimental groups	Total protein, g/L	Urea, mmol/L	Creatinine, μmol/L	Calcium, mmol/L	Iron ions, μmol/L	Sodium, mmol/L	Chloride ions, mmol/L
Control	75.8 ± 3.2	4.8 ± 0.4	74.6 ± 2.6	2.47 ± 0.45	37.7 ± 2.2	127.5 ± 13.2	117.8 ± 14.4
Les-3833	50.3 ± 2.7	2.6 ± 0.4	67.1 ± 2.9	2.60 ± 0.41	15.0 ± 6.2*	322.5 ± 12.1*	120.7 ± 9.5
Les-3833 + PNC	81.4 ± 4.4■	3.9 ± 0.6■	70.7 ± 3.4	3.15 ± 0.33■	29.3 ± 3.2■	189.7 ± 12.3■	102.9 ± 10.2
Dox (positive control)	55.8 ± 4.1*	1.9 ± 0.2*	56.7 ± 2.9*	3.60 ± 0.39*	31.4 ± 2.9	340.0 ± 16.1*	192.2 ± 9.5*
Dox + PNC	71.8 ± 4.3■	3.5 ± 0.4■	77.35 ± 3.9■	2.49 ± 0.28■	38.4 ± 2.8	159.7 ± 11.3■	184.6 ± 11.2
PNC (negative control)	67.5 ± 3.2	5.1 ± 0.3	70.2 ± 2.9	3.22 ± 0.51	42.5 ± 3.2	141.0 ± 9.8	119.8 ± 12.8

* – $P < 0.05$ compared to control (untreated) group;
■ – $P < 0.05$ compared to the group treated with free drug

Many chemotherapeutic agents kill tumor cells by damaging the mitochondria, inducing pore formation in the mitochondrial membrane (permeability transition pore), membrane depolarization, osmotic swelling, and release of cytochrome c mechanisms. The anticancer drugs can also act indirectly via damaging the myocardium that is realized with the participation of free radicals which start a cascade of the enzymatic reactions in the myocytes. As a result, the Dox molecule is transformed into semiquinone radicals, which generate a superoxide anion radical and hydrogen peroxide. The last one in the presence of ferrous iron (Fe^{2+}) contributes to the formation of the hydroxyl radical ($OH^{\bullet}$) (Kim et al., 2002; Matés & Sánchez-Jiménez, 2000). Another mechanism of the cardiotoxic action of Dox is associated with the formation of its complex by the Fe^{3+} cation, which, by attaching an electron, is transformed into a complex of Dox-divalent iron. Subsequently, this complex forms hydroxyl radicals which initiate lipid peroxidation and that is not enough to be inactivated by the enzymes of antioxidant protection. Antitumor drugs, including Dox, cause oxidative stress not only in tumors but also in intact cells, which adversely affects the function of the respiratory chain in mitochondria, leading to cell death by apoptosis (Sullivan & Chandel, 2014).

Dox is used to treat many types of cancer, including leukemia, lymphoma, neuroblastoma, sarcoma, Wilms tumor, and cancer of the lung, breast, stomach, ovaries, thyroid, and bladder (Joshi et al., 2015). In the cardiomyocytes, it induces an increase in ROS levels, DNA damage, activation of the ATM signaling pathway, and p53 accumulation leading to their death. Inhibition of ROS formation completely suppresses the toxic effects of Dox. Cardiolipin, a phospholipid localized on the inner mitochondrial membrane, possesses high affinity to Dox (Goormaghtigh et al., 1980). The cardiomyocytes are rich in mitochondria, thus, Dox accumulates there, leading to oxidative stress in these organelles. As a consequence, Dox causes a release of cytochrome c, which binds cardiolipin in the mitochondrial membrane and causes the activation of the proapoptotic caspase-3 (Sharifi et al., 2015). A large number of mitochondria in the cardiomyocytes is necessary for providing energy for supporting a contractile function of the myocardium (Joshi et al., 2015; Shi et al., 2011).

The vast majority of studies aimed at preventing the toxicity of the anthracycline antibiotics, including Dox, involve inhibiting the processes of free radical oxidation (FRO) and restoring energy metabolism, as well as limiting the "reload" of myocytes by calcium ions that prevent the development of Mates 2000 heart disease. However, many drugs considered as antioxidants and antiradical compounds do not always demonstrate a specific cardioprotective effect when used in a combination with anthracycline compounds. Therefore, the activation of FRO is not the main mechanism for the development of anthracycline-induced cardiomyopathy (Shi et al., 2011).

Among the biochemical indicators of the cardiotoxic action of anticancer agents, the activity of the following enzymes in rat blood serum was shown to be the most informative: creatine kinase, lactate dehydrogenase, aspartate

aminotransferase, and alanine aminotransferase (Kobylinska et al., 2014). While 10 times injection of Dox in a dose of 5.5 mg/kg of weight caused rats' death, the Les-3833 compound did not possess such toxic action. The application of Dox as a complex with a synthetic polymeric carrier prolonged animal survival time to 20 days. Thus, the injection of anticancer agents in a complex with the polymeric carrier provides a significant decrease in their cardiotoxicity, which was also confirmed by the results of measuring changes in the activity of the corresponding marker enzymes. We revealed that lower antineoplastic activity of synthetic 4-thiazolidinone derivative Les-3833 (comparing with such activity of Dox) correlates with lower cardiotoxicity of these derivatives in the experimental rats. Application of Les-3833 compound and Dox as complexes with a PEG-containing polymeric nanocarrier considerably decreased the cardiotoxicity of these anticancer agents in laboratory rats. Such conclusion was confirmed by the results of measuring the enzymatic activity of the creatine kinase, lactate dehydrogenase, aspartate aminotransferase, and alanine aminotransferase in blood serum of the treated rats (Figs. 6 and 7).

12   Nephrotoxicity

Nephrotoxicity of chemical compounds is based on their ability to cause structural and functional impairments in the kidney that are primarily associated with lesions in the proximal, rarely distal tubules, and glomerulus of the kidney (Naughton, 1984). The most common pathophysiological mechanisms of drug nephrotoxicity are disorders of hemodynamics in the glomeruli, the toxic effects in the epithelium of the tubules, as well as the inflammation, nephropathy, crystalluria, rhabdomyolysis, and microangiopathy, the immune and the autoimmune reactions (Perry & Doll, 2012). The adverse nephrotoxic reaction to drug application can be both renal (at the level of glomerular filtration, tubular reabsorption, and secretion), and pre- and postrenal. The kidney is an organ with high sensitivity to various regulatory mechanisms, as well as to the effects of endogenous and exogenous agents. The high blood supply and long tubular apparatus cause a long-term contact of toxicants and their metabolites with the vascular endothelial cells and the renal tubule epithelium.

Nephrotoxicity is characteristic of a large proportion of drugs (Perry & Doll, 2012). About 20–30% of the reported cases of acute renal failure and almost a third of the cases of chronic renal failure occur due to the action of chemical agents, including medicines. Therefore, nephrotoxicity is also a factor that limits adequate cytostatic chemotherapy in the oncological practice (Perry & Doll, 2012). Nephrotoxicity as an important side effect of a number of anticancer drugs is most commonly associated with lesions of the proximal, rarely distal tubules, and the glomeruli. A damage to the renal tubules is due to the re-absorption of high doses of drugs and their metabolites from the glomerular filtrate. Among the most

widespread pathophysiological mechanisms of the nephrotoxicity of medicines are disorders of hemodynamics in the glomeruli of the kidney, toxic effects on the cells of the epithelium of tubules, inflammation with nephropathy caused by the formation of crystals, and thrombotic microangiopathy (Perry & Doll, 2012). First of all, the nephrotoxic effect of anticancer drugs is manifested as a reduction in creatinine clearance, which, in turn, increases the duration of circulation in blood of agents that are excreted or metabolized by the kidney. That leads to a prolongation of the action of drugs on the organs and tissues and, as a consequence, enhances all types of toxic effects of the anticancer drugs (Perry & Doll, 2012).

The mechanisms of renal failure caused by the introduction of cytostatics include vascular damage and renal morphology leading to hemolytic and uremic syndromes (Naughton, 1984). The creatinine clearance that indicates the glomerular filtration status is a characteristic indicator of kidney functional status. The nephrotoxicity caused by the anticancer drugs is manifested as an increase in blood serum creatinine, which is due to a decrease in the level of the glomerular filtration in the kidney (Naughton, 1984). Even one injection of Dox can cause proteinuria in rats and damage kidney glomerular (Naughton, 1984). Dox-induced nephrotoxicity is, at least in part, due to an oxidative stress, which subsequently leads to an inflammatory process in the kidney (Naughton, 1984).

Nephrotoxicity is manifested differently when using various antitumor drugs, namely, cisplatin causes tubular necrosis, mitomycin–glomerular vasculitis, ifosfamide–proximal tubular defect, hematuria and chemical cystitis, and platinum preparations were shown to be the most nephrotoxic (Naughton, 1984). When exposed to cisplatin, a marked decrease in the glomerular filtration with an increase in blood serum creatinine and a decrease in the effective renal plasma flow were often observed. The combination of the irinotecan with cisplatin that is used to treat patients with small cell lung cancer caused kidney damage in 25% of cases, requiring a reduction in the dose of cisplatin at different stages of treatment (Perry & Doll, 2012). In the same study, it was noted that the combined effect of cisplatin with docetaxel caused nephrotoxic pathology in 21% of cases and etoposide in 23%, while the combination of anticancer drugs in the absence of platinum is less likely to damage the kidney (Naughton, 1984; Perry & Doll, 2012).

At the final stage of detoxification, water-soluble derivatives of toxins form complexes with bile acids and are removed with feces, or they enter blood serum and are removed through the kidney in the form of urine. Most anticancer drugs are excreted by the kidney, and some (cisplatin, thiophosphamide, methotrexate, bleomycin) are metabolized in the kidney tissues. The main mechanisms of the adverse effects of antitumor drugs on the kidney include their direct cytotoxicity and autoimmune complications (Perry & Doll, 2012). A degree of toxic damage to the kidney by the cytostatics depends on a dose of the drug, concomitant renal pathology, creatinine clearance, and diuresis. For example, cisplatin is characterized by high accumulation in kidney tissue, as well as dose-dependent and cumulative nephrotoxicity (Naughton, 1984).

We have found that after injection of anticancer compounds, the concentration of sodium cations and chloride anions in blood serum increased, compared to the control group (untreated animals) (Table 1) (Kobylinska et al., 2016). Dox's injection was also accompanied by a decrease in the concentration of the iron cations. The concentration of total protein, urea, and creatinine decreased under the influence of the 4-thiazolidinone derivative, the Les-3833, and Dox (positive control), while the complexation of these drugs with a synthetic polymeric nanocarrier normalized the concentration of total protein and that of the investigated metabolites (Table 1).

A balance between the anticancer activity of novel and/or traditional drugs and oxidative stress is required to study at the appearance of side effects. The value of such effects significantly depends on free radical oxidation and the balance between the reactive oxidant species and the activity of the antioxidant system. The nanoparticles of various size and chemical composition can enter into cells and target their mitochondria. This can lead to a disruption of the mitochondrial electron transduction chain that leads to excess O_2^- production. Besides, the nanoparticles may perturb the mitochondrial permeability transition pore, which leads to a release of the pro-apoptotic agents and a programmed cell death. Drug conjugation with nanocarriers affects the mechanisms of induced apoptosis.

13 Concluding Notes

In this chapter, we have established that the immobilization of the water-insoluble 4-thiazolidinone derivatives on the nanosized polymeric carrier functionalized with PEG provided for the formation of water-soluble complexes of those derivatives with improved stability. The created complexes penetrated the cells more rapidly than free derivatives, facilitated their accumulation in the target tissue or organ, retained their biological activity for a longer time, and enhanced cytotoxic action in vitro. Such complexes reduced the viability of mammalian tumor cells in vitro more effectively than what was done by the derivatives in free form. It should be stressed that the complexation of 4-thiazolidinone derivatives (e.g., Les-3833) or the doxorubicin (used as a positive control) with polymeric carriers reduced considerably the side effects, in particular cardio-, hepato-, and nephrotoxic effects in the body of treated laboratory animals, namely mice with implanted experimental tumor—NK/Ly lymphoma.

It is known that most of the anticancer drugs approved for clinical use have distinct signaling instruments, which include (a) monoclonal antibodies designed to bind to specific proteins in cancer cells, so that the immune system can recognize and attack them, or specifically stick to and block the signals from the receptors of growth factor(s) overexpressed in tumor cells; (b) small molecules, like the tyrosine kinase inhibitors that are used to block signaling pathways involved in the

regulation of abnormal growth; (c) antiapoptotic molecules; (d) blockers of tumoral neo-angiogenesis. The platforms that allow for the transportation of the highly toxic anticancer drugs to specific molecular targets overexpressed in tumor cells might be conjugated via chemical linkers with monoclonal antibodies or peptide ligands which assist in tumor permeability by targeting specific moieties on the surface of tumor cells and also help overcome the multidrug resistance barrier on cell surface.

The liposomes and polymer conjugates were the first nanocarriers approved by the FDA; however, to date, only five liposomal drugs and two polymer-protein conjugates are available in the market (Novel Drug Approvals for 2020. U.S. Food and Drug Administration, 2021). There are no polymeric micelles, polymer-drug conjugates, dendrimers, carbon nanotubes, or polymeric nanoparticles ready for clinical use, except for the Abraxane, an albumin-bound paclitaxel nanoparticle approved by the FDA in 2005 and recommended for the treatment of metastatic breast cancer. It got the approval for the first-line treatment of advanced non-small-cell lung cancer (2012) and for metastatic pancreatic cancer (2013). The corresponding clinical trials are currently in progress, which makes these new nano-platforms the promising carriers to passive or active delivery of various anticancer drugs, improving their clinical efficacy and reducing their general toxicity.

The polymeric nanoparticles have a huge potential in cancer chemotherapy, being one of the most widely tested nano-platforms for drug delivery and offering a more effective and less toxic options to onco-patients. However, because of the small number of clinical trials in current operation, only one formulation has received FDA approval (Novel Drug Approvals for 2020. U.S. Food and Drug Administration, 2021). This clinical failure is due to numerous challenges that need to be solved, such as the non-addressed action leading to the accumulation of carriers in liver and spleen, their still low therapeutic efficiency inside the tumors, and the existence of different biological barriers that have to be crossed to reach and enter the cancer cells. Thus, a search for new anticancer ligands or targeting moieties for driving the drug carrier to specific organ(s) or tumor(s) in order to achieve the site-specific delivery of the chemotherapy-containing nanocarriers to cancerous tissue is an important task in the oncopharmacology.

It should be noted that tumor cells possess high adaptation capacities expressing plasma membrane (e.g., transporters responsible for the multidrug resistance) and intracellular (e.g., inactivating mutations in *p53* gene) mechanisms causing the resistance of tumor cells to traditional anticancer drugs. Thus, the drug carriers capable of circumventing such mechanisms are of special importance. Another innovation task needed for improvement of the polymeric nanocarrier is to achieve a release of the anticancer agents by stimuli-sensitive carriers in a controlled way under the microenvironment conditions.

References

Bamrungsap, S., Zhao, Z., Chen, T., Wang, L., Li, C., Fu, T., & Tan, W. (2012). Nanotechnology in therapeutics: A focus on nanoparticles as a drug delivery system. *Nanomedicine, 7*(8), 1253–1271. https://doi.org/10.2217/nnm.12.87

Barraud, L., Merle, P., Soma, E., Lefrançois, L., Guerret, S., Chevallier, M., Dubernet, C., et al. (2005). Increase of doxorubicin sensitivity by doxorubicin-loading into nanoparticles for hepatocellular carcinoma cells in vitro and in vivo. *Journal of Hepatology, 42*(5), 736–743. https://doi.org/10.1016/j.jhep.2004.12.035

Beechinor, R., & Gonzalez, D. (2017). Book review: Introduction to drug disposition and pharmacokinetics. *Clinical Pharmacology & Therapeutics, 102*(6), 893–893. https://doi.org/10.1002/cpt.806

Bilia, A., Piazzini, V., Risaliti, L., Vanti, G., Casamonti, M., Wang, M., & Bergonzi, M. (2019). Nanocarriers: A successful tool to increase solubility, stability and optimise bioefficacy of natural constituents. *Current Medicinal Chemistry, 26*(24), 4631–4656. https://doi.org/10.2174/0929867325666181101110050

Boyd, M., & Paull, K. (1995). Some practical considerations and applications of the national cancer institute in vitro anticancer drug discovery screen. *Drug Development Research, 34*(2), 91–109. https://doi.org/10.1002/ddr.430340203

Brigger, I., Dubernet, C., & Couvreur, P. (2012). Nanoparticles in cancer therapy and diagnosis. *Advanced Drug Delivery Reviews, 64*, 24–36. https://doi.org/10.1016/j.addr.2012.09.006

Bunker, A. (2012). Poly(ethylene glycol) in drug delivery, why does it work, and can we do better? All atom molecular dynamics simulation provides some answers. *Physics Procedia, 34*, 24–33. https://doi.org/10.1016/j.phpro.2012.05.004

Cabral, H., Matsumoto, Y., Mizuno, K., Chen, Q., Murakami, M., Kimura, M., et al. (2011). Accumulation of sub-100 nm polymeric micelles in poorly permeable tumours depends on size. *Nature Nanotechnology, 6*(12), 815–823. https://doi.org/10.1038/nnano.2011.166

Couvreur, P., Kante, B., Roland, M., & Speiser, P. (1979). Adsorption of antineoplastic drugs to polyalkylcyanoacrylate nanoparticles and their release in calf serum. *Journal of Pharmaceutical Sciences, 68*(12), 1521–1524. https://doi.org/10.1002/jps.2600681215

de Jong. (2008). Drug delivery and nanoparticles: Applications and hazards. *International Journal of Nanomedicine, 133*. https://doi.org/10.2147/ijn.s596

Dutta, R. (2007). Drug carriers in pharmaceutical design: Promises and progress. *Current Pharmaceutical Design, 13*(7), 761–769. https://doi.org/10.2174/138161207780249119

Feng, R., Zhu, W., Teng, F., Liu, N., Yang, F., Meng, N., & Song, Z. (2015). Poly(ethylene glycol) amphiphilic copolymer for anticancer drugs delivery. *Anti-Cancer Agents in Medicinal Chemistry, 15*(2), 176–188. https://doi.org/10.2174/1871520614666141124102347

Finiuk, N., Boiko, N., Klyuchivska, O., Kobylinska, L., Kril, I., Zimenkovsky, B., et al. (2017). 4-Thiazolidinone derivative Les-3833 effectively inhibits viability of human melanoma cells through activating apoptotic mechanisms. *Croatian Medical Journal, 58*(2), 129–139. https://doi.org/10.3325/cmj.2017.58.129

Gong, J., Chen, M., Zheng, Y., Wang, S., & Wang, Y. (2012). Polymeric micelles drug delivery system in oncology. *Journal of Controlled Release, 159*(3), 312–323. https://doi.org/10.1016/j.jconrel.2011.12.012

Goormaghtigh, E., Chatelain, P., Caspers, J., & Ruysschaert, J. (1980). Evidence of a specific complex between adriamycin and negatively-charged phospholipids. *Biochimica et Biophysica Acta (BBA) – Biomembranes, 597*(1), 1–14. https://doi.org/10.1016/0005-2736(80)90145-5

Hamaguchi, T., Doi, T., Eguchi-Nakajima, T., Kato, K., Yamada, Y., Shimada, Y., et al. (2010). Phase I study of NK012, a novel SN-38-incorporating micellar nanoparticle, in adult patients with solid tumors. *Clinical Cancer Research, 16*(20), 5058–5066. https://doi.org/10.1158/1078-0432.ccr-10-0387

Hamaguchi, T., Kato, K., Yasui, H., Morizane, C., Ikeda, M., Ueno, H., et al. (2007). A phase I and pharmacokinetic study of NK105, a paclitaxel-incorporating micellar nanoparticle formulation. *British Journal of Cancer, 97*(2), 170–176. https://doi.org/10.1038/sj.bjc.6603855

Havrylyuk, D., Zimenkovsky, B., Vasylenko, O., Gzella, A., & Lesyk, R. (2012). Synthesis of new 4-thiazolidinone-, pyrazoline-, and isatin-based conjugates with promising antitumor activity. *Journal of Medicinal Chemistry, 55*(20), 8630–8641. https://doi.org/10.1021/jm300789g

Hillaireau, H., & Couvreur, P. (2009). Nanocarriers' entry into the cell: Relevance to drug delivery. *Cellular and Molecular Life Sciences, 66*(17), 2873–2896. https://doi.org/10.1007/s00018-009-0053-z

Hu, C., Aryal, S., & Zhang, L. (2010). Nanoparticle-assisted combination therapies for effective cancer treatment. *Therapeutic Delivery, 1*(2), 323–334. https://doi.org/10.4155/tde.10.13

Iwamoto, T. (2013). Clinical application of drug delivery systems in cancer chemotherapy: Review of the efficacy and side effects of approved drugs. *Biological and Pharmaceutical Bulletin, 36*(5), 715–718. https://doi.org/10.1248/bpb.b12-01102

Joshi, M., Sodhi, K., Pandey, R., Singh, J., & Goyal, S. (2015). Doxorubicin-induced cardiotoxicity. *International Journal of Basic & Clinical Pharmacology, 4*(1), 6. https://doi.org/10.5455/2319-2003.ijbcp20150203

Jabir, N. R., Tabrez, S., Ashraf, G. M., Shakil, S., Damanhouri, G. A., & Kamal, M. A. (2012, 4391). Nanotechnology-based approaches in anticancer research. *International Journal of Nanomedicine*. https://doi.org/10.2147/ijn.s33838

Kato, K., Chin, K., Yoshikawa, T., Yamaguchi, K., Tsuji, Y., Esaki, T., et al. (2011). Phase II study of NK105, a paclitaxel-incorporating micellar nanoparticle, for previously treated advanced or recurrent gastric cancer. *Investigational New Drugs, 30*(4), 1621–1627. https://doi.org/10.1007/s10637-011-9709-2

Kim, R., Tanabe, K., Uchida, Y., Emi, M., Inoue, H., & Toge, T. (2002). Current status of the molecular mechanisms of anticancer drug-induced apoptosis. *Cancer Chemotherapy and Pharmacology, 50*(5), 343–352. https://doi.org/10.1007/s00280-002-0522-7

Kobylinska, L., Boiko, N., Panchuk, R., Grytsyna, I., Klyuchivska, O., Biletska, L., et al. (2016). Putative anticancer potential of novel 4-thiazolidinone derivatives: Cytotoxicity toward rat C6 glioma in vitro and correlation of general toxicity with the balance of free radical oxidation in rats. *Croatian Medical Journal, 57*(2), 151–163. https://doi.org/10.3325/cmj.2016.57.151

Kobylinska, L., Havrylyuk, D., Mitina, N., et al. (2014). Study of rat blood serum biochemical indicators of cardiotoxic action of novel antitumor 4-thiazolidinone derivatives and doxorubicin in complexes with polyethylenglycol-containing polymeric carrier in the rat blood serum. *The Ukrainian Biochemical Journal, 86*(6), 84–95. https://doi.org/10.15407/ubj86.06.084

Kobylinska, L., Havrylyuk, D., Mitina, N., et al. (2016). Biochemical indicators of nephrotoxicity in blood serum of rats treated with novel 4-thiazolidinone derivatives or their complexes with polyethylene glycol-containing nanoscale polymeric carrier. *The Ukrainian Biochemical Journal, 88*(1), 51–60. https://doi.org/10.15407/ubj88.01.051

Kobylinska, L., Havrylyuk, D., Ryabtseva, A., Mitina, N., Zaichenko, O., Lesyk, R., et al. (2015). Biochemical indicators of hepatotoxicity in blood serum of rats under the effect. *The Ukrainian Biochemical Journal, 87*(2), 122–132. https://doi.org/10.15407/ubj87.02.122

Kobylinska, L., Ivasechko, I., Skorokhyd, N., Panchuk, R., Riabtseva, A., Mitina, N., et al. (2019). Enhanced proapoptotic effects of water dispersed complexes of 4-thiazolidinone-based chemotherapeutics with a PEG-containing polymeric nanocarrier. *Nanoscale Research Letters, 14*(1). https://doi.org/10.1186/s11671-019-2945-7

Kobylinska, L., Lozynskii, A., Lesyk, R., Stoika, R., & Vari, S. (2020). Biodistribution and anticancer characteristics of Les-3833, a novel 4-thiazolidinone-based lead compound. *Scientia Pharmaceutica, 88*(2), 18. https://doi.org/10.3390/scipharm88020018

Kobylinska, L., Patereha, I., Finiuk, N., Mitina, N., Riabtseva, A., Kotsyumbas, I., et al. (2018). Comb-like PEG-containing polymeric composition as low toxic drug nanocarrier. *Cancer Nanotechnology, 9*(1). https://doi.org/10.1186/s12645-018-0045-5

Kobylinska, L., Skorohyd, N., Klyuchivska, O., Mitina, N., Zaichenko, A., Lesyk, R., et al. (2018). Increased antitumor efficiency and reduced negative side effects in laboratory mice of 4-thiazolidinone derivatives in complexes with PEG-containing polymeric nanocarrier. *Biopolymers and Cell, 34*(4), 313–328. https://doi.org/10.7124/bc.000985

Kwon, G. (2003). Polymeric micelles for delivery of poorly water-soluble compounds. *Critical Reviews in Therapeutic Drug Carrier Systems, 20*(5), 357–403. https://doi.org/10.1615/crit-revtherdrugcarriersyst.v20.i5.20

Kwon, G., & Kataoka, K. (2012). Block copolymer micelles as long-circulating drug vehicles. *Advanced Drug Delivery Reviews, 64*, 237–245. https://doi.org/10.1016/j.addr.2012.09.016

Lammers, T., Kiessling, F., Hennink, W., & Storm, G. (2012). Drug targeting to tumors: Principles, pitfalls and (pre-) clinical progress. *Journal of Controlled Release, 161*(2), 175–187. https://doi.org/10.1016/j.jconrel.2011.09.063

Langer, R. (1999). Selected advances in drug delivery and tissue engineering. *Journal of Controlled Release, 62*(1–2), 7–11. https://doi.org/10.1016/s0168-3659(99)00057-7

Langer, R., & Folkman, J. (1976). Polymers for the sustained release of proteins and other macromolecules. *Nature, 263*(5580), 797–800. https://doi.org/10.1038/263797a0

Lee, S., Yun, M., Jeong, S., In, C., Kim, J., Seo, M., et al. (2011). Development of docetaxel-loaded intravenous formulation, Nanoxel-PM™ using polymer-based delivery system. *Journal of Controlled Release, 155*(2), 262–271. https://doi.org/10.1016/j.jconrel.2011.06.012

Li, Y. (2003). Nanoparticles bearing polyethyleneglycol-coupled transferrin as gene carriers: Preparation and in vitro evaluation. *International Journal of Pharmaceutics, 259*(1–2), 93–101. https://doi.org/10.1016/s0378-5173(03)00211-4

Liu, D., & Auguste, D. (2015). Cancer targeted therapeutics: From molecules to drug delivery vehicles. *Journal of Controlled Release, 219*, 632–643. https://doi.org/10.1016/j.jconrel.2015.08.041

Liu, Z., Jiao, Y., Wang, Y., Zhou, C., & Zhang, Z. (2008). Polysaccharides-based nanoparticles as drug delivery systems. *Advanced Drug Delivery Reviews, 60*(15), 1650–1662. https://doi.org/10.1016/j.addr.2008.09.001

Lu, Y., & Park, K. (2013). Polymeric micelles and alternative nanonized delivery vehicles for poorly soluble drugs. *International Journal of Pharmaceutics, 453*(1), 198–214. https://doi.org/10.1016/j.ijpharm.2012.08.042

Ma, P. (2013). Paclitaxel nano-delivery systems: A comprehensive review. *Journal of Nanomedicine & Nanotechnology, 04*(02). https://doi.org/10.4172/2157-7439.1000164

Marenberg, B. (2004). FDA issues final rule on patent listing requirements and 30-month stays of approval following submission of abbreviated new drug applications. *Biotechnology Law Report, 23*(1), 48–51. https://doi.org/10.1089/073003104322838240

Matés, J., & Sánchez-Jiménez, F. (2000). Role of reactive oxygen species in apoptosis: Implications for cancer therapy. *The International Journal of Biochemistry & Cell Biology, 32*(2), 157–170. https://doi.org/10.1016/s1357-2725(99)00088-6

Matsumura, Y., Hamaguchi, T., Ura, T., Muro, K., Yamada, Y., Shimada, Y., et al. (2004). Phase I clinical trial and pharmacokinetic evaluation of NK911, a micelle-encapsulated doxorubicin. *British Journal of Cancer, 91*(10), 1775–1781. https://doi.org/10.1038/sj.bjc.6602204

Milane, L., Duan, Z., & Amiji M. (2011) Therapeutic efficacy and safety of paclitaxel/lonidamine loaded EGFR-targeted nanoparticles for the treatment of multi-drug resistant cancer. *PLoS One. 6(9): e24075.* https://doi.org/10.1371/journal.pone.0024075

Min, Y., Caster, J., Eblan, M., & Wang, A. (2015). Clinical translation of nanomedicine. *Chemical Reviews, 115*(19), 11147–11190. https://doi.org/10.1021/acs.chemrev.5b00116

Mishra, P., Nayak, B., & Dey, R. (2016). PEGylation in anti-cancer therapy: An overview. *Asian Journal of Pharmaceutical Sciences, 11*(3), 337–348. https://doi.org/10.1016/j.ajps.2015.08.011

Mitra, S., Gaur, U., Ghosh, P., & Maitra, A. (2001). Tumour targeted delivery of encapsulated dextran–doxorubicin conjugate using chitosan nanoparticles as carrier. *Journal of Controlled Release, 74*(1–3), 317–323. https://doi.org/10.1016/s0168-3659(01)00342-x

Mitry, M., & Edwards, J. (2016). Doxorubicin induced heart failure: Phenotype and molecular mechanisms. *IJC Heart & Vasculature, 10*, 17–24. https://doi.org/10.1016/j.ijcha.2015.11.004

Narvekar, M., Xue, H., Eoh, J., & Wong, H. (2014). Nanocarrier for poorly water-soluble anticancer drugs—Barriers of translation and solutions. *AAPS PharmSciTech, 15*(4), 822–833. https://doi.org/10.1208/s12249-014-0107-x

Nath Roy, D., Goswami, R., & Pal, A. (2016). Nanomaterial and toxicity: What can proteomics tell us about the nanotoxicology? *Xenobiotica, 47*(7), 632–643. https://doi.org/10.1080/00498254.2016.1205762

Naughton, C. A. (1984). Drug-induced nephrotoxicity. *Reactions, 94*(1), 11–12. https://doi.org/10.1007/bf03273412

Navarro, V., & Senior, J. (2006). Drug-related hepatotoxicity. *New England Journal of Medicine, 354*(7), 731–739. https://doi.org/10.1056/nejmra052270

Novel Drug Approvals for 2020. U.S. Food and Drug Administration [cited 22 January 2021]. Available from: https://www.fda.gov/drugs/new-drugs-fda-cders-new-molecular-entities-and-new-therapeutic-biological-products/novel-drug-approvals-2020

Onishi, H., Machida, Y., & Machida, Y. (2003). Antitumor properties of irinotecan-containing nanoparticles prepared using poly(DL-lactic acid) and poly(ethylene glycol)-block-poly(propylene glycol)-block-poly(ethylene glycol). *Biological & Pharmaceutical Bulletin, 26*(1), 116–119. https://doi.org/10.1248/bpb.26.116

Otsuka, H., Nagasaki, Y., & Kataoka, K. (2003). PEGylated nanoparticles for biological and pharmaceutical applications. *Advanced Drug Delivery Reviews, 55*(3), 403–419. https://doi.org/10.1016/s0169-409x(02)00226-0

Park, K., Lee, G., Kim, Y., Yu, M., Park, R., Kim, I., et al. (2006). Heparin–deoxycholic acid chemical conjugate as an anticancer drug carrier and its antitumor activity. *Journal of Controlled Release, 114*(3), 300–306. https://doi.org/10.1016/j.jconrel.2006.05.017

Pérez-Herrero, E., & Fernández-Medarde, A. (2015). Advanced targeted therapies in cancer: Drug nanocarriers, the future of chemotherapy. *European Journal of Pharmaceutics and Biopharmaceutics, 93*, 52–79. https://doi.org/10.1016/j.ejpb.2015.03.018

Perry, M., & Doll, D. (2012). *Perry's the chemotherapy source book*. Lipincott Williams & Wilkins.

Plummer, R., Wilson, R., Calvert, H., Boddy, A., Griffin, M., Sludden, J., et al. (2011). A Phase I clinical study of cisplatin-incorporated polymeric micelles (NC-6004) in patients with solid tumours. *British Journal of Cancer, 104*(4), 593–598. https://doi.org/10.1038/bjc.2011.6

Rahman, A., Fumagalli, A., Barbieri, B., Schein, P., & Casazza, A. (1986). Antitumor and toxicity evaluation of free doxorubicin and doxorubicin entrapped in cardiolipin liposomes. *Cancer Chemotherapy and Pharmacology, 16*(1). https://doi.org/10.1007/bf00255281

Ramadori, G., & Cameron, S. (2010). Effects of systemic chemotherapy on the liver. *Annals of Hepatology, 9*(2), 133–143. https://doi.org/10.1016/s1665-2681(19)31651-5

Ravi Kumar, M., & Kumar, N. (2001). Polymeric controlled drug-delivery systems: Perspective issues and opportunities. *Drug Development and Industrial Pharmacy, 27*(1), 1–30. https://doi.org/10.1081/ddc-100000124

Riabtseva, A., Mitina, N., Boiko, N., Garasevich, S., Yanchuk, I., Stoika, R., et al. (2012). Structural and colloidal-chemical characteristics of nanosized drug delivery systems based on pegylated comb-like carriers. *Chemistry & Chemical Technology, 6*(3), 291–295. https://doi.org/10.23939/chcht06.03.291

Rollerova, E., Tulinska, J., Liskova, A., Kuricova, M., Kovriznych, J., Mlynarcikova, A., et al. (2015). Titanium dioxide nanoparticles: Some aspects of toxicity/focus on the development. *Endocrine Regulations, 49*(02), 97–112. https://doi.org/10.4149/endo_2015_02_97

Sahoo, S., & Labhasetwar, V. (2003). Nanotech approaches to drug delivery and imaging. *Drug Discovery Today, 8*(24), 1112–1120. https://doi.org/10.1016/s1359-6446(03)02903-9

Savjani, K., Gajjar, A., & Savjani, J. (2012). Drug solubility: Importance and enhancement techniques. *ISRN Pharmaceutics, 2012*, 1–10. https://doi.org/10.5402/2012/195727

Sharifi, S., Barar, J., Hejazi, M., & Samadi, N. (2015). Doxorubicin changes Bax/Bcl-xL ratio, caspase-8 and 9 in breast cancer cells. *Advanced Pharmaceutical Bulletin, 5*(3), 351–359. https://doi.org/10.15171/apb.2015.049

Shi, Y., Moon, M., Dawood, S., McManus, B., & Liu, P. (2011). Mechanisms and management of doxorubicin cardiotoxicity. *Herz, 36*(4), 296–305. https://doi.org/10.1007/s00059-011-3470-3

Shoemaker, R. (2006). The NCI60 human tumour cell line anticancer drug screen. *Nature Reviews Cancer, 6*(10), 813–823. https://doi.org/10.1038/nrc1951

Soppimath, K., Aminabhavi, T., Kulkarni, A., & Rudzinski, W. (2001). Biodegradable polymeric nanoparticles as drug delivery devices. *Journal of Controlled Release, 70*(1–2), 1–20. https://doi.org/10.1016/s0168-3659(00)00339-4

Sullivan, L., & Chandel, N. (2014). Mitochondrial reactive oxygen species and cancer. *Cancer & Metabolism, 2*(1). https://doi.org/10.1186/2049-3002-2-17

Talelli, M., Rijcken, C., Hennink, W., & Lammers, T. (2012). Polymeric micelles for cancer therapy: 3 C's to enhance efficacy. *Current Opinion in Solid State and Materials Science, 16*(6), 302–309. https://doi.org/10.1016/j.cossms.2012.10.003

Talukder, R., Reed, C., Dürig, T., & Hussain, M. (2011). Dissolution and solid-state characterization of poorly water-soluble drugs in the presence of a hydrophilic carrier. *AAPS PharmSciTech, 12*(4), 1227–1233. https://doi.org/10.1208/s12249-011-9697-8

Tang, M., Lei, L., Guo, S., & Huang, W. (2010). Recent progress in nanotechnology for cancer therapy. *Chinese Journal of Cancer, 29*(9), 775–780. https://doi.org/10.5732/cjc.010.10075

Tomao, S. (2009). Albumin-bound formulation of paclitaxel (Abraxane® ABI-007) in the treatment of breast cancer. *International Journal of Nanomedicine, 99*. https://doi.org/10.2147/ijn.s3061

Tong, R., & Cheng, J. (2007). Anticancer polymeric nanomedicines. *Polymer Reviews, 47*(3), 345–381. https://doi.org/10.1080/15583720701455079

Torchilin, V. (2001). Structure and design of polymeric surfactant-based drug delivery systems. *Journal of Controlled Release, 73*(2–3), 137–172. https://doi.org/10.1016/s0168-3659(01)00299-1

Torchilin, V. (2007). Nanocarriers. *Pharmaceutical Research, 24*(12), 2333–2334. https://doi.org/10.1007/s11095-007-9463-5

Ulbrich, K. (2004). Polymeric anticancer drugs with pH-controlled activation. *Advanced Drug Delivery Reviews, 56*(7), 1023–1050. https://doi.org/10.1016/j.addr.2003.10.040

Wang, L., Du, J., Zhou, Y., & Wang, Y. (2017). Safety of nanosuspensions in drug delivery. *Nanomedicine: Nanotechnology, Biology and Medicine, 13*(2), 455–469. https://doi.org/10.1016/j.nano.2016.08.007

Wang, X., Wang, Y., Chen, Z., & Shin, D. (2009). Advances of cancer therapy by nanotechnology. *Cancer Research and Treatment, 41*(1), 1. https://doi.org/10.4143/crt.2009.41.1.1

Wilczewska, A., Niemirowicz, K., Markiewicz, K., & Car, H. (2012). Nanoparticles as drug delivery systems. *Pharmacological Reports, 64*(5), 1020–1037. https://doi.org/10.1016/s1734-1140(12)70901-5

Wilsker, D., Barrett, A., Dull, A., Lawrence, S., Hollingshead, M., Chen, A., et al. (2019). Evaluation of pharmacodynamic responses to cancer therapeutic agents using DNA damage markers. *Clinical Cancer Research, 25*(10), 3084–3095. https://doi.org/10.1158/1078-0432.ccr-18-2523

Zhang, J., Li, S., & Li, X. (2009). Polymeric nano-assemblies as emerging delivery carriers for therapeutic applications: A review of recent patents. *Recent Patents on Nanotechnology, 3*(3), 225–231. https://doi.org/10.2174/187221009789177803

Zimmerman, H. (1999). *Hepatotoxicity*. Lippincott Williams & Wilkins.

Nano- and Microparticles and Their Role in Inflammation and Immune Response: Focus on Neutrophil Extracellular Traps

Galyna Bila, Andrii Rabets, and Rostyslav Bilyy

Abbreviations

Abs   Absorbance
AKI   Acute kidney inflammation
FL   Fluorescence
MPO   Myeloperoxidase
MPTP   Mitochondria permeability transition pore
MSU   Monosodium urate crystals
NE   Neutrophil elastase
NETs   Neutrophil extracellular traps
NOX-2   NADPH-oxidase 2
NP   Nanoparticle
PAD4   Peptidylarginine deiminase 4
Pfif   Peptidylprolyl isomerase F
PMN   Polymorphonuclear neutrophilic granulocytes
RBC   Red blood cells
ROS   Reactive oxygen species

1 Introduction

Nano- and microparticles when they contact with the body trigger a response, which is managed by the immune system, since most of the nanoparticles are "foreign" and are "antigens" to human body. This makes our immune system active. Soot from fires, asbestos, cementum, smog, and other particles in the air are the most spread, and many other immune-related interactions were summarized in recent

G. Bila · A. Rabets · R. Bilyy (✉)
Danylo Halytsky Lviv National Medical University, Lviv, Ukraine

research (Anders et al., 2019). Immediately, we will recall the increasing number of allergies, respiratory diseases, and other related problems distinguishing the life in metropolies and countryside.

However, the forest fires took place before first lungs have developed in course of evolution. Naturally occurring nano-sized pollutants like extraterrestrial nanodiamonds (originating from meteors entering the atmosphere) served as prototypes of nanodiamonds derived from modern polishing machines. Therefore, it is not surprising that human tissues have developed mechanisms to cope with the exposure to nanoparticles without triggering pathological responses. Moreover, nanoparticles are often a natural form of interaction which is common in the body—low and high-density lipoproteins, immune complexes involving IgM molecules (>1 MDa) are typical natural occurring nanoparticles.

Indeed, phagocytosis, excretion, catabolism, isolation, and immobilization are strategies of the body to appropriately handle or ideally clear heterogeneous nanoparticles. Several cells orchestrate the response to particulate agents. Epithelial cells constitute physical barriers, mononuclear phagocytes engulf and clear, and granulocytes immobilize and sequester. Although this process is usually silent, there are conditions causing mostly mild but sometimes severe pathologies, relating to conditions when engulfed nanoparticles cannot be digested, oxidized, dissolved or excreted (either due to inert chemistry, absence of specific receptors or other reasons). In this case, our body should select the strategy of sequestration—isolation of potentially harmful objects in one place and limiting their further contact with body tissues. The mechanism of object sequestration was developed by our immune cells, namely polymorphonuclear neutrophilic granulocytes (neutrophils or PMN), after prolonged contact with particles they were not able to destroy by other means. For decades, it was known among pathologists observing granulomas and other material isolated with fibrous or adipose tissue. However, molecular and cellular mechanism started to be deciphered when we learned in 2004 about the ability of PMNs to produce neutrophil extracellular traps (NETs), and then the team of Martin Herrmann demonstrated the ability of NETs to aggregate and isolate the causative agent of gout—naturally occurring monosodium urate crystals (MSU), with elongated needle-shaped morphology, thus revealing a century-old mystery of why gout stops as rapidly as it starts (Schauer et al., 2014).

2   Neutrophils and NETs

Neutrophils Polymorphonuclear neutrophilic granulocytes (PMN) in the blood have been known to patrol our tissues, epithelia of body surfaces, and the lumina of various ducts (Leppkes et al., 2016) for infections threats, phagocytose it and activate a cascade of reactive oxygen species (ROS) to destroy or neutralize pathogens. Neutrophils are a primary working horse of innate immune system and our organism produces at least 100 billion of these cells every day (Dancey et al., 1976). Neutrophils can protect us in three different ways: they can phagocytize pathogens,

produce chemicals that can mediate pathogens' death and suicide to form NETs. DNA in NETs can interact with bacterial membrane and immobilize them (Brinkmann & Zychlinsky, 2012), therefore making bacteria better exposed to cytotoxic molecules. Cytotoxic molecules localize in granules that are divided into four types. Primary or azurophilic granules contain a cocktail of proteinases like neutrophil elastase, cathepsin G, and myeloperoxidase. Secondary (specific) granules contain lysozyme, lactoferrin, and collagenase, and tertiary granules display high amounts of gelatinase and secretory vesicles (Borregaard & Cowland, 1997). Just to clarify how dangerous those proteins are, we would like to remind the readers that neutrophil myeloperoxidase is producing HClO, hypochlorous acid, upon radical oxidation events (we know its solution as "bleach") with the aim to destroy most dangerous pathogens (Winterbourn & Kettle, 2013). The lifespan of "healthy" PMNs is approximately 8 hours, with their nuclei becoming progressively more "branched" with ageing, a feature helping neutrophils to extravasate and reach tissues and duct surfaces, wound surfaces, and mucosa linings (Daniel et al., 2019; Silvestre-Roig et al., 2016). Thus, it is not surprising, that with no possibility to proliferate, living very short time, and having a tremendously powerful weapon, PMNs tend to sacrifice themselves with the aim to kill the pathogens and protect the body. Usually, this is realized by phagocytosis, but when it fails, or when pathogens prevail (nanoparticles can serve as pathogens and usually appear in the body in high number due to directed administration), neutrophils utilize the strategy of NET formation by transforming their body into pathogen-trapping and killing net.

General Characteristics of NETs and NETosis In 1996, a new mechanism of neutrophil death was described. It occurs over several hours, includes stepwise chromatin decondensation, nuclei swelling, nucleoplasm leakage, and following perforation of the cellular membrane (Takei et al., 1996). In 2004, Brinkmann et al. showed that this phenomenon is of critical importance for antimicrobial immunity and it was later called Neutrophil Extracellular Traps (NETs), yet another valuable addition to the neutrophil granulocytes weapon (Brinkmann, 2004). Neutrophil extracellular traps are, as the name implies, net-like structures mainly consisting of nuclear DNA, histones, and granules that contain a variety of proteolytic proteins. NETs generally can be seen as long filaments ranging from 15 to 17 nm in diameter intersected by globular domains of around 25 nm in diameter. Filaments and globular domains are further aggregated into larger thread-like structures around 50 nm in diameter. NETs formation is typically suicidal, which means that the neutrophil dies. However, under certain conditions, neutrophils can even survive NET release (Yipp & Kubes, 2013). Although NETs release usually results in neutrophils death, these aggregates are not surrounded by membranes. Besides, NETs are richly decorated with granule-derived proteins. These proteins include neutrophil elastase, cathepsin G, myeloperoxidase, lactoferrin, and gelatinase. Membrane-bound and cytoplasmic proteins have not yet been detected as part of NETs protein assembly (Brinkmann, 2004).

    NETs formation is an extremely complicated process that involves a variety of molecular mechanisms. Neutrophil DNA release is a ROS-dependent process. H. Parker and C. C. Winterbourn got into great detail about ROS and their role in NETosis (Parker & Winterbourn, 2012). However, there are several things that should be mentioned. Most of the known NETosis forms rely on NADPH-oxidase 2 (NOX-2) for ROS production (Parker & Winterbourn, 2012)—one of the better-studied enzymes in neutrophils that produces large quantities of superoxide (O_2^-) that are later dismutated into hydrogen peroxide (H_2O_2). However, recently, a NOX-2-independent NETosis was demonstrated, which depends on mitochondria-derived ROS for NETosis (Douda et al., 2015). Myeloperoxidase, another prominent enzyme in azurophilic granules, is usually also activated and released during NETs formation. NETs mainly consist of DNA, derived from nuclei or its parts (Brinkmann, 2004). Some researchers reported that DNA can also originate from mitochondria; however its amount in the cells is lower compared to nuclear DNA (Yousefi et al., 2009). NETosis, in response to various stimuli, majorly depends on chromatin decondensation for DNA externalization (Wang et al., 2009). Most of the known data points at the important role of peptidylarginine deiminases in NETosis. Peptidylarginine deiminase 4 (PAD4) is essential for histone citrullination. By reducing positive charge of histones, it weakens DNA-protein interaction and hence, takes part in chromatin decondensation (P. Li et al., 2010). However, PAD4 is not required for NETosis, a PAD4 independent NETosis was also reported, and PAD2 and other enzymes can be involved in the process as well (Claushuis et al., 2018; Kenny et al., 2017). Neutrophil elastase (NE) is a serine protease that is involved in pathogen clearance (Belaaouaj et al., 2000). NE is essential for NETosis, as it promotes chromatin cleavage and it is strongly enhanced by MPO independently of MPO enzymatic activity (Papayannopoulos et al., 2010). In a subset of proteins of azurophilic granules (MPO, azurocidin, cathepsin G, eosinophil cationic protein, defensin-1, lysozyme, and lactoferrin) forms a membrane-bound azurophilic granule complex (azurosome) that can be activated by ROS in the form of H_2O_2 (Metzler et al., 2014). Interestingly, it has been shown that NE can localize to the membrane and upon azurosome activation, MPO mediates protein release from intact granules. NE, cathepsin G, and azurocidin release as complex and bind to F-actin. When NE is activated by H_2O_2/MPO, it degrades F-actin and proceeds to the nucleus to help in degradation of chromatin (Metzler et al., 2014). Examples of NETs under low and high magnifications, isolated from murine gallbladder material, demonstrating patrolling neutrophils producing extensive NETs, and being decorated with granules and binding bacteria are shown in Fig. 1. The same figure demonstrates the results of DNA intensity evaluation visualized by ImageJ software using 14-bit images with an ultrasensitive camera. As can be seen, DNA decondensation immediately results in rapid degradation of DNA-specific signal, making NETs so difficult to detect, and making fluorescent microscopy the best approach for their detection. Since many of NETs components are also involved in other neutrophil functions, in the recent NET Consensus meeting, it was agreed upon voting that to prove NETs formation one would need three independent morphological (microscopic) features to be proven: (1) presence of extracellular decondensed DNA; (2)
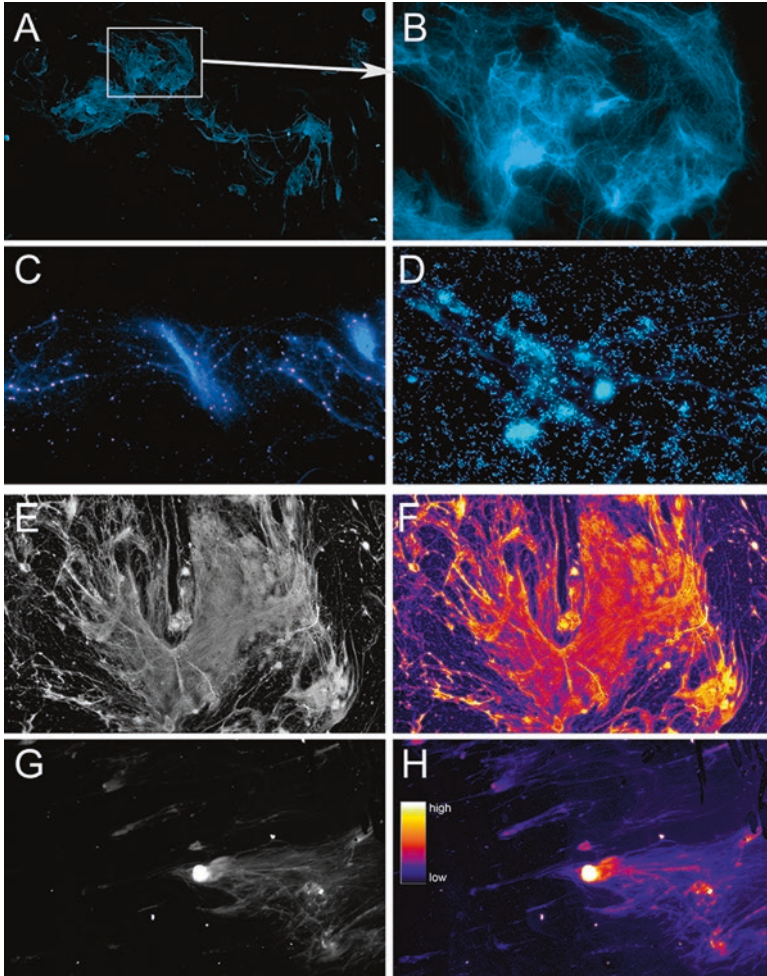
Fig. 1 Neutrophil extracellular traps made by patrolling neutrophils in the gall bladder. (**a**, **b**) Low and high magnification. (**c**) Neutrophilic granules (pink) are decorating NETs. (**d**) NETs bind and immobilize bacterial invasion. (**e**, **g**) Visualization of NETs by the amount of corresponding DNA signal obtained under 14-bit depth imaging and processing (**f**, **h**, correspondingly)

presence of NE or MPO; and (3) presence of citrullinated histone H3—a very specific modification of histone molecule, currently attributable only to NET formation (Boeltz et al., 2019).

Good or Bad? NETs are also capable of isolating exogenic materials like the nanodiamonds (Muñoz et al., 2016), asbestos (Desai et al., 2017), and monosodium urate (Schauer et al., 2014). Since many of them are often encountered as microparticulate matter, we will discuss this interaction in detail in the next paragraphs. They can sequester toxic agents, for example, from certain staphylococci and shield loci

of necrosis, and granulomas (Bilyy et al., 2016). In some cases, NET-born proteases can even diminish a pool of proinflammatory cytokines, promoting inflammation resolution (Reinwald et al., 2017; Schauer et al., 2014) or destruction of the circulating immune complexes.

Passivation of big/foreign/toxic objects is beneficial to the body, but it also provides another challenge to the immune system. When NETs are released on relatively small areas, they are easily removed/cleared by macrophage system, forming a precise balance between NET formation and their silent clearance. Should this clearance be disrupted either due to overproduction of NETs of failure of macrophage system, the body will face a huge amount of oxidized by NET-derived ROS, and thus immunologically "new" epitopes (Podolska et al., 2018). One should remember that the appearance of NETs is often the choice when phagocytosis fails, thus, upon abundant NET formation, there are high chances of inappropriate clearance. The latter will result in the formation of the antibodies to histones, DNA, and cytoplasmic components of neutrophils (ANCA), all being the hallmarks of the autoimmune disorders like SLE and rheumatoid arthritis (Podolska et al., 2018).

At the same time a combination of excessive NETs formation and their subsequent aggregation create another danger of mechanical blocking ducts and vessels. This was true for occluding blood vessels (von Brühl et al., 2012), pancreatic ducts (Leppkes et al., 2016), initiating gallstone formation with bile duct occlusion (Muñoz et al., 2019), and some other implications. Interestingly, neutrophils tend to form extracellular traps at their high concentrations even in the absence of a specific infectious trigger (or the trigger being not currently known). Therefore, uncontrolled or excessive production of NET can lead to an aggravation of inflammation and the development of an autoimmune response, the spread of tumor metastases, and thrombosis (Mitsios et al., 2017). Usually, we have a protective mechanism against clotting, circulating host DNase 1 and DNase 3 (Jiménez-Alcázar et al., 2017) preventing NET formation in the circulation, and failure of both enzyme in genetically modified organisms increase blood occlusion and thrombosis of small vessels (the smallest vessels in our body are in brain and lungs). Recent findings suggest the possibility of NETs involvement in severe malaria, with NETs being a dominant vasculopathy factor (Boeltz et al., 2017). We hypothesize that NETs are also the cause of multiple organ failure usually accompanying SIRS or sepsis, as we have observed many "basophilic," DNA-containing clots in distant, presumably non-affected organs in autopsy samples under multiple organ failure conditions. We hope that recent advances of the pioneers of aggregated NET research (Bilyy et al., 2016; Daniel et al., 2019; Muñoz et al., 2019) will eventually help to treat many conditions, whose clinical cause was not previously understood. Figure 2 summarizes current physiological and pathological NET involvement, with nanoparticle being one important stimulus, which can, in fact, trigger any of the described above consequences with either positive or negative results for the organisms.
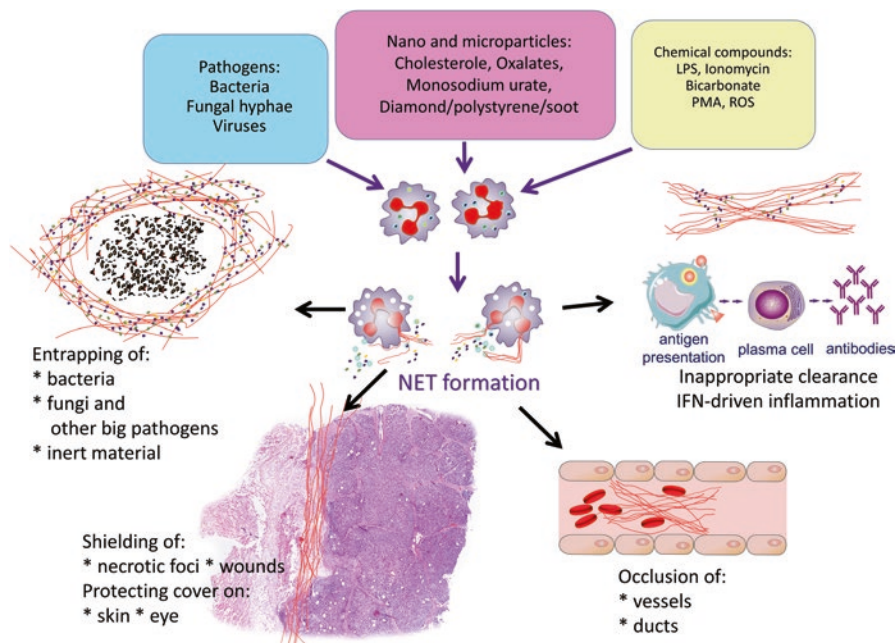
Fig. 2 Presentation of current data about causative agents and consequences of NETs formation. As can be seen, any from the group of three NET inducers can trigger either beneficial or detrimental effect. (Based on data of Podolska et al. (2018))

3   Interaction of Neutrophils and Nano-/Microparticles

There are a variety of nanoparticles of different sizes, chemistry and biocompatibility/degradability. We can imagine that if a bacteria-sized nanoparticle composed of biodegradable material, like polylactic acid, were to encounter the neutrophil, it would be engulfed into phagosome, merged with lysosome, and degraded into smaller bricks; the latter of which would be metabolized. Should the chemistry of nanoparticle be more complicated, the ROS-related machinery can be involved in oxidations. However, it is important to know what will happen if the nanoparticle is of the following nature:

- Made of a single element
- Is chemically resistant
- Is hydrophobic

In this case, one immediately realizes that there is no receptor for engulfment, the ROS machinery will not work, and hydrophobic nature will be incompatible with hydrophilic intercellular content. Indeed, many inert nano- and microparticles were reported to not be cleared by the immune system, thereby triggering regulated

or passive-mechanical cellular death (Agudo-Canalejo & Lipowsky, 2015; Desai et al., 2017; Muñoz et al., 2016).

Nanodiamonds that possess all three above-mentioned features allowed us to establish this mechanical type of interaction causing dangerous immunological consequences (Muñoz et al., 2016). It turned out that the size of hydrophobic nanoparticle is critical. Plasma membrane itself is 6–9 nm thick. Since lipids of plasma membrane are hydrophobic, they will be absorbed in the surface of nanoparticles. Thus, nanoparticles with sizes less than the thickness of plasma membrane (e.g., 3 nm) will be embedded between its bilayers (Fig. 3a), nanoparticles with much bigger sizes (e.g., 50 nm) will interact with the bilayer, making the curvature around the nanoparticles (Fig. 3c), but nanoparticles with sizes comparable to that of plasma membrane will cause bilipid layer curvature with points of sterical conflicts or, simply speaking, just leaking holes in the plasma membrane (Fig. 3b, indicated with arrows). This rough modeling with balls and stick was also confirmed by more precise mathematical calculations (Agudo-Canalejo & Lipowsky, 2015).

If the cell will sense the hole or leakage in the plasma membrane, it will immediately start the recycling machinery to isolate the affected part of plasma membrane and engulf it into endosome (Alberts et al., 2014). This endosome will be later merged with the lysosome, with the formation of secondary lysosome, and recycled; the leakage will be replaced with the intact bilayer. But if the hydrophobic nanoparticle is still in the lipid bilayer, the leakage will not be liquidated. Instead, it will be converted into the lysosomal leakage (Fig. 4) and the lysosomal content will be released into the cytoplasm. To our estimates, the most damaging size of hydrophobic nanoparticles is in the range of 10–40 nm (Muñoz et al., 2016). In fact, cell exposure to the NPs with sharp, protruding Lancet or, otherwise, irregular shapes will cause membrane damage and induce cellular death. For instance, MSU, asbestos, and CaOx can induce cellular death, yet can be significantly bigger than 10 nm (Desai et al., 2017).

To Form NETs or to Die? Till this moment, the interaction of nanoparticles and membrane recycling was governed by universal chemical features and cell structure. The latter response will be different in different cells; actually, we know for sure that neutrophils will produce NETs, while many cancer cells, human blood-derived macrophages, and some others will die. RBC will leak their hemoglobin content. Figure 5 demonstrates micro- and macrovacuoles formed soon after imme-
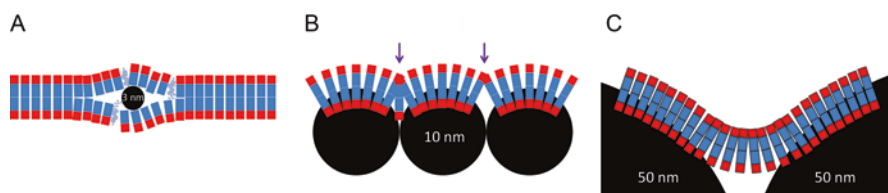
Fig. 3 Interaction of hydrophobic nanoparticles (black) of indicated size with the cell plasma membrane. (**a**) 3 nm; (**b**) 10 nm; (**c**) 50 nm
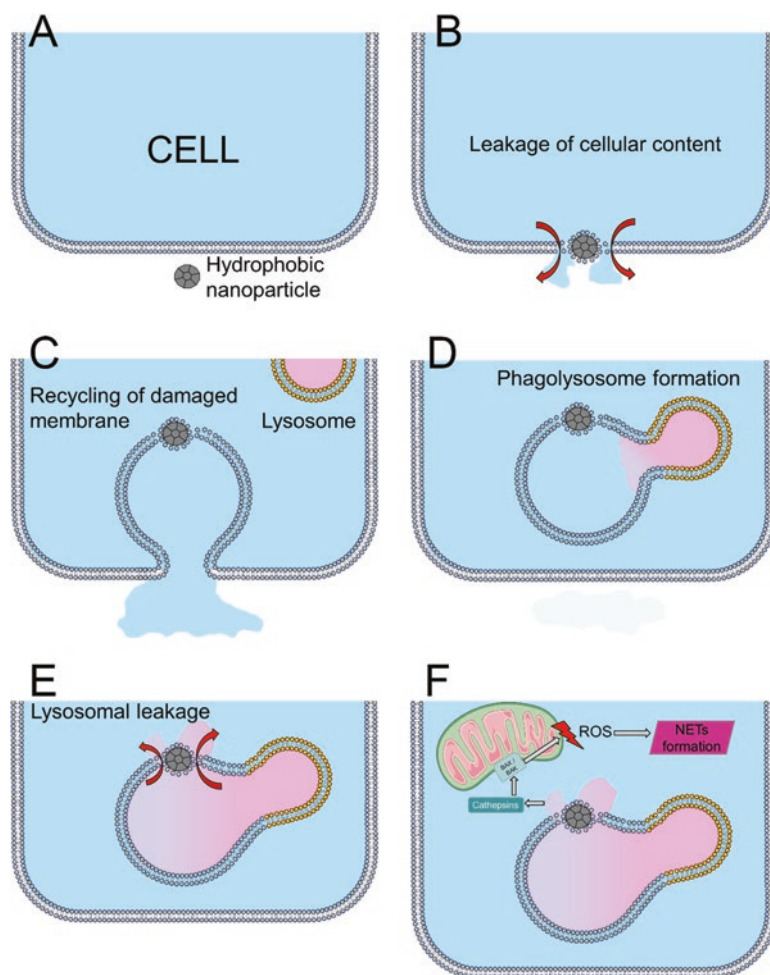
Fig. 4 Interaction of hydrophobic nanoparticles with cell surface leading to cell damage or formation of NETs. A to F indicate the sequence of events upon nanoparticle contacting neutrophil surface. (Based on data of Mulay et al. (2019), Muñoz et al. (2016))

diate contact on neutrophils or HeLa cells upon the contact with nanoparticles. In neutrophils, this will later cause lysosomal leakage and NETs formation, while HeLa cells will lose membrane integrity and die.

Recently, Mulay et al. demonstrated that in acute kidney inflammation (AKI) crystal-induced necroptosis occurs with involving mitochondria permeability transition (Mulay et al., 2019). After the secondary lysosome leaks cathepsins into the cytoplasm, the cell produces ROS. This is paired with a mitochondrial
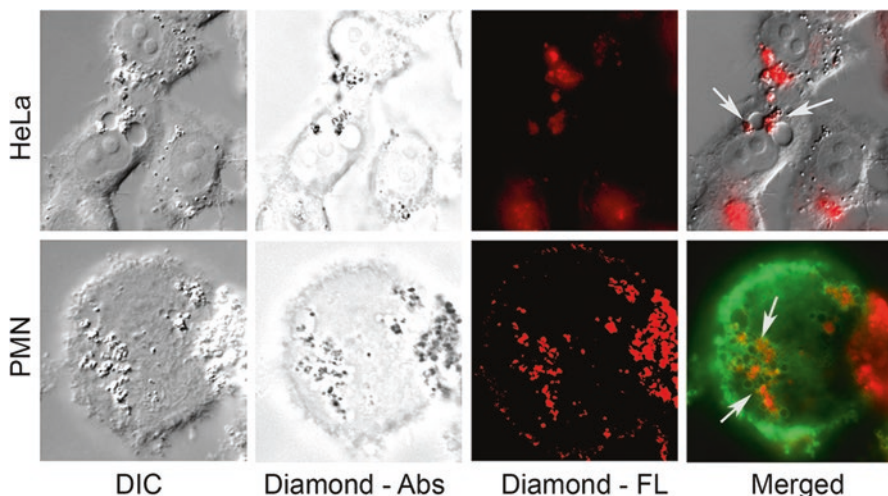
Fig. 5 Formation of micro- and macrovacuoles in PMN and HeLa cells, correspondingly, upon contact with 10 nm nanodiamonds. Nanodiamonds are visualized by absorbance (Abs) and fluorescence (FL)

damage because a mitochondrial swelling, loss of mitochondrial outer membrane potential, and loss of cristae can be detected. Seemingly, it is connected with the formation of MPTP (mitochondria permeability transition pore), which in turn induces even higher ROS production. Moreover, another crucial protein in crystal-induced necroptosis was identified. Peptidylprolyl isomerase F (Pfif) plays an important role in the formation of MPTP. PPIF inhibition can reduce MTPT formation, hence diminishing some of the crystal-induced effects like loss of membrane potential (Mulay et al., 2019). Mitochondria, therefore, is protected from further damage and does not produce more ROS, which would otherwise lead to cellular death.

The released NETs and granular component will attract more neutrophils to the place of nanoparticle contact until their concentration will be enough to form aggregated NETs; the latter will form a shield or envelop around nanoparticles and initially damaged cells, causing local inflammation. As was perfectly shown in the work of Schauer et al. (2014), formation of aggregated NETs will be accompanied by the release of cytokine-degrading proteases (Schauer et al., 2014) as well as enzymes degrading circulating immune complexes (Paryzhak et al., 2018), making the inflammation self-limiting. Indeed, even sterile nanoparticles are causing self-limiting inflammation, as was shown by Biermann et al. (2016). The formed granuloma-like structure will sequester nanomaterial and will stop its spread and damaging action in the body (Fig. 6).

Fig. 6 Sequestration of nanoparticles with NETs during sterile self-limiting inflammation. (Based on the data of Biermann et al. (2016))
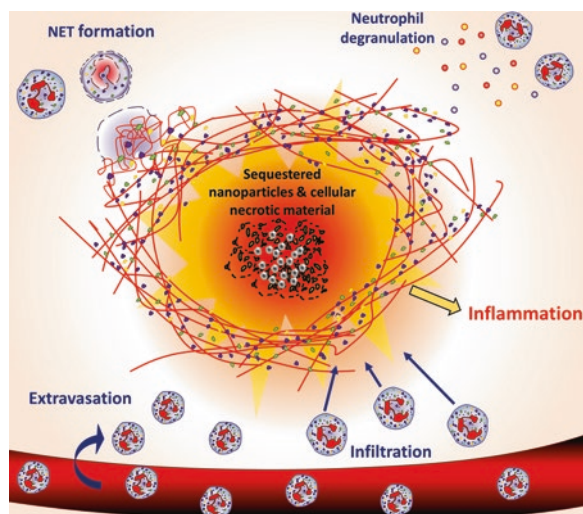
4   Nanoparticles and NETs

Among a plethora of nano- and microparticles, that our body comes in contact with, we can define the following main groups: (1) naturally occurring—those that arise in our body upon normal or pathological metabolic processes: monosodium urate (MSU), cholesterol NP, and oxalates are the best examples. Usually, these are materials which, upon precipitation due to excess formation, form natural nanoparticles/nanocrystals; (2) nanoparticles that we encounter as a result of technological development—for instance, carbon dust, soot, nanodiamonds, asbestos, and silica nanoparticles; (3) those we intentionally put into the body, like aluminum salts in vaccine adjuvants. All the above-mentioned nanoparticles were reported to cause NETs formation and some of their pictures can be seen in Fig. 7.

4.1   MSU

Uric acid is one of the major byproducts of the human catabolism, also being a good antioxidant byproduct of metabolism. The normal concentration range of uric acid (or hydrogen urate ion) in the human blood is 25–80 mg/L for men and 15–60 mg/L for women, while even numbers of 96 mg/L do not cause gout (Tausche et al., 2006); the solubility of uric acid is 60 mg/L at 20 °C. The cellular concentration of uric acid can be even higher, but the intercellular milieu is low in sodium. However, when uric acid binds with sodium, MSU forms with much lower solubility and it tends to precipitate into needle-like crystals (Martillo et al., 2014) initiating gout. The action of MSU is mediated through the uptake of MSU crystals by monocytes and following formation of NALP3 inflammasome with following IL-1B release
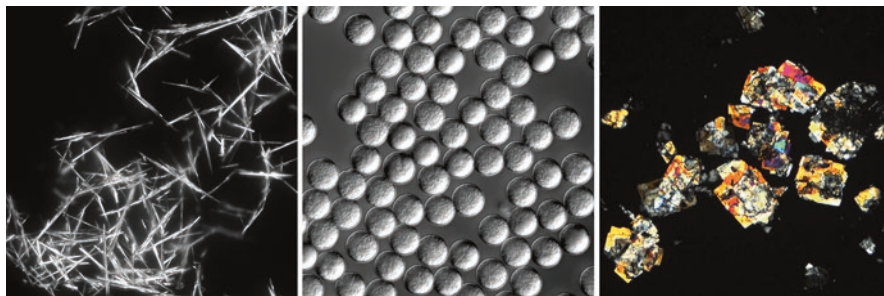
Fig. 7 Nanoparticles of (left to right) MSU, silica microspheres, and cholesterol

(Schorn et al., 2011). IL-1B serves as an alarm and activates neutrophils along with other immune cells. Besides, neutrophils directly ingest MSU crystals starting inflammasome-dependent NET-formation pathway (Mulay et al., 2016; Schett et al., 2015). This eventually envelopes MSU with aggregated NETs and provoking self-limiting inflammation reaction leading to gout attack resolution (should neutrophils be functional and generate enough ROS) (Schauer et al., 2014).

4.2 Cholesterol

Cholesterol crystals, the fist liquid crystals discovered at Lviv University (Ukraine) more than 150 years ago (Bilyy & Lutsyk, 2010), are common crystals in the human body. They can spontaneously and quite naturally appear in the gallbladder and its lumina (Admirand & Small, 1968). On the other hand, neutrophils are extremely common in an organism and patrol it for signs of pathogenicity, with bile duct being one of the hot areas, as it connects vital organs—liver with intestine—full of bacteria (some animals do not have bile duct and release bile directly to the intestine). Hydrophobic cholesterol crystal can cause cellular death (Desai et al., 2017), which makes for a perfect trouble combination. Cholesterol crystals in gallbladder lumina can cause NETosis and consequently lead to lumina occlusion (Muñoz et al., 2019). Moreover, it seems that it is an autocatalytic process—the more NETs you have, the bigger the stone grows, since aggregated NETs are impregnated with calcium and other salts in hypersaturated bile. Our recent finding proves that NETs are initiating gall stone formation (Muñoz et al., 2019). Here, for the first time, we demonstrate how NETs are entrapping cholesterol crystals in animal lithogenic diet model (Fig. 8). DNA in NETs entraps cholesterol nanocrystals (Bila et al., 2019); it serves as a glue and was shown to be present in large amounts on the surface of gallstones. Indeed, the cross-section of gallstones from mice on a fat-rich diet revealed concentrated circles and displayed high neutrophil elastase activity. Elastase activity also seems to be related to the crystal ages, meaning that the younger the crystals, the higher the elastase activity (Muñoz et al., 2019). Active
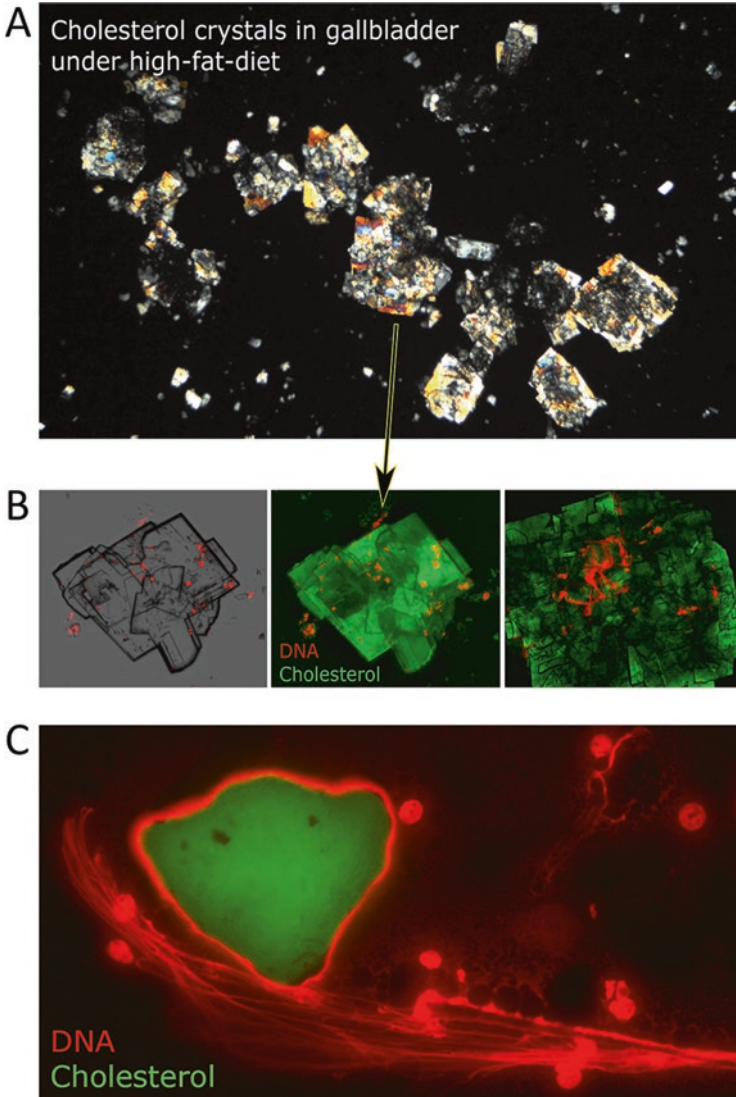
Fig. 8 At a high-fat, high-cholesterol diet, NETs formation is induced by cholesterol nanocrystals isolated from gallbladder material of mice and analyzed by polarization microscopy (**a**). The latter contains DNA material (**b**). High magnification image at (**c**) demonstrated that NETs (red) entrap and later, glue together cholesterol nanocrystals (green)

inhibition of NETs formation significantly reduced the development and growth of gallstones (Muñoz et al., 2019).

4.3   Oxalates

Calcium oxalates, mono- or hydrates, are another type of naturally occurring crystals in the human body. Diets rich in oxalates, vitamin C supplements, and ethylene glycol poisoning can greatly contribute to the CaOx formation and acute kidney injury. CaOx crystals are irregularly shaped and can induce RIPK3- and MLKL-depended necroptosis (Desai et al., 2017). CaOx crystals can also induce NETosis (Muñoz et al., 2016) and contribute to neutrophil associated necroinflammation (Mulay et al., 2019). Recently, Mulay et al. described another type of crystal-mediated necrosis present in tubular epithelial cells (Mulay et al., 2019). Interestingly, CaOx crystals can induce inflammation similarly to MSU's. Secretion of IL-1β can be induced by CaOx via NLRP3 inflammasome and caspase-1- dependent mechanism, which has been shown to play an important role in acute kidney injury (Mulay et al., 2013). Generally, NETs have demonstrated the ability to agglomerate particles during their sequestration. Although there is no direct evidence, it can be suggested that NETs can also promote CaOx development and growth.

4.4   Artificial Nanocrystals

4.4.1   Asbestos, Soot, and Other Air Pollutants

Asbestos and soot (carbon nanoparticles) are common air pollutants and can cause a variety of diseases (Agarwal et al., 2013; Büchner et al., 2013). Recent big fires all around the world caused worsening of symptoms with chronic inflammation, well known to the doctors, and not only lung-related ailments like asthma (Meldrum et al., 2017) but also cardiac disorders (Saber et al., 2013) and brain cells damage (Borisova et al., 2017). Systemic inflammatory effects resulting from soot inhalation were reproduced in animal models (Chu et al., 2019). Song et al. demonstrated that nanoparticles are a contributing factor to pleural effusion, pulmonary fibrosis, and granuloma (Song et al., 2009). Among the responsible nanomaterials polluting the air are also silica microparticles causing silicosis, particles of laser printer's toners, cigarette smoke, and related air-born pollutants, all known to cause lung tissue damage. Asbestos was demonstrated to directly induce NETs (Desai et al., 2017). In other words, lungs are not fond of nanoparticle exposure and incorporate a number of defensive mechanisms. Clearly, due to their inert nature, most of the nanomaterials cannot be degraded by enzymes present in leucocytes (Paryzhak et al., 2019). Dust cells, macrophages in the lungs, got their name due to the accumulation of dust particles inside. However, stimulation of ROS-producing machinery in the lungs is

harmful to this sensitive organ (Niranjan & Thakur, 2017). Elastases from inflammatory and dendritic cells were reported to mediate ultrafine carbon black-induced acute lung destruction in mice (Chang et al., 2011). Particle-induced pulmonary acute phase response correlates with the neutrophil influx and it was reported to link inhaled particles and cardiovascular risk (Saber et al., 2013). Particles can be connected to cardiac vessel obstruction with NETs. In the ongoing project, we evaluate NETs formation in lungs upon soot inhalation. We reported on the appearance of neutrophil elastase around the dark areas of soot deposition found in autopsy lung samples (Bila et al., 2020).

4.4.2   Carbon Derivatives and Nanodiamonds

Carbon derivatives like graphene, nanodiamonds, or carbon blacks are also major contributors to a variety of lung diseases (Niranjan & Thakur, 2017; Paryzhak et al., 2019; Song et al., 2009). They are found in a variety of sizes and shapes and represent a serious threat for an organism, being a byproduct of polishing processes, grinding, etc. We directly demonstrated the ability of nanodiamonds to cause NETs in the lungs (Muñoz et al., 2016). As stated throughout the article, nanodiamonds are potent inducers of cellular death, NETosis, and are usually extremely immunogenic (Muñoz et al., 2016). Nanodiamonds of 10 nm size are among the most dangerous non-polar nanoparticles. As was previously mentioned, they can easily induce cellular death through membrane damage and subsequent lysosome leakage, provoking self-limiting inflammation (Agudo-Canalejo & Lipowsky, 2015; Desai et al., 2017; Muñoz et al., 2016). They are also effective at stimulating NET formation (Muñoz et al., 2016). Surprisingly, graphene was not able to cause NET formation in many tested setups (Paryzhak et al., 2019). This is important since this carbon-based material is now widely applied as a nanoparticle for thermal heating in medicine (Altinbasak et al., 2018; Li et al., 2017; Turcheniuk et al., 2016). Fullerenes C60 were shown to induce membrane leakage (Prylutska et al., 2012) and aggregated NET formation (Paryzhak et al., 2019). Although inflammatory properties are mainly contributed to the necrosis-induction properties of NPs, it is unclear whether NPs can induce reactions similar to those produced by natural crystals. It is also unclear whether artificially derived NPs can adsorb various serum elements like immunoglobulins and complement parts and, therefore, cause an immune response.

4.5   Beneficial Application of Nanoparticle-Induced Immune Response: Aluminum Nanofibers

One of the ways to use the ability of nanoparticles to induce NET formation with subsequent sequestering of nanoparticles and self-limiting nature of inflammation is to apply them in vaccines. Aluminum-based salts (Alum) have been used in

vaccines for almost 90 years mainly in the form of aluminum oxyhydroxide (AlOOH) or aluminum hydroxide (Al(OH)₃) (Baylor et al., 2002; Digne et al., 2002; Vinogradov & Vinogradov, 2014). The adjuvanticity of Al-containing particles depends on their chemical and physical nature (Song et al., 2009). Aluminum can be shaped in a variety of forms and sizes. Modified aluminum oxyhydroxide has been reported to yield significantly better immune response in comparison to traditional Alum (Sun et al., 2013). Aluminum oxide (Al₂O₃) is not usually used as an adjuvant due to its robustness and significantly lower efficacy. Actually, aluminum oxides are effective absorbents of antigen and act as microdepos of antigen for effective immune cell stimulation, including phagocytosis. Only recently, it was directly demonstrated that alum in the vaccine composition causes local formation of NETs. Artificial NPs due to high immunogenicity can serve as highly effective adjuvant for vaccines (Stephen et al., 2017). Knowing the feature of nanoparticles to induce NETs formation, we used synthesized (Lei et al., 2017) ultralong aluminum oxide nanowires, with a thickness of 20–40 nm and length of 20–60μm (~1000 aspect ratio), making them small enough to induce NETs in neutrophils, but too long to be engulfed by macrophages. In the model immunization experiments, aluminum oxide in the form of nanowires provided the immune response, measured in humoral response of antibody titers, which was 32 times higher than that of aluminum oxide in the form of amorphous powder. These nanowires were shown to effectively induce NET-driven, self-limiting inflammation and were proposed as novel adjuvants (Bilyy et al., 2019) as demonstrated in Fig. 9.
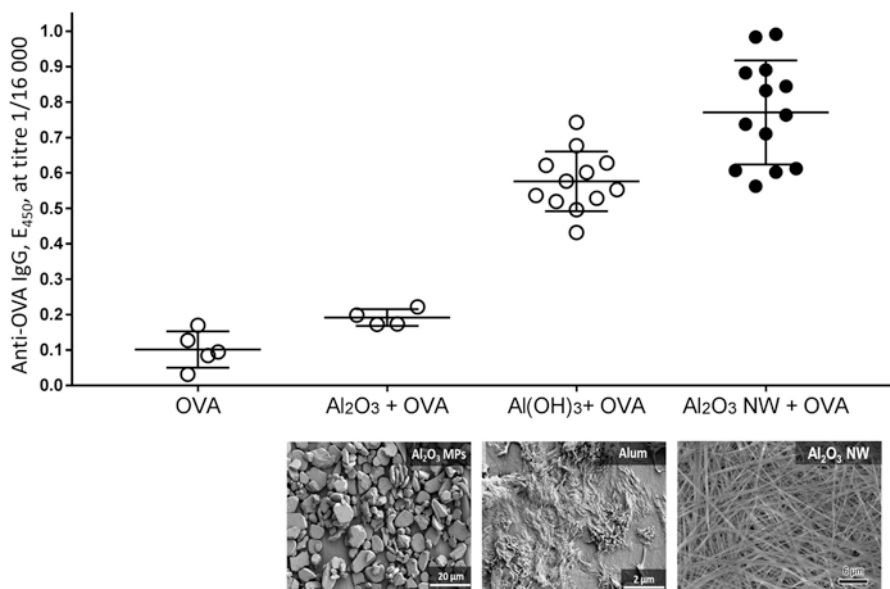
Fig. 9 Humoral response towards ovalbumin (OVA) induced in mice using different aluminum compounds as adjuvants. SEM photos demonstrate the shape of microparticulate objects. (Based on the data of Bilyy et al. (2019))

Thus, just changing the shape of particulate matter is enough to provoke neutrophil for hyperactivation and produce NETs; this ability can be used as a beneficial factor for developing effective vaccine adjuvants.

5   Summary

Neutrophilic granulocytes use the weaponry designed to immobilize and kill bacteria to sequester and isolate harmful micro- and nanoparticles. It is accomplished by NETs formation by neutrophils upon their contact with some nanoparticles. Usually, that provokes inflammation, which can be self-limiting.

References

Admirand, W. H., & Small, D. M. (1968). The physicochemical basis of cholesterol gallstone formation in man. *The Journal of Clinical Investigation, 47*(5), 1043–1052. https://doi.org/10.1172/JCI105794

Agarwal, R., Awasthi, A., Singh, N., Mittal, S. K., & Gupta, P. K. (2013). Epidemiological study on healthy subjects affected by agriculture crop-residue burning episodes and its relation with their pulmonary function tests. *International Journal of Environmental Health Research, 23*(4), 281–295. https://doi.org/10.1080/09603123.2012.733933

Agudo-Canalejo, J., & Lipowsky, R. (2015). Critical particle sizes for the engulfment of nanoparticles by membranes and vesicles with bilayer asymmetry. *ACS Nano, 9*(4), 3704–3720. https://doi.org/10.1021/acsnano.5b01285

Alberts, B., Johnson, A. D., Lewis, J., Morgan, D., Raff, M., Roberts, K., & Walter, P. (2014). *Molecular biology of the cell: Sixth international student edition*. Garland Science, Taylor and Francis Group.

Altinbasak, I., Jijie, R., Barras, A., Golba, B., Sanyal, R., Bouckaert, J., Drider, D., Bilyy, R., Dumych, T., Paryzhak, S., Vovk, V., Boukherroub, R., Sanyal, A., & Szunerits, S. (2018). Reduced graphene-oxide-embedded polymeric nanofiber mats: An "on-demand" photother-

mally triggered antibiotic release platform. *ACS Applied Materials & Interfaces, 10*(48), 41098–41106. https://doi.org/10.1021/acsami.8b14784

Anders, H.-J., Mulay, S. R., Herrmann, M., Bilyy, R., & Gabibov, G. G. (2019). Editorial on the research topic: Nano-and microparticle-induced cell death, inflammation and immune responses. *Frontiers in Immunology, 10*, 844.

Baylor, N. W., Egan, W., & Richman, P. (2002). Aluminum salts in vaccines – US perspective. *Vaccine, 20*(Suppl. 3), 18–23. https://doi.org/10.1016/S0264-410X(02)00166-4

Belaaouaj, A. A., Kim, K. S., & Shapiro, S. D. (2000). Degradation of outer membrane protein A in Escherichia coli killing by neutrophil elastase. *Science, 289*(5482), 1185–1187. https://doi.org/10.1126/science.289.5482.1185

Biermann, M. H. C., Podolska, M. J., Knopf, J., Reinwald, C., Weidner, D., Maueröder, C., Hahn, J., Kienhöfer, D., Barras, A., Boukherroub, R., Szunerits, S., Bilyy, R., Hoffmann, M., Zhao, Y., Schett, G., Herrmann, M., & Munoz, L. E. (2016). Oxidative burst-dependent NETosis is implicated in the resolution of necrosis-associated sterile inflammation. *Frontiers in Immunology, 7*, 557. https://doi.org/10.3389/fimmu.2016.00557

Bila, G., Peshkova, S., Dumych, T., & Bilyy, R. (2019). Natural cholesterol nanocrystals in gall material and their interaction with neutrophilic granulocytes. *PhoBiA Annual Nanophotonics International Conference, 1*, 62.

Bila, G., Peshkova, S., Vovk, V., Borysov, A., Borisova, T., & Bilyy, R. (2020). Soot-derived carbon nanoparticles are encapsulated in the lungs upon inhalation. In S. G. Vari (Ed.), *RECOOP bridges in life science annual conference* (p. 015). RECOOP HST Assosiation.

Bilyy, R., Fedorov, V., Vovk, V., Leppkes, M., Dumych, T., Chopyak, V., Schett, G., & Herrmann, M. (2016). Neutrophil extracellular traps form a barrier between necrotic and viable areas in acute abdominal inflammation. *Frontiers in Immunology, 7*, 424. https://doi.org/10.3389/fimmu.2016.00424

Bilyy, R., & Lutsyk, A. D. (2010). A brief account of Julius Planer's life and research. *Condensed Matter Physics, 13*(3), 37003. https://doi.org/10.5488/cmp.13.37003

Bilyy, R., Paryzhak, S., Turcheniuk, K., Dumych, T., Barras, A., Boukherroub, R., Wang, F., Yushin, G., & Szunerits, S. (2019). Aluminum oxide nanowires as safe and effective adjuvants for next-generation vaccines. *Materials Today, 22*, 58–66. https://doi.org/10.1016/j.mattod.2018.10.034

Boeltz, S., Amini, P., Anders, H. J., Andrade, F., Bilyy, R., Chatfield, S., Cichon, I., Clancy, D. M., Desai, J., Dumych, T., Dwivedi, N., Gordon, R. A., Hahn, J., Hidalgo, A., Hoffmann, M. H., Kaplan, M. J., Knight, J. S., Kolaczkowska, E., Kubes, P., … Herrmann, M. (2019). To NET or not to NET:current opinions and state of the science regarding the formation of neutrophil extracellular traps. *Cell Death and Differentiation, 26*(3), 395–408. https://doi.org/10.1038/s41418-018-0261-x

Boeltz, S., Muñoz, L. E., Fuchs, T. A., & Herrmann, M. (2017). Neutrophil extracellular traps open the Pandora's box in severe malaria. *Frontiers in Immunology, 8*, 2–5. https://doi.org/10.3389/fimmu.2017.00874

Borisova, T., Dekaliuk, M., Pozdnyakova, N., Pastukhov, A., Dudarenko, M., Borysov, A., Vari, S. G., & Demchenko, A. P. (2017). Harmful impact on presynaptic glutamate and GABA transport by carbon dots synthesized from sulfur-containing carbohydrate precursor. *Environmental Science and Pollution Research International, 24*(21), 17688–17700. https://doi.org/10.1007/s11356-017-9414-6

Borregaard, N., & Cowland, J. B. (1997). Granules of the human neutrophilic polymorphonuclear leukocyte. *Blood, 89*(10), 3503–3521. https://doi.org/10.1182/blood.v89.10.3503

Brinkmann, V. (2004). Neutrophil extracellular traps kill bacteria. *Science, 303*(5663), 1532–1535. https://doi.org/10.1126/science.1092385

Brinkmann, V., & Zychlinsky, A. (2012). Neutrophil extracellular traps: Is immunity the second function of chromatin? *Journal of Cell Biology, 198*(5), 773–783. https://doi.org/10.1083/jcb.201203170

Büchner, N., Ale-Agha, N., Jakob, S., Sydlik, U., Kunze, K., Unfried, K., Altschmied, J., & Haendeler, J. (2013). Unhealthy diet and ultrafine carbon black particles induce senescence

and disease associated phenotypic changes. *Experimental Gerontology, 48*(1), 8–16. https://doi.org/10.1016/j.exger.2012.03.017

Chang, C.-C., Chen, C.-Y., Chiu, H.-F., Dai, S.-X., Liu, M.-Y., & Yang, C.-Y. (2011). Elastases from inflammatory and dendritic cells mediate ultrafine carbon black induced acute lung destruction in mice. *Inhalation Toxicology, 23*(10), 616–626. https://doi.org/10.3109/08958378.2011.598965

Chu, C., Zhou, L., Xie, H., Pei, Z., Zhang, M., Wu, M., Zhang, S., Wang, L., Zhao, C., Shi, L., Zhang, N., Niu, Y., Zheng, Y., & Zhang, R. (2019). Pulmonary toxicities from a 90-day chronic inhalation study with carbon black nanoparticles in rats related to the systemical immune effects. *International Journal of Nanomedicine, 14*, 2995–3013. https://doi.org/10.2147/IJN.S198376

Claushuis, T. A. M., van der Donk, L. E. H., Luitse, A. L., van Veen, H. A., van der Wel, N. N., van Vught, L. A., Roelofs, J. J. T. H., de Boer, O. J., Lankelma, J. M., Boon, L., de Vos, A. F., van 't Veer, C., & van der Poll, T. (2018). Role of peptidylarginine deiminase-4 in neutrophil extracellular trap formation and host defense during Klebsiella pneumoniae – Induced pneumonia-derived sepsis. *The Journal of Immunology, 201*(4), 1241–1252. https://doi.org/10.4049/jimmunol.1800314

Dancey, J. T., Deubelbeiss, K. A., Harker, L. A., & Finch, C. A. (1976). Neutrophil kinetics in man. *Journal of Clinical Investigation, 58*(3), 705–715. https://doi.org/10.1172/JCI108517

Daniel, C., Leppkes, M., Muñoz, L. E., Schley, G., Schett, G., & Herrmann, M. (2019). Extracellular DNA traps in inflammation, injury and healing. *Nature Reviews Nephrology, 15*(9), 559–575. https://doi.org/10.1038/s41581-019-0163-2

Desai, J., Foresto-Neto, O., Honarpisheh, M., Steiger, S., Nakazawa, D., Popper, B., Buhl, E. M., Boor, P., Mulay, S. R., & Anders, H. J. (2017). Particles of different sizes and shapes induce neutrophil necroptosis followed by the release of neutrophil extracellular trap-like chromatin. *Scientific Reports, 7*(1), 1–10. https://doi.org/10.1038/s41598-017-15106-0

Digne, M., Sautet, P., Raybaud, P., Toulhoat, H., & Artacho, E. (2002). Structure and stability of aluminum hydroxides: A theoretical study. *The Journal of Physical Chemistry B, 106*(20), 5155–5162. https://doi.org/10.1021/jp014182a

Douda, D. N., Khan, M. A., Grasemann, H., & Palaniyar, N. (2015). SK3 channel and mitochondrial ROS mediate NADPH oxidase-independent NETosis induced by calcium influx. *PNAS, 112*(9), 2817–2822. https://doi.org/10.1073/pnas.1414055112

Jiménez-Alcázar, M., Rangaswamy, C., Panda, R., Bitterling, J., Simsek, Y. J., Long, A. T., Bilyy, R., Krenn, V., Renné, C., Renné, T., Kluge, S., Panzer, U., Mizuta, R., Mannherz, H. G., Kitamura, D., Herrmann, M., Napirei, M., & Fuchs, T. A. (2017). Host DNases prevent vascular occlusion by neutrophil extracellular traps. *Science, 358*(6367), 1202–1206. https://doi.org/10.1126/science.aam8897

Kenny, E. F., Herzig, A., Krüger, R., Muth, A., Mondal, S., Thompson, P. R., Brinkmann, V., von Bernuth, H., & Zychlinsky, A. (2017). Diverse stimuli engage different neutrophil extracellular trap pathways. *eLife, 6*, 1–21. https://doi.org/10.7554/eLife.24437

Lei, D., Benson, J., Magasinski, A., Berdichevsky, G., & Yushin, G. (2017). Transformation of bulk alloys to oxide nanowires. *Science (New York, N.Y.), 355*(6322), 267–271. https://doi.org/10.1126/science.aal2239

Leppkes, M., Maueröder, C., Hirth, S., Nowecki, S., Günther, C., Billmeier, U., Paulus, S., Biermann, M., Munoz, L. E., Hoffmann, M., Wildner, D., Croxford, A. L., Waisman, A., Mowen, K., Jenne, D. E., Krenn, V., Mayerle, J., Lerch, M. M., Schett, G., … Becker, C. (2016). Externalized decondensed neutrophil chromatin occludes pancreatic ducts and drives pancreatitis. *Nature Communications, 7*(1), 10973. https://doi.org/10.1038/ncomms10973

Li, C., Ye, R., Bouckaert, J., Zurutuza, A., Drider, D., Dumych, T., Paryzhak, S., Vovk, V., Bilyy, R. O., Melinte, S., Li, M., Boukherroub, R., & Szunerits, S. (2017). Flexible nanoholey patches for antibiotic-free treatments of skin infections. *ACS Applied Materials & Interfaces, 9*(42), 36665–36674. https://doi.org/10.1021/acsami.7b12949

Li, P., Li, M., Lindberg, M. R., Kennett, M. J., Xiong, N., & Wang, Y. (2010). PAD4 is essential for antibacterial innate immunity mediated by neutrophil extracellular traps. *Journal of Experimental Medicine, 207*(9), 1853–1862. https://doi.org/10.1084/jem.20100239

Martillo, M. A., Nazzal, L., & Crittenden, D. B. (2014). The crystallization of monosodium urate. *Current Rheumatology Reports, 16*(2), 400. https://doi.org/10.1007/s11926-013-0400-9

Meldrum, K., Guo, C., Marczylo, E. L., Gant, T. W., Smith, R., & Leonard, M. O. (2017). Mechanistic insight into the impact of nanomaterials on asthma and allergic airway disease. *Particle and Fibre Toxicology, 14*(1), 1–35. https://doi.org/10.1186/s12989-017-0228-y

Metzler, K. D., Goosmann, C., Lubojemska, A., Zychlinsky, A., & Papayannopoulos, V. (2014). Myeloperoxidase-containing complex regulates neutrophil elastase release and actin dynamics during NETosis. *Cell Reports, 8*(3), 883–896. https://doi.org/10.1016/j.celrep.2014.06.044

Mitsios, A., Arampatzioglou, A., Arelaki, S., Mitroulis, I., & Ritis, K. (2017). NETopathies? Unraveling the dark side of old diseases through neutrophils. *Frontiers in Immunology, 7*, 1–13. https://doi.org/10.3389/fimmu.2016.00678

Mulay, S. R., Desai, J., Kumar, S. V., Eberhard, J. N., Thomasova, D., Romoli, S., Grigorescu, M., Kulkarni, O. P., Popper, B., Vielhauer, V., Zuchtriegel, G., Reichel, C., Brasen, J. H., Romagnani, P., Bilyy, R., Munoz, L. E., Herrmann, M., Liapis, H., Krautwald, S., … Anders, H.-J. (2016). Cytotoxicity of crystals involves RIPK3-MLKL-mediated necroptosis. *Nature Communications, 7*, 10274. https://doi.org/10.1038/ncomms10274

Mulay, S. R., Honarpisheh, M. M., Foresto-Neto, O., Shi, C., Desai, J., Zhao, Z. B., Marschner, J. A., Popper, B., Buhl, E. M., Boor, P., Linkermann, A., Liapis, H., Bilyy, R., Herrmann, M., Romagnani, P., Belevich, I., Jokitalo, E., Becker, J. U., & Anders, H.-J. (2019). Mitochondria permeability transition versus necroptosis in oxalate-induced AKI. *Journal of the American Society of Nephrology, 30*(10), 1857–1869. https://doi.org/10.1681/ASN.2018121218

Mulay, S. R., Kulkarni, O. P., Rupanagudi, K. V., Migliorini, A., Darisipudi, M. N., Vilaysane, A., Muruve, D., Shi, Y., Munro, F., Liapis, H., & Anders, H. J. (2013). Calcium oxalate crystals induce renal inflammation by NLRP3-mediated IL-1β secretion. *Journal of Clinical Investigation, 123*(1), 236–246. https://doi.org/10.1172/JCI63679

Muñoz, L. E., Bilyy, R., Biermann, M. H. C., Kienhöfer, D., Maueröder, C., Hahn, J., Brauner, J. M., Weidner, D., Chen, J., Scharin-Mehlmann, M., Janko, C., Friedrich, R. P., Mielenz, D., Dumych, T., Lootsik, M. D., Schauer, C., Schett, G., Hoffmann, M., Zhao, Y., & Herrmann, M. (2016). Nanoparticles size-dependently initiate self-limiting NETosis-driven inflammation. *PNAS, 113*(40), E5856–E5865. https://doi.org/10.1073/pnas.1602230113

Muñoz, L. E., Boeltz, S., Bilyy, R., Schauer, C., Mahajan, A., Widulin, N., Grüneboom, A., Herrmann, I., Boada, E., Rauh, M., Krenn, V., Biermann, M. H. C., Podolska, M. J., Hahn, J., Knopf, J., Maueröder, C., Paryzhak, S., Dumych, T., Zhao, Y., … Herrmann, M. (2019). Neutrophil extracellular traps initiate gallstone formation. *Immunity, 51*(3), 443–450. https://doi.org/10.1016/j.immuni.2019.07.002

Niranjan, R., & Thakur, A. K. (2017). The toxicological mechanisms of environmental soot (black carbon) and carbon black: Focus on oxidative stress and inflammatory pathways. *Frontiers in Immunology, 8*, 1–20. https://doi.org/10.3389/fimmu.2017.00763

Papayannopoulos, V., Metzler, K. D., Hakkim, A., & Zychlinsky, A. (2010). Neutrophil elastase and myeloperoxidase regulate the formation of neutrophil extracellular traps. *Journal of Cell Biology, 191*(3), 677–691. https://doi.org/10.1083/jcb.201006052

Parker, H., & Winterbourn, C. C. (2012). Reactive oxidants and myeloperoxidase and their involvement in neutrophil extracellular traps. *Frontiers in Immunology, 3*, 1–6. https://doi.org/10.3389/fimmu.2012.00424

Paryzhak, S., Dumych, T., Mahorivska, I., Boichuk, M., Bila, G., Peshkova, S., Nehrych, T., & Bilyy, R. (2018). Neutrophil-released enzymes can influence composition of circulating immune complexes in multiple sclerosis. *Autoimmunity, 51*(6), 297–303. https://doi.org/10.1080/08916934.2018.1514390

Paryzhak, S., Dumych, T. I., Peshkova, S. M., Bila, E. E., Lutsyk, A. D., Barras, A., Boukherroub, R., Szunerits, S., & Bilyy, R. O. (2019). Interaction of 4 allotropic modifications of carbon

nanoparticles with living tissues. *Ukrainian Biochemical Journal, 91*(2), 41–50. https://doi.org/10.15407/UBJ91.02.041

Podolska, M. J., Mahajan, A., Knopf, J., Hahn, J., Boeltz, S., Munoz, L., Bilyy, R., & Herrmann, M. (2018). Autoimmune, rheumatic, chronic inflammatory diseases: Neutrophil extracellular traps on parade. *Autoimmunity, 51*(6), 281–287. https://doi.org/10.1080/08916934.2018.1519804

Prylutska, S., Bilyy, R., Overchuk, M., Bychko, A., Andreichenko, K., Stoika, R., Rybalchenko, V., Prylutskyy, Y., Tsierkezos, N. G., & Ritter, U. (2012). Water-soluble pristine fullerenes C60 increase the specific conductivity and capacity of lipid model membrane and form the channels in cellular plasma membrane. *Journal of Biomedical Nanotechnology, 8*(3), 522–527. https://doi.org/10.1166/jbn.2012.1404

Reinwald, C., Schauer, C., Csepregi, J. Z., Kienhöfer, D., Weidner, D., Malissen, M., Mocsai, A., Schett, G., Herrmann, M., & Hoffmann, M. (2017). Erratum: Reply to "Neutrophils are not required for resolution of acute gouty arthritis in mice". *Nature Medicine, 23*(4), 526–526. https://doi.org/10.1038/nm0417-526b

Saber, A. T., Lamson, J. S., Jacobsen, N. R., Ravn-Haren, G., Hougaard, K. S., Nyendi, A. N., Wahlberg, P., Madsen, A. M., Jackson, P., Wallin, H., & Vogel, U. (2013). Particle-induced pulmonary acute phase response correlates with neutrophil influx linking inhaled particles and cardiovascular risk. *PLoS One, 8*(7), e69020. https://doi.org/10.1371/journal.pone.0069020

Schauer, C., Janko, C., Munoz, L. E., Zhao, Y., Kienhöfer, D., Frey, B., Lell, M., Manger, B., Rech, J., Naschberger, E., Holmdahl, R., Krenn, V., Harrer, T., Jeremic, I., Bilyy, R., Schett, G., Hoffmann, M., & Herrmann, M. (2014). Aggregated neutrophil extracellular traps limit inflammation by degrading cytokines and chemokines. *Nature Medicine, 20*(5), 511–517. https://doi.org/10.1038/nm.3547

Schett, G., Schauer, C., Hoffmann, M., & Herrmann, M. (2015). Why does the gout attack stop? A roadmap for the immune pathogenesis of gout. *RMD Open, 1*(1), e000046. https://doi.org/10.1136/rmdopen-2015-000046

Schorn, C., Frey, B., Lauber, K., Janko, C., Strysio, M., Keppeler, H., Gaipl, U. S., Voll, R. E., Springer, E., Munoz, L. E., Schett, G., & Herrmann, M. (2011). Sodium overload and water influx activate the NALP3 inflammasome. *Journal of Biological Chemistry, 286*(1), 35–41. https://doi.org/10.1074/jbc.M110.139048

Silvestre-Roig, C., Hidalgo, A., & Soehnlein, O. (2016). Neutrophil heterogeneity: Implications for homeostasis and pathogenesis. *Blood, 127*(18), 2173–2181. https://doi.org/10.1182/blood-2016-01-688887

Song, Y., Li, X., & Du, X. (2009). Exposure to nanoparticles is related to pleural effusion, pulmonary fibrosis and granuloma. *European Respiratory Journal, 34*(3), 559–567. https://doi.org/10.1183/09031936.00178308

Stephen, J., Scales, H. E., Benson, R. A., Erben, D., Garside, P., & Brewer, J. M. (2017). Neutrophil swarming and extracellular trap formation play a significant role in Alum adjuvant activity. *NPJ Vaccines, 2*(1), 1. https://doi.org/10.1038/s41541-016-0001-5

Sun, B., Ji, Z., Liao, Y.-P., Wang, M., Wang, X., Dong, J., Chang, C. H., Li, R., Zhang, H., Nel, A. E., & Xia, T. (2013). Engineering an effective immune adjuvant by designed control of shape and crystallinity of aluminum oxyhydroxide nanoparticles. *ACS Nano, 7*(12), 10834–10849. https://doi.org/10.1021/nn404211j

Takei, H., Araki, A., Watanabe, H., Ichinose, A., & Sendo, F. (1996). Rapid killing of human neutrophils by the potent activator phorbol 12-myristate 13-acetate (PMA) accompanied by changes different from typical apoptosis or necrosis. *Journal of Leukocyte Biology, 59*(2), 229–240.

Tausche, A. K., Unger, S., Richter, K., Wunderlich, C., Grässler, J., Roch, B., & Schröder, H. E. (2006). Hyperuricemia and gout: Diagnosis and therapy. *Der Internist, 47*(5), 509–520; quiz 521. https://doi.org/10.1007/s00108-006-1578-y

Turcheniuk, K., Dumych, T., Bilyy, R., Turcheniuk, V., Bouckaert, J., Vovk, V., Chopyak, V., Zaitsev, V., Mariot, P., Prevarskaya, N., Boukherroub, R., & Szunerits, S. (2016). Plasmonic

photothermal cancer therapy with gold nanorods/reduced graphene oxide core/shell nanocomposites. *RSC Advances, 6*(2), 1600–1610. https://doi.org/10.1039/C5RA24662H

Vinogradov, A. V., & Vinogradov, V. V. (2014). Low-temperature sol-gel synthesis of crystalline materials. *RSC Advances, 4*(86), 45903–45919. https://doi.org/10.1039/c4ra04454a

von Brühl, M.-L., Stark, K., Steinhart, A., Chandraratne, S., Konrad, I., Lorenz, M., Khandoga, A., Tirniceriu, A., Coletti, R., Köllnberger, M., Byrne, R. A., Laitinen, I., Walch, A., Brill, A., Pfeiler, S., Manukyan, D., Braun, S., Lange, P., Riegger, J., … Massberg, S. (2012). Monocytes, neutrophils, and platelets cooperate to initiate and propagate venous thrombosis in mice in vivo. *The Journal of Experimental Medicine, 209*(4), 819–835. https://doi.org/10.1084/jem.20112322

Wang, Y., Li, M., Stadler, S., Correll, S., Li, P., Wang, D., Hayama, R., Leonelli, L., Han, H., Grigoryev, S. A., Allis, C. D., & Coonrod, S. A. (2009). Histone hypercitrullination mediates chromatin decondensation and neutrophil extracellular trap formation. *Journal of Cell Biology, 184*(2), 205–213. https://doi.org/10.1083/jcb.200806072

Winterbourn, C. C., & Kettle, A. J. (2013). Redox reactions and microbial killing in the neutrophil phagosome. *Antioxidants and Redox Signaling, 18*(6), 642–660. https://doi.org/10.1089/ars.2012.4827

Yipp, B. G., & Kubes, P. (2013). NETosis: How vital is it? *Blood, 122*(16), 2784–2794. https://doi.org/10.1182/blood-2013-04-457671

Yousefi, S., Mihalache, C., Kozlowski, E., Schmid, I., & Simon, H. U. (2009). Viable neutrophils release mitochondrial DNA to form neutrophil extracellular traps. *Cell Death and Differentiation, 16*(11), 1438–1444. https://doi.org/10.1038/cdd.2009.96

Basic Principles of Nanotoxicology

Rostyslav S. Stoika

Abbreviations

ALT	Alanine aminotransferase
AST	Aspartate aminotransferase
AST/ALT	De Ritis coefficient
BBB	Blood-brain barrier
BTB	Blood-tumor barrier
CPP	Cell-penetrating peptide
DMAEM	2-(Dimethylamino)ethyl methacrylate
DNA	Deoxyribonucleic acid
D-Pt	D-pantethine
ED50	Half-maximal effective dose
EGF-R	Epidermal growth factor receptor
EPR	Enhanced Permeability and Retention
EROD	Microsomal 7-ethoxyresorufin O-deethylase
FDA	Food and Drug Administration
FITC	Fluorescein isothiocyanate
HER-2	Human epidermal growth factor receptor 2
LDH	Lactate dehydrogenase
MDR	Multiple drug resistance
Me-NC	Metal-containing nanocomposite
miRNA	Micro ribonucleic acid
MPS	Mononuclear phagocytic system
mRNA	Messenger ribonucleic acid
MRP	Multidrug resistance associated protein
MTs	Metallothioneins
NA	Nuclear abnormalities
NC	Nanocomposite
p53KO	Knock-out in p53 gene
PARP	Poly (ADP-ribose) polymerase
PD	Pharmacodynamics

R. S. Stoika (✉)
Institute of Cell Biology, NAS of Ukraine, Lviv, Ukraine

PEG   Polyethylene glycol
Pgp   P-glycoprotein
PK   Pharmacokinetics
poly(VEP-GMA)-graft-PEG   Synthetic polymer
RECOOP HST   Regional Cooperation in the Fields of Health,
                                 Science and Technology
ROS   Reactive oxygen species
SeMet   Selenomethionine
Sna   Snail, zinc-finger transcription factor
TD50   Half-maximal toxic dose
TNF   Tumor necrosis factor
Vtg-LP   Vitellogenin-like proteins

1 Introduction

The development of novel nanomaterials and nanotechnologies for industry, agri-culture, and medicine is rapidly growing; however, besides many benefits, their use is also accompanied by considerable risks. The interaction of nanomaterials with other potential toxicants can either enhance or reduce health risks and also influence the adverse environmental effects caused by nanomaterials' pollution. Nanotoxicology is the multidisciplinary field of toxicology that is focused on defin-ing the hazards of nanomaterials (<100 nm in at least one dimension) to human organism or environment. The nanoscale and quantum size effects, as well as large ratio of surface area to volume of these materials, may lead to biological effects which differ from such effects that are induced by their large parts (Haynes & Pedersen, 2020).

Of course, one cannot simply state that all nanomaterials necessarily elicit new specific toxicities because they are of the nano-scale size (Donaldson & Poland, 2013). However, with respect to nanomedicine, much evidence exists that the nano-materials function as a "double-edged sword" with both negative and positive effects. The nanomaterials are used as carriers of drugs and such delivery often enhances the toxicity of drugs toward the pathological (e.g., tumor) cells in vitro due to an improved water solubility, increased uptake, and higher stability, circum-venting multidrug resistance of target cells and other mechanisms (Senkiv et al., 2014; Heffeter et al., 2014). When applied to experimental animals and at treatment of patients, the anticancer drugs trigger general toxicity (Kobylinska et al., 2014, 2015, 2016, 2018; Walker, 2006), while the immobilization of these medicines with the nanomaterials may decrease the toxicity, probably due to the improved charac-teristics of the medicines and more addressed action in the organism.

Nanotoxicology can be defined as the multidisciplinary branch of toxicology focused on answering the question, "Why do nanomaterials create more hazard to human and environment?" It is known that their small size and large ratio of surface

area to volume may result in the unique biological effects. As a new branch of the biological science, it has its own journal, "*Nanotoxicology*," which is an international journal of Q1 Quartile with an impact factor 6.310, updated in 2020, and current volume number 14.

There are several monographs published with the term, "Nanotoxicology," in their titles (Hobson & Guy, 2014; van der Merwe & Pickrell, 2018; Kumar et al., 2018; Simón-Vázquez et al., 2012). Finally, there are scientific institutions whose research activity is focused on the problems of nanotoxicology (e.g., Center for Nanotechnology and Nanotoxicology at Harvard T.H. Chan School of Public Health, with a principal office located at: 90 Smith Street Fourth Floor, Boston, MA 02120, USA).

In this chapter, we address the basic principles of nanotoxicology, as well as problems and perspectives of this novel branch of toxicology. It should be stressed that the role of nanotoxicology is rapidly growing due to the development of novel nanomaterials and nanotechnologies that are used in industry and human life.

2 Impact of Physico-chemical Properties of Nanomaterials on Their Toxicity

It is known that "classic" medicines consist of a drug substance to which a certain filler substance is added. Mostly, the filler is inert and non-toxic, but completely unnecessary to provide a therapeutic effect. This filler is used because many drugs are applied in mini (micro) amounts, which is inconvenient to administer them to the patient. In new generations of drugs, the active drug substance is combined non-covalently with a "smart" delivery platform (carrier). Most often, certain nanoparticles perform the role of such platform. Due to the inclusion of special vector molecules in the carrier (e.g., specific monoclonal antibodies to certain antigens on the surface of target cells), the nanocomplex acquires the ability to "recognize" specific pathological cells.

Thus, "smart" (also called "intelligent") drugs are a kind of molecular nano-robots that contain a drug substance and transport it in the patient's body. At the same time, they protect the drug from its uncontrolled release and destruction, as well as "recognize" certain biological targets in the body. These properties allow "smart" drugs to influence on certain molecular targets in the body and, if necessary, monitor the action of the drug substance in vivo. Such monitoring is achieved by the incorporation of the bio-compatible label (usually fluorescent or luminescent dye) in the carrier molecule. In addition, "smart" nanomaterials often possess an ability to change their size, shape, color or other characteristics in response to certain extreme factors, such as temperature, pH, pressure, radiation, ultraviolet, ultrasound, humidity, specific chemicals, and mechanical action among others.

"Smart" nanocarriers (nanoplatforms) are classified according to various characteristics, such as size, morphology, and chemical nature. Taking into account the

morphologic characteristics, "smart" nanomaterials used in biology and medicine are divided into: (1) nanoparticles (nano-spheres); (2) surfaces covered with nano-materials ("envelope," film, biosensor); (3) micelles. The size of particles might be of "nano" or "micro" scale. The first (1–100 nm) are used mainly for delivery of drugs or genetic materials (plasmid DNA or mi-RNA), as well as in cell biotesting, for example, estimation of the phagocytic activity. While the larger particles whose diameters are >1–2μm are typically used to recognize and bind cells (diagnostics), as well as for isolating them from cell mixtures (research and cell engineering). It should be noted that the diameter of typical animal cells is >10μm.

Characterizing factors that influence the toxicity of nanomaterials, it is reasonable to mention the effect of stimulation of permeability and retention of particles (Enhanced Permeability and Retention, EPR) (Nakamura et al., 2015). This physical phenomenon can explain why the nanoparticles are selectively accumulated in tumor tissue, while drug molecules (<500 Da) are not concentrated there. As established, when small molecules (e.g., drugs) begin to reach the central part of tumor, their removal (clearance) is already taking place on its periphery. Due to the EPR effect, the larger nanoparticles gradually accumulate in the tumor and their concentration there continues to increase even after 24 h from the onset of their application.

The main characteristics which determine the behavior of nanoparticles in the living systems (cells) are as follows:

- Size and morphology (important for particle clearance in the body)
- The core (determines the biodegradability of particles)
- The shell (important for ensuring the biocompatibility of particles)
- Active groups on the surface (necessary for the bio-functionalization of particles)
- Bio-functionalization (provides a possibility of particle's recognition by specific cells and targeted action of particles in the body)
- Presence of a label (optional property that is important for detecting particles and monitoring their behavior in the body—bio-imaging)

The behavior (including the toxicity) of the aggregates of nanomaterials often differs from such behavior of the nanomaterials of their primary size. In the environment, due to physical, chemical, and biological transformations, the nanomaterials may change their properties, such as the reactivity, biological activities (e.g., toxicity), and bioavailability (Tong, 2018). Thus, a possibility of the environmental transformations should be taken into account when predicting the toxicity and other features of the nanomaterials.

The core part of nanoparticles used in biology and medicine consists of the following: (1) organic polymers, for example, synthetic polystyrene and polyacrylate materials, polymers of natural compounds such as malate, lactate and others (chitosan), linear and branched oligoelectrolyte surfactant polymers, and other natural compounds (phospholipid liposomes); (2) mineral substances, for example, nanoparticles based on SiO_2, iron oxides (Fe_3O_4, Fe_2O_3), as well as metals such as Au, Ag, Pd, Cu, Zn, Ni, Co, others, and oxides of other metals (TiO_2, Zr_2O_3). Mineral nanoparticles are used not only for drug delivery, but also as a diagnostic tool or for research purposes, such as biomedical imaging.

The polymers used for biomedical application can be of linear or dendrimeric morphology. Polycefin is an example of a linear polymer used for drug delivery (b-poly-(L-malic acid)) (Fujita et al., 2007; Ljubimova et al., 2008), while the polymer described by Kanika Madaan et al. (2014) is an example of nanocarrier of the dendrimeric structure that is also used for drug delivery purpose. Both of these polymers satisfy the requirements mentioned in the above list of characteristics of nanomaterials used for drug delivery.

As an example of the comb-like polymeric (formally dendrimeric) nanocarrier for drug delivery use could be a co-polymer of the unsaturated peroxide of 2-tret-butylperoxy-2-methyl-5-hexen-3-in (VEP, l) and glycidyl metacrylate (GMA, m) and polyethylene glycole (PEG, n) side chains (mol. mass = 245,000 g/mol, $D = 61$ nm). This nanocarrier considerably improves the delivery of doxorubicin and other compounds to mammalian cells (Riabtseva et al., 2012; Senkiv et al., 2014). In more detail, this polymeric system is described in Chap. 2 of our monograph.

Size and chemical composition are two features that are the most important for the toxicity of nanoparticles. Usually, a reduction in size of nanoparticles leads to an increase in their surface area and more molecules of various chemical substances may attach to this surface, thus, enhancing its reactivity and increasing its potential toxic effects (Ai et al., 2011; Suh et al., 2009). After absorption by the mucus, nanoparticles migrate through the blood stream and are spread in the tissues. Nearly 33% of 50 nm, 26% of 100 nm, and 10% of 500 nm particles were discovered in the mucosal and lymphatic tissues of the intestine (Ai et al., 2011).

It was concluded that the smaller nanoparticles (<100 nm) are absorbed by the intestinal cells better than the larger nanoparticles (>300 nm), and cells of the lymphatic tissue absorb the nanoparticles of <100 nm size better than cells of the intestine tissue. The nanoparticles of >400 nm size cannot penetrate into the intestinal cells and the circulatory system (Suh et al., 2009). Due to small size, the nanoparticles get a bigger surface to volume ratio and thus, more molecules of these compounds are present on cell surface that might explain why the smaller nanoparticles possess higher toxicity than the larger ones, even of the same chemical composition. This was confirmed by the results of study of carbon and titanium oxide particles of different sizes showing that a reduction in their sizes was accompanied by the increased toxicity in the lungs (Ai et al., 2011).

Water solubility is a critical feature for many medicines, especially the anticancer ones, since they are soluble only in the organic solvents (e.g., dimethyl sulfoxide or alcohol) that surely are not biocompatible. More than 40% of newly developed medicines and approximately 90% of medicines under development are poorly soluble or insoluble in water (Savjani et al., 2012; Loftsson & Brewster, 2010). Thus, the enhancement of drug solubility and bioavailability (permeability) is a very important challenge in the development of pharmaceutical formulations. The application of water insoluble medicines requires the use of specific approaches. Below, we will focus in more detail, on the encapsulation of medicines into the amphiphilic surface-active nanomaterials, particularly, of the polymeric nature, which could be a perspective approach.

3 Impact of Surface Characteristics of Nanomaterials on Their Toxicity

The shell of nanoparticles serves to improve their stability and biocompatibility. A specific coating on the surface of the particles can be created by different substances, such as vinyl-pyrrolidone, vinyl alcohol, oxyethylated, and fluorinated copolymers and their complexes with various biopolymers, for example, with blood serum albumin. Besides, some bio-surfactants of the microbial origin and other substances can be used for this purpose. Immobilization of certain materials on the surface of the particles is called opsonization. It has been shown that opsonization of latex nanoparticles with the lectin (concanavalin A) and, in particular, proteins of blood serum improve the recognition and absorption of these particles by the phagocytic blood cells (our observation). Immobilization of antibody molecules on the surface of microparticles also provides their stabilization and protects them from destruction by various agents.

The activation of chemical groups on the surface of nanoparticles is also necessary for their bio-functionalization. This activation occurs through reactive groups (hydroxyl, carboxyl, amino, aldehyde or epoxy) introduced into the linear chain of the polymer or its branches (Ljubimova et al., 2008; Torchilin, 2014).

The biocompatibility of nanomaterials is mainly determined by: (a) unimodality of nanoparticle sizes; (b) number, distribution, and composition of active groups on the surface of nanoparticles; (c) opsonization of the surface of the particles by the biocompatible macromolecules. Chemistry of nanoparticles' surface and their capability to induce the oxidative stress, as well as the crystallinity and longevity, are also important characteristics that determine their toxicity and switching on the inflammation in the respiratory system (Zhang et al., 1998). The biocompatibility of nanomaterials in vivo depends on their immunogenicity. In order to diminish the immunogenicity of nanomaterials, the number and variety of amino acid residues in the polymer chain should be minimum. Usually, the nanomaterials possess maximum biological activity at their minimum immunogenicity in the body (Ljubimova et al., 2008).

The biodegradability of nanomaterials is an important characteristic that determines the possibilities of their use in medicine, in particular as nanoplatforms for the delivery of drugs and genetic materials. The biodegradability of nanomaterials is related to their biocompatibility. Polymeric materials are considered to be biodegradable when they contain $-O-$, $-NH-$, $-S-$, $-S-S-$ bonds in the main chain (Ljubimova et al., 2008). Therefore, poly-aspartate, poly-glutamate, poly-malate, poly-lactate, some polysaccharides, and other natural and synthetic polymers are considered to be the most promising nanocarriers. While the polymeric materials containing $-C-C-$ bonds in the main chain, as well as mineral nanomaterials are usually not biodegradable, that is important to know at evaluating their excretion from the body.

4   Role of Interaction of Nanomaterials with Biological Matrices

The bio-functionalization of nanomaterials plays a crucial role in providing them with an addressed action toward the molecular and cellular targets and thus, diminishing their potential negative side effects in the treated organism. Such bio-functionalization is necessary for (Ljubimova et al., 2008; Torchilin, 2014):

(a) Providing bioactivity (drug, antisense oligonucleotides against mRNA for HER-2 or EGF-R) to nanomaterials.
(b) Crossing the barriers of the endothelial system, such as blood-brain-barrier (BBB) or blood-tumor-barrier (BTB) with the help of monoclonal antibodies against transferrin receptor
(c) Addressed action through recognition of the pathological cells (specific antibody, specific peptide, cytokine (TNF), folic acid)
(d) Blocking the undesirable uptake of particles by the macrophages (via decoration of the particles by the polyethylene glycol (PEG))
(e) Proper trafficking of the up-taken nanocomposites within the targeted cells (via controlling drug release at pH present in the endosomes)
(f) Bio-imaging (necessary for monitoring of drug action and release (clearance) in the organism)

"Smart" nanomaterials are also named "intelligent" primarily due to the peculiarities of bio-functionalization of chemical groups available on their surfaces. The ability for addressed action is the main property of "smart" nanomaterials, which is determined by vectors included in structure of these nanomaterials. The following vectors are described:

• Specific immunoglobulins (antibodies) that recognize the structure of specific protein antigens (receptors) on the surface of target cells and macromolecules (Ljubimova et al., 2008; Torchilin, 2014)
• Specific lectins that recognize carbohydrate determinants in the glycocalyx on the surface of target cells and in the composition of various molecules (Tarbell & Cancel, 2016)
• Vectors based on specific peptides (e.g., cell-penetrating peptides (CPPs which unlike other peptides can cross plasma membrane) that consist of <50 amino acids and can be applied as a delivery system for different therapeutic agents (Cerrato et al., 2014)
• Lipids that improve the interaction of nanoparticles with a double lipid layer on the surface of target cells

The effectiveness of action of functionalized nanomaterials is ensured by the following properties of the plasma membrane of target cells (Ljubimova et al., 2008):

- Ratio of lipids to proteins at approximately 1:1 level
- Presence of phospholipids in the plasma membrane providing the properties of a semi-liquid phase
- Plasticity of the plasma membrane provided by the phospholipids present in it, while its rigidity depends on cholesterol content
- Protein receptors in plasma membrane that play a role of "sense organs" of the cell and also determine the specificity of the action of ligand-functionalized nanomaterials with these receptors

The "intelligence" and behavior of drug nanocarriers are determined by such main functional modules (Ljubimova et al., 2008):

- Active drug substance(s) or prodrugs acting on specific molecular targets in pathological cells
- Module(s) recognizing specific target cells in the organism, for example, monoclonal antibodies or peptides that interact with surface antigens often overexpressed in tumor cells
- Polyethylene glycol (PEG), a protective module that prevents cleavage of nanomaterials by enzymes and their resorption by the reticuloendothelial system
- Module that promotes the release of a drug substance in the endosomes of the target cell; the action of this module depends on the pH (in the endosomes, optimal pH is 5.2) and is realized through hydrolysis of the hydrazone bond
- Module that promotes the release of a drug substance from endosomes when they maturate to lysosomes (protonated and, therefore, neutralized carboxylates and hydrophobic groups play the main role here)
- Module that promotes the release of a drug substance in the cytoplasm (cytosolic glutathione often destroys the bond between the nanocarrier and the drug)
- Optional module required for bio-imaging of the nanoconjugate in the tissue (e.g., fluorescent dye) (Ljubimova et al., 2008)

PEG is included in the shell of many drug carriers, both polymeric micelles and nanoparticles. Since the surface of most cells has a negative electric charge, the nanoparticles with a cationic shell can more easily penetrate into the cells together with a delivered drug. PEG is an electroneutral molecule capable of reducing binding to plasma protein particles, as well as inhibiting the uptake of particles by the mononuclear phagocytic system (MPS) (Jokerst et al., 2011). Due to this, the duration of life of nanoparticles in bloodstream increases, which also facilitates them to reach their target cells in the body. Binding of proteins to nanoparticles, as well as their distribution in the body, depends on the length of the polymeric chain of PEG, as well as the density of the PEG coating on the nanoparticles (Jokerst et al., 2011).

Doxorubicin (another brand name, Adriamycin), due to its extremely strong antitumor effect, is often called a "golden standard" drug among the existing anticancer drugs. However, along with such treatment effect, doxorubicin also possesses severe negative side effects, such as cardio-, nephro-, and hepatotoxicity (Kobylinska et al., 2014, 2015, 2016, 2018; Walker, 2006). To reduce these effects, doxorubicin was encapsulated into the liposomes that improve significantly its biocompatibility

in cancer patients. "Ben Venue Laboratories" manufactures for "Johnson & Johnson" a nanomedicine Doxil, in which doxorubicin is encapsulated in the liposomes that are additionally functionalized with PEG (Zhang et al., 2011). The lifespan of Doxil in the body of cancer patients is 600 times longer compared to free doxorubicin. Besides, Doxil is better concentrated in blood vessels and tumors. The cardiotoxicity of doxorubicin in Doxil nanocomplex is decreased by ten times. Of course, such characteristics of Doxil are definitely reflected in its price, compared to the price of free doxorubicin. Due to such advantages of Doxil, there is a significant reduction in the effective therapeutic doses of this drug, as well as a reduction in the negative side effects of its action. Probably, that is caused by "masking" of the toxic drug substance which prevents its non-addressed action in the patients' body. However, in some cancer patients treated with Doxil, immunogenic effect of this nano-drug was found (Zhang et al., 2011). As assumed, such an immunogenic effect of Doxil was caused by the presence of PEG in this nanomedicine.

"Drug vectorization" of nanocarriers is synonymous to their bio-functionalization. The vectorization term was proposed for the reverse immobilization of various biologically active substances on different nanomaterials, such as polymers, nanoparticles, or liposomes (Su et al., 2014; Secret et al., 2013). Vectorization permits a simultaneous delivery of substances that act synergetically, like drugs and miRNA to mRNA coding for specific proteins in tumors or other pathologic loci. Such action provides more effective and addressed action of the nanomedicine, as well as a circumvention of the barrier of multiple drug resistances in the organism. The immunoglobulins belong to the most specific vectors attached to nanocarriers of drugs. Instead of traditional antibodies that recognize the bio-markers on the pathological cells, low molecular weight, low immunogenic and, low allergenic camel immunoglobulins or immunoglobulin fragments were proposed. Besides, the monoclonal antibodies to transferrin receptor were recommended for crossing of the endothelial system, namely blood-brain barrier (BBB) and blood-tumor barrier (BTB) (Su et al., 2014; Secret et al., 2013).

In addition to the negative side effects of medicines in the organism, oncologists constantly face no less important problem that appears at using such potent antitumor factors as doxorubicin, cisplatin, vincristine, and others. This is due to the development of resistance to these drugs in more than 50% of cancer patients (Holohan et al., 2013). Similarly, drug resistance also develops in tuberculosis patients. Obviously, malignant cells, like cells of tuberculosis-causing bacteria, become resistant to chemotherapeutic factors due to the rapid selection of drug-resistant cell strains (Furin et al., 2019).

The transport system that functions in the plasma membrane of most cells is the main mechanism that inhibits the action of drugs, which are actually xenobiotics. This system protects cells from the entry of various toxic substances with a molecular weight of <1000 Da, that in general corresponds to the molecule size of most drugs (<500 Da). Thus, its functioning can provide a multiple drug resistance (MDR). Genes that encode the corresponding membrane proteins are often activated in tumor cells (Holohan et al., 2013). Therefore, the transportation of drugs in

a "masked" state under the guise of a nanocarrier might circumvent such protection of tumor cells and the antitumor drugs can get into these cells.

A multilevel system of biological barriers protects the living organisms from the action of various xenobiotics naturally by preventing them from penetrating into living cells and by stopping the biological action of foreign agents, including highly toxic drugs. They are as follows:

- Tissue-organ barriers (blood-brain or placenta-fetus) that exist in order to protect the brain or fetus from the action of dangerous substances
- Transport membrane system of the multiple drug resistances located on the surface of the cells and aimed at the removal of xenobiotics, including highly toxic medicines, from the cell
- Molecular barriers working through various mechanisms in order to neutralize the negative effects of cytotoxic agents, including drugs, on the biomolecules inside the cell; as examples are the systems of antioxidant and antiradical protection of biomolecules, as well as systems of protection of the genetic apparatus, such as p53 protein, Sna repair systems, PARP reparation enzyme, and others

Thus, due to the existence of blood-brain barrier, a problem appears with the delivery of drugs to the brain. In this case, multifunctional nanocomposites can be useful, because they can be "programmed" to pass through such a barrier to successfully deliver the drug substance to the affected area, such as brain tumor (Ljubimova et al., 2008).

In order to visualize the behavior of nanocomposites in biological systems of varying complexities (cells, tissues, organism), these composites may include special labels that are convenient to detect using microscopic (in vitro) or special bioimaging (in vivo) techniques (Jenjob et al., 2020; Pratiwi et al., 2019). The following labels are proposed for this purpose: (1) optically dense substances, such as gold, silver, nickel, magnetite, magnetite, specific dyes, and others; (2) fluorescent substances (fluorescein, FITC, Texas red, and others); (3) luminescent substances (cations of rare earth elements, such as Ce (III), Eu (III), Nd (III), as well as pyrene and other substances).

5   Action of Nanomaterials on Mammalian Cells In Vitro

Here we addressed, preferentially, drug delivery systems of the polymeric nature that provide more opportunities for conjugation of functional components, comparing with other types of nanomaterials, such as mineral nanoparticles or liposomes. We also presented our data on the use of Fulleren C60 as a biocompatible nanocarrier for drugs, since promising results in targeting tumor cells in vitro and in vivo have been obtained. Other nanomaterials for the biomedical application are described in detail in four volumes encyclopedia edited by Vladimir Torchilin (2014).

To evaluate the cytotoxic action of the comb-like polymeric nano-carrier (poly(VEP-GMA)-graft-PEG) at delivery of traditional anticancer drug

doxorubicin and clinical trial metal-containing medicine KP-1019, the Enhancement coefficient was calculated. It is a ratio of the IC50 at the action of drug in the encapsulated versus free form—$IC50_{carrier-drug}/IC50_{drug}$. Ten human and two murine tumor cell lines and their drug resistant sub-lines with defects in specific genes (p53KO, p53 mutation or overexpression of Pgp, MRP) were treated for 72 h with encapsulated or free doxorubicin. It was found that the Enhancement coefficient varied from 2 to 18 that distinctly indicates the increase in drug toxicity after its complexation with the polymeric nanocarrier (Senkiv et al., 2014). The Enhancement coefficient varied from 1.6 to 22.7 when ten human tumor cell lines and their drug resistant sub-lines with defects in specific genes responsible for drug resistance were treated with clinical trial metal-containing anticancer compound—KP-1019 (Heffeter et al., 2014).

Encapsulation of drug compounds with polymeric nanocarriers increases the water solubility of water-insoluble drug substances, which in turn improves drug application, prolongs the stability of anticancer drug, and accelerates drug delivery into targeted cells (Senkiv et al., 2014; Heffeter et al., 2014). In addition to that, such encapsulation also significantly enhances the effectiveness of drug action both in vitro and in vivo (see next sub-chapter of this book). What is particularly important is that it permits the circumvention of the multidrug resistance barrier in tumor cells.

6   Toxicity of Nanomaterials In Vivo

Taking into account the results of the bio-imaging of distribution of fluorescently labeled drugs in the body, it was suggested that only 0.01% of drugs applied intravenously can reach its biological targets in the organism, while 99.99% are practically useless. Moreover, they create a potential danger of negative side effects in the treated organism (Fujita et al., 2007; Ljubimova et al., 2008). Thus, one can reduce (theoretically, up to 10,000 times) the acting concentration of highly toxic drug substance, if there is an addressed action of the drug. "Masking" (hiding) of the toxic drug provides a possibility to decrease its negative side effects in an organism, and using nanocarriers for drug encapsulation and delivery seems to be the best way to achieve the above-mentioned aims (Ljubimova et al., 2008).

Below, we describe how the encapsulation of traditional (doxorubicin and cisplatin) and experimental (derivatives of novel heterocyclic compounds with a potential anticancer activity) antitumor drugs with the poly(VEP-GMA)-graft-PEG comb-like polymer and Fulleren C60 improve the action of these agents toward tumor-bearing (NK/Ly lymphoma, L1210 leukemia and Lewis lung carcinoma) mice. Besides, a decrease in negative side effects (cardiotoxicity, hepatotoxicity, nephrotoxicity, and immune toxicity) in mice and rats is briefly described.

It was found that immobilization of doxorubicin by organic (polymer) or mineral (fullerene C60) nanocarriers decreased the acting concentration of this drug. Such effect was best pronounced in mice with NK/Ly lymphoma and L1210 leukemia

treated with the polymer-encapsulated doxorubicin. The Enhancement coefficient ($IC50_{carrier-drug}/IC50_{drug}$) was increased by up to ten times (Senkiv et al., 2014). It was shown that treatment effect of the encapsulated doxorubicin in 0.1µg/mL dose was comparable with such effect of free doxorubicin in 1.0µg/mL dose. The volume of Lewis carcinoma tumor in mice was significantly decreased and the survival of tumor-bearing animals was prolonged at their treatment with Doxorubicin-Fulleren C60 (Panchuk et al., 2015) or Cisplatin-Fulleren C60 (Prylutska et al., 2017) nano-complexes comparing with these indicators in mice treated with free form of these anticancer drugs.

The immobilization of doxorubicin or cisplatin on Fullerene C60 resulted in an average twofold increase in the therapeutic effect of these drugs in Lewis carcinoma model in mice (Panchuk et al., 2015). It is known that both tumor growth and anti-cancer drug cause general toxicity in tumor-bearing animals and cancer patients that is expressed in the form of cachexia (loss of body weight). We observed a reduction in body weight from 18.1 ± 0.9 g per mouse in the untreated animals to $13.0 \pm 1.1^*$ g per mouse with Lewis carcinoma and $11.7 \pm 0.9^*$ g per mouse under Cisplatin treatment (Prylutska et al., 2017). Whereas the body weight of tumor-bearing animals treated with Cisplatin-Fulleren C60 nanocomposite was partly restored to $15.3 \pm 1.2^*$ g per mouse (Prylutska et al., 2017). Note: *statistically significant ($p < 0.05$).

Total volume of lung metastases (mm^3) per mice with Lewis carcinoma was 112 ± 8, and an average volume of a single metastatic focus (mm^3) in those mice was 8.6 ± 0.6. After Cisplatin treatment, the first indicator decreased to $48 \pm 3^*$ and after treatment with Cisplatin-Fulleren C60 nanocomplex, it decreased to $28 \pm 2^*$. Values of second indicator were $4.0 \pm 0.3^*$ and $3.1 \pm 0.2^*$, correspondingly (Prylutska et al., 2017).

Thus, the antimetastatic action of Cisplatin-Fulleren C60 nanocomplex in Lewis carcinoma-bearing mice was more efficient compared to that of free cisplatin (Prylutska et al., 2017). Higher effectiveness of action doxorubicin-Fulleren C60 nanocomplex comparing with the effectiveness of action of free doxorubicin was also observed at treatment of tumor-bearing experimental animals (Panchuk et al., 2015).

The antioxidants selenomethionine (SeMet, 1200µg/kg) and D-pantethine (D-Pt, 500 mg/kg) demonstrated tissue-protective action against the adverse effects of doxorubicin (Dx, 10 mg/kg) in mice with B16 melanoma (Panchuk et al., 2017b). These antioxidants significantly reduced tumor and Dx-induced neutrophilia, lym-phocytopenia, and leukocytosis. They also decreased other negative side effects of Dx action, for example, elevated creatinine level in blood and monocytosis, thus normalizing health conditions in B16 melanoma-bearing animals. However, these tissue-protective effects of SeMet and D-Pt in melanoma-bearing mice under Dx treatment had no major impact on animal survival. Thus, ROS scavenging potential of the applied antioxidants does not directly affect the antitumor action of Dx. The intrinsic antioxidant activity of fullerene C60 can also reduce the potential adverse effects of drugs caused by the induced excessive production of ROS, since it hinders the inflammatory processes caused by tumor growth in experimental animals and,

consequently, improves the prognosis of animal survival. A similar conclusion was made by us on the effect of landomycin A toward the redox status and anticancer activity in tumor cells (Panchuk et al., 2017a).

As mentioned above, the adverse effects of most anticancer medicines caused by their non-addressed action in the organism create the main problems for their application in chemotherapy. The hepato-, cardio-, and nephrotoxicities of these drugs were described (Kobylinska et al., 2014, 2015, 2016, 2018; Walker, 2006). Besides, their immune- (Panchuk et al., 2017b) and neurotoxicities (Teleanu et al., 2019) were also detected. The potential genotoxicity of nanomaterials of biomedical use was also noted (see next sub-chapter). It was revealed that in many cases these adverse effects could be, at least, partially blocked when the anticancer drugs were immobilized on the nanoplatforms used for their delivery. Below, we briefly describe the results of our studies devoted to the negative side effects of highly toxic anticancer drugs and their decrease by the applied drug delivery system.

Changes in the activity of creatine phosphokinase, aspartate aminotransferase, alanine aminotransferase, and lactate dehydrogenase (LDH) were monitored by the automatic biochemical analyzer (Humalyzer 3000 Germany) in blood serum of white laboratory rats for evaluation of the cardiotoxicity effects caused by the doxorubicin and novel 4-tiazolidinone derivatives with potential anticancer action (Kobylinska et al., 2014). For such study, the redistribution of heart- and muscle-specific isozymes of LDH has been also recommended (Walker, 2006). Doxorubicin and 4-tiazolidinone derivatives, as well as the nanocomplexes of these agents with poly(VEP-GMA)-graft-PEG comb-like polymer were used to treat laboratory rats. It was found that the rats survived for 10 days after treatment with doxorubicin, but they died after 20 days treatment (Kobylinska et al., 2014, 2015, 2016). Doxorubicin induced the elevation of activity of creatine phosphokinase (enzymatic indicator of cardiotoxicity) in rat blood serum from 124.5 + 0.01 to 207.9 + 0.04 units/L, while application of this drug as a nanocomplex decreased this activity to 128.4 + 0.01 units/L. The content of LDH-1 and LDH-2 isozymes in blood serum of control (untreated) and NL/Ly lymphoma-bearing mice did not differ considerably, but the content of LDH-2 isozyme was elevated significantly after doxorubicin injections (5×1.0 mg/kg). This data suggests a release of heart-specific isoforms of LDH from heart muscle into blood of animals treated with doxorubicin. The application of doxorubicin as a complex with poly(VEP-GMA)-graft-PEG comb-like polymer normalized the ratio LDG-1/LDH-2 in blood serum of the treated mice.

The estimated enzymatic indicators of hepatotoxic action of anticancer drugs and their nanocomplexes with poly(VEP-GMA)-graft-PEG comb-like polymer are as follows: alkaline phosphatase, α-amylase, gamma-glutamyltransferase, lactate dehydrogenase, alanine (ALT) and aspartate (AST) aminotransferases, and De Ritis coefficient (AST/ALT) (Kobylinska et al., 2015). The measured activities of gamma-glutamyltransferase in blood serum of rats, which shows doxorubicin-induced hepatotoxicity, are as follows: control, 0.3 microcat/L; doxorubicin, 1.3 microcat/L; and doxorubicin-polymeric nanocarrier, 0.2 microcat/L. Similar dynamics of

changes were revealed when the activities of alkaline phosphatase and α-amylase were monitored.

The following metabolic indicators of nephrotoxicity were estimated: urea, creatinine, glucose, cations of calcium, iron, sodium, and anions of chlorine. Besides, the level of total protein was measured in blood serum of treated laboratory rats (Kobylinska et al., 2016). The results of total protein are as follows: control, 75.8 + 3.2 g/L; doxorubicin, 55.8 + 4.1 g/L; and doxorubicin-polymeric nanocarrier, 71.8 + 4.3 g/L. The results of sodium content in the serum of rats are as follows: control, 127.5 + 13.2 mmol/L; doxorubicin, 340.0 + 16.1 mmol/L; and doxorubicin-polymeric nanocarrier, 159.7 + 11.3 mmol/L. The results of chlorine content are as follows: control, 117.8 + 14.4 mmol/L; doxorubicin, 192.2 + 9.5 mmol/L; and doxorubicin-polymeric nanocarrier, 184.6 + 11.2 mmol/L.

Thus, analysis of most frequently studied indicators that characterize cardio-, hepato-, and nephrotoxicities demonstrated that doxorubicin induced significant changes in the levels of those indicators, while its nanocomplex with poly(VEP-GMA)-graft-PEG comb-like polymer normalized those levels. As an explanation for such effect of encapsulation of doxorubicin, the "masking" of this highly toxic anticancer drug that prevented its direct interaction with cells of normal tissues and organs could be proposed. Thus, such encapsulation hindered the non-addressed action of the doxorubicin in the treated organism. As a result, the negative side effects of the anticancer drug, namely cardio-, hepato-, and nephrotoxicities were significantly decreased. It should be noted that the protective effect of drug immobilization on this nanocarrier was also found when other toxic compounds such as 4-tiazolidinone derivatives with potential anticancer activity were used (Kobylinska et al., 2014, 2015, 2016, 2018; Walker, 2006).

We have found that the complexation of anticancer drug with a perspective mineral nanocarrier (fullerene C60) also enhanced cytotoxic (pro-apoptotic) action of the drug. It should be noted that the immunotoxicity of this nanocarrier was also described (Turabekova et al., 2014); therefore, further investigations are needed.

The reactive oxygen species (ROS) induced by many anticancer drugs, at least partly, might be responsible for their cytotoxic action via the programmed cell death (Elmore, 2007; Johnstone et al., 2002; Lin & Beal, 2006; Ling et al., 2003). ROS accumulation results either from increased production or reduced scavenging by cellular detoxifying systems, or both. Direct influence of ROS on the apoptotic processes correlates to their damaging effects on cellular structures, resulting in the necrotic cell death, or to a more limited action on mitochondria, such as an impairment of the mitochondrial transmembrane potential and respiratory chain, leading to apoptosis (Elmore, 2007; Johnstone et al., 2002; Lin & Beal, 2006; Ling et al., 2003). Thus, the amount of drug-induced ROS can correlate with negative side effects caused by drug action.

Therapeutic index (π) is a principal indicator of the effectiveness of medicine action (Muller & Milton, 2012). The concentration range of the highly effective medicine (ED_{50}) targeting the pathologic cells (e.g., tumor ones) should be as far as possible from the concentration range of TD_{50} showing general toxicity of the

medicine in the treated organism. A medicine whose ED_{50} is below 1μM is considered effective.

Pharmacology, which studies the interactions between drugs and body, has two branches: pharmacokinetics (PK) and pharmacodynamics (PD). Whereas the aim of pharmacokinetics is to analyze the status of drugs in the body (absorption, distribution, bioavailability/bioequivalence, metabolism, and excretion), pharmacodynamics characterizes the biological responses to drug action in the body (molecular interactions of drugs in tissues and organs) (Li & Hickman, 2011; Sandritter et al., 2017; Zhao & Iyengar, 2012). The inter-relationships of the exposure-response (PK/PD) is a key issue at the development of new drugs. The relationships concentration-effect is of critical significance in pharmacodynamics. The bio-safety margins versus efficacy characteristics (therapeutic window) permit to define dosing thresholds for specific drugs. It should be noted that long ago, the medieval naturalist, alchemist, and astrologer, Paracelsus, (1493–1541) who is considered by some people as the father of toxicology, wrote "*Sola dosis facit venenum.*" ("The dose makes the poison.") PK/PD modeling and compartmental simulation allow one to better understand drug's distribution and action, for example, to answer a question, "How much of the drug might get into the brain?" In ecotoxicology, pharmacokinetics and pharmacodynamics, also termed as toxicokinetics and toxicodynamics, affect the therapeutic window (Li & Hickman, 2011), which can differ in various organisms. It should be noted that Springer publishes the "Journal of Pharmacokinetics and Pharmacodynamics" (Editor-in-Chief—Peter Bonate, Volume 47 in 2020, 6 Issues yearly, Impact factor equaled 2.461 in 2019).

In the United States of America, Food and Drug Administration (FDA) is responsible for safe consumption by humans of any new medicine and for taking a decision whether a drug might be proposed for or taken off the market. Such decision also includes veterinary drugs and biological products. Thus, the bio-safety and efficacy of drugs depend significantly upon the pharmacokinetics and pharmacodynamics. Materials such as blood serum, plasma, urine, saliva, tears, sweat, and others (surgical samples) can be used for such analysis, and the objects for analysis include rodents, non-human primates, and humans. The unwished biological effects of drug may include the following: (a) a mutation that can lead to carcinogenic effect; (b) simultaneous multiple actions that are deleterious (toxic) for the organism; (c) interactions that lead to uncontrolled proliferation or metabolic disorders; (d) induction of physiological damage or chronic disorders (Marcato, 2014).

The pharmacokinetic and pharmacodynamic approaches are also valid for nanoparticles used for drug delivery (Marcato, 2014). The application of the nanoparticles can provide a site-specific delivery of drug, diminish the unwanted toxicity caused by its nonspecific distribution, increase tissue-specific accumulation, and improve patient's compliance and clinical outcomes. Besides, the nanocarriers can increase the bioavailability of drug, sustain its effect in tissue target, provide water solubility of drugs that is important for their intravenous delivery, and improve the stability of therapeutics in tissue or blood microenvironment. Thus, understanding pharmacokinetic and pharmacodynamic characteristics of the

nanoparticles during their interaction with biological systems helps in designing "smarter" nanomaterials for the biomedical application. The physico-chemical properties of nanomaterials (size, surface charge and modifications for targeting the ligands, PEGylation, and other functionalizations) that are needed for better pharmacokinetics and pharmacodynamics of these nanomaterials are also described in Chap. 2 of this book. These modifications of the nanoparticles provide them with a longer circulation time in the bloodstream, increased cellular uptake, and accumulation in tissue and organ targets, which enhance their therapeutic efficiency.

There is a need in the development of test methods for standardization and/or validation of the potential hazards of nanomaterials. In addition to the existing methods of in vitro and in vivo studies enabling risk assessment of nanomaterials for humans, the corresponding test methods are necessary for the environment (see sub-chapter below). In silico approaches might promote classification of nanomaterials in order to predict their toxicological risks. The collaboration between the research teams working in the nanosafety area should accelerate the development of the nanosafety guidelines. This will not only improve methods and experimental models in nanotoxicology but also increase the quality of research in nanotoxicology.

7 Genotoxicity of Nanomaterials

Genotoxicity is a set of destructive genetic changes caused by different (physical, chemical, and biological) agents (genotoxins) that lead to gene mutations, chromosomal aberrations, and gene recombination (Shah, 2012). The potential genotoxic action of the nanomaterials should be taken into account when they are planned for use either as drugs or as gene delivery systems. Such action can significantly decrease the advantages of application of nanocarriers in medicine.

Basing on their biological effects, genotoxins can be classified into three categories: (1) agents causing cancer (carcinogens); (2) agents inducing mutations (mutagens); (3) agents causing defects of birth (teratogens) (Mohamed et al., 2017). The most convenient methods developed on best practices of in vitro study of genotoxicity are as follows: (1) Ames test (bacterial reverse mutation); (2) mammalian assays for detection of mutations; (3) ana-telophase assay in onion (*Allium cepa*) for detection of chromosomal aberrations, (4) comet assay (DNA strand breaks in nuclear DNA of individual cells). The in vivo assays for evaluation of genetic damage include micronucleus detection, comet (DNA fragmentation) analysis, and detection of transgenic mutations (Elespuru et al., 2018). Of course, the list of methods for evaluation of genotoxic effects is much longer (Elespuru et al., 2018). Most studies devoted to genotoxicity in the mammalian cells were conducted using human breast adenocarcinoma cells of MCF-7 and MDA-MB-231 lines, while the mononuclear cells of human peripheral blood (lymphocytes) were used as a test system of normal cells.

In Ames test for mutagenicity, two *Salmonella typhimurium* strains are used: TA98 (his D 3052, rfa, uvr B, +R, pKm 101 that detects the reading frameshift mutations) and TA100 (his G46, rfa, uvrB bio, pKm 101 that detects base pair substitution mutations in the histidine operon (mis-mutation his G46)). The mutagenic index is counted as the ratio of number of colonies in experiment samples to number of colonies in negative control. The histidine revertant colonies are counted after incubation of plates for 48 h at 37 °C. A significant increase was detected in the number of *S. typhimurium* revertants (mutant frequency reached 4.72–5.44) that appeared at the action of the known mutagenic compounds (benzidine, nitrosoguanidine or sodium azide) (Finiuk et al., 2020). The mutagenic index due to the action of DMAEM-based polymers used for gene delivery was only 0.81–1.18 for TA98 and 0.82–1.17 for TA100 in the presence of S9 fraction (Finiuk et al., 2020). The mutagenic index of PEG (0.0025%) in the presence of S9 fraction was 1.21–1.47; however, it increased to 1.85 after a tenfold increase in PEG concentration (0.025%).

The *Allium* assay is a highly sensitive system used for the evaluation of both cytotoxic and genotoxic activities of different agents. This ana-telophase assay is based on the detection of chromosomal aberrations caused by the examined substances in the meristematic cells of onion (*Allium cepa*) roots after seeds germination (Fiskesjo, 1995; Kiełkowska, 1993). As a positive control, sodium azide is used, and the distilled water is used as a negative control.

The mitotic index (MI, %, the ratio of number of dividing cells to total number of cells) was determined in crushed preparations of root tips analyzed under a light microscope (Finiuk et al., 2020). The amount (%) of ana-telophases was calculated as the ratio of the sum of selected ana- and telophases to the sum of ana- and telophases. To detect the blocking effect of tested substances on a particular phase of mitosis (cell division), the ratio of the number of cells in metaphase to the sum of cells in anaphase and telophase (M/(A + T)) and the ratio of cells in metaphase to the number of cells in prophase (M/P) (Finiuk et al., 2020; Kiełkowska, 1993) were calculated.

When onion (*A. cepa*) seeds were grown in a solution containing polymers (0.0025%) optimal for transformation of plant cells, the inhibition of root growth by poly-DMAEMA carriers varied at 8.7–17.4% (Finiuk et al., 2020). However, at the action of PEG-6000 in such concentration, much higher level (30.3%) of growth inhibition of onion roots was observed. It should be noted that PEG-containing polymers used for gene delivery demonstrated stronger inhibitory effects on the growth of onion roots and seed germination compared with polymers without the PEG in their structures (Finiuk et al., 2020). Thus, the poly-DMAEMA polymeric carriers in 0.0025% concentration are more biocompatible and less genotoxic than the PEG that is traditionally applied for gene delivery because these carriers induce much less chromosomal aberrations in the meristem cells of *A. cepa* roots.

The comet assay is widely used for the evaluation of DNA damage in the eukaryotic cells (Olive & Banáth, 2006). This assay is conducted by means of electrophoresis of studied cells in the agarose gel at alkaline or neutral pH. Most investigators use electrophoresis at alkaline conditions to measure single-strand breaks in nuclear DNA, while double-strand breaks in DNA might be detected during electrophoresis

at neutral conditions. Other modifications of this method also allow to monitor cross-links in DNA, nucleotide base damage, DNA repair capacity, and appearance of the apoptotic nuclei.

DNA damage can be classified into five levels of genotoxicity according to the comet tail size: 0 (0–5% damage), 1 (5–25% damage), 2 (25–45% damage), 3 (45–70% damage), and 4 (more than 70% damage) (Singh et al., 1988).

The alkaline comet assay allows the detection of single-strand DNA breaks in alkaline-labile DNA sites. The obtained results are estimated using the mean value of the Olive tail moment (OTL) (Mozaffarieh et al., 2008). These results are also estimated using the mean value of the TailDNA% (Mozaffarieh et al., 2008). In the addition to comet category, both indicators are applied for quantification of DNA breaks during comet assay. As recommended, minimum 50 cells on each slide should be subjected to random quantification of DNA damage by the computer software. The tail moment is calculated as the length of DNA tail multiplied by % of total DNA in the tail, while the Olive tail moment represents the percentage of total DNA in the tail and the distance between the centers of the comet head and tail regions. These parameters are calculated automatically.

The results of our studies on targeting of tumor cells with the anticancer agents demonstrated that both quantitative indicators (Olive tail moment and TailDNA%) of DNA damage measured by comet assay, as well as a category of genotoxicity according to five levels of the comet tail size showed the increased value of all three indicators at the cytotoxic action of the examined anticancer agents when they were applied in complex with the nanocarrier (Kobylinska et al., 2019).

8   Environmental Toxicity of Nanomaterials

Ecotoxicology of nanomaterials is widely explored. We advise the readers to refer to a series of excellent reviews and experimental papers devoted to that issue (Tong, 2018; Batley et al., 2013; Farré et al., 2009; Handy et al., 2008; Fadeel et al., 2013). Here, we conducted only a brief analysis of probably several hundreds of publications in order to assist the readers in more detailed and specialized investigations.

The physico-chemical characteristics of nanomaterials are the most important for predicting the fate and behavior of the nanomaterials in the environment. The fate of mineral nanomaterials might differ significantly from the fate of the organic (e.g., polymeric) nanomaterials. The interactions of nanomaterials with other toxicants or chemical compounds in the environment are critical for their fate. Besides, the nanomaterials might be uptaken by different organisms (bacteria, algae, plants, invertebrate animals, fish, reptiles, amphibians, and mammals) that can transform the nanomaterials in more or less toxic agents. The aquatic (mainly freshwater) organisms are better studied in respect to ecotoxicologic features, comparing with the terrestrial organisms. In this book, there are two special Chaps. 9 and 10 devoted to the marine and freshwater organisms, correspondingly. The uptake and distribution of the nanomaterials within the organisms significantly depend upon the

formation of bio-corona on the surface of the nanomaterials that consists of different materials (including pollutants) present in the micro- and macroenvironment, capable of enhancing or inhibiting the toxicity (Docter et al., 2015; Nel et al., 2009; Stauber et al., 2020; Monopoli et al., 2012). This issue has been addressed in more detail in the Chap. 11, devoted to the role of environmental nanoparticles as multi-pollutant agents with a risk to human health. The potential detoxification mechanisms of the organisms subjected to the nanomaterials acting as pollutants should be taken into account when considering the bio-risks for the organisms and environment. Below, such a mechanism (metallothioneins (MTs), the intracellular metal-buffering proteins) is described in more detail, since it was a subject of our studies on ecotoxicity of metal-containing nanomaterials for the freshwater organisms—mollusk (Falfushynska et al., 2012), fish (Falfushynska et al., 2014), and amphibia (Falfushynska et al., 2015).

Cobalt is an essential element for health in animals and humans, since it is a component of vitamin B12. Cobalt is also widely used in industry for producing high performance alloys, in batteries (Lithium-Cobalt oxide ($LiCoO_2$)), in chemical reactions as oxidation catalysts, in production of pigments and colorings for glass, smalt, ceramics, inks, paints, and varnishes, and as a radioisotope (Co^{60}) in X-ray source. In our experiments (Falfushynska et al., 2012, 2014, 2015), we used Cobalt as $CoCl_2$ or nanocomposite with concentration of Co^{2+} that is ecologically relevant and corresponds to Co^{2+} concentrations (50μg/l) in the blood of persons with worn implants. Synthesis of initial polymer substances (PS) was performed via radical copolymerization of vinyl pyrrolidone (NVP), 5-(*tert*butylperoxy)-5-methyl-1-hexene-3-yne (VEP), and dimethyl aminoethyl methacrylate (DMAEM) (molar ration = 1:1:1) in the dimethyl formamide solution (Zaichenko et al., 1998). Synthesis of coordinated Me-NC was carried out in the reaction of Me^{2+} with PS.

Different fresh water organisms—mollusk (Falfushynska et al., 2012), fish (Falfushynska et al., 2014), and amphibia (Falfushynska et al., 2015)—were subjected to the action of $CoCl_2$ or Cobalt-containing nanocomposite. Selected biomarkers of the oxidative stress, cytotoxicity (lysosomal membrane stability) in the digestive gland of *A. cygnea* mollusk, genotoxicity (hemocytes with nuclear abnormalities (NA) and micronuclei (MN)), endocrine disruption (content of vitellogenin-like proteins (Vtg-LP)), and microsomal 7-ethoxyresorufin *O*-deethylase (EROD) activity, which is cytochrome *P*-450-dependent were measured (Falfushynska et al., 2012). The responses of the mollusk to metal (Co) and the corresponding metal-containing nanocomposite suggest an existence of the potential protection mechanism(s) against toxic metal action in the mollusk organism (Falfushynska et al., 2012).

At the same time, the responses of fish to metal (Co) and the corresponding metal-containing nanocomposites (Me-NC) suggests that these nanocomposites did not provide significant protection against the toxic effects of the metal (Falfushynska et al., 2014). This toxicity could be due to metabolic changes in the Me-NC and release of toxic metal, unlike shown previously in the freshwater mussels (Falfushynska et al., 2012). The response of frog to metal (Co) and the

corresponding metal-containing nanocomposite (Me-NC) was similar to that observed in fish but more complicated (Falfushynska et al., 2015).

Thus, the protective effect of the polymeric coating of cytotoxic substances encapsulated in the nanoscale composites depends significantly on the tested organisms (e.g., mollusk versus fish and frog).

In Chap. 10, we have demonstrated that targeting metallothioneins is a sensitive approach for assessing the bio-risks associated with using metal-containing nanoscale composites, both in the mammalian microenvironment and the aquatic macroenvironment. Metallothioneins (MTs) belong to a family of cysteine-rich (30% of all amino acid residues), low-molecular-weight (0.5–14 kDa) proteins, localized in the membranes of the Golgi apparatus of cells. In addition to physiological metals (zinc, copper) and selenium, they are also capable of binding xenobiotics such as cadmium, hydrargium, and argentum (Falfushynska et al., 2012). Here, we demonstrated that the MTs can serve as potential molecular targets for Co and Zn if they are released from the NCs in the metabolically active tissues such as the liver. They can also function as scavengers of the reactive oxygen species, and these activities of the MTs are species-specific (Falfushynska et al., 2012, 2014, 2015).

9   Concluding Notes

With respect to nanomedicine, nanomaterials are generally viewed as only potential carriers of conventional drugs. However, as pointed out in recent reviews, nanomaterials can also possess the intrinsic therapeutic properties and, thus, may be considered as drugs per se (Yang et al., 2014; Świętek et al., 2020; Vasylechko et al., 2020).

Although big progress was achieved in the use of nanomaterials as macromolecular medicines or drugs per se, the unsolved problems still exist in drug delivery with the nanocarriers, namely:

- Nonspecific bio-distribution of drug substances that leads to hepato-, cardio-, nephro-, neuro-, immune-, and genotoxic actions
- Low therapeutic index (range between ED50 and TD50) of nanomedicines
- Poor water solubility of many drug substances
- Low stability of drug substances due to preterm biodegradation that decreases their effectiveness
- Multiple drug resistance of the biological systems under treatment
- Immunogenic and allergic actions of many drugs and drug delivery systems are still poorly studied
- Genotoxicity (drug effect on the expression of genes that may lead to hereditary consequences)
- Standardization of validation methods in vitro and in vivo studies used for the assessment of potential bio-hazards of existing and novel nanomaterials
- The risks of application of nanomaterials to human health should also be evaluated in parallel with the assessment of such risks to the environment

- FDA certification should be taken into account since a development of many medicinal remedies based on drug carriers is blocked by low reproducibility of synthesis of those carriers, as well as synthesis of drug nanocomposites

Thus, moving to nano-world is not a guarantee of the unappealable creation of all new properties. Although these properties are different from those in the macro-world, often the nano-specific toxicity of the nanomaterials might not be easily detectable (Donaldson & Poland, 2013). The aim of this chapter was to show that one cannot assume that all nanomaterials possess their specific features, including toxicities, because of their nano-size. Many properties of the nanomaterials might also be due to nanoscale interactions of the nanomaterials with the targeted biological systems. Therefore, experimental studies should be combined with bioinformatic (in silico) approaches to better understand the behavior and function of nanomaterials.

References

Ai, J., Biazar, E., Jafarpour, M., Montazeri, M., Majdi, A., Aminifard, S., et al. (2011). Nanotoxicology and nanoparticle safety in biomedical designs. *International Journal of Nanomedicine, 6*, 1117–1127. https://doi.org/10.2147/IJN.S16603

Batley, G. E., Kirby, J. K., & McLaughlin, M. J. (2013). Fate and risks of nanomaterials in aquatic and terrestrial environments. *Accounts of Chemical Research, 46*(3), 854–862. https://doi.org/10.1021/ar2003368

Cerrato, C. P., Lehto, T., & Langel, Ü. (2014). Peptide-based vectors: Recent developments. *Biomolecular Concepts, 5*(6), 479–488. https://doi.org/10.1515/bmc-2014-0024

Docter, D., Strieth, S., Westmeier, D., Hayden, O., Gao, M., Knauer, S. K., & Stauber, R. H. (2015). No king without a crown--impact of the nanomaterial-protein corona on nanobiomedicine. *Nanomedicine (London, England), 10*(3), 503–519. https://doi.org/10.2217/nnm.14.184

Donaldson, K., & Poland, C. A. (2013). Nanotoxicity: Challenging the myth of nano-specific toxicity. *Current Opinion in Biotechnology, 24*(4), 724–734. https://doi.org/10.1016/j.copbio.2013.05.003

Elespuru, R., Pfuhler, S., Aardema, M. J., Chen, T., Doak, S. H., Doherty, A., et al. (2018). Genotoxicity assessment of nanomaterials: Recommendations on best practices, assays, and methods. *Toxicological Sciences, 164*(2), 391–416. https://doi.org/10.1093/toxsci/kfy100

Elmore, S. (2007). Apoptosis: A review of programmed cell death. *Toxicologic Pathology, 35*(4), 495–516. https://doi.org/10.1080/01926230701320337

Fadeel, B., Feliu, N., Vogt, C., Abdelmonem, A. M., & Parak, W. J. (2013). Bridge over troubled waters: Understanding the synthetic and biological identities of engineered nanomaterials. *Wiley Interdisciplinary Reviews. Nanomedicine and Nanobiotechnology, 5*(2), 111–129. https://doi.org/10.1002/wnan.1206

Falfushynska, H., Gnatyshyna, L., Fedoruk, O., Mitina, N., Zaichenko, A., Stoliar, O., & Stoika, R. (2015). Hepatic metallothioneins in molecular responses to cobalt, zinc, and their

nanoscale polymeric composites in frog Rana ridibunda. *Comparative Biochemistry and Physiology. Toxicology & Pharmacology: CBP, 172–173*, 45–56. https://doi.org/10.1016/j.cbpc.2015.04.006

Falfushynska, H., Gnatyshyna, L., Stoliar, O., Mitina, N., Skorokhoda, T., Filyak, Y., et al. (2012). Evaluation of biotargeting and ecotoxicity of Co^{2+}-containing nanoscale polymeric complex by applying multi-marker approach in bivalve mollusk Anodonta cygnea. *Chemosphere, 88*(8), 925–936. https://doi.org/10.1016/j.chemosphere.2012.02.087

Falfushynska, H., Gnatyshyna, L., Turta, O., Stoliar, O., Mitina, N., Zaichenko, A., & Stoika, R. (2014). Responses of hepatic metallothioneins and apoptotic activity in Carassius auratus gibelio witness a release of cobalt and zinc from waterborne nanoscale composites. *Comparative Biochemistry and Physiology. Toxicology & Pharmacology: CBP, 160*, 66–74. https://doi.org/10.1016/j.cbpc.2013.11.009

Farré, M., Gajda-Schrantz, K., Kantiani, L., & Barceló, D. (2009). Ecotoxicity and analysis of nanomaterials in the aquatic environment. *Analytical and Bioanalytical Chemistry, 393*(1), 81–95. https://doi.org/10.1007/s00216-008-2458-1

Finiuk, N., Romanyuk, N., Mitina, N., Lobachevska, O., Zaichenko, A., Terek, O., & Stoika, R. (2020). Evaluation of phytotoxicity and mutagenicity of novel DMAEMA-containing gene carriers. *Cytology and Genetics, 54*(5), 437–448. https://doi.org/10.3103/S0095452720050096

Fiskesjo, G. (1995). Allium test. *Methods in Molecular Biology, 43*, 119–127.

Fujita, M., Lee, B. S., Khazenzon, N. M., Penichet, M. L., Wawrowsky, K. A., Patil, R., et al. (2007). Brain tumor tandem targeting using a combination of monoclonal antibodies attached to biopoly(beta-L-malic acid). *Journal of Controlled Release: Official Journal of the Controlled Release Society, 122*(3), 356–363. https://doi.org/10.1016/j.jconrel.2007.05.032

Furin, J., Cox, H., & Pai, M. (2019). Tuberculosis. *Lancet (London, England), 393*(10181), 1642–1656. https://doi.org/10.1016/S0140-6736(19)30308-3

Handy, R. D., Owen, R., & Valsami-Jones, E. (2008). The ecotoxicology of nanoparticles and nanomaterials: Current status, knowledge gaps, challenges, and future needs. *Ecotoxicology (London, England), 17*(5), 315–325. https://doi.org/10.1007/s10646-008-0206-0

Haynes, C. L., & Pedersen, J. A. (2020). *Nanotoxicology guidelines*. ACS Publications. https://pubs.acs.org/page/virtual_issue/nanotoxicology.

Heffeter, P., Riabtseva, A., Senkiv, Y., Kowol, C. R., Körner, W., Jungwith, U., et al. (2014). Nanoformulation improves activity of the (pre)clinical anticancer ruthenium complex KP1019. *Journal of Biomedical Nanotechnology, 10*(5), 877–884. https://doi.org/10.1166/jbn.2014.1763

Hobson, D. W., & Guy, R. C. (2014). Nanotoxicology. In P. Wexler (Ed.), *Encyclopedia of toxicology* (3rd ed., pp. 434–436). Academic Press. https://doi.org/10.1016/B978-0-12-386454-3.01045-9

Holohan, C., Van Schaeybroeck, S., Longley, D. B., & Johnston, P. G. (2013). Cancer drug resistance: An evolving paradigm. *Nature Reviews. Cancer, 13*(10), 714–726. https://doi.org/10.1038/nrc3599

Jenjob, R., Phakkeeree, T., & Crespy, D. (2020). Core-shell particles for drug-delivery, bioimaging, sensing, and tissue engineering. *Biomaterials Science, 8*(10), 2756–2770. https://doi.org/10.1039/c9bm01872g

Johnstone, R. W., Ruefli, A. A., & Lowe, S. W. (2002). Apoptosis: A link between cancer genetics and chemotherapy. *Cell, 108*(2), 153–164. https://doi.org/10.1016/s0092-8674(02)00625-6

Jokerst, J. V., Lobovkina, T., Zare, R. N., & Gambhir, S. S. (2011). Nanoparticle PEGylation for imaging and therapy. *Nanomedicine (London, England), 6*(4), 715–728. https://doi.org/10.2217/nnm.11.19

Kiełkowska, A. (1993). Allium cepa root meristem cells under osmotic (sorbitol) and salt (NaCl) stress *in vitro*. *Acta Botanica Croatica, 76*(2), 146–153. https://doi.org/10.1515/botcro-2017-0009

Kobylinska, L., Ivasechko, I., Skorokhyd, N., Panchuk, R., Riabtseva, A., Mitina, N., et al. (2019). Enhanced proapoptotic effects of water dispersed complexes of 4-thiazolidinone-based chemotherapeutics with a peg-containing polymeric nanocarrier. *Nanoscale Research Letters, 14*(1), 140. https://doi.org/10.1186/s11671-019-2945-7

Kobylinska, L., Patereha, I., Finiuk, N., Mitina, N., Riabtseva, A., Kotsyumbas, I., et al. (2018). Comb-like PEG-containing polymeric composition as low toxic drug nanocarrier. *Cancer Nanotechnology, 9*(1), 11. https://doi.org/10.1186/s12645-018-0045-5

Kobylinska, L. I., Havrylyuk, D., Riabtseva, A. O., Mitina, N., Zaichenko, O. S., Zimenkovskyi, B. S., & Stoika, R. S. (2014). Study of rat blood serum biochemical indicators of cardiotoxic action of novel antitumor 4-thiazolidinone derivatives and doxorubicin in complexes with polyethylene glycol-containing polymeric carrier in the rat blood serum. *Ukrainian Biochemical Journal, 86*(6), 84–95. [Article published in Ukrainian].

Kobylinska, L. I., Havrylyuk, D. Y., Mitina, N. E., Zaichenko, A. S., Lesyk, R. B., Zimenkovsky, B. S., & Stoika, R. S. (2016). Biochemical indicators of nephrotoxicity in blood serum of rats treated with novel 4-thiazolidinone derivatives or their complexes with polyethylene glycol-containing nanoscale polymeric carrier. *Ukrainian Biochemical Journal, 88*(1), 51–60. https://doi.org/10.15407/ubj88.01.051

Kobylinska, L. I., Havrylyuk, D. Y., Ryabtseva, A. O., Mitina, N. E., Zaichenko, O. S., Lesyk, R. B., Zimenkovsky, B. S., & Stoika, R. S. (2015). Biochemical indicators of hepatotoxicity in blood serum of rats under the effect of novel 4-thiazolidinone derivatives and doxorubicin and their complexes with polyethyleneglycol-containing nanoscale polymeric carrier. *Ukrainian Biochemical Journal, 87*(2), 122–132. https://doi.org/10.15407/ubj87.02.122

Kumar, V., Dasgupta, N., & Ranjan, S. (2018). *Nanotoxicology. Toxicity evaluation, risk assessment and management* (702 p). CRC Press, Taylor & Francis Group.

Li, Q., & Hickman, M. (2011). Toxicokinetic and toxicodynamic (TK/TD) evaluation to determine and predict the neurotoxicity of artemisinins. *Toxicology, 279*(1–3), 1–9. https://doi.org/10.1016/j.tox.2010.09.005

Lin, M. T., & Beal, M. F. (2006). Mitochondrial dysfunction and oxidative stress in neurodegenerative diseases. *Nature, 443*(7113), 787–795. https://doi.org/10.1038/nature05292

Ling, Y. H., Liebes, L., Zou, Y., & Perez-Soler, R. (2003). Reactive oxygen species generation and mitochondrial dysfunction in the apoptotic response to Bortezomib, a novel proteasome inhibitor, in human H460 non-small cell lung cancer cells. *The Journal of Biological Chemistry, 278*(36), 33714–33723. https://doi.org/10.1074/jbc.M302559200

Ljubimova, J. Y., Fujita, M., Khazenzon, N. M., Lee, B. S., Wachsmann-Hogiu, S., Farkas, D. L., et al. (2008). Nanoconjugate based on polymalic acid for tumor targeting. *Chemico-Biological Interactions, 171*(2), 195–203. https://doi.org/10.1016/j.cbi.2007.01.015

Loftsson, T., & Brewster, M. E. (2010). Pharmaceutical applications of cyclodextrins: Basic science and product development. *The Journal of Pharmacy and Pharmacology, 62*(11), 1607–1621. https://doi.org/10.1111/j.2042-7158.2010.01030.x

Madaan, K., Kumar, S., Poonia, N., Lather, V., & Pandita, D. (2014). Dendrimers in drug delivery and targeting: Drug-dendrimer interactions and toxicity issues. *Journal of Pharmacy & Bioallied Sciences, 6*(3), 139–150. https://doi.org/10.4103/0975-7406.130965

Marcato, P. D. (2014). Pharmacokinetics and pharmacodynamics of nanomaterials. In N. Durán, S. Guterres, & O. Alves (Eds.), *Nanotoxicology. Nanomedicine and nanotoxicology* (pp. 97–110). Springer. https://doi.org/10.1007/978-1-4614-8993-1_4

Mohamed, S., Sabita, U., Rajendra, S., & Raman, D. (2017). Genotoxicity: Mechanisms, testing guidelines and methods. *Global Journal of Pharmacy & Pharmaceutical Sciences, 1*, 1–6. https://doi.org/10.19080/GJPPS.2017.01.555575

Monopoli, M. P., Aberg, C., Salvati, A., & Dawson, K. A. (2012). Biomolecular coronas provide the biological identity of nanosized materials. *Nature Nanotechnology, 7*(12), 779–786. https://doi.org/10.1038/nnano.2012.207

Mozaffarieh, M., Schoetzau, A., Sauter, M., Grieshaber, M., Orgül, S., Golubnitschaja, O., & Flammer, J. (2008). Comet assay analysis of single-stranded DNA breaks in circulating leukocytes of glaucoma patients. *Molecular Vision, 14*, 1584–1588.

Muller, P. Y., & Milton, M. N. (2012). The determination and interpretation of the therapeutic index in drug development. *Nature Reviews. Drug Discovery, 11*(10), 751–761. https://doi.org/10.1038/nrd3801

Nakamura, H., Jun, F., & Maeda, H. (2015). Correction to: Development of next-generation macromolecular drugs based on the EPR effect: Challenges and pitfalls. *Expert Opinion on Drug Delivery, 12*(4), 691. https://doi.org/10.1517/17425247.2015.1024483

Nel, A. E., Mädler, L., Velegol, D., Xia, T., Hoek, E. M., Somasundaran, P., et al. (2009). Understanding biophysicochemical interactions at the nano-bio interface. *Nature Materials, 8*(7), 543–557. https://doi.org/10.1038/nmat2442

Olive, P. L., & Banáth, J. P. (2006). The comet assay: A method to measure DNA damage in individual cells. *Nature Protocols, 1*, 23–29. https://doi.org/10.1038/nprot.2006.5

Panchuk, R. R., Lehka, L. V., Terenzi, A., Matselyukh, B. P., Rohr, J., Jha, A. K., et al. (2017a). Rapid generation of hydrogen peroxide contributes to the complex cell death induction by the angucycline antibiotic landomycin E. *Free Radical Biology & Medicine, 106*, 134–147. https://doi.org/10.1016/j.freeradbiomed.2017.02.024

Panchuk, R. R., Prylutska, S. V., Chumakl, V. V., Skorokhyd, N. R., Lehka, L. V., Evstigneev, M. P., et al. (2015). Application of C60 fullerene-doxorubicin complex for tumor cell treatment *in vitro* and *in vivo*. *Journal of Biomedical Nanotechnology, 11*(7), 1139–1152. https://doi.org/10.1166/jbn.2015.2058

Panchuk, R. R., Skorokhyd, N. R., Kozak, Y. S., Lehka, L. V., Moiseenok, A. G., & Stoika, R. S. (2017b). Tissue-protective activity of selenomethionine and D-panthetine in B16 melanoma-bearing mice under doxorubicin treatment is not connected with their ROS scavenging potential. *Croatian Medical Journal, 58*(2), 171–184. https://doi.org/10.3325/cmj.2017.58.171

Pratiwi, F. W., Kuo, C. W., Chen, B. C., & Chen, P. (2019). Recent advances in the use of fluorescent nanoparticles for bioimaging. *Nanomedicine (London, England), 14*(13), 1759–1769. https://doi.org/10.2217/nnm-2019-0105

Prylutska, S., Panchuk, R., Gołuński, G., Skivka, L., Prylutskyy, Y., Hurmach, V., et al. (2017). C60 fullerene enhances cisplatin anticancer activity and overcomes tumor cell drug resistance. *Nano Research, 10*, 652–671. https://doi.org/10.1007/s12274-016-1324-2

Riabtseva, A., Mitina, N., Boiko, N., Garasevich, S., Yanchuk, I., Stoika, R., et al. (2012). Structural and colloidal-chemical characteristics of nanosized drug delivery systems based on pegylated comb-like carriers. *Chemistry and Chemical Technology, 6*(3), 291–295. https://doi.org/10.23939/chcht06.03.291

Sandritter, T. L., McLaughlin, M., Artman, M., & Lowry, J. (2017). The Interplay between pharmacokinetics and pharmacodynamics. *Pediatrics in Review, 38*(5), 195–206. https://doi.org/10.1542/pir.2016-0101

Savjani, K. T., Gajjar, A. K., & Savjani, J. K. (2012). Drug solubility: Importance and enhancement techniques. *ISRN Pharmaceutics, 2012*, 195727. https://doi.org/10.5402/2012/195727

Secret, E., Smith, K., Dubljevic, V., Moore, E., Macardle, P., Delalat, B., et al. (2013). Antibody-functionalized porous silicon nanoparticles for vectorization of hydrophobic drugs. *Advanced Healthcare Materials, 2*(5), 718–727. https://doi.org/10.1002/adhm.201200335

Senkiv, Y., Riabtseva, A., Heffeter, P., Boiko, N., Kowol, C. R., Jungwith, U., et al. (2014). Enhanced anticancer activity and circumvention of resistance mechanisms by novel polymeric/phospholipidic nanocarriers of doxorubicin. *Journal of Biomedical Nanotechnology, 10*(7), 1369–1381. https://doi.org/10.1166/jbn.2014.1864

Shah, S. (2012). Importance of genotoxicity & S2A guidelines for genotoxicity testing for pharmaceuticals. *IOSR Journal of Pharmacy and Biological Science, 1*, 43–54. https://doi.org/10.9790/3008-0124354

Simón-Vázquez, R., Peleteiro, M., Lozano, T., González-Fernández, A., & Casal, A. (2012). Nanotoxicology. In J. M. de la Fuente & V. Grazu (Eds.), *Nanobiotechnology: Inorganic nanoparticles vs organic nanoparticles* (pp. 443–485). Elsevier. https://doi.org/10.13140/2.1.1881.6003

Singh, N. P., McCoy, M. T., Tice, R. R., & Schneider, E. L. (1988). A simple technique for quantitation of low levels of DNA damage in individual cells. *Experimental Cell Research, 175*(1), 184–191. https://doi.org/10.1016/0014-4827(88)90265-0

Stauber, R. H., Westmeier, D., Wandrey, M., Becker, S., Docter, D., Ding, G. B., et al. (2020). Mechanisms of nanotoxicity – Biomolecule coronas protect pathological fungi against nanoparticle-based eradication. *Nanotoxicology, 14*(9), 1157–1174. https://doi.org/10.108 0/17435390.2020.1808251

Su, C. W., Chiang, C. S., Li, W. M., Hu, S. H., & Chen, S. Y. (2014). Multifunctional nanocarriers for simultaneous encapsulation of hydrophobic and hydrophilic drugs in cancer treatment. *Nanomedicine (London, England), 9*(10), 1499–1515. https://doi.org/10.2217/nnm.14.97

Suh, W. H., Suslick, K. S., Stucky, G. D., & Suh, Y. H. (2009). Nanotechnology, nanotoxicology, and neuroscience. *Progress in Neurobiology, 87*(3), 133–170. https://doi.org/10.1016/j. pneurobio.2008.09.009

Świętek, M., Panchuk, R., Skorokhyd, N., Černoch, P., Finiuk, N., Klyuchivska, O., et al. (2020). Magnetic temperature-sensitive solid-lipid particles for targeting and killing tumor cells. *Frontiers in Chemistry, 8*, 205. https://doi.org/10.3389/fchem.2020.00205

Tarbell, J. M., & Cancel, L. M. (2016). The glycocalyx and its significance in human medicine. *Journal of Internal Medicine, 280*(1), 97–113. https://doi.org/10.1111/joim.12465

Teleanu, D. M., Chircov, C., Grumezescu, A. M., & Teleanu, R. I. (2019). Neurotoxicity of nanomaterials: An up-to-date overview. *Nanomaterials (Basel, Switzerland), 9*(1), 96. https://doi. org/10.3390/nano9010096

Tong, T. (2018). Environmental nanotoxicology: Where are we now? *Journal of Industrial and Environmental Chemistry, 2*(1), 11–13.

Torchilin, V. (2014). *Handbook of nano biomedical research: Fundamentals, applications and recent developments* (2332 p). Imperial College Press.

Turabekova, M., Rasulev, B., Theodore, M., Jackman, J., Leszczynska, D., & Leszczynski, J. (2014). Immunotoxity of nanoparticles: A computational study suggests that CNTs and C60 fullerenes might be recognized as pathogens by Toll-like receptors. *Nanoscale, 6*(7), 3488–3495. https://doi.org/10.1039/c3nr05772k

van der Merwe, D., & Pickrell, J. A. (2018). Toxicity of nanomaterials. In R. C. Gupta (Ed.), *Veterinary toxicology* (3rd ed., pp. 319–326). Academic Press. https://doi.org/10.1016/B978-0 -12-811410-0.00018-0

Vasylechko, V. O., Klyuchivska, O. Y., Manko, N. O., Gryshchouk, G. V., Kalychak, Y. M., Zhmurko, I. I., & Stoika, R. S. (2020). Novel nanocomposite materials of silver-exchanged clinoptilolite with pre-concentration of $Ag(NH3)^{2+}$ in water possess enhanced anticancer action. *Applied Nanoscience, 10*, 4869–4878. https://doi.org/10.1007/s13204-020-01353-7

Walker, D. B. (2006). Serum chemical biomarkers of cardiac injury for nonclinical safety testing. *Toxicologic Pathology, 34*(1), 94–104. https://doi.org/10.1080/01926230500519816

Yang, Z., Kang, S. G., & Zhou, R. (2014). Nanomedicine: de novo design of nanodrugs. *Nanoscale, 6*(2), 663–677. https://doi.org/10.1039/c3nr04535h

Zaichenko, A. S., Voronov, S. A., Kuzayev, A. I., Shevchuk, O. M., & Vasilyev, V. P. (1998). Control of microstructure and molecular weight distribution of carbon-chain heterofunctional oligoperoxidic curing agents. *Journal of Applied Polymer Science, 70*(12), 2449–2455. https:// doi.org/10.1002/(SICI)1097-4628(19981219)70:12<2449:AID-APP17>3.0.CO;2-D

Zhang, F., Zhu, L., Liu, G., Hida, N., Lu, G., Eden, H. S., et al. (2011). Multimodality imaging of tumor response to doxil. *Theranostics, 1*, 302–309. https://doi.org/10.7150/thno/v01p0302

Zhang, Q., Kusaka, Y., Sato, K., Nakakuki, K., Kohyama, N., & Donaldson, K. (1998). Differences in the extent of inflammation caused by intratracheal exposure to three ultrafine metals: Role of free radicals. *Journal of Toxicology and Environmental Health. Part A, 53*(6), 423–438. https:// doi.org/10.1080/009841098159169

Zhao, S., & Iyengar, R. (2012). Systems pharmacology: Network analysis to identify multiscale mechanisms of drug action. *Annual Review of Pharmacology and Toxicology, 52*, 505–521. https://doi.org/10.1146/annurev-pharmtox-010611-134520

Bioimaging, Biocompatibility, and Functioning of Polymeric Nanocarriers for Gene Delivery

Nataliya Finiuk, Nataliya Mitina, Alexander Zaichenko, and Rostyslav S. Stoika

Abbreviations

AEM	aminoethyl methacrylate
BA	butyl acrylate
CMV	cytomegalovirus
DEAE	diethylethanolamine
DMAEMA	(2-dimethylamino)ethyl methacrylate
DNA	deoxyribonucleic acid
F8MA	octafluoropentyl methacrylate
FA	folic acid
GARD	Genetic and Rare Diseases Information Center
GFP	Green Fluorescent Protein
GMA	glycidyl methacrylate
GO	graphene oxide
LB media	Luria-Bertani media
LMA	lauryl methacrylate
MA	maleic acid
miRNA	microRNA
MP	1-isopropyl-3(4)-[1-(tert-butyl peroxy)-1-methylethyl] benzene
mPEG	poly(ethylene glycol) methyl ether
mRNA	messenger ribonucleic acid
NCATS	National Center for Advancing Translational Sciences
NVP	N-vinylpyrrolidone
PAH	polyallylamine hydrochloride

N. Finiuk · R. S. Stoika (✉)
Institute of Cell Biology of National Academy of Sciences of Ukraine, Lviv, Ukraine

N. Mitina · A. Zaichenko
Lviv Polytechnic National University, Lviv, Ukraine

pDNA   plasmid DNA
PEG   poly(ethylene glycol)
PEGMA   poly(ethylene glycol)monomethyl ether methacrylate
PEI   polyethyleneimine
pHEMA   poly(2-hydroxyethyl methacrylate)
PLGA   poly(lactide-co-glycolide)
siRNA   small interfering ribonucleic acid
VA   vinyl acetate
VEP   5-tert butylperoxy-5-methyl-l-hexene-3-yne.

1   Introduction

According to the Genetic and Rare Diseases Information Center (GARD) and Global Genes®, dysfunctional genes are responsible for 80% of the reported 7136 diseases. Approximately, 30 million people in the United States and more than 300 million people in the rest of the world suffer from genetic diseases, and half of them are children. According to the National Center for Advancing Translational Sciences (NCATS), only 500 human diseases are sensitive to treatment with available 10,000 drugs. Thus, a necessity in developing new drugs and treatment remedies exists. The gene therapy provides a treatment option by rewriting or fixing errors in the natural genetic pattern. Currently, gene therapy covers less than one percent of the total $1.2 trillion world annual pharmaceutical market, and this market extends. The market of anticancer gene therapy products had reached $289 million in 2016, and it is expected to reach $2082 million by 2023. Typically, DNA, anti-sense oligonucleotides, mRNA, siRNA, and miRNA are the genetic materials most frequently used for therapeutic delivery into a defective target cell or tissue in order to restore a specific gene function or turn off a gene responsible for the development of disease or disorder (Goswami et al., 2019). In 2026, a financial forecast for the development of the world market of nano-pharmaceutical products is expected to increase to over 79 billion USD ('Global Nanopharmaceutical Drugs Market—Analysis and Forecast, 2018–2026' reported by BIS Research, https://www.prnewswire.com/news-releases/global-nanopharmaceutical-drugs-market-is-expected-to-reach-79-29-billion-by-2026-832020991.html).

As of March 19, 2021, in the international PubMed database, there were 167,910 articles noted with the keywords "drug delivery systems" and 207,304 articles with "gene delivery systems." The first article on the "gene delivery system" topic was published in 1997. Thus, gene delivery is really a hot topic in both the academic research and world pharmaceutical market.

The main consumers of systems proposed for the delivery of genetic materials to cells are biotechnology and medicine. The main goal of biotechnology is to create new products and increase the production of well-known products that are scarce and/or in accordance with the demands of the market. The microorganisms capable of producing biologically active and technologically important substances are in the

first place among such producers. Plants rank second, after microorganisms, as commonly used producers. However, there are some problems when applying the constructs of the microbial origin for the delivery of genetic materials at creating new biological products. There is a gradual increase in such production by the mammalian cells, but methodological problems still exist.

In medicine, gene therapy based on the delivery of genetic materials into human cells is undoubtedly the most effective treatment, especially for patients with hereditary and oncological diseases, whose pathological conditions are directly associated with a deficiency or damage of specific gene(s), which results in lack of active protein product or expression of the product with inappropriate functions. The creation of the gene bank of extinct organisms for further reproducing the gene pool of those organisms is another promising biotechnological direction that is based on a delivery of the alien genes to cells.

2 Principal Methods for Delivery of Nucleic Acids Into Target Cells

A big problem that is encountered during the delivery of nucleic acid to cells is the presence of the phosphoric acid residues in the nucleotides causing a negative electric charge of the nucleic acids. Due to the glycol epitopes that are a part of the membrane components, the plasma membrane that surrounds the cells also possesses a negative charge, which impedes the penetration of the molecules of the nucleic acids into the cells (Fig. 1). Besides, the cells covered with a double layer of
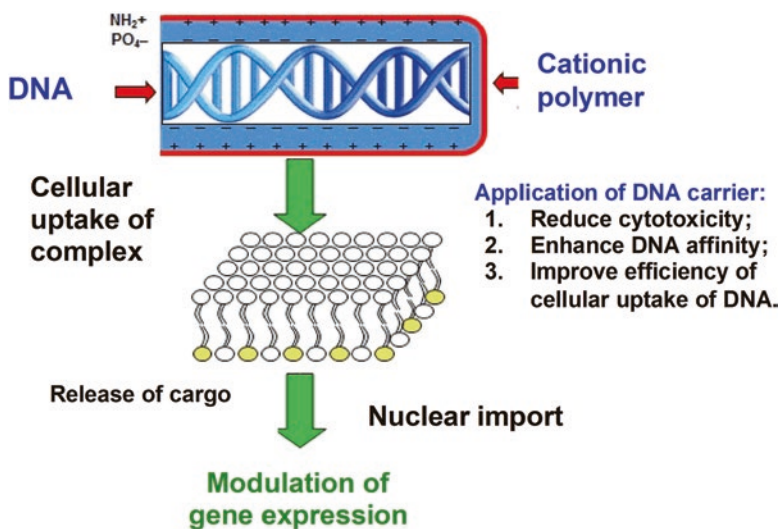
Fig. 1 Schematic structure and principle of the application of the nanoscale carrier for DNA delivery into cells. (Reproduced with permission of Stoika (2018))

Biological methods	Physical methods	Chemical methods
• Viral vectors	• Electroporation • Microinjection • Biolistic gene delivery • Magnetofection	• Calcium phosphate • Cationic polymers • Cationic lipids • DEAE-Dextran • Dendrimers

Fig. 2 Different methods for gene delivery to target cells

phospholipids possessing hydrophobic properties are unpenetratable for the nucleic acids which have pronounced hydrophilic properties. Therefore, the nucleic acids under delivery should overcome this natural barrier in order to modulate gene expression (Upadhyay, 2014; Cunningham et al., 2018; Glover et al., 2007).

Several approaches have been proposed to promote the penetration of different biomolecules, including foreign genetic material, through the cell surface (Fig. 2). In our analysis, only the transportation of nucleic acids inside the cell will be discussed.

Viruses are known to inject their nucleic acid into the infected cells. The *biological methods* of delivery of nucleic acid to cells using viral constructs that avoid a direct viral infection were developed. Up until now, the viral-related methods of gene delivery were shown to be the most effective methods of genetic transformation (Goswami et al., 2019; Jayant et al., 2016). However, there is a minimal, but a theoretically possible, risk of the effect of viral genetic elements (promotors) on the expression of cellular genes at the transportation of a nucleic acid by the carrier inside the cell. Therefore, despite the several advantages of viral delivery of genetic materials (high efficiency of transfection, including the transfection of cells that are difficult to be transformed), this method has serious drawbacks, in particular, associated with the biosafety issues, technical complexity, and the need for specially trained personnel and isolated laboratory facilities, as well as a long time needed to carry out such experiments (Sung & Kim, 2019; Jayant et al., 2016).

There are several *physical methods* used for the delivery of nucleic acids to cells. They require application of special equipment, sometimes very expensive, that is considered a big drawback of these methods. Another disadvantage of physical methods is a high possibility of damaging target cells that may lead to their death, thereby reducing the transfection efficiency. Electroporation is the most common among the physical methods used for gene delivery. The principle of this method is

to put cells into a special chamber (cuvette) with aluminum electrodes, where for a short time pores arise in the bilayer lipid membrane of cells under electric field, and at that moment, the macromolecules that are present in the medium (e.g., DNA or RNA) can enter into the cells. Electroporation is applied to treat cells resistant to transfection. Despite the need for using electroporation devices, this method is relatively simple and quick in implementation. The disadvantages of this method are: requirement of special equipment, the necessity to optimize the parameters of the transfection process for cells of a certain type, and a possibility of irreversible damage to cellular membrane that can lead to cell destruction (Shi et al., 2018; Wells, 2004).

The biolistic method of DNA delivery uses "shooting" of the particles with the so-called "gene gun," providing a possibility of rapid transient transfection of cells (the advantage of this method). The major drawbacks are the need for rather expensive equipment, the "gene gun," high rate of death of target cells, and often low efficiency of cell transfection (Wells, 2004).

Based on the literature data, the *chemical transfection methods* look to be optimal in terms of their price/quality and advantages/drawbacks characteristics. The advantages of DNA delivery with *calcium phosphate* or *DEAE-dextran* carriers are low cost of reagents and a versatility of application for different cell types, while the disadvantages are the lack of stability of the reagents, often low efficiency of the transfection, the lack of reproducibility of transfection results, and, in some cases, their toxicity in target cells (Kumar et al., 2018; Onishi et al., 2007). The DEAE-dextran is suitable only for transient transfection and calcium phosphate is not applicable for in vivo transfection.

Application of the *cationic lipids* provides some advantages in the achievement of reproducibility of transfection results. These DNA carriers are suitable for different cell lines, they provide high transfection efficiency, are easy to use, and allow rapid transfection procedure. The disadvantages include the need of optimization of the transfection conditions, as well as a resistance to transfection in some types of cells. In addition, the transfection efficiency may vary significantly for different cell types, and some of these polymers are toxic to individual types of target cells.

The *cationic polymers* were suggested to be the most promising carriers for gene delivery into target cells (Rai et al., 2019; Santo et al., 2017; Bae et al., 2017; Agarwal et al., 2012). These carriers are safer than the viral ones and efficient enough in cell transfection. In addition, the polymeric carriers possess greater flexibility in choosing the size of gene cargo, and they cause less immunological and allergenic responses in the organism. The poly(L-lysine) (Byrne et al., 2013), polyethyleneimine (PEI) (Xiao et al., 2019), diethylaminoethyl-dextran (Onishi et al., 2007), poly(amidoamine) dendrimers, poly(2-dimethylamino)ethyl methacrylate (poly-DMAEMA) (Agarwal et al., 2012), chitosan (Lebre et al., 2016), and polyplexes (DNA complexes with the cationic polymers) are the synthetic polymers most widely used for gene delivery into the mammalian cells (Table 1). The literature search for the "non-viral vectors" showed that these carriers were effective at fighting cancer and cardiovascular diseases (Hidai & Kitano, 2018; Hardee et al., 2017).

Table 1 Overview of different polymeric carriers for gene delivery

Polymer	Cargo	Target	References
Polyethyleneimine and PEI-based	DNA, siRNA, oligonucleotides	Mammalian cells in vitro and in vivo, neurodegenerative disease	Conte et al. (2020), Daryabari et al. (2020), Hao et al. (2019), Helmschrodt et al. (2017), Jayant et al. (2016), Kong et al. (2017), Lungwitz et al. (2005), Nimesh (2012), Plianwong et al. (2020), Sahin et al. (2014), Wang et al. (2016), Xiao et al. (2019), Zhupanyn et al. (2019)
Poly(L-lysine)	DNA, siRNA	Mammalian cells in vitro and in vivo	Kodama et al. (2017), Pichon et al. (2002), Wang et al. (2018)
Poly(lactide-co-glycolide) (PLGA)-based	DNA, miRNA	Mammalian cells in vitro	Gwak et al. (2017), Mishra et al. (2011, 2014)
Poly(amino amine)-based	DNA	Mammalian cells in vitro	Mateos-Timoneda et al. (2008), Ping et al. (2013), Sun et al. (2017), van der Aa et al. (2014), Xing et al. (2019)
Poly(N,N-dimethylaminoethyl methacrylate)-based	DNA, miRNA, siRNA	Mammalian cells in vitro, primary human T cells	Cordeiro et al. (2017), Mendrek et al. (2014, 2015), Newland et al. (2013), Olden et al. (2018), Qian et al. (2013, 2014), Tan et al. (2015), Werfel et al. (2017), Xie et al. (2018). Zhang et al. (2012, 2013)
Poly(β-amino ester)s	DNA	Mammalian cells in vitro and in vivo	Cordeiro et al. (2017, 2019), Liu, et al. (2019b), Zhou et al. (2016a, (2016b)
Dendrimers (e.g., poly(amidoamine))	siRNA, DNA	Mammalian cells in vitro and in vivo	Arima et al. (2010), Kong et al. (2016), Nam et al. (2012)
Chitosan	DNA	Mammalian cells in vitro and in vivo	Arima et al. (2010), Kashkouli et al. (2019), Kulkarni et al. (2017), Liu et al. (2019a), Rahmani et al. (2019)

3   Novel Synthetic Poly-DMAEMA Carriers for Delivery of Plasmid DNA Into Target Cells: Characteristics and Activity

Earlier, a series of poly-DMAEMA carriers were synthesized at the Department of Organic Chemistry at Lviv National Polytechnic University (Zaichenko et al., 2000, 2001, 2008; Miagkota et al., 2014; Paiuk et al., 2019) (Fig. 3). They demonstrated high effectiveness in gene delivery to yeast (Filyak et al., 2013), plant cells (Finiuk et al., 2017; Buziashvili et al., 2015; Finiuk et al., 2014), and mammalian cells (Paiuk et al., 2019; Ficen et al., 2013) (Table 2).
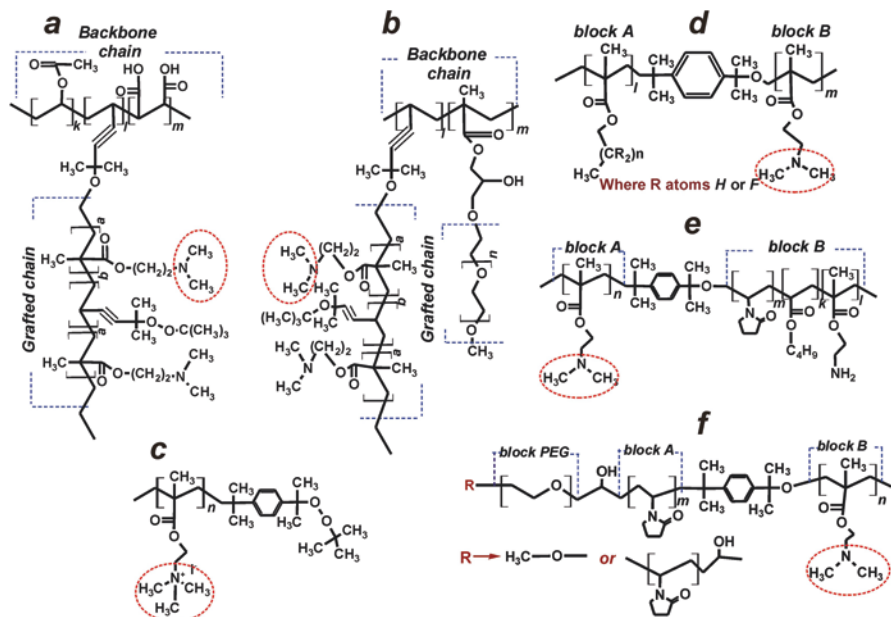
Fig. 3 Poly-DMAEMA copolymers used for DNA (oligonucleotides) delivery (the choice of copolymers was done due to the possibility of their additional functionalization): (**a**) poly(VA-*co*-VEP-*co*-MA)-*graft*-poly(DMAEMA-*co*-VEP) (BG-2 with M_n = 10 kDa and BG-2l with M_n = 30 kDa) (basic chain – anionic, side – cationic); (**b**) poly(VEP-*co*-GMA)-*graft*-mPEG-graft-poly(DMAEMA-*co*-VEP) (BG-2m with M_n = 250 kDa); (**c**) quaternized poly(DMAEMA)-MP (5Dq with M_n = 5 kDa); (**d**) poly(LMA)-*block*-poly(DMAEMA) (LA-DM with M_n = 32 kDa) or poly(F8MA)-*block*-poly(DMAEMA) (FMA8-DM with M_n = 18 kDa); (**e**) poly(DMAEMA)-*block*-poly(NVP-*co*-BA-*co*-AEM) (TN 83/5c with Mn = 11 kDa); (**f**) mPEG(PEG)-*block*-poly(NVP)-*block*-poly(DMAEMA) (LM-8-DM with M_n = 4 kDa and DLM-9-DM with M_n = 5 kDa). Red circle indicates potential centers of polymer–plasmid DNA binding. *Comments*: polymer links: VA vinyl acetate, VEP 5-tert butylperoxy-5-methyl-l-hexene-3-yne, MA maleic acid, GMA glycidyl methacrylate, mPEG poly(ethylene glycol) methyl ether, M_n = 750 Da, PEG poly(ethylene glycol), M_n = 600 Da, LMA lauryl methacrylate, F8MA octafluoropentyl methacrylate, NVP N-vinylpyrrolidone, BA butyl acrylate, AEM aminoethyl methacrylate, MP 1-isopropyl-3(4)-[1-(tert-butyl peroxy)-1-methylethyl] benzene. In round circles on the scheme are chemical groups with positive charge

Chemical structures of different poly-DMAEMA carriers capable of gene delivery to cells of various types of organisms—from bacteria, to yeast, plants, and mammals—are shown in Fig. 3. As one can see, all these polymers contain the primary amine group or its methylated derivatives, which provide a positive charge of the corresponding polymers necessary for the interaction and binding with negatively charged phosphoric groups of the nucleotides in the structure of DNA or RNA.

The physicochemical characteristics of novel poly-DMAEMA carriers and their complexes with DNA demonstrate a higher surface activity of such complexes compared to the surface activity of the solution of native DNA. That contributes to better

Table 2 Examples of application of poly-DMAEMA polymers for gene delivery

Polymer	Target	Gene delivery efficacy	Reference
Low molecular weight cationic poly(DMAEMA) carrier	Mouse lymphocytic leukemia L1210 cells	Poly-DMAEMA in the complexes with antisense-oligodeoxynucleotides (asODNs) caused reduction of cellular prion (PrPC) expression level content by 70–90% in L1210 cells in vitro	Ivanytska et al. (2011)
Copolymer of DMAEMA with vinyl acetate (VA), 5-(tertbutylperoxy)-5-methyl-1-hexen-3-yne (VEP), and maleic anhydride (MA) (marked as BG-2)	Yeasts *Hansenula (Ogataea) polymorpha, Pichia pastoris, Saccharomyces cerevisiae*	Polymer was more efficient and reproducible than Lithium acetate and electroporation methods of genetic transformation of yeast	Filyak et al. (2013)
BG-2 polymer	Human cervix epithelioid carcinoma HeLa cells	BG-2 at 7.5μg/mL showed transfection efficiency of 6×10^4 RLU/mg protein. The GFP expression was detected after HeLa transfection with BG-2/pEGFP-N1 complex	Ficen et al. (2013)
PEGylated BG-2 polymer (marked as BG-2m)	Moss *Ceratodon purpureus* (Hedw.) Brid. protoplasts	One stable moss transformant was selected under application of BG-2m and 5Dq carriers, and 11 transformants – under application of 83/5 polymer	Finiuk et al. (2014)
Poly(DMAEMA)-MP (1-isopropyl-3(4)-[1-(tert-butylperoxy)-1-methylethyl] benzene) (marked as 5Dq)			
Poly(DMAEMA)-block-oligo(N-vinylpyrrolidone (NVP)-co-butyl acrylate(BA)-co-2-aminoethyl methacrylate hydrochloride (AEM) (marked as 83/5)			
BG-2, BG-2q (with quaternary amine groups), BG-2f (with phosphatidylcholine), BG-2c (synthesized in ethanol), BG-2cq, BG-2cf	Tobacco *Nicotiana tabacum* L. protoplasts	*N. tabacum* protoplasts efficiency was 1–10.5% under application of BG-2cf, BG-2c, BG-2f, BG-2q, BG-2cq, BG-2 polymers	Buziashvili et al. (2015)

Table 2 (continued)

Polymer	Target	Gene delivery efficacy	Reference
Poly(DMAEMA)-block-oligo(NVP-co-BA-co-AEM) (TN83/6)	Moss *C. purpureus,* and tobacco *N. tabacum* protoplasts	Carriers were effective in plasmid DNA delivery into moss and tobacco protoplasts. Polymers 83/6 and 84/5 were more effective for moss and tobacco transformation than PEG-containing block polymers DLM-9-DM and LM-8-DM	Finiuk et al. (2017)
Poly(NVP-co-VA-co-HEMA)-block- oligo(NVP-co-BA-co-AEM) (TN 84/5)			
PEG-block-poly(NVP)-block-poly(DMAEM) (LM-8-DM)			
Poly(NVP)-blok-PEG-block-poly(NVP)- block-poly(DMAEM) (DLM-9-DM)			
Poly(fluoropentyl methacrylate)-block-poly(DMAEMA)-isopropyl benzene (FMA-DM)	Human breast adenocarcinoma MCF-7 cells	Polymer with less number of fluorine atoms and higher length of poly-DMAEMA was more effective in MCF-7 transfection with pEGFPc-1 plasmid	Paiuk et al. (2019)
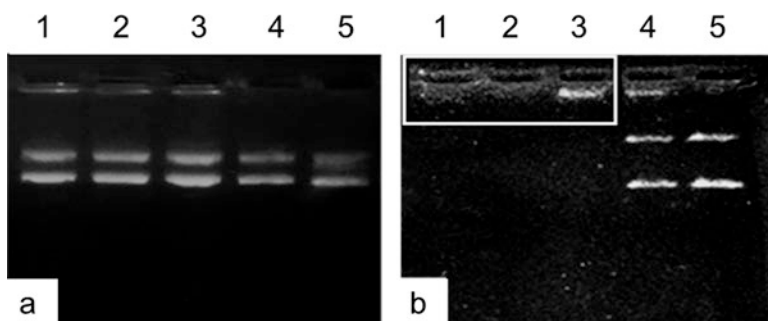
Fig. 4 Comparison of DNA binding properties of polymeric carriers BG-4 and 83/5: (**a**) BG-4 that does not bind DNA; (**b**) 83/5c that binds with plasmid DNA at the concentration of 0.01% and, therefore, inhibits DNA movement during electrophoresis. Lane 1—0.1%, 2—0.03%, 3—0.01%, 4—0.003%, 5—plasmid DNA pEGFPc-1

interaction of the DNA-loaded carriers with the surface of the target cells. A comparative study of the structure (scanning electron microscopy), colloid-chemical (electrophoresis), and spectral (turbidimetry, spectroscopy, dynamical light scattering) characteristics of new poly-ampholytic poly-DMAEMA-based carriers of the BG-2 type were conducted (Ficen et al., 2013; Filyak et al., 2013; Finiuk et al., 2012).

It was shown that poly-DMAEMA-based carriers effectively bound plasmid DNA (pDNA) with forming polyplexes and shielding the surface negative charge of the plasmid DNA (Fig. 4). The results of measuring zeta-potential of plasmid DNA, poly-ampholytic polymeric carriers, and their complexes with plasmid DNA are
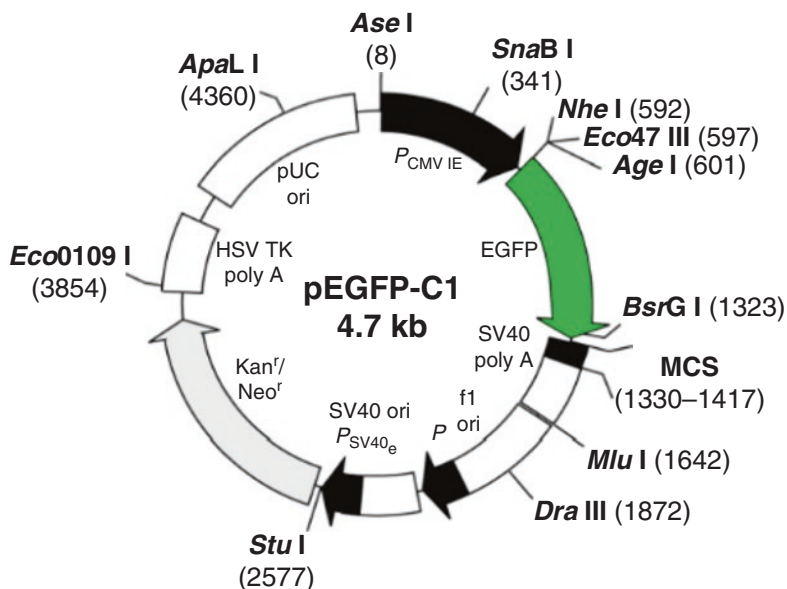
Fig. 5 Structure of the pEGFP-c1 plasmid DNA that encodes enhanced green fluorescence protein (GFP) under cytomegalovirus (CMV) promoter. (Data taken from https://www.addgene.org/44212/)

Table 3 Zeta-potential of synthetic poly-ampholytic nanocarriers and their complexes with plasmid DNA (pEGFPc-1)

	Size, nm	Zeta-potential, mV
BG-2	19.16	+30.6
BG-2/DNA	95.60	+35.4
BG-2c	27.29	+21.9
BG-2c/DNA	67.92	+40.8
BG-2l	20.46	+18.3
BG-2l/DNA	65.89	+26.4
Plasmid DNA	390.20	−2.98

presented in Table 3. As one can see, the pDNA in complex with the polymeric carrier (BG-2) possesses positive charge and also achieves more compact size (shape). Both these changes in pDNA properties contribute to its better uptake by the target cells. We have found that the polymer/pDNA complexes used for transfection of the mammalian cells were formed more effectively in culture medium without blood serum. In order to determine the efficiency of formation of such complexes of the polymeric carriers BG-4 and 83/5c, and plasmid DNA, the electrophoresis in the agarose gel was conducted (Fig. 4). In cases of the formation of these complexes, the retardation of plasmid DNA can be observed on the electrophoregram (Fig. 4b).

The lower the concentration of the polymer, the higher the effectiveness of its binding of the plasmid DNA for gene delivery.

In order to monitor the efficiency of incorporation of plasmid DNA in the nuclear chromatin and its functioning, such DNA is fused with the gene of GFP protein (Fig. 5).

The results of the expression of GFP as a fluorescent signal inside the treated MCF-7 cells are shown in Fig. 6. The ratio of GFP-labeled cells in total population of cells treated with the polymeric carrier loaded with plasmid DNA is an indicator of the efficiency of cell transfection (Table 4). As one can see, the human embryonic kidney cells of HEK293 line were the most sensitive to transfection by the applied plasmid DNA pEGFPc-1 delivered by the designed poly-DMAEMA carrier 83/5c. Human breast adenocarcinoma cells of MCF-7 line were also well accepting and expressing DNA delivered by the poly-DMAEMA carriers.

A comparison of the transfection efficiency of the traditional reagent, linear polyethyleneimine (PEI), and poly-DMAEMA 83/5c carrier in different human cell lines was conducted (Table 4). Both these transfection reagents demonstrated similar efficiencies. Another peculiarity is that the mammalian cell lines that are more resistant to poly-DMAEMA-based transfection, were also more resistant to PEI-based transfection.

The application of the GFP-based technique for monitoring cells transformed with a fused target gene is a convenient method that is also used for visualization of expression of specific gene(s) not only in cell culture, but also in tissues and organs of the organism. The discovery of green fluorescent protein provided a decisive impetus to the development of genetic engineering and biotechnology. Due to this discovery, it is possible to observe cells under the fluorescent microscope or use a mini-tomograph to visualize tissues and organs of the laboratory animals in which the foreign gene functions (this foreign gene should be fused with the *GFP* gene). There are also other approaches to reveal the function of foreign gene delivered by the polymeric platform. The enzymatic activity (if available in gene product) can be measured, or the immunodetection based on Western-blot analysis can be applied. Figure 7 presents the results of expression of growth inhibitor (p21 protein) whose DNA was delivered to human breast adenocarcinoma MCF-7 cells by means of the poly-DMAEMA carrier 83/5c.

The results of application of poly-DMAEMA-based carriers for delivery of plasmid DNA to the bacterial and yeast cells, correspondingly, are presented in Figs. 8 and 9. At using these carriers, in both types of the targeted cells, the effectiveness of genetic transformation was significantly higher than such effectiveness at using chemical method (PEI for bacteria or Lithium acetate for yeasts) or electroporation.

It was much more complicated to conduct a delivery of plasmid DNA to plant cells. In order to target plant cells, one first needs to destroy their outer cellulose shell, which can be done with the help of special hydrolytic enzymes. First, we have demonstrated the capacity of poly-DMAEMA-based carriers to target moss *Ceratodon purpureus* (Hedw.) Brid. (Finiuk et al., 2014; Finiuk et al., 2017) and then higher-organized plants such as tobacco (*Nicotiana tabacum* L.) (Buziashvili et al., 2015;
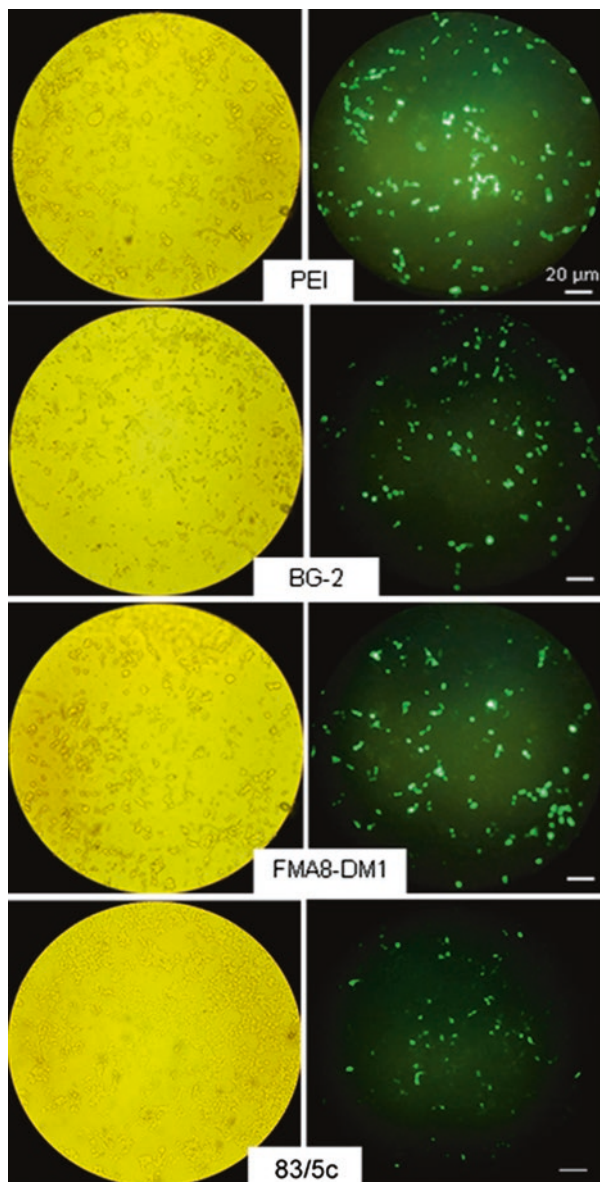
Fig. 6 Transfection efficiency of poly(DMAEMA) carriers (BG-2, FMA8-DM1, and 83/5c) and PEI complexed with plasmid pEGFPc-1 in human breast adenocarcinoma MCF-7 cells (48 h after transfection). Bar equals 20µm

Table 4 The efficiency of transfection of mammalian cells with different polymeric carriers of plasmid DNA

Cell line	Transfection efficiency	
	Carrier 83/5c, %	PEI, %
HEK 293 (human embryonic kidney cells)	44.5 ± 5.8	64.0 ± 7.9
MCF-7 (human breast adenocarcinoma cells)	34.5 ± 5.1	48.6 ± 5.7
HeLa (human cervical cancer cells)	14.6 ± 1.8	20.0 ± 2.4
HepG2 (human hepatocarcinoma cells)	12.0 ± 0.3	18.5 ± 2.3
U251 (human glioblastoma cells)	5.4 ± 0.9	14.7 ± 2.0
HCT 116 (human colon carcinoma cells)	2.0 ± 0.5	3.1 ± 0.5
A549 (human lung carcinoma cells)	2.0 ± 0.3	2.6 ± 0.8
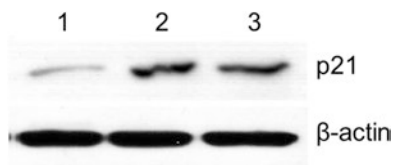
Fig. 7 The expression of p21 protein (inhibitor of cell growth) in human breast adenocarcinoma MCF-7 cells after transfection with poly-DMAEMA carrier 83/5c (2), PEI (3) on 48 h after transfection, and in not-transfected MCF-7 cells (1). Results of Western-blot analysis are presented
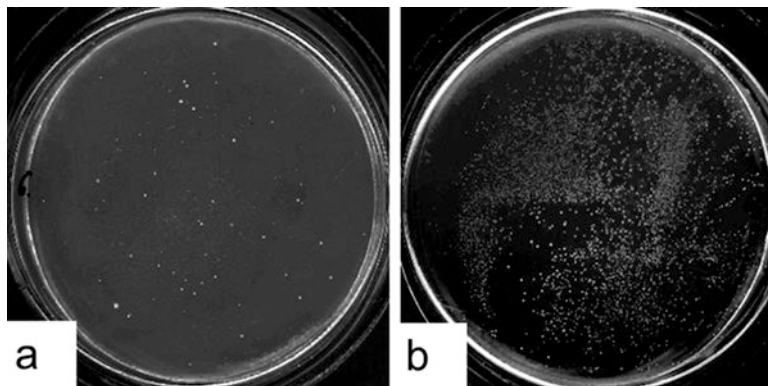
Fig. 8 The results of genetic transformation of *Escherichia coli DH5* after application of PEI (**a**) and 83/5c polymer (**b**) complexed with plasmid DNA (pPIC3.5). Bacteria transformants were selected on Luria-Bertani (LB) media supplemented with ampicillin antibiotic
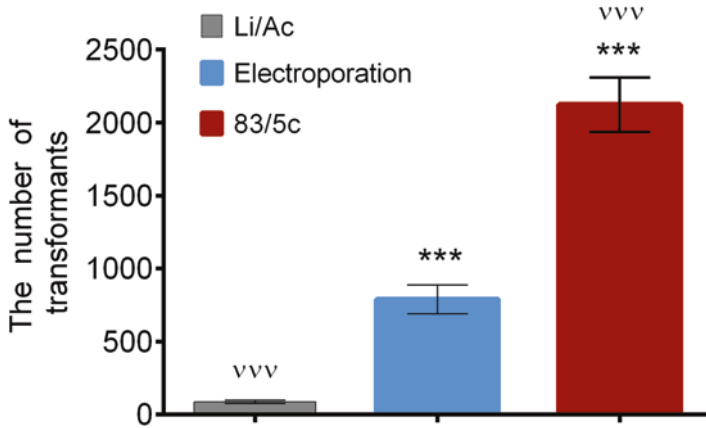
Fig. 9 Number of *Ogataea polymorpha* NCYC 495 leu1-1 yeast transformants obtained through different transformation methods. Lithium acetate (Li/Ac), electroporation, and 83/5c polymer-based transformation methods were compared using the circular plasmid pGLG578. Yeasts transformants were selected on G418 antibiotic-containing medium. ***$P < 0.001$ compare to Li/Ac transformation; $^{vvv}P < 0.001$ compare to electroporation
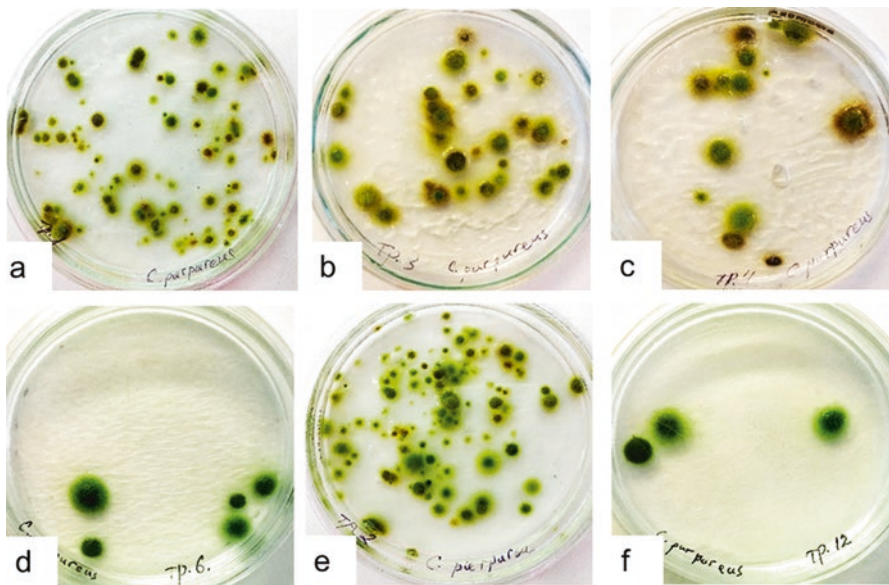
Fig. 10 Stable transformants of *C. purpureus* moss obtained by transformation with plasmid pSF3 complexed with different polymeric carriers: 83/5c (**a**), TN 83/6 (**b**); TN 84/5 (**c**), DLM-9-DM 9 (**d**), FMA8-DM1 (**e**), BG-2 (**f**). Selection of stable transformants was carried out on a selective medium containing hygromycin B antibiotic
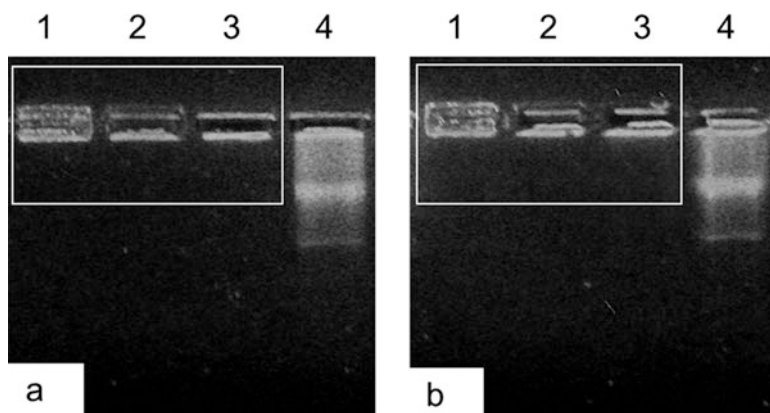
Fig. 11 Results of electrophoresis in the agarose gel of 0.1% polymers 83/5 (**a**), FMA8-DM1 (**b**) and their pDNA pEGFPc-1 complexes after incubation for 30 min with different concentrations of the DNase I. Lane 1—polymer/pDNA complex; 2—polymer/pDNA complex incubated with DNase I at 0.05 U/μg pDNA; 3—polymer/pDNA complex incubated with DNase I at 0.5 U/μg pDNA; 4—pDNA incubated with DNase I at 0.05 U/μg pDNA

Finiuk et al., 2017). The colonies of moss cells transformed with plasmid DNA pSF3 by means of various poly-DMAEMA 83/5c, TN 83/6, TN 84/5, DLM-9-DM 9, FMA8-DM1, BG-2 carriers to moss *C. purpureus* are shown in Fig. 10.

We have demonstrated that in complex with the poly-DMAEMA carriers, plasmid DNA is fully protected against the action of nucleases (Fig. 11).

Summarizing the results of characterization (structural, colloidal, chemical, and spectral) and evaluation of the transfection efficiency (gene delivery to cells of organisms of various taxonomic groups) of the synthetic poly-DMAEMA carriers, the following conclusions can be done: (1) poly-DMAEMA carriers form the micellar structures in a liquid medium; (2) due to the formation of a surface with electropositive charge, these micellar carriers form complexes with plasmid DNA; (3) as a part of such complexes, plasmid DNA is fully protected against the action of nucleases; (4) poly-DMAEMA carriers and polyethyleneimine possess similar efficiencies at transfection of different mammalian cells, including tumor cells.

4 Biosafety of Polymeric Nanoscale Carriers for Gene Delivery

The interrelations of biosafety versus transformation efficacy and biospecificity are the most important criteria for successful gene delivery to target cells. The gene delivery vector must interact with the therapeutic gene in such a way that it should provide stability to the cargo gene in the cellular environment (Jayant et al., 2016). The size, surface charge, shape, and surface functionality of gene carriers are
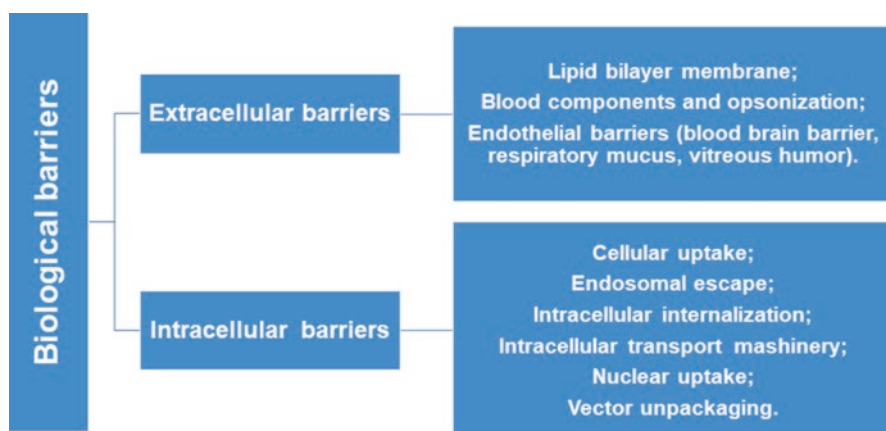
Fig. 12 The biological barriers that are crossed at gene delivery

critical for their efficient delivery, increased circulation time, and specific cellular entry (Cordeiro et al., 2019; Olden et al., 2018; Sunshine et al., 2011; Xie et al., 2018). Thus, the success of the nonviral gene transfer is dependent on enhanced crossing of various extra- and intracellular barriers (Fig. 12).

The carrier forms a stable complex with its nucleic acid (DNA or RNA) in order to protect it from extracellular degradation, circumvent cell barriers and be internalized (typically via receptor-mediated endocytosis and/or nonspecific endocytosis), escape the degradation in endosomes and lysosomes, and release its cargo in the nucleus or cytoplasm (Sunshine et al., 2011). The breakdown of nuclear membrane (during mitosis or under special agent/instrument) might improve cell transfection efficiency. The plasmid DNA can enter the nucleus through the nuclear pore complexes (NPCs) when these complexes are coupled to nuclear localization signals (Lam & Dean, 2010).

The poly-DMAEMA carriers and polyethyleneimine were shown to possess similar cytotoxicity at doses used for DNA delivery; however, at higher doses, the polyethyleneimine was more toxic (Fig. 13, Finiuk et al., 2013; Ficen et al., 2013; Paiuk et al., 2019).

The gene delivery carriers should not possess the genotoxicity that destroys the effectiveness of their action. To measure potential genotoxic effects, the Ames and ana-telophase tests are used. It was shown that the poly-DMAEMA carriers do not possess a mutagenic effect that could be dangerous for the mammalian cells (Finiuk et al., 2013, 2017, 2020).

The poly-DMAEMA carriers did not trigger gene mutations in *Salmonella typhimurium,* namely TA98 and TA100, in the Ames test (Fig. 14; Finiuk et al., 2013, 2020). At the action of the studied polymeric carriers FMA8-DM1, 83/5c, DLM-9-DM 9, no mutagenic effect was revealed, since the mutagenicity coefficient did not exceed 1.3 in the Ames test (either in the absence or presence of S9 metabolic microsomal activation). While the PEG-6000 at 0.025% concentration is a
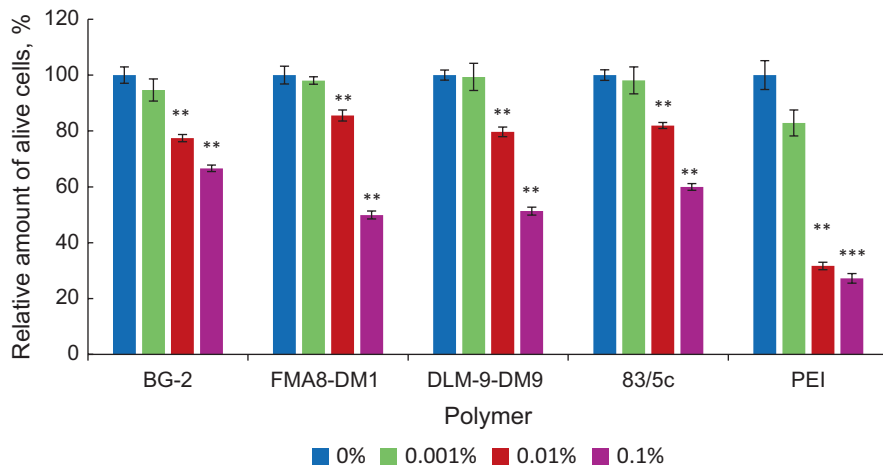
Fig. 13 Comparison of toxic effects of poly-DMAEMA carriers and polyethyleneimine (PEI) towards human breast adenocarcinoma MCF-7 cells on 48 h. $**P \leq 0.01$; $***P \leq 0.001$
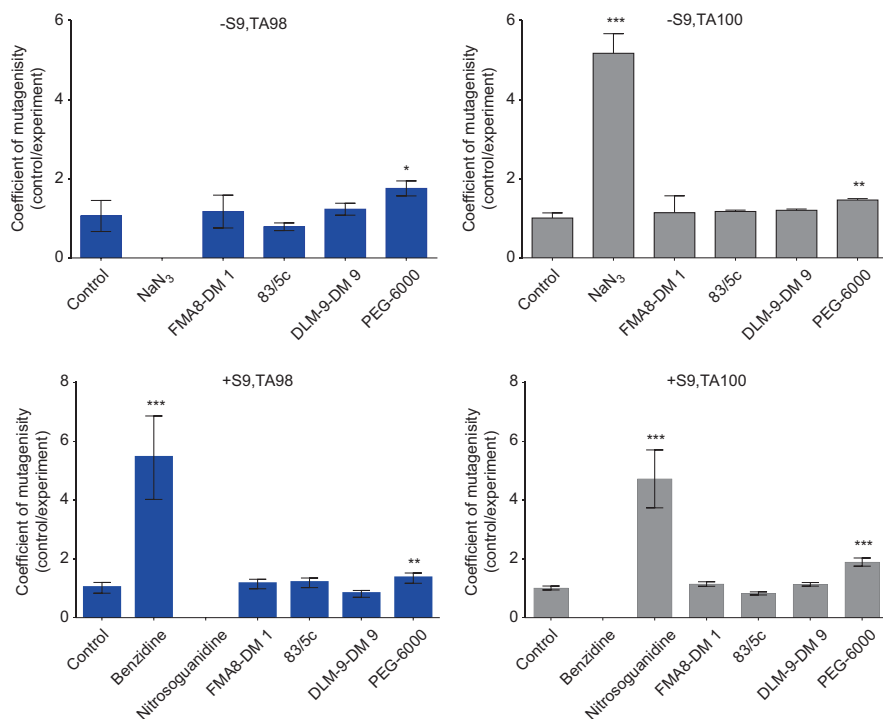
Fig. 14 The effect of poly-DMAEMA carriers (0.025%) toward growth and spontaneous mutation background in *S. typhimurium* TA 98 i TA 100 stains without S9 metabolic microsomal activation (-S9) and under the S9 metabolic microsomal activation (+S9). Benzidine (100 μg/plate), nitrosoguanidine (1 mg/plate), sodium azide (100 μg/plate), and PEG-6000 (0.025%) were used as positive controls. $*P \leq 0.05$; $**P \leq 0.01$; $***P \leq 0.001$

potentially mutagenic agent, the mutagenicity coefficient of PEG-6000 (0.025%) reached 1.89 for TA100 in the presence of S9 activation and 1.76 in the absence of S9 activation.

The results of the ana-telophase test in *Alium cepa* showed that PEG-containing block polymers DLM-9-DM and LM-8-DM used for gene delivery into plant cells possessed higher cytotoxicity and increased levels of the chromosomal aberrations compared to such effects of TN 83/6 and TN 84/5 polymeric carriers used in 0.001–0.1% concentrations. We suggested that the presence of PEG blocks in the structure of DLM-9-DM and LM-8-DM carriers could be responsible for the increased toxicity of these carriers for plant cells (Finiuk et al., 2017). The application of PEG as protoplast transformation agent was associated with an increased damage of protoplasts due to PEG-induced reversible destabilization of cell membrane (Assani et al., 2005; Burris et al., 2016; Masani et al., 2014). The copolymer of DMAEMA and poly(ethylene glycol)monomethyl ether methacrylate (PEGMA) was not stable and disintegrated into monomers at high salt concentrations or at a lower or physiological pH (Mazumder et al., 2014). Chemical modification or using branched structures, as well as low molecular weight of the polymers were shown to be favorable characteristics of the carriers (Agarwal et al., 2012; Samsonova et al., 2011; Schallon et al., 2010). Besides, poly(2-hydroxyethyl methacrylate) (pHEMA) blocks were reported to have additional fusogenic effects during interactions with cellular membranes enhancing the uptake of the polyplexes (Samsonova et al., 2011; Sunshine et al., 2011). The DLM-9-DM and LM-8-DM polymers possessing higher molecular weight demonstrated less effective binding of pDNA molecule with the carriers, comparing to TN 83/6 and TN 84/5 polymers (Finiuk et al., 2017).

Although many studies used nonviral gene delivery systems based on poly-DMAEMA, PEGylation of poly-DMAEMA reduced the cytotoxicity of these carriers for the mammalian cells (Agarwal et al., 2012; Guo et al., 2011). We did not reveal a significant difference in the toxicity of the PEGylated and non-PEGylated poly-DMAEMA toward the mammalian cells.

5 Hybrid Multifunctional Nanocarriers for Delivery of Drugs and Genetic Materials

Gene therapy has several mandatory requirements for nucleic acid (DNA, RNA) carriers. In particular, DNA molecules should penetrate the plasma membrane of the recipient cells, retain their structural and functional properties inside the cell after absorption by endocytosis, and penetrate the nucleus where DNA must be integrated into chromatin and transcribed to the informational RNA (Barry et al., 1999). A number of such carriers for the delivery of nucleic acids have been described, including polyethyleneimine (Lungwitz et al., 2005; Rudolph et al., 2005; Wang et al., 2006) [14-16], poly-L-lysine (Liu et al., 2010), dendrimers

(Marvaniya et al., 2010; Kong et al., 2016), liposomes (Tros de Larduya et al., 2010; Vhora et al., 2018), metal-containing nanomaterials (Riley & Vermerris, 2017), and this list is far from complete. The polymeric nanoscale carrier does not only provide high efficiency of delivery of nucleic acids to target cells, but also protects these biomolecules from the cleavage by the extracellular and intracellular nucleases, and assists in the addressed delivery of the targeted gene to cells.

The dendrimers are immensely branched, three-dimensional nanoscale macromolecules. They have chemical functional groups at the exterior terminal surface that offer wide opportunities for multiple interactions with several cargos (Fig. 15). This multifunctionality is necessary for the formation of various carrier-cargo complexes of wide applications (Madaan et al., 2014). The polymeric dendrimer used as a multifunctional drug delivery platform contains (Madaan et al., 2014): (1) small interfering RNA that blocks the functioning of matrix RNA that encodes the structure of a specific gene; (2) poly-ethylene glycol that prevents premature removal of drug complex by immune system cells; (3) an antibody as immunoglobulin molecule that recognizes a specific receptor on the surface of target cells; (4) folic acid that contributes to the effect of the complex on tumor cells; (5) a certain peptide that improves targeted action; (6) fluorescent dye, an optional element that is used for better visualization of the delivery, performance, and removing complex in the body; (7) contrasting factors used for identification of the complex by magnetic resonance imaging.

Another multifunctional hybrid nanocarrier was created on the basis of modified multilayer graphene oxide (GO) for gene therapy of the pancreatic cancer in the mouse (Yin et al., 2017). This nanocarrier (FA/PEG/GO) was proposed for delivery of the nucleic acids; however, it also contained the folic acid (FA, provides a predominant effect on tumor cells) attached to the amine group of the polyethylene glycol (NH_2-mPEG-NH_2), which improved water-solubility and biocompatibility of the nanocomplexes. For delivery of siRNA, graphene oxide containing attached FA/PEG complex was further functionalized with the PAH (polyallylamine
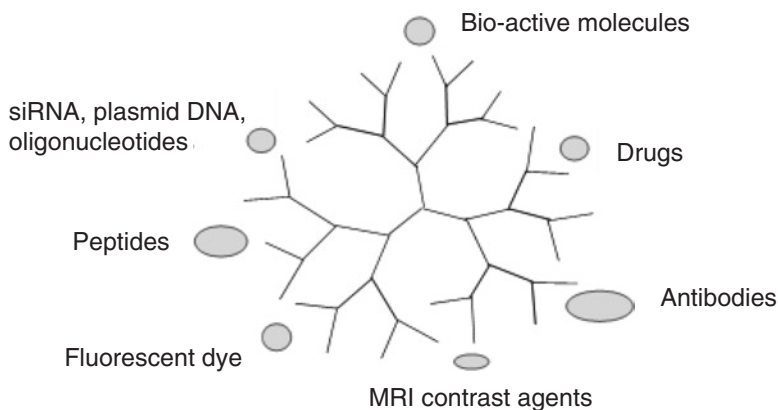
Fig. 15 Dendrimers as multifunctional nanoscale platforms for cargo delivery

hydrochloride) polymer with a positive charge. This GO/PEG/FA/PAH complex capable of delivering siRNA electrostatically interacts with the target cell surface, which has a negative charge (Yin et al., 2017).

The delivery of RNAs is more problematic than the DNA transfer, since RNA molecules are more susceptible to the destruction by the RNA-digesting enzymes that are present not only inside the cell, but also in the extracellular micro-environment. Thus, the multifunctional systems for simultaneous delivery of a drug and nucleic acid might be considered as peculiar biological nano-robots whose application is intended to improve, significantly, the efficiency and targeting of the therapeutic agents, and reduce their negative side effects in the body.

6   Conclusions

Despite high efficiency of transfection at using various multifunctional nanoscale polymeric carriers, a number of problems stay unsolved: (1) still low specificity of biodistribution of such carriers in the body; (2) premature biodegradation of cargo that significantly reduces the effectiveness of gene delivery; (3) immunogenicity and allergenicity of drug and gene delivery systems (this problem is poorly studied, unlike the cardio-, hepato-, nephro-, or neurotoxicity); (4) not enough information on the impact of nanomaterials on gene expression with hereditary consequences; (5) low reproducibility of preparation of both the synthetic and natural origin nano-carriers, which blocks their approval as medicines by the Food and Drug Administration (FDA); (6) delivery of small noncoding therapeutic RNAs still remains at the initial stage of development.

The polymeric nanoscale carriers demonstrated high effectiveness of binding plasmid DNA, transfection efficiency, as well as a potential for additional biofunc-tionalization to improve their addressed action.

The genotoxic action of novel polymeric nanoscale carriers for gene delivery should stop their further development, since otherwise, the biological sense in trans-porting the genetic materials is lost. At present, two known tests (Ames and Ana-telophase) are widely used to evaluate the genotoxic (mutagenic) effects of the carriers for gene delivery. The results of both these tests demonstrated the absence of such action in the created poly-DMAEMA carriers.

Chemical modifications of these carries allowed creating the universal gene delivery systems that possess high effectiveness of the genetic transformation of cell belonging to various taxonomic types, such as bacteria, yeast, plants, and mammals.

References

Agarwal, S., Zhang, Y., Maji, S., & Greiner, A. (2012). PDMAEMA based gene delivery materials. *Materials Today, 15*, 388–393. https://doi.org/10.1016/S1369-7021(12)70165-7

Arima, H., Yamashita, S., Mori, Y., Hayashi, Y., Motoyama, K., Hattori, K., … Uekama, K. (2010). *In vitro* and *in vivo* gene delivery mediated by Lactosylated dendrimer/alpha-cyclodextrin conjugates (G2) into hepatocytes. *Journal of Controlled Release, 146*(1), 106–117. https://doi.org/10.1016/j.jconrel.2010.05.030

Assani, A., Chabane, D., Haïcour, R., Bakry, F., Wenzel, G., & Foroughi-Wehr, B. (2005). Protoplast fusion in banana (Musa spp.): Comparison of chemical (PEG:polyethylene glycol) and electrical procedure. *Plant Cell. Tissue and Organ Culture, 83*, 145–151. https://doi.org/10.1007/s11240-005-4633-9

Bae, Y., Rhim, H., Lee, S., Ko, K., Han, J., & Choi, J. (2017). Apoptin gene delivery by the functionalized polyamidoamine dendrimer derivatives induces cell death of U87-MG glioblastoma cells. *Journal of Pharmaceutical Sciences, 106*, 1618–1633. https://doi.org/10.1016/j.xphs.2017.01.034

Barry, M. E., Pinto-Gonzalez, D., Orson, F. M., McKenzie, G. J., Petry, G. R., & Barry, M. A. (1999). Role of endogenous endonucleases and tissue site in transfection and CpG-mediated immune activation after naked DNA injection. *Human Gene Therapy, 10*(15), 2461–2480. https://doi.org/10.1089/10430349950016816

Burris, K., Dlugosz, E., Collins, G., Stewart, N., & Lenaghan, S. (2016). Development of a rapid, low-cost protoplast transfection system for switch grass (*Panicum virgatum* L.). *Plant Cell Reports, 35*, 693–704. https://doi.org/10.1007/s00299-015-1913-7

Buziashvili, A. Y., Finiuk, N. S., Stoika, R. S., Blume, Y. A. B., & Yemets, A. I. (2015). PDMAEMA based nanopolymers are promising vectors for delivery of genetic material into plant cells. *Factors of Experimental Evolution of Organisms, 17*, 117–120.

Byrne, M., Victory, D., Hibbitts, A., Lanigan, M., Heise, A., & Cryan, S. A. (2013). Molecular weight and architectural dependence of well-defined star-shaped poly(Lysine) as a gene delivery vector. *Biomaterials Science, 1*, 1223–1234. https://doi.org/10.1039/C3BM60123D

Conte, R., Valentino, A., Di Cristo, F., Peluso, G., Cerruti, P., Di Salle, A., & Calarco, A. (2020). Cationic polymer nanoparticles-mediated delivery of miR-124 impairs tumorigenicity of prostate cancer cells. *International Journal of Molecular Sciences, 21*(3), pii: E869. https://doi.org/10.3390/ijms21030869

Cordeiro, R. A., Santo, D., Farinha, D., Serra, A., Faneca, H., & Coelho, J. F. J. (2017). High transfection efficiency promoted by tailor-made cationic tri-block copolymer-based nanoparticles. *Acta Biomaterials, 47*, 113–123. https://doi.org/10.1016/j.actbio.2016.10.015

Cordeiro, R. A., Serra, A., Coelho, J. F. J., & Faneca, H. (2019). Poly(β-amino ester)-based gene delivery systems: From discovery to therapeutic applications. *Journal of Controlled Release, 310*, 155–187. https://doi.org/10.1016/j.jconrel.2019.08.024

Cunningham, F. J., Goh, N. S., Demirer, G. S., Matos, J. L., & Landry, M. P. (2018). Nanoparticle-mediated delivery towards advancing plant genetic engineering. *Trends in Biotechnology, 36*(9), 882–897. https://doi.org/10.1016/j.tibtech.2018.03.009

Daryabari, S. S., Fathi, M., Mahdavi, M., Moaddab, Y., Hosseinpour Feizi, M. A., Shokoohi, B., & Safaralizadeh, R. (2020). Overexpression of CFL1 in gastric cancer and the effects of its

silencing by siRNA with a nanoparticle delivery system in the gastric cancer cell line. *Journal of Cellular Physiology, 235*(10), 6660–6672. https://doi.org/10.1002/jcp.29562

Ficen, S. Z., Guler, Z., Mitina, N., Finiuk, N., Stoika, R., Zaichenko, A., & Ceylan, S. E. (2013). Biophysical study of novel oligoelectrolyte based non-viral gene delivery systems to mammalian cells. *Journal of Gene Medicine, 15*(5), 193–204. https://doi.org/10.1002/jgm.2710

Filyak, Y., Finiuk, N., Mitina, N., Bilyk, O., Titorenko, V., Hrydzhuk, O., … Stoika, R. (2013). A novel method for genetic transformation of yeast cells using oligoelectrolyte polymeric nanoscale carriers. *BioTechniques, 54*(1), 35–43. https://doi.org/10.2144/000113980

Finiuk, N. S., Vitak, T. Y., Mitina, N. Y., Filyak, Y. Z., Zaichenko, O. S., & Stoika, R. S. (2012). Polyplex formation by novel surface-active comb-like polyamfolytes and plasmid DNA. *Biotechnologia, 5*(6), 66–72. (in Ukrainian).

Finiuk, N. S., Filyak, Y. Z., Boiko, N. M., Mitina, N. Y., Zaichenko, O. S., & Stoika, R. S. (2013). Evaluation of cytotoxic and mutagenic action of novel surface-active comb-like polyampholytes that are used for delivery of nucleic acids to target cells. *Studia Biologica, 7*(2), 27–36. (in Ukrainian). https://doi.org/10.30970/sbi.0702.288

Finiuk, N., Chaplya, A., Mitina, N., Boiko, N., Lobachevska, O., Miahkota, O., Yemets, A. I., Blume, Y. B., Zaichenko, O. S., & Stoika, R. S. (2014). Genetic transformation of moss *Ceratodon purpureus* by means of polycationic carriers of DNA. *Cytology and Genetics, 48*(6), 345–351. https://doi.org/10.3103/S0095452714060048

Finiuk, N., Buziashvili, A., Burlaka, O., Zaichenko, A., Mitina, N., Miagkota, O., … Yemets, A. (2017). Investigation of novel oligoelectrolyte polymer carriers for their capacity of DNA delivery into plant cells. *Plant Cell, Tissue and Organ Culture, 131*(1), 27–39. https://doi.org/10.1007/s11240-017-1259-7

Finiuk, N., Romanyuk, N., Mitina, N., Lobachevska, O., Zaichenko, A., Terek, O., & Stoika, R. (2020). Evaluation of phytotoxicity and mutagenicity of novel DMAEMA-containing gene carriers. *Cytology and Genetics, 54*(5), 437–448. https://doi.org/10.3103/S0095452720050096

Glover, D. J., Glouchkova, L., Lipps, H. J., & Jans, D. A. (2007). Overcoming barriers to achieve safe, sustained and efficient non-viral gene therapy. *Advances in Gene, Molecular and Cell Therapy, 1*(2), 126–140.

Goswami, R., Subramanian, G., Silayeva, L., Newkirk, I., Doctor, D., Chawla, K., Chattopadhyay, S., Chandra, D., Chilukuri, N., & Betapudi, V. (2019). Gene therapy leaves a vicious cycle. *Frontiers in Oncology, 9*, 297. https://doi.org/10.3389/fonc.2019.00297

Guo, S., Huang, Y., Wei, T., Zhang, W., Wang, W., Lin, D., … Liang, X. J. (2011). Amphiphilic and biodegradable methoxy polyethylene glycol-block-(polycaprolactone-graft-poly(2-(dimethylamino)ethyl methacrylate)) as an effective gene carrier. *Biomaterials, 32*(3), 879–889. https://doi.org/10.1016/j.biomaterials.2010.09.052

Gwak, S. J., Macks, C., Bae, S., Cecil, N., & Lee, J. S. (2017). Physicochemical stability and transfection efficiency of cationic amphiphilic copolymer/pDNA polyplexes for spinal cord injury repair. *Scientific Reports, 7*(1), 11247. https://doi.org/10.1038/s41598-017-10982-y

Hao, F., Li, Y., Zhu, J., Sun, J., Marshall, B., Lee, R. J., Teng, L., Yang, Z., & Xie, J. (2019). Polyethylenimine-based formulations for delivery of oligonucleotides. *Current Medicinal Chemistry, 26*(13), 2264–2284. https://doi.org/10.2174/0929867325666181031094759

Hardee, C. L., Arévalo-Solizm, L. M., Hornsteinm, B. D., & Zechiedrich, L. (2017). Advances in non-viral DNA vectors for gene therapy. *Genes (Basel), 8*(2), pii: E65. https://doi.org/10.3390/genes8020065

Helmschrodt, C., Höbel, S., Schöniger, S., Bauer, A., Bonicelli, J., Gringmuth, M., Fietz, S. A., Aigner, A., Richter, A., & Richter, F. (2017). Polyethylenimine nanoparticle-mediated siRNA delivery to reduce α-Synuclein expression in a model of Parkinson's disease. *Molecular Therapy. Nucleic Acids, 9*, 57–68. https://doi.org/10.1016/j.omtn.2017.08.013

Hidai, C., & Kitano, H. (2018). Nonviral gene therapy for cancer: A review. *Diseases (Basel, Switzerland), 6*(3), 57. https://doi.org/10.3390/diseases6030057

Ivanytska, L. A., Stadnyk, V. V., Martyn, Y. V., Kozak, M. R., Fedorova, S. V., Shtapenko, O. V., … Vlizlo, V. V. (2011). Efficient method of prion gene silencing *in vitro* and *in vivo*

by antisense-oligodeoxynucleotides conjugated with new dimethylaminoethylmethacrylate oligoelectrolite. *Studia Biologica, 5*(3), 77–88. (in Ukrainian). https://doi.org/10.30970/sbi.0503.168

Jayant, R. D., Sosa, D., Kaushik, A., Atluri, V., Vashist, A., Tomitaka, A., & Nair, M. (2016). Current status of non-viral gene therapy for CNS disorders. *Expert Opinion on Drug Delivery, 13*(10), 1433–1445. https://doi.org/10.1080/17425247.2016.1188802

Kashkouli, K. I., Torkzadeh-Mahani, M., & Mosaddegh, E. (2019). Synthesis and characterization of a novel organosilane-functionalized chitosan nanocarrier as an efficient gene delivery system: Expression of green fluorescent protein. *International Journal of Biological Macromolecules, 125*, 143–148. https://doi.org/10.1016/j.ijbiomac.2018.11.145

Kodama, Y., Kuramoto, H., Mieda, Y., Muro, T., Nakagawa, H., Kurosaki, T., … Sasaki, H. (2017). Application of biodegradable dendrigraft poly-l-lysine to a small interfering RNA delivery system. *Journal of Drug Targeting, 25*, 49–57. https://doi.org/10.1080/1061186X.2016.1184670

Kong, L., Wu, Y., Alves, C. S., & Shi, X. (2016). Efficient delivery of therapeutic siRNA into glioblastoma cells using multifunctional dendrimer-entrapped gold nanoparticles. *Nanomedicine (London), 11*(23), 3103–3115. https://doi.org/10.2217/nnm-2016-0240

Kong, L., Qiu, J., Sun, W., Yang, J., Shen, M., Wang, L., & Shi, X. (2017). Multifunctional PEI-entrapped gold nanoparticles enable efficient delivery of therapeutic siRNA into glioblastoma cells. *Biomaterials Science, 5*(2), 258–266. https://doi.org/10.1039/c6bm00708b

Kulkarni, A. D., Patel, H. M., Surana, S. J., Vanjari, Y. H., Belgamwar, V. S., & Pardeshi, C. V. (2017). N,N,N-Trimethyl chitosan: An advanced polymer with myriad of opportunities in nanomedicine. *Carbohydrate Polymers, 157*, 875–902. https://doi.org/10.1016/j.carbpol.2016.10.041

Kumar, P., Nagarajan, A., & Uchil, P. D. (2018). DEAE-Dextran transfection. *Cold Spring Harbor Protocols, 2018*(7). https://doi.org/10.1101/pdb.top096263

Lam, A. P., & Dean, D. A. (2010). Progress and prospects: Nuclear import of nonviral vectors. *Gene Therapy, 17*(4), 439–447. https://doi.org/10.1038/gt.2010.31

Lebre, F., Borchard, G., Faneca, H., Pedroso de Lima, M. C., & Borges, O. (2016). Intranasal administration of novel chitosan nanoparticle/DNA complexes induces antibody response to hepatitis B surface antigen in mice. *Molecular Pharmaceutics, 13*, 472–482. https://doi.org/10.1021/acs.molpharmaceut.5b00707

Liu, G., Swierczewska, M., Lee, S., & Chen, X. (2010). Functional nanoparticles for molecular imaging guided gene delivery. *NanoToday, 5*(6), 524–539. https://doi.org/10.1016/j.nantod.2010.10.005

Liu, Q., Jin, Z., Huang, W., Sheng, Y., Wang, Z., & Guo, S. (2019a). Tailor-made ternary nanopolyplexes of thiolated trimethylated chitosan with pDNA and folate conjugated cis-aconitic amide-polyethylenimine for efficient gene delivery. *International Journal of Biological Macromolecules, pii S0141-8130*(19), 34853–34856. https://doi.org/10.1016/j.ijbiomac.2019.10.212

Liu, S., Gao, Y., Zhou, D., Zeng, M., Alshehri, F., Newland, B., … Wang, W. (2019b). Highly branched poly(β-amino ester) delivery of minicircle DNA for transfection of neurodegenerative disease related cells. *Nature Communications, 10*(1), 3307. https://doi.org/10.1038/s41467-019-11190-0

Lungwitz, U., Breunig, M., Blunk, T., & Göpferich, A. (2005). Polyethylenimine-based non-viral gene delivery systems. *European Journal of Pharmaceutics and Biopharmaceutics, 60*(2), 247–266. https://doi.org/10.1016/j.ejpb.2004.11.011

Madaan, K., Kumar, S., Poonia, N., Lather, V., & Pandita, D. (2014). Dendrimers in drug delivery and targeting: Drug-dendrimer interactions and toxicity issues. *Journal of Pharmacy and Bioallied Sciences, 6*(3), 139–150. https://doi.org/10.4103/0975-7406.130965

Marvaniya, H. M., Parikh, P. K., Patel, V. R., Modi, K. N., & Sen, D. J. (2010). Dendrimer nanocarriers as versatile vectors in gene delivery. *Journal of Chemical and Pharmaceutical Research, 2*(3), 97–108.

Masani, A., Noll, G., Kadir, G., Sambanthamurthi, R., & Prufer, D. (2014). Efficient transformation of oil palm protoplasts by PEG-mediated transfection and DNA microinjection. *PLoS One, 9*, e96831. https://doi.org/10.1371/journal.pone.0096831

Mateos-Timoneda, M. A., Lok, M. C., Hennink, W. E., Feijen, J., & Engbersen, J. F. (2008). Poly(amido amine)s as gene delivery vectors: Effects of quaternary nicotinamide moieties in the side chains. *ChemMedChem, 3*(3), 478–486. https://doi.org/10.1002/cmdc.200700279

Mazumder, M. A. J., Zahir, H., & Zaman, S. F. (2014). Advanced materials for gene delivery. *Advanced Materials Research, 995*, 29–47. https://doi.org/10.4028/www.scientific.net/AMR.995.29

Mendrek, B., Sieroń, L., Libera, M., Smet, M., Trzebicka, B., Sieroń, A. L., … Kowalczuk, A. (2014). Polycationic star polymers with hyperbranched cores for gene delivery. *Polymers, 55*(18), 4551–4562. https://doi.org/10.1016/j.polymer.2014.07.013

Mendrek, B., Sieroń, Ł., Żymełka-Miara, I., Binkiewicz, P., Libera, M., Smet, M., … Dworak, A. (2015). Nonviral plasmid DNA carriers based on N,N'-dimethylaminoethyl methacrylate and di(ethylene glycol) methyl ether methacrylate star copolymers. *Biomacromolecules, 16*(10), 3275–3285. https://doi.org/10.1021/acs.biomac.5b00948

Miagkota, O., Mitina, N., Nadashkevych, Z., Yanchuk, I., Greschuk, O., Hevus, O., & Zaichenko, A. (2014). Novel peroxide containing pegylated polyampholytic block copolymers. *Chemistry and Chemical Technology, 8*(1), 61–66.

Mishra, D., Kang, H. C., & Bae, Y. H. (2011). Reconstitutable charged polymeric (PLGA)(2)-b-PEI micelles for gene therapeutics delivery. *Biomaterials, 32*(15), 3845–3854. https://doi.org/10.1016/j.biomaterials.2011.01.077

Mishra, D., Kang, H. C., Cho, H., & Bae, Y. H. (2014). Dexamethasone-loaded reconstitutable charged polymeric (PLGA)n -b-bPEI micelles for enhanced nuclear delivery of gene therapeutics. *Macromolecular Bioscience, 14*(6), 831–841. https://doi.org/10.1002/mabi.201300432

Nam, H. Y., Nam, K., Lee, M., Kim, S. W., & Bull, D. A. (2012). Dendrimer type bio-reducible polymer for efficient gene delivery. *Journal of Controlled Release, 160*(3), 592–600. https://doi.org/10.1016/j.jconrel.2012.04.025

Newland, B., Abu-Rub, M., Naughton, M., Zheng, Y., Pinoncely, A. V., Collin, E., … Pandit, A. (2013). GDNF gene delivery via a 2-(dimethylamino)ethyl methacrylate based cyclized knot polymer for neuronal cell applications. *ACS Chemical Neuroscience, 4*(4), 540–546. https://doi.org/10.1021/cn4000023

Nimesh, S. (2012). Polyethylenimine as a promising vector for targeted siRNA delivery. *Current Clinical Pharmacology, 7*(2), 121–130.

Olden, B. R., Cheng, Y., Yu, J. L., & Pun, S. H. (2018). Cationic polymers for non-viral gene delivery to human T cells. *Journal of Controlled Release, 282*, 140–147. https://doi.org/10.1016/j.jconrel.2018.02.043

Onishi, Y., Eshita, Y., Murashita, A., Mizuno, M., & Yoshida, J. (2007). Characteristics of DEAE-dextran-MMA graft copolymer as a nonviral gene carrier. *Nanomedicine, 3*(3), 184–191. https://doi.org/10.1016/j.nano.2007.07.002

Paiuk, O., Mitina, N., Slouf, M., Pavlova, E., Finiuk, N., Kinash, N., … Zaichenko, A. (2019). Fluorine-containing block/branched polyamphiphiles forming bioinspired complexes with biopolymers. *Colloids and Surfaces B: Biointerfaces, 174*, 393–400. https://doi.org/10.1016/j.colsurfb.2018.11.047

Pichon, C., LeCam, E., Guérin, B., Coulaud, D., Delain, E., & Midoux, P. (2002). Poly[Lys-(AEDTP)]: A cationic polymer that allows dissociation of pDNA/cationic polymer complexes in a reductive medium and enhances polyfection. *Bioconjugate Chemistry, 13*(1), 76–82. https://doi.org/10.1021/bc015503o

Ping, Y., Wu, D., Kumar, J. N., Cheng, W., Lay, C. L., & Liu, Y. (2013). Redox-responsive hyperbranched poly(amido amine)s with tertiary amino cores for gene delivery. *Biomacromolecules, 14*(6), 2083–2094. https://doi.org/10.1021/bm400460r

Plianwong, S., Thapa, B., Kc, R. B., Kucharski, C., Rojanarata, T., & Uludağ, H. (2020). Enabling combinatorial siRNA delivery against apoptosis-related proteins with linoleic acid and

α-linoleic acid substituted low molecular weight polyethylenimines. *Pharmaceutical Research, 37*(3), 46. https://doi.org/10.1007/s11095-020-2770-9

Qian, Y., Zha, Y., Feng, B., Pang, Z., Zhang, B., Sun, X., … Jiang, X. (2013). PEGylated poly(2-(dimethylamino) ethyl methacrylate)/DNA polyplex micelles decorated with phage-displayed TGN peptide for brain-targeted gene delivery. *Biomaterials, 34*(8), 2117–2129. https://doi.org/10.1016/j.biomaterials.2012.11.050

Qian, X., Long, L., Shi, Z., Liu, C., Qiu, M., Sheng, J., … Kang, C. (2014). Star-branched amphiphilic PLA-b-PDMAEMA copolymers for co-delivery of miR-21 inhibitor and doxorubicin to treat glioma. *Biomaterials, 35*(7), 2322–2335. https://doi.org/10.1016/j.biomaterials.2013.11.039

Rahmani, S., Hakimi, S., Esmaeily, A., Samadi, F. Y., Mortazavian, E., Nazari, M., … Tehrani, M. R. (2019). Novel chitosan-based nanoparticles as gene delivery systems to cancerous and noncancerous cells. *International Journal of Pharmaceutics, 560*, 306–314. https://doi.org/10.1016/j.ijpharm.2019.02.016

Rai, R., Alwani, S., & Badea, I. (2019). Polymeric nanoparticles in gene therapy: New avenues of design and optimization for delivery applications. *Polymers, 11*, 745. https://doi.org/10.3390/polym11040745

Riley, M. K., & Vermerris, W. (2017). Recent advances in nanomaterials for gene delivery - a review. *Nanomaterials (Basel, Switzerland), 7*(5), 94. https://doi.org/10.3390/nano7050094

Rudolph, C., Ortiz, A., Schillinger, U., Jauernig, J., Plank, C., & Rosenecker, J. (2005). Methodological optimization of polyethyleneimine (PEI)-based gene delivery to the lungs of mice via aerosol application. *Journal of Gene Medicine, 7*(1), 59–66. https://doi.org/10.1002/jgm.646

Sahin, B., Fife, J., Parmar, M. B., Valencia-Serna, J., Gul-Uludağ, H., Jiang, X., Weinfeld, M., … Uludağ, H. (2014). siRNA therapy in cutaneous T-cell lymphoma cells using polymeric carriers. *Biomaterials, 35*(34), 9382–9394. https://doi.org/10.1016/j.biomaterials.2014.07.029

Samsonova, O., Pfeiffer, C., Hellmund, M., Merkel, O., & Kissel, T. (2011). Low molecular weight pDMAEMA-block-pHEMA block-copolymers synthesized via RAFT-polymerization: Potential non-viral gene delivery agents? *Polymers, 3*, 693–718. https://doi.org/10.3390/polym3020693

Santo, D., Cordeiro, R. A., Sousa, A., Serra, A., Coelho, J. F. J., & Faneca, H. (2017). Combination of poly[(2-dimethylamino)ethyl methacrylate] and poly(β-amino ester) results in a strong and synergistic transfection activity. *Biomacromolecules, 18*, 3331–3342. https://doi.org/10.1021/acs.biomac.7b00983

Schallon, A., Jérôme, V., Walther, A., Synatschke, C., Müller, A., & Freitag, R. (2010). Performance of three PDMAEMA-based polycation architectures as gene delivery agents in comparison to linear and branched PEI. *Reactive and Functional Polymers, 70*, 1–10. https://doi.org/10.1016/j.reactfunctpolym.2009.09.006

Shi, J., Ma, Y., Zhu, J., Chen, Y., Sun, Y., Yao, Y., … Xie, J. (2018). A review on electroporation-based intracellular delivery. *Molecules (Basel, Switzerland), 23*(11), 3044. https://doi.org/10.3390/molecules23113044

Stoika, R. S. (2018). Perspectives of development of the nanocarriers for delivery of genetic materials into cells. *Visnyk of National Academy of Sciences of Ukraine, 3*, 19–32. (in Ukrainian). https://doi.org/10.15407/visn2018.03.019

Sun, Y., Xian, L., Yu, J., Yang, T., Zhang, J., Yang, Z., … Ding, P. (2017). Structure-function correlations of poly(amido amine)s for gene delivery. *Macromolecular Bioscience, 17*(3). https://doi.org/10.1002/mabi.201600297

Sung, Y. K., & Kim, S. W. (2019). Recent advances in the development of gene delivery systems. *Biomaterials Research, 23*, 8. https://doi.org/10.1186/s40824-019-0156-z

Sunshine, J. C., Bishop, C. J., & Green, J. J. (2011). Advances in polymeric and inorganic vectors for nonviral nucleic acid delivery. *Therapeutic Delivery, 2*(4), 493–521. https://doi.org/10.4155/tde.11.14

Tan, J. K., Choi, J. L., Wei, H., Schellinger, J. G., & Pun, S. H. (2015). Reducible, dibromomaleimide-linked polymers for gene delivery. *Biomaterials Science, 3*(1), 112–120. https://doi.org/10.1039/c4bm00240g

Tros de Larduya, C., Sun, Y., & Düzgüneş, N. (2010). Gene delivery by lipoplexes and polyplexes. *European Journal of Pharmaceutical Sciences, 40*(3), 159–170. https://doi.org/10.1016/j.ejps.2010.03.019

Upadhyay, R. K. (2014). Drug delivery systems, CNS protection, and the blood brain barrier. *BioMed Research International, 2014*, 1–37. https://doi.org/10.1155/2014/869269

van der Aa, L. J., Vader, P., Storm, G., Schiffelers, R. M., & Engbersen, J. F. (2014). Intercalating quaternary nicotinamide-based poly(amido amine)s for gene delivery. *Journal of Controlled Release, 195*, 11–20. https://doi.org/10.1016/j.jconrel.2014.08.005

Vhora, I., Lalani, R., Bhatt, P., Patil, S., Patel, H., Patel, V., & Misra, A. (2018). Colloidally stable small unilamellar stearyl amine lipoplexes for effective BMP-9 gene delivery to stem cells for osteogenic differentiation. *AAPS PharmSciTech (An Official Journal of the American Association of Pharmaceutical Scientists), 19*(8), 3550–3560. https://doi.org/10.1016/10.1208/s12249-018-1161-6

Wang, Y., Chen, P., & Shen, J. (2006). The development and characterization of a glutathione-sensitive cross-linked polyethyleneimine gene vector. *Biomaterials, 27*(30), 5292–5298. https://doi.org/10.1016/j.biomaterials.2006.05.049

Wang, S., Zhang, J., Wang, Y., & Chen, M. (2016). Hyaluronic acid-coated PEI-PLGA nanoparticles mediated co-delivery of doxorubicin and miR-542-3p for triple negative breast cancer therapy. *Nanomedicine, 12*(2), 411–420. https://doi.org/10.1016/j.nano.2015.09.014

Wang, F., Pang, J. D., Huang, L. L., Wang, R., Li, D., Sun, K., Wang, L., & Zhang, L. M. (2018). Nanoscale polysaccharide derivative as an AEG-1 siRNA carrier for effective osteosarcoma therapy. *International Journal of Nanomedicine, 13*, 857–875. https://doi.org/10.2147/IJN.S147747

Wells, D. (2004). Gene therapy Progress and prospects: Electroporation and other physical methods. *Gene Therapy, 11*, 1363–1369. https://doi.org/10.1038/sj.gt.3302337

Werfel, T. A., Jackson, M. A., Kavanaugh, T. E., Kirkbride, K. C., Miteva, M., Giorgio, T. D., & Duvall, C. (2017). Combinatorial optimization of PEG architecture and hydrophobic content improves ternary siRNA polyplex stability, pharmacokinetics, and potency *in vivo*. *Journal of Controlled Release (Official Journal of the Controlled Release Society), 255*, 12–26. https://doi.org/10.1016/j.jconrel.2017.03.389

Xiao, Y. P., Zhang, J., Liu, Y. H., Zhang, J. H., Yu, Q. Y., Huang, Z., & Yu, X. Q. (2019). Low molecular weight PEI-based fluorinated polymers for efficient gene delivery. *European Journal of Medicinal Chemistry, 162*, 602–611. https://doi.org/10.1016/j.ejmech.2018.11.041

Xie, Y., Yu, F., Tang, W., Alade, B. O., Peng, Z. H., Wang, Y., … Oupický, D. (2018). Synthesis and evaluation of chloroquine-containing DMAEMA copolymers as efficient anti-miRNA delivery vectors with improved endosomal escape and antimigratory activity in cancer cells. *Macromolecular Bioscience, 18*(1). https://doi.org/10.1002/mabi.201700194

Xing, H., Cheng, L., Lu, M., Liu, H., Lang, L., Yang, T., … Ding, P. (2019). A biodegradable poly(amido amine) based on the antimicrobial polymer polyhexamethylene biguanide for efficient and safe gene delivery. *Colloids and Surfaces B: Biointerfaces, 182*, 110355. https://doi.org/10.1016/j.colsurfb.2019.110355

Yin, F., Hu, K., Chen, Y., Yu, M., Wang, D., Wang, Q., … Li, Z. (2017). SiRNA delivery with PEGylated graphene oxide nanosheets for combined photothermal and gene therapy for pancreatic cancer. *Theranostics, 7*(5), 1133–1148. https://doi.org/10.7150/thno.17841

Zaichenko, A., Mitina, N., Kovbuz, M., Artym, I., & Voronov, S. (2000). Surface-active metal-coordinated Oligoperoxidic radical initiators. *Journal of Polymer Science, Part A: Polymer Chemistry and Journal of Polymer Science, 38*, 516–527. https://doi.org/10.1002/(SICI)1099-0518(20000201)38:3<516::AID-POLA18>3.0.CO;2-R

Zaichenko, A., Mitina, N., Kovbuz, M., Artym, I., & Voronov, S. (2001). Low-temperature surface-active complex-radical oligo (di-tert.alkyl) peroxide initiators and curing agents. *Wiley-VCH, 164*, 47–71.

Zaichenko, A., Mitina, N., Shevchuk, O., Rayevska, K., Lobaz, V., Skorokhoda, T., & Stoika, R. (2008). Development of novel linear, block and branched oligoelectrolytes and functionally

targeting nanoparticles. *Pure and Applied Chemistry, 80*, 2309–2326. https://doi.org/10.1351/pac200880112309

Zhang, Y., Zheng, M., Kissel, T., & Agarwal, S. (2012). Design and biophysical characterization of bioresponsive degradable poly(dimethylaminoethyl methacrylate) based polymers for *in vitro* DNA transfection. *Biomacromolecules, 13*(2), 313–322. https://doi.org/10.1021/bm2015174

Zhang, Y., Aigner, A., & Agarwal, S. (2013). Degradable and biocompatible poly(N,N-dimethylaminoethyl methacrylate-co-caprolactone)s as DNA transfection agents. *Macromolecular Bioscience, 13*(9), 1267–1275. https://doi.org/10.1002/mabi.201300043

Zhou, D., Cutlar, L., Gao, Y., Wang, W., O'Keeffe-Ahern, J., McMahon, S., … Wang, W. (2016a). The transition from linear to highly branched poly(β-amino ester)s: Branching matters for gene delivery. *Science Advances, 2*(6), e1600102. https://doi.org/10.1126/sciadv.1600102

Zhou, D., Gao, Y., Aied, A., Cutlar, L., Igoucheva, O., Newland, B., … Wang, W. (2016b). Highly branched poly(β-amino ester)s for skin gene therapy. *Journal of Controlled Release, 244*(Pt B), 336–346. https://doi.org/10.1016/j.jconrel.2016.06.014

Zhupanyn, P., Ewe, A., Büch, T., Malek, A., Rademacher, P., Müller, C., … Aigner, A. (2019). Extracellular vesicle (ECV)-modified polyethylenimine (PEI) complexes for enhanced siRNA delivery *in vitro* and *in vivo*. *Journal of Controlled Release, 319*, 63–76. https://doi.org/10.1016/j.jconrel.2019.12.032

Part IV
Environmental Impacts of Nanomaterials

Uptake, Biodistribution, and Mechanisms of Toxicity of Metal-Containing Nanoparticles in Aquatic Invertebrates and Vertebrates

Halina Falfushynska, Inna Sokolova, and Rostyslav S. Stoika

Abbreviations

ATP	Adenosine triphosphate
C3q	Complement component
CAT	Catalase
COX	Cyclooxygenase
EROD	Ethoxyresorufin-O-deethylase
ETS	Electron transport system
GSH	Glutathione
GST	Glutathione transferase
IEP	Isoelectric point
LPO	Lipid peroxidation
MDA	Malondialdehyde
MTs	Metallothioneins
NO	Nitric oxide
NPs	Nanoparticles
NR	Nanorods
nZnO	Nano-zinc oxide
PC	Protein carbonyls
ROS	Reactive oxygen species

H. Falfushynska (✉)
Department of Physical Rehabilitation, Ternopil V. Hnatiuk National Pedagogical University, Ternopil, Ukraine
e-mail: falfushynska@tnpu.edu.ua

I. Sokolova
Department of Marine Biology, Institute of Biological Sciences, University of Rostock, Rostock, Germany
e-mail: inna.sokolova@uni-rostock.de

R. S. Stoika
Department of Regulation of Cell Proliferation and Apoptosis, Institute of Cell Biology of National Academy of Sciences of Ukraine, Lviv, Ukraine

SOD   Superoxide dismutase
TBARS   Thiobarbituric acid reactive substances
TLR   Toll-like receptor
TSH   Thyroid-stimulating hormone

1 Introduction

The modern advance of nanotechnologies leads to an exponential growth in the production of novel nanomaterials broadly used in industrial applications, manufacturing, agriculture, medicine, cosmetics, and food production (Wright, 2016). The economic value of nanotechnologies was estimated at $1 trillion USD in 2015 and was expected to reach ~$3 trillion USD in 2020 (Roco, 2018). According to the Project on Emerging Nanotechnologies (Graca et al., 2018), the number of nanotechnology-based consumer products increased by 125% each year between 2008 and 2010 (Graca et al., 2018). To date, approximately 1800 registered industrial products contain nanomaterials (Vance et al., 2015). Nanoparticles (the particles with at least one dimension <100 nm) are incorporated in optical devices, textiles, plastics, personal care products, food additives and packaging films, solar batteries, water disinfection systems, smart drug delivery systems, greener engineering, and environmental sensors, and also used for remediation puposes (Wright, 2016). A large fraction of engineered nanoparticles (10–40% of the production volume, depending on the nanoparticle) (Coll et al., 2016; Gottschalk et al., 2015) enter the aquatic ecosystems through wastewater treatment plants, aerial transport, and directly due to human recreational activities. The nanoparticles then accumulate in the water and sediments of the coastal zones of the ocean as well as in the freshwater bodies presenting a potential threat to the aquatic ecosystems and humans as the end users.

Due to their small size, the NPs exhibit distinctive physicochemical characteristics (different from the bulk form of the same material) such as the large specific surface area, high reactivity, catalytic activity, photostability or photoreactivity, UV shielding function, and unique quantum and electron-tunneling effects (Gatoo et al., 2014). The size, shape, surface properties, and reactivity of NPs can influence their uptake by cells and modulate their toxic effects. Generally, NPs are considered more toxic than the respective bulk substances (Wright, 2016) and are more likely to be transferred up the food web ultimately reaching humans and other top-level consumers (Mattsson et al., 2017). The nanoscale size of NPs (shown in Fig. 1 for ZnO nanoparticles and nanorods) allows them to penetrate into cells, bind to specific biomolecules, and affect cellular metabolism. Thus, the issue of the biosafety of nanomaterials for the biota, humans, and environment is becoming a matter of scientific and public concern. Ideally, the development of nanomaterials should incorporate a safety-by-design approach, which should reduce their potential impact on human health and the environment (Wright, 2016).
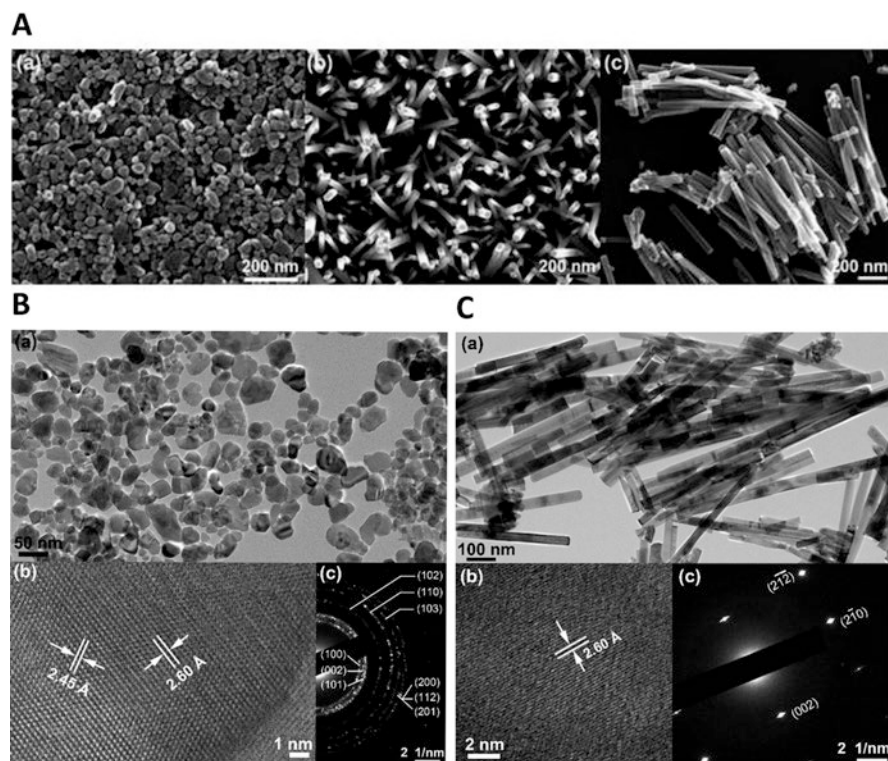
Fig. 1 Images of ZnO nanomaterials (Reproduced with permission [Falfushynska et al. (2019b)]]). (**a**) Scanning electron micrograph (SEM) of (a) ZnO nanoparticles, (b) ZnO nanorods on a glass substrate, and (c) free suspended ZnO nanorods. (**b**) Transmission electron micrographs (TEM) of (a) ZnO nanoparticles, (b) high-resolution imaging of a single ZnO nanoparticle, and (c) selected area diffraction (SAED) pattern from ZnO nanoparticles. (**c**) Transmission electron micrographs (TEM) of (a) ZnO nanorods, (b) high-resolution imaging of one nanorod, and (c) SAED pattern from a single ZnO nanorod

Nano-zinc oxide (nZnO; Fig. 1) occupies third place in the list of worldwide products based on NPs with an annual production of 550–10,000 tons (Piccinno et al., 2012). The nZnO is extensively used in industry, manufacturing, agriculture, pharmaceutical, and personal care products (Gottschalk et al., 2009; Wu et al., 2019). Multifunctional uses of nZnO reflect the unique antibacterial, anticorrosive, antifungal, and UV filtering properties of these NPs. nZnO strongly absorbs UVA (320–400 nm) and UVB (290–320 nm) radiation, while being optically transparent, and is broadly used as an UV filter in textiles, cosmetics, and sunscreens. ZnO NPs are also used as antimicrobial and anticorrosion agents, polymer additives, and catalysts in the manufacturing of paints, coatings, textiles, and electronics. About 10% of all produced nZnO is released from the technosphere into the environment, and >95% of it into the aquatic ecosystems (Gottschalk et al., 2015). The predicted concentrations of nZnO in the environment (derived from the simulation statistics and

mathematical modeling) range from 0.001 to 0.058 μg L^{-1} in surface waters and from 0.22 to 1.42 μg L^{-1} in the industrial sewage effluent in the USA, Europe, and Switzerland (Gottschalk et al., 2009). The predicted present-day concentrations of nZnO in freshwater and marine sediments exceed 100–300 μg kg^{-1} (Gottschalk et al., 2015). The environmental concentrations of nZnO increase exponentially reflecting the increase in the production and use of these NPs (Gottschalk et al., 2009; Wu et al., 2019). ZnO NPs belong to the most toxic metallic NPs (Watson et al., 2014), likely due to their ion-shedding ability (Liu et al., 2016). Zinc oxide has been classified by the EU hazard classification as N; R50-53 (ecotoxic) (Siddiqi et al., 2018) and is considered extremely toxic (50% lethal effect concentration LC_{50} <0.1 mg L^{-1}) to aquatic organisms (Kahru & Dubourguier, 2010).

In water, NPs including nZnO agglomerate and sink to the bottom, making the benthic biota a key target for the potential NPs toxicity. Benthic animals, including epi- and infaunal species, are exposed to NPs via direct body contact with the sinking and sediment-associated NPs and/or through ingestion of NPs associated with the sediment, biofilms, or other food sources (Selck et al., 2016). Benthic filter-feeding organisms (such as bivalve mollusks and corals) are especially vulnerable to NPs, as they can ingest and internalize NPs and their agglomerates from the water column and resuspended sediments, facilitated by the large surface area of the filtration organs. Because of this, benthic filter feeders such as the bivalve mollusks are commonly used as bioindicators of different types of pollutants including NPs. Bivalves are keystone species in freshwater and marine ecosystems due to their habitat forming, filtration, and bioturbation activities. They have high filtration rates, ability to bioaccumulate and bioconcentrate pollutants, and low rate of excretion of pollutants via the kidney (Oehlmann & Schulte-Oehlmann, 2003). These traits make mussels an important target and sentinels for the toxicity of NPs in the aquatic environments (Canesi et al., 2012; Tedesco et al., 2010; Falfushynska et al., 2012, 2019a; Wu et al., 2020).

Among the aquatic vertebrate groups, fish are the most commonly used bioindicator species for water quality because of their abundance in marine and freshwater ecosystems, high susceptibility to pollution, and the relatively long life span that enhances bioaccumulation of the pollutants (Chovanec et al., 2003). Because of the similarity of the physiological and molecular stress responses in fish and other vertebrates (including the mammalian model species), the toxicological studies in fish benefit from the experimental and molecular toolbox developed in biomedicine as well as provide insights into the possible off-target effects of NPs in humans and other vertebrates. Thus, along with the bivalves, fish are important model organisms to investigate the toxic mechanisms and environmental impacts of nanopollutants (Wong et al., 2010; Teles et al., 2016; Wang et al., 2017).

This review focuses on the pathways of exposure, toxicity mechanisms, and physiological effects of NPs (emphasizing nZnO) in aquatic organisms, including the key sentinel groups such as the bivalves and fish. We have chosen nZnO as the focal nanopollutant because of its high production volume, wide distribution in the environment, and relatively well-studied mechanisms of toxicity. We also discuss the influence of other abiotic factors (such as temperature, salinity, or presence of

other pollutants) on the bioavailability, bioaccumulation, and toxicity of nanomaterials and emphasize the shared toxicity mechanisms between nZnO and other types of metal-containing nanoparticles in aquatic organisms.

2   Physicochemical Characteristics and Behavior of Metal-Containing Nanoparticles in Aquatic Environments

The environmental distribution, behavior, and toxicity of metal-based NPs depend on their physical (e.g., size and shape) and chemical (acid–base character and hydrophilicity of the surface, surface coating, and water solubility) characteristics (Tourinho et al., 2012). The physicochemical characteristics of NPs together with the conditions of the surrounding environment (such as the temperature, ionic strength, oxygen level, and natural organic matter) influence the behavior and transport of NPs in the aquatic systems (Gottschalk et al., 2013). Zeta potential of NPs (i.e., the difference in potential between the medium in which the particles are suspended and the fluid layer at the particle surface) is a key determinant of the stability of NPs in suspension. The particles with high absolute zeta potential (>30 mV) tend to remain suspended, while the particles with low zeta potential aggregate and sink more rapidly (Barba et al., 2019).

Zeta potential of the nanoparticles depends on the particle size and the surface charge and is modified depending on the properties of the aquatic environment. In low ionic strength media (such as freshwater), zeta potential changes nonlinearly with pH so that the absolute zeta potential is the lowest (and the size of the particle aggregates—the largest) near the so-called isoelectric point (IEP), where there is no net charge on the surface of the particle (Berg et al., 2009). The IEP depends on the chemical properties of the particle; thus, for ZnO, Al_2O_3, and CeO_2 NPs, the IEP is near the neutral pH (7.13, 7.06, and 6.71, respectively), whereas the IEP of TiO_2 and Fe_2O_3 is shifted toward the more acidic pH (5.19 and 4.24, respectively) (Berg et al., 2009).

The zeta potential and aggregation behavior of the metal-containing NPs is also affected by the seawater salinity and pH. The absolute zeta potential typically decreases (i.e., becomes closer to zero) with increasing salinity and ionic strength of the water, likely reflecting the change-driven binding of the ions to the surface of the nanoparticle. As a result, higher salinity and ionic strength increase the aggregation and the rate of sedimentation of nanoparticles (Praetorius et al., 2014; Yung et al., 2015). The studies on the effects of pH on zeta -potential and aggregation of nanoparticles in the environmentally relevant pH range are rare. Thus, zeta potential of nano-TiO_2 ($nTiO_2$) increases with seawater acidification leading to the higher hydrodynamic diameter (334.8, 439.8, and 537.1 nm at pH 8.1, 7.8, and 7.4, respectively) and stronger aggregation of $nTiO_2$ at low pH (Shi et al., 2019). Given that the toxicity of nanoparticles increases with the decreasing size of their aggregates,

changes in ambient salinity and pH have important implications for the toxicity of metal-containing NPs.

The presence of the natural organic matter in the water further modifies the surface charge and zeta potential of the nanoparticles thereby affecting their aggregation behavior (Keller et al., 2010; Li & Chen, 2012; Praetorius et al., 2014) and mobility in the water and sediments (Yecheskel et al., 2016). NPs can interact with the natural organic matter that adsorbs on the surface of NPs and stimulates their aggregation due to the so-called bridging effects (Canesi & Corsi, 2016). For instance, exopolymeric substances (the colloidal polymers produced by algae) influence aggregation and transformation of NPs in aqueous media, mainly as a function of the hydrophobic and electrostatic interactions between NPs and exopolymeric substances (Adeleye et al., 2014; Kadar et al., 2014). The binding of NPs to hydrophobic aquatic pollutants may increase their lipophilicity and therefore, the bioavailability and cellular uptake (Velzeboer et al., 2014). NPs uptake can also be modified by the presence of extracellular excreted proteins in the water. The binding of the proteins to the surface of NPs leads to the formation of the so-called eco-corona (similar to the protein corona around the internalized NPs inside the cell or the extracellular fluid) that regulates the NP interactions with the cell membranes and receptors and ultimately affects the uptake of NPs, biological activity, and toxicity (Xiao & Gao, 2018).

Nanoparticle dissolution in the water can modulate the toxicity of NPs by decreasing the concentration of nanoparticles but releasing the ionic metals that might also be toxic. The solubility of NPs strongly depends on the salinity, pH, ionic strength, and temperature of the ambient water. Thus, nZnO has a high solubility in acidic environments but limited solubility at the neutral and basic pH (Liu et al., 2016). ZnO NPs are also more soluble in seawater than in freshwater (Li et al., 2018a). The bioavailability of ionic Zn released by the dissolution of nZnO can be further modified by the complexation of Zn^{2+} with other ions, the organic matter, or the sediment. This complexation decreases the amount of free ionic Zn thereby reducing its toxicity. As a result, the toxicity of nZnO and ionic Zn tends to be higher in the freshwater compared with the seawater and is further decreased in the presence of the sediment (Poynton et al., 2019). Thus, in the freshwater exposure, the pristine and phosphate transformed ZnO NPs were more toxic to epibenthic amphipod *Hyalella azteca* (LC_{50} = 0.11–0.18 mg L^{-1}) than $ZnSO_4$ (LC_{50} = 0.26 mg L^{-1}) and the ZnS nano-clusters (LC_{50} = 0.29 mg L^{-1}) (Poynton et al., 2019). When salinity increased, the toxicity of Zn^{2+} and ZnO NPs to *H. azteca* decreased. The presence of the sediment decreased the concentrations of dissolved Zn in the water column by the factor of 10 and was associated with a ~10-fold reduction in toxicity (measured as LC_{50}) of nZnO and $ZnSO_4$ for *H. azteca* (Poynton et al., 2019).

Due to the complexity of NP interactions with the environmental matrices and implications of these interactions for the uptake and toxicity of NPs, it is essential to characterize the size distribution, shape, surface properties, and aggregation behavior of NPs under environmental and experimental exposure conditions. As a minimum, the size distribution, shape, zeta potential, hydrodynamic radius (or

aggregate size), and dissolution of NPs should be reported to interpret the toxicity data and compare them across different studies. Furthermore, investigations of the toxicity of NPs at high, environmentally unrealistic concentrations should be discouraged because the biologically relevant characteristics of NPs (especially the aggregation and agglomeration behavior) are strongly concentration dependent (Skjolding et al., 2016). Presently, the amount of the available data is insufficient for the broad generalizations about the potential relationships between the physico-chemical characteristics of NPs and their toxicity. However, as the field of NPs ecotoxicology matures and the data accumulate, future meta-analyses should reveal the relative importance of the core characteristics such as size, shape, surface charge, and aggregation behavior of NPs in determining their toxicity to aquatic organisms.

3   Environmental Concentrations and Fate of Nanoparticles

Assessment of the environmental concentrations of engineered nanomaterials represents a significant challenge for ecotoxicology and environmental science. The information about the actual environmental concentrations of NPs in aquatic environments is extremely limited since detection and identification of NPs requires sophisticated techniques such as dynamic light scattering, laser and X-ray diffraction, nanoparticle tracking analysis, or high-resolution imaging techniques such as electron microscopy (Graca et al., 2018). These techniques are expensive, time- and effort consuming, and hard to use in complex environmental matrices such as surface water, wastewater plant effluents, biosolids, sediments, or soil. Therefore, the assessment of the environmental concentrations of NPs heavily depends on the modeling based on probability distributions of production volumes, use, environmental release, and transfer between compartments to predict the accumulation of engineered nanomaterials across environmental media (Boxall et al., 2007; Gottschalk et al., 2013).

Recent model predicts high but variable concentrations of engineered NPs in the environmental compartments (Coll et al., 2016; Garner et al., 2017; Gottschalk et al., 2015; Piccinno et al., 2012). High concentrations in the aquatic systems are predicted for carbon black, photostable TiO_2 (Gottschalk et al., 2015), and nZnO (Coll et al., 2016; Piccinno et al., 2012). Unlike TiO_2, ZnO NPs are partially transformed during water treatments that reduce their concentrations and releases ionic Zn^{2+}; however, direct inputs of nZnO from the sunscreens into the aquatic environments may bypass this transformation route. Notably, even soluble nanometal oxides may accumulate as nanoparticles in the environment in sufficient concentrations to cause toxicity, though this is more likely to occur for high-production volume of NPs such as TiO_2 and ZnO (Coll et al., 2016; Garner et al., 2017). Current models predict that a large fraction of the released NPs ends up in the aquatic compartment. Thus, 56% and 41% of the released nZnO end up in the marine and freshwaters, respectively, with only ~2% accumulating in soils (Gottschalk et al., 2015). For photostable TiO_2 (such as used in sunscreens), soils are the main receiving

compartment taking up ~63% of the released nTiO$_2$, followed by the marine and freshwaters (21% and 16%, respectively) (Gottschalk et al., 2015).

Due to the particle sedimentation and surface interactions, NPs commonly aggregate in sediments and soils. Modeled average sediment concentrations of NPs are often several orders of magnitude higher than in the overlying water (Garner et al., 2017). For example, the average concentration of NPs in surface waters ranged from 10^{-3} to $10^{-5}\mu g\ L^{-1}$, while their concentrations in sediments ranged from $1\mu g\ kg^{-1}$ to $1\ mg\ kg^{-1}$ (Selck et al., 2016). The predicted environmental concentrations of ZnO NPs in the USA and Europe were ranging from $1–10\ ng\ L^{-1}$ in natural surface water to $300–432\ ng\ L^{-1}$ in the effluents from sewage treatment plants (Gottschalk et al., 2009) that were lower than estimated environmental concentrations of Au $(0.14\ mg\ L^{-1})$ and SiO$_2$ $(0.7\mu g\ L^{-1})$ NPs in surface water (Tiede et al., 2009). Within the sediment, the concentrations of NPs typically decrease with the increasing depth indicating slow burial. Thus, ^{67}Zn concentrations (used as a marker for ZnO NPs) in the sediment from an intertidal mudflat in the Bay of Bourgneuf showed higher levels in the upper section of the sediment (2.59 mg kg^{-1} at 1 cm depth), decreasing progressively with the depth (1.63, 0.90, 0.67, and 0.31 mg kg^{-1} at the 2, 3, 4, and 5 cm depth, respectively) (Buffet et al., 2012).

Similar to the NPs in sediments and soil, suspended NPs commonly exist in the form of aggregates or agglomerates in the water column (Graca et al., 2018). Thus, a study in the Baltic Sea showed that NPs occurred as the nanofibers (among them silica, asbestos, iron, and manganese), nanotubes, and nanospheres (among them pyrite) in seawater (Graca et al., 2018). Some fibers appeared in the form of separate entangled structures, and the concentration of NPs was season- and site-specific ranging from not detectable amounts to 360×10^2 particles cm^{-3}. The NPs' number decreased in the order: nanofibers > nanotubes ≫ nanospheres. Many of the NPs were found as structures that were initially considered to be agglomerates of the nanofibers (Graca et al., 2018).

4 Uptake and Accumulation of Metal-Based Nanoparticles in Aquatic Organisms

4.1 Invertebrates

Aquatic invertebrates (especially filter-feeders such as bivalves and sediment-dwelling mollusks and annelids) are considered vulnerable to harmful effects of the nanopollutants. These organisms are therefore recognized as key bioindicator species for the assessment of the water NPs pollution. Nevertheless, the mechanisms of uptake, accumulation, and toxicity of NPs in aquatic invertebrates are not well understood and the existing data are sometimes controversial.

Accumulation of dissolved metals is well studied in aquatic invertebrates including bivalves (Canesi et al., 2012; Canesi & Corsi, 2016; Falfushynska et al., 2012,

2015b, 2018, 2019a, 2019b, 2019c; Xu et al., 2020), and the models exist to predict the bioavailability of the dissolved metals depending on the physicochemical parameters of the water such as the salinity, temperature, pH, and organic matter content (Schlekat et al., 2020). In contrast, the uptake, accumulation, and elimination of the metal-based NPs have not been extensively studied in aquatic invertebrates (Falfushynska et al., 2015b, 2018; Gnatyshyna et al., 2019). In bivalves, NPs can be taken up directly from the water phase (e.g., by endocytosis in the gills and hemocytes) or ingested as particulate matter or as NPs associated with the phytoplankton and other food sources. The direct uptake route through endocytosis has been demonstrated by in vitro studies of isolated hemocytes (Katsumiti et al., 2014); however, the role of this route in the uptake of NPs during in vivo exposures is yet to be demonstrated.

The ingestion of NPs has been postulated as the main uptake route for the filter feeders such as the bivalves. However, due to the size selectivity of the bivalve filtration apparatus, the efficiency of the uptake of NPs uptake likely to strongly depends on the size and the aggregation behavior of NPs. For example, mussels cannot take up the particles of the diameter <1 μm with great efficiency (Ward & Kach, 2009). Nevertheless, there is ample evidence that mussels accumulate metal-containing NPs from the environment including ZnO, TiO_2, Au, and CeO_2 NPs (Pan et al., 2012; Bergami et al., 2016; Volland et al., 2015; Shi et al., 2019). For example, after treatment of *Mytilus galloprovincialis* with $nCeO_2$ and ZnO NPs (1–10 mg L^{-1}), the mussels accumulated 62 μg Ce g^{-1} and 880 μg Zn g^{-1} on a dry tissue basis and rejected 21,000 μg Ce g^{-1} dry mass and 63,000 μg Zn g^{-1} dry mass in the pseudofeces (Montes et al., 2012). Sea urchins Paracentrotus lividus accumulated SnO_2, CeO_2, and Fe_3O_4 in the coelomocytes after in vivo exposures to the suspended SnO_2, CeO_2, and Fe_3O_4 NPs (Falugi et al., 2012). While metal accumulation indicates uptake of NPs, the toxicity of NPs is not always directly related to the accumulated metal burdens. For examples, studies with nZnO NPs showed a strong signature of cytotoxicity and inflammation (discussed in Sect. 5.3 below) in the blue mussels *Mytilus edulis* and swollen river mussel *Unio tumidus* in the absence of significant Zn accumulation (Falfushynska et al., 2015b; Wu et al., 2019).

Additional stressors such as salinity or ocean acidification can affect the uptake of metal-containing NPs by invertebrates. In bivalves, ocean acidification due to the elevated CO_2 levels increased the accumulation of TiO_2 NPs (Shi et al., 2019). After 21-day exposure to 100μg L^{-1} $nTiO_2$, Ti levels accumulated in the gills, foot, and mantle tissues of the blood clam (*Tegillarca granosa*), the hard clam (*Meretrix meretrix*), and the venus clam (*Cyclina sinensis*) were ~34% and 16% greater at pH 7.4 and 7.8, respectively, than in the clams kept at the ambient pH of 8.1 (Shi et al., 2019). The influence of ocean acidification on the uptake of other types of NPs including nZnO has not been studied, but synergistic effects of seawater acidification and ZnO NPs on the physiological performance were reported in the thick shell mussel *Mytilus coruscus* (Shang et al., 2018). Furthermore, ambient salinity modulated the immunotoxic effects of nZnO in the blue mussels *M. edulis* (Wu et al., 2019). These findings suggest that the interactive effects of NPs with other abiotic

stressors are common in the bivalves and require further investigation to determine the mechanisms and the role of the modulated NP uptake in these interactions.

4.2   Vertebrates

Depending on the size and physicochemical properties of NPs, they can penetrate the bodies of aquatic vertebrates via gills, chorion, intestinal, or blood–brain barrier, as well as in a transcutaneous manner (Handy et al., 2008; Klaine et al., 2008; Johnston et al., 2010; Canesi et al., 2012). Water-breathing vertebrates such as fish and amphibians are especially vulnerable due to the high surface area of the permeable epithelia in the gills and the skin. Owing to their small size, NPs can be taken up intracellularly by endocytosis and transfer from cell to cell by transcytosis (Handy et al., 2008; Lammel et al., 2019). Metal accumulation is commonly used as a marker of NP uptake in the aquatic vertebrates exposed to NPs. Thus, in medaka (*Oryzias melastigma*) and rainbow trout (*Oncorhynchus mykiss*), Zn accumulated in the gills and intestine during exposure to the waterborne ZnO NPs (Connolly et al., 2016; Wang et al., 2017). Depuration of Zn from nZnO in fish is slow, and the Zn levels in tissues remain at a stable elevated level for 28 days of the depuration phase (Connolly et al., 2016). In fish co-exposed to ZnO and CuO NPs, the accumulated levels of Cu and Zn increased with the increasing concentrations of CuO NPs indicating that the presence of CuO NPs facilitates nZnO (and/or dissolved Zn) entry (Hernández-Moreno et al., 2019). Accumulation of the waterborne hematite and CuO NPs was also demonstrated in zebrafish (Huang et al., 2020; Tesser et al., 2020). Notably, the rate of accumulation of well-dispersed hematite NPs by zebrafish differed between different life stages that increase in the order: embryo > larva > adult (Huang et al., 2020). The accumulation of hematite NPs increased linearly with the exposure time until reaching a peak and decreased afterward, indicating the excretion of NPs or accumulation of metal (Huang et al., 2020). Overall, like in invertebrates, the empirical studies clearly demonstrate the uptake of NPs by aquatic vertebrates, but the precise mechanisms of this uptake remain to be elucidated.

5   The Toxicity Mechanisms of Nanoparticles in Aquatic Organisms

5.1   Biological Targets of the Toxicity of Nanoparticles

Adverse effects of NPs on the biological systems depend on their physicochemical properties and can include direct toxic effects, changes in the bioavailability of nutrients and toxins, and indirect effects resulting from NP interactions with biomolecules (Klaine et al., 2008; Graca et al., 2018). The common mechanisms of the

toxicity of NPs found in aquatic invertebrates and vertebrates include oxidative stress, immune system alterations, inflammation, and dysregulation of the cell cycle and apoptosis/autophagy (Fig. 2). Furthermore, the interaction of the NPs with mitochondria can cause mitochondrial depolarization and swelling in isolated cells including monocytes and keratinocytes (Maurer & Meyer, 2016); however, currently, little is known about the mitochondrial toxicity of NPs during in vivo exposures of invertebrates (Ciacci et al., 2012; Trevisana et al., 2014; Falfushynska et al., 2019a, 2019b) or lower vertebrates such as amphibians and fish.

The size and shape of NPs determine the efficiency of their uptake by the target cells (Tedesco et al., 2010). Typically, smaller NPs enter the cell more easily than larger ones. Spherical NPs are more likely to be incorporated into the cell than the rod and cylindrical NPs. Furthermore, positively charged NPs show higher rates of endocytosis than negatively charged or neutral NPs and remain longer in the cell (Oh & Park, 2014). Finer particles may be able to pass through the membrane by passive diffusion (Liu et al., 2016).

The solubility of NPs and the nature of the constituent metal are important factors of their toxicity. Highly soluble NPs can release metals in intra- and extracellular compartments of the body thereby causing adverse effects through the dual mechanisms, as NPs and as toxic metals. Therefore, a high surface area to volume ratio of NPs and an elevated ratio of dissolved to nanoparticulate metal may facilitate the toxicity of NP similar to nZnO (Liu et al., 2016). The toxicity mechanisms of highly soluble NPs such as Ag, CuO, and ZnO NPs also depend on the different nature of the released metals (Bondarenko et al., 2013; Scherzad et al., 2017). For
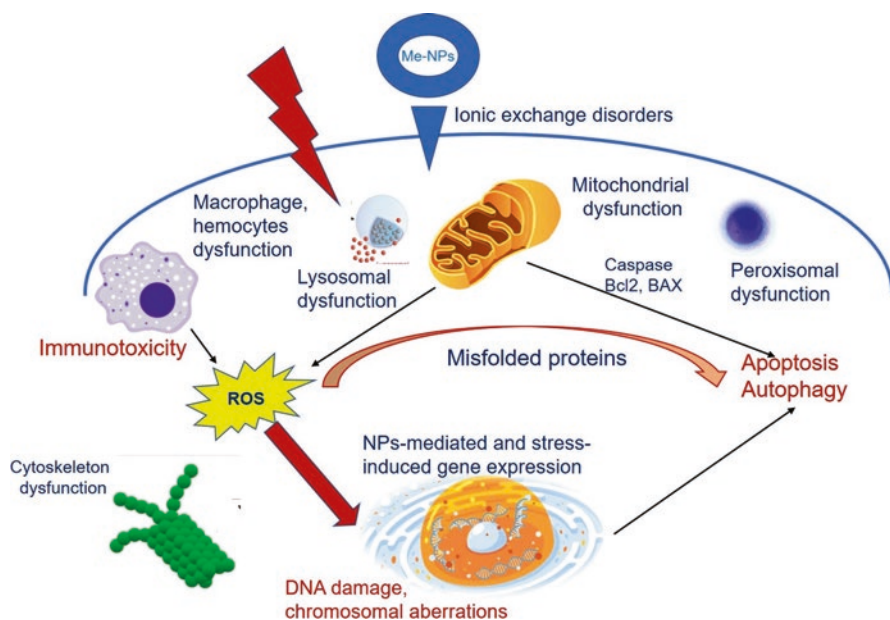
Fig. 2 The putative intracellular targets and key toxicity mechanisms of NPs in animal cells

example, Zn and Cu are essential metals, tightly regulated in the cell, and involved in multiple intracellular processes such as the electron transfer (Cu), metabolic and antioxidant enzyme activities (Cu and Zn), and DNA transcription (Zn) (Festa & Thiele, 2011; Maret, 2017). In contrast, Ag is a nonessential metal that is not involved in any cellular processes and poorly regulated through the cellular transport mechanisms (Maurer & Meyer, 2016). Therefore, Ag can accumulate in the high levels in the cell and cause stronger toxicity than Cu or Zn. Dissolved Cu and Zn can enter the cells through the specialized ion transport mechanisms such as CTR1 and CTR2 for Cu^{2+}, the Zrt- and Irt-like proteins, and zinc transporters of ZIP family for Zn (Maret, 2017). Dissolved Ag hijacks monovalent transport mechanisms such as Na^+ channel situated on the branchial apical membrane of aquatic vertebrate and can penetrate by basolateral membrane vesicle silver transport system (Bury et al., 1999).

Once inside the body, NPs interact with the intra- or extracellular proteins forming the so-called protein-coated corona complex (Xiao & Gao, 2018). The formation of the protein corona around the internalized NPs has been observed in mammalian cells, as well as in terrestrial, freshwater, and marine invertebrates including the rugworm *Eisena fetida* and *Daphnia magna* (Nasser & Lynch, 2016; Canesi & Corsi, 2016). The protein-coated corona complex also affects the binding of NPs to the cell surface receptors and may facilitate the uptake of NPs from the bloodstream and/or environment by endocytosis (Salvati et al., 2013). Furthermore, the protein corona-coated NPs are readily taken up and digested by the lysosomes contributing to the release of metals and lysosomal damage (Cho et al., 2012).

Table 1 summarizes the known biological targets and toxicity mechanisms of nZnO as a model NP in aquatic animals. In the subsequent Sections (5.2, 5.3, and 5.4), we discussed the key toxic mechanisms of nZnO and compared them to other NPs as appropriate.

5.2   Induction of Oxidative Stress by Nanoparticles in Aquatic Animals

5.2.1   Invertebrates

Oxidative stress has been proposed as a major mechanism of the toxicity for metal-containing NPs (Vandebriel & De Jong, 2012; Xia et al., 2008), presumably elicited by the release of the constituent metals from NPs (Baker et al., 2014). The available studies on the NP-induced oxidative stress in aquatic invertebrates show controversial results and do not provide evidence for a strong oxidative stress response at low, environmentally relevant NP concentrations. Thus, exposure to the blue mussel *M. edulis* for 14 days to environmentally relevant concentrations of ZnO NPs and nanorods (10 and 100 μg L^{-1} Zn) did not result in a consistent, concentration-dependent increase in the levels of oxidative lesions (thiobarbituric acid reactive substances (TBARS) and protein carbonyls) in the mussels' tissues (Falfushynska

Table 1 Hazardous effects of nano-zinc oxide on aquatic animals

Test organism	Applied concentration	Acute toxicity	Hazardous effect	Time of exposure	References
Freshwater invertebrates					
Daphnia magna	0.2–50 ppm		GSH↑, MDA↑	72 h	Ates et al. (2019)
Biomphalaria alexandrina	7 mg L⁻¹	LC₅₀ = 145 mg L⁻¹	MDA↑, NO↑, GST↓		Fahmy et al. (2014)
Unio tumidus	3.1 μM		Autophagy↑, ATP~	14 days	Falfushynska et al. (2019b)
Unio tumidus	3.1 μM		Multixenobiotic-resistance protein activity↓	14 days	Falfushynska et al. (2018)
Elliptio complanata	0.5 mg L⁻¹		Body mass ↓ COX↑, AcetylCoA↑	7 days	Gagné et al. (2015)
Elliptio complanata	1 and 10 μg L⁻¹		Zn accumulation↑, GST↓, MTs↑, DNA damage↑	21 days	Gagnon et al. (2016)
Dreissena polymorpha	25 μg L⁻¹		Zn accumulation↓, oxidative stress↑ after combine exposure with brown water and diluted municipal effluent Air-time survival ↓	96 h	Gagné et al. (2019)
Marine and saltwater invertebrates					
Artemia salina	0.2–50 ppm	LC₅₀ = 89.4 mg L⁻¹ for nZnO (10–30 nm).	GSH↑, MDA↑	72 h	Ates et al. (2019)
Mytilus edulis	100 μg L⁻¹		TLRb↓, TLRc↓, C-lectin↓, C3q↓, pathogen recognition↓, defensin↑	21 days	Wu et al. (2020)
Mytilus edulis	10 and 100 μg L⁻¹		TBARS↑, PC↑, autophagy↑, lysosomal membrane destabilization↑, apoptosis- and inflammation-related genes↑	14 days	Falfushynska et al. (2019a)

Table 1 (continued)

Test organism	Applied concentration	Acute toxicity	Hazardous effect	Time of exposure	References
Mytilus coruscus	2.5 and 10 mg L^{-1}		respiration rate↓, absorption efficiency↓, clearance rate↓, O:N ratio↓, the scope for growth↓, ammonium excretion rate↑	14 days	Shang et al. (2018)
Ruditapes philippinarum	10 μg L^{-1}		DNA damage↑ Total lipids↑ Cholesterol↑	7 days	Marisa et al. (2016)
Crassostrea gigas	4 mg L^{-1}	LC50(96) = 30 mg L^{-1}	Zn accumulation↑, mitochondrial disruption, GSH↓, LPO↑	48 h	Trevisana et al. (2014)
Mytilus galloprovincialis	0.1–2 mg L^{-1}		Zn accumulation↑, respiration rate↑	12 weeks	Hanna et al. (2013)
Freshwater vertebrates					
Danio rerio	8 mg L^{-1}		Zn accumulation ↑	120 h	Wu et al. (2019)
Danio rerio		LC50 = 1.79 ÷ 4.92 mg L^{-1}			Bondarenko et al. (2013)
Carassius auratus	10 and 100 μg L^{-1}		SOD↑, CAT↑, GST↑, LPO↑, gill hyperplasia, liver degeneration	14 days	Benavides et al. (2016)
Catostomus commersonii	1 mg L^{-1}		LPO↑, Caspase3/7↑, HSP↑, Na(+)/K(+)-ATPase↑, heart rate↓	24 h	Bessemer et al. (2015)
Pelophylax ridibundus	3.1 μM		LPO↑, Vtg↑, Cu(MTs)↑, Zn(MTs)↑, Lactate/Pyruvate↑	14 days	Falfushynska et al. (2019d)
Pelophylax ridibundus	3.1μM		Zn accumulation↑, MT-Me↑, MT-SH↑, Deiodinase↑, TSH↓, lipofuscin↑, DNA damage↑	14 days	Falfushynska et al. (2017)

Marine and brackish water vertebrates				
Oryzias melastigma	4 and 40 mg L^{-1}		HSP70↑, MT-I↑, SOD↑	96 h	Wong et al. (2010)
Mugilogobius chulae	1–25 mg L^{-1}	LC50 = 45.4 mg L^{-1}	Hatching↓, spinal bending↑, oedema↑, hypoplasia↑	96 h	Li et al. (2018a)
Sparus aurata	1 mg L^{-1}		Lipid vacuolation, necrosis of hepatic and pancreatic tissues, blood congestion, melano-macrophages diffusion	96 h	Beegam et al. (2019)

GSH glutathione, *MDA* malondialdehyde, *NO* nitric oxide, *GST* Glutathione S-transferases, *COX* cyclooxygenase, *ATP* adenosine triphosphate, *MTs* metallo-thioneins, *TLR* Toll-like receptor, *C3q* complement component, *TBARS* thiobarbituric acid reactive substances, *PC* protein carbonyls, *LPO* lipid peroxidation, *SOD* superoxide dismutase, *CAT* catalase, *TSH* thyroid-stimulating hormone

et al., 2019c). An increase in TBARS levels was found in the tissues of the mussels exposed to low concentration of ZnO NPs and ionic Zn^{2+} (10 μg L^{-1} Zn) and to the high concentration of ZnO nanorods (100 μg L^{-1} Zn) but not in other experimental exposure groups. The elevated levels of protein carbonyls were detected only in tissues of mussels exposed to 10 μg L^{-1} of the ionic Zn^{2+} and to 100 μg Zn L^{-1} of ZnO NPs and nanorods (Falfushynska et al., 2019c). In a marine clam *Ruditapes philippinarum,* exposure to 1–10 μg Zn L^{-1} of ZnO NPs for 7 days did not result in the accumulation of TBARS or protein carbonyls (Marisa et al., 2016). In contrast, high concentrations of ZnO NPs (0.5–5 mg Zn L^{-1}) led to an elevated ROS production in the embryos of a sea urchin Lytechinus variegatus (Wu et al., 2015).

Similar to nZnO, exposures to other types of NPs do not reveal a clear oxidative stress signature in aquatic invertebrates. Thus, in vitro and in vivo exposure to different metal-containing NPs including CdS quantum dots (0.001–100 mg Cd L^{-1}), nCuO (10 μg L^{-1}), and nAu (0.75 μg L^{-1}) provoked unbalanced changes in antioxidant–prooxidant system of marine invertebrates including bivalves *M. galloprovincialis, Scrobicularia plana, R. philippinarum*, and an annelid *H. diversicolor* (Buffet et al., 2011; Katsumiti et al., 2014; Volland et al., 2015). Under these conditions, no other common toxicity biomarkers (including DNA damage, catalase activity, glutathione transferase activity, tissue levels of metallothioneins, acid phosphatase activity, and multixenobiotic resistance protein (MXR) transport) changed in the isolated hemocytes and gill cells of *M. galloprovincialis, S. plana, R. philippinarum*, and *H. diversicolor* (Buffet et al., 2012; Katsumiti et al., 2014; Volland et al., 2015). In a marine bivalve *S. plana* and an annelid *H. diversicolor,* 10 μg L^{-1} CuO NPs exposure for 16 days induced elevated catalase and glutathione-S-transferase activities but no change in lipid peroxidation (Buffet et al., 2011).

A short-term exposure (24 h) to $nTiO_2$ and n-SiO_2 (0.05, 0.2, 1, and 5 mg L^{-1}) induced variations in catalase and glutathione transferase activities in the gills of the blue mussels *Mytilus* sp., but no clear trend with regard to the type or concentration of NPs was observed (Canesi et al., 2010). The treatment of *M. galloprovincialis* (96 h), marine epibenthic copepods Tisbe battagliai (5 weeks), and marine algae *Skeletonema pseudocostatum* with $nTiO_2$ (0.1 mg L^{-1}) resulted in the higher level of ROS production in *Skeletonema pseudocostatum*, sensitivity to mortality in Tisbe battagliai and elevated production of nitric oxide (NO) in *M. galloprovincialis* possibly reflecting hemocyte infiltration (Canesi & Corsi, 2016; Georgantzopoulou et al., 2018). Exposure of a freshwater bivalve *Unio tumidus* for 14 days to 100 μg L^{-1} $nTiO_2$ led to a decrease in the ROS production and upregulation of the reduced glutathione levels, lipofuscin, and TBARS (Gnatyshyna et al., 2019). Overall, the available data on marine and freshwater invertebrates indicate that the antioxidant system and ROS-producing pathways of these organisms are not major targets for toxicity of the metal-containing NPs at the environmentally relevant, low concentrations.

ZnO nanomaterials have been shown to negatively affect mitochondria of aquatic invertebrates, which are the main ROS generating organelles. However, the mitochondrial injury depends on the type of exposure and the concentration of the NPs. For example, in vitro exposure of isolated hemocytes of *M. galloprovintialis* to

10 mg L^{-1} nZnO led to a decrease in the mitochondrial abundance and mitochondrial membrane potential while other tested NPs (TiO$_2$, SiO$_2$, and CeO$_2$ at 10 mg L^{-1}) had no effect on these mitochondrial traits (Ciacci et al., 2012). In the oysters *Crassostrea gigas*, exposure to ZnO NPs (4 mg Zn L^{-1}) resulted in swelling and rupture of the mitochondria and loss of the mitochondrial cristae (Trevisana et al., 2014). In the mussels *M. edulis*, environmentally relevant ZnO exposures (10 and 100 μg Zn L^{-1}) suppressed the mitochondrial capacity shown by a decline in the mitochondrial electron transport system activity (Falfushynska et al., 2019c). A decrease in the mitochondrial electron transport system activity indicates the negative impacts of nano-ZnO on the bioenergetics of the mussels, since the ETS activity tightly correlates with a maximum capacity for the ATP synthesis (Falfushynska et al., 2019a; Haider et al., 2018; Sokolov & Sokolova, 2019). However, the effects of the nano-ZnO NPs and nanorods on the ETS activity in mussels were not concentration-dependent, and statistically significant modest declines were observed only in the groups exposed to 10 μg L^{-1} ZnO NPs and 100 μg L^{-1} ZnO nanorods (Falfushynska et al., 2019c).

Overall, the results of published studies demonstrate that the effects of the metal-containing NPs on the redox balance of the aquatic invertebrates are modest and variable, at least in the range of low, environmentally relevant concentrations. The concentration-independent variability and the lack of consistency of the oxidative stress response to NPs indicate that disruptions of the redox balance caused by the low levels of the metal-containing NPs are insufficient to cause major cell and tissue damage. Therefore, the oxidative stress-related markers (such as the levels of oxidative lesions, activities of antioxidant enzymes or ROS productions) cannot be recommended as the biomarkers of choice to assess the exposure or the effects of NPs in aquatic invertebrates in the field.

5.2.2 Vertebrates

Similar to the invertebrates, oxidative damage due to the overproduction of ROS and/or suppression of the antioxidant defenses has been proposed as a putative mechanism for the toxicity of NPs in vertebrates (Golbamaki et al., 2015; García-Gómez et al., 2020). Furthermore, ROS generation during particle-induced inflammation can cause DNA damage and secondary genotoxicity (Golbamaki et al., 2015). The available data show multiple signs of redox misbalance induced by exposures of NP in aquatic vertebrates such as fish and amphibians. Specifically, the signs of both oxidative stress (i.e., the initiation of measures to reduce elevated ROS such as elevated expression or activity of antioxidants) and oxidative distress (i.e., the accumulation of intracellular lesions that accompany excessive ROS) (Olson, 2020) have been reported in the NP-exposed fish.

Exposure to ZnO NPs (2.5 mg L^{-1}) for 24 h induced elevated ROS generation in cell culture of Balb/c mice by depleting antioxidant enzymes, increasing lipid peroxidation, and protein carbonyl contents in the macrophages (Roy et al., 2014).

These oxidative (di)stress markers were associated with the inhibited release of the Nrf2 transcription factor and followed by a low rate of apoptosis and autophagy (Roy et al., 2014). ZnO NPs of different morphology (rod-shaped and spherical) had different effects on the oxidative stress markers in fish cells (García-Gómez et al., 2020). Rod-shaped ZnO NPs inhibited the activity of reductase enzyme (measured as Alamar Blue test) and, to a lesser extent, enhanced the levels of the ROS in fish cells, while the spherical nZnO NPs and nZnO coated with (3-aminopropyl) triethoxysilane affected mainly ROS generation. In particular, the parameter increased up to 20% when compared to the control (García-Gómez et al., 2020).

Elevated ROS generation in the NP-exposed fish is commonly counteracted by the upregulation of enzymatic antioxidants. Thus, chronic dietary exposure to nZnO ($80 \, mg \, kg^{-1}$) significantly enhanced the antioxidant defenses in medaka, with no negative effect on fish growth (Wang et al., 2017). These beneficial effects disappeared, and the growth was suppressed at the high dietary nZnO ($300 \, mg \, kg^{-1}$) treatment indicating that the protective systems of the fish became overwhelmed (Wang et al., 2017). In the rainbow trout and a freshwater teleost *Prochilodus lineatus,* exposure for 96 h to $1.25 \, mg \, L^{-1}$ of ZnO NPs in combination with Cu NPs (0.04–$0.34 \, mg \, L^{-1}$) provoked an increase in the activity of GST and the GSH/GSSG ratio in the liver and gills but didn't alter significantly lipid peroxidation and EROD activity (Hernández-Moreno et al., 2019; Tesser et al., 2020). Similarly, in the striped catfish *Pangasianodon hypophthalmu*s, exposure to 16–$30 \, mg \, L^{-1}$ ZnO NPs for 96 h led to an increase in SOD, catalase and GST activity, and elevated levels of lipid peroxidation (Kumar et al., 2019). In zebrafish *Danio rerio*, acute exposure of embryos (96 h postfertilization) to 12.5–$50 \, mg \, L^{-1}$ ZnO NPs led to a concentration-dependent increase in the activity of SOD and GPx but suppressed CAT activity and led to the elevated LPO (Du et al., 2017). A concentration-dependent increase in activities of SOD, CAT, and GPx was also found in zebrafish embryos exposed to increasing concentrations of ZnO NPs in the range of 1–$100 \, mg \, L^{-1}$ (Zhao et al., 2013). A short-term exposure (6 h) of primary hepatocytes of the magur catfish *Clarias magur* to 5 or $10 \, mg \, L^{-1}$ of ZnO NPs led to a sharp rise in the intracellular concentrations of H_2O_2, production of NO (as a consequence of the increase in activity of inducible nitric oxide synthase (iNOS), higher expression of *nos*2 gene and iNOS protein) and accumulation of malondialdehyde indicating lipid peroxidation (Koner et al., 2019). This increase in the reactive oxygen and nitrogen species production during the early stage of nZnO exposure was accompanied by a decrease in SOD and CAT activities (Koner et al., 2019). Longer exposure led to a gradual return of the levels of these parameters to the baseline levels in *C. magur* hepatocytes indicating that the redox homeostasis was restored (Koner et al., 2019). In the opposite case, in the marsh frog *Pelophylax ridibundus* exposure for 14 d to $100 \, \mu g \, L^{-1}$ of ZnO NPs caused an increase in DNA fragmentation, lipofuscin accumulation as well as upregulation of caspase-3 and CYP450 levels reflecting cytotoxicity of the studied compounds in the liver (Falfushynska et al., 2017).

Studies of the transcriptional response of the antioxidant genes to the exposure of NP in fish show less consistent findings. Thus, in *S. aurata* exposed for 96 h to $4 \, \mu g \, L^{-1}$ of Au NPs coated with citrate or polyvinylpyrrolidone, mRNA levels *GPx1*,

CAT, MT, and *GST3* were upregulated in the blood plasma, but the total antioxidant capacity of the plasma did not change (Teles et al., 2016). In isolated hepatocytes of the magur catfish *Clarias magur* exposed to 5 or 10 mg L^{-1} of nZnO, mRNA levels of *CAT* and *SOD* decreased after 6 h of exposure and returned to the near-baseline levels afterward, closely tracked by the activities of the respective enzymes (Koner et al., 2019). In the Japanese medaka *Oryzias melastigma,* acute exposure to nZnO (4 or 40 mg L^{-1}) had no clear effect on the mRNA expression of *SOD* or metallothionein (Wong et al., 2010). These data indicate a variable transcriptional response of antioxidants to the exposure of NPs in fish and lack of the clear correlation between the transcript level and the antioxidant activity at least in some cases. However, the limited dataset does not yet permit broad generalizations. Further studies are needed to determine the involvement of transcriptional regulation in the oxidative stress response of the NP-exposed fish.

Overall, the exposure to metal-containing NPs appears to induce a consistent oxidative stress response (indicated by the modulation of the antioxidant activities), and in some cases, oxidative distress (indicated by the accumulation of oxidative lesions in proteins and lipids) in fish and frog. However, it is worth noting that most exposures in fish used high NP concentrations (in the mg L^{-1} range) so that the environmental relevance of these findings remains unclear. Further studies are needed to test the effect of nanopollutants on fish that use lower, environmentally relevant concentrations of NPs to resolve the question about the involvement of oxidative stress in the ecotoxicity of NPs in aquatic vertebrates.

5.3 Cyto- and Genotoxicity of Nanoparticles in Aquatic Animals

5.3.1 Invertebrates

Lysosomal membrane stability of the hemocytes is commonly used as a marker of general stress response in the bivalves (Moore et al., 2006; Nigro et al., 2006). Because endocytosis is considered a key route of the uptake of NPs, lysosomes are an important intracellular target for NP toxicity. Earlier studies in marine bivalves *M. galloprovincialis* showed that exposure to nTiO$_2$ and nSiO$_2$ suspensions induced destabilization of the lysosomal membrane and accumulation of lipofuscin (the lipid-containing residues of lysosomal digestion) in the hemocytes and the digestive gland cells of the mussels (Canesi et al., 2010). The uptake of the Neutral Red (a vital dye localizing to the lysosomes) was also modulated by the nZnO in *M. edulis*; however, the response was variable and both decrease (Falfushynska et al., 2019c) and increase (Wu et al., 2020) has been reported. A decrease in the Neutral Red uptake in response to nZnO exposures was also found in a freshwater bivalve *U. tumidus* (Falfushynska et al., 2018). It is worth noting that the Neutral Red uptake is dependent on the lysosomal abundance in the cell as well as the lysosomal membrane stability, and a decrease in this parameter may reflect destabilization of the lysosomal membrane, a loss in the

lysosomal volume, or both. A decrease in the lysosomal volume (measured with a LysoTracker dye) was observed in the hemocytes of *Mytilus coruscus* exposed to 2.5 and 10 mg L^{-1} nZnO (Wu et al., 2018). Alternatively, an increase in the Neutral Red uptake may reflect lysosomal proliferation and enlargement (Wu et al., 2020). Further investigations are needed to disentangle the effects of the metal-containing NPs on the lysosomal quantity and quality in aquatic invertebrates.

DNA damage is likewise considered an important toxicity mechanism for metal-containing NPs due to the direct effects of the NPs binding to the DNA, as well as the indirect effect of oxidative damage. DNA damage was reported in the immune cells of the adult sea urchins *Paracentrotus lividus* exposed to 14 and 100 nm nZnO (10 mg Zn kg^{-1}) through the diet; 64% and 33% of the immune cells contained damaged nuclei, respectively (Manzo et al., 2017). The DNA damage of the gametes is also thought to be responsible for the malformations of the offspring of the NP-exposed urchins. Thus, 85% and 75% of larvae were malformed in the offspring of the urchins fed a diet containing nZnO of different sizes (14 and 100 nm, respectively) (Manzo et al., 2017). Manzo et al. (2017) ascribed the negative effects on the larval development to the genotoxic effects on nZnO in the sperm cells (Manzo et al., 2017). This hypothesis is supported by the study of Oliviero et al. (2019) showing that ZnO NPs in the ecologically relevant concentration induced DNA damages in spermatozoa of Paracentrotus lividus after 30 min of exposure. While the capability of sperm fertilization was not affected, morphological alterations (skeletal alterations) in offspring were observed, and a positive correlation between sperm DNA damage and offspring quality was reported (Oliviero et al., 2019).

Accumulated DNA damage may activate the DNA repair mechanisms during exposures of NPs. Thus, in the blue mussel *M. galloprovincialis* exposure to 10—100,000 μg L^{-1} of nZnO led to a strong upregulation of mRNA levels of DNA repair enzymes such as *p53* and *PDRP* (Li et al., 2018a). Notably, after the prolonged exposure to the concentrations of 1 mg L^{-1} and higher, the expression levels of *p53* and *PDRP* declined followed by the onset of the mass mortality of the mussels (Li et al., 2018a). This indicates that the compensatory response to maintain the DNA integrity is overwhelmed at the high exposure concentrations and/or prolonged exposures to nZnO.

Cytogenetic analysis showed that nZnO exposures can interfere with the cell cycle in invertebrates (Mahmoudi et al., 2011). DNA damage and cell cycle arrest might contribute to the developmental toxicity, and effects were also reported for nZnO and other metal-based NPs. In particular, the larval development of the Mediterranean sea urchin *Paracentrotus lividus* was negatively affected by ZnO NPs (EC50 = 0.46 [0.30–0.63] μM [Zn]) in a concentration-dependent way and disclosed as retarded larvae, malformed larvae, and developmental arrest (Manzo et al., 2013). Exposure of the *Bombyx mori* to ZnO NPs (2 mg per individual) resulted in alteration of hemocyte dynamics including an immediate increase in total hemocytes count, possibly due to the release of these hemocytes either from enhanced rate of cell divisions or from attached hemocyte populations, and decline in the percentage of prohemocytes and increase in the percentage of two professional phagocytes, that is, granulocytes and plasmatocytes, possibly due to the

differentiation of prohemocytes into phagocytes in response to a perceived immune challenge posed by ZnO NPs (Mir et al., 2020). The developmental toxicity of $nTiO_2$ was dependent on its "nano" condition and influenced by the exposure to light. That supported an increase in the number of pre-D shell stage (retarded) larvae compared to the malformed ones, especially at the maximum effect concentrations (4 and 8 mg $nTiO_2$ L^{-1}) (Libralato et al., 2013). The embryonic development of *Arbacia lixula* and *Sphaerechinus granularis* was also sensitive to exposures of Ag NPs with *A. lixula* showing the embryonic abnormalities in a lower concentration range of Ag NPs (1–10 μg L^{-1}) compared with *S. granularis* (10–50 μg L^{-1}) (Burić et al., 2015). Severe morphological malformations and defects in the skeletal parts were found in the developing embryos of Paracentrotus *lividus* exposed to high (300 μg L^{-1}) concentrations of Ag NPs (Siller et al., 2013).

Accumulated cellular damage from mitochondrial dysfunction, oxidative stress (described in Sect. 5.2), lysosomal, and DNA damage can result in the induction of the cell death pathways such as autophagy and apoptosis. Damage to other subcellular compartments and suppression of the cellular protective pathways may also contribute to the widespread cellular damage, as shown in the sea urchin *Paracentrotus lividus* exposed to 0.1 and 10 mg L^{-1} SnO_2, CeO_2, and Fe_3O_4 NPs via oral gavage (Falugi et al., 2012). Harmful modifications in the trans-Golgi and endoplasmic reticulum, inhibition of the acetylcholinesterase activity, and reduction in the expression levels of molecular chaperones HSC70 and GRP78 were found in these exposures (Falugi et al., 2012).

Consistent with the notion of the cellular damage leading to cell death, exposure of *M. edulis* to ZnO NPs and NRs (10 and 100 μg Zn L^{-1}) led to the stimulation of the activity of an important autophagic enzyme, cathepsin D, and upregulation of mRNA expression of several key genes in the apoptosis pathways including caspase 2, caspase 3, and Bcl-2 in the digestive gland of the mussels (Falfushynska et al., 2019c). Notably, this transcriptional upregulation of apoptotic pathways was found only in exposures to ZnO nanomaterials but not in dissolved Zn (Fig. 3). Similarly, activation of cathepsin D was found in the digestive gland of a freshwater bivalve *U. tumidus* exposed to 3.1μM nZnO (Falfushynska et al., 2015b, 2019b) or to 1.25 μM $nTiO_2$ (Gnatyshyna et al., 2019). In the blue mussels *M. edulis*, nZnO-induced activation of apoptosis and autophagy coincided with the onset of the inflammation (indicated by the upregulation of the inflammation markers such as NF-κB mRNA) (Fig. 3) (Falfushynska et al., 2019c). This indicates that the programmed cell death pathways cannot fully contain the spillover effects from the cellular injury in the nZnO-exposed mussels so that the inflammatory stress signal can propagate resulting in tissue-wide damage.

5.3.2   Vertebrates

Like in invertebrates, exposure to the metal-based NPs induces the cytotoxic and genotoxic pathways and causes developmental abnormalities in aquatic vertebrates. For example, treatment of zebrafish embryos with nZnO (1.79–120 mg L^{-1}) for 96 h
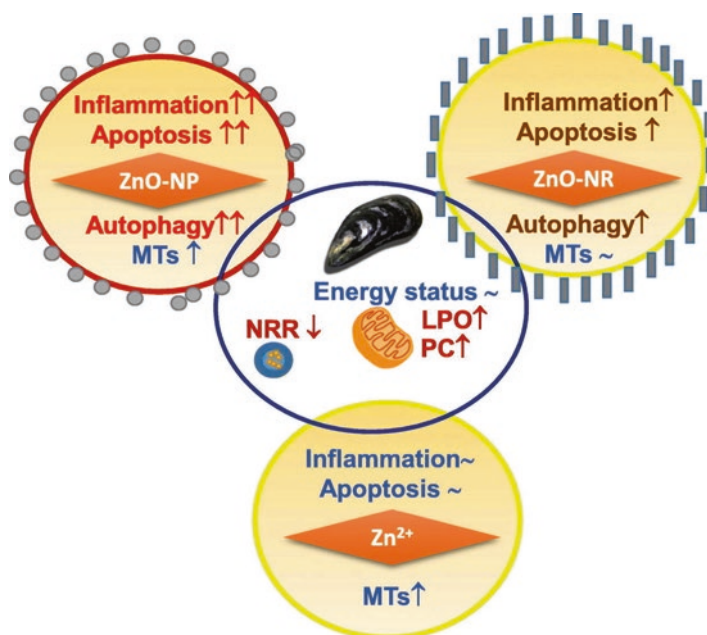
Fig. 3 A schematic representation of the effects of ZnO NPs of different morphology including spherical NPs, nanorods (NR), and dissolved Zn on the digestive gland cells of the blue mussels *M. edulis* (Reproduced with permission [Falfushynska et al. (2019c)]). Note that the two types of nanomaterials induced strong apoptotic and inflammatory responses that were not observed during the exposure to the equivalent concentrations of dissolved Zn

caused larval mortality and teratogenic effects, such as retarded hatching, increased heart rates, reduced larval body length, and tail malformation (Zhu et al., 2008, 2009; Zhao et al., 2016). Similarly, acute exposure to nZnO (1–25 mg L^{-1}) inhibited hatching and induced spinal bending, edema, hypoplasia, and other deformities in the embryos and larvae of the yellowstripe goby *Mugilogobius chulae* (Li et al., 2018b). A histopathologic study of the malformed larvae revealed vacuolar degeneration, enlargement of hepatocytes and enterocytes, and morphological abnormalities of the vertebrae (Li et al., 2018b).

The embryonic and larval teratogenic effects of nZnO in fish have been attributed to the disruption of the cell cycle and induction of oxidative stress due to excessive ROS generation (Zhao et al., 2016; Hou et al., 2019). In zebrafish, nZnO altered the expression of cyclins (Cyc), cyclin-dependent kinases (CDK), and the mini-chromosome maintenance (MCM) protein complex leading to the activation of Cyc/CDK complexes and suppression of the MCM (Zhao et al., 2016; Hou et al., 2019). This resulted in a disorder of the DNA replication in G1, M, and G2 phases of the cell cycle, as well as initiated the expression of antioxidant defense genes (*SOD1, CAT, GPx1a*, and *PPARα*) (Zhao et al., 2016; Hou et al., 2019). Besides, an altered transcriptional regulation of the pro-apoptotic genes (*BAX, PUMA,* and APAF-1) and the antiapoptotic genes (*Bcl-2*) indicated the activation of apoptosis during the

embryonic and larval development of the nZnO-exposed zebrafish likely contributing to mortality and malformation (Zhao et al., 2016). Embryonic and larval lethality and malformations were also reported for zebrafish exposed to Cu NPs. Thus, acute exposures to nano-Cu induced delay in zebrafish hatching and caused deformities and lethal effects on the gastrula stage (Bai et al., 2010). Notably, after the treatment of Cu and CuO NP suspensions in a municipal wastewater treatment system, no embryonic toxicity of the transformed Cu-containing NPs to zebrafish was observed (Lin et al., 2015).

Activation of autophagy and apoptosis are important pathways of nZnO-induced cellular toxicity in vertebrates including fish and frog and may contribute to the adverse developmental effects of nZnO exposure (Scherzad et al., 2017; Falfushynska et al., 2014, 2015a, 2016a, 2016b, 2017; Du et al., 2017; Zhao et al., 2013). ROS generation is considered as a major trigger of the autophagy induction in response to nZnO, associated with the increased autophagosome formation and upregulation of autophagy marker proteins such as microtubule-associated protein 1 light chain 3-isoform II (MAP-LC3-II), and Beclin 1 (Roy et al., 2014). In fact, ZnO NP-induced oxidative DNA damage stimulates autophagy pathways and thus may influence the balance between cell survival and cytotoxicity (Scherzad et al., 2017). Pati et al. (2016) demonstrated inhibition of DNA repair mechanisms. The reduction in the macrophage cell viability was due to the arrest of the cell cycle at the G0/G1 phase, the inhibition of superoxide dismutase, catalase, and eventually ROS. Moreover, exposure of immune cells of C57BL/6J mice to ZnO NPs resulted in autophagic death and increased levels of LC3A, an essential component of autophagic vacuoles. When cells were pretreated with 3-methyladenine (3-MA), a known inhibitor of autophagy, $ZnCl_2$, and ZnO NPs-induced SupT1 cell death was potently inhibited. This indicated that ZnO NP-mediated toxicity of immune cells is due to autophagic death (Brandon et al., 2015).

Apoptosis (likely due to the NP-induced damage of biomolecules including proteins, lipids, and DNA) has also been demonstrated in aquatic vertebrates exposed to metal-containing NPs. This exposure of the zebrafish embryos (96 h postfertilization) to 12.5–50 mg L^{-1} nZnO led to a strong increase in the activity of the apoptotic caspase 3 and (at the highest tested concentration) caspase 9 (Du et al., 2017). At 50 mg L^{-1} nZnO, mRNA expression of the proapoptotic tumor suppressor *p53, BAX*, and *caspases 3* and *9* was upregulated, whereas the transcript levels of an antiapoptotic *Bcl-2* were suppressed in the zebrafish embryos (Du et al., 2017). Suppression of the mRNA expression of an antiapoptotic regulator Bcl-2 was also found in another study in the zebrafish embryos exposed to 10–100 mg L^{-1} nZnO (Zhao et al., 2013). Exposure to Au NP in the ecologically relevant concentration (0.25 μg L^{-1} for *Danio rerio* and 0.5, 4, and 80 μg L^{-1} Au NPs for *S. aurata*) induced apoptosis shown by upregulation of the mRNA expression of the proapoptotic genes, *BAX* and *CASP3* (Dedeh et al., 2015; Teles et al., 2016, 2018). A concomitant upregulation of the transcripts related to the DNA repair (including Fanconi anemia group F protein (FANCF), mismatch repair protein (Msh6), *gaad*, and *rad 51*) indicates that the apoptosis induction in nZnO-exposed *S. aurata* and *D. rerio* might be induced by the elevated DNA damage (Dedeh et al., 2015; Teles et al., 2016, 2018).

Exposure to metal-containing NPs results in cell and tissue damage in adult fish, likely through the same cytotoxic mechanisms as in the embryos and larvae. The gills and the blood cells appear to be the key targets of the toxicity of NPs in fish. Thus, hyperplasia, lamellar fusion, dilation, epithelial lifting, necrosis, and alterations in the secondary structure of the gills were as found in *Cyprinus carpio* after 21 days of exposure to nZnO at three sub-lethal concentrations (5, 10, and 20% of the 96-h LC50 = 4.897 mg L^{-1}) (Subashkumar & Selvanayagam, 2014). Sublethal exposures to nZnO (LC50: 100–110 ppm) and nTiO$_2$ (LC50: 80–90 ppm) NPs also induced a decrease in red blood cells count, hematocrit, and hemoglobin levels and suppressed the oxygen-carrying capacity of red blood cells in the euryhaline fish, the Mozambique tilapia *Oreochromis mossambicus* (Suganthi et al., 2019). A concentration-dependent increase in the number of neutrophils and monocytes and a decreased number of lymphocytes were found in the NP-exposed *O. mossambicus* indicating an inflammatory response (Suganthi et al., 2019). Based on the changes in the blood characteristics, nZnO appeared more toxic than nTiO$_2$ in the *Mozambique tilapia* (Suganthi et al., 2019). Unlike the gills and the blood, the muscle tissue did not show the signs of damage during NP exposure as shown in the perch *Rutilus rutilus* after 96 h exposure to 4.8–48 mg L^{-1} nZnO NPs (Khosravi-Katuli et al., 2018).

5.4 Effect of Nanoparticles on the Immune System of Marine Invertebrates

The innate immune system of invertebrates and lower vertebrates such as fish is a key target for the toxicity of nanomaterials. The immunotoxic effects of NPs in fish have been discussed in a recent comprehensive review (Torrealba et al., 2019). Therefore, in our review, we focused on the effects of NPs on the immune system of marine invertebrates.

The innate immune system of aquatic invertebrates including bivalves relies heavily on circulating hemocytes for immune surveillance. Hemocytes play a key role in pathogen and nonself recognition, phagocytosis and subsequent destruction of the pathogens through cytotoxic reactions and lysosomal degradation, encapsulation of the foreign materials, and production of the humoral immune functions secreted into the hemolymph (Sokolova, 2009). Therefore, modulation of the hemocyte abundance, as well as the functions of the hemocytes (including phagocytosis, adhesion capacity and expression of immune recognition receptors, enzymes, humoral defense, and opsonizing molecules), by the NPs exposure can have important implication for the immune defense of invertebrates and thus for their performance and survival in the aquatic environments, where they exposed to a large number of protozoan, bacterial, and viral pathogens.

Abundance of the circulating hemocytes reflects the balance between hemocyte mortality, hematopoiesis, and migration of the hemocytes between the blood and other body compartments (Allam & Raftos, 2015; Pila et al., 2016). Hemocytes

readily engulf different types of NPs (including different nanosized metal oxides, carbon black, and fullerenes), at least during in vitro exposures as was shown in the blue mussels (Canesi & Corsi, 2016). The uptake of the NPs by the hemocytes during in vivo exposures has not been directly demonstrated but the effects of NPs on the hemocyte functions during in vivo and in vitro exposures indicate a strong impact. Thus, nZnO (0.001–100 mg L^{-1}) as well as other metal-containing NPs including CdS (0.001–100 mg Cd L^{-1}), nAu (0.1–100 mg L^{-1}), nAg (up to 120 ppb), and nTiO$_2$ (1–10 mg L^{-1}) are capable of increasing hemocytes mortality and reducing phagocytosis in *Crassostrea virginica, Mytilus galloprovincialis*, and *R. philippinarum (*Abbott Chalew et al., 2012; Katsumiti et al., 2014; Marisa et al., 2015*)*. Meanwhile, the ionic Zn was more toxic to the hemocytes mussels than ZnO NPs, followed by the ZnO < 130-EcoP90 NPs < ZnO < 280-EcoP90 NPs, and, finally, bulk ZnO, which showed relatively low toxicity (Katsumiti et al., 2014).

We have shown that ZnO NPs in the environmentally relevant concentration affected the immune system of *Mytilus edulis* invading functional parameters such as increased mortality of the mussels' hemocytes, their adhesion capacity and phagocytosis, as well as gene expression profiles (Fig. 4). Moreover, these responses were modulated by a salinity regime (Wu et al., 2020). At salinity equal 15, nZnO suppressed the mRNA expression of the Toll-like receptors TLRb and c, C-lectin, and the complement system component C3q indicating an impaired ability for pathogen recognition. In contrast, the mRNA levels of an antimicrobial peptide defensin increased during nZnO exposure at a salinity of 15. At fluctuating salinity (5–15), nZnO exposure increased an expression of multiple immune-related genes in hemocytes including the complement system components C1 and C3q, and the Toll-like receptors TLRa, b, and c. Low salinity equal 5 had strong
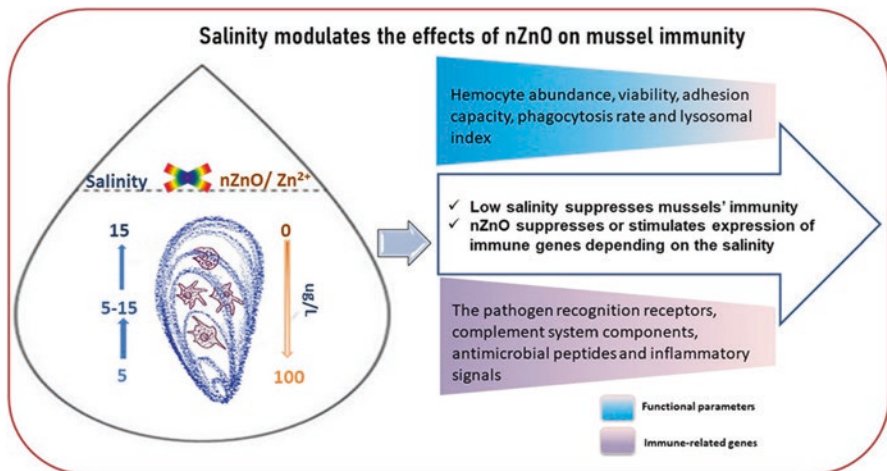
Fig. 4 An overview of the interactive effects of salinity variation and exposure to ZnO nanoparticles on the innate immune system of a sentinel marine bivalve, *M. edulis.* (Reproduced with permission [Wu et al. (2020)])

immunosuppressive effects on functional and molecular immune traits of *M. edulis* that overshadowed the effects of nZnO. They were able to compensate the negative effects of nZnO on the hemocyte viability at normal and fluctuating salinity. So, the abundance of circulating hemocytes remained at a normal level. This might reflect elevated hematopoiesis and/or recruitment of the resident hemocytes from the tissues of nZnO-exposed mussels. A salinity-dependent modulation of the immune response to nZnO cannot be attributed to differences in the aggregation or solubility of nZnO, and it likely reflects the interaction of the toxic effects of NPs and physiological effects of the osmotic stress (Wu et al., 2020).

Different metal-containing NPs were shown to affect the phagocytic activity in the hemocytes of oyster *C. gigas* (Abbott Chalew et al., 2012) and of the clam *Ruditapes decussatus* (Marisa et al., 2015). Interestingly, the induction of functional responses, as well as of cellular damage and apoptotic processes, was particularly rapid, occurring within 1 h of exposure. This corresponds to a physiological role of the bivalve hemocytes representing the first line of defense against the nonself materials (Canesi & Prochàzovà, 2013). The exposure of blood clam, *Tegillarca granosa,* to $0.1–10$ mg L^{-1} of ZnO NPs as well as nFe_2O_3 and nCuO resulted in reduced total counts, altered cell composition, and constrained phagocytic activities of the hemocytes. The intracellular contents of the reactive oxygen species and a degree of DNA damage of the hemocytes were significantly induced, whereas the hemocyte viability was suppressed. Furthermore, exposures of NPs led to significant increases in the in vivo content of neurotransmitters and downregulations of the expression of immune- and neurotransmitter-related genes (Zha et al., 2019). A similar pattern was disclosed also for $nTiO_2$ and silver NPs. In particular, different doses of $nTiO_2$ $(0.05, 0.2, 1.0, 5.0$ mg $L^{-1})$ of $nTiO_2$ decreased lysosomal membrane stability and phagocytosis, increased oxyradical production, transcription of antimicrobial peptides, and suppressed the immune system in *M. galloprovincialis* (Canesi et al., 2010). This was in agreement with a decrease in total hemocytes count, phagocytic activity, and esterase and lysosomal contents in mussel *M. coruscus* after 14-day exposure to $nTiO_2$ (Huang et al., 2016). Moreover, $nTiO_2$ (1, 10 and 100 μg L^{-1}) and silver NPs stimulated the pre-apoptotic processes and phenoloxidase activity in vivo in *M. galloprovincialis, C. virginica*, and *S. plana* (Abbott Chalew et al., 2012).

6   Conclusions

NPs are widely used substances with numerous beneficial properties; however, they can be released in the environment and threaten the nontarget organisms. NPs can provoke various toxic effects related to their physicochemical characteristics, namely, small size and shape, acid–base character of surface, surface coating, and aqueous solubility of the metal (in case of metal-based NPs) (see Fig. 5). NPs can be absorbed via a variety of exposure routes, including gills, chorion, intestinal, or blood–brain barrier, as well as using transcutaneous routes, and then be translocated to target organs. Numerous studies concerning the effects of NPs on the biota have
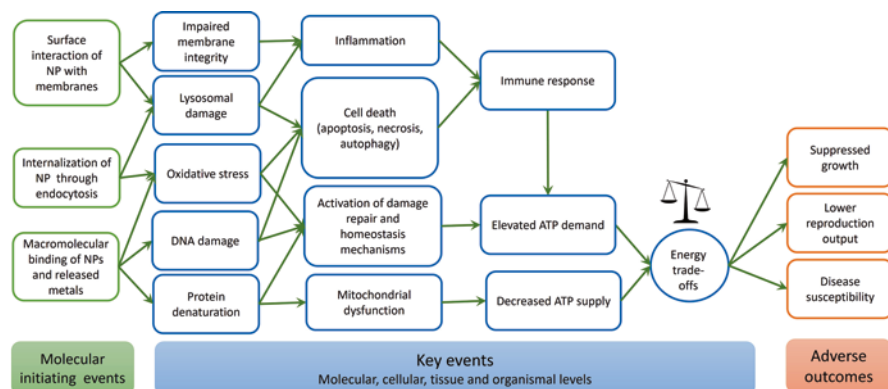
Fig. 5 A scheme of possible events on different levels of biological organization under the effect of ZnO NPs

proven that the oxidative stress, immunomodulation, and inflammation are the major mechanisms of their toxicity. Taking into consideration the above-mentioned issues, the application of the NPs in real-life requires actual standards and specific regulations of their manufacturing, use, and waste handle. Furthermore, a toxicological profile of the metal-based NPs in marine fish at the environmentally relevant concentrations requires further elucidation.

References

Abbott Chalew, T. E., Galloway, J. F., & Graczyk, T. K. (2012). Pilot study on effects of nanoparticle exposure on Crassostrea virginica hemocyte phagocytosis. *Marine Pollution Bulletin, 64*(10), 2251–2253. https://doi.org/10.1016/j.marpolbul.2012.06.026

Adeleye, A. S., Conway, J. R., Perez, T., Rutten, P., & Keller, A. A. (2014). Influence of extracellular polymeric substances onthe long-term fate, dissolution, and speciation of copper-based nanoparticles. *Environmental Science & Technology, 48*(21), 12561–12568. https://doi.org/10.1021/es5033426

Allam, B., & Raftos, D. (2015). Immune responses to infectious diseases in bivalves. *Journal of Invertebrate Pathology, 131*, 121–136. https://doi.org/10.1016/j.jip.2015.05.005

Ates, M., Danabas, D., Ertit Tastan, B., Unal, I., Cicek Cimen, I. C., Aksu, O., Kutlu, B., & Arslan, Z. (2019). Assessment of oxidative stress on artemia salina and *Daphnia magna* after exposure to Zn and ZnO nanoparticles. *Bulletin of Environmental Contamination and Toxicology, 104*, 206–214. https://doi.org/10.1007/s00128-019-02751-6

Bai, W., Tian, W., Zhang, Z., He, X., Ma, Y., Liu, N., & Chai, Z. (2010). Effects of copper nanoparticles on the development of zebrafish embryos. *Journal of Nanoscience and Nanotechnology, 10*(12), 8670–8676. https://doi.org/10.1166/jnn.2010.2686

Baker, T. J., Tyler, C. R., & Galloway, T. S. (2014). Impacts of metal and metal oxide nanoparticles on marine organisms. *Environmental Pollution, 186*, 257–271.

Barba, A. A., Bochicchio, S., Dalmoro, A., Caccavo, D., Cascone, S., & Lamberti, G. (2019). Chapter 10 – Polymeric and lipid-based systems for controlled drug release: An engineering point of view. In A. M. Grumezescu (Ed.), *Nanomaterials for drug delivery and therapy* (pp. 267–304). William Andrew Publishing.

Beegam, A., Lopes, M., Fernandes, T., Jose, J., Barreto, A., Oliveira, M., Soares, A. M. V. M., Trindade, T., Thomas, S., & Pereira, M. L. (2019). Multiorgan histopathological changes in the juvenile seabream Sparus aurata as a biomarker for zinc oxide particles toxicity. *Environmental Science and Pollution Research International, 27*(25), 30907–30917. https://doi.org/10.1007/s11356-019-05949-7

Benavides, M., Fernández-Lodeiro, J., Coelho, P., Lodeiro, C., & Diniz, M. S. (2016). Single and combined effects of aluminum (Al2O3) and zinc (ZnO) oxide nanoparticles in a freshwater fish, *Carassius auratus*. *Environmental Science and Pollution Research International, 23*(24), 24578–24591. https://doi.org/10.1007/s11356-016-7915-3

Berg, J. M., Romoser, A., Banerjee, N., Zebda, R., & Sayes, C. M. (2009). The relationship between pH and zeta potential of ∼ 30 nm metal oxide nanoparticle suspensions relevant to in vitro toxicological evaluations. *Nanotoxicology, 3*(4), 276–283. https://doi.org/10.3109/17435390903276941

Bergami, E., Bocci, E., Vannuccini, M. L., Monopoli, M., Salvati, A., Dawson, K. A., & Corsi, I. (2016). Nano-sized polystyrene affects feeding, behavior and physiology of brine shrimp Artemia franciscana larvae. *Ecotoxicology and Environmental Safety, 123*, 18–25. https://doi.org/10.1016/j.ecoenv.2015.09.021

Bessemer, R. A., Butler, K. M., Tunnah, L., Callaghan, N. I., Rundle, A., Currie, S., Dieni, C. A., & MacCormack, T. J. (2015). Cardiorespiratory toxicity of environmentally relevant zinc oxide nanoparticles in the freshwater fish Catostomus commersonii. *Nanotoxicology, 9*(7), 861–870. https://doi.org/10.3109/17435390.2014.982737

Bondarenko, O., Juganson, K., Ivask, A., Kasemets, K., Mortimer, M., & Kahru, A. (2013). Toxicity of Ag, CuO and ZnO nanoparticles to selected environmentally relevant test organisms and mammalian cells in vitro: A critical review. *Archives of Toxicology, 87*(8), 1181–1200. https://doi.org/10.1007/s00204-013-1079-4

Boxall, A. B. A., Chaudhry, Q., Sinclair, C., Jones, A. D., Aitken, R., Jefferson, B., & Watts, C. (2007). *Current and future predicted environmental exposure to engineered nanoparticles*. Central Science Laboratory.

Brandon, M. J., Fraietta, J. A., Gracias, D. T., Hope, J. L., Stairiker, C. J., Patel, P. R., Mueller, Y. M., McHugh, M. D., Jablonowski, L. J., Wheatley, M. A., & Katsikis, P. D. (2015). Acute exposure to ZnO nanoparticles induces autophagic immune cell death. *Nanotoxicology, 9*(6), 737–748. https://doi.org/10.3109/17435390.2014.974709

Buffet, P. E., Amiard-Triquet, C., Dybowska, A., Risso-de Faverney, C., Guibbolini, M., Valsami-Jones, E., & Mouneyrac, C. (2012). Fate of isotopically labeled zinc oxide nanoparticles in sediment and effects on two endobenthic species, the clam *Scrobicularia plana* and the ragworm Hediste diversicolor. *Ecotoxicology and Environmental Safety, 84*, 191–198. https://doi.org/10.1016/j.ecoenv.2012.07.010

Buffet, P. E., Tankoua, O. F., Pan, J. F., Berhanu, D., Herrenknecht, C., Poirier, L., Amiard-Triquet, C., Amiard, J. C., Bérard, J. B., Risso, C., Guibbolini, M., Roméo, M., Reip, P., Valsami-Jones, E., & Mouneyrac, C. (2011). Behavioural and biochemical responses of two marine invertebrates Scrobicularia plana and Hediste diversicolor to copper oxide nanoparticles. *Chemosphere, 84*(1), 166–174. https://doi.org/10.1016/j.chemosphere.2011.02.003

Burić, P., Jakšić, Ž., Štajner, L., Dutour Sikirić, M., Jurašin, D., Cascio, C., Calzolai, L., & Lyons, D. M. (2015). Effect of silver nanoparticles on Mediterranean sea urchin embryonal development is species specific and depends on moment of first exposure. *Marine Environmental Research, 111*, 50–59. https://doi.org/10.1016/j.marenvres.2015.06.015

Bury, N. R., Grosell, M., Grover, A. K., & Wood, C. M. (1999). ATP-dependent silver transport across the basolateral membrane of rainbow trout gills. *Toxicology and Applied Pharmacology, 159*(1), 1–8.

Canesi, L., & Procházková, P. (2014). Chapter 7 - The Invertebrate Immune System as a Model for Investigating the Environmental Impact of Nanoparticles. In D.Boraschi, & A. Duschl (Eds.), *Nanoparticles and the Immune System* (pp. 91-112). Academic Press. https://doi.org/10.1016/B978-0-12-408085-0.00007-8

Canesi, L., & Corsi, I. (2016). Effects of nanomaterials on marine invertebrates. *Science of the Total Environment, 565*, 933–940. https://doi.org/10.1016/j.scitotenv.2016.01.085

Canesi, L., Ciacci, C., Fabbri, R., Marcomini, A., Pojana, G., & Gallo, G. (2012). Bivalve molluscs as a unique target group for nanoparticle toxicity. *Marine Environmental Research, 76*, 16–21. https://doi.org/10.1016/j.marenvres.2011.06.005

Canesi, L., Fabbri, R., Gallo, G., Vallotto, D., Marcomini, A., & Pojana, G. (2010). Biomarkers in *Mytilus galloprovincialis* exposed to suspensions of selected nanoparticles (nano carbon black, C60 fullerene, nano-TiO2, nano-SiO2). *Aquatic Toxicology, 100*(2), 168–177. https://doi.org/10.1016/j.aquatox.2010.04.009

Cho, W. S., Duffin, R., Thielbeer, F., Bradley, M., Megson, I. L., MacNee, W., Poland, C. A., Lang Tran, C., & Donaldson, K. (2012). Zeta potential and solubility to toxic ions as mechanisms of lung inflammation caused by metal/metal oxide nanoparticles. *Toxicological Sciences, 126*(2), 469–477.

Chovanec, A., Hofer, R., & Schiemer, F. (2003). Chapter 18. Fish as bioindicators. In *Trace metals and other contaminants in the environment* (Vol. 6, pp. 639–676). Elsevier. https://doi.org/10.1016/S0927-5215(03)80148-0

Ciacci, C., Canonico, B., Bilaniĉovă, D., Fabbri, R., Cortese, K., Gallo, G., Marcomini, A., Pojana, G., & Canesi, L. (2012). Immunomodulation by different types of N-oxides in the hemocytes of the marine bivalve Mytilus galloprovincialis. *PLoS One, 7*(5), e36937. https://doi.org/10.1371/journal.pone.0036937

Coll, C., Notter, D., Gottschalk, F., Sun, T., Som, C., & Nowack, B. (2016). Probabilistic environmental risk assessment of five nanomaterials (nano-TiO2, nano-Ag, nano-ZnO, CNT, and fullerenes). *Nanotoxicology, 10*(4), 436–444. https://doi.org/10.3109/17435390.2015

Connolly, M., Fernández, M., Conde, E., Torrent, F., Navas, J. M., & Fernández-Cruz, M. L. (2016). Tissue distribution of zinc and subtle oxidative stress effects after dietary administration of ZnO nanoparticles to rainbow trout. *Science of the Total Environment, 551–552*, 334–343. https://doi.org/10.1016/j.scitotenv.2016.01.186

Dedeh, A., Ciutat, A., Treguer-Delapierre, M., & Bourdineaud, J. P. (2015). Impact of gold nanoparticles on zebrafish exposed to a spiked sediment. *Nanotoxicology, 9*, 71–80. https://doi.org/10.3109/17435390.2014.889238

Du, J., Cai, J., Wang, S., & You, H. (2017). Oxidative stress and apoptosis to zebrafish (Danio rerio) embryos exposed to perfluorooctane sulfonate (PFOS) and ZnO nanoparticles. *International Journal of Occupational Medicine and Environmental Health, 30*, 213–229. https://doi.org/10.13075/ijomeh.1896.00669

Fahmy, S. R., Abdel-Ghaffar, F., Bakry, F. A., & Sayed, D. A. (2014). Ecotoxicological effect of sublethal exposure to zinc oxide nanoparticles on freshwater snail Biomphalaria alexandrina. *Archives of Environmental Contamination and Toxicology, 67*(2), 192–202. https://doi.org/10.1007/s00244-014-0020-z

Falfushynska, H. I., Gnatyshyna, L. L., Ivanina, A. V., Khoma, V. V., Stoliar, O. B., & Sokolova, I. M. (2019a). Bioenergetic responses of freshwater mussels *Unio tumidus* to the combined effects of nano-ZnO and temperature regime. *Science of the Total Environment, 650*, 1440–1450. https://doi.org/10.1016/j.scitotenv.2018.09.136

Falfushynska, H. I., Wu, F., Ye, F., Kasianchuk, N., Dutta, J., Dobretsov, S., & Sokolova, I. M. (2019b). The effects of ZnO nanostructures of different morphology on bioenergetics and stress response biomarkers of the blue mussels *Mytilus edulis*. *Science of the Total Environment, 694*, 133717. https://doi.org/10.1016/j.scitotenv.2019.133717

Falfushynska, H., Gnatyshyna, L., Fedoruk, O., Mitina, N., Zaichenko, A., Stoliar, O., & Stoika, R. (2015a). Hepatic metallothioneins in molecular responses to cobalt, zinc, and their nanoscale polymeric composites in frog Rana ridibunda. *Comparative Biochemistry and Physiology, 172–173C*, 45–56. https://doi.org/10.1016/j.cbpc.2015.04.006

Falfushynska, H., Gnatyshyna, L., Fedoruk, O., Sokolova, I. M., & Stoliar, O. (2016a). Endocrine activities and cellular stress responses in the marsh frog *Pelophylax ridibundus* exposed to cobalt, zinc and their organic nanocomplexes. *Aquatic Toxicology, 170*, 62–71. https://doi.org/10.1016/j.aquatox.2015.11.006

Falfushynska, H., Gnatyshyna, L., Horyn, O., Shulgai, A., & Stoliar, O. (2019c). A calcium channel blocker nifedipine distorts the effects of nano-zinc oxide on metal metabolism in the marsh frog *Pelophylax ridibundus*. *Saudi Journal of Biological Sciences, 26*(3), 481–489. https://doi.org/10.1016/j.sjbs.2017.10.004

Falfushynska, H., Gnatyshyna, L., Horyn, O., Sokolova, I., & Stoliar, O. (2017). Endocrine and cellular stress effects of zinc oxide nanoparticles and nifedipine in marsh frogs *Pelophylax ridibundus*. *Aquatic Toxicology, 185*, 171–182. https://doi.org/10.1016/j.aquatox.2017.02.009

Falfushynska, H., Gnatyshyna, L., Ivanina, A., Sokolova, I. M., & Stoliar, O. B. (2018). Detoxification and cellular stress responses of unionid mussels *Unio tumidus* from two cooling ponds to combined nano-ZnO and temperature stress. *Chemosphere, 193*, 1127–1142. https://doi.org/10.1016/j.chemosphere.2017.11.079

Falfushynska, H., Gnatyshyna, L., Myhalska, V., Romanchuk, L., & Stoliar, O. (2016b). Reductive and endocrine effects of zinc oxide nanoparticles in marsh frog *Pelophylax ridibundus* and their modulation in combine exposures. *Visnyk of L'viv Univ Biology Series, 73*, 213–216.

Falfushynska, H., Gnatyshyna, L., Stoliar, O., Mitina, N., Skorokhoda, T., Filyak, Y., Zaichenko, A., & Stoika, R. (2012). Evaluation of biotargeting and ecotoxicity of Co^{2+}-containing nanoscale polymeric complex by applying multi-marker approach in bivalve mollusk *Anodonta cygnea*. *Chemosphere, 88*(8), 925–936. https://doi.org/10.1016/j.chemosphere.2012.02.087

Falfushynska, H., Gnatyshyna, L., Turta, O., Stoliar, O., Mitina, N., Zaichenko, A., & Stoika, R. (2014). Responses of hepatic metallothioneins and apoptotic activity in *Carassius auratus gibelio* witness a release of cobalt and zinc from waterborne nanoscale composites. *Comparative Biochemistry and Physiology, 160C*, 66–74.

Falfushynska, H., Gnatyshyna, L., Yurchak, I., Sokolova, I., & Stoliar, O. (2015b). The effects of zinc nanooxide on cellular stress responses of the freshwater mussels *Unio tumidus* are modulated by elevated temperature and organic pollutants. *Aquatic Toxicology, 162*, 82–93. https://doi.org/10.1016/j.aquatox.2015.03.006

Falfushynska, H., Sokolov, E. P., Haider, F., Oppermann, C., Kragl, U., Ruth, W., Stock, M., Glufke, S., Winkel, E. J., & Sokolova, I. M. (2019d). Effects of a common pharmaceutical, atorvastatin, on energy metabolism and detoxification mechanisms of a marine bivalve *Mytilus edulis*. *Aquatic Toxicology, 208*, 47–61. https://doi.org/10.1016/j.aquatox.2018.12.022

Falugi, C., Aluigi, M. G., Chiantore, M. C., Privitera, D., Ramoino, P., Gatti, M. A., Fabrizi, A., Pinsino, A., & Matranga, V. (2012). Toxicity of metal oxide nanoparticles in immune cells of the sea urchin. *Marine Environmental Research, 76*, 114–121. https://doi.org/10.1016/j.marenvres.2011.10.003

Festa, R. A., & Thiele, D. J. (2011). Copper: An essential metal in biology. *Current Biology, 21*(21), R877–R883. https://doi.org/10.1016/j.cub.2011.09.040

Gagné, F., Auclair, J., Turcotte, P., Gagnon, C., Peyrot, C., & Wilkinson, K. (2019). The influence of surface waters on the bioavailability and toxicity of zinc oxidenanoparticles in freshwater mussels. *Comparative Biochemistry and Physiology Part C: Toxicology and Pharmacology, 219*, 1–11. https://doi.org/10.1016/j.cbpc.2019.01.005

Gagné, F., Auclair, J., Peyrot, C., & Wilkinson, K. J. (2015). The influence of zinc chloride and zinc oxide nanoparticles on air-time survival in freshwater mussels. *Comparative Biochemistry and Physiology Part C: Toxicology & Pharmacology, 172–173*, 36–44. https://doi.org/10.1016/j.cbpc.2015.04.005

Gagnon, C., Pilote, M., Turcotte, P., André, C., & Gagné, F. (2016). Effects of exposure to zinc oxide nanoparticles in freshwater mussels in the presence of municipal effluents. *Invertebrate Survival Journal, 13*(1), 140–152.

García-Gómez, C., García, S., Obrador, A., Almendros, P., González, D., & Fernández, M. D. (2020). Effect of ageing of bare and coated nanoparticles of zinc oxide applied to soil on the Zn behaviour and toxicity to fish cells due to transfer from soil to water bodies. *Science of the Total Environment, 706*, 135713. https://doi.org/10.1016/j.scitotenv.2019.135713

Garner, K. L., Suh, S., & Keller, A. A. (2017). Assessing the risk of engineered nanomaterials in the environment: Development and application of the nanoFate model. *Environmental Science & Technology, 51*(10), 5541–5551. https://doi.org/10.1021/acs.est.6b05279

Gatoo, M. A., Naseem, S., Arfat, M. Y., Dar, A. M., Qasim, K., & Zubair, S. (2014). Physicochemical properties of nanomaterials: Implication in associated toxic manifestations. *BioMed Research International, 2014*, 498420. https://doi.org/10.1155/2014/498420

Georgantzopoulou, A., Almeida Carvalho, P., Vogelsang, C., Tilahun, M., Ndungu, K., Booth, A. M., Thomas, K. V., & Macken, A. (2018). Ecotoxicological effects of transformed silver and titanium dioxide nanoparticles in the effluent from a lab-scale wastewater treatment system. *Environmental Science & Technology, 52*(16), 9431–9441. https://doi.org/10.1021/acs.est.8b01663

Gnatyshyna, L., Falfushynska, H., Horyn, O., Khoma, V., Martinyuk, V., Mishchuk, O., Mishchuk, N., & Stoliar, O. (2019). Biochemical responses of freshwater mussel *Unio tumidus* to titanium oxide nanoparticles, Bisphenol A, and their combination. *Ecotoxicology, 28*, 923–937. https://doi.org/10.17632/cnhjzb2x49.1

Golbamaki, N., Rasulev, B., Cassano, A., Marchese Robinson, R. L., Benfenati, E., Leszczynski, J., & Cronin, M. T. (2015). Genotoxicity of metal oxide nanomaterials: Review of recent data and discussion of possible mechanisms. *Nanoscale, 7*(6), 2154–2198. https://doi.org/10.1039/c4nr06670g

Gottschalk, F., Lassen, C., Kjoelholt, J., Christensen, F., & Nowack, B. (2015). Modeling flows and concentrations of nine engineered nanomaterials in the danish environment. *International Journal of Environmental Research and Public Health, 12*(5), 5581–5602. https://doi.org/10.3390/ijerph120505581

Gottschalk, F., Sonderer, T., Scholz, R. W., & Nowack, B. (2009). Modeled environmental concentrations of engineered nanomaterials (TiO_2, ZnO, Ag, CNT, fullerenes) for different regions. *Environmental Science & Technology, 43*, 9216–9222. https://doi.org/10.1021/es9015553

Gottschalk, F., Sun, T., & Nowack, B. (2013). Environmental concentrations of engineered nanomaterials: Review of modeling and analytical studies. *Environmental Pollution, 181*, 287–300. https://doi.org/10.1016/j.envpol.2013.06.003

Graca, B., Zgrundo, A., Zakrzewska, D., Rzodkiewicz, M., & Karczewski, J. (2018). Origin and fate of nanoparticles in marine water – Preliminary results. *Chemosphere, 206*, 359–368. https://doi.org/10.1016/j.chemosphere.2018.05.022

Haider, F., Sokolov, E. P., & Sokolova, I. M. (2018). Effects of mechanical disturbance and salinity stress on bioenergetics and burrowing behavior of the soft-shell clam *Mya arenaria*. *Journal of Experimental Biology, 221*(Pt 4), jeb172643. https://doi.org/10.1242/jeb.172643

Handy, R. D., Henry, T. B., Scown, T. M., Johnston, B. D., & Tyler, C. R. (2008). Manufactured nanoparticles: Their uptake and effects on fish–a mechanistic analysis. *Ecotoxicology, 17*(5), 396–409. https://doi.org/10.1007/s10646-008-0205-1

Hanna, S. K., Miller, R. J., Muller, E. B., Nisbet, R. M., & Lenihan, H. S. (2013). Impact of engineered zinc oxide nanoparticles on the individual performance of *Mytilus galloprovincialis*. *PLoS One, 8*(4), e61800. https://doi.org/10.1371/journal.pone.0061800

Hernández-Moreno, D., Valdehita, A., Conde, E., Rucandio, I., Navas, J.M., & Fernández-Cruz, M.L. (2019). Acute toxic effects caused by the co-exposure ofnanoparticles of ZnO and Cu in rainbow trout. *Science Total Environment, 687*, 24–33. https://doi.org/10.1016/j.scitotenv.2019.06.084

Hou, J., Liu, H., Zhang, S., Liu, X., Hayat, T., Alsaedi, A., & Wang, X. (2019). Mechanism of toxic effects of Nano-ZnO on cell cycle of zebrafish (*Danio rerio*). *Chemosphere, 229*, 206–213. https://doi.org/10.1016/j.chemosphere.2019.04.217

Huang, X., Lin, D., Ning, K., Sui, Y., Hu, M., Lu, W., & Wang, Y. (2016). Hemocyte responses of the thick shell mussel *Mytilus coruscus* exposed to nano-TiO2 and seawater acidification. *Aquatic Toxicology, 180*, 1–10. https://doi.org/10.1016/j.aquatox.2016.09.008

Huang, B., Cui, Y.Q., Guo, W.B., Yang, L., & Miao, A.J. (2020). Waterborne and dietary accumulation of well-dispersible hematite nanoparticles by zebrafish atdifferent life stages. *Environmental Pollution, 259*, 113852. https://doi.org/10.1016/j.envpol.2019.113852

Johnston, B. D., Scown, T. M., Moger, J., Cumberland, S., Baalousha, M., Linge, K., van Aerle, R., Jarvis, K., Lead, J. R., & Tyler, C. R. (2010). Bioavailability of nanoscale metal oxides, TiO2, CeO2, and ZnO to fish. *Environmental Science and Technology, 44*(3), 1144–1151. https://doi.org/10.1021/es901971a

Kadar, E., Cunliffe, M., Fisher, A., Stolpe, B., Lead, J., & Shi, Z. (2014). Chemical interaction of atmospheric mineral dust-derived nanoparticles with natural seawater-EPS and sunlight-mediated changes. *Science of the Total Environment, 468–469*, 265–271. https://doi.org/10.1016/j.scitotenv.2013.08.059

Kahru, A., & Dubourguier, H.-C. (2010). From ecotoxicology to nanoecotoxicology. *Toxicology, 269*, 105–119.

Katsumiti, A., Gilliland, D., Arostegui, I., & Cajaraville, M. P. (2014). Cytotoxicity and cellular mechanisms involved in the toxicity of CdS quantum dots in hemocytes and gill cells of the mussel *Mytilus galloprovincialis*. *Aquatic Toxicology, 153*, 39–52. https://doi.org/10.1016/j.aquatox.2014.02.003

Keller, A. A., Wang, H. T., Zhou, D. X., Lenihan, H. S., Cherr, G., Cardinale, B. J., & Miller, & R., Ji, Z. X. (2010). Stability and aggregation of metal oxide nanoparticles in natural aqueous matrices. *Environmental Science & Technology, 44*, 1962–1967.

Khosravi-Katuli, K., Lofrano, G., Pak Nezhad, H., Giorgio, A., Guida, M., Aliberti, F., Siciliano, A., Carotenuto, M., Galdiero, E., Rahimi, E., & Libralato, G. (2018). Effects of ZnO nanoparticles in the Caspian roach (*Rutilus rutilus caspicus*). *Science of the Total Environment, 626*, 30–41. https://doi.org/10.1016/j.scitotenv.2018.01.085

Klaine, S. J., Alvarez, P. J. J., Batley, G. E., Fernandes, T. F., Handy, R. D., Lyon, D. Y., Mahendra, S., McLaughlin, M. J., & Lead, J. R. (2008). Nanomaterials in the environment: Behavior, fate, bioavailability, and effects. *Environmental Toxicology and Chemistry, 27*, 1825–1851.

Koner, D., Banerjee, B., Hasan, R., & Saha, N. (2019). Antioxidant activity of endogenously produced nitric oxide against the zinc oxide nanoparticle-induced oxidative stress in primary hepatocytes of air-breathing catfish, Clarias magur. *Nitric Oxide, 84*, 7–15. https://doi.org/10.1016/j.niox.2018.12.010

Kumar, N., Chandan, N. K., Wakchaure, G. C., & Singh, N. P. (2019). Synergistic effect of zinc nanoparticles and temperature on acute toxicity with response to biochemical markers and histopathological attributes in fish. *Comparative Biochemistry and Physiology Part C: Toxicology & Pharmacology, 229*, 108678. https://doi.org/10.1016/j.cbpc.2019.108678

Lammel, T., Mackevica, A., Johansson, B. R., & Sturve, J. (2019). Endocytosis, intracellular fate, accumulation, and agglomeration of titanium dioxide (TiO$_2$) nanoparticles in the rainbow trout liver cell line RTL-W1. *Environmental Science and Pollution Research, 26*, 15354–15372. https://doi.org/10.1007/s11356-019-04856-1

Li, J., Chen, Z., Huang, R., Miao, Z., Cai, L., & Du, Q. (2018a). Toxicity assessment and histopathological analysis of nano-ZnO against marine fish (*Mugilogobius chulae*) embryos. *Journal of Environmental Sciences (China), 73*, 78–88. https://doi.org/10.1016/j.jes.2018.01.015

Li, J., Schiavo, S., Xiangli, D., Rametta, G., Miglietta, M. L., Oliviero, M., Changwen, W., & Manzo, S. (2018b). Early ecotoxic effects of ZnO nanoparticle chronic exposure in *Mytilus galloprovincialis* revealed by transcription of apoptosis and antioxidant-related genes. *Ecotoxicology, 27*(3), 369–384. https://doi.org/10.1007/s10646-018-1901-0

Li, K. G., & Chen, Y. S. (2012). Effect of natural organic matter on the aggregation kinetics of CeO2 nanoparticles in KCl and CaCl2 solutions: Measurements and modeling. *Journal of Hazardous Materials, 209–210*, 264–270. https://doi.org/10.1016/j.jhazmat.2012.01.013

Libralato, G., Minetto, D., Totaro, S., Mičetić, I., Pigozzo, A., Sabbioni, E., Marcomini, A., & Ghirardini, A. V. (2013). Embryotoxicity of TiO2 nanoparticles to Mytilus galloprovincialis (Lmk). *Marine Environmental Research, 92*, 71–78. https://doi.org/10.1016/j.marenvres.2013.08.015

Lin, S., Taylor, A. A., Ji, Z., Chang, C. H., Kinsinger, N. M., Ueng, W., Walker, S. L., & Nel, A. E. (2015). Understanding the transformation, speciation, and hazard potential of copper particles in a model septic tank system using zebrafish to monitor the effluent. *ACS Nano, 9*(2), 2038–2048. https://doi.org/10.1021/nn507216f

Liu, J., Feng, X., Wei, L., Chen, L., Song, B., & Shao, L. (2016). The toxicology of ion-shedding zinc oxide nanoparticles. *Critical Reviews in Toxicology, 46*(4), 348–384. https://doi.org/10.3109/10408444.2015.1137864

Mahmoudi, M., Azadmanesh, K., Shokrgozar, M. A., Journeay, W. S., & Laurent, S. (2011). Effect of nanoparticles on the cell life cycle. *Chemical Reviews, 111*(5), 3407–3432. https://doi.org/10.1021/cr1003166

Manzo, S., Miglietta, M. L., Rametta, G., Buono, S., & Di Francia, G. (2013). Embryotoxicity and spermiotoxicity of nanosized ZnO for Mediterranean sea urchin Paracentrotus lividus. *Journal of Hazardous Materials, 254–255*, 1–9.

Manzo, S., Schiavo, S., Oliviero, M., Toscano, A., Ciaravolo, M., & Cirino, P. (2017). Immune and reproductive system impairment in adult sea urchin exposed to nanosized ZnO via food. *Science of the Total Environment, 599–600*, 9–13. https://doi.org/10.1016/j.scitotenv.2017.04.173

Maret, W. (2017). Zinc in cellular regulation: The nature and significance of "zinc signals". *International Journal of Molecular Sciences, 18*(11), E2285. https://doi.org/10.3390/ijms18112285

Marisa, I., Marin, M. G., Caicci, F., Franceschinis, E., Martucci, A., & Matozzo, V. (2015). In vitro exposure of haemocytes of the clam Ruditapes philippinarum to titanium dioxide (TiO2) nanoparticles: Nanoparticle characterisation, effects on phagocytic activity and internalisation of nanoparticles into haemocytes. *Marine Environmental Research, 103*, 11–17. https://doi.org/10.1016/j.marenvres.2014.11.002

Marisa, I., Matozzo, V., Munari, M., Binelli, A., Parolini, M., Martucci, A., Franceschinis, E., Brianese, N., & Marin, M. G. (2016). In vivo exposure of the marine clam Ruditapes philippinarum to zinc oxide nanoparticles: Responses in gills, digestive gland and haemolymph. *Environmental Science and Pollution Research International, 23*(15), 15275–15293. https://doi.org/10.1007/s11356-016-6690-5

Mattsson, K., Johnson, E. V., & Malmendal, A. (2017). Brain damage and behavioural disorders in fish induced by plastic nanoparticles delivered through the food chain. *Scientific Reports, 7*, 11452. https://doi.org/10.1038/s41598-017-10813-0

Maurer, L. L., & Meyer, J. N. (2016). A systematic review of evidence for silver nanoparticle-induced mitochondrial toxicity. *Environmental Science: Nano, 3*, 311.

Mir, A. H., Qamar, A., Qadir, I., Naqvi, A. H., & Begum, R. (2020). Accumulation and trafficking of zinc oxide nanoparticles in an invertebrate model, Bombyx mori, with insights on their effects on immuno-competent cells. *Scientific Reports, 10*(1), 1617. https://doi.org/10.1038/s41598-020-58526-1

Montes, M. O., Hanna, S. K., Lenihan, H. S., & Keller, A. A. (2012). Uptake, accumulation, and biotransformation of metal oxide nanoparticles by a marine suspension-feeder. *Journal of Hazardous Materials, 225–226*, 139–145. https://doi.org/10.1016/j.jhazmat.2012.05.009

Moore, M. N., Icarus Allen, J., & McVeigh, A. (2006). Environmental prognostics: An integrated model supporting lysosomal stress responses as predictive biomarkers of animal health status. *Marine Environmental Research, 61*, 278–304. https://doi.org/10.1016/j.marenvres.2005.10.005

Nasser, F., & Lynch, I. (2016). Secreted protein eco-corona mediates uptake and impacts of poly-styrene nanoparticles on *Daphnia magna*. *Journal of Proteomics, 137*, 45–51. https://doi.org/10.1016/j.jprot.2015.09.005

Nigro, M., Falleni, A., Barga, I. D., Scarcelli, V., Lucchesi, P., Regoli, F., & Frenzilli, G. (2006). Cellular biomarkers for monitoring estuarine environments: Transplanted versus native mussels. *Aquatic Toxicology, 77*, 339–347. https://doi.org/10.1016/j.aquatox.2005.12.013

Oehlmann, J., & Schulte-Oehlmann, U. (2003). Molluscs as bioindicators. In *Trace metals and other contaminants in the environment* (Vol. 6, pp. 577–635). Elsevier.

Oh, N., & Park, J.-H. (2014). Endocytosis and exocytosis of nanoparticles in mammalian cells. *International Journal of Nanomedicine, 9*, 51.

Oliviero, M., Schiavo, S., Dumontet, S., & Manzo, S. (2019). DNA damages and offspring quality in sea urchin Paracentrotus lividus sperms exposed to ZnO nanoparticles. *Science of the Total Environment, 651*(Pt 1), 756–765. https://doi.org/10.1016/j.scitotenv.2018.09.243

Olson, K. R. (2020). Reactive oxygen species or reactive sulfur species: Why we should consider the latter. *The Journal of Experimental Biology, 223*, jeb196352. https://doi.org/10.1242/jeb.196352

Pan, J. F., Buffet, P. E., Poirier, L., Amiard-Triquet, C., Gilliland, D., Joubert, Y., Pilet, P., Guibbolini, M., Risso de Faverney, C., Roméo, M., Valsami-Jones, E., & Mouneyrac, C. (2012). Size dependent bioaccumulation and ecotoxicity of gold nanoparticles in an endobenthic invertebrate: The Tellinid clam Scrobicularia plana. *Environmental Pollution, 168*, 37–43. https://doi.org/10.1016/j.envpol.2012.03.051

Pati, R., Das, I., Mehta, R. K., Sahu, R., & Sonawane, A. (2016). Zinc-oxide nanoparticles exhibit genotoxic, clastogenic, cytotoxic and actin depolymerization effects by inducing oxidative stress responses in macrophages and adult mice. *Toxicological Sciences, 150*, 454–472.

Piccinno, F., Gottschalk, F., Seeger, S., & Nowack, B. (2012). Industrial production quantities and uses of ten engineered nanomaterials in Europe and the world. *Journal of Nanoparticle Research, 14*, 1109. https://doi.org/10.1007/s11051-012-1109-9

Pila, E. A., Sullivan, J. T., Wu, X. Z., Fang, J., Rudko, S. P., Gordy, M. A., & Hanington, P. C. (2016). Haematopoiesis in molluscs: A review of haemocyte development and function in gastropods, cephalopods and bivalves. *Developmental & Comparative Immunology, 58*, 119–128. https://doi.org/10.1016/j.dci.2015.11.010

Poynton, H. C., Chen, C., Alexander, S. L., Major, K. M., Blalock, B. J., & Unrine, J. M. (2019). Enhanced toxicity of environmentally transformed ZnO nanoparticles relative to Zn ions in the epibenthic amphipod Hyalella Azteca. *Environmental Science: Nano, 6*(1), 325–340. https://doi.org/10.1039/C8EN00755A

Praetorius, A., Labille, J., Scheringer, M., Thill, A., Hungerbühler, K., & Bottero, J. Y. (2014). Heteroaggregation of titanium dioxide nanoparticles with model natural colloids under environmentally relevant conditions. *Environmental Science & Technology, 48*(18), 10690–10698. https://doi.org/10.1021/es501655v

Roco, M. C. (2018). Overview: Affirmation of nanotechnology between 2000 and 2030. In T. O. Mensah, B. Wang, G. Bothun, J. Winter, & V. Davis (Eds.), *Nanotechnology commercialization: Manufacturing processes and products*. Wiley.

Roy, R., Singh, S. K., Chauhan, L. K., Das, M., Tripathi, A., & Dwivedi, P. D. (2014). Zinc oxide nanoparticles induce apoptosis by enhancement of autophagy via PI3K/Akt/mTOR inhibition. *Toxicology Letters, 227*(1), 29–40. https://doi.org/10.1016/j.toxlet.2014.02.024

Salvati, A., Pitek, A. S., Monopoli, M. P., Prapainop, K., Bombelli, F. B., Hristov, D. R., Kelly, P. M., Åberg, C., Mahon, E., & Dawson, K. A. (2013). Transferrin-functionalized nanoparticles lose their targeting capabilities when a biomolecule corona adsorbs on the surface. *Nature Nanotechnology, 8*(2), 137–143. https://doi.org/10.1038/nnano.2012.237

Scherzad, A., Meyer, T., Kleinsasser, N., & Hackenberg, S. (2017). Molecular mechanisms of zinc oxide nanoparticle-induced genotoxicity short running title: Genotoxicity of ZnO NPs. *Materials (Basel), 10*(12), E1427. https://doi.org/10.3390/ma10121427

Schlekat, C., Stubblefield, W., & Gallagher, K. (2020). State of the science on metal bioavailability modeling: Introduction to the outcome of a society of environmental toxicology and chemistry technical workshop. *Environmental Toxicology and Chemistry, 39*, 42–47. https://doi.org/10.1002/etc.4561

Selck, H., Handy, R. D., Fernandes, T. F., Klaine, S. J., & Petersen, E. J. (2016). Nanomaterials in the aquatic environment: A European Union-United States perspective on the status of ecotoxicity testing, research priorities, and challenges ahead. *Environmental Toxicology and Chemistry, 35*(5), 1055–1067. https://doi.org/10.1002/etc.3385

Shang, Y., Lan, Y., Liu, Z., Kong, H., Huang, X., Wu, F., Liu, L., Hu, M., Huang, W., & Wang, Y. (2018). Synergistic effects of nano-ZnO and low pH of sea water on the physiological energetics of the thick shell mussel Mytilus coruscus. *Frontiers in Physiology, 9*, 757. https://doi.org/10.3389/fphys.2018.00757

Shi, W., Han, Y., Guo, C., Su, W., Zhao, X., Zha, S., Wang, Y., & Liu, G. (2019). Ocean acidification increases the accumulation of titanium dioxide nanoparticles (nTiO2) in edible bivalve mollusks and poses a potential threat to seafood safety. *Scientific Reports, 9*(1), 3516. https://doi.org/10.1038/s41598-019-40047-1

Siddiqi, K. S., Ur Rahman, A., & Husen, A. (2018). Properties of zinc oxide nanoparticles and their activity against microbes. *Nanoscale Research Letters, 13*(1), 141. https://doi.org/10.1186/s11671-018-2532-3

Siller, L., Lemloh, M. L., Piticharoenphun, S., Mendis, B. G., Horrocks, B. R., Brümmer, F., & Medaković, D. (2013). Silver nanoparticle toxicity in sea urchin Paracentrotus lividus. *Environmental Pollution, 178*, 498–502. https://doi.org/10.1016/j.envpol.2013.03.010

Skjolding, L. M., Sørensen, S. N., Hartmann, N. B., Hjorth, R., Hansen, S. F., & Baun, A. (2016). Aquatic ecotoxicity testing of nanoparticles-the quest to disclose nanoparticle effects. *Angewandte Chemie (International Ed. in English), 55*, 15224–15239. https://doi.org/10.1002/anie.201604964

Sokolov, E. P., & Sokolova, I. M. (2019). Compatible osmolytes modulate mitochondrial function in a marine osmoconformer Crassostrea gigas (Thunberg, 1793). *Mitochondrion, 45*, 29–37. https://doi.org/10.1016/j.mito.2018.02.002

Sokolova, I. M. (2009). Apoptosis in molluscan immune defense. *Invertebrate Survival Journal, 6*(1), 49–58.

Subashkumar, S., & Selvanayagam, M. (2014). Zinc oxide (ZnO) nanoparticles induced histopathological changes in the liver of freshwater fish (*Cyprinus carpio*). *Cibtech Journal of Zoology, 3*(3), 74–77.

Suganthi, P., Murali, M., Athif, P., Sadiq Bukhari, A., Syed Mohamed, H. E., Basu, H., & Singhal, R. K. (2019). Haemato-immunological studies in ZnO and TiO2 nanoparticles exposed euryhaline fish, Oreochromis mossambicus. *Environmental Toxicology and Pharmacology, 66*, 55–61. https://doi.org/10.1016/j.etap.2018.12.011

Tedesco, S., Doyle, H., Blasco, J., Redmond, G., & Sheehan, D. (2010). Oxidative stress and toxicity of gold nanoparticles in *Mytilus edulis*. *Aquatic Toxicology, 100*(2), 178–186. https://doi.org/10.1016/j.aquatox.2010.03.001

Teles, M., Fierro-Castro, C., Na-Phatthalung, P., Tvarijonaviciute, A., Trindade, T., Soares, A. M., Tort, L., & Oliveira, M. (2016). Assessment of gold nanoparticle effects in a marine teleost (Sparus aurata) using molecular and biochemical biomarkers. *Aquatic Toxicology, 177*, 125–135. https://doi.org/10.1016/j.aquatox.2016.05.015

Teles, M., Reyes-López, F., Balasch, J. C., Guimarães, L., Tort, M., & Oliveira, M. (2018). Toxicogenomics of gold nanoparticles in a marine fish: Linkage to established biomarkers. *Toxicology Letters, 295*(1), S82. https://doi.org/10.1016/j.toxlet.2018.06.555

Tesser, M. E., de Paula, A. A., Risso, W. E., Monteiro, R. A., do Espirito Santo Pereira, A., Fraceto, L. F., & Bueno Dos Reis Martinez, C. (2020). Sublethal effects of waterborne copper and copper nanoparticles on the freshwater Neotropical teleost Prochilodus lineatus: A comparative approach. *Science of the Total Environment, 704*, 135332. https://doi.org/10.1016/j.scitotenv.2019.135332

Tiede, K., Hassellöv, M., Breitbarth, E., Chaudhry, Q., & Boxall, A. B. (2009). Considerations for environmental fate and ecotoxicity testing to support environmental risk assessments for engineered nanoparticles. *Journal of Chromatography. A, 1216*(3), 503–509. https://doi.org/10.1016/j.chroma.2008.09.008

Torrealba, D., More-Bayona, J. A., Wakaruk, J., & Barreda, D. R. (2019). Innate immunity provides biomarkers of health for teleosts exposed to nanoparticles. *Frontiers in Immunology, 9*, 3074–3074. https://doi.org/10.3389/fimmu.2018.03074

Tourinho, P. S., van Gestel, C. A., Lofts, S., Svendsen, C., Soares, A. M., & Loureiro, S. (2012). Metal-based nanoparticles in soil: Fate, behavior, and effects on soil invertebrates. *Environmental Toxicology and Chemistry, 31*(8), 1679–1692. https://doi.org/10.1002/etc.1880

Trevisana, R., Delapedra, G., Mello, D. F., Arl, M., Schmidt, É. C., Meder, F., Monopoli, M., Cargnin-Ferreira, E., Bouzon, Z. L., Fisher, A. S., Sheehan, D., & Dafr, A. L. (2014). Gills are an initial target of zinc oxide nanoparticles in oysters *Crassostrea gigas,* leading to mitochondrial disruption and oxidative stress. *Aquatic Toxicology, 153*, 27–38. https://doi.org/10.1016/j.aquatox.2014.03.018

Vance, M. E., Kuiken, T., Vejerano, E. P., McGinnis, S. P., Hochella, M. F., Jr., Rejeski, D., & Hull, M. S. (2015). Nanotechnology in the real world: Redeveloping the nanomaterial consumer products inventory. *Beilstein Journal of Nanotechnology, 6*, 1769–1780. https://doi.org/10.3762/bjnano.6.181

Vandebriel, R. J., & De Jong, W. H. (2012). A review of mammalian toxicity of ZnO nanoparticles. *Nanotechnology, Science and Applications, 5*, 61–71. https://doi.org/10.2147/NSA.S23932

Velzeboer, I., Kwadijk, C. J., & Koelmans, A. A. (2014). Strong sorption of PCBs to nanoplastics, microplastics, carbon nanotubes, and fullerenes. *Environmental Science & Technology, 48*(9), 4869–4876. https://doi.org/10.1021/es405721v

Volland, M., Hampel, M., Martos-Sitcha, J. A., Trombini, C., Martínez-Rodríguez, G., & Blasco, J. (2015). Citrate gold nanoparticle exposure in the marine bivalve Ruditapes philippinarum: Uptake, elimination and oxidative stress response. *Environmental Science and Pollution Research International, 22*(22), 17414–17424. https://doi.org/10.1007/s11356-015-4718-x

Wang, J., Wang, A., & Wang, W. X. (2017). Evaluation of nano-ZnOs as a novel Zn source for marine fish: Importance of digestive physiology. *Nanotoxicology, 11*(8), 1026–1039. https://doi.org/10.1080/17435390.2017.1388865

Ward, J. E., & Kach, D. J. (2009). Marine aggregates facilitate ingestion of nanoparticles by suspension-feeding bivalves. *Marine Environmental Research, 68*(3), 137–142. https://doi.org/10.1016/j.marenvres.2009.05.002

Watson, C., Ge, J., Cohen, J., Pyrgiotakis, G., Engelward, B. P., & Demokritou, P. (2014). High-throughput screening platform for engineered nanoparticle-mediated genotoxicity using CometChip technology. *ACS Nano, 8*, 2118–2133.

Wong, S. W., Leung, P. T., Djurisić, A. B., & Leung, K. M. (2010). Toxicities of nano zinc oxide to five marine organisms: Influences of aggregate size and ion solubility. *Analytical and Bioanalytical Chemistry, 396*(2), 609–618. https://doi.org/10.1007/s00216-009-3249-z

Wright, P. F. (2016). Potential risks and benefits of nanotechnology: Perceptions of risk in sunscreens. *The Medical Journal of Australia, 204*(10), 369–370. https://doi.org/10.5694/mja15.01128

Wu, B., Torres-Duarte, C., Cole, B. J., & Cherr, G. N. (2015). Copper oxide and zinc oxide nanomaterials act as inhibitors of multidrug resistance transport in sea urchin embryos: Their role as chemosensitizers. *Environmental Science & Technology, 49*(9), 5760–5770. https://doi.org/10.1021/acs.est.5b00345

Wu, F., Falfushynska, H., Dellwig, O., Piontkivska, H., & Sokolova, I. M. (2020). Interactive effects of salinity variation and exposure to ZnO nanoparticles on the innate immune system of a sentinel marine bivalve, *Mytilus edulis*. *Science of the Total Environment, 712*, 136473. https://doi.org/10.1016/j.scitotenv.2019.136473

Wu, F., Harper, B. J., & Harper, S. L. (2019). Comparative dissolution, uptake, and toxicity of zinc oxide particles in individual aquatic species and mixed populations. *Environmental Toxicology and Chemistry, 38*(3), 591–602. https://doi.org/10.1002/etc.4349

Xia, T., Kovochich, M., Liong, M., Mädler, L., Gilbert, B., Shi, H., Yeh, J. I., Zink, J. I., & Nel, A. E. (2008). Comparison of the mechanism of toxicity of zinc oxide and cerium oxide nanoparticles based on dissolution and oxidative stress properties. *ACS Nano, 2*, 2121–2134. https://doi.org/10.1021/nn800511k

Xiao, W., & Gao, H. (2018). The impact of protein corona on the behavior and targeting capability of nanoparticle-based delivery system. *International Journal of Pharmaceutics, 552*, 328–339. https://doi.org/10.1016/j.ijpharm.2018.10.011

Xu, L., Wang, Z., Zhao, J., Lin, M., & Xing, B. (2020). Accumulation of metal-based nanoparticles in marine bivalve mollusks from offshore aquaculture as detected by single particle ICP-MS. *Environmental Pollution, 260*, 114043. https://doi.org/10.1016/j.envpol.2020.114043

Yecheskel, Y., Dror, I., & Berkowitz, B. (2016). Transport of engineered nanoparticles in partially saturated sand columns. *Journal of Hazardous Materials, 311*, 254–262. https://doi.org/10.1016/j.jhazmat.2016.03.027

Yung, M. M. N., Mouneyrac, C., & Leung, K. M. Y. (2015). Ecotoxicity of zinc oxide nanoparticles in the marine environment. In *Encyclopedia of nanotechnology* (pp. 1–17). Springer. https://doi.org/10.1007/978-94-007-6178-0_100970-1

Zha, S., Rong, J., Guan, X., Tang, Y., Han, Y., & Liu, G. (2019). Immunotoxicity of four nanoparticles to a marine bivalve species, Tegillarca granosa. *Journal of Hazardous Materials, 377*, 237–248. https://doi.org/10.1016/j.jhazmat.2019.05.071

Zhao, X., Wang, S., Wu, Y., You, H., & Lv, L. (2013). Acute ZnO nanoparticles exposure induces developmental toxicity, oxidative stress and DNA damage in embryo-larval zebrafish. *Aquatic Toxicology (Amsterdam, Netherlands), 136–137C*, 49–59. https://doi.org/10.1016/j.aquatox.2013.03.019

Zhao, X., Ren, X., Zhu, R., Luo, Z., & Ren, B. (2016). Zinc oxide nanoparticles induce oxidative DNA damage and ROS-triggered mitochondria-mediated apoptosis in zebrafish embryos. *Aquatic Toxicology, 180*, 56–70. https://doi.org/10.1016/j.aquatox.2016.09.013

Zhu, X., Wang, J., Zhang, X., Chang, Y., & Chen, Y. (2009). The impact of ZnO nanoparticle aggregates on the embryonic development of zebrafish (*Danio rerio*). *Nanotechnology, 20*(19), 195103. https://doi.org/10.1088/0957-4484/20/19/195103

Zhu, X., Zhu, L., Duan, Z., Qi, R., Li, Y., & Lang, Y. (2008). Comparative toxicity of several metal oxide nanoparticle aqueous suspensions to Zebrafish (*Danio rerio*) early developmental stage. *Journal of Environmental Science and Health. Part A, Toxic/Hazardous Substances & Environmental Engineering, 43*(3), 278–284. https://doi.org/10.1080/10934520701792779

Metallothioneins' Responses on Impact of Metal-Based Nanomaterials for Biomedical Use

Oksana Stoliar and Rostyslav S. Stoika

Abbreviations

Me-NPs	Metal-containing nanoparticles
MTs	Metallothioneins
MT-SH	MTs protein total concentration
QDs	Quantum dots
TPPs	Thermal power plants
Zn, Cu, Cd-MTs	Metalated metallothioneins

1 Introduction

Metal-containing nanoparticles (Me-NPs) belong to the most applicable category of nanomaterials. They include semiconductor nanocrystals (quantum dots, QDs) that contain noble, transition, or post-transitional metals, such as CdSe, CdTe, CdSeTe, ZnSe, InAs, or PbSe in their core, CdS or ZnS in their shell, and an organic coating, atomic forms (Ag, Au, Fe, Cu), and metal oxides (ZnO, TiO_2, FeO, Fe_3O_4, ZrO_2, CeO_2) (Klębowski et al., 2018; Mauricio et al., 2018). Each type of Me-NPs possesses unique physicochemical properties, which, in turn, determine their potential application, toxicity, or lack thereof. Nevertheless, growing scales of their application in the pharmaceutical production and medicine cause a concern relating to their toxicity and ecotoxicity, since the Me-NPs or their compounds can penetrate surface waters (Khan et al., 2019; Singla et al., 2016; Yang et al., 2017).

Rapidly increasing application of nanoscale silver particles due to their antibacterial and odor-fighting properties can lead to considerable bio-risks. Silver NPs have been extensively used in detergents and wound dressings that can enter

O. Stoliar (✉)
Ternopil Volodymyr Hnatiuk National Pedagogical University, Ternopil, Ukraine
e-mail: Oksana.Stolyar@tnpu.edu.ua

R. S. Stoika
Institute of Cell Biology, NAS of Ukraine, Lviv, Ukraine

the environment during waste disposal (Asz et al., 2006). Each tube of toothpaste contains approximately 91 mg of silver nanoparticles; thus, approximately 3.9 tons of silver nanoparticles enter the environment annually (Junevičius et al., 2015). These materials may possess unusual physicochemical properties (e.g., colloid chemistry) and behavior in water media that are less familiar to ecotoxicologists compared to the properties of traditional forms of contaminating metals (Handy et al., 2008).

Due to poor effectiveness of their elimination by water purification plants, the Me-NPs can influence the wildlife, primarily on aquatic ecosystems that causes a great concern. As a result, aquatic animals are not only suitable models for the elucidation of impact of metal-contained nanoparticles on biological systems but also nontargeted organisms of this impact. Therefore, evaluation of the bioavailability of these particles seems to be crucial to understandthe mechanisms of their biological activity and/or toxicity (Asharani et al., 2008; Gagné, Auclair, Fortier, et al., 2013; Griffitt et al., 2008; Peyrot et al., 2009).

Two main characteristics can be selected for evaluating ecotoxicity of the nanoparticles. In particular, their size as well as surface properties determine their aggregation behavior, and, thus, affect their mobility in the aquatic and terrestrial systems ang the interactions with algae, plants, and animals (Navarro et al., 2008). Me-NPs with large surface area relative to small particle volume might be reactive and possess a particular aggregation behavior (Klaine et al., 2008; Navarro et al., 2008). With decreasing particle size, its penetration is eased and the bioavailability is increased (Kim et al., 2010; Pan et al., 2012). However, the aggregation of nanoparticles can also impact the environment. The available data suggest that a risk of the nanostructured titanium dioxide (TiO_2-NPs) or zinc oxide (ZnO-NPs) on humans is negligible due to particles' aggregation (Schilling et al., 2010). The distribution and persistence of the nanostructured metal oxides are the same compared to larger pigment-grade (i.e., >100 nm) particles, which demonstrate equivalence in the recognition and elimination of such material from the body. However, when the *Elliptio complanata* mussels were exposed for 24 h to increasing concentrations (up to 8 mg Cd L^{-1}) of quantum dots (QDs) CdTe, approximately 80% of Cd was retained by a 450 nm pore filter (aggregates), and only 14% of the Cd was in a dissolved phase (i.e., eluted through a 1 kDa ultrafiltration membrane). These results suggest that the uncoated CdTe QDs were not stable in freshwater (Peyrot et al., 2009).

Generally, it was shown that the Me-NPs are stable in the in vivo conditions (King-Heiden et al., 2009). However, the environment can weaken this stability leading to the release of metal ions. Thus, it is probable that some of the resulting adverse effects might be caused by the dissolved metal species (Chae et al., 2009). In different systems, the instability of Me-NPs depending on pH (Mauricio et al., 2018) and buffering system (Eixenberger et al., 2017) was accompanied by a release of free metals (Landa et al., 2015). Metals incorporated in the nanoparticles can be potentially toxic (Stohs & Bagchi, 1995; Valko et al., 2005). For example, once Ag enters the environment, it is oxidized to Ag^+ (Yu et al., 2013). Therefore, the main

problem in the ecotoxicology of Me-NPs is to elucidate the effect of these nanomaterials on the molecular targets of metals within the organism.

The intracellular metal-binding proteins, metallothioneins (MTs), might be potential molecular targets for these metals. MTs constitute a diverse family of thermostable intracellular proteins, which are enriched in cysteines and bind transition and post-transition metals in metal-thiolate clusters. MTs were discovered by Margoshes and Vallee (1957) as cadmium-keeping proteins in horse kidney. At present, they are considered to participate in storage and detoxification of metals, such as zinc (Zn), copper (Cu), and cadmium (Cd), and in scavenging of the reactive oxygen species in a wide range of living organisms (Isani & Carpenè, 2014). They are rapidly induced in the digestive gland/liver by a wide range of metals, drugs, and inflammatory mediators. They are also involved in human metalloneurochemistry and were identified (MT-3) as an inhibitor of neuronal growth (Atrián-Blasco et al., 2017; McGee et al., 2010; Ziller & Fraissinet-Tachet, 2018). Association of MTs with several diseases, including cancer, circulatory and septic shock, coronary artery disease, Alzheimer's disease, and immune disorders has been found (for the review, see Krizkova et al., 2012). PubMed search (August 19, 2021) revealed numerous publications devoted to MTs: 13,259 documents with "metallothioneins" keywords, their biological functions, role in the organism, and possible applications for the diagnostics and bioindication. Such definitions as "elusive function," "puzzling role," "opaque/pazzing/two faced" proteins remain popular for the MTs.

MTs received special attention as a biomarker for metal toxicity in the aquatic animals, and they are included in the recommended set of biomarkers for the aquatic ecotoxicological and environmental risk assessment (Amiard et al., 2006; Viarengo et al., 2007). Due to their properties, MTs can be a target for Me-NPs or products of their destruction. Particularly, the metals derived from Me-NPs can impact metal composition of MTs. Moreover, attempts to use transgenic MTs as the Me-NPs were accomplished (see later). Since Me-NPs can provoke the generation of the reactive oxygen species and oxidative stress, MTs as highly reactive thiols can also be involved in the scavenging of the reactive oxygen species (ROS) induced by Me-NPs. Further, the MTs are highly inducible by some ionic metals and different stress-related agents. However, the items of the biocompatibility, bioavailability, and bio-decomposition of the Me-NPs were not discussed earlier regarding the metal-bufferingfunctions of MTs

In the ecotoxicological studies, it was crucial to investigate the environmentally relevant concentrations of the nanoparticles (Busch et al., 2010; Figgitt et al., 2010), whereas in the toxicology, the lethality indices (L(E)C50 values) of synthetic Me-NPs based on measuring ppm (part per million) concentrations are explored (Hardman, 2005; Kahru & Dubourguier, 2010; Kim et al., 2010). In the environment, Me-NPs have been also found to act as the carriers of coexisting contaminants and natural nanoparticles, and such interaction can alter a toxicity of specific chemicals toward indicator organisms (Baun et al., 2008).

The scope of our work is to discuss problems and methodological approaches that appear while utilizing MTs for indication and application of Me-NPs in ecotoxicology, medicine, and pharmaceutic industry.

2   Metal-Based Nanoparticles as Inducers of Metallothionein Expression

2.1   General Characteristics

The main attention while studying the adverse effects of different agents (actions) is usually paid to their impact on gene expression and/or genotoxicity. Different Me-NPs were shown to cause genotoxic effects, such as chromosomal fragmentation, DNA strand breaks, and alterations in gene expression profiles (Magdolenova et al., 2014). It was proved by random amplified polymorphism DNA polymerase chain reaction (RAPD-PCR) technique, DNA microarrays, and real-time PCR (RT-PCR) that basal level of expression of MT genes remains relatively low; however, the MTs belong to highly inducible proteins (Mahaye et al., 2017). The induction of MTs genes is driven by a number of transition and post-transitional metals, particularly by Cd, as well as physiological mediators through several response elements in the MTs gene promoter (Cho et al., 2008; Davis & Cousins, 2000; Rhee et al., 2009; Wu et al., 2008; Zafarullah et al., 1988). Besides, the induction of MTs gene can be specifically caused by the Me-NPs in carcinogenesis that serves as a defense mechanism and provides protection by acting as free radical scavengers, anti-inflammatory agents, and antiapoptotic agents. It can also mediate zinc-dependent gene expression involved in apoptosis, cell proliferation, or differentiation (Heger et al., 2016; Penkowa, 2006; Sharma et al., 2013). Targeting human adenocarcinomic alveolar basal epithelial cells of A549 line with the nanoparticles caused a specific activation of the metallothionein 2A (MT2A) gene in case of ZnO, CuO, and Bi_2O_3 exposure among six kinds of metal oxide nanoparticles (Horie et al., 2018). On the other hand, the relation of MTs to an enhanced resistance of tumor cells was also reported, for example, in murine leukemia L1210 cell sub-lines resistant to cisplatin (Falfushynska, Gnatyshyna, et al., 2012; Si & Lang, 2018).

A sensitivity of the MTs to inducers and consequences of this inducibility were shown to be species-dependent. Generally, fish MTs are considered as a kind of stress protein responsive to different stress signals. However, the MTs of mollusks seem to be more specifically involved in a response to heavy metals and demonstrate higher resistance to stress signals (Viarengo et al., 1999). This is one of the reasons that could explain high variability of responses of MTs expression depending on species and particular Me-NPs. For example, due to high inducibility, liposome-encapsulated MT-1 promoter has been used extensively to induce growth hormone or other genes in cell cultures and gene-manipulated animals (Sharma et al., 2013).

Below, the available information concerning the inducibility of MTs genes by specific Me-NPs has been analyzed.

2.2 Cd-Nanoparticles

As noted by Si and Lang (2018), MTs expression can be used as early and sensitive biomarker to assess the effectiveness and environmental safety of newly developed NPs. This is of particular importance when well-known inducer of MTs, Cd (II) is presented in the Me-MPs composition. For example, the stability of the novel synthesized surfactant-coated semiconductor silica-coated NPs was elucidated based on the detection of well-known upregulation of MTs by Cd. These NPs were developed for the biomedical applications. They consist of Cd/Se core and Zn sulfide or Cd sulfide shell. After illumination with the UV light, these NPs were effectively induced MTs in cell-based therapies. Moreover, the induction of MTs by Cd was utilized for decreasing toxicity of novel Cd/Se/Tellurium (Te)-based ODs (QD-705) developed for a potential biomedical application (Lin et al., 2009).

On the other hand, the long-term exposure (85 days) of reproductive fish *Fundulus heteroclitus* to lecithin-encapsulated CdSe/ZnS QD (1–10μg/day) day, or a diet containing 5.9μg CdCl$_2$/day for 85 days did not reveal significant changes in the hepatic expression of genes involved in metal metabolism or oxidative stress including the MTs. It was suggested that minimal Cd release from the QD (less than 0.01% of the QD's Cd was retained in the liver or intestinal tissues; Blickley et al., 2014).

In the study of King-Heiden et al. (2009), the embryos of zebrafish *Danio rerio* were exposed to aqueous suspensions of CdSe(core)/ZnS(shell) QDs functionalized with either poly-L-lysine or poly(ethylene glycol) terminated with methoxy, carboxylate, or amine groups. At sublethal concentrations, many QD preparations produced characteristic signs of Cd toxicity that weakly correlated with MT expression, thus, indicating that QDs are slightly degraded *in vivo*. QDs also produced distinctly different toxicity that could not be explained by Cd release. (King-Heiden et al., 2009). Hence, the absence of MTs induction confirms stability of these NPs.

2.3 Ag-Nanoparticles

Unlike CdSe/ZnS QDs, Ag-NPs seem to easily release Ag from their structure. Indeed, there are data that confirm an inadvertent release of Ag into the environment, owing to increasing commercial use of Ag-NPs. Benn and Westerhoff (2008) had shown that a release of Ag from the Ag-NPs contained in "anti-bacterial socks" into the aquatic ecosystems and its fate in municipal wastewater treatment plants can be of high concern. They demonstrated that the socks containing up to 1400μg Ag•g^{-1} released as much as 650μg Ag in 500 mL of distilled water. Ag is one of the

most favorable metals for binding with MTs (Amiard et al., 2006). It was shown to impact gene expression. For example, in a liver of the fish Oncorhynchus mykiss, both Ag-NPs and silver nitrate led to significant changes in gene expression for 13% of 207 stress-related genes. About 12% of genes responded specifically to Ag-NPs, while 10% of total gene targets responded specifically to a dissolved Ag (ionic form). However, the expression of MTs was not assessed in that study (Gagné et al., 2012).

In cultured primary astrocytes incubated for 4 h in the presence of Ag-NPs, concentration-dependent increase in the specific cellular Ag content for up to 46 nmol•mg^{-1} protein was detected and it remained almost constant for up to 7 days. Western-blot analysis and immunocytochemical staining revealed that Ag-NP-treated astrocytes strongly upregulated the expression of the MTs. However, no delayed cell toxicity including the redox state of glutathione was detected. Thus, the authors evaluated this manifestation as a successful strategy for preventing Ag NP-mediated toxicity of the Ag ion (Luther et al., 2012). In opposite, in the *in vitro* experiment in human hepatoma cells, the expression of metal-responsive MT1b mRNA was not induced in the Ag-NP-treated cells (in the concentrations 0.1–2 mg Ag•mL^{-1}), while it was induced in AgNO$_3$-treated cells in the same concentrations of Ag. These results indicate that Ag-NP-treated cells have a limited exposure to Ag$^+$ ions, despite a potential release of Ag$^+$ ions from the Ag-NPs in cell culture (Kim et al., 2009).

The exposures of the aquatic animals to Ag-NPs also demonstrated a variability of responses in the MTs gene activities. The investigation of the impact of Ag nanoparticles (Ag-NPs) was conducted in Japanese medaka *Oryzias latipes* by studying changes in the expression of stress-related genes using real-time RT-PCR of liver extracts. Comparing these results with those of medaka exposed to soluble Ag ions suggests that these two forms of Ag have distinguishable toxic fingerprints. While the Ag-NPs led to cellular and DNA damage, as well as carcinogenic and oxidative stresses, the expression of genes related to metal detoxification/metabolism regulation and radical scavenging action was also induced. A significant induction of MT expression (6.0-fold increase) was observed 1 day after the fish was exposed to 25μg•L^{-1} Ag-NPs (high dosage), which was much higher than the response seen with an equivalent mass of the metallic Ag from AgNO$_3$ (2.2-fold). However, a depressed mRNA level (about 3.5-fold) was seen after 4-day exposure. In contrast, the ionic Ag led to a repressed expression of this gene at all tested dosages up to a 2-day exposure compared to control (Chae et al., 2009).

At the exposure of marine mussels, *Mytilus galloprovincialis*, to maltose-stabilized Ag-NPs of different sizes (20 and 100 nm), bulk or aqueous forms of the metal, the MTs expression in the digestive gland after 1 and 21 days of exposure was determined (Jimeno-Romero et al., 2017). The 0.75 μg Ag L^{-1} concentration was selected as low best effective one. In that study, transcription levels of MTs genes mt20IV and mt10IIIa did not change significantly in comparison with controls, regardless of the form of the metal or exposure time and despite the elevated level of Ag in the tissue after 1 day exposure.

However, in the study of Ringwood et al. (2010), the effect of similar concentration (0.16 μg L−1) of Ag-NP on the oysters, Crassostrea virginica, for 48 h caused significant increases in the MTs mRNA levels, both in embryos and adults mollusks. In Ag-NP-exposed adult oysters, the MT mRNA levels increased approximately by 2.4-fold. Importantly, in control oyster embryos, the MT mRNA levels were negligible, but highly significant increases were observed, an approximately 80-fold increase over control embryo levels.

In plant Yellow-lupin (*Lupinus luteus L.*) that was grown on soils contaminated with Ag-NPs (25 mg kg^{-1}), the expression of MTs was not changed, whereas a single metal including Cd, Pb, Zn, Ni (in nitrate form), and Ag (in nitrate form) induced a statistically significant increase in the expression levels of the MTs (Jaskulak et al., 2019).

The exposures of the nematode, *Caenorhabditis elegans,* to three Ag-NPs with different sizes and polyvinylpyrrolidone (PVP) or citrate coatings were investigated using wild-type (N2) *C. elegans* and strains expected to be sensitive to the oxidative stress (nth-1, sod-2 and mev-1), genotoxins (xpa-1 and nth-1), and metals (mtl-2). A MT-deficient (mtl-2) strain was the only mutant tested that exhibited a consistently higher sensitivity to the Ag-NP than the wild-type at the exposure to 25 mg L^{-1} during 3 days and according to the growth inhibition. Although all tested Ag-NPs were internalized (passed cell membranes) in *C. elegans*, at least part of the observed toxicity was mediated by the ionic Ag. That conclusion was confirmed by the detection of the dissolved silver, particularly for the PVP-coated particles (Meyer et al., 2010).

In general, due to a particular popularity of Ag-NPs in different applications (Junevičius et al., 2015), as well as their easy decomposition in the environment and cells, the impact of these Me-NPs on the MTs expression is of great concern. Nevertheless, even little difference in the concentrations or time of detection and particular model organism can give different results in the expression of MTs in a response to Ag-NPs.

2.4 *TiO$_2$-Nanoparticles*

TiO$_2$-NPs are manufactured worldwide in the increasing quantities for a wide range of applications, including medicine (e.g., in biomedical implants and cancer therapy) (Chen & Mao, 2007; Giese et al., 2018). Therefore, within the xenobiotics found in surface waters, TiO$_2$-NPs are arguably among the most worrisome (Baun et al., 2008). The recorded concentrations of TiO$_2$-NPs in the surface waters are at the magnitudes of ng·L^{-1} (Sun et al., 2017), and exposures are continuous. The persistence of stable residual TiO$_2$-NPs in the aquatic environments for extended periods was demonstrated by Zhang et al. (2017). Moreover, in water, the bulk form of TiO$_2$, derived from the TiO$_2$ pigments, can produce nanoparticles (Botta et al., 2011). However, titanium does not belong to typical inducers of the MTs. In the study of D'Agata et al. (2014), a significant overexpression of the inducible mt20

gene was detected in the digestive gland of *M. galloprovincialis* exposed to bulk TiO_2 high concentration (10 mg L^{-1}), while TiO_2-NPs (fresh, or aged under simulated sun light for 7 days) did not change the expression of *mt* genes in this tissue. Despite the TiO_2-NPs showed greater accumulation than bulk TiO_2, irrespective of ageing, particularly in digestive gland (>sixfold higher), histology and histochemical analysis suggested that the bulk material was more toxic (D'Agata et al., 2014). Similarly, a combined exposure to 0.1 mg•L^{-1} TiO_2-NPs and $CdCl_2$ in the *in vivo* exposure of *M. galloprovincialis* for 96 h caused a significant upregulation of *mt-20* gene expression, compared to controls. However, it was proved that this effect was caused by Cd, whereas the $CdCl_2$ (0.1 mg•L^{-1}) in the exposures alone provoked same in magnitude effect (Della Torre et al., 2015). These results confirm the non-sensitivity of MTs expression to the impact of TiO_2-NPs.

2.5   ZnO-Nanoparticles

In the experiments with the ZnO-NPs, it was proved that the induction of the MTs is dependent on a partial release of Zn from the nanoparticles (Boran & Ulutas, 2016). In that study, the effects of ZnO-NPs and corresponding concentrations of the water-soluble $ZnCl_2$ on the larval zebrafish *Danio rerio* (72 h post-fertilization) were compared. A significant induction in the *mt2* gene of larvae exposed to highest Zn and ZnO-NPs concentrations was shown. However, the effect of soluble Zn was substantially greater than the effect of ZnO-NPs (of 20.5 ± 1.9-fold and 2.5 ± 0.8-fold change compare to control, respectively). A similarity in the upregulation of expression of MTs gene to Zno-NPs and ionic Zn was demonstrated in other experimental models, namely human cell lines derived from colon and skin tumors (Moos et al., 2011) as well as mice lung (Wesselkamper et al., 2001). It seems that ZnO-NPs are of high biodecomposition that might lead to the MTs induction by soluble Zn. However, it should be noted that in those exposures rather high concentrations of the particles were applied, for example, 3 and 6 mg L^{-1} in the study of Boran and Ulutas (2016).

2.6   Au-Nanoparticles

Gold nanoparticles (Au-NPs) attract an extreme attention in medicine (Elahi et al., 2018). Their intrinsic features, such as optical, electronic, physicochemical and surface plasmon resonance (SPR), can be altered by changing the characteristics of particles such as shape, size, aspect ratio, or environment. The Au-NPs are easy to be synthesized and functionalized resulting in various application in different fields of biomedicine such as sensing, targeted drug delivery, imaging, photothermal, and photodynamic therapy, as well as the modulation of two or three applications. Therefore, it is important to predict safety and evaluate therapeutic efficiency of the

Au-NPs. It is necessary to establish proper approaches for the study of their toxicity and biomedical effects. However, their impact on the MTs expression is almost unknown. It was reported that the Au-NPs of 5 and 40 nm size during 16-day laboratory exposure at 100μg Au•L^{-1} caused MTs induction in the marine bivalve *Scrobicularia plana.* A successfulness of such response in the prevention of oxidative stress was confirmed by the absence in the activation of lipid peroxidation, detected as TBARS (Pan et al., 2012).

2.7   Cu-Based Nanoparticles

Cu$_2$O-NPs are increasingly used in various medical preparations, for example, anti-microbial remedies or intrauterine contraceptive devices. In the study of Chen et al. (2011), the toxic effects of Cu$_2$O-NPs were investigated in zebrafish *Danio rerio* larvae and zebrafish liver cell-line. The comparison of the effects of elevated Cu$_2$O-NPs and CuCl$_2$ concentrations in the water on the expression of several copper-related genes in zebrafish larvae by using real-time quantitative polymerase chain reaction revealed that both forms of Cu induced the mRNA levels of MTs, and also Cu/Zn superoxide dismutase, metal regulatory transcription factor 1 (MTF1) and copper transporters, ATP7A and 7B, but downregulated the mRNA levels of glutathione S-transferase. The concentrations were selected according to the 96 h LC50 values. The expression of the MTs in the cell lines was increased after the application of 55 ppm of Cu$_2$O-NPs or 11.5 ppm of CuCl$_2$ during 96 h, but was not changed after the application of 28 and 5.8 ppm of the corresponding substances. In the larvae, the MTs were induced after all applied concentrations during 96 h (30, 60, and 121 ppb for Cu$_2$O-NPs and 11, 22, 43 ppb for CuCl$_2$. (Chen et al., 2011). In the reviewed literature, only this study was addressed to testing the Me-NPs as more prominent inducer of the MTs than the corresponding metal.

The study of the effects of manufactured Cu-NPs in soils was applied with the utilization of the earthworm *Eisenia fetida* exposed to a series of concentrations of commercially produced Cu-NPs labeled as 20- to 40-nm or < 100-nm Cu in the artificial soil media. Ecologically, relevant concentrations of CuNPs up to 65 mg kg^{-1} caused no adverse effects. However, an increase in MTs expression occurred at concentrations exceeding 20 mg kg^{-1} of Cu-NPs and 10 mg kg^{-1} of CuSO$_4$. Based on the relationship of Cu tissue concentration to MTs expression level and the spatial distribution and chemical speciation of Cu in the tissues, it was concluded that Cu ions and oxidized CuNPs were taken up by the earthworms. In that study, the upregulation of the MT1 genes was an indication that Cu ions have been delivered intracellularly through cellular uptake of Cu ions or through an uptake of Cu-containing particles and subsequent dissolution. Whereas the concentration-dependent increases in mtl expression were observed due to CuSO$_4$ exposure, as well as exposure to Cu-NPs, the reason for the MTs inducibility can be a release of Cu from the nanoparticles. Moreover, when mtl expression was plotted versus soil concentrations, it was clear that CuSO$_4$ was a more potent inducer of mtl than

Cu-NPs. It is also apparent that the 20- to 40-nm Cu-NPs were more effective in inducing mtl than the <100-nmCu-NPs. In any case, the equivalent Cu tissue concentrations from the Cu-NP treatments did not produce as much mtl expression as the CuSO₄ treatment did. This suggests that accumulated Cu was present partially in the form of Cu-NPs that did not dissolve in the tissue to release Cu ions (Unrine et al., 2010).

2.8   NiO-Nanoparticles

The study of the effect of NiO-NPs on the MTs expression in rats was reported. Male Wistar rats received nano-NiO (0.015, 0.06 or 0.24 mg/kg body weight (b.w.)) or micro-NiO (0.24 mg/kg b.w.) by intratracheal instilling twice a week for 6 weeks. The obtained results demonstrated that MT-1 mRNA expression levels were down-regulated in the 0.24 mg/kg nano- and micro-NiO exposure groups compared with control group suggesting a deficient antioxidant and detoxification capacity induced by the NiO-NPs impact. However, based on these results, it is impossible to determine whether this effect is caused by high concentration of NiO independent on the form of substance.

2.9   Reactive Oxygen Species Mediated Effect of me-Nanoparticles on Metallothioneins Expression

Me-NPs can influence the MTs expression via the oxidative stress generation (Manke et al., 2013). Generation of reactive oxygen species (ROS) is one of the most discussed nanotoxicity mechanism in literature (Manke et al., 2013; Vale et al., 2016). Particularly, it was shown to be caused by the reactive surface of NPs (Schins, 2002). Consequently, ROS over-production can trigger the induction of antioxidants (Vale et al., 2016). The induction of the MT as a stress protein can be a part of common stress response released via the activation of signaling pathways, transcription factors, and cytokine cascade contributing to a diverse range of cellular responses. It was also proposed that Me-NPs can influence intracellular calcium concentrations, activate transcription factors, and modulate cytokine production via ROS production. There are studies in which Me-NPs have been reported to induce the oxidative stress ($O_2^{\bullet-}$ and $OH^{\bullet}$), for example, via Fenton-type reaction (Valko et al., 2006). Some Me-NPs (Ar, Be, Co, and Ni) promote the activation of intercellular radical-inducing system such as the MAPK and NF-κB pathways (Manke et al., 2013). However, to the best of our knowledge, the relation between this activation and the expression of MTs was not studied in detail.

Generally, the presented scant experience of investigation of the MTs expression under the exposures to Me-NPs, either in vivo or in vitro, attests the inability of stable nanoparticles to induce the MTs expression directly. Mainly the ionic metals

released from instable Me-NPs might affect the MTs genes in a wide range of experimental model systems, firstly in the aquatic organisms.

3   Metallothioneins—Metal-Based Nanoparticles of New Generation

3.1   *Dual Roles of Metallothioneins Functionality*

When cellular targets of Me-NPs and/or corresponding metals are analyzed, the primary targets seem to be thiol compounds. Whereas MTs represent a substantial compound of so-called soluble thiolome (Rubino, 2015), their metal and Me-NPs binding behavior must be in the focus of the investigation of Me-NPs toxicity. Expectedly, the upregulation of the MTs expression is manifested in the increased concentration of these thiols within the cell. However, there are many examples which indicate that the upregulation of the MTs gene expression is not accompanied by the elevation of MTs protein and its metal-binding. For example, the presence of MT genes in two icefish species was not accompanied by their expression at protein level (Bargelloni et al., 1999). In brown trout *Salmo trutta* obtained from some polluted areas, the MTs content was not elevated even when the MTs gene transcription was increased (Hansen et al., 2006). A discrepancy between the MT mRNA and protein levels was also found in the juvenile Pacific oyster *Crassostrea gigas* (Marie et al., 2006). Moreover, on the post-translation level, the metalated, partially metalated, or super-metalated forms or apoform (reduced and oxidized) of the MTs protein can coexist in different patterns depending on the conditions of the environmental or model exposure and species-dependent sensitivity of redox state of the MTs-related functional thiol groups (Sutherland & Stillman, 2014; Ngu & Stillman, 2009; Duncan et al., 2006; Jayawardena et al., 2017; Krężel & Maret, 2017; Maret, 2017; Haase & Maret, 2008) (Fig. 1). Therefore, the results of the detection of total MTs protein cannot be the enough characteristic of its metal-binding activity. It was reported that in the conditions of highly loaded by Zn or Cd organism (16 or 24 h after the injection of $CdCl_2$ (0.6 mg Cd/kg) or $ZnSO_4$ (10 mg Zn/kg) to rats), application of the polarographic and Cd saturation methods showed good agreement in liver and kidney (Onosaka & Cherian, 1982).

However, when different methods of assessment of the MTs protein are applied in the cases of the environmentally relevant exposures, the results of two methods can be distinct. Even the application in the same study of two different methods of MT-associated thiols had shown a noncorrespondence. In particular, when the SH-groups in the MTs were detected by two alternative methods, certainly by pulse polarography (DPP) and spectrophotometry (with Ellman reagent), the results were not similar (Zorita et al., 2005). In mussels exposed to Cd in laboratory experiment and in mussels sampled in different seasons from field sites, the MTs values detected with the DPP were 9 (in the laboratory) and 34 to 38-fold (in the field) higher than
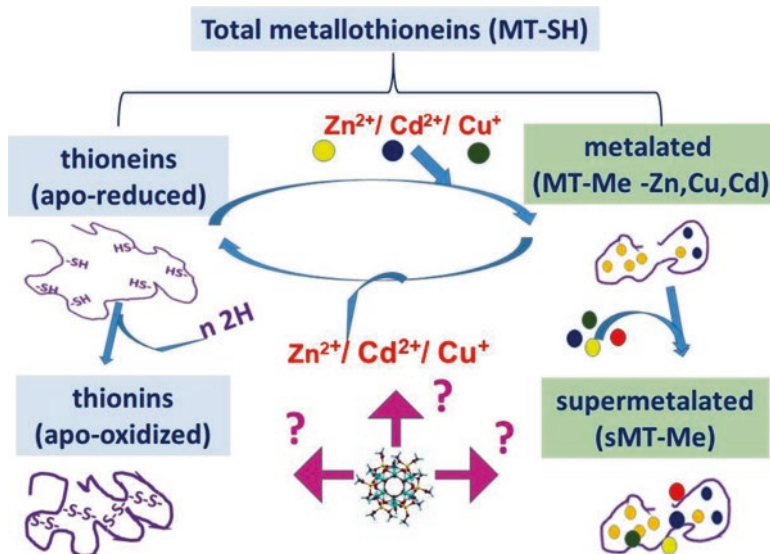
Fig. 1 A scheme of the transformation of the post-translational forms of metallothioneins (metalated and apo-forms) and probable directions of metal-based nanoparticles impact

such values detected with spectrophotometry. More expectedly, a discrepancy was detected when the concentrations of metalated MTs and total MTs protein were compared in the same study. For example, there was no correspondence between the metalated form of MTs (MT-Me) and the MTs total protein concentration determined from thiols in some field studies for the talitrid amphipod, *Orchestia gammarellus,* (Mouneyrac et al., 2001), crabs, *Pachygrapsus marmoratus*, (Münger et al., 1985), fish, *Carassius carassius,* (Falfushynska et al., 2010a, b).

The SH-groups of MTs react with the 5,5′-dithiobis-(2-nitrobenzoic acid) (DTNB or Ellman's reagent) in order to release 5-thio-2-nitrobenzoate and metal ions. It was shown that only the simply coordinated cysteinyl groups in the MTs reacted fast with DTNB, while slow phase of the reaction corresponded to bridging of cysteine thiolate ions (Saito & Hunziker, 1996). Therefore, it was assumed that tightly binding of metal ions in the thiolate cluster decreased the reactivity of SH-groups.

It was proved that in the mammalian tissues under physiological conditions, the levels of thionein could be rather high and enough to harbor important implications for the MTs functionality in Zn and redox metabolism (Capdevila et al., 1997, 2010; Duncan et al., 2006). In the MTs of fish, higher Zn mobility was demonstrated in compared to that of in mouse (Capasso et al., 2005). The mussel MTs were even more reactive than the fish protein regarding metal transfer from Cd-saturated MT to 4-(2-pyridylazo)resorcinol (Vergani et al., 2005). The MTs of frog were also found to be easily oxidized with the loss of metal ions from the metal-thiolate

clusters (Falfushynska et al., 2010a, b). These species-related peculiarities should be taken into consideration when the effect of Me-NPs is investigated in different animal models.

Probably, high levels of the MTs-associated thiols unsaturated by metals might confer some advantage to specimens in a situation of the oxidative stress (Chen et al., 2015), whereas tightly binding of metals by the MTs may supply the bounding of ionic metals in a low toxic form. For evaluation of the oxidized part of the MTs, MTs are reduced by Tris (2-carboxyethyl) phosphine (Haase & Maret, 2004). Difference between the phosphine-treated and untreated MTs corresponds to the oxidized form of the MTs (Gagné, Maysinger, et al., 2008).

Generally, the analysis of the discrepancy between concentrations of total and metalated MTs could be useful for better understanding of their targeting by the Me-NPs or derived metals depending on the species-specific reactivity of these proteins. Investigation of the impact of Me-NPs on the living systems demonstrated high variety of responses of the MTs protein (Table 1). As mentioned above, the expected MTs response to Me-NPs can depend on the level of stability of the Me-NPs, as well as species-related reactivity of the SH-groups in MTs.

3.2 Implication of Metallothioneins as Metal-Based Nanoparticles

It was shown that MTs *per se* can create the Me-NPs with the metal ions entering the cells (Aryal et al., 2006). These nano-crystals can play a role in the organ toxicity of accumulated metals, especially in the kidney of higher vertebrates. Moreover, based on their properties, MT-capped semiconductor NPs are further developed for their theranostic applications as a third-generation Me-NPs (Sharma et al., 2013). It was developed as MT-capped Cd/Se NPs, in which up to eight MTs could be attached as detected by an increase in the fluorescence intensity (Aryal et al., 2006). These NPs were successfully used for labeling of bone marrow-derived mononuclear stem cells while determining their biodistribution, pharmacokinetics, and therapeutic potential in the experimental model of the acute ischemic stroke (Sharma et al., 2013). Moreover, Sharma et al. (2013) and Sharma and Ebadi (2014) discovered multilamellar, electron-dense membrane stacks in the developing Purkinje neurons in rats and in the hippocampal CA-3, which were named "Charnoly bodies." The studies strongly support MTs as potent antioxidant neuroprotective factors in the progressive neurodegenerative disorders, including the inhibition of the Charnoly bodies in brain. Based on these findings, the perspective of the detailed pharmacological properties of NPs using MTs as a sensitive biomarker and antioxidant is expected.

The yeast *Saccharomyces cerevisiae* served as a host for the heterologous expression for a variety of the MTs from different species. Therefore, the technological

Table 1 The effects of metal-based nanoparticles on the metallothioneins in different experimental model systems

Me-NPs	Effect on MTs	Model	Reference
CdSe nanoparticles	Interact with recombinant MT-based peptides	In vitro	Aryal et al. (2006)
ZnS-coated CdSe nanoparticles	Interact with recombinant MT-based peptides	In vitro	Aryal et al. (2006)
"Aged" positively coated CdTe QD, 0.1 mg•L^{-1}, 48 h	Elevated MT total concentration (Cd release?)	Primary cultures of rainbow trout hepatocytes	Gagné, Maysinger, et al. (2008)
CdTe QD, 4 mg•L^{-1}, 24 h	Elevated MT total concentration (Cd release?)	Freshwater mussel, *Elliptio complanata*	Peyrot et al. (2009)
Functionalized nano-magnetic particles (Fe$_3$O$_4$@ Au nanoparticles)	Bound MTs (Au–S interaction)	In vitro	Xin-Yu et al. (2018)
MSA-capped CdTe QDs capped with mercaptosuccinic acid	Electrostatic interaction	In vitro	Tmejova et al. (2015)
Ag-NPs and ionic form of Ag, 1 and 10μg•L^{-1}, 96 h	Increased MTs total (release of Ag?)	Freshwater mussel *Elliptio complanata*	Gagné, Auclair, Turcotte, and Gagnon (2013)
Co-N-vinyl-2-pyrrolidone (NVP)-based Me-NPs 50μg co·L^{-1}, ~ 0.85μM, 14 days	Co from Co-NCs does not bind with MTs, only Co-NCs increase MT total	Bivalve *Anodonta cygnea*	Falfushynska, Filyak, et al. (2012)
Co-(NVP)-based Me-NPs 50μg Co·L^{-1} ~ 0.85μM, 14 days	Co from both Co-NCs and ionic Co bounds with MTs and increase MT total	Fish *Carassius auratus gibelio*	Falfushynska et al. (2014)
Co-(NVP)-based Me-NPs 50μg Co·L^{-1}, ~ 0.85μM, 14 days	Co from Co-NCs does not bind with MTs, unlike ionic Co, both Co-NCs and Co increase MT total	Frog *Pelophylax ridibundus*	Falfushynska, Gnatyshyna, Fedoruk, et al. (2015)
Zn-(NVP)-based Me-NPs 100μg Zn·L^{-1}, ~ 1.54μM, 14 days	Zn from both Zn-NCs and ionic Zn bounds with MTs, decrease MT total	Fish *Carassius auratus gibelio*	Falfushynska et al. (2014)
Zn-(NVP)-based Me-NPs 100μg Zn·L^{-1}, ~ 1.54μM, 14 days	Zn from Zn-NCs does not bind with MTs, Zn-NCs increase MT total	Frog *Pelophylax ridibundus*	Falfushynska, Gnatyshyna, Fedoruk, et al. (2015),
ZnO NPs, bulk ZnO or Zn^{2+}, ~ 30.8μM, 2 mg•L^{-1}	MTs bound Zn^{2+}, metal-rich granules bound ZnO-NPs	Goldfish *Carassius auratus*	Fan et al. (2013)

Table 1 (continued)

Me-NPs	Effect on MTs	Model	Reference
^{67}ZnO-NP in diethylene glycol, 3 mg kg(−1) sediment, ~ 37.04μmol kg^{-1}, 16 d	Does not change MT concentration	Bivalve mollusk *Scrobicularia plana*	Buffet et al. (2012)
ZnO-NPs, 2μg/L, (~0.02μM) in different combinations with municipal effluent and alone, 21 days	Does not change total MT in any combination	Freshwater mussels, *Elliptio complanata*	Gagné, Auclair, Fortier, et al. (2013)
ZnO-NPs or Zn^{2+} (3.1μM) alone and in combination with nifedipine, thiocarbamate tattoo, elevated temperature, 14 days	ZnO-NPs did not affect MT-Me; Zn^{2+} decreased MT-Me; different combinations cause increasd response in total MT	Mussel *Unio tumidus* from pristine site	Falfushynska, Gnatyshyna, Yurchak, et al. (2015)
ZnO-NPs or Zn^{2+} (3.1μM) at 18 or 25 °C, 14 days	MT-Me increased by all exposures, except BTPP group (25 °C); MT-SH increased in all exposures, except BTPP (ZnO-NPs)	Mussel *Unio tumidus* from reservoirs of thermal power plants (DTPP and BTPP)	Falfushynska et al. (2018)
ZnO-NPs or Zn^{2+} (3.1μM) alone and in different combinations with nifedipine. 14 days	MT-Me increased in ZnO-NPs and Zn^{2+-} exposed frogs, except nifedipine combined exposure, total MT elevated in all groups	Frog *Pelophylax ridibundus*	Falfushynska et al. (2017)
TiO$_2$-NPs (1.25μM), TiO$_2$-NPs + BPA, TiCl$_4$ (Ti, 1.25μM), 14 days	MT-Me increased, MT-SH decreased by Ti, TiO$_2$, and TiO$_2$ + BPA	Bivalve mollusk *Unio tumidus*	Gnatyshyna et al. (2019)

implications for the overexpression of the recombinant MTs expressing in yeast were developed with the aim to use these transgenic cells in heavy metal-related biotechnologies, including synthesis of clonable Me-NPs. The MTs use *per se* for creation of the clonable Me-NPs for medicine was experimentally approved based on the unique properties of these proteins However, practical applications of that idea stay unknown (Farcasanu & Ruta, 2017; Ni et al., 2015).

3.3   *Evidence of Direct Interactions of Metallothioneins with Metal-Based Nanoparticles*

Direct interactions of the MTs and nanoparticles were proposed for rapid detection of the MTs desirable for clinical monitoring, for example, early diagnosis of heavy metal poisoning and malignancies, based on the enzyme-mimetic activity

of the nanoparticles and protein corona-based recognition. Zhang et al. (2019) developed insufficient polyhedral oligomeric silsesquioxane polymer-caged gold nanoparticles (denoted as PP-AuNPs) for protein corona-based recognition. As the authors stated, in the presence of the MTs, the catalytic reduction in yellow 4-nitrophenol to a colorless 4-aminophenol is inhibited due to masking of the exposed PP-AuNPs catalytic surface with the MTs corona. According to that approach, the MTs can be quantified by the presence of color contrast with a superior sensitivity up to a 1.5 nM detection limit. The transitional and post-transitional metal ion- and aptamer-free PP-AuNPs platform exhibits an excellent selectivity toward MTs over various ions, neutral biomolecules, and protein species, and successful applications were demonstrated by the detection of MTs in complex biological samples.

The ability of MTs to interact with the functionalized nano-magnetic particles confirms the ability of a direct interaction of MTs with the Me-NPs within the cells. In the study of Xin-Yu et al. (2018), MTs in the mixture with bovine serum albumin interacted with the Fe3O4@Au NPs. It was shown that this effect is realized through a simple Au–S interaction, and the detection limit could be as low as 10 fg mL^{-1}. Purified proteins were determined by matrix-assisted laser desorption ionization time-of-flight mass spectrometry.

Raz et al. (2012) showed that both Ag-NPs and the ionic Ag bound the MTs. This interaction was utilized for the developing of the surface plasmon resonance (SPR) sensor for rapid detection of Ag-NPs. Incorporation of human MT-1A to sensor surface enables screening for potentially biologically active silver nanoparticles at parts per billion sensitivity. Other protein ligands (ovalbumin and immunoglobulin G) were also tested for binding capacity of the Ag-NPs. They were found to be an inferior of the MTs (almost no binding activity or threefold lower dose-dependent binding activity correspondingly) toward the Ag-NPs.

A unique property of MTs to bind Cd makes these proteins a potential target of Cd-NPs. Indeed, it was shown that the toxicity of CdSe-NPs is mediated by the MTs. In particular, recombinant MT-based peptides are capable of removing surface Cd^{2+} ions from the thiocarboxylate-capped CdSe nanoparticles, while surface Zn^{2+} ion depletion from ZnS-coated CdSe nanoparticles was more difficult (Aryal et al., 2006). A depletion of Cd or Zn by MT peptides also occurred over time, suggesting that slow depletion of Cd and Zn at the surface of the nanoparticles initiates their toxicity in cells.

The interaction between semiconductor nanocrystals, CdTe QDs capped with the mercaptosuccinic acid (MSA) and MTs was investigated by various analytical methods, such as tris-tricine gel electrophoresis, fluorescence evaluation, and electrochemical detection of catalyzed hydrogen evolution. The obtained results demonstrate that the MSA-capped CdTe QDs and MT do not create firmly bound stable complex. However, weak electrostatic interactions contribute to the interaction of the MT with the MSA-capped CdTeQDs. The smallest QDs possessed the highest affinity to MTs and *vice versa* (Tmejova et al., 2015).

4   Responses of Metallothionein Protein in Organism Exposed to Metal-Based Nanoparticles

4.1   Exposures to Cd- and Ag-Based Nanoparticles

Due to particular affinity of MTs to Cd, the analysis of these proteins is a relevant tool in the study of the biostability of Cd-NPs. For example, the instability of QDs of aged cadmium telluride (CdTe) was reflected in the increased level of the MTs in primary cultures of hepatocytes of the rainbow trout under exposure for 48 h of such cultures to positively coated and aged (2 months and 2 years) CdTe QDs at a threshold concentration of 0.1 mg•L^{-1}. Partially, that was explained by the liberation of Cd^{2+} from the NPs, and not from a direct effect of the QDs (Gagné, Maysinger, et al., 2008). However, a direct binding of Cd to the MTs was not investigated in that work. Similarly, the levels of MTs protein were elevated in both a digestive gland (reaching a 1.8-fold) and gonads (2.2-fold) in comparison to control of the freshwater mussel, *E. complanata*, exposed to 4 mg•L^{-1} CdTe for 24 h. But it returned to control at higher concentrations. In the gills, the level of MTs was readily decreased by both CdTe QDs and CdSO$_4$ at a threshold concentration of 5.6 mg•L^{-1} CdTe (Peyrot et al., 2009). Probably, these results indicate the indirect effect of extremely high concentrations of nanoparticles on MTs functionality.

At the exposures of the aquatic animals, rainbow trout *O. mykiss* and freshwater mussel *E. complanata,* to low nanomolar concentrations of Ag-NPs, a relation of the effect of nanoparticles on the MTs to a release of Ag was evident (Gagné et al., 2012; Gagné, Auclair, Fortier, et al., 2013; Gagné, Auclair, Turcotte, & Gagnon, 2013). For example, an adverse effect of Me-NPs on the MTs was demonstrated at the exposure of the rainbow trout *O. mykiss* to the Ag-NPs and ionic form of Ag (in 0.06, 0.6 and 6μg L^{-1} concentrations for 96 h) (Gagné et al., 2012). It showed significant reduction in the total level of the hepatic MTs, accompanied by an increased proportion of the oxidized MTs. Importantly, the effect was caused by either form of Ag; however, the Ag-NPs were less potent than the dissolved Ag. In marine mussels exposed to 1 and 10μg/L of Ag-NPs for 96 h, a significant increase in Ag in whole tissues was observed accompanied with the increased levels of the MTs. In particular, 20 and 80 nm (diameter) citrate-coated Ag-NPs and ionic Ag were able to increase the levels of the MTs and LPO that suggest that ionic Ag was able to explain partly the toxicity of the Ag-NPs (Gagné, Auclair, Fortier, et al., 2013).

In conclusion, the investigated Cd- and Ag-NPs in high ranges of concentrations caused the responses of the aquatic organisms similar to the effects of the ionic forms. The MTs were sensitive to those exposures; however, the changes in their concentrations were contradictive and likely caused by the indirect effects, namely by the oxidative stress. The content of metals in the MTs was not detected in those studies.

4.2   Species-Dependent Responses of Metallothioneins at Animal Exposure to Nanoscale Composites of N-Vinyl Pyrrolidone Copolymer

The responses of the MTs to the Me-NPs can be different depending on the animal species. This regularity is illustrated by the examples of bivalve mollusks, cyprinidae fish, and anuran frogs exposed to Cobalt and Zinc-containing nanoscale composytes of the N-vinyl pyrrolidone copolymer. Due to low toxicity, easy film formation, and adhesive characteristics, the N-vinyl-2-pyrrolidone (NVP)-based Me-NPs are widely used in industry, personal care products, and medicine (Abraham et al., 2001; Luther et al., 2012; Parambil et al., 2012; Xiong et al., 2006; Zhang et al., 2012).

A particular interest to Zn- and Co-NCs is stimulated by the essential functions of these transition metals in the organism (Downward et al., 2012; Kim et al., 2011; Miao et al., 2013; Yang et al., 2011). Zn is a second after iron most abundant transition metal in the organism. It is known as a metal involved in various processes of the molecular stabilization, catalysis, and cell signaling (Krężel & Maret, 2007; Outten & O'Halloran, 2001). However, the ionic Co plays crucial role in regulation of numerous vital functions. It is present in the cyanocobalamin and at least eight noncorrin-Co-containing enzymes and Co transporter (Kobayashi & Shimizu, 1999). Besides, it is present in many nanoscaled materials, particularly created for medical applications (Colognato et al., 2008). A particular concern to the biomedical application of Co-NPs is related to a danger of early failure of metal-on-metal hip resurfacings secondary to an adverse reaction to metal debris. Co concentrations higher than $20 \mu g \cdot L^{-1}$ (up to $50 \mu g \cdot L^{-1}$) in the blood of patients are frequently associated with that effect (Langton et al., 2013).

Therefore, to assess the bioavailability and biostability of these NVP-based Me-NPs in different model organisms, aquatic animals (mollusk *Anodonta cygnea*, fish *Carassius auratus gibelio*, and frog *Pelophylax ridibundus)* were investigated (Falfushynska et al., 2014; Falfushynska, Filyak, et al., 2012; Falfushynska, Gnatyshyna, et al., 2012; Falfushynska, Gnatyshyna, Fedoruk, et al., 2015). Concentrations of Me-NP used in those studies were corresponding to $50 \mu g \cdot L{-}1$ of Co and $100 \mu g \cdot L{-}1$ of Zn. For the analysis of metalated MTs (MT-Me), these proteins were isolated as thermostable proteins by a size-exclusion chromatography, as described (Falfushynska, Filyak, et al., 2012; Falfushynska, Gnatyshyna, et al., 2012). Metal (Zn, Co, Cu, and Cd) concentrations were analyzed in the eluted MTs-contained peak and in tissue by the atomic absorption spectrometry. Total concentration of the MTs protein (MT-SH) was assayed according to Viarengo et al. (1999).

Importantly, in those studies, the concentrations of Co^{2+} and Zn^{2+} and their NVP-derived polymeric substance were corresponded to the limits found in the freshwater areas or physiological conditions applied to the animals during 14 days. Particularly, Co concentration was based on the limits found in freshwater ($4–110 \mu g \bullet L^{-1}$), where the lower concentration is considered to be not harmful for

the freshwater organisms, while higher concentrations corresponded to the acute toxicity (US EPA).

Co^{2+} is well-known pro-oxidant that can directly generate the reactive oxygen species in Fenton reaction (Kubrak et al., 2011; Simonsen et al., 2012; Valko et al., 2005). Indeed, the exposure to ionic Co was accompanied with the elevated toxicity and oxidative stress (Figgitt et al., 2010; Gaitanaki et al., 2007; Kubrak et al., 2011; Simonsen et al., 2012; Valko et al., 2005). Those pro-oxidant activities suggest its possible impact on the MTs. However, Co contribution in the toxicity of Co-NPs has not been clarified definitely (Unfried et al., 2007). A selection of the MTs as a principal molecular target of Co-NC was grounded on a possibility of Co incorporation in the metal-thiolate structure of these proteins. Owing to Co similarity to Zn in its coordination properties and its conspicuous chromophoric and magnetic characteristics, Co(II) serves as a reliable and convenient probe of the coordination geometry of zinc in proteins and has been employed to explore the structure of the metal-binding sites in MTs (Overnell et al., 1988; Vasak & Kägi, 1981). Additionally, Co directly induced MTs synthesis *in vitro* in rat hepatic tissue (Bracken & Klaassen, 1987; Murata et al., 1999). Despite that, only several studies were devoted to the effect of Co on the MTs function in the *in vivo* (Falfushynska et al., 2014; Falfushynska, Filyak, et al., 2012; Falfushynska, Gnatyshyna, et al., 2012; Falfushynska, Gnatyshyna, Fedoruk, et al., 2015; Piotrowski & Szymańska, 1976; Rosenberg & Kappas, 1989).

These studies suggest the ability of ionic Co to elevate the concentration of total MTs protein and metalated MTs (Zn, Cu, Cd-MTs) in the digestive gland of mussels compare to control (up to10 times) confirming the results in vitro, mentioned above. Moreover, these MTs had the increased level of Co in their composition, despite the total level of Co in the tissue was corresponding to control value. However, the results exist that only the ionic Co-treated specimens accumulated an excess of Co in MTs of bivalve mollusk and had the increased level of metalated MTs, whereas in the Co-NPs exposed group, the level of Co-MTs was not changed (Fig. 3; Falfushynska, Filyak, et al., 2012; Falfushynska, Gnatyshyna, et al., 2012).

In opposite, the mollusks, exposed to Co-NPs, showed the increase in the total level of Co in the tissue compare to control. However, it was not accompanied by the substantial changes in the MT-Me and Co-MTs (Falfushynska, Filyak, et al., 2012; Falfushynska, Gnatyshyna, et al., 2012). Interestingly, total MTs protein concentration (MT-SH) was upregulated. Consequently, Co-NPs directly (due to elevated level of Co in the tissue) or indirectly (for example, by means of reactive oxygen species) were able to upregulate MTs concentration. However, this excess of MTs was not metalated. The VNP-derived polymeric substance *per se* did not provoke significant changes in metal concentration or distribution within the digestive gland tissue of mollusks. Therefore, this study indicated the different responses to Co and Co-NPs confirming stability of the Co-VNP-derived substance in the organism of the bivalve mollusk.
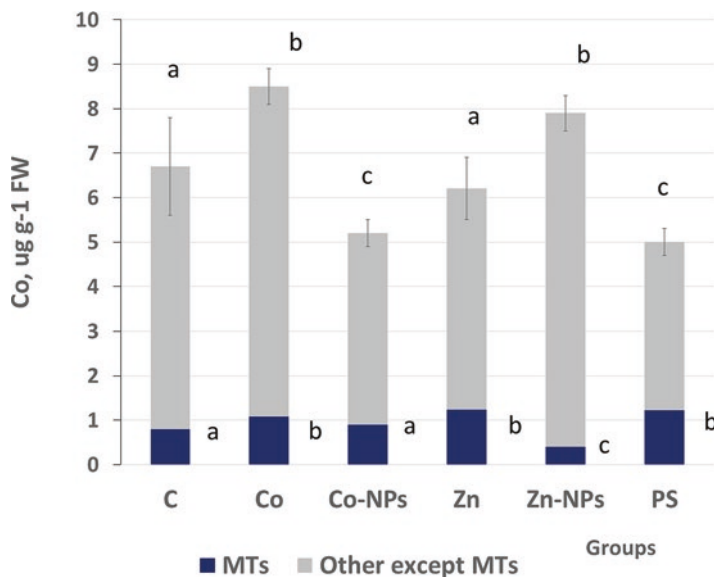
Fig. 2 Concentration of Co in the metallothioneins of the liver of frog *P. ridibundus* exposed to the VNP-derived Me-NPs (Co-NC, Zn-NC), Co^{2+} or Zn^{2+} or polymeric substance (PS). In this and the next figures, the same letters indicate the values of biomarkers that do not differ significantly ($P > 0.05$). (Reproduced with permission (Falfushynska, Gnatyshyna, Fedoruk, et al., 2015))

Interestingly, similar ability to accumulate Co in the MTs only at the exposure to soluble ionic Co, but not at the exposure to Co-NPs, was detected in frog *P. ridibundus* (Fig. 2, Falfushynska, Gnatyshyna, Fedoruk, et al., 2015). However, in frog, this binding of Co was accompanied by the elevation of total MTs concentration without the increase in MT-Me level, as in mollusk (Fig. 3). In opposite, the MT-Me concentration was decreased at both Co-related exposures. Moreover, in contrary to the response of mollusk, Co-NPs did not cause the elevation of the level of this element in the tissue. The effect of Co-NC on the accumulation of Co in the tissues and MTs in fish was different from that in mollusk and frog (Falfushynska et al., 2014). In the liver of fish, the levels of Co in the tissue, Co-MTs, MT-Me, and MT-SH were elevated similarly in the exposures to nanocomposite and free Co.

Total ability to concentrate Co from the medium and the level of MT-Me were the highest in fish, in comparison with mollusk and frog. That peculiarity can be explained by the highest rate of degradation of the metal-organic substance in fish.

The fish and frog were also investigated on their ability to release Zn ($100\mu g\ L^{-1}$ of Zn either as a cation or a nanocomposite) from the VNP-derived nanocomposite (Falfushynska et al., 2014; Falfushynska, Gnatyshyna, Fedoruk, et al., 2015). Similar to Co, there was the species-dependent difference in the response of the MTs, and only fish was able to release Zn from the Zn-NPs and increase its level in the MTs (by 2.4 and 2.9 times, correspondingly) both at the exposure to the ionic Zn
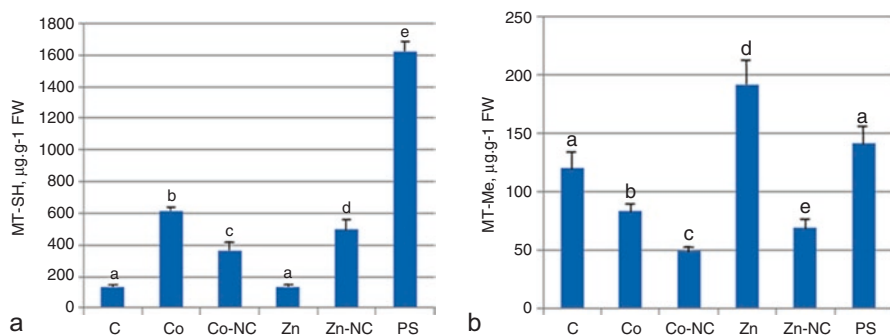
Fig. 3 Concentrations of total metallothionein protein (**a**) and its metalated form (**b**) in the liver of frog *Pelophylax ridibundus* exposed to the VNP-derived Me-NPs (Co-NC, Zn-NC), Co^{2+} or Zn^{2+} or polymeric substance (PS) ($\mu g \cdot g^{-1}$ FW, M ± SD, $n = 8$). (Reproduced with permission (Falfushynska, Gnatyshyna, Fedoruk, et al., 2015))

and Zn-NCs. This and other peculiarities that are common for metal and Me-NPs witness a release of metal from the NP in fish. In opposite, in frog only Zn^{2+} caused an elevation of the concentration of Zn in the MTs (corresponding to the MT-Me because of the main Zn contribution in the metal composition of MTs) (Fig. 3).

As a conclusion, the tissues and organs of studied mussels and frogs were not able to accumulate Co (except mollusk) or Zn in the form of VNP-derived nano-composites, or release metal from this form, while that was possible in fish. Detection of concentration of Co and Zn bound with the MTs indicates different species-related responses.

According to our studies (Falfushynska et al., 2014; Falfushynska, Filyak, et al., 2012; Falfushynska, Gnatyshyna, et al., 2012; Falfushynska, Gnatyshyna, Fedoruk, et al., 2015; Falfushynska, Gnatyshyna, Yurchak, et al., 2015), the comparison of the concentration of total MTs protein and its metalated form MT-Me deeper analysis of the vulnerability of metallothioneins is possible. Whereas the metalation of the MTs (MT-Me) can be caused by free ionic metals or higher affinity of the MTs to metal than in the Me-NPs, total concentration of the MTs (MT-SH) is probably corresponding to the expression of that protein. The comparison of the MT-SH and the MT-Me gives the arguments that concern the oxidative change of MTs and their involving in the antioxidant defense (Krężel & Maret, 2016). This kind of response can be induced by the pro-oxidant activity of the nanoparticles. Indeed, the comparison with the indices of the oxidative stress allow one to suggest that in all cases of the Me-NVP-derived nanocomposites, the oxidative stress was the reason for that MT-SH elevation. It was caused by the Co-NPs, NPs *per se* in all species and by the ionic Co in fish and frog. Moreover, a rise of the nonmetalated MTs proportion was accompanied by a successful antioxidative defense. It was confirmed by low level of the oxyradical formation and absence of elevated carbonylation of proteins only in the Co-NC-exposed group of mollusks, and in all, except Zn-exposed groups of frogs (Falfushynska, Filyak, et al., 2012; Falfushynska, Gnatyshyna, et al., 2012;

Falfushynska, Gnatyshyna, Fedoruk, et al., 2015; Falfushynska, Gnatyshyna, Yurchak, et al., 2015). In fish, the opposite relation—a decreased level of the MT-SH accompanied with low level of the oxyradical generation was detected, whereas at all other exposures, these parameters were not changed (Falfushynska et al., 2014). Thus, in mollusk and frog, the MT-SH/oxyradical ratio was opposite to that detected in fish. High vulnerability of the SH-groups to the oxidation in mollusk and frog, comparing to fish, was observed. These data confirm a canonical reactivity of MTs with more tight binding of metal ions in α- than in β-domain and their species-depending specificity (Vergani et al., 2005). The MTs of frog demonstrate high oxidizability associated with the creation of the oligomeric forms with spectral features typical for –S-S- groups (Falfushynska et al., 2010a, b).

Generally, a comparison of the effect of the same NVP-derived nanoparticles in different animal models demonstrated high species-dependent variability of the responses with a participation of the MTs. Thus, the MTs can be a biomarker for evaluation of the bioavailability of the Me-NPs in different species and their application of the experimental models for medicine.

4.3   Responses of Metallothioneins at Combined Exposures of Model Animals to ZnO-Nanoparticles

The ability of the aquatic animals to release metals from the NC in the combined exposures was studied for the ZnO-NPs. A toxicity of the ZnO-NPs has often been ascribed to a release of zinc ions from the NPs. However, it is not understood to which extent these ions contribute to the toxicity of ZnO-NP and which are the underlying mechanisms (Buerki-Thurnherr et al., 2013). This particularity can be explained by a very strong binding of Zn to the MTs (Krężel & Maret, 2016). Therefore, MTs represent a highly expected intracellular target for the accumulation of Zn from Zn-NPs. However, it was shown that in the tissues of goldfish (Carassius auratus) MTs accumulated mostly free Zn ions from the medium, whereas Zn from ZnONPs and bulk ZnO was bound by the metal-rich granules. Different results on subcellular distributions revealed that the mechanisms of metal detoxification in the liver of fish were different for those three forms of Zn (Fan et al., 2013). An approach of stable isotope labeling was applied to investigate the bio-uptake of ZnO-NPs in the estuarine clam *Scrobicularia plana*. An exposure to 3 mg kg^{-1} sediment ZnO-NPs in the diethylene glycol was selected since that level is a realistic prediction of the environmental concentration in the sediments. An exposure of 16 days to glycol led to a significant increase in levels of the MTs (determined by a differential pulse polarography analysis) in clams, compared with those exposed to ^{67}ZnO-NPs or controls, detecting the absence of a response to NPs (Buffet et al., 2012).

It was proposed that a combined exposure can influence the bioavailability of ZnO-NPs. To model the environmentally realistic effect of ZnO-NPs, the freshwater mussels *E. complanata* were exposed for 21 days to the environmentally realistic

concentration of the ZnO-NPs ($2\mu g \cdot L^{-1}$) and the ionic Zn, or to a physically and chemically treated municipal effluents, alone and in the presence of each form of Zn, and the levels of the MTs were characterized in gill, digestive gland, and gonad tissues (Gagné, Auclair, Fortier, et al., 2013). In a similar study, 1 and $10\mu g \cdot L^{-1}$ concentrations of the ZnO-NPs were utilized (Gagné et al., 2016). According to the reported data, only the municipal effluents at the concentration of $2\mu g \cdot L^{-1}$ increased the level of the MTs protein (Gagné, Auclair, Fortier, et al., 2013). However, the exposure to 1 and $10\mu g \cdot L^{-1}$ of ZnO-NPs or $10\mu g \cdot L^{-1}$ of the ionic Zn increased total concentration of the MTs in gill in the absence of the municipal effluents (Gagné et al., 2016). The municipal effluent concentration was indicated as a dominant factor because the presence of the municipal effluent eliminated the effect of the ZnO-NPs (Gagné et al., 2016). However, the results of those two studies were contradictory concerning the effect of the effluents. The elevation of MTs concentration was accompanied by a decrease in the level of the lipid peroxidation, indicating the antioxidant activity of the MTs. The analysis of these data makes it evident that the effects of the ZnO-NPs and the ionic Zn on the MTs are different. This inference supports the hypothesis that a toxicity of the ZnO-NPs in mollusk is not associated solely with a release of Zn^{2+} ions in its tissues. In those works, the binding of Zn to MTs was not indicated.

The effects of ZnO-NPs in a model organism, *U. tumidus* mussel, and a potential modulation of these effects by common co-occurring environmental stressors were studied utilizing the exposure to the ZnO-NPs or Zn^{2+} ($3.1\mu M$) and a combined exposure of ZnO-NPs with traditional drug Ca-channel blocker nifedipine, thiocarbamate pesticide Tattoo, or with the elevated temperature (25 °C) during 14 days. All these combinations and concentrations were assumed to be typical for the realistic environment. Some cellular responses to Zn^{2+} and ZnO-NPs were different, indicating that the effect of ZnO-NPs was not due exclusively to Zn release (Falfushynska, Gnatyshyna, Fedoruk, et al., 2015; Falfushynska, Gnatyshyna, Yurchak, et al., 2015). In that study, ZnO-NPs did not affect the level of the MTs metalation, whereas the ionic Zn and all combined exposures to ZnO-NPs affected the MT metalation.

In opposite, all experimental exposures at 18 °C induced a significant upregulation of the MT-SH, and only the elevated temperature (25 °C) reduced such increase (Fig. 4). Thus, the ZnO-NPs were not a source of the available Zn for its incorporation in the MTs, the same as in the experiments of (Gagné et al., 2016; Gagné, Auclair, Fortier, et al., 2013). However, all exposures were able to increase the total MT-SH level, probably, via inducing its synthesis.

To summarize, all exposures caused stress-response of the MT-SH. A comparison of the MT-SH and MT-Me values (Fig. 4b) demonstrates that in all Zn-related exposures, an excess of the nonmetalated protein was present, attesting the involving of the MTs in the oxidative response.

The same exposures to ZnO-NPs were applied for the mollusks from two cooling reservoirs of the thermal power plants (TPPs) that were highly (BTPP) or moderately (DTPP) polluted. The responses of their MTs to applied exposures (ZnO-NPs
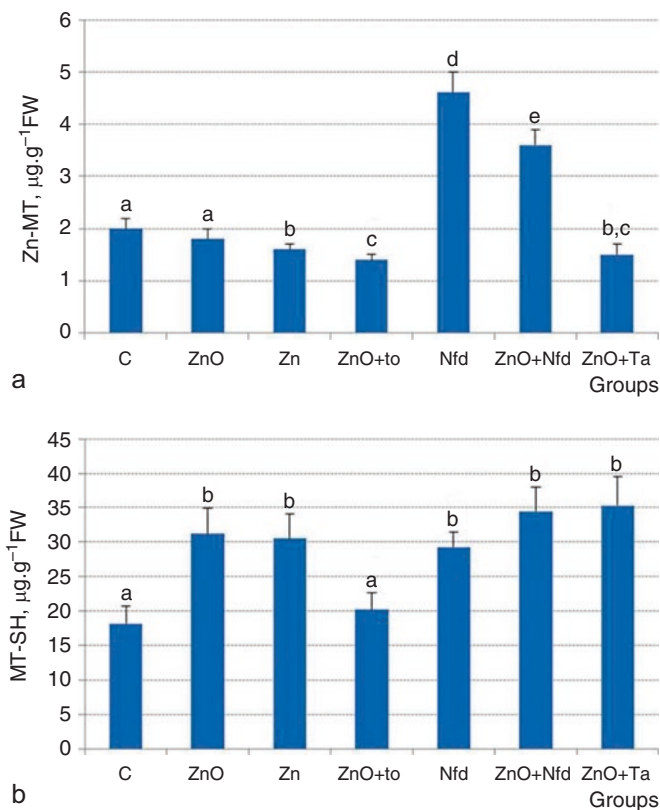
Fig. 4 Effects of the experimental exposures to Zn, Zn nanoparticles, and the organic pollutants on tissue levels of the metallothionein in *Unio tumidus* Experimental exposures: C-control, ZnO—ZnO-NPs; Zn—Zn^{2+}; Nfd—nifedipine; ZnO + Nfd—combination of ZnO-NPs and Nfd; ZnO + Ta—combination of ZnO-NPs and fungicide Tattoo, all conducted at 18 °C; ZnO-NPs + t°—at 25 °C. All exposures lasted for 14 days. Data are presented as the means ± SD. (Reproduced with permission (Falfushynska, Gnatyshyna, Yurchak, et al., 2015))

at two temperature regimes and the ionic Zn) were different from those in the mollusks from a pristine site mentioned above (Fig. 5; Falfushynska et al., 2018).

In the DTPP mussels, no particular responses to the ZnO-NPs or only to ZnO-NPs and to the ionic Zn were detected. While in the BTPP mussels the accumulation of Zn in the MTs was more specific and appeared in all groups exposed to Zn-contained substances, unlike at the exposure to heating only. Probably, the populations of mollusks from sites highly polluted with metal and dust possessed certain adaptations to the Zn-contained substances. Thus, in those populations, mollusks were also more susceptible to different additional stressors than the mussels from the pristine site. However, at all exposures of mollusks to ZnO-NPs, the MTs in the digestive gland were not targeted directly or particularly by the ZnO-NPs or Zn derived from the nanoparticles. Only the coexposures to other adverse challenges
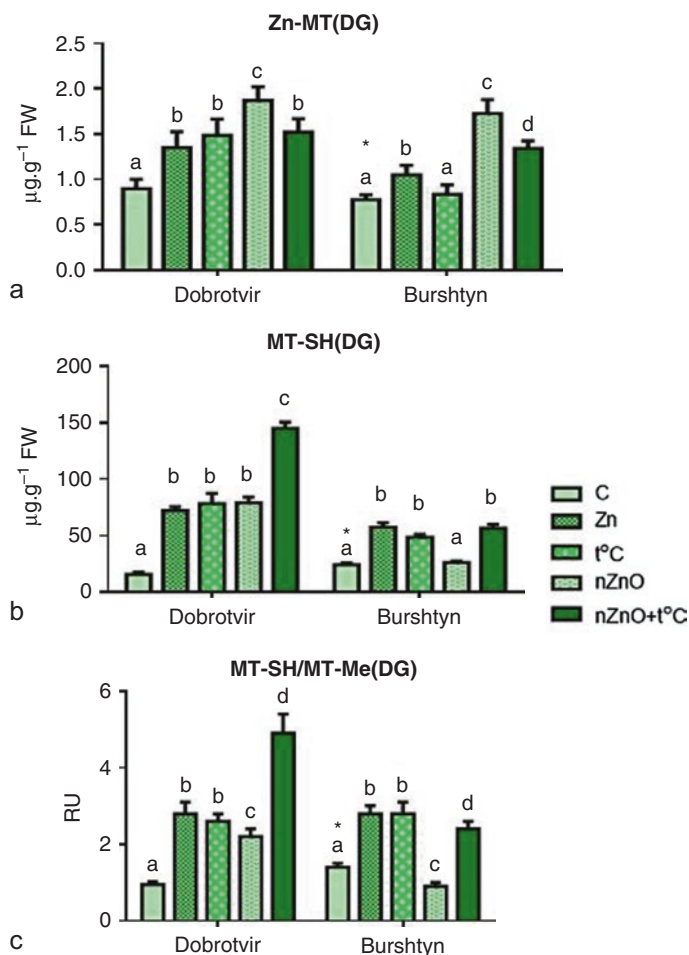
Fig. 5 Effects of the experimental exposures to nanosized ZnO (ZnO-NPs), ionic zinc (Zn), elevated temperature (T), and the combination of ZnO-NPs + T on the levels of the metallothionein in a digestive gland (DG) of *U. tumidus* from two cooling reservoirs (Dobrotvir and Burshtyn in Ukraine). Experimental exposures: C—control, ZnO—ZnO-NPs; Zn—Zn²⁺; all conducted at 18 °C; ZnO-NPs + tº –at 25 °C. Asterisks indicate the control values of the traits that significantly differ between the DTPP and BTPP mussels ($P < 0.05$). (Reproduced with permission (Falfushynska et al., 2018))

enhanced such sensitivity of MTs. Particularly, a long-term acclimatization to a warm metal-polluted environment (such as the cooling ponds of the TPP) enhanced metal-detoxification capacities of mussels over a broad range of the environmental temperatures and compensated the negative effects of the acute warming on metal homeostasis (Sokolova & Lannig, 2008).

The combined exposures to ZnO-NPs were also studied in marsh frog *P. ridibundus* exposed to the same treatments as the bivalve mollusk (Falfushynska et al.,

2017): to ZnO-NPs or Zn^{2+} (3.1μM), nifedipine (10μM), and combination of ZnO-NPs and nifedipine during 14 days. All experimental exposures led to an increase in total levels of the MTs (MT-SH), which were the highest in Zn^{2+} and nifedipine-exposed groups (Fig. 6).

Thus, a response of the MT-SH was a common stress response. However, the amount of MT-Me was elevated in ZnO-NPs and Zn^{2+}-exposed frogs, but significantly suppressed in their nifedipine-exposed counterparts, compared to control detecting common responses to Zn-related exposures. The ratio of the MT-SH/MT-Me in Zn^{2+} and ZnO-NPs-exposed frogs remained at control levels, reflecting a concomitant increase in the total MT-SH and metal-bound MT-Me, similar for both Zn-contained substances. A comparison of the bivalve mollusk and frog at a combined exposure to ZnO-NPs and ionic Zn shows that the direction and potentially the mechanisms of pollutant interactions (such as ZnO-NPs and nifedipine) might differ between mollusks and amphibians.
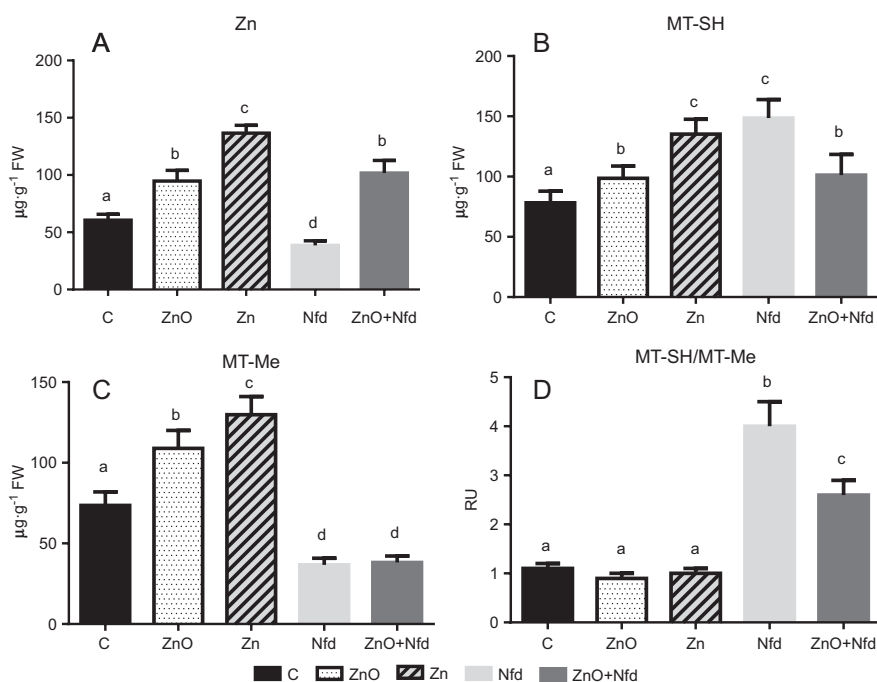
Fig. 6 Effects of experimental exposures to the nanoform of ZnO (nZnO), zinc (Zn), nifedipine (Nfd), and the combination of nZnO+Nfd on tissue levels of Zn (**a**), metallothionein total (MT-SH) (**b**), and metalated (MT-Me) (**c**) concentrations and the ratio of the concentrations of MT-SH/MT-Me in the liver of frog *P. ridibundus*. Data are presented as the means ± SD. (Reproduced with permission (Falfushynska et al., 2017))

4.4 Reflection of TiO₂-Nanoparticles Impact on the Organism by Characteristics of Metallothionein

According to the results of analysis of the TiO$_2$-NPs effects (see Sect. 2.4), MTs expression does not belong to the expected cellular targets of these particles. The effects of titanium compounds on the MTs concentration are contradictory. In a study of *M. galloprovincialis*, an acute exposure to TiO$_2$-containing sunscreen led to a progressive and dose-dependent increase in the MT-SH in gill (Sureda et al., 2018). On the other hand, TiO$_2$-NPs brought down the MT-SH level in the gill of *M. galloprovincialis*, previously elevated as a result of cadmium exposure (Della Torre et al., 2015).

The effect on the MTs protein via the produced ROS was expected. Indeed, the reported effects of n-TiO$_2$ toward various organisms are related to the generation of ROS, resulting in the oxidative stress and oxidative damage (Barmo et al., 2013; Diniz et al., 2013; Federici et al., 2007; Khene et al., 2017; Reeves et al., 2008). These expectations regarding MTs were verified in the study of Tan and Wang (2014). After the exposures to TiO$_2$-NPs at various concentrations (0.05, 0.1, 0.2, 0.5, and 1 mg•L^{-1}) of 14-day-old *Daphnia magna* and subsequent depuration for 2 h, the MTs concentration measured using a modified silver saturation assay was not changed in comparison to the control. It was also indicated that the TiO$_2$-NPs did not produce ROS in daphnids over the concentrations employed in that study (Tan & Wang, 2014). Only 2 mg•L^{-1} of TiO$_2$-NPs (the concentration generally considered to be safe in the environment) caused a substantial impact on the ability of the MTs to bind metals and on common concentration of the MTs in tissues of *Daphnia magna* (Fan et al., 2011).

One of the major ways of utilizing n-TiO$_2$ is related to its unique photocatalytic activity (Chen et al., 2003). This activity is applied in wastewater purification due to relatively low cost and high stability (Khalilova et al., 2018). On the other hand, the photocatalytic activity of n-TiO$_2$ could provoke changes in the biotopes based on different sensitivity to that activity (Binh et al., 2015). Therefore, the investigations of complex exposures to TiO$_2$-NPs are highly actual. Indeed, it was shown that coexposures to TiO$_2$-NPs and other substances in in vitro or in vivo test models comprise almost half of the 151 published studies devoted to coexposures of the nanoparticles (Naasz et al., 2018). Frequently, the "Trojan-horse effect" was shown for those coexposures, when the interactions of the compounds in the environment or their effects in the organism led to an occurrence of the mixed effects (Naasz et al., 2018).

A study of the MTs indicates such distortion of the effects to certain substance in the coexposures with Me-NPs. In particular, in the combined exposures, TiO$_2$-NPs decreased the upregulation of MTs caused by Cu (100μg L^{-1}) in comparison with the effect of Cu alone. However, at lower concentrations of Cu (10, 20, 30, 40, 50, 70μg L^{-1}), TiO$_2$-NPs did not modulate an increase in MTs concentration caused by Cu. The authors explained such impact of the TiO$_2$-NPs by the adsorption of Cu onto the TiO$_2$-NPs. As a result, Cu ability to impact MTs got weaker. Hence, whereas

the evidence of a direct impact of the TiO_2-NPs on the molecules of the MTs seems to be weak, they are able to distort the effect of other known impacts on the MTs (Fan et al., 2011).

The consequences of complex exposure to TiO_2-NPs and Bisphenol A (BPA) were studied in a bivalve mollusk *U. tumidus* (Gnatyshyna et al., 2019). The specimens of *U. tumidus* were subjected to 14-day exposure to: 1) TiO_2-NPs (1.25μM), 2) BPA (0.88 nM), 3) TiO_2-NPs + BPA, or 4) $TiCl_4$ (Ti, 1.25μM, as a positive control for TiO_2-NPs). In this study, coexposure to TiO_2-NPs and BPA caused a specific response, namely, a depletion of the total MTs protein concentration (Fig. 7). The determination of MTs metalated concentration allowed to show another important effect of titanium. An exposure to all Ti-containing compounds resulted in the hypermetalation of the MTs detected from Zn and Cu content in those proteins and without an increase in total protein concentration of the MTs.

The authors proposed as explanation a so-called hypermetalation of the MTs that was observed for all titanium-containing treatments. They considered a unique protein-binding behavior of the titanium (IV), namely, its ability to polymerize through the oxo bridges (Rozes et al., 2006), providing additional metal binding by the MTs (Sutherland et al., 2012). That attribute of the titanium (IV) is used in the anticancer chemotherapy (Wang et al., 2013). In a recent study, it was demonstrated that TiO_2 strongly interacted with different cellular proteins, selective to specific amino acid side chains (Ranjan et al., 2018).

Fig. 7 Metallothionein concentrations in a digestive gland of *Unio tumidus* exposed to $TiCl_4$ (Ti), n-TiO_2, BPA, and n-TiO_2 + BPA for 14 days, in comparison with control (C). (Reproduced with permission (Gnatyshyna et al., 2019))
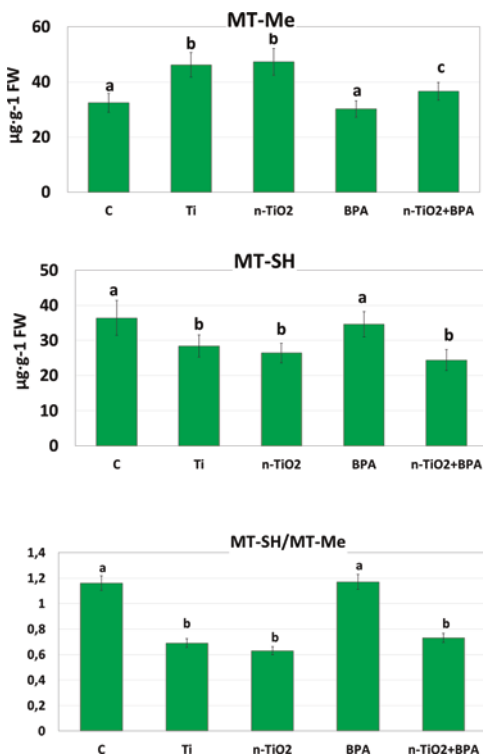
5   Conclusions and Perspectives

In this chapter, specific responses of the MTs to Me-NPs are discussed based on the results of experiments conducted by the authors, as well as the results available in the reviewed literature. To date, most existing data are related to studies conducted on *in vitro* experimental models and lower animals, namely, the aquatic organisms. The metalated MTs *per se* can be regarded and utilized as Me-NPs of novel generation due to their ability to bind metal ions in the nanoscale particles and, expectedly, provide their transfer to other cellular targets. Their direct interaction with Me-NPs is also perspective for use in nanomedicine. The performed comparison has shown that in the invertebrate species and amphibia, the MTs are less responsible to the biodegradation of Me-NPs than the MTs in fish. Particular attention was paid to the effect of the Me-NPs at the combined exposures with other confounding impacts, namely, drugs, fungicides, municipal wastes, and elevated temperature causing a so-called Trojan-horse effect. For the adequate estimation of the environmental exposures, these interrelations should be considered in different models used in study. It is evident that there are not enough investigations of the MTs in higher vertebrates and human, regarding their implication in the understanding of the Me-NPs toxicity. Such studies of the MTs can provide a valuable expertise on the application of the Me-NPs in medicine and pharmacology.

References

Abraham, G. A., De Queiroz, A. A., & San Roman, J. (2001). Hydrophilic hybrid IPNs of segmented polyurethanes and copolymers of vinylpyrrolidone for applications in medicine. *Biomaterials, 22*(14), 1971–1985. https://doi.org/10.1016/S0142-9612(00)00381-1

Amiard, J. C., Amiard-Triquet, C., Barka, S., Pellerin, J., & Rainbow, P. S. (2006). Metallothioneins in aquatic invertebrates: Their role in metal detoxification and their use as biomarkers. *Aquatic Toxicology, 76*(2), 160–202. https://doi.org/10.1016/j.aquatox.2005.08.015

Aryal, B. P., Neupane, K. P., Sandros, M. G., & Benson, D. E. (2006). Metallothioneins initiate semiconducting nanoparticle cellular toxicity. *Small, 2*(10), 1159–1163. https://doi.org/10.1002/smll.200500527

Asharani, P. V., Wu, Y. L., Gong, Z., & Valiyaveettil, S. (2008). Toxicity of silver nanoparticles in zebrafish models. *Nanotechnology, 19*(25), 255102. https://doi.org/10.1088/0957-4484/19/25/255102

Asz, J., Asz, D., Moushey, R., Seigel, J., Mallory, S. B., & Foglia, R. P. (2006). Treatment of toxic epidermal necrolysis in a pediatric patient with a nanocrystalline silver dressing. *Journal of Pediatric Surgery, 41*(12), e9–e12. https://doi.org/10.1016/j.jpedsurg.2006.08.043

Atrián-Blasco, E., Santoro, A., Pountney, D. L., Meloni, G., Hureau, C., & Faller, P. (2017). Chemistry of mammalian metallothioneins and their interaction with amyloidogenic peptides and proteins. *Chemical Society Reviews, 46*(24), 7683–7693. https://doi.org/10.1039/C7CS00448F

Bargelloni, L., Scudiero, R., Parisi, E., Carginale, V., Capasso, C., & Patarnello, T. (1999). Metallothioneins in Antarctic fish: Evidence for independent duplication and gene conversion. *Molecular Biology and Evolution, 16*(7), 885–897. https://doi.org/10.1093/oxfordjournals.molbev.a026178

Barmo, C., Ciacci, C., Canonico, B., Fabbri, R., Cortese, K., Balbi, T., Marcomini, A., Pojana, G., Gallo, G., & Canesi, L. (2013). In vivo effects of n-TiO2 on digestive gland and immune function of the marine bivalve *Mytilus galloprovincialis*. *Aquatic Toxicology, 132–133*, 9–18. https://doi.org/10.1016/j.aquatox.2013.01.014/

Baun, A., Hartmann, N. B., Grieger, K., & Kusk, K. O. (2008). Ecotoxicity of engineered nanoparticles to aquatic invertebrates: A brief review and recommendations for future toxicity testing. *Ecotoxicology, 17*(5), 387–395. https://doi.org/10.1007/s10646-008-0208-y

Benn, T. M., & Westerhoff, P. (2008). Nanoparticle silver released into water from commercially available sock fabrics. *Environmental Science & Technology, 42*(11), 4133–4139. https://doi.org/10.1021/es801501j

Binh, C. T. T., Peterson, C. G., Tong, T., Gray, K. A., Gaillard, J.-F., & Kelly, J. J. (2015). Comparing acute effects of a nano-TiO2 pigment on cosmopolitan freshwater phototrophic microbes using high-throughput screening. *PLoS One, 10*, e0125613. http://dx.doi.org/10.13/journal.pone.0125613

Blickley, T. M., Matson, C. W., Vreeland, W. N., Rittschof, D., Di Giulio, R. T., & McClellan-Green, P. D. (2014). Dietary CdSe/ZnS quantum dot exposure in estuarine fish: Bioavailability, oxidative stress responses, reproduction, and maternal transfer. *Aquatic Toxicology, 148*, 27–39. https://doi.org/10.1016/j.aquatox.2013.12.021

Boran, H., & Ulutas, G. (2016). Genotoxic effects and gene expression changes in larval zebrafish after exposure to ZnCl2 and ZnO nanoparticles. *Diseases of Aquatic Organisms, 117*(3), 205–214. https://doi.org/10.3354/dao02943

Botta, C., Labille, J., Auffan, M., Borschneck, D., Miche, H., Cabié, M., et al. (2011). TiO2-based nanoparticles released in water from commercialized sunscreens in a life-cycle perspective: Structures and quantities. *Environmental Pollution, 159*(6), 1543–1550. https://doi.org/10.1016/j.envpol.2011.03.003

Bracken, W. M., & Klaassen, C. D. (1987). Induction of metallothionein in rat primary hepatocyte cultures: Evidence for direct and indirect induction. *Journal of Toxicology and Environmental Health, Part A Current Issues, 22*(2), 163–174. https://doi.org/10.1080/15287398709531060

Buerki-Thurnherr, T., Xiao, L., Diener, L., Arslan, O., Hirsch, C., Maeder-Althaus, X., et al. (2013). In vitro mechanistic study towards a better understanding of ZnO nanoparticle toxicity. *Nanotoxicology, 7*(4), 402–416. https://doi.org/10.3109/17435390.2012.666575

Buffet, P. E., Amiard-Triquet, C., Dybowska, A., Risso-de Faverney, C., Guibbolini, M., Valsami-Jones, E., & Mouneyrac, C. (2012). Fate of isotopically labeled zinc oxide nanoparticles in sediment and effects on two endobenthic species, the clam Scrobicularia plana and the ragworm Hediste diversicolor. *Ecotoxicology and Environmental Safety, 84*, 191–198. https://doi.org/10.1016/j.ecoenv.2012.07.010

Busch, W., Kühnel, D., Schirmer, K., & Scholz, S. (2010). Tungsten carbide cobalt nanoparticles exert hypoxia-like effects on the gene expression level in human keratinocytes. *BMC Genomics, 11*(1), 65. https://doi.org/10.1186/1471-2164-11-65

Canesi, L., & Corsi, I. (2016). Effects of nanomaterials on marine invertebrates. *Science of the Total Environment, 565*, 933–940. https://doi.org/10.1016/j.scitotenv.2016.01.085

Capasso, C., Carginale, V., Crescenzi, O., Di Maro, D., Spadaccini, R., Temussi, P. A., & Parisi, E. (2005). Structural and functional studies of vertebrate metallothioneins: Cross-talk between domains in the absence of physical contact. *Biochemical Journal, 391*(1), 95–103. https://doi.org/10.1042/BJ20050335

Capdevila, M., Cols, N., Romero-Isart, N., Gonzalez-Duarte, R., Atrian, S., & Gonzalez-Duarte, P. (1997). Recombinant synthesis of mouse Zn3-β and Zn4-α metallothionein 1 domains and characterization of their cadmium (II) binding capacity. *Cellular and Molecular Life Sciences CMLS, 53*(8), 681–688. https://doi.org/10.1007/s000180050088

Capdevila, M., Palacios, O., & Atrian, S. (2010). The Zn-or Cu-thionein character of a metallothionein determines its metal load when synthesized in physiological (metal-unsupplemented) conditions. *Bioinorganic Chemistry and Applications, 2010*. https://doi.org/10.1155/2010/541829

Chae, Y. J., Pham, C. H., Lee, J., Bae, E., Yi, J., & Gu, M. B. (2009). Evaluation of the toxic impact of silver nanoparticles on Japanese medaka (Oryzias latipes). *Aquatic Toxicology, 94*(4), 320–327. https://doi.org/10.1016/j.aquatox.2009.07.019

Chen, D., Zhang, D., Jimmy, C. Y., & Chan, K. M. (2011). Effects of Cu_2O nanoparticle and $CuCl_2$ on zebrafish larvae and a liver cell-line. *Aquatic Toxicology, 105*(3–4), 344–354. https://doi.org/10.1016/j.aquatox.2011.07.005

Chen, J., Liu, M., Zhang, L., Zhang, J., & Jin, L. (2003). Application of nano TiO2 towards polluted water treatment combined with electro-photochemical method. *Water Research, 37*, 3815–3820. https://doi.org/10.1016/s0043-1354(03)00332-4

Chen, S., Han, J., & Liu, Y. (2015). Dual opposing roles of metallothionein overexpression in C57BL/6J mouse pancreatic β-cells. *PLoS One, 10*(9), e0137583. https://doi.org/10.1371/journal.pone.0137583

Chen, X., & Mao, S. S. (2007). Titanium dioxide nanomaterials: Synthesis, properties, modifications, and applications. *Chemical Reviews, 107*(7), 2891–2959. https://doi.org/10.1021/cr0500535

Cho, Y. S., Lee, S. Y., Kim, K. Y., Bang, I. C., Kim, D. S., & Nam, Y. K. (2008). Gene structure and expression of metallothionein during metal exposures in Hemibarbus mylodon. *Ecotoxicology and Environmental Safety, 71*(1), 125–137. https://doi.org/10.1016/j.ecoenv.2007.08.005

Colognato, R., Bonelli, A., Ponti, J., Farina, M., Bergamaschi, E., Sabbioni, E., & Migliore, L. (2008). Comparative genotoxicity of cobalt nanoparticles and ions on human peripheral leukocytes in vitro. *Mutagenesis, 23*(5), 377–382. https://doi.org/10.1093/mutage/gen024

D'Agata, A., Fasulo, S., Dallas, L. J., Fisher, A. S., Maisano, M., Readman, J. W., & Jha, A. N. (2014). Enhanced toxicity of 'bulk' titanium dioxide compared to 'fresh' and 'aged' nano-TiO2 in marine mussels (Mytilus galloprovincialis). *Nanotoxicology, 8*(5), 549–558. https://doi.org/10.3109/17435390.2013.807446

Davis, S. R., & Cousins, R. J. (2000). Metallothionein expression in animals: A physiological perspective on function. *The Journal of Nutrition, 130*(5), 1085–1088. https://doi.org/10.1093/jn/130.5.1085

Della Torre, C., Balbi, T., Grassi, G., Frenzilli, G., Bernardeschi, M., Smerilli, A., et al. (2015). Titanium dioxide nanoparticles modulate the toxicological response to cadmium in the gills of Mytilus galloprovincialis. *Journal of Hazardous Materials, 297*, 92–100. https://doi.org/10.1016/j.jhazmat.2015.04.072

Diniz, M. S., de Matos, A. P., Lourenço, J., Castro, L., Peres, I., Mendonça, E., & Picado, A. (2013). Liver alterations in two freshwater fish species (*Carassius auratus* and *Danio rerio*) following exposure to different TiO2 nanoparticle concentrations. *Microscopy and Microanalysis, 19*, 1131–1140. https://doi.org/10.1017/s1431927613013238

Downward, A. M., Jane, R. T., Polson, M. I., Moore, E. G., & Hartshorn, R. M. (2012). Heterodinuclear ruthenium (II)–cobalt (III) complexes as models for a new approach to selective cancer treatment. *Dalton Transactions, 41*(47), 14425–14432. https://doi.org/10.1039/C2DT31986A

Dumont, E., Johnson, A. C., Keller, V. D., & Williams, R. J. (2015). Nano silver and nano zinc-oxide in surface waters–exposure estimation for Europe at high spatial and temporal resolution. *Environmental Pollution, 196*, 341–349. https://doi.org/10.1016/j.envpol.2014.10.022

Duncan, K. E. R., Ngu, T. T., Chan, J., Salgado, M. T., Merrifield, M. E., & Stillman, M. J. (2006). Peptide folding, metal-binding mechanisms, and binding site structures in metallothioneins. *Experimental Biology and Medicine, 231*(9), 1488–1499. https://doi.org/10.1177/153537020623100907

Eixenberger, J. E., Anders, C. B., Hermann, R. J., Brown, R. J., Reddy, K. M., Punnoose, A., & Wingett, D. G. (2017). Rapid dissolution of ZnO nanoparticles induced by biological buffers significantly impacts cytotoxicity. *Chemical Research in Toxicology, 30*(8), 1641–1651. https://doi.org/10.1021/acs.chemrestox.7b00136

Elahi, N., Kamali, M., & Baghersad, M. H. (2018). Recent biomedical applications of gold nanoparticles: A review. *Talanta, 184*, 537–556. https://doi.org/10.1016/j.talanta.2018.02.088

Falfushynska, H., Filyak, Y., Stoliar, O., & Stoika, R. (2012). Study of interrelations between resistance to cisplatin and composition of low molecular weight thiols in murine leukemia L1210 cell lines. *Studia Biologica, 6*(3), 5–14. https://doi.org/10.30970/sbi.0603.251

Falfushynska, H., Gnatyshyna, L., Fedoruk, O., Mitina, N., Zaichenko, A., Stoliar, O., & Stoika, R. (2015). Hepatic metallothioneins in molecular responses to cobalt, zinc, and their nanoscale polymeric composites in frog *Rana ridibunda*. *Comparative Biochemistry and Physiology Part C: Toxicology & Pharmacology, 172*, 45–56. https://doi.org/10.1016/j.cbpc.2015.04.006

Falfushynska, H., Gnatyshyna, L., Horyn, O., Sokolova, I., & Stoliar, O. (2017). Endocrine and cellular stress effects of zinc oxide nanoparticles and nifedipine in marsh frogs *Pelophylax ridibundus*. *Aquatic Toxicology, 185*, 171–182. https://doi.org/10.1016/j.aquatox.2017.02.009

Falfushynska, H., Gnatyshyna, L., Stoliar, O., Mitina, N., Skorokhoda, T., Filyak, Y., et al. (2012). Evaluation of biotargeting and ecotoxicity of Co^{2+}-containing nanoscale polymeric complex by applying multi-marker approach in bivalve mollusk *Anodonta cygnea*. *Chemosphere, 88*(8), 925–936. https://doi.org/10.1016/j.chemosphere.2012.02.087

Falfushynska, H., Gnatyshyna, L., Turta, O., Stoliar, O., Mitina, N., Zaichenko, A., & Stoika, R. (2014). Responses of hepatic metallothioneins and apoptotic activity in *Carassius auratus gibelio* witness a release of cobalt and zinc from waterborne nanoscale composites. *Comparative Biochemistry and Physiology Part C: Toxicology & Pharmacology, 160*, 66–74. https://doi.org/10.1016/j.cbpc.2013.11.009

Falfushynska, H., Gnatyshyna, L., Yurchak, I., Sokolova, I., & Stoliar, O. (2015). The effects of zinc nanooxide on cellular stress responses of the freshwater mussels *Unio tumidus* are modulated by elevated temperature and organic pollutants. *Aquatic Toxicology, 162*, 82–93. https://doi.org/10.1016/j.aquatox.2015.03.006

Falfushynska, H. I., Gnatyshyna, L. L., Ivanina, A. V., Sokolova, I. M., & Stoliar, O. B. (2018). Detoxification and cellular stress responses of unionid mussels *Unio tumidus* from two cooling ponds to combined nano-ZnO and temperature stress. *Chemosphere, 193*, 1127–1142. https://doi.org/10.1016/j.chemosphere.2017.11.079

Falfushynska, H. I., Gnatyshyna, L. L., Priydun, C. V., Stoliar, O. B., & Nam, Y. K. (2010a). Variability of responses in the crucian carp Carassius carassius from two Ukrainian ponds determined by multi-marker approach. *Ecotoxicology and Environmental Safety, 73*(8), 1896–1906. https://doi.org/10.1016/j.ecoenv.2010.08.029

Falfushynska, H. I., Romanchuk, L. D., & Stoliar, O. B. (2010b). Reactivity of metallothioneins in frog Rana ridibunda treated by copper and zinc ions. *Ukrainian Biochemical Journal, 82*(N3), 31–40. http://nbuv.gov.ua/UJRN/BioChem_2010_82_3_6

Fan, W., Cui, M., Liu, H., Wang, C., Shi, Z., Tan, C., & Yang, X. (2011). Nano-TiO2 enhances the toxicity of copper in natural water to Daphnia magna. *Environmental Pollution, 159*(3), 729–734. https://doi.org/10.1016/j.envpol.2010.11.030

Fan, W., Li, Q., Yang, X., & Zhang, L. (2013). Zn subcellular distribution in liver of goldfish (Carassius auratus) with exposure to zinc oxide nanoparticles and mechanism of hepatic detoxification. *PLoS One, 8*(11), e78123. https://doi.org/10.1371/journal.pone.0078123

Farcasanu, I. C., & Ruta, L. L. (2017). Metallothioneins, Saccharomyces cerevisiae, and heavy metals: A biotechnology triad? In *Old yeasts-new questions*. IntechOpen. https://doi.org/10.5772/intechopen.70340

Federici, G., Shaw, B. J., & Handy, R. D. (2007). Toxicity of titanium dioxide nanoparticles to rainbow trout (*Oncorhynchus mykiss*): Gill injury, oxidative stress, and other physiological effects. *Aquatic Toxicology, 84*, 415–430. https://doi.org/10.1016/j.aquatox.2007.07.009

Figgitt, M., Newson, R., Leslie, I. J., Fisher, J., Ingham, E., & Case, C. P. (2010). The genotoxicity of physiological concentrations of chromium (Cr (III) and Cr (VI)) and cobalt (Co (II)): An in vitro study. *Mutation Research/Fundamental and Molecular Mechanisms of Mutagenesis, 688*(1–2), 53–61. https://doi.org/10.1016/j.mrfmmm.2010.03.008

Gagné, F., André, C., Skirrow, R., Gélinas, M., Auclair, J., Van Aggelen, G., et al. (2012). Toxicity of silver nanoparticles to rainbow trout: A toxicogenomic approach. *Chemosphere, 89*(5), 615–622. https://doi.org/10.1016/j.chemosphere.2012.05.063

Gagné, F., Auclair, J., Fortier, M., Bruneau, A., Fournier, M., Turcotte, P., et al. (2013). Bioavailability and immunotoxicity of silver nanoparticles to the freshwater mussel *Elliptio complanata*. *Journal of Toxicology and Environmental Health, Part A, 76*(13), 767–777. https://doi.org/10.1080/15287394.2013.818602

Gagné, F., Auclair, J., Trépanier, S., Turcotte, P., Pilote, M., & Gagnon, C. (2016). The impact of zinc oxide nanoparticles in freshwater mussels exposed to municipal effluents. *Invertebrate Survival Journal, 13*(1), 281–290. https://doi.org/10.25431/1824-307X/isj.v13i1.281-290

Gagné, F., Auclair, J., Turcotte, P., & Gagnon, C. (2013). Sublethal effects of silver nanoparticles and dissolved silver in freshwater mussels. *Journal of Toxicology and Environmental Health, Part A, 76*(8), 479–490. https://doi.org/10.1080/15287394.2013.779561

Gagné, F., Maysinger, D., André, C., & Blaise, C. (2008). Cytotoxicity of aged cadmium-telluride quantum dots to rainbow trout hepatocytes. *Nanotoxicology, 2*(3), 113–120. https://doi.org/10.1080/17435390802245708

Gaitanaki, C., Pliatska, M., Stathopoulou, K., & Beis, I. (2007). Cu2+ and acute thermal stress induce protective events via the p38-MAPK signalling pathway in the perfused Rana ridibunda heart. *Journal of Experimental Biology, 210*(3), 438–446. https://doi.org/10.1242/jeb.02680

Giese, B., Klaessig, F., Park, B., Kaegi, R., Steinfeldt, M., Wigger, H., et al. (2018). Risks, release and concentrations of engineered nanomaterial in the environment. *Scientific Reports, 8*(1), 1565. https://doi.org/10.1038/s41598-018-19275-4

Gnatyshyna, L., Falfushynska, H., Horyn, O., Khoma, V., Martynyuk, V., Mishchuk, O., et al. (2019). Biochemical responses of freshwater mussel Unio tumidus to titanium oxide nanoparticles, Bisphenol A, and their combination. *Ecotoxicology, 28*(8), 923–937. https://doi.org/10.1007/s10646-019-02090-6

Griffitt, R. J., Hyndman, K., Denslow, N. D., & Barber, D. S. (2008). Comparison of molecular and histological changes in zebrafish gills exposed to metallic nanoparticles. *Toxicological Sciences, 107*(2), 404–415. https://doi.org/10.1093/toxsci/kfn256

Haase, H., & Maret, W. (2004). A differential assay for the reduced and oxidized states of metallothionein and thionein. *Analytical Biochemistry, 333*(1), 19–26. https://doi.org/10.1016/j.ab.2004.04.039

Haase, H., & Maret, W. (2008). Partial oxidation and oxidative polymerization of metallothionein. *Electrophoresis, 29*(20), 4169–4176. https://doi.org/10.1002/elps.200700922

Handy, R. D., Von der Kammer, F., Lead, J. R., Hassellöv, M., Owen, R., & Crane, M. (2008). The ecotoxicology and chemistry of manufactured nanoparticles. *Ecotoxicology, 17*(4), 287–314. https://doi.org/10.1007/s10646-008-0199-8

Hansen, B. H., Rømma, S., Søfteland, L. I., Olsvik, P. A., & Andersen, R. A. (2006). Induction and activity of oxidative stress-related proteins during waterborne Cu-exposure in brown trout (Salmo trutta). *Chemosphere, 65*(10), 1707–1714. https://doi.org/10.1016/j.chemosphere.2006.04.088

Hardman, R. (2005). A toxicologic review of quantum dots: Toxicity depends on physicochemical and environmental factors. *Environmental Health Perspectives, 114*(2), 165–172. https://doi.org/10.1289/ehp.8284

Heger, Z., Angel Merlos Rodrigo, M., Krizkova, S., Ruttkay-Nedecky, B., Zalewska, M., Maria Planells del Pozo, E., et al. (2016). Metallothionein as a scavenger of free radicals-new cardioprotective therapeutic agent or initiator of tumor chemoresistance? *Current Drug Targets, 17*(12), 1438–1451. https://doi.org/10.2174/1389450116666151001113304

Horie, M., Shimizu, K., & Tabei, Y. (2018). Validation of metallothionein, interleukin-8, and heme oxygenase-1 as markers for the evaluation of cytotoxicity caused by metal oxide nanoparticles. *Toxicology Mechanisms and Methods, 28*(8), 630–638. https://doi.org/10.1080/15376516.2018.1486931

Isani, G., & Carpenè, E. (2014). Metallothioneins, unconventional proteins from unconventional animals: A long journey from nematodes to mammals. *Biomolecules, 4*(2), 435–457. https://doi.org/10.3390/biom4020435

Jaskulak, M., Rorat, A., Grobelak, A., Chaabene, Z., Kacprzak, M., & Vandenbulcke, F. (2019). Bioaccumulation, antioxidative response, and metallothionein expression in Lupinus luteus L. exposed to heavy metals and silver nanoparticles. *Environmental Science and Pollution Research, 26*(16), 16040–16052. https://doi.org/10.1007/s11356-019-04972-y

Jayawardena, D. P., Heinemann, I. U., & Stillman, M. J. (2017). Zinc binds non-cooperatively to human liver metallothionein 2a at physiological pH. *Biochemical and Biophysical Research Communications, 493*(1), 650–653. https://doi.org/10.1016/j.bbrc.2017.08.137

Jimeno-Romero, A., Bilbao, E., Izagirre, U., Cajaraville, M. P., Marigómez, I., & Soto, M. (2017). Digestive cell lysosomes as main targets for Ag accumulation and toxicity in marine mussels, Mytilus galloprovincialis, exposed to maltose-stabilised Ag nanoparticles of different sizes. *Nanotoxicology, 11*(2), 168–183. https://doi.org/10.1080/17435390.2017.1279358

Junevičius, J., Žilinskas, J., Česaitis, K., Česaitienė, G., Gleiznys, D., & Maželienė, Ž. (2015). Antimicrobial activity of silver and gold in toothpastes: A comparative analysis. *Stomatologija, 17*(1), 9–12.

Kahru, A., & Dubourguier, H. C. (2010). From ecotoxicology to nanoecotoxicology. *Toxicology, 269*(2–3), 105–119. https://doi.org/10.1016/j.tox.2009.08.016

Khalilova, H. K., Hasanova, S. A., & Aliyev, F. G. (2018). Photocatalytic removal of organic pollutants from industrial wastewater using TiO2 catalyst. *Journal of Environmental Protection, 9*, 691–698. https://di.oorg/10.4236/jep.2018.96043

Khan, I., Saeed, K., & Khan, I. (2019). Nanoparticles: Properties, applications and toxicities. *Arabian Journal of Chemistry, 12*(7), 908–931. https://doi.org/10.1016/j.arabjc.2017.05.011

Khene, L., Berrebbah, H., Yahyaoui, A., Bouarroudj, T., Zouainia, S., Kahli, H., & Bourayou, C. (2017). Biomarkers of oxidative stress, lipid peroxidation and ROS production induced by TiO$_2$ microparticles on snails. *Helix aspersa. Studia Universitatis "Vasile Goldiş", 27*, 127–133.

Kim, J. H., Bae, S. N., Lee, C. W., Song, M. J., Lee, S. J., Yoon, J. H., et al. (2011). A pilot study to investigate the treatment of cervical human papillomavirus infection with zinc-citrate compound (CIZAR®). *Gynecologic Oncology, 122*(2), 303–306. https://doi.org/10.1016/j.ygyno.2011.04.026

Kim, K. T., Klaine, S. J., Cho, J., Kim, S. H., & Kim, S. D. (2010). Oxidative stress responses of Daphnia magna exposed to TiO2 nanoparticles according to size fraction. *Science of the Total Environment, 408*(10), 2268–2272. https://doi.org/10.1016/j.scitotenv.2010.01.041

Kim, S., Choi, J. E., Choi, J., Chung, K. H., Park, K., Yi, J., & Ryu, D. Y. (2009). Oxidative stress-dependent toxicity of silver nanoparticles in human hepatoma cells. *Toxicology In Vitro, 23*(6), 1076–1084. https://doi.org/10.1016/j.tiv.2009.06.001

King-Heiden, T. C., Wiecinski, P. N., Mangham, A. N., Metz, K. M., Nesbit, D., Pedersen, J. A., et al. (2009). Quantum dot nanotoxicity assessment using the zebrafish embryo. *Environmental Science & Technology, 43*(5), 1605–1611. https://doi.org/10.1021/es801925c

Klaine, S. J., Alvarez, P. J., Batley, G. E., Fernandes, T. F., Handy, R. D., Lyon, D. Y., et al. (2008). Nanomaterials in the environment: Behavior, fate, bioavailability, and effects. *Environmental Toxicology and Chemistry, 27*(9), 1825–1851. https://doi.org/10.1897/08-090.1

Klębowski, B., Depciuch, J., Parlińska-Wojtan, M., & Baran, J. (2018). Applications of noble metal-based nanoparticles in medicine. *International Journal of Molecular Sciences, 19*(12), 4031. https://doi.org/10.3390/ijms19124031

Kobayashi, M., & Shimizu, S. (1999). Cobalt proteins. *European Journal of Biochemistry, 261*(1), 1–9. https://doi.org/10.1046/j.1432-1327.1999.00186.x

Krężel, A., & Maret, W. (2007). Different redox states of metallothionein/thionein in biological tissue. *Biochemical Journal, 402*(3), 551–558. https://doi.org/10.1042/BJ20061044

Krężel, A., & Maret, W. (2016). The biological inorganic chemistry of zinc ions. *Archives of Biochemistry and Biophysics, 611*, 3–19. https://doi.org/10.1016/j.abb.2016.04.010

Krężel, A., & Maret, W. (2017). The functions of metamorphic metallothioneins in zinc and copper metabolism. *International Journal of Molecular Sciences, 18*(6), 1237. https://doi.org/10.3390/ijms18061237

Krizkova, S., Ryvolova, M., Hrabeta, J., Adam, V., Stiborova, M., Eckschlager, T., & Kizek, R. (2012). Metallothioneins and zinc in cancer diagnosis and therapy. *Drug Metabolism Reviews, 44*(4), 287–301. https://doi.org/10.3109/03602532.2012.725414

Kubrak, O. I., Husak, V. V., Rovenko, B. M., Storey, J. M., Storey, K. B., & Lushchak, V. I. (2011). Cobalt-induced oxidative stress in brain, liver and kidney of goldfish Carassius auratus. *Chemosphere, 85*(6), 983–989. https://doi.org/10.1016/j.chemosphere.2011.06.078

Landa, P., Prerostova, S., Petrova, S., Knirsch, V., Vankova, R., & Vanek, T. (2015). The transcriptomic response of Arabidopsis thaliana to zinc oxide: A comparison of the impact of nanoparticle, bulk, and ionic zinc. *Environmental Science & Technology, 49*(24), 14537–14545. https://doi.org/10.1021/acs.est.5b03330

Langton, D. J., Sidaginamale, R. P., Joyce, T. J., Natu, S., Blain, P., Jefferson, R. D., et al. (2013). The clinical implications of elevated blood metal ion concentrations in asymptomatic patients with MoM hip resurfacings: A cohort study. *BMJ Open, 3*(3), e001541. https://doi.org/10.1136/bmjopen-2012-001541

Lin, C. H., Chang, L. W., Chang, H., Yang, M. H., Yang, C. S., Lai, W. H., et al. (2009). The chemical fate of the Cd/Se/Te-based quantum dot 705 in the biological system: Toxicity implications. *Nanotechnology, 20*(21), 215101. https://doi.org/10.1088/0957-4484/20/21/215101

Luther, E. M., Schmidt, M. M., Diendorf, J., Epple, M., & Dringen, R. (2012). Upregulation of metallothioneins after exposure of cultured primary astrocytes to silver nanoparticles. *Neurochemical Research, 37*(8), 1639–1648. https://doi.org/10.1007/s11064-012-0767-4

Magdolenova, Z., Collins, A., Kumar, A., Dhawan, A., Stone, V., & Dusinska, M. (2014). Mechanisms of genotoxicity. A review of in vitro and in vivo studies with engineered nanoparticles. *Nanotoxicology, 8*(3), 233–278. https://doi.org/10.3109/17435390.2013.773464

Mahaye, N., Thwala, M., Cowan, D. A., & Musee, N. (2017). Genotoxicity of metal based engineered nanoparticles in aquatic organisms: A review. *Mutation Research/Reviews in Mutation Research, 773*, 134–160. https://doi.org/10.1016/j.mrrev.2017.05.004

Manke, A., Wang, L., & Rojanasakul, Y. (2013). Mechanisms of nanoparticle-induced oxidative stress and toxicity. *BioMed Research International, 1*, 1–15. https://doi.org/10.1155/2013/942916

Maret, W. (2017). Zinc in cellular regulation: The nature and significance of "zinc signals". *International Journal of Molecular Sciences, 18*(11), 2285. https://doi.org/10.3390/ijms18112285

Margoshes, M., & Vallee, B. L. (1957). A cadmium protein from equine kidney cortex. *Journal of the American Chemical Society, 79*(17), 4813–4814. https://doi.org/10.1021/ja01574a064

Marie, V., Gonzalez, P., Baudrimont, M., Boutet, I., Moraga, D., Bourdineaud, J. P., & Boudou, A. (2006). Metallothionein gene expression and protein levels in triploid and diploid oysters Crassostrea gigas after exposure to cadmium and zinc. *Environmental Toxicology and Chemistry: An International Journal, 25*(2), 412–418. https://doi.org/10.1897/05-114R.1

Mauricio, M. D., Guerra-Ojeda, S., Marchio, P., Valles, S. L., Aldasoro, M., Escribano-Lopez, I., et al. (2018). Nanoparticles in medicine: A focus on vascular oxidative stress. *Oxidative Medicine and Cellular Longevity, 2018*. https://doi.org/10.1155/2018/6231482

McGee, H. M., Woods, G. M., Bennett, B., & Chung, R. S. (2010). The two faces of metallothionein in carcinogenesis: Photoprotection against UVR-induced cancer and promotion of tumour survival. *Photochemical & Photobiological Sciences, 9*(4), 586–596. https://doi.org/10.1002/mc.22846

Meyer, J. N., Lord, C. A., Yang, X. Y., Turner, E. A., Badireddy, A. R., Marinakos, S. M., et al. (2010). Intracellular uptake and associated toxicity of silver nanoparticles in Caenorhabditis elegans. *Aquatic Toxicology, 100*(2), 140–150. https://doi.org/10.1016/j.aquatox.2010.07.016

Miao, X., Wang, Y., Sun, J., Sun, W., Tan, Y., Cai, L., et al. (2013). Zinc protects against diabetes-induced pathogenic changes in the aorta: Roles of metallothionein and nuclear factor (erythroid-derived 2)-like 2. *Cardiovascular Diabetology, 12*(1), 54. https://doi.org/10.1186/1475-2840-12-54

Moos, P. J., Olszewski, K., Honeggar, M., Cassidy, P., Leachman, S., Woessner, D., et al. (2011). Responses of human cells to ZnO nanoparticles: A gene transcription study. *Metallomics, 3*(11), 1199–1211. https://doi.org/10.1039/c1mt00061f

Mouneyrac, C., Amiard-Triquet, C., Amiard, J. C., & Rainbow, P. S. (2001). Comparison of metallothionein concentrations and tissue distribution of trace metals in crabs (Pachygrapsus marmoratus) from a metal-rich estuary, in and out of the reproductive season. *Comparative Biochemistry and Physiology Part C: Toxicology & Pharmacology, 129*(3), 193–209. https://doi.org/10.1016/S1532-0456(01)00193-4

Münger, K., Germann, U. A., Beltramini, M., Niedermann, D., Baitella-Eberle, G., Kägi, J. H., & Lerch, K. (1985). (Cu, Zn)-metallothioneins from fetal bovine liver. Chemical and spectroscopic properties. *Journal of Biological Chemistry, 260*(18), 10032–10038.

Murata, M., Gong, P., Suzuki, K., & Koizumi, S. (1999). Differential metal response and regulation of human heavy metal-inducible genes. *Journal of Cellular Physiology, 180*(1), 105–113. https://doi.org/10.1002/(SICI)1097-4652(199907)180:1<105::AID-JCP12>3.0.CO;2-5

Naasz, S., Altenburger, R., & Kühnel, D. (2018). Environmental mixtures of nanomaterials and chemicals: The Trojan-horse phenomenon and its relevance for ecotoxicity. *Science of the Total Environment, 635*, 1170–1181. https://doi.org/10.1016/j.scitotenv.2018.04.180

Navarro, E., Baun, A., Behra, R., Hartmann, N. B., Filser, J., Miao, A. J., et al. (2008). Environmental behavior and ecotoxicity of engineered nanoparticles to algae, plants, and fungi. *Ecotoxicology, 17*(5), 372–386. https://doi.org/10.1007/s10646-008-0214-0

Ngu, T. T., & Stillman, M. J. (2009). Metalation of metallothioneins. *IUBMB Life, 61*(4), 438–446. https://doi.org/10.1002/iub.182

Ni, T. W., Staicu, L. C., Nemeth, R. S., Schwartz, C. L., Crawford, D., Seligman, J. D., et al. (2015). Progress toward clonable inorganic nanoparticles. *Nanoscale, 7*(41), 17320–17327. https://doi.org/10.1039/C5NR04097C

Onosaka, S., & Cherian, M. G. (1982). Comparison of metallothionein determination by polarographic and cadmium-saturation methods. *Toxicology and Applied Pharmacology, 63*(2), 270–274. https://doi.org/10.1016/0041-008X(82)90049-7

Outten, C. E., & O'Halloran, T. V. (2001). Femtomolar sensitivity of metalloregulatory proteins controlling zinc homeostasis. *Science, 292*(5526), 2488–2492. https://doi.org/10.1126/science.1060331

Overnell, J., Good, M., & Vašàk, M. (1988). Spectroscopic studies on cadmium (II)-and cobalt (II)-substituted metallothionein from the crab Cancer pagurus: Evidence for one additional low-affinity metal-binding site. *European Journal of Biochemistry, 172*(1), 171–177. https://doi.org/10.1111/j.1432-1033.1988.tb13869.x

Pan, J. F., Buffet, P. E., Poirier, L., Amiard-Triquet, C., Gilliland, D., Joubert, Y., et al. (2012). Size dependent bioaccumulation and ecotoxicity of gold nanoparticles in an endobenthic invertebrate: The Tellinid clam Scrobicularia plana. *Environmental Pollution, 168*, 37–43. https://doi.org/10.1016/j.envpol.2012.03.051

Parambil, A. M., Puttaiahgowda, Y. M., & Shankarappa, P. (2012). Copolymerization of N-vinyl pyrrolidone with methyl methacrylate by Ti (III)-DMG redox initiator. *Turkish Journal of Chemistry, 36*(3), 397–409. https://doi.org/10.3906/kim-1111-21

Penkowa, M. (2006). Metallothioneins are multipurpose neuroprotectants during brain pathology. *The FEBS Journal, 273*(9), 1857–1870. https://doi.org/10.1111/j.1742-4658.2006.05207.x

Peyrot, C., Gagnon, C., Gagné, F., Willkinson, K. J., Turcotte, P., & Sauvé, S. (2009). Effects of cadmium telluride quantum dots on cadmium bioaccumulation and metallothionein production to the freshwater mussel, *Elliptio complanata*. *Comparative Biochemistry and Physiology, Part C, 150*(2), 246–251. https://doi.org/10.1016/j.cbpc.2009.05.002

Piotrowski, J. K., & Szymańska, J. A. (1976). Influence of certain metals on the level of metallothionein-like proteins in the liver and kidneys of rats. *Journal of Toxicology and Environmental Health, Part A Current Issues, 1*(6), 991–1002. https://doi.org/10.1080/15287397609529402

Ranjan, S., Dasgupta, N., Sudandiradoss, C., Ramalingam, C., & Kumar, A. (2018). Titanium dioxide nanoparticle–protein interaction explained by docking approach. *International Journal of Nanomedicine, 13*(T-NANO 2014 Abstracts), 47. https://doi.org/10.2147/IJN.S125008

Raz, S. R., Leontaridou, M., Bremer, M. G., Peters, R., & Weigel, S. (2012). Development of surface plasmon resonance-based sensor for detection of silver nanoparticles in food and the environment. *Analytical and Bioanalytical Chemistry, 403*(10), 2843–2850. https://doi.org/10.1007/s00216-012-5920-z

Reeves, J. F., Davies, S. J., Dodd, N. J., & Jha, A. N. (2008). Hydroxyl radicals (OH) are associated with titanium dioxide (TiO2) nanoparticle-induced cytotoxicity and oxidative DNA damage in fish cells. *Mutation Research, 640*, 113–122. https://doi.org/10.1016/j.mrfmmm.2007.12.010

Rhee, J. S., Raisuddin, S., Hwang, D. S., Lee, K. W., Kim, I. C., & Lee, J. S. (2009). Differential expression of metallothionein (MT) gene by trace metals and endocrine-disrupting chemicals in the hermaphroditic mangrove killifish, Kryptolebias marmoratus. *Ecotoxicology and Environmental Safety, 72*(1), 206–212. https://doi.org/10.1016/j.ecoenv.2008.06.001

Ringwood, A. H., McCarthy, M., Bates, T. C., & Carroll, D. L. (2010). The effects of silver nanoparticles on oyster embryos. *Marine Environmental Research, 69*, S49–S51. https://doi.org/10.1016/j.marenvres.2009.10.011

Rosenberg, D. W., & Kappas, A. (1989). Trace metal interactions in vivo: Inorganic cobalt enhances urinary copper excretion without producing an associated zincuresis in rats. *The Journal of Nutrition, 119*(9), 1259–1268. https://doi.org/10.1093/jn/119.9.1259

Rozes, L., Steunou, N., Fornasieri, G., & Sanchez, C. (2006). Titanium-oxo clusters, versatile nanobuilding blocks for the design of advanced hybrid materials. *Monatshefte für Chemie/ Chemical Monthly, 137*(5), 501–528. https://doi.org/10.1007/s00706-006-0464-6

Rubino, F. (2015). Toxicity of glutathione-binding metals: A review of targets and mechanisms. *Toxics, 3*(1), 20–62. https://doi.org/10.3390/toxics3010020

Saito, S., & Hunziker, P. E. (1996). Differential sensitivity of metallothionein-1 and -2 in liver of zinc-injected rat toward proteolysis. *Biochimica et Biophysica Acta, General Subjects, 1289*, 65–70.

Schilling, K., Bradford, B., Castelli, D., Dufour, E., Nash, J. F., Pape, W., et al. (2010). Human safety review of "nano" titanium dioxide and zinc oxide. *Photochemical & Photobiological Sciences, 9*(4), 495–509. https://doi.org/10.1039/B9PP00180H

Schins, R. P. (2002). Mechanisms of genotoxicity of particles and fibers. *Inhalation Toxicology, 14*(1), 57–78. https://doi.org/10.1080/089583701753338631

Senapati, V. A., & Kumar, A. (2018). ZnO nanoparticles dissolution, penetration and toxicity in human epidermal cells. Influence of pH. *Environmental Chemistry Letters, 16*(3), 1129–1135. https://doi.org/10.1007/s10311-018-0736-5

Sharma, S., & Ebadi, M. (2014). The Charnoly body as a universal biomarker of cell injury. *Biomarkers and Genomic Medicine, 6*(3), 89–98. https://doi.org/10.1016/j.bgm.2014.03.004

Sharma, S., Rais, A., Sandhu, R., Nel, W., & Ebadi, M. (2013). Clinical significance of metallothioneins in cell therapy and nanomedicine. *International Journal of Nanomedicine, 8*, 1477. https://doi.org/10.2147/IJN.S42019

Si, M., & Lang, J. (2018). The roles of metallothioneins in carcinogenesis. *Journal of Hematology & Oncology, 11*(1), 107. https://doi.org/10.1186/s13045-018-0645-x

Simonsen, L. O., Harbak, H., & Bennekou, P. (2012). Cobalt metabolism and toxicology—A brief update. *Science of the Total Environment, 432*, 210–215. https://doi.org/10.1016/j.scitotenv.2012.06.009

Singla, R., Guliani, A., Kumari, A., & Yadav, S. K. (2016). Metallic nanoparticles, toxicity issues and applications in medicine. In *Nanoscale materials in targeted drug delivery, theragnosis and tissue regeneration* (pp. 41–80). Springer. https://doi.org/10.1007/978-981-10-0818-4_3

Sokolova, I. M., & Lannig, G. (2008). Interactive effects of metal pollution and temperature on metabolism in aquatic ectotherms: Implications of global climate change. *Climate Research, 37*(2–3), 181–201. https://doi.org/10.3354/cr00764

Stohs, S. J., & Bagchi, D. (1995). Oxidative mechanisms in the toxicity of metal ions. *Free Radical Biology and Medicine, 18*(2), 321–336. https://doi.org/10.1016/0891-5849(94)00159-H

Sun, T. Y., Mitrano, D. M., Bornhöft, N. A., Scheringer, M., Hungerbühler, K., & Nowack, B. (2017). Envisioning nano release dynamics in a changing world: Using dynamic probabilistic modeling to assess future environmental emissions of engineered nanomaterials. *Environmental Science & Technology, 51*(5), 2854–2863. https://doi.org/10.1021/acs.est.6b05702

Sureda, A., Capó, X., Busquets-Cortés, C., & Tejada, S. (2018). Acute exposure to sunscreen containing titanium induces an adaptive response and oxidative stress in Mytillus galloprovincialis. *Ecotoxicology and Environmental Safety, 149*, 58–63. https://doi.org/10.1016/j.ecoenv.2017.11.014

Sutherland, D. E., & Stillman, M. J. (2014). Challenging conventional wisdom: Single domain metallothioneins. *Metallomics, 6*(4), 702–728. https://doi.org/10.1039/C3MT00216K

Sutherland, D. E., Summers, K. L., & Stillman, M. J. (2012). Noncooperative metalation of metallothionein 1A and its isolated domains with zinc. *Biochemistry, 51*(33), 6690–6700. https://doi.org/10.1021/bi3004523

Tan, C., & Wang, W. X. (2014). Modification of metal bioaccumulation and toxicity in Daphnia magna by titanium dioxide nanoparticles. *Environmental Pollution, 186*, 36–42. https://doi.org/10.1016/j.envpol.2013.11.015

Tmejova, K., Hynek, D., Kopel, P., Gumulec, J., Krizkova, S., Guran, R., et al. (2015). Structural effects and nanoparticle size are essential for quantum dots–metallothionein complex formation. *Colloids and Surfaces B: Biointerfaces, 134*, 262–272. https://doi.org/10.1016/j.colsurfb.2015.06.045

Unfried, K., Albrecht, C., Klotz, L. O., Von Mikecz, A., Grether-Beck, S., & Schins, R. P. (2007). Cellular responses to nanoparticles: Target structures and mechanisms. *Nanotoxicology, 1*(1), 52–71. https://doi.org/10.1080/00222930701314932

Unrine, J. M., Tsyusko, O. V., Hunyadi, S. E., Judy, J. D., & Bertsch, P. M. (2010). Effects of particle size on chemical speciation and bioavailability of copper to earthworms (Eisenia fetida) exposed to copper nanoparticles. *Journal of Environmental Quality, 39*(6), 1942–1953. https://doi.org/10.2134/jeq2009.0387

Vale, G., Mehennaoui, K., Cambier, S., Libralato, G., Jomini, S., & Domingos, R. F. (2016). Manufactured nanoparticles in the aquatic environment-biochemical responses on freshwater organisms: A critical overview. *Aquatic Toxicology, 170*, 162–174. https://doi.org/10.1016/j.aquatox.2015.11.019

Valko, M., Rhodes, C., Moncol, J., Izakovic, M. M., & Mazur, M. (2006). Free radicals, metals and antioxidants in oxidative stress-induced cancer. *Chemico-Biological Interactions, 160*(1), 1–40. https://doi.org/10.1016/j.cbi.2005.12.009

Valko, M. M. H. C. M., Morris, H., & Cronin, M. T. D. (2005). Metals, toxicity and oxidative stress. *Current Medicinal Chemistry, 12*(10), 1161–1208. https://doi.org/10.2174/0929867053764635

Vasak, M., & Kägi, J. H. (1981). Metal thiolate clusters in cobalt (II)-metallothionein. *Proceedings of the National Academy of Sciences, 78*(11), 6709–6713. https://doi.org/10.1073/pnas.78.11.6709

Vergani, L., Grattarola, M., Borghi, C., Dondero, F., & Viarengo, A. (2005). Fish and molluscan metallothioneins: A structural and functional comparison. *The FEBS Journal, 272*(23), 6014–6023. https://doi.org/10.1111/j.1742-4658.2005.04993.x

Viarengo, A., Burlando, B., Dondero, F., Marro, A., & Fabbri, R. (1999). Metallothionein as a tool in biomonitoring programmes. *Biomarkers, 4*(6), 455–466. https://doi.org/10.1080/135475099230615

Viarengo, A., Lowe, D., Bolognesi, C., Fabbri, E., & Koehler, A. (2007). The use of biomarkers in biomonitoring: A 2-tier approach assessing the level of pollutant-induced stress syndrome in sentinel organisms. *Comparative Biochemistry and Physiology Part C: Toxicology & Pharmacology, 146*(3), 281–300. https://doi.org/10.1016/j.cbpc.2007.04.011

Wang, J., Hou, Y., & Ma, J. (2013). Titanium(IV) intake by apotransferrin. In R. H. Kretsinger, V. N. Uversky, & E. A. Permyakov (Eds.), *Encyclopedia of metalloproteins* (pp. 81–89). Springer. https://doi.org/10.1007/978-1-4614-1533-6_200033

Wesselkamper, S. C., Chen, L. C., & Gordon, T. (2001). Development of pulmonary tolerance in mice exposed to zinc oxide fumes. *Toxicological Sciences, 60*(1), 144–151. https://doi.org/10.1093/toxsci/60.1.144

Wu, S. M., Da Zheng, Y., & Kuo, C. H. (2008). Expression of mt2 and smt-B upon cadmium exposure and cold shock in zebrafish (Danio rerio). *Comparative Biochemistry and Physiology Part C: Toxicology & Pharmacology, 148*(2), 184–193. https://doi.org/10.1016/j.cbpc.2008.05.007

Xin-Yu, H. E., Bing, W. A. N. G., Yang-Yang, Z. H. O. U., Xiao-Jun, B. I. A. N., & Juan, Y. A. N. (2018). Enrichment and identification of metallothionein by functionalized nanomagnetic particles and matrix assisted laser desorption ionization time-of-flight mass spectrometry. *Chinese Journal of Analytical Chemistry, 46*(7), 1069–1076. https://doi.org/10.1016/S1872-2040(18)61096-5

Xiong, Y., Washio, I., Chen, J., Cai, H., Li, Z. Y., & Xia, Y. (2006). Poly (vinyl pyrrolidone): A dual functional reductant and stabilizer for the facile synthesis of noble metal nanoplates in aqueous solutions. *Langmuir, 22*(20), 8563–8570. https://doi.org/10.1021/la061323x

Yang, J. J., Cheng, H., & Frost, R. L. (2011). Synthesis and characterisation of cobalt hydroxy carbonate Co2CO3 (OH) 2 nanomaterials. *Spectrochimica Acta Part A: Molecular and Biomolecular Spectroscopy, 78*(1), 420–428. https://doi.org/10.1016/j.saa.2010.11.004

Yang, Y., Qin, Z., Zeng, W., Yang, T., Cao, Y., Mei, C., & Kuang, Y. (2017). Toxicity assessment of nanoparticles in various systems and organs. *Nanotechnology Reviews, 6*(3), 279–289.

Yu, S. J., Yin, Y. G., & Liu, J. F. (2013). Silver nanoparticles in the environment. *Environmental Science: Processes & Impacts, 15*(1), 78–92. https://doi.org/10.1039/C2EM30595J

Zafarullah, M., Bonham, K., & Gedamu, L. (1988). Structure of the rainbow trout metallothionein B gene and characterization of its metal-responsive region. *Molecular and Cellular Biology, 8*(10), 4469–4476. https://doi.org/10.1128/MCB.8.10.4469

Zhang, C., Lohwacharin, J., & Takizawa, S. (2017). Properties of residual titanium dioxide nanoparticles after extended periods of mixing and settling in synthetic and natural waters. *Scientific Reports, 7*(1), 9943. https://doi.org/10.1038/s41598-017-09699-9

Zhang, W., Rosano-Ortega, G., Hu, Y., Bai, L., & Qin, L. (2012). New investigation in PVP-mediated synthesis of noble metallic nanomaterials. *Journal of Nanoscience and Nanotechnology, 12*(3), 2634–2639. https://doi.org/10.1166/jnn.2012.5800

Zhang, Y., Hao, J., Xu, X., Chen, X., & Wang, J.-H. (2019). Protein Corona-triggered catalytic inhibition of insufficient POSS polymer-caged gold nanoparticles for sensitive colorimetric detection of Metallothioneins. *Analytical Chemistry*, s1–s13. https://doi.org/10.1021/acs.analchem.9b04593

Ziller, A., & Fraissinet-Tachet, L. (2018). Metallothionein diversity and distribution in the tree of life: A multifunctional protein. *Metallomics, 10*(11), 1549–1559. https://doi.org/10.1039/C8MT00165K

Zorita, I., Strogyloudi, E., Buxens, A., Mazon, L. I., Papathanassiou, E., Soto, M., & Cajaraville, M. P. (2005). Application of two SH-based methods for metallothionein determination in mussels and intercalibration of the spectrophotometric method: Laboratory and field studies in the Mediterranean Sea. *Biomarkers, 10*(5), 342–359. https://doi.org/10.1080/13547500500264645

Environmental Nanoparticles: Focus on Multipollutant Strategy for Environmental Quality and Health Risk Estimations

Tatiana Borisova

1 Rationale: Environmental Pollution and Health Hazard

Pollution is the largest environmental cause of disease and premature deaths in the world. Diseases caused by environmental pollution were responsible for estimated 16% (9 million premature deaths in 2015) of all deaths worldwide. This number of deaths is threefold more than a combined death number caused by AIDS, tuberculosis, and malaria. Importantly, low-dose exposures of children to pollutants can result in disability, disease, and even death, and so children are at high risk of pollution-related health hazard. In the most severely polluted countries, the environment pollution might be responsible for diseases resulted in more than one death in four. However, despite significant effects of pollution on human health, this fact has been neglected, especially in low- and middle-income countries. Moreover, it is considered that the health effects related to pollution are underestimated. Pollution not only jeopardizes public health and abolishes ecosystems, it is closely linked to global climate change (Landrigan et al., 2018; Borisova, 2018).

Environmental pollution is getting worse in many territories worldwide. Pollution of ambient air, chemical and soil pollution produced by industry, mining, electricity generation, mechanized agriculture, and petroleum-powered vehicles are increased, especially in rapidly developing and industrialized countries with low- and middle-sized income (Landrigan et al., 2018; Borisova, 2018).

The Lancet Commission recommended to establish special systems for monitoring pollution and its effects on health. New technologies, such as satellite imaging and data mining, widely used in pollution monitoring may increase its efficiency and drive changes in pollution policy. It was recommended that the pollution-related research should: (1) reveal causal links between pollution, disease, and subclinical

T. Borisova (✉)

Palladin Institute of Biochemistry, National Academy of Sciences of Ukraine, Kyiv, Ukraine
e-mail: tborisov@biochem.kiev.ua

impairment, for example, between air pollution and dysfunction of the central nervous system in children and the elder people; (2) estimate the global burden of disease associated with known chemical pollutants (lead, mercury, copper, chromium, arsenic, asbestos, benzene, others); (3) characterize the adverse health outcomes (e.g. developmental neurotoxicity or endocrine disruption) caused by chemical pollutants (novel insecticides, chemical herbicides, and pharmaceutical wastes) (Landrigan et al., 2018). Detailed analysis of health effects of different pollutants should improve prognosis of health risks as well as strategy of health protection.

2   Environmental Air Pollution Particulate Matter

Among the "classical" environmental pollutants, heavy metals, persistent organic pollutants, harmful gaseous compounds, pollution-associated particles are of special attention to the environmental scientists with regard to the health impact these particles create. The particulate matter of air pollution is a global problem since it can move across borders of countries, oceans and continents (Jiang et al., 2015; Zhang et al., 2017).

During evolution and in modern life, humans are permanently exposed to environmentally derived particles, for example, components of volcanic ash during eruptions, dust storms, and particles from disasters, other natural processes, and space (Fig. 1). The nanoparticles from the eruptions of volcanoes and volcanic ash possess toxic effects. Both acute and chronic health effects of the volcanic ash
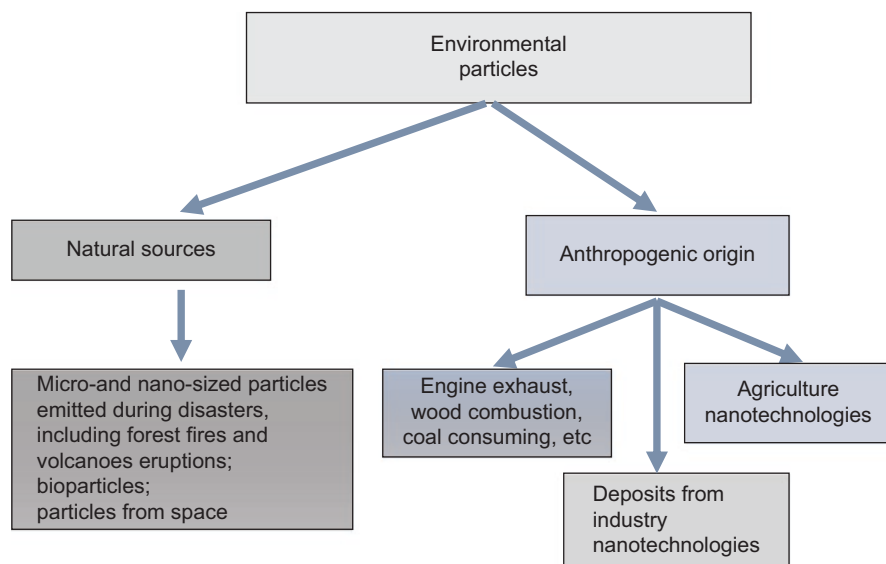
Fig. 1 Origin of environmental air pollution particles

depend upon the size, mineralogical composition and the surface physicochemical properties of ash particles. These characteristics vary between different volcanoes, and even in the eruptions of the same volcano. The acute respiratory symptoms incidences, such as asthma and bronchitis, varied after ash falls from very few reported cases to population outbreaks of asthma. Patients with the pre-existing lung diseases, including asthma, are at augmented risk symptoms after falls of fine ash (Horwell & Baxter, 2006). A long-term silicosis hazard has been identified; however, additional and a more systematic study is required (Horwell & Baxter, 2006). Using different volcanic ash preparations, an increase in excitatory neurotransmitter glutamate binding to isolated brain nerve terminals in low sodium media and at low temperature was demonstrated in the in vitro experiments. The capability to increase glutamate binding to the brain nerve terminals can be explained by specific sharp angles of particles in the volcanic ash preparation. In human organisms, this feature of the volcanic ash can lead to changes in the extracellular level of the neurotransmitter in the synaptic cleft and extracellular glutamate homeostasis in a whole. Simultaneously, the plasma membrane potential of nerve terminal and synaptic vesicle acidification remained unchanged in presence of the volcanic ash preparations (Pozdnyakova et al., 2017).

It should be noted that the microorganisms (bacteria, archaea, algae, and fungi), fungal spores, pollen, viruses, different biological fragments can act themselves as the aerosol bioparticles. Aerosol bioparticle sizes vary for viruses between 0.05 and 0.15μm, for bacteria 0.1–4.0μm, for fungal spores 0.5–15.0μm, and for pollen 10–30μm (Després et al., 2012). The concentrations of the aerosol bioparticles depend on their location and season, and as a part of total global aerosol mass they are consisted of ~25% (Jaenicke, 2005; Lang-Yona et al., 2012).

The environmental particles can also originate from the anthropogenic activity, where smoke from wood, coal and waste combustion, engine exhaust, industry waste deposites and nanotechnologies augmente air pollution with particulate matter (Fig. 1). Wood and biomass burning contribute to organic carbon in Europe region by approximately 30–75% (Gilardoni et al., 2016). Besides, wood combustion for heating of individual houses is in use in developed (Fuzzi et al., 2015), and especially in the undeveloped countries. Chemical and physical features of the organic combustion particles vary in dependence on the precursor materials and burning conditions (Gilardoni et al., 2016; Fuzzi et al., 2015).

Use of modern agriculture technologies leads to the production of various nanoparticles of different composition that, in turn, contribute to air pollution. Precision farming techniques based on accurate material delivery to the plants to increase plant capability to absorb nutrients and detection of plant disease, etc. are developed, and in those technologies, the nanoparticles are used (Singh et al., 2015; Duhan et al., 2017). Conventional fertilizers, pesticides and herbicides encapsulated in the nanoparticle form provide a dosage release of agrochemicals to the plants (Singh et al., 2015; Duhan et al., 2017). Therefore, it is crucial to be aware regarding dust-forming capability and biodegradation cycle of nanoparticles from the agriculture technologies.

The increasing amount of nanoparticles' production, potential of their release into the environment, and their effects on the ecosystem and human health have become a great problem. The engineered nanomaterials enter the environment through the atmospheric emissions and solid/liquid waste streams from production facilities. The paints, fabrics, personal health care products, sunscreens, cosmetics containing nanomaterials enter the environment directly during usage of these products (Ray et al., 2009). The emitted nanomaterials deposit on land and in water, and can also form the dust. After reaching the land, the nanoparticles can contaminate soil, and then migrate into the surface and ground waters (Ray et al., 2009; Tranvik, 2018). Due to their small size, the engineered nanoparticles can be transferred to the air pollution particulate matter. These nanoparticles can agglomerate into larger particles and longer fiber chains and vice versa that, in turn, can change their physical and chemical properties, as well as their behavior in both indoor and outdoor environments and also their potential entry into the human body with subsequent health effects (Ray et al., 2009).

3   Health Threats from Nano-sized Environmentally Derived Air Pollution Particulate Matter

The emission of fine particles (PM2.5, the particulate matter the size of which is less than 2.5μm) into the atmosphere establishes serious problems to human health and is accompanied with growing amount of deaths associated with air pollution (Landrigan et al., 2018; Hata et al., 2014; Pope et al., 2011; Lelieveld et al., 2015). Minuscule size of nanoparticles, smaller than cells and cellular organelles, is the key to understand their toxicity and it allows them to penetrate into basic biological structures, thereby disrupting their normal functioning (Buzea et al., 2007). Toxicology knowledge of "bulk" materials could not precisely predict toxic properties of particles, and so detailed study on nanotoxicity is necessary (Buzea et al., 2007; Borysov et al., 2014; Pozdnyakova et al., 2016, 2017). Human hazard associated with exposure to toxic particles can be reduced by identifying their exposure pathways and mechanisms of their effects in human organism.

Air pollution with PM2.5 is associated with cardiovascular and pulmonary diseases, asthma attacks, increase in rates of lung cancer and premature death (Valavanidis et al., 2008; Kelly & Fussell, 2015). Lowered cognitive function, attention deficit/hyperactivity disorders in children, autism, neurodegenerative disease, including dementia in adults and stroke have causal association with PM2.5 pollution (Landrigan et al., 2018). In particular, burning plastic waste emission components were shown to increase the risk of heart disease, aggravate respiratory diseases, for example, asthma and emphysema, and cause rashes, nausea or headaches, and nervous system damages (Verma et al., 2016). The World Health Organization noted (2006) that the PM2.5 average concentrations should not exceed 10μg/m^3 annually and 25μg/m^3 daily, but these thresholds are exceeded in many of the world's cities

(Hey et al., 2018; Guerreiro et al., 2014; He et al., 2017). In this context, a sustainable step towards healthier environment requires immediate attention of the environmental and biomedical scientists (Verma et al., 2016).

It was underlined that the lesser is the size of nanoparticle, the more health hazard they cause (Borisova, 2018). Particle toxicity has been shown to be higher for smaller in size particles on a per unit mass basis (Oberdörster & Utell, 2002; Li et al., 2002); thus, more attention has been focused on fine and ultrafine particulate matter (Fine et al., 2004). A stronger association between health effects and exposure to ultrafine particles as compared to fine or coarse ones was demonstrated (Peters et al., 1997). Epidemiological and toxicological evidences link respiratory health effects and exposures to ultrafine particles, for example associations between fine and ultrafine particles and the incidence of asthma in children (Fine et al., 2004; Pekkanen et al., 1997). When the epithelial cells of human airways were subjected to the different modes of air particulate matter on an equal mass basis, ultrafine particles caused a greater degree of response (Fine et al., 2004; Li et al., 2003). Fine and ultrafine particles can penetrate deeper than larger ones into the airways of the respiratory tract, can reach the alveoli in which 50% are retained in the lung parenchyma and cause damage to the most important components of the respiratory system (Valavanidis et al., 2008; Fine et al., 2004; Anna, 2009).

The intranasally instilled nanoparticles can directly target the central nervous system. They can be accumulated in nasal region of the mammalian organisms, and transported to the central nervous system along sensory axons of the olfactory nerve (Oberdörster et al., 2004, 2005; Kao et al., 2012). The epidemiological, observational, clinical, and experimental evidences suggested that neurological diseases, that is, stroke, Alzheimer's and Parkinson's disease, and autism can be strongly associated with ambient air pollution (Genc et al., 2012). The titanium oxide nanoparticles were detected in brain of the exposed mice (Takeda et al., 2009). The magnetite nanoparticles were found in the human brain that proved significant environmental nanoparticle-associated health hazard (Maher et al., 2016).

The deposition site and, thus, the clearance time of the inhaled particles changes with particle size, leading to differences in toxicity, even for particles of the same composition. Therefore, the chemical composition of the particles should be analyzed with respect to their size, predominantly for the nanoparticles (Hata et al., 2014). However, it is not clear whether particle number, mass, surface area or chemical constituent concentrations pose the greatest health risk (Fine et al., 2004). It was shown that the size of the airborne particles and their surface area determine the potential to provoke inflammatory injury, oxidative damage, and other biological effects. The airborne particulate matter has several mechanisms of cellular effects, such as cytotoxicity through oxidative stress, oxygen-free radical-generating activity, mutagenicity, DNA oxidative damage, and stimulation of proinflammatory factors. The smaller the size of particulate matter, the higher is the toxicity through mechanisms of oxidative stress and inflammation (Valavanidis et al., 2008).

In general, nanoparticles' influence on human health depends on several individual aspects, such as genetics of the organism, existing diseases, the exposure manner, and nanoparticles' properties, namely their chemistry, size, shape,

agglomeration state, and electromagnetic properties (Buzea et al., 2007). Besides, the ability of particles to form dust is very important.

The environmental monitoring is carried out mainly via measuring air pollution particulate matter whose size is of 1, 2.5 and 10μm that identifies them as PM1, PM2.5 and PM10. The ultrafine particles have toxic effects and controlling ambient PM2.5 mass via national air quality standards may not necessarily show human exposure to the ultrafine particles (Fine et al., 2004). Health effects of the atmospheric ultrafine particulate matter have refocused attention on particle number rather than particle mass concentrations as a relevant measurement of particulate matter pollution (Fine et al., 2004). Thus, the nano-sized aerosol particles have received a scientific and even political attention due to data that they directly affect human health (Lee & Bae, 2016; Kuklinska et al., 2015).

4   Carbon-Containing Environmental Nanoparticles Are the Main Components of Air Pollution Particulate Matter

Carbon-containing nanoparticles produced during combustion of carbohydrate-based products, such as fuel, oil, wood, turf and garbage are the most potent air pollutants. They possess different size, composition and surface properties, which makes them difficult object for precise investigation regarding their health effects.

The available literature data are rather contradictory. It was shown that synthesized carbon nanodots exhibited cytotoxicity in HepG2 liver cell lines (DorcÉna et al., 2013). However, Wang et al. (2013) did not demonstrate carbon-nanodot-mediated abnormalities and lesions in mice organs and concluded that carbon nanodots were not toxic at any dose. The environmental carbon-containing nanoparticles are often enriched with the heteroatoms including sulfur. Being prepared from different organic precursors, carbon nanoparticles expose different atoms at their surface and, thus, a variety of functional chemical groups.

The neuroactive properties of sulfur-containing carbon nanodots synthesized from thiourea and citric acid were revealed in studies, when animal brain nerve terminals have been analyzed (Borisova, 2018, 2019). Monitoring key characteristics of excitatory and inhibitory, glutamatergic and γ-aminobutyric acid (GABA), neurotransmission revealed that carbon nanodots from the thiourea and citric acid at the concentrations of 0.5–1.0 mg/mL decreased the initial rate of transporter-mediated uptake of glutamate and GABA by nerve terminals and augmented the ambient level of these neurotransmitters. These carbon nanodots depolarized the plasma membrane of nerve terminals and caused a step-like decrease in synaptic vesicle acidification. Despite different surface and fluorescent features of carbon nanodots synthesized from various precursor materials, namely thiourea/citric acid and β-alanine, they possessed unidirectional neurotoxic effects that were displayed at a different level of efficiency. Sulfur-containing carbon nanodots exhibited 30% lower effects on glutamate and GABA transport in nerve terminals in comparison

with sulfur-free, that is, β-alanine, ones (Borisova, 2019). The presence of the abandoned carbon-containing particles as air pollution components caused a neurotoxicity risk for human health (Borisova, 2018).

5   Methodological Approach for Assessment of Toxicity of Smoke Aerosol Particulate Matter

Laboratory synthesis and characterization of water-suspended smoke aerosol preparations were performed for detailed assessment of smoke aerosol effects and toxicity of different smoke preparations (Borysov et al., 2020; Shelestov et al., 2019). Water-suspended efficacy for the wood smoke particulate matter was calculated taking into account the amount of PM2.5 before and after suspending procedure, that was 800 and 500μg/m^3, respectively. Therefore, efficacy of water-suspended matter consisted of ~60%. Size of the particulate matter of water-suspended wood smoke aerosol preparations was analyzed using dynamic light scattering with Zetasizer (Malvern Instruments, UK), and heterogeneity of the particulate matter was shown. The overall mean of particles in the preparations was 809 nm, where three main populations of particles possessed the size of 53, 727, and 2211 nm (Shelestov et al., 2019). Water-suspended preparations from plastic smoke aerosols have been obtained in a similar way (Borysov et al., 2020).

    Measuring of the membrane potential of brain nerve terminals revealed that the minimal dose of wood smoke particulate matter that caused changes in this parameter and, thus, could initiate harmful health effects, was 40μg/mL (Shelestov et al., 2019). Plastic smoke particulate matter as a component of water-suspended preparations was also capable of the depolarizing plasma membrane of brain nerve terminals (Borysov et al., 2020).

6   Multipollutant Strategies for Environmental Quality and Health Risk Estimations

6.1   *Multipollutant Strategies in Health Hazard Estimations: Interaction of Environmental Factors and Their Combined Effects on Human Health*

An improvement of quality of health risk prognosis based on the multipollutant approach and advanced emerging essential variables is of great importance. A combination of a number of chemical, physical, and biological environmental agents can lead to the combined health effects, which can significantly differ from the effects of particular agents. In general, the combined action of the environmental agents can demonstrate either their interactions or no relations (Fig. 2).
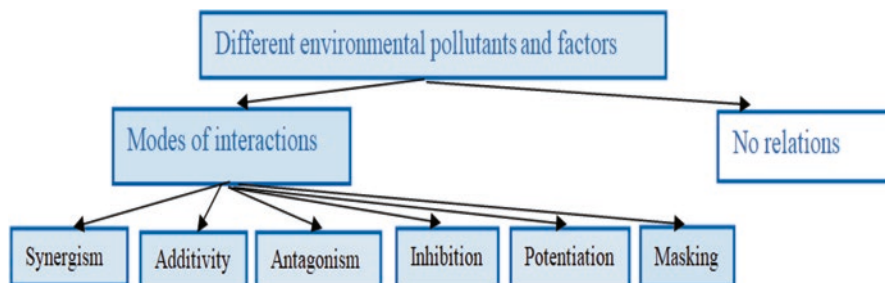
Fig. 2 Potential interrelations between the pollutants

According to Mauderly and Samet (2009), potential interactions between the pollutants include: (1) additivity (the effect of the combination equals the sum of individual effects); (2) synergism (the effect of the combination is greater than the sum of individual effects); (3) antagonism (the effect of the combination is less than the sum of individual effects); (4) inhibition (the component having no effect reduces the effect of another component); (5) potentiation (the component having no effect increases the effect of another component); (6) masking (two components have opposite, cancelling effects, such that no effect is observed from the combination). Statistical modelling defines the interaction as the interdependence of health effects of two or more environmental variables. To test the interaction impact, new environmental variables have to be introduced into the analytical models (Mauderly & Samet, 2009).

Among different modes of environmental pollutants and factors interactions, synergism is of special interest because it can result in the underestimation of health hazard feasibility. Individual chemical compounds, environmental pollutants, are usually naturally present in low concentrations. However, they can interact with each other resulting in synergistic combined health effects of the pollutant mixture. Therefore, determination of a quantitative index of synergism, and also the assessment of additivity, antagonism, inhibition, potentiation and masking can significantly improve the prognosis of health hazards in environmental monitoring.

The results of the epidemiologic investigations suggested that for several environmental pollutants and factors, the effects of the combined exposures were more considerable than the effects of the exposure to a single pollutant or factor.

Recently, it was found that sunlight and electromagnetic fields could change the effects of pesticides and metal trace elements on human health. The degradation of a parent molecule can result in several by-products which can trigger various toxic effects. For example, sunlight-irradiated pesticide sulcotrione has a greater cytotoxicity and genotoxicity than the parent molecule, the sulcotrione. Other elements, metals or biological products can augment cellular toxicity of pesticides suggesting a synergy in the living organisms (Ledoigt et al., 2015).

A widespread repeated exposure to pesticides and heavy metals of the occupational and environmental origin has indicated that a combination of heavy metals and pesticides can provoke more severe impact on human health as compared to individual effects. Several studies have revealed the synergistic interactions and synergistic toxic effects of various heavy metals and pesticides in animals and humans (Singh et al., 2017). Thus, it might be suggested that air pollution particulate matter and other environmental nanoparticles can interact with heavy metals, pesticides and other pollutants, and these pollutants during their interactions can provoke more severe complex health impacts, as compared to those of the individual pollutant per se.

Using epidemiologic approaches for an assessment of synergism among the pollutants requires certain information, such as estimation of exposure or dose for two or more pollutants. The synergism is assessed using multivariable models that include the terms representing the effects of the individual pollutants and one or more interaction terms that represent potential joint effects (Greenland, 1983; Rothman et al., 2008; Mauderly & Samet, 2009). A model for interaction of two pollutants can be expressed as follows: $Y = \alpha + \beta_1 x_1 + \beta_2 x_2 + \beta_3 x_1 x_2 + \varepsilon$, where Y is the outcome, x_1 and x_2 are two specific pollutants, β_1 and β_2 estimate the pollutant-specific effects of x_1 and x_2, and β_3 estimates the joint effect of x_1 and x_2, and ε is the error term. At the existence of interaction (synergism is a positive interaction), β_3 is not zero (the value indicating no interaction), and the effect of x_1 is $x_1(\beta_1 + \beta_3 x_1 x_2)$ and that of x_2 is $x_2(\beta_2 + \beta_3 x_1 x_2)$ (Mauderly & Samet, 2009).

6.2   Feasible Synergistic Neurotoxic Effects of Different Environmental Pollutants

In addition to the epidemiological studies, laboratorial studies conducted *in vitro* are important for: (1) identification of essential environmental variables for advanced multipollutant strategies in estimation of health treats and identification of cellular targets of pollutant actions; (2) analysis of possibility of interaction of the environmental pollutants and factors; and (3) interpretation of the epidemiological modelling data.

If the targets of the pollutant action are defined, the preliminary health effect prognosis can be done and potential synergism and additivity of pollutant effects can be predicted. A quantitative test of synergism and additivity obliges investigators to perform related measurement of health effects of each pollution component and component mixture under identical experimental conditions (Fig. 3).
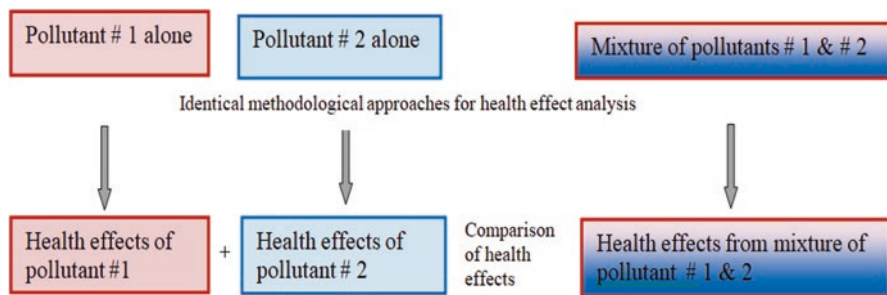
Fig. 3 Algorithm of evaluation of synergism between the pollutants. All measurements should be performed using identical methodological approach

6.3 Feasible Synergistic Toxic Effects of Air Pollution Particulate Matter with Heavy Metals and Other Environmental Pollutants

As shown earlier, aerosols play a significant role in the atmosphere and influence directly on global climate and human health. Satellite images confirm the existence of the particulate matter from both the anthropogenic and natural sources (Buzea et al., 2007), and, thus, the estimation of air quality is an important stream of the environmental science based on the computational analyses (Eisen et al., 2011; Block et al., 2012; Karmakar et al., 2014). The environmental micro- and nano-sized particles and natural organic matter derived from air, soil, and water may interact with each other and act together. These particles can also closely interact with plant organic compounds, animal residues, and microbial products. The environmental particles might serve as a platform for immobilization of microorganisms and viruses, and such immobilization can make the particles more stable. It should be emphasized that the interaction of the environmental nanoparticles with natural organic matter might alter their general toxicity (Lin et al., 2017; Borisova & Komisarenko, 2020).

It was shown (Borisova, 2018) that air pollution particulate matter might possess severe neurotoxic features because these particles can move along the olfactory nerve directly to the central nervous system, avoiding the blood brain barrier and altering brain functioning (Oberdörster et al., 2004, 2005). In this context, the interaction between different neurotoxic environmental pollutants, such as air pollution particulate matter and heavy metals, can be predicted. Moreover, before interaction with the air pollution particulate matter, several heavy metals can interact with each other and have the synergetic effects. The presynaptic mechanisms underlying neurotoxic effects of heavy metals cadmium and lead have been analyzed. We revealed that the synaptic malfunctioning associated with the influence of cadmium and lead can result from a partial dissipation of the synaptic vesicle proton gradient. This effect leads to a decrease in stimulated exocytosis, which is associated not only with the blockage of voltage-gated calcium channels but also with incomplete filling of

synaptic vesicles and the attenuation of transporter-mediated uptake of glutamate, the major excitatory neurotransmitter in the central nervous system (Borisova, 2014).

Based on these experimental data (Borisova, 2014), we suggested that the effects of cadmium and lead might be additive or even synergistic within a definite range of pollutant concentrations. In favor of this suggestion, it was shown that glutamate transporters, whose functioning determines proper extracellular level of this neurotransmitter, are among the targets influenced by both heavy metals in the nerve cells (Borisova, 2016; Borisova & Borysov, 2016; Tarasenko et al., 2010).

The interaction and even synergism between the environmental pollutants, for example cadmium and lead, on one hand, and mercury on the other hand, could take place because they act at the same biochemical pathway in the nerve cells. Assuming that the metal cations occupy most likely SH groups of the same key functional membrane proteins, for example neurotransmitter transporters, located in the plasma membrane of nerve cells, one could predict that the occupation of the neurotransmitter transporters by the less toxic metal, for example cadmium and lead, may partially prevent the interaction of more toxic metal, for example mercury, with those proteins, thus, causing a protective effect.

The results of measuring an acute lethality in rats under the action of different combinations of cadmium, mercury and lead salts indicate that particular combinations could be synergistic, antagonistic or additive, depending on the relative doses of employed metal cations (Schubert et al., 1978).

A use of pairwise and triple metal combinations demonstrated that heavy metals displayed synergistic killing effects towards nematode *Caenorhabditis elegans*. Severe increase in the mortality was registered on application of low metal concentrations. This fact shows a complexity of the toxicity tests in the biological systems (Wah Chu & Chow, 2002).

Importantly, potential interactions can be predicted for other severe environmental pollutants with proved or suggested neurotoxic effects. Special attention might be focused at the combined application of heavy metals, persistent organic pollutants, for example polychlorinated biphenyls, and insecticides of the neonicotinoid type, as they all have targets in plasma membrane of the nerve cells.

The synergistic effects of the environmental pollutants might be realized at the different levels of the biological organization, namely organ, tissue and cellular level. Different pollutants, namely air pollution particulate matter, heavy metals, persistent organic pollutants, the polychlorinated biphenyls and neonicotinoids demonstrated neurotoxic action; however, their interactions need to be investigated in more detail. Besides, the mechanisms of action of air pollution particulate matter at the cellular level remain unclear. It was demonstrated that various types of micro- and nano-sized particles interacted with the cellular plasma membrane and some of them penetrated it and reached the intracellular compartments (Borisova, 2018). So, the abovementioned pollutants are potentially capable of interacting with membrane-associated proteins of the nerve cells. In this context, the additivity and synergism of the effects of air pollution particulate matter, heavy metals, polychlorinated biphenyls and neonicotinoids might be also predicted.

The black carbon from fuel exhaust, wood, coal, garbage and plastic combustion is known to be the main component of air pollution particulate matter (Tranvik, 2018; Long et al., 2013). As shown in Fig. 3, an assessment of interaction of different pollutants can be carried out using identical methodological approach. To perform such experiments, one should have water-suspended aerosol preparations appropriate for the biological experiments (the method for synthesis of those preparations was described above). Different water-suspended smoke preparations can be used for establishment of relations of air quality with health hazards. Selection of a set of essential variables for estimation of air quality is still staying at early stage of Group on Earth Observations (GEO).

It should be noted that synergistic effect is very specific. For example, combined exposure to air pollution particulate matter and/or several heavy metals can have synergistic effects regarding one cellular target, but no such effects for another target. Besides, these pollutants can have synergistic action in one tissue, but lack such action in other tissues (Schubert et al., 1978; Wah Chu & Chow, 2002; Buzea et al., 2007). Therefore, the interaction of the environmental pollutants and factors, as well as health threat prognosis, should be considered separately for each tissue, organ and system of human organism.

The analysis of these indicators might be based on the dose-response curves of the pollutant actions. The additive and synergistic effects could be monitored only at a definite concentration range of each pollutant. Moreover, these effects can be lost beyond definite concentration interval (Schubert et al., 1978; Wah Chu & Chow, 2002; Buzea et al., 2007). In this context, even proven additivity and synergism of the combined action of pollutants toward one cellular target can be actual only within their definite concentration range. This fact should be taken into consideration at the estimation of environmental impact and health threat prognosis. Specific algorithms have to be developed for each type of interaction of the environmental pollutants and factors. Therefore, single pollutant strategy in the estimation of the environmental health hazard should be replaced by the multipollutant one.

6.4   Multipollutant Information Technologies

Recognizing multipollutant strategies and related parameter changes in models and risk assessment programs led to development of the multipollutant information technologies that are better addressing the overall air quality objectives. Pearson correlation coefficients between the pairs of pollutants and ratios of the average correlations for each pollutant with other pollutants (Levy et al., 2014) can be computed based on the experimental and monitoring data. The experimental data from in vitro and in vivo experiments, as well as from the epidemiological studies and monitoring, are necessary for determination of different pollutant interrelations. It should be noted that actual exposures underlying the epidemiological studies are multipollutant *pes se* (Scheffe et al., 2007). The health effects of air pollution may be the result of a single pollutant toxicity or the product of several pollutants

interacting in the unknown manner (Scheffe et al., 2007). These interactions might be established in in vitro experiments and may be existing between the pollutants themselves or interacting via complex biological mechanisms and even through common cellular pathways (Scheffe et al., 2007).

A platform offering the analysis of the environmental information, modern controlling technologies, and models for risk assessment should be developed for neurotoxicity prognosis and interference of air pollution particulate matter with other neurotoxic environmental pollutants (heavy metals, for example, mercury, cadmium, lead, copper, etc., persistent organic pollutants, for example, polychlorinated biphenyls, and neonicotinoids). Regulatory dispersion model, AERMOD (Revision to the Guideline on Air Quality Models, 2005), provides a discrete source- and local-scale characterization for primary species (air toxics and a significant fraction of urban scale particulate matter). The US Environmental Protection Agency has developed several risk assessment tools, including the Total Risk Integrated Methodology (TRIM). It uses a compartmental mass balance model that describes the movement and transformation of pollutants over time through a user-defined system and includes both biotic and abiotic compartments (Scheffe et al., 2007). The Co-Benefits Risk Assessment (COBRA) model (Environmental Protection Agency, 2004) which uses built-in source-receptor atmospheric sensitivity matrices in place of atmospheric modelling, allows quick estimates of health impacts from various emission sources (Chestnut et al., 2006).

In summary, the action of the environmental pollutants and factors towards human organisms is complex. A combination of different chemical, physical, and biological environmental agents and factors can lead to the combined health effects that can significantly differ from the effects of particular agent or factor. Synergism of pollutant health effects is of special attention because it can result in underestimation of health hazard feasibility. Prediction of synergistic toxic effects of the environmental pollutants, and determination of a quantitative index of the synergism, as well as the additivity, antagonism, inhibition, potentiation and masking can significantly improve the prognosis of health hazards in the environmental monitoring. The additive and synergistic effects of combinations of air pollution particulate matter and heavy metals, for instance, mercury, cadmium, lead, copper, etc., persistent organic pollutants, for example, polychlorinated biphenyls, and insecticide neonicotinoids on the nervous system were suggested.

References

Anna, A. D. (2009). *Combustion-formed nanoparticles*. Accessed 9 Aug 2018. https://doi.org/10.1016/j.proci.2008.09.005

Block, M. L., Elder, A., Auten, R. L., et al. (2012). The outdoor air pollution and brain health workshop. *Neurotoxicology, 33*, 972–984.

Borisova, T. (2014). The neurotoxic effects of heavy metals: Alterations in acidification of synaptic vesicles and glutamate transport in brain nerve terminals. In A. Costa & E. Villalba (Eds.), *Horizons in neuroscience research* (Vol. 14, pp. 89–112). Nova Science Publisher, Inc.

Borisova, T. (2016). Permanent dynamic transporter-mediated turnover of glutamate across the plasma membrane of presynaptic nerve terminals: Arguments in favour and against. *Reviews in the Neurosciences, 27*, 71–81.

Borisova, T. (2018). Nervous system injury in response to contact with environmental, engineered and planetary micro- and nano-sized particles. *Frontiers in Physiology, 728*. https://doi.org/10.3389/fphys.2018.00728

Borisova, T. (2019). Express assessment of neurotoxicity of particles of planetary and interstellar dust. *npj Microgravity, 5*, Article number: 2.

Borisova, T., & Borysov, A. (2016). Putative duality of presynaptic events. *Reviews in the Neurosciences, 27*, 377–383.

Borisova, T., & Komisarenko, S. (2020). Air pollution particulate matter as a potential carrier of SARS-CoV-2 to the nervous system and/or neurological symptom enhancer: Arguments in favor. *Environmental Science and Pollution Research*. https://doi.org/10.1007/s11356-020-11183-3

Borysov, A., Krisanova, N., Chunihin, O., Ostapchenko, L., Pozdnyakova, N., & Borisova, T. (2014). A comparative study of neurotoxic potential of synthesized polysaccharide-coated and native ferritin-based magnetic nanoparticles. *Croatian Medical Journal, 55*, 195–205.

Borysov, A., Tarasenko, A., Krisanova, N., Pozdnyakova, N., Pastukhov, A., Dudarenko, M., Paliienko, K., & Borisova, T. (2020). Plastic smoke aerosol: Nano-sized particle distribution, absorption/fluorescent properties, dysregulation of oxidative processes and synaptic transmission in rat brain nerve terminals. *Environmental Pollution, 263*, Part A, 114502.

Buzea, C., Pacheco, I. I., & Robbie, K. (2007). Nanomaterials and nanoparticles: Sources and toxicity. *Biointerphases, 2*(4), MR17–MR71. https://doi.org/10.1116/1.2815690

Chestnut, L. G., Mills, D. M., & Cohan, D. S. (2006). Cost-benefit analysis in the selection of efficient multipollutant strategies. ISSN 1047-3289. *Journal of the Air & Waste Management Association, 56*, 530–536.

Després, V., Huffman, J. A., Burrows, S. M., Hoose, C., Safatov, A., Buryak, G., Fröhlich-Nowoisky, J., et al. (2012). Primary biological aerosol particles in the atmosphere: A review. *Tellus Series B: Chemical and Physical Meteorology, 64*, 15598.

DorcÉna, C. J., Olesik, K. M., Wetta, O. J., & Winter, J. O. (2013). Characterization and toxicity of carbon dot-poly(lactic-co-glycolic acid) nanocomposites for biomedical imaging. *Nano LIFE, 03*(01), 1340002. https://doi.org/10.1142/S1793984413400023

Duhan, J. S., Kumar, R., Kumar, N., Kaur, P., Nehra, K., & Duhan, S. (2017). Nanotechnology: The new perspective in precision agriculture. *Biotechnology Reports, 15*, 11–23.

Eisen, E. A., Costello, S., Chevrier, J., & Picciotto, S. (2011). Epidemiologic challenges for studies of occupational exposure to engineered nanoparticles; a commentary. *Journal of Occupational and Environmental Medicine, 53*, S57–S61.

Fine, P. M., Shen, S., & Sioutas, C. (2004). Inferring the sources of fine and ultrafine particulate matter at downwind receptor sites in the Los Angeles Basin using multiple continuous measurements special issue of *Aerosol Science and Technology* on findings from the fine particulate matter supersites program. *Aerosol Science and Technology, 38*(sup1), 182–195. https://doi.org/10.1080/02786820390229499

Fuzzi, S., Baltensperger, U., Carslaw, K., Decesari, S., Denier van der Gon, H., Facchini, M. C., Fowler, D., et al. (2015). Particulate matter, air quality and climate: Lessons learned and future needs. *Atmospheric Chemistry and Physics, 15*, 8217–8299.

Genc, S., Zadeoglulari, Z., Fuss, S. H., & Genc, K. (2012). The adverse effects of air pollution on the nervous system. *Journal of Toxicology, 2012*, 782462. https://doi.org/10.1155/2012/782462

Gilardoni, S., Massoli, P., Paglione, M., Giulianelli, L., Carbone, C., Rinaldi, M., Decesari, S., et al. (2016). Direct observation of aqueous secondary organic aerosol from biomass-burning emissions. *Proceedings of the National Academy of Sciences, 113*(36) http://www.pnas.org/content/113/36/10013

Greenland, S. (1983). Tests for interaction in epidemiologic studies: A review and study of power. *Statistics in Medicine, 83*, 243–251.

Guerreiro, C. B. B., Foltescu, V., & de Leeuw, F. (2014). Air quality status and trends in Europe. *Atmospheric Environment, 98*(December), 376–384. https://doi.org/10.1016/J.ATMOSENV.2014.09.017

Hata, M., Chomanee, J., Thongyen, T., Bao, L., Tekasakul, S., Tekasakul, P., Otani, Y., & Furuuchi, M. (2014). Characteristics of nanoparticles emitted from burning of biomass fuels. *Journal of Environmental Sciences, 26*(9), 1913–1920. https://doi.org/10.1016/J.JES.2014.07.005

He, M., Zeng, X., Zhang, K., & Kinney, P. (2017). Fine particulate matter concentrations in urban Chinese cities, 2005–2016: A systematic review. *International Journal of Environmental Research and Public Health, 14*(2), 191. https://doi.org/10.3390/ijerph14020191

Hey, J. D. V., Sonderfeld, H., Jeanjean, A. P. R., Panchal, R., Leigh, R. J., Allen, M. A., Dawson, M., & Monks, P. S. (2018). Experimental and modelling assessment of a novel automotive Cabin PM$_{2.5}$ removal system. *Aerosol Science and Technology*, 1–50. https://doi.org/10.1080/02786826.2018.1490694

Horwell, C. J., & Baxter, P. J. (2006). The respiratory health hazards of volcanic ash: A review for volcanic risk mitigation. *Bulletin of Volcanology, 69*, 1–24. https://doi.org/10.1007/s00445-006-0052-y

Jaenicke, R. (2005). Abundance of cellular material and proteins in the atmosphere. *Science. 80, 308*, 73.

Jiang, X., Zhang, Q., Zhao, H., Geng, G., Peng, L., Guan, D., Kan, H., et al. (2015). Revealing the hidden health costs embodied in Chinese exports. *Environmental Science & Technology, 49*, 4381–4388.

Kao, Y.-Y., Cheng, T.-J., Yang, D.-M., Wang, C.-T., Chiung, Y.-M., & Liu, P.-S. (2012). Demonstration of an Olfactory Bulb–Brain translocation pathway for ZnO nanoparticles in rodent cells in vitro and in vivo. *Journal of Molecular Neuroscience, 48*, 464–471.

Karmakar, A., Zhang, Q., & Zhang, Y. (2014). Neurotoxicity of nanoscale materials. *Journal of Food and Drug Analysis, 22*, 147–160.

Kelly, F. J., & Fussell, J. C. (2015). Air pollution and public health: Emerging hazards and improved understanding of risk. *Environmental Geochemistry and Health, 37*(4), 631–649. https://doi.org/10.1007/s10653-015-9720-1

Kuklinska, K., Wolska, L., & Namiesnik, J. (2015). Air quality policy in the U.S. and the EU – A review. *Atmospheric Pollution Research, 6*(1), 129–137. https://doi.org/10.5094/APR.2015.015

Landrigan, P. J., Fuller, R., Acosta, N. J. R., Adeyi, O., Arnold, R., Basu, et al. (2018). The Lancet Commission on pollution and health. *The Lancet, 391*(10119), 462–512. https://doi.org/10.1016/S0140-6736(17)32345-0

Lang-Yona, N., Dannemiller, K., Yamamoto, N., Burshtein, N., Peccia, J., Yarden, O., & Rudich, Y. (2012). Annual distribution of allergenic fungal spores in atmospheric particulate matter in the Eastern Mediterranean; a comparative study between ergosterol and quantitative PCR analysis. *Atmospheric Chemistry and Physics, 12*, 2681–2690. https://doi.org/10.5194/acp-12-2681-2012

Ledoigt, G., Sta, C., Goujon, E., Souguir, D., & El Ferjani, E. (2015). Synergistic health effects between chemical pollutants and electromagnetic fields. *Reviews on Environmental Health, 30*(4), 305–309.

Lee, B. U., & Bae, G. N. (2016). Measurement of aerosol nanoparticles from a combustion particle generator by using three types of dilutors. *Atmospheric Pollution Research, 7*(2), 303–306. https://doi.org/10.1016/J.APR.2015.10.012

Lelieveld, J., Evans, J. S., Fnais, M., Giannadaki, D., & Pozzer, A. (2015). The contribution of outdoor air pollution sources to premature mortality on a global scale. *Nature, 525*(7569), 367–371. https://doi.org/10.1038/nature15371

Levy, I., Mihele, C., Lu, G., Narayan, J., & Brook, J. R. (2014). Evaluating multipollutant exposure and urban air quality: Pollutant interrelationships, neighborhood variability, and nitrogen dioxide as a proxy pollutant. *Environmental Health Perspectives, 122*, 65–72.

Li, N., Kim, S., Wang, M., Froines, J., Sioutas, C., & Nel, A. (2002). Use of a stratified oxidative stress model to study the biological effects of ambient concentrated and diesel exhaust particulate matter. *Inhalation Toxicology, 14*(5), 459–486. https://doi.org/10.1080/089583701753678571

Li, N., Sioutas, C., Cho, A., Schmitz, D., Misra, C., Sempf, J., Wang, M., Oberley, T., Froines, J., & Nel, A. (2003). Ultrafine particulate pollutants induce oxidative stress and mitochondrial damage. *Environmental Health Perspectives, 111*(4), 455–460. http://www.ncbi.nlm.nih.gov/pubmed/12676598

Lin, S., Mortimer, M., Chen, R., Kakinen, A., Riviere, J. E., Davis, T. P., Ding, F., et al. (2017). NanoEHS beyond toxicity – Focusing on biocorona. *Environmental Science. Nano, 4*, 1433–1454.

Long, C. M., Nascarella, M. A., & Valberg, P. A. (2013). Carbon black vs. black carbon and other airborne materials containing elemental carbon: Physical and chemical distinctions. *Environmental Pollution, 181*, 271–286.

Maher, B. A., Ahmed, I. A. M., Karloukovski, V., MacLaren, D. A., Foulds, P. G., Allsop, D., Mann, D. M. A., Torres-Jardón, R., & Calderon-Garciduenas, L. (2016). Magnetite pollution nanoparticles in the human brain. *Proceedings of the National Academy of Sciences of the United States of America, 113*, 10797–10801.

Mauderly, J. L., & Samet, J. M. (2009). Is there evidence for synergy among air pollutants in causing health effects? *Environmental Health Perspectives, 117*(1), 1–6.

Oberdörster, G., & Utell, M. J. (2002). Ultrafine particles in the urban air: To the respiratory tract--and beyond? *Environmental Health Perspectives, 110*(8), A440–A441. http://www.ncbi.nlm.nih.gov/pubmed/12153769

Oberdörster, G., Sharp, Z., Atudorei, V., Elder, A., Gelein, R., Kreyling, W., & Cox, C. (2004). Translocation of inhaled ultrafine particles to the brain. *Inhalation Toxicology, 16*, 437–445.

Oberdörster, G., Oberdörster, E., & Oberdörster, J. (2005). Nanotoxicology: An emerging discipline evolving from studies of ultrafine particles. *Environmental Health Perspectives, 113*, 823–839.

Pekkanen, J., Timonen, K. L., Ruuskanen, J., Reponen, A., & Mirme, A. (1997). Effects of ultrafine and fine particles in urban air on peak expiratory flow among children with asthmatic symptoms 1. https://pdfs.semanticscholar.org/0f23/6424c6cefe3890f033f13a2c417f79c3bee4.pdf.

Peters, A., Wichmann, H. E., Tuch, T., Heinrich, J., & Heyder, J. (1997). Respiratory effects are associated with the number of ultrafine particles. *American Journal of Respiratory and Critical Care Medicine, 155*(4), 1376–1383. https://doi.org/10.1164/ajrccm.155.4.9105082

Pope, C. A., Burnett, R. T., Turner, M. C., Cohen, A., Krewski, D., Jerrett, M., Gapstur, S. M., & Thun, M. J. (2011). Lung cancer and cardiovascular disease mortality associated with ambient air pollution and cigarette smoke: Shape of the exposure–response relationships. *Environmental Health Perspectives, 119*, 1616–1621.

Pozdnyakova, N., Pastukhov, A., Dudarenko, M., Galkin, M., Borysov, A., Borisova, T. (2016). Neuroactivity of detonation nanodiamonds: dose-dependent changes in transporter-mediated uptake and ambient level of excitatory/inhibitory neurotransmitters in brain nerve terminals. *Journal of Nanobiotechnology*. https://doi.org/10.1186/s12951-016-0176-y

Pozdnyakova, N., Pastukhov, A., Dudarenko, M., Borysov, A., Krisanova, N., Nazarova, A., & Borisova, T. (2017). Enrichment of inorganic Martian dust simulant with carbon component can provoke neurotoxicity. *Microgravity Science and Technology, 29*, 133–144.

Ray, P. C., Yu, H., & Fu, P. P. (2009). Toxicity and environmental risks of nanomaterials: Challenges and future needs. *Journal of Environmental Science and Health. Part*

C, Environmental Carcinogenesis & Ecotoxicology Reviews, 27(1), 1–35. https://doi.org/10.1080/10590500802708267

Revision to the Guideline on Air Quality Models: Adoption of a Preferred General Purpose (Flat and Complex Terrain) Dispersion Model, 40 CFR Part 51. (2005).

Rothman, K. J., Greenland, S., & Last, T. L. (2008). *Modern Epidemiology*. Lippincott Williams & Evans.

Scheffe, R., Hubbell, B., Fox, T., Rao, V., & Pennell, W. (2007). *The rationale for a multipollutant, multimedia air quality management framework*, EPA, NARSTO, awma.org.

Schubert, J., Riley, E. J., & Tyler, S. A. (1978). Combined effects in toxicology--a rapid systematic testing procedure: Cadmium, mercury, and lead. *Journal of Toxicology and Environmental Health, 4*(5–6), 763–776.

Shelestov, A., Kolotii, A., Borisova, T., Turos, O., Milinevsky, G., Gomilko, I., Bulanay, T., Fedorov, O., Shumilo, L., Pidgorodetska, L., Kolos, L., Borysov, A., Pozdnyakova, N., Chunikhin, A., Dudarenko, M., Petrosian, A., Danylevsky, V., Miatselskaya, N., & Choli, V. (2019). Essential variables for air quality estimation. *International Journal of Digital Earth, 13*, 1–22. https://doi.org/10.1080/17538947.2019.1620881

Singh, S., Singh, B. K., Yadav, S. M., & Gupta, A. K. (2015). Applications of nanotechnology in agricultural and their role in disease management. *Research Journal of Nanoscience and Nanotechnology, 5*, 1–5.

Singh, N., Gupta, V. K., Kumar, A., & Sharma, B. (2017). Synergistic effects of heavy metals and pesticides in living systems. *Frontiers in Chemistry*. https://doi.org/10.3389/fchem.2017.00070

Takeda, K., Suzuki, K., Ishihara, A., Kubo-Irie, M., Fujimoto, R., Tabata, M., Oshio, S., Nihei, Y., Ihara, T., & Sugamata, M. (2009). Nanoparticles transferred from pregnant mice to their offspring can damage the genital and cranial nerve systems. *Journal of Health Science, 55*, 95–102.

Tarasenko, A. S., Sivko, R. V., Krisanova, N. V., Himmelreich, N. H., Borisova , T. A. (2010). Cholesterol depletion from the plasma membrane impairs proton and glutamate storage in synaptic vesicles of nerve terminals. *Journal of Molecular Neuroscience, 41*(3), 358–367.

Tranvik, L. J. (2018). New light on black carbon. *Nature Geoscience, 11*(8), 547–548. https://doi.org/10.1038/s41561-018-0181-x

User's Manual for the National Co-Benefits Risk Assessment Model; Abt Associates. (2004). : U.S. Environmental Protection Agency.

Valavanidis, A., Fiotakis, K., & Vlachogianni, T. (2008). Airborne particulate matter and human health: Toxicological assessment and importance of size and composition of particles for oxidative damage and carcinogenic mechanisms. *Journal of Environmental Science and Health, Part C, 26*(4), 339–362. https://doi.org/10.1080/10590500802494538

Verma, R., Vinoda, K. S., Papireddy, M., & Gowda, A. N. S. (2016). Toxic pollutants from plastic waste- a review. *Procedia Environmental Sciences, 35*(January), 701–708. https://doi.org/10.1016/J.PROENV.2016.07.069

Wah Chu, K., & Chow, K. L. (2002). Synergistic toxicity of multiple heavy metals is revealed by a biological assay using a nematode and its transgenic derivative. *Aquatic Toxicology, 61*, 53–64.

Wang, K., Gao, Z., Gao, G., Wo, Y., Wang, Y., Shen, G., & Cui, D. (2013). Systematic safety evaluation on photoluminescent carbon dots. *Nanoscale Research Letters, 8*(1), 122. https://doi.org/10.1186/1556-276X-8-122

Zhang, Q., Jiang, X., Tong, D., Davis, S. J., Zhao, H., Geng, G., Feng, T., et al. (2017). Transboundary health impacts of transported global air pollution and international trade. *Nature, 543*, 705–709.

Index